CORA Cork Open Research Archive
Cartlann Taighde Oscailte Chorcaí

Title	An evaluation of orogenic kinematic evolution utilizing crystalline and magnetic anisotropy in granitoids
Authors	McCarthy, William J.
Publication date	2013
Original Citation	McCarthy, W. J. 2013. An evaluation of orogenic kinematic evolution utilizing crystalline and magnetic anisotropy in granitoids. PhD Thesis, University College Cork.
Type of publication	Doctoral thesis
Rights	© 2013, William J. McCarthy - http://creativecommons.org/licenses/by-nc-nd/3.0/
Download date	2026-10-16 06:02:47
Item downloaded from	https://hdl.handle.net/10468/1669



UCC
University College Cork, Ireland
Coláiste na hOllscoile Corcaigh

An Evaluation of Orogenic Kinematic Evolution Utilizing Crystalline and Magnetic Anisotropy in Granitoids

---

Volume 1 of 2 (Main Text)

William J. McCarthy

A thesis submitted for the degree of

Doctor of Philosophy

June 2013

Research Supervisors:

Dr. R.J. Reavy

Prof. M.S. Petronis

National University of Ireland, Cork
School of Biological, Earth & Environmental Sciences (Discipline of Geology)
College of Science, Engineering and Food Science
Head of School: Prof. John O'Halloran

Table of Contents

Table of Contents i
Declaration v
Acknowledgements vi
Abstract vii
Prologue ix
Notes for the Reader x

Chapter 1:
Controls on Granite Ascent and Emplacement

1.1 Introduction 1
1.2 Factors controlling ascent and emplacement 4
1.2.1 The Role of Buoyancy 4
1.2.2 Viscosity and Magma Pressure 6
1.2.3 Excess Magma Pressure 7
1.2.4 Ambient Stress 8
1.2.5 The Role of Crustal Anisotropy 9
1.2.6 Summary 12
1.3 Validity of Passive and Forceful Terminology 13
1.4 Emplacement Mechanisms 15
1.4.1 Diapirism 16
1.4.2 Ballooning and Inflation 17
1.4.3 Intrusion into Active Shear Zones 18
1.4.4 Laccoliths 19
1.4.5 Cauldron Subsidence 22
1.4.6 Role of Stoping 24
1.5 Conclusions 25

Chapter 2:
The Caledonian and Acadian Orogenies

2.1 Introduction 27
2.2 Definition of the Caledonian Orogeny 27
2.3 Summary of Opening the Iapetus Ocean 29
2.3.1 Initiation of the Iapetus Ocean 29
2.3.2 The Dalradian Supergroup 32
2.3.2.1 Summary of Stratigraphy 34
2.3.2.2 Temporal Constraints 36
2.4 Closure of the Iapetus Ocean 36
2.4.1 The Penobscotian Orogenic Phase 37
2.4.2 The Grampian Orogenic Phase 38
2.4.3 The Shelveian Orogenic Phase 40
2.4.4 The Scandian Orogenic Phase 42
2.4.5 Suturing of Laurentia and Avalonia 45
2.4.6 Transcurrent Lockup 47
2.5 The Acadian Orogeny 55
2.6 Summary of Key Tectonic Parameters 58

Chapter 3:
Background Geology; The Connemara Metamorphic Complex

3.1 Introduction 59
3.2 Dalradian Stratigraphy of Connemara 62
3.3 Grampian Magmatism 64
3.3.1 Metagabbros 65
3.3.2 Orthogneisses 66
3.4 Oughterard Granite 67
3.5 Regional Metamorphism 69
3.6 Structural Evolution of the CMC 71
3.7 Connemara; Ominously South of the Highland Boundary Fault 76
3.8 Conclusions 78
3.8.1 Main Structural Features 79

Chapter 4:
Caledonian Granites of Britain and Ireland

4.1 Introduction 81
4.2 Categorising the Caledonian Granites 82
4.2.1 The Northern Granites 84
4.2.2 The Trans-Suture Suite 86
4.3 Regional Petrogenetic Models Applied to Irish Granites 88

Chapter 5:
The Galway Granite Complex

5.1 Introduction 91
5.2 Clarification of the Nomenclature 91
5.3 Constituents of the Galway Granite Complex 93
5.3.1 The Earlier Plutons 93
5.3.1.1 The Inish Pluton 94
5.3.1.2 The Letterfrack Pluton 94
5.3.1.3 The Omey Pluton 94
5.3.1.4 The Roundstone Pluton 96
5.3.2 The Main Batholith 98
5.3.2.1 The Carna Pluton 98
5.3.2.2 The Kilkieran Pluton 102
5.4 Summary and Objectives 106
5.4.1 Key Questions 108

Chapter 6:
A Review of Applied Theory

6.1 Introduction 110
6.2 Geochronology 110
6.2.1 Analytical Process 113
6.3 Rheology; Magmatic, Sub-magmatic and Solid State Fabrics 114
6.3.1 Rheology 114
6.3.2 Microstructural Analysis of Granite 116
6.3.2.1 Microstructures of Common Granitic Minerals 116
6.3.3 Classification of Rheological State Based on Microstructure 121
6.3.3.1 Magmatic Flow 122
6.3.3.2 Sub-magmatic Deformation 123

6.3.3.3 Solid State Deformation 124
6.4 The Strain Record in Granite 124
6.4.1 Quantifying Strain 126
6.4.2 Field Based Fabric Analysis 127
6.4.3 Inclusions as Strain Markers 127
6.4.4 Shear Sense Indicators 129
6.4.5 Deformation of the Country Rock 130
6.5 Anisotropy of Magnetic Susceptibility 131
6.5.1 AMS Parameters and Data Manipulation 133
6.5.2 AMS of some Minerals 137
6.5.3 Caveats of AMS 140
6.6 Characterising the Magnetic Properties of a Specimen 143
6.6.1 Rock Magnetic Experiments 144
6.6.1.1 Temperature vs. Low Field Susceptibility (T vs. K) 144
6.6.1.2 The Lowrie - Fuller Test 145
6.6.1.3 IRM Acquisition Curves 146
6.6.1.4 Thermomagnetic Analysis of Three-Component IRM 147
6.7 Summary 148
6.7.1 The use of Rock Magnetics in this Thesis 149

Chapter 7:
The Omey Pluton; A Discordant Phacolith
7.1 Introduction 152
7.2 Geological Background 152
7.3 Petrographic and Field Descriptions 154
7.3.1 Facies Descriptions and Distribution 155
7.3.2 Contact Relationships 160
7.3.2.1 External Contact Relationships 160
7.3.2.2 Internal Contacts 166
7.3.3 Late Stage Minor Intrusions 169
7.3.4 Fabrics in the Omey Pluton 173
7.3.5 Summary of Field Observations 180
7.4 Rock Magnetic Analysis 181
7.4.1 Sampling 182
7.4.2 Results of Rock Magnetic Experiments 182
7.4.3 Anisotropy of Magnetic Susceptibility Results 190
7.5 General Discussion of Magnetic Data 191
7.5.1 Rock Magnetic Properties 191
7.5.2 Controls over AMS Vectors 192
7.5.3 Symmetry and Attitude of Magnetic Fabrics 195
7.5.4 Summary of AMS fabrics 198
7.6 The Emplacement and Tectonic History of the Omey Pluton 198
7.6.1 Tectonic Overprint of an Emplacement Foliation 199
7.6.2 Controls on the Emplacement of the Omey Pluton 204
7.7 Conclusion 207

Chapter 8:
The Roundstone Pluton; A Punched Laccolith
8.1 Introduction 210
8.2 Geological Setting 211

8.3 Field Relationships 211
8.3.1 External Contact Relationships 212
8.3.2 Facies Distribution 215
8.3.3 Fabric Development 221
8.3.4 Summary of Field Data 225
8.4 Rock Magnetic Investigation 226
8.4.1 Sampling 226
8.4.2 Results of Rock Magnetic Experiments 226
8.4.3 Anisotropy of Magnetic Susceptibility Results 233
8.5 Discussion 237
8.5.1 Characterising Magnetic Mineralogy 237
8.5.2 Comparison of Field and Magnetic Data 239
8.6 An Emplacement Model for the Roundstone Pluton 242
8.6.1 Interaction Between Regional Transpression and Local Structures 243
8.6.2 Controls on Ascent and Emplacement 245
8.7 Conclusions 249

Chapter 9:
The Carna Pluton; Evidence for a Regional Kinematic Transition
9.1 Introduction 251
9.2 Field Data 252
9.3 Geochronology 259
9.3.1 Sampling and Methodology 259
9.3.2 Results 259
9.3.3 Discussion 261
9.4 Rock Magnetic Analysis 263
9.4.1 Sampling 263
9.4.2 Results of Rock Magnetic Experiments 264
9.4.3 Anisotropy of Magnetic Susceptibility Results 276
9.5 Discussion of Magnetic Data 277
9.5.1 Magnetic Assemblage 278
9.5.2 Genesis of Ferromagnetic Assemblage 280
9.5.3 Overview of AMS Data 283
9.6 Interpretation 284
9.6.1 Syn to Post Emplacement Shearing 284
9.6.2 Tectonic Controls Over Siting of the Carna Pluton 289
9.7 Conclusion 293

Chapter 10:
Synthesis; The Kinematic Evolution of the Galway Granite Complex and Conclusions
10.1 Introduction 295
10.2 Late Caledonian Transtension - Transpression Transition 296
10.3 Dynamics of Transpression and Transtension 298
10.4 Summary of Emplacement Models Pertaining to GGC Constituents 300
10.5 Tectonic Controls over the GGC 303
10.6 Conclusions 310
10.6.1 Kinematic Controls on the Galway Granite Complex 310
10.6.2 Comment on Large Scale Petrogenic Models 311
10.6.3 The Caveats of AMS and Implications for Other Studies 312
10.6.4 Publications arising from this Study 315

Declaration

I hereby declare that this thesis has not been submitted for another degree at University College Cork or any other university. The work described in this thesis is entirely that of the author except where otherwise stated.

This thesis is submitted in fulfilment of the requirement of the degree of Doctor of Philosophy at the National University of Ireland, Cork in the School of Biological, Earth and Environmental Sciences (Discipline of Geology), College of Science, Engineering and Food Science.

Signed …….. (William McCarthy)

Date ……..

Acknowledgements

Every Ph.D. starts with a B.Sc., the quality of my B.Sc. is directly attributed to the guidance, support and professional tuition I received from the former Geology Department at U.C.C.. For this, I am indebted to all of the teaching staff including Prof. J.A. Gamble, Prof. K.T. Higgs, Dr. A.R. Allen, Dr. B. Higgs, Dr. P.A. Meere, Dr. I. McCarthy, Dr. D.E. Jarvis, Dr. R.J. Reavy, Dr. (now Prof.) A.J. Wheeler and of course the lovely Ms. Mary McSweeney, for keeping all of the above on the straight and narrow.

I would not have undertaken, never mind completed, the current work without the assistance of my supervisors. Dr. R.J. Reavy has been outstandingly supportive and has always made himself available despite having a very busy schedule (it's great that we have figured out how the magma emplaced….). Prof. M.S. Petronis is thanked for introducing me to deep fried turkey, permitting me to used his laboratory in Highlands University New Mexico and above all for guiding me through the convoluted dark art that is rock magnetics. Dr. C.T. Stevenson provided ongoing support for AMS analysis and interpretation and offered guidance during the application of several innovative techniques (including the infamous "one up one down").

I would also like to thank Prof. Q. Crowley who selflessly committed his time, and applied his unique skill set, to the geochronology aspect of this project. Prof. M. Feely is also acknowledged for his kind words of support and financial assistance. Prof. B.E. Leake amiably made his personal field notes and maps available to the current author in the interest of science, his contribution to the current work is obvious and graciously acknowledged. Dr. D. Brown is thanked for the covert operations carried out in of Glasgow University.

Dr. C. Magee, Dr. K. McDermott Dr. K.F. Mulchrone and proto-Dr. Dave McCarthy endured various discussions and ramblings in the field of rock magnetics and structural geology throughout the project. Adam Brister, Rhonda Trujillo, Marine Foucher and Kate Zeigler provided altruistic lab assistance, advice and refreshments during rock magnetic analytical work. Stoicism is an ancient Greek school of thought that suggests one should remain indifferent toward the vicissitudes of fortune, pleasure and pain - thanks to Chloe, Cora, Caroline, Marian, Dave, Mark and Junior (aka Arron) for practicing this while sharing office space with me.

Special thanks are extended to all who contributed to this work in a general way, especially those who have absolutely no interest in rocks at all. Ruth Stevenson, John and Ruth Hunt, Matt O'Sullivan, Yvonne McGillycuddy and the Doyle family provided free accommodation, food and sympathetic ears over the last three years. I take my hat off to all members of Waterville 11 (as well as honorary members) who are rumoured to be capable of turning water to wine (or beer). Odhran McCarthy and Sarah Broderick are thanked for tireless data validation and John McCarthy, Daithí Power and Timmy Power for their patience and engineering talent in drill press design. Special thanks are extended to Conrad Daly who endured my ramblings for over a month in a caravan, in February, in deep dark Connemara, and also assisted in precarious offshore and monotonous onshore block sampling.

On a personal note, thanks to my parents, brothers and unfortunate sister for providing ongoing financial and moral support. Last but not least thanks to Kate who has endured countless, arduous, one sided "*discussions*" about rocks and magnets that are too small to see and yet still always helped out with colouring in.

Abstract

The Silurian-Devonian Galway Granite Complex (GGC ~425-380Ma) is defined here as a suite of granitoid plutons that comprise the *Main Galway Granite Batholith* and the *Earlier Plutons*. The Main Batholith is a composite of the Carna Pluton in the west and the Kilkieran Pluton in the east and extends from Galway City ~130km to the west. The Earlier Plutons are spatially, temporally and structurally distinct, situated northwest of the Main Batholith and include the Roundstone, Omey, Inis and Letterfrack Plutons.

The majority of isotopic and structural data currently available pertain to the Kilkieran Pluton, several tectonic models have already been devised for this part of the complex. These relate emplacement of the Kilkieran Pluton to extension across a large east-west Caledonian lineament, i.e. the Skird Rocks Fault, during late Caledonian transtension.

No chronological data have been published that directly and accurately date the emplacement of the Carna Pluton or any of the Earlier Plutons. There is also a lack of data pertaining to the internal structure of these intrusions. Accordingly, no previous study has established the mechanisms of emplacement for the Earlier Plutons and only limited work is available for the Carna Pluton. As a consequense of this, constituents of the GGC have not previously been placed in a context relative to each other or to regional scale Silurio-Devonian kinematics.

The current work focuses on the Omey, Roundstone and Carna Plutons. Here, results of detailed field and Anisotropy of Magnetic Susceptibiliy (AMS) fabric studies are presented. This work is complemented by geological mapping that focuses on fault dynamics and contact relationships. Interpretation of AMS data is aided by rock magnetic experiment data and petrographic microstructural evaluations of representative samples.

A new geological map of the the Omey Pluton demonstrates that this intrusion has a defined roof and base which are gently inclined parallel to the fold hinge of the Connemara Antiform. AMS and petrographic data show the intrusion is cross cut by NNW-SSE shear zones that extend into the country rock. These pre-date and were active during magma emplacement. It is proposed that the Omey pluton was emplaced as a discordant phacolith. Pre-existing subvertical D5 faults in the host rock were reactived during emplacement, due to regional sinistral transpression, and served as centralised ascent conduits.

A central portion of the Roundstone Pluton was mapped in detail for the first time. Two facies are identified, G1 forms the majority of the pluton and coeval G2 sheets cross cut G1 at the core of the pluton. NNW-SSE D5 faults mapped in the country rock extend across the pluton. These share a geometrical relationship with the distribution of submagmatic strain in the pluton and parallel the majoity of mapped subvertical G2 dykes. These data indicate that magma ascent was controlled by NNW-SSE conduits that are inherently related to those identifed in the Omey Pluton. It is proposed that the Roundstone Pluton is a punched laccolith, the symmetry and structure of which was controlled by pre-exising host rock structures and regional sinistral transpressive stress which presided during emplacement.

Field relationships show the long axis of the Carna Pluton lies parallel to mulitple NNW-SSE shear zones. These are represented on a regional scale by the Clifden-Mace Fault which cross cuts the core of this intrusion. AMS and petrographic data show concentric emplacement fabrics were tectonically overprinted as magma cooled from the magmatic state due to this faulting. It is proposed that the Clifden-Mace Fault system was active during ascent and emplacement of the magma and that pluton inflation only terminated as this controlling structure went into compression due to the onset of regional transtension.

U-Pb zircon laser ablation inductively coupled mass spectrometry (LA-ICP-MS) data has been compiled from four sample sites. New geochronological data from the Roundstone Pluton (RD1 =

423.8 ± 3.2Ma) represent the oldest age determination obtained from any member of the GGC and demonstrates that this pluton predates the Carna Pluton by ~10Ma and probably intruded synchronously with the Omey Pluton (~422.5 ± 1.7Ma). Chronological data from the Carna Pluton (CN2 = 412.9 ± 2.5Ma; CN3 = 409.8 ± 7.2Ma; CN4 = 409.6 ± 3.6Ma) represent the first precise magma crystallisation age for this intrusion. This work shows this pluton is 10Ma older than the Kilkieran Pluton and that the supply of magma into the Carna Pluton had terminated by ~409Ma.

Chronological, magnetic and field data have been utilised to evaluate the kinematic evolution of the Caledonides of western Ireland throughout the construction of the GGC. It is proposed that the GGC was constructed during four distinct episodes. The style of emplacement and the conduits used for magma transport to the site of emplacement was dependent on the orientation of local structures relative to the regional ambiant stress field. This philosophy is used to critically evaluate and progress existing hypotheses on the transition from regional transpression to regional transtension at the end of the Caledonian Orogeny.

Prologue

Multidisciplinary research on granitoid complexes can generate not only critical data which facilitate the construction of viable ascent and emplacement models but also, when combined with detailed structural and accurate geochronological information, allow an unprecedented opportunity to assess the regional kinematic framework at the time of magmatism.

The Silurian-Devonian granitoids in Connemara, Western Ireland, consist of a suite of spatially distinct plutons that were emplaced into the highly deformed Connemara Metamorphic Complex between ~425-380Ma concurrent with the culmination of the Caledonian Orogeny and the duration of Acadian Orogeny which followed. Previous authors have recognised and named several discrete granite intrusions, carried out substantial detailed facies mapping, produced voluminous petrological and geochemical data and proposed local individual emplacement models for some of these bodies. However, there is a dearth of information on the internal architecture of the majority of these intrusions. As a consequence of this, no attempts have been made to assess the controls over the ascent and emplacement of individual plutons. Despite decades of research, the structural relationship between this suite of intrusions remains enigmatic and therefore, they cannot be utilised to evaluate the evolution of kinematic processes concomitant with their siting and emplacement. This topic is addressed here.

Essentially the current work may be regarded as two parts:

The first part, comprising Chapters 1-5, is an appraisal of relevant literature in the areas of magma transport, regional orogenesis, geological setting of the area under consideration, Caledonian magmatism in general and finally the Siluro-Devonian granitoids of Connemara, which are the subject of the current work.

The second part contains a discussion of the methods used and three chapters that present data which allow novel and innovative geological models regarding magma emplacement and pluton architecture to be constructed in the context of both local structures and regional tectonics.

Finally a first synthesis is proposed which integrates the data generated with current kinematic models on an orogenic scale and shows that the Galway Granite Complex provides crucial evidence for the Siluro-Devonian tectonic evolution of the British and Irish Caledonides.

Notes for the reader

All grid co-ordinates used in this thesis refer to the Irish Grid Reference system. All co-ordinates quoted refer to the grid square "L", this is omitted as a full reference is provided in all cases.

Abbreviations and Symbols			
CMC	Connemara Metamorphic Complex	EMP/P_E	Excess Magma Pressure
CSB	Connemara Steep Belt	ΔP_B	Buoyancy overpressure
GGC	Galway Granite Complex	ΔP_V	Volume-related hydraulic pressure
MT	Mannin Thrust	Q_C	Conduit flux
BF	Barna Fault	Q_U	Under-burden flux
SRF	Skird Rocks Fault	σ_H	Horizontal (confining) stress
HBF	Highland Boundary Fault	EMV	Excess Magma Volume
CMF	Clifden-Mace Fault	φ	Coefficient of excess EMV
OM	Omey Pluton	η	Coefficient of EMV relaxation by cracking
RD	Roundstone Pluton	σ_P	Internal magma pressure
CN	Carna Pluton	σ_L	Local stress field
KK	Kilkieran Pluton	σ_i	Local stress field at the time of magma ingress
CMG	Costelloe Murvey Granite	**v**	Poisson coefficient
ETG	Errisbeg Townland Granite	σ3	Minimum principal stress axis
LLG	Lough Lurgan Granite	σ2	Intermediate principal stress axis
MMZ	Magma Mixing Zone	σ1	Maximum principal stress axis
KKG	Knock Granite	ε3	Minimum stretching direction
CWG	Callowfinish Granite	ε2	Intermediate stretching direction
KMG	Kilkieran Murvey Granite	ε1	Maximum stretching direction
SPG	Shannapheasteen Granite	K1	Maximum susceptibility axis
		K2	Intermediate susceptibility axis
		K3	Minimum susceptibility axis
		K_{mean}	Mean susceptibility
		Tj	Shape Factor (Jelinek 1981)
		Pj	Corrected anisotropy degree (Jelinek 1981)
		H	Total anisotropy (Owens 1974)
		L	Lineation (Khan 1962)
		F	Foliation (Khan 1962)
		M_S	Magnetic saturation
		M_R	Magnetic remanence
		H_{CR}	Coercivity of remanence
		H_C	Coercive force
		T_C	Curie Temperature
		T_N	Néel Temperature
		T_V	Verwey Temperature

Chapter 1:

Controls on Granite Ascent and Emplacement

1.1 Introduction

The generation of granitoid bodies is driven by four fundamental process, melting, segregation, ascent & emplacement (Petford *et al.* 1997; Petford and Clemens 2000). The role of the mantle in the provision of stress and heat, is considered by Vigneresse (2005). Energy derived from advected or diffused mantle heat and radioactive decay, promotes lithospheric melting by the breakdown of hydrous minerals. Segregation of melt and residue occurs in punctuated bursts due to matrix relaxation - compression cycles and magma is transported from the source via a network of increasingly larger conduits to an ascent site. Melt progressively and episodically ascends along crustal lineaments as discrete batches and ultimately amalgamates at the site of emplacement to form plutonic structures (see Vigneresse (2005)).

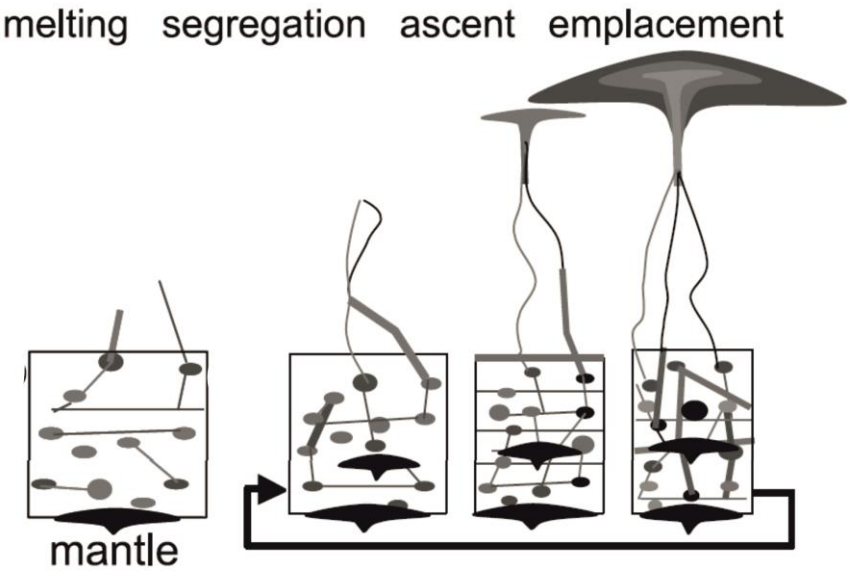


Fig. 1.1 The four fundamental processes, melting, segregation, ascent and emplacement, involved in granite generation (from Vigneresse (2005)). The four stages are discrete and may occur episodically or continuously during a protracted tectonic event. In this paradigm the mantel represents a fifth factor, that of a heat source and chemical reservoir.

The construction of plutons and batholiths occurs by the episodic influx of magma into progressively inflating structures (Bergantz 2000; Petford *et al.* 2000). The process of magma generation and migration is fundamentally linked with major tectonic events (Pitcher 1993). The intrusion of igneous bodies unavoidably alters the local stress field into which they intrude (Vigneresse *et al.* 1999) and the strain recorded in an igneous body may reflect stress field fluctuations that occur during crystallisation (e.g. Hutton (1988b)). As a result of this, analysis of the internal architecture of a suite of granitoids across space and time can reveal details regarding

the evolution of an orogenic kinematic regime on a local and regional scale (e.g. Brown *et al.* (2008); Neilson *et al.* (2009)). This principle will be applied to the Galway Granites in western Ireland to attempt to unravel the relationship between granite intrusion and the evolving strain regime into which these granitoids were emplaced.

The distinction between *Ascent* and *Emplacement* is fundamental to understanding how granites intrude the earth's crust; fortunately this is a fairly easy concept to grasp. *Ascent* is the process by which segregated melt rises up through the crust, *Emplacement* is the process of melt accumulation in the mid to upper crust as a large mass where it crystallises and ultimately forms voluminous intrusive bodies such as plutons or batholiths (Jacques and Reavy 1994). More simply, *Ascent* is the upward movement of melt toward the site of emplacement, *Emplacement* is the accumulation of melt in the mid to upper crust to form large intrusions (Fig. 1.2).

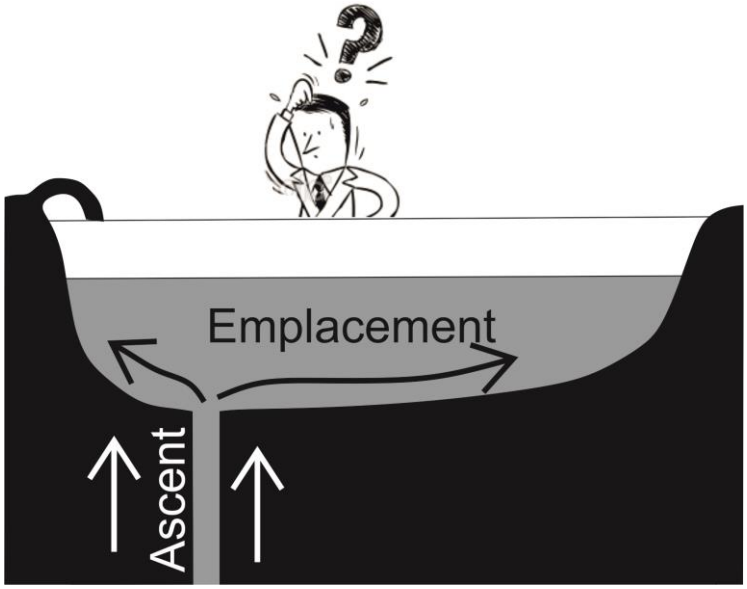


Fig. 1.2 Fundamental distinction between Ascent and Emplacement

In this chapter the causative forces behind magma transport are discussed and contrasting models for magma emplacement summarised. Section 1.2 is a discussion on the forces which drive and control magma transport in general. Section 1.3 examines the basic principle that all fluids can only migrate orthogonal to local σ3, thus the concept of *Passive* and *Forceful* emplacement is challenged. Section 1.4 summarises pluton emplacement models.

Section 1.5 summarises the fundamental controls over magma transport in the crust and pluton construction. The chapter concludes by applying these principles to examples where careful analysis has been used to assess regional stress field fluctuations and identifying the work

required to carry out a similar evaluation on the Siluro-Devonian granites in Co. Galway, Ireland, which is the focal point of this thesis.

1.2 Factors controlling ascent and emplacement

Owing to the timescale and depth at which granite petrogenesis takes place and the spatial scale of granitoid intrusion, direct observation of the role played by each of the forces in dictating the ascent route and emplacement is not possible. Direct observations are limited to fieldwork, the collection of structural data and geochemical analyses (as reviewed in Cruden (1998); Petford *et al.* (2000); Vigneresse (2005); Thomson and Petford (2008)). Such studies are most often restricted to a single surface that is representative of only a fraction of the entire pluton that may extend for several kilometres on the vertical axis. Indirect methods of observation include gravity, magnetic and seismic geophysical methods which facilitate the interpretation of intrusion shape, and basic composition, at depth and under vegetation or water cover (e.g. Murphy (1952); Max *et al.* (1978); Max *et al.* (1983)). Analogue and numerical modelling provides a means by which one may directly observe the ascent and emplacement process using a scaled down model in a controlled environment with materials that are representative of a specified host medium and intruding magma (Weinberg and Podladchikov 1994; Burov *et al.* 2003; Ablay *et al.* 2008). Experimental modelling is an effective tool in determining the active role played by specific body forces under contrasting rheological, pressure and temperature conditions and so characterise forces which are universal to all intrusions by elimination of local complexities (e.g. structural anisotropies).

1.2.1 The Role of Buoyancy

Early analogue experimentation typically modelled ascent of a viscous fluid through a ductile medium and returned the classic tear-drop shaped diapir of almost equi-dimensional x-y-z axis, this led to the diapiric ascent hypothesis (Ramberg 1981; Cruden 1988; Weinberg and Podladchikov 1994). Several authors have applied inertia models in an attempt to refine the feasibility of this process using Stokes flow, Rayleigh-Taylor (RT) or other instability modelling techniques (Coward 1981; Marsh 1982; Van den Eckhout *et al.* 1986; Cruden 1988; Mahon *et al.* 1988; Weinberg 1996). Results suggest that the buoyancy contrast between an ascending magma

and a ductile host is the primary driving force behind granitoid ascent while a low viscosity contrast between the two media cause upward movement of a single large diapir (Fig. 1.3). However, where a viscous body intruded a brittle medium or a realistically ductile host (brittle or highly viscous) diapiric ascent was substituted in favour of brittle dyke propagated intrusion (Ramberg 1981; Mahon *et al.* 1988; Barnichon *et al.* 1999). Thus buoyancy is shown to be the main driving force only when unrealistic viscosity contrasts between host and magma were applied to analytical tests.

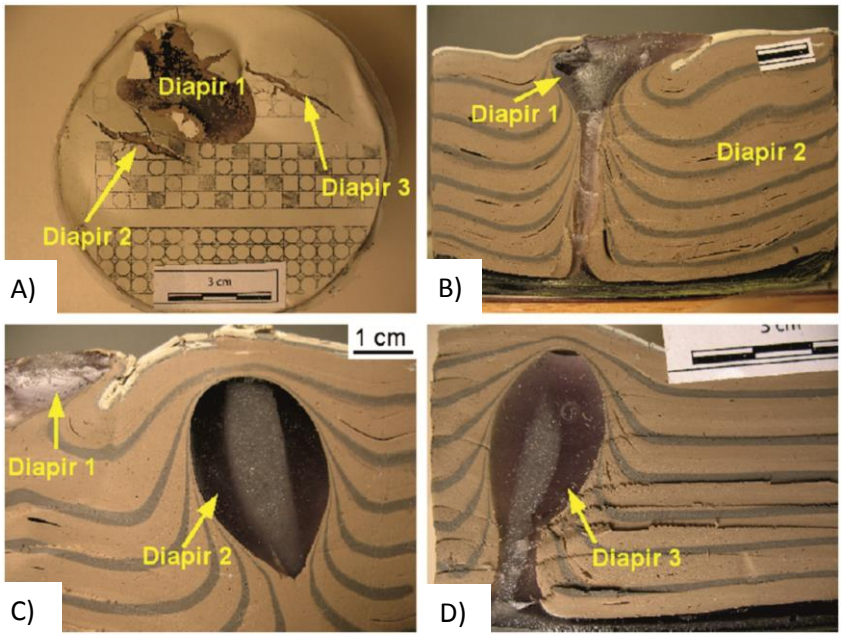


Fig. 1.3 Results of centrifuge analogue experiments using plasticine-silicone materials of differing density (Dietl and Koyi (2011)). Many of the structures recognised are comparable to real field observations (isoclinal folds, doming and fracturing of overburden, concentric internal architecture of diapir, rim synclines). In this model "magma" ascent is achieved due to a buoyancy contrast between the plasticine and silicone. However, in reality a buoyancy contrast between host and magma is not always present, or magma may be denser than the host. As such, this model cannot account for the ascent and emplacement of all intrusive bodies.

However, if buoyancy is the primary driver it follows that ascent should terminate once a neutrally buoyant rock unit is intruded. Several published works clearly show plutons with felsic facies intruded by later relatively mafic, denser magma (e.g. El-Desouky *et al.* (1996); Zaniewski *et al.* (2006); McLeod *et al.* (2011) however see Cruden *et al.* (1995)). Gravity data also show successive intrusions emplaced at a similar crustal level indiscriminate of positive or negative gravity anomalies; this suggests that batches of magma stopped ascending due to factors other than reaching buoyancy equilibrium (Vigneresse and Clemens 2000).

1.2.2 Viscosity and Magma Pressure

Weertman (1971) proposed a model of fracture propagation driven by magma viscosity in analogy to the transport of water through glaciers via the Peach-Koehler force. In this model, fluid transfer was promoted by magma viscosity at the fracture tip and intrinsic magma pressure which would equal the elastic response of the fracturing rock (Pollard and Muller 1976; Rubin 1998). Améglio and Vigneresse (1999) interpreted narrow gravity anomalies at depth around large granitoid intrusions as feeder dykes in support of a fracture propagation model. However Vigneresse (2005) argues that structures of this size could only supply a limited volume of magma and that the diameter of feeder dykes is generally insufficient to facilitate the migration of highly viscous granitic melt from the deep crust to the emplacement level (Clemens *et al.* 1997; Petford *et al.* 1997).

Some early models attributed the transition between ascent and emplacement and the final geometry of laccolithic intrusions to magma viscosity. Emerman and Marrett (1990) argued that viscosity was a critical controlling factor over intrusion morphology and that higher and lower viscosity melts result in higher and lower aspect ratio intrusions respectively. Ryan (1993) applies a similar philosophy in evaluating the controls over the symmetry of picritic to tholeiitic intrusions in mid-ocean ridge settings but places more emphasis on the role of neutral buoyancy and host structure.

Vigneresse *et al.* (1999) suggested that viscosity alone cannot explain the spectrum of laccolithic morphologies observed around the world (Corry 1988; McCaffrey and Petford 1997). Qualitative and quantitative data derived from the field, petrographic and magnetic fabric analysis illustrate that fabric development in many intrusions occurred by the rotation of mega - phenocryst phases in a ductile medium (e.g. Stevenson *et al.* (2007a); Petronis *et al.* (2012), methods reviewed in Hutton (1988b); Tarling and Hrouda (1993); Bouchez (1997); Paterson *et al.* (2004); Vernon (2004); Passchier and Trouw (2005)). Such observations are supported by analogue experiments which show fabric development in a viscous medium to be a product of particle rotation under shear flow (Arbaret *et al.* 1997). These works demonstrate that large viscosity contrasts between magma in ascent and emplacement mode is not a characteristic universal to all intrusions. Therefore, the viscosity attributes of a system do not independently control the mode of magma transport or the symmetry of plutonic structures because there is no observed link between magma viscosity values and the shape or orientation of magma conduits.

1.2.3 Excess Magma Pressure

Ablay *et al.* (2008) recently emphasised the fundamental controls over magma driven juvenile hydraulic fracturing. This paper highlighted buoyancy overpressure (ΔP_B) and volume-related hydraulic pressure (ΔP_v), both derived from the volume increase during melt production, as primary components to Excess Magma Pressure (i.e. P_E or EMP) where;

$$\Delta P_B + \Delta P_v = P_E$$

Uplift related extension, crustal strength, and confining stress are identified as key mechanical factors that control deformation of the host strata during magma driven juvenile fracture propagation, hydraulic inflation and buoyancy pumping which are driven by EMP (Ablay *et al.* 2008). Their findings show that with varying degrees of EMP characteristic vertical ascent and tabular emplacement geometries may be predicted through a medium with a horizontally homogenous and vertically gradational structure (Fig. 1.4).

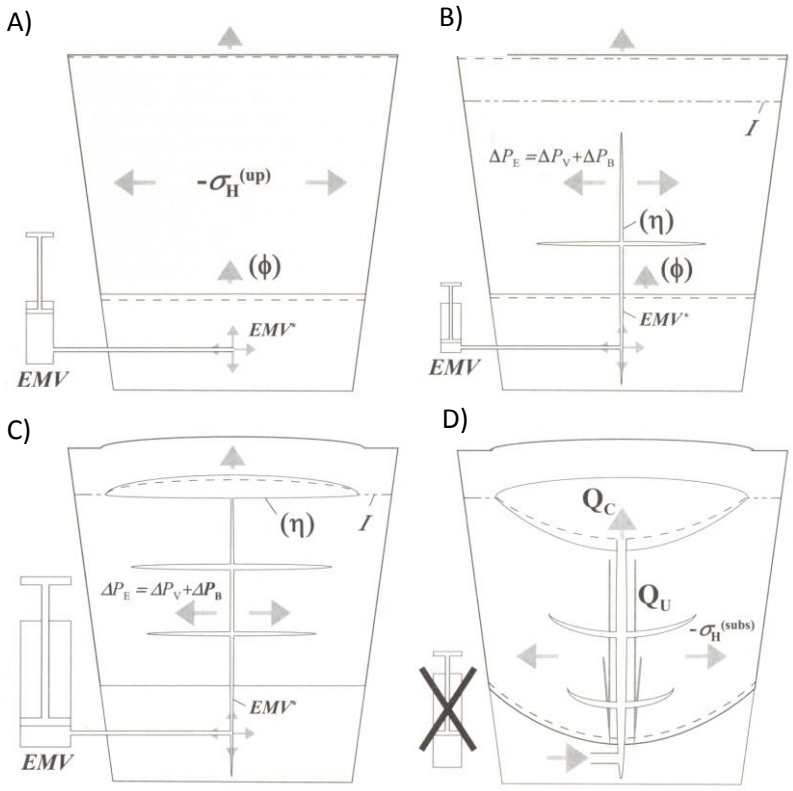


Fig. 1.4 Fracture-mediated intrusion model driven by Excess Magma Pressure as proposed by Ablay *et al.* (2008). A) Pre-rupture stresses. B, C & D) Low and high EMV (excess magma volume) and buoyancy pumping regime generate distinct conduit morphologies i.e. sills and dykes, christmas-tree laccolith and a lopolith respectively. Q_C; conduit flux , Q_U; under-burden flux , $-\sigma_H$; horizontal (confining) stress, ϕ; Coefficient of EMV relaxation by inelastic deformation, η; Coefficient of EMV relaxation by crack growth.

The transition from ascent (σ3 is orthogonal to a subvertical plane), to emplacement (σ3 is orthogonal to a subhorizontal plane) occurs with the reorientation of the plane of opening (σ1-σ2). This transition occurs due to the reduction in hydrostatic stress along the vertical axis but not the horizontal, caused by the shallower level of intrusion reached during vertical ascent. By this means, Ablay *et al.* (2008) show that the level of emplacement of tabular laccoliths was controlled by the degree of EMP available. These results imply that the common mechanical force universal to all granitoid intrusion is EMP, that this force is intrinsic to magma production, and that this force can be attributed to the generation of the generic shape of granitoid intrusions around the world (McCaffrey and Petford 1997) and assign the role of host rock structure as "*ad hoc*" which need not be considered for universal models.

1.2.4 Ambient Stress

Anderson (1951) established a model for dyke intrusion in a straight forward setting whereby fracture mediated intrusion is achieved in a tensional regime along the σ1- σ2 plane, orthogonal to σ3 (Andersonian dykes). In an isotropic medium, elevated lithostatic stress at depth favours vertical ascent while at shallower depths reduced overburden stress rotates σ3 to the vertical plane facilitating the emplacement of horizontal sills. The above work follows the basic principle that in the absence of structural anisotropy, magma will intrude perpendicular to the least compressive stress (Jeager and Cook 1979) but does not consider the interaction of excess magma pressure upon the strain regime into which it intrudes.

During fracture mediated intrusion, excess magma pressure will interact with the local stress regime into which it intrudes. This will always modify the stress field's principal vectors to some degree and may ultimately generate intrusive geometries which are inconsistent with the original stress field (Parsons and Thompson 1991). By means of numerical modelling, Vigneresse *et al.* (1999) investigated the contrasting styles of emplacement produced in differing stress regimes in structurally isotropic medium. This work showed that across tensional, simple shear and compressional regimes the orientation of the three principal stress axes are altered by intruding magma and that predictable intrusive morphologies are produced (Fig. 1.5). Vigneresse *et al.* (1999) argued that the dynamic interaction between magma intrusion and local stress controlled conduit geometry, not density or viscosity-driven overpressure.

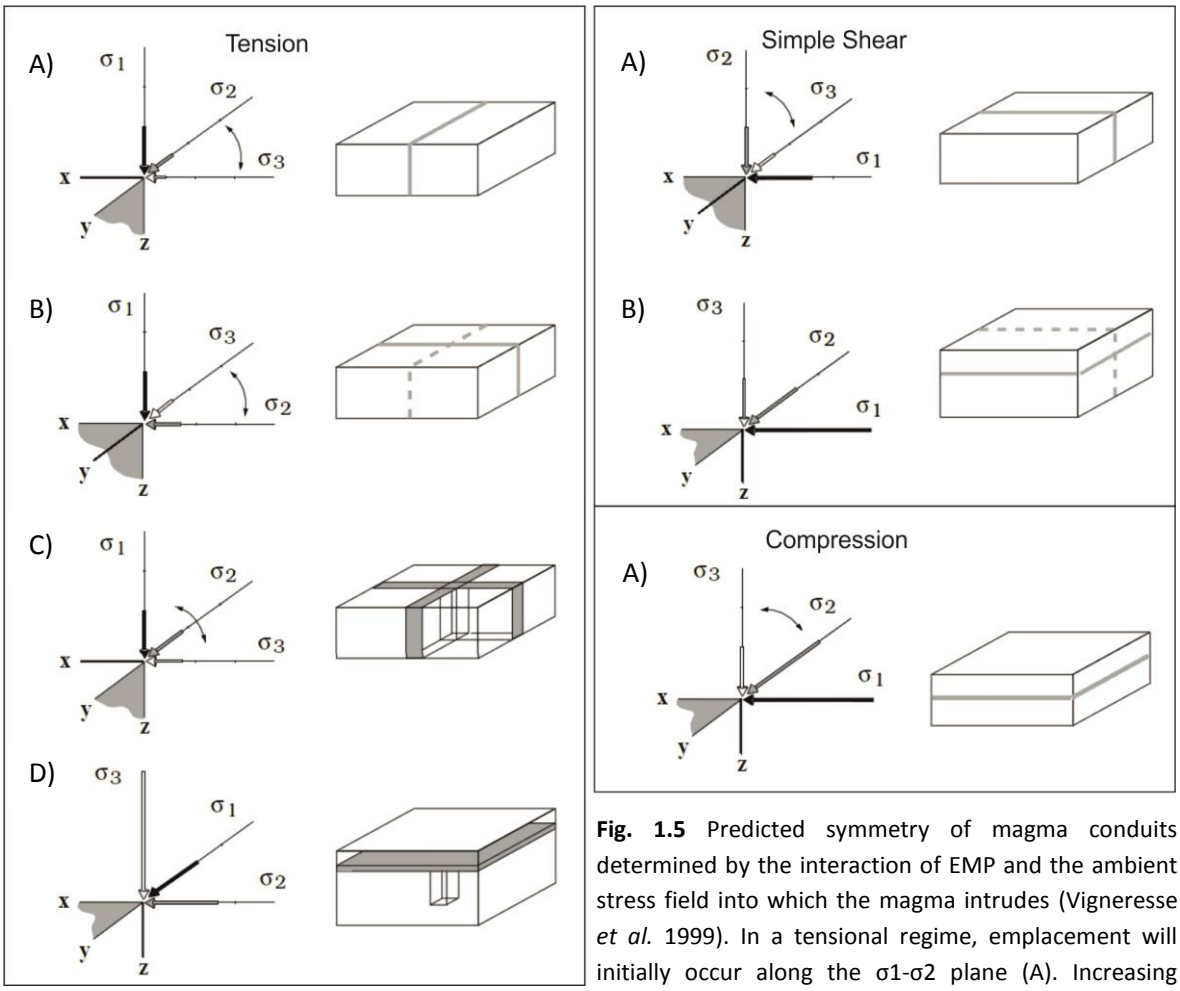


Fig. 1.5 Predicted symmetry of magma conduits determined by the interaction of EMP and the ambient stress field into which the magma intrudes (Vigneresse *et al.* 1999). In a tensional regime, emplacement will initially occur along the σ1-σ2 plane (A). Increasing pressure can manipulate the local stress field causing σ2-σ3 to swap orientation (B) or if they are close in magnitude form a central vertical conduit (C). If EMP exceeds the lithostatic load and not the confining stress, subhorizontal emplacement is achieved (D). In a simple shear regime a conduit will initially develop along a single discrete shear zone (A) but may rotate to the horizontal plane with increasing EMP or reduction in lithostatic load (B). In a compressive regime, presuming the vertical load < confining pressure, conduits will always propagate in a horizontal plane (A). Host structure is not considered.

1.2.5 The Role of Crustal Anisotropy

The spatial association between large igneous bodies and major crustal structures has long been recognised and with it a tectonic control over granitoid intrusion implied (e.g. Pitcher and Bussell (1977); Leake (1978); Pitcher (1979); Pitcher (1982). Field based studies through the 1980's identified that emplacement into pre-existing brittle and ductile crustal structures is often achieved during regional orogenesis (e.g. Brun and Pons (1981); Hutton (1982); Reavy (1989); Brun *et al.* (1990)). Examination of the internal architecture of plutonic bodies and their host rock via mapping and structural analysis (reviewed in Hutton (1988b); Bouchez (1997); Vernon (2004);

Borradaile and Jackson (2010)) confirms a syn-orogenic relationship between intrusion, crustal structure and strain regime into which emplacement occurred. By such methods, it has become apparent that in many cases granites intrude as syn-orogenic bodies into pre-existing reactivated structures (Hutton 1988b; Hutton 1997), and that ascent may be facilitated via subvertical sheeting along crustal lineaments (Hutton 1992; McCaffrey 1992) or via steep tensional voids between intersecting lineaments (Jacques and Reavy 1994) while emplacement is often controlled by a combination of outward ballooning and sub-horizontal intrusion into the wall rocks of the ascent conduit guided by planes of weakness (e.g. Cruden (2008)).

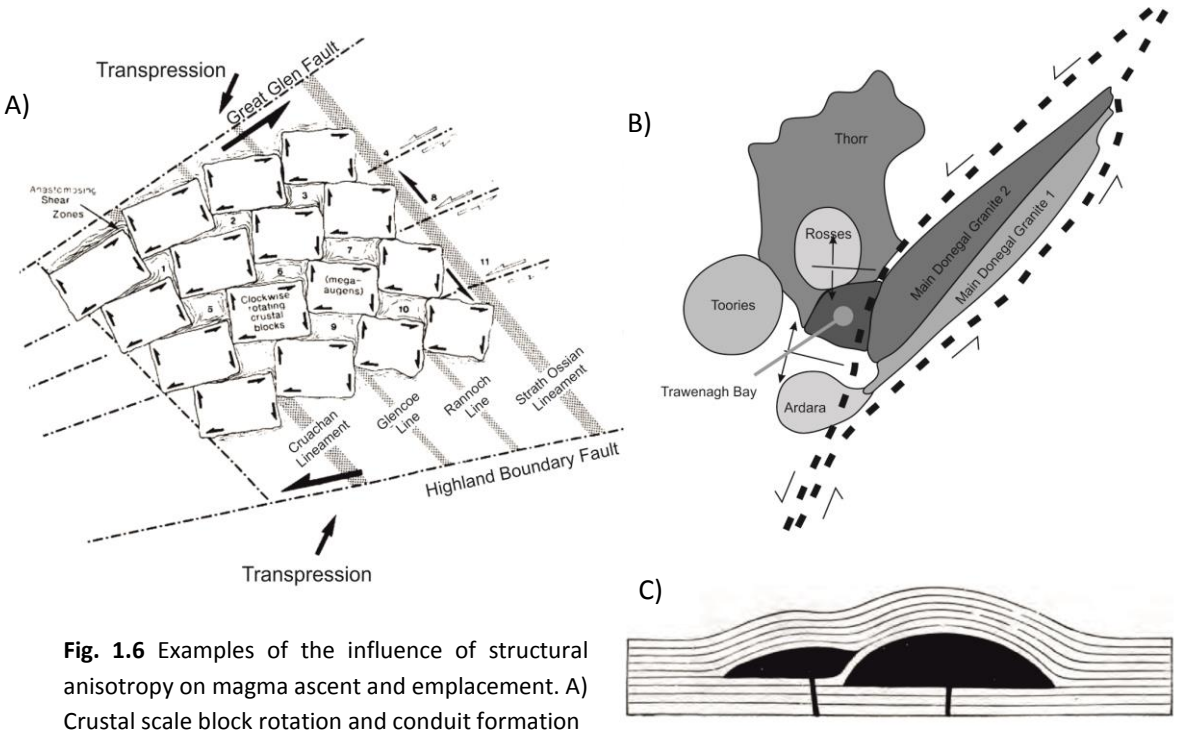


Fig. 1.6 Examples of the influence of structural anisotropy on magma ascent and emplacement. A) Crustal scale block rotation and conduit formation after Jacques and Reavy (1994). B) Influence of active shear zones on the Donegal batholith (Hutton 1982). C) relatively local scale influence of bedding on laccolith formation in Mount Holmes (Gilbert 1877).

It is now well established that space can be created for granitoid intrusions by reactivation of local/regional structures in all stress regimes (Hutton 1992). Emplacement into transcurrent structures such as the crustal pull aparts (Galway Granite Batholith, Ireland (El-Desouky *et al.* 1996)), extensional terminations at transcurrent faults (Strontian Granite, Scotland (Hutton 1988a)), transpressional tension gashes (Central Extremadura batholith, Spain (Castro 1986)) or dilation associated with differential displacement (Donegal Batholith (Hutton 1982)) are the most common. Examples of space generation within extensional regimes are also reasonably easy to envisage and include re-activation of low angle faults in extensional hanging walls (Coastal Cordillera, Chilean Andes (Grocott *et al.* 2009), intrusion into ramp flat geometries (the Xanthi

Pluton, Greece (Koukouvelas and Pe-piper 1991)) and uplift of overburden into the free surface partially facilitated by ongoing tectonic extension (examples from Tuscany, Italy in Acocella and Rossetti (2002)). Counterintuitive space creation models within compressive regimes have also been documented this include the Great Tonalite Sill, Alaska (intrusion into the median plane of an high angle reverse fault (Hutton and Ingram 1992; Ingram and Hutton 1994)), Sierra Morena, Spain (plutonic ballooning during co-axial deformation (Brun and Pons 1981)) and Vosges Massif, France (Variscan aged magmatic state deformation of granitoids in sub-horizontal compressive shear zones (Blumenfeld and Bouchez 1988)).

By comparison of the Great Tonalite Sill (Hutton and Ingram 1992), the main Donegal Granite (Hutton 1982; Stevenson *et al.* 2008a) and the south Greenland Rapakivi granites (Bridgwater *et al.* 1974; Hutton *et al.* 1990), Hutton (1992) illustrated that magma commonly intrudes highly oblique to the regional plane of maximum compressive stress and consequently coined the term "non-Andersonian sheets" (intrude contrary to the Andersonian Dyke model (Anderson 1951; Jeager and Cook 1979)). On this basis Hutton (1992) proposed that space creation, for granites concordant with planes of weakness in the crust, is geometrically controlled by the shapes and attitudes of their bounding structures and generally not by the orientation and magnitudes of the crustal stress system. Additionally, this work also highlights that a dilation zone is not always necessary (plutonic development in compressive regimes) as intrusion can be accomplished into structures which intuitively appear to be "space denying" (Hutton 1997). Hence, the role of magma pressure in generating space for the intrusion of granite varies depending on the stress regime i.e. in extension and transcurrent scenarios space may be created by tectonic opening while in compressive scenarios internal magma pressure must exceed the regional compressive stress field in order for intrusion (ascent or emplacement) to occur (Hutton 1996).

The ultimate concept implied by this model is that pre-existing structures in the crust provide zones of strain concentration that energetically favours sheet-tip propagation. Therefore, in practical circumstances, i.e. in the structurally anisotropic and rheologically inhomogeneous crust, magma is likely to migrate via the exploitation of pre-existing structures; even if these structures are at high angles to the regional σ1-σ2 plane (Hutton 1996, 1997).

1.2.6 Summary

Granitoid production in the continental crust is inherently linked to orogenic events (Pitcher 1993) and so structural anisotropy and stress fluctuation complexities are inherent to the medium into which granitoids intrude.

Filtering out of such parameters through numerical and analogue modelling facilitates identification of specific factors that are a common causative mechanical force to all intrusions (e.g. (Takada 1989; Clemens and Mawer 1992; Roman-Berdiel *et al.* 1995; Petford 1996; Roman Berdiel *et al.* 1997; Kerr and Pollard 1998; Rubin 1998; Ablay *et al.* 2008)). Combining the results of such experiments aids in constraining the principal driving forces behind ascent and emplacement. From the above discussions it is clear that magma intrusion may be driven via any one of the body forces proposed by Hutton (1997). However, one need not emphasise the fact that body forces act in synchrony and that, in the dynamic crust, the potential for any one of these forces to independently drive magma migration through the crust is most likely nil. Therefore the validity of the analytical and numerical modelling approach is limited to constraining the role played by particular forces in artificial scenarios. None the less, controlled experiments have inspired a general consensus; that magma migration is driven by internal magma pressure (derived from any combination of the body forces), that conduits form via juvenile hydraulic fracturing or re-fracturing of pre-existing structures and that this is a mechanism universal to all intrusive bodies (Vigneresse and Clemens 2000; Thomson and Petford 2008). Most significantly, the existing literature show that simple diapiric models are infeasible for magma propagation through the brittle crust (Petford and Clemens 2000; Vigneresse and Clemens 2000; Vigneresse 2005).

The argument for structural control over granite intrusion is based on the fact that the continental crust is abundant in structural anisotropies (compositional and secondary) that serve to concentrate strain and that these provide energetically favourable means for conduit propagation (Hutton 1992). The fundamental contributors to magma pressure and the same fracture propagation mechanisms are common to both experimental modelling and nature, but it must be emphasised that the removal of structural anisotropies in numerical and analogue models result in the redundancy of such work in holistic realistic applications. Models based on field observations and associated structural data (Hutton 1982; Reavy 1989; Hutton 1992; Jacques and Reavy 1994; Hutton 1997; Stevenson *et al.* 2008b; Petronis *et al.* 2012) are unable to obtain the same quantitative data of the intrusion process that lab based modelling provides, however

this approach has been effective in demonstrating the critical role of host rock structure in guiding internal magma pressure and the regional stress during magma ingress.

In conclusion, data derived from both experimental and field based work has shown that as magma intrudes a host it will alter the local stress regime in some way. In the great majority of cases, the local stress field will also interact with pre-existing zones of contrasting structural integrity (brittle or ductile shear zones, lithological boundaries, hydrated areas) which serve to manipulate regional stress and typically re-orientate the local σ1-σ2 plane into parallelism with a pre-existing planer structure (for example). This dynamic (stress applied by intruding magma + regional tectonic stress + localised concentration of stress) controls conduit propagation. In all cases the transition from ascent to emplacement is controlled by re-orientating the local σ3 principal stress axis from the sub-horizontal plane to the sub-vertical, either permanently (sill) or in a temporally dynamic manner (ballooning). Alteration of the hydrostatic field, the regional stress regime, interaction regional stress with host structural anisotropies or, more likely, a combination of all three factors facilitate the transition from vertical ascent to lateral emplacement.

1.3 Validity of Passive and Forceful Terminology

Recognising the significant role of tectonic structures and stress in the emplacement of granite Hutton (1988b) defined two terms to describe the manner in which igneous rocks may intrude host strata, i.e. by *Passive* or *Forceful* emplacement. *Senso stricto* passive emplacement refers to the scenario where space creation exceeds the rate of magma supply facilitating the passive flow of magma into the tectonic structure. Forceful emplacement is used to describe the scenario where the magma pressure is greater than the rate of tectonic space creation and magma ingress is achieved by forceful manipulation of the country rock through magma pressure (Hutton 1988b; Paterson and Fowler 1993; Stevenson 2009).

Production of granitic melt generates excess magma pressure (EMP) which drives melt migration through the crust (Ablay *et al.* 2008). Most often, structural features in the crust guide conduit propagation via manipulation of the local stress field and EMP (Hutton 1997; Vigneresse 2005; Brown 2007). During magma ingress, the rate of tectonic opening is generally less than that of magma supply (Paterson and Tobisch 1992), thus a magmatic overpressure is predicted. Analogue and numerical modelling demonstrates that the magnitude and orientation of the three

local principal stress axes are susceptible to manipulation during the intrusion process due to the presence of EMP and local structures (Vigneresse *et al.* 1999; Ablay *et al.* 2008).

Internal magma pressure (σ_P) will modify the local stress field (σ_L) into which it emplaces creating a new local stress field at the time of intrusion (σ_i). Ultimately the $\sigma3_i$ determines the melt conduit opening and propagation direction. Vigneresse *et al.* (1999) established the simple relationships;

$$\sigma3_i = \sigma3_L + \sigma_P \qquad \text{and} \qquad \sigma2_i = \sigma2_L + \nu\,\sigma_P,$$

where ν is the Poisson coefficient. Therefore the stress regime at the time of intrusion is subject to σ_P and σ_L, and magma overpressure serves to push the conduits walls toward $\sigma3_i$. By this reasoning it is apparent that internal magma pressure will positively contribute to space creation and promote conduit propagation orthogonal to $\sigma3_i$ in all cases regardless of the local tectonic stress field. Depending on the relative magnitude of $\sigma3_L$ and σ_P conduit propagation will be variably dependant on magmatic or tectonic stress contributors but in all cases magma pressure contributes to the forceful intrusion of magma. By this reasoning the term passive emplacement is negated as magma transport in the crust is always forceful *sensu* Hutton (1988b).

Hutton (1997) and Stevenson (2004) emphasise that passive emplacement is achieved by magma flow into zones of lower strain and not actual voids in the crust, while forceful emplacement is achieved by "magma pushing or shouldering aside the wall rocks". This implies that passive is distinct from forceful emplacement as magma propagation toward a zone of low strain is exclusive to the former term. On the contrary, analytical data (discussed above) conclusively illustrate that melt will always propagate in that direction. This is an intuitively acceptable concept given that fracture propagation will only occur along a plane orthogonal to $\sigma3_L$ (Engelder 1993). Therefore the orientation of $\sigma3_i$ does not differ, relative of opening direction, between passive or forceful emplacement and so should not be used as defining criteria. In all circumstances where magma intrudes the crust EMP contributes to the propagation of the magma conduit and hence all emplacement is forceful and at the same time occurs towards a zone of lower stress (i.e. the least compressive stress).

Therefore, it is argued that while the rate of tectonic opening may promote plutonic development, EMP (which is always present) will proactively influence the rate of space creation

in all scenarios. Therefore, regardless of tectonic setting, all plutonic bodies forcefully intrude *senso* Hutton (1988b) & Stevenson (2009).

Hutton (1992) points out that the Great Tonalite Sill, Alaska, was able to overcome contractional orogenic stresses during emplacement and that space must have been made by some forceful mechanism, yet in many other instances the inferred primary space-creating mechanism for intrusions was attributed to dilation associated with crustal structures. In reference to this point he asks "Given this contrast, is there anything which is common to all three tectonic settings in terms of emplacement processes?". The current author proposes that the answer is yes; all fluids will propagate perpendicular to the $\sigma3_i$ at the scale of the magma conduit, a product of the interaction between $\sigma3_i$ and σ_P, which may or may not be parallel to $\sigma3_L$. It is critical to note that in any scenarios $\sigma3_L/\sigma3_i$ may be highly oblique to regional crustal scale far field stress parameters which are subject to manipulation by terrane scale or local scale planar anisotropies.

1.4 Emplacement Mechanisms

Working from the principle that the earths' crust becomes increasing brittle and so structurally anisotropic at shallower levels (Hutton 1988b), Hutton (1996) put forward a simple scheme which proposed three broad depth defined realms of characteristic emplacement styles (Fig. 1.7). This model suggests that, due to decreasing magma connectivity and lithostatic pressure at shallower depths and increased fluid connectivity at depth in the ductile crust, space for plutonic development is facilitated in contrasting styles. For example diapiric and deep seated shear zone mechanisms favour the deep crust and deflection of the free surface and lateral intrusion along brittle structures favour the upper crust. Below is a discussion on the main models proposed for granite emplacement and some of the controversies associated with these.

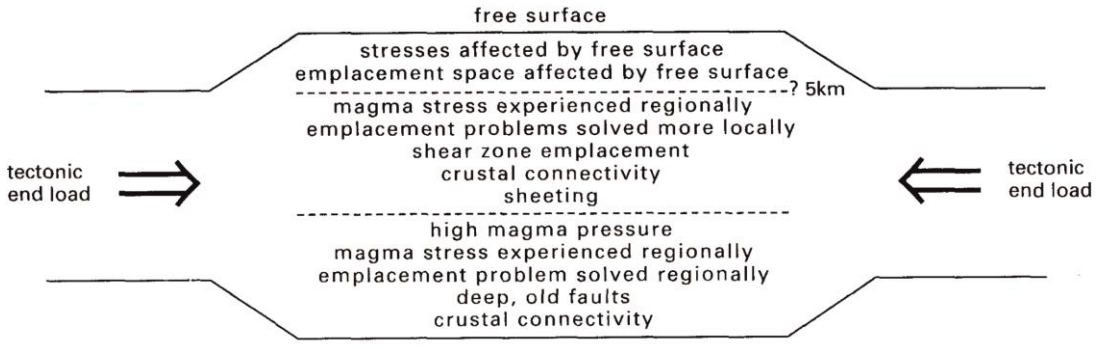


Fig. 1.7 Simplified diagram illustrating the contrast in emplacement styles expected at diffent crustal depths (Hutton 1996).

1.4.1 Diapirism

The word *diapir* is taken from the Greek word to *pierce* and has been used since its first application in a geological context in 1927 (Marzec 1927; Petford 1996) to refer to the buoyant rise of a large crudely equi-dimensional inverted teardrop shaped body of salt or magma through the crust. Since then, several modifications of this model have been suggested including piercing, non-piercing, ballooning and nested diapiric models (Ramberg 1970; Brun and Pons 1981; Ramberg 1981; Van den Eckhout *et al.* 1986; Mahon *et al.* 1988; Weinberg and Podladchikov 1994; Paterson and Vernon 1995; Cruden 1998; Burov *et al.* 2003; Forien and Dietl 2009; Dietl and Koyi 2011).

Field evidence for diapirism includes;

1. Crude concentric facies zoning
2. Concentric foliations with radiating increasing strain profile
3. Shortening of host strata perpendicular to plutonic contacts
4. Non-coaxial shear sense indicators that preferentially indicate diapiric growth
5. Strain in country rocks exposed below the midpoint of an ascending diapir should not be purely oblate but rather show a steep stretching lineation and pluton up shear indicators.

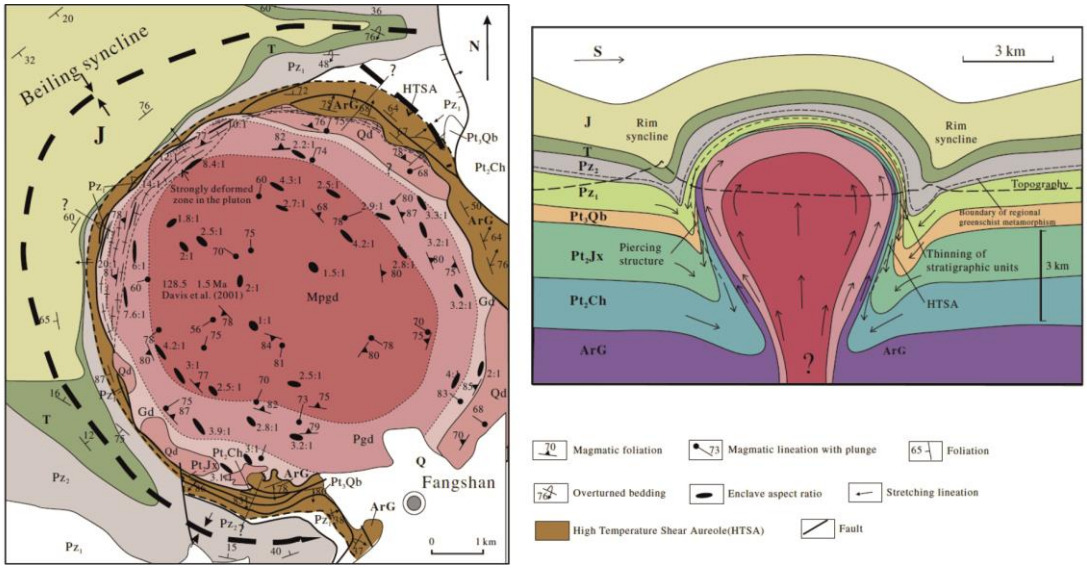


Fig. 1.8 The Fangshan Pluton, Baijing, exhibits features which are consistent with that of a diapir (He *et al.* 2009). The internal architecture is similar to that of an inflated laccolith. Host strata are a series of bedded sediments.

(e.g. Paterson *et al.* (1988); England (1990); He *et al.* (2009)). Such features are observed in many real examples such as those illustrated in Figure 1.8 (He *et al.* 2009). With the exception of the

final point, such characteristics are not exclusive to the diapiric mechanism and equally support plutonic inflation/ballooning (e.g. Molyneux and Hutton (2000) vs. Paterson and Vernon (1995), also Courrioux (1987); Corry (1988); England (1992); Hutton (1996); McCaffrey and Petford (1997); Améglio and Vigneresse (1999)).

It has been demonstrated that the heat required to induce sufficient viscosity contrasts in host strata would expel an excess amount of energy from the diapir and stall ascent before mid crustal levels are broached (Marsh 1982; Mahon *et al.* 1988). The nested diapir hypothesis (Paterson and Vernon 1995) is also debunked as the degree of mixing and mingling required for heat transfer is not supported by field observations of distinctly zoned plutons (Hutton 1996).

Although popular through the previous century, the diapiric model has been largely discredited as a mid to shallow crust emplacement mechanism (e.g. Petford (1996); Pitcher (1997); Vigneresse (2005); Brown (2007) although is not completely dismissed (e.g. Miller and Paterson (1999) *vs.* Petford and Clemens (2000)).

1.4.2 Ballooning and Inflation

Ballooning is the incremental inflation of an intrusive body driven by the continued build up of excess magma pressure which progressively forces dilation of the country rock at the site of emplacement. Hutton (1996) typifies this space generation mechanism as a mid crustal process as it requires continued ductile deformation of the country rock.

The concept of ballooning as an emplacement mechanism was inspired by the observation that the strain record within many plutonic bodies shows concentric pure shear flattening (e.g. Holder (1979); Ramsay (1989)). Brun *et al.* (1990) identified "pillow balloons" characterised by marginal sub-lateral stretching lineations and a plutonic geometry which exhibits a lateral axis greater than the vertical. The Ardara pluton is a classic example of a ballooned pluton (Molyneux and Hutton 2000) which exhibits a definite concordant magmatic state foliation (Vernon and Paterson 1993). Jacques and Reavy (1994), and later Brown and McClelland (2000), considered ballooning as a likely style of emplacement over sub-vertical ascent conduits at intersecting crustal lineaments. The dynamic between plutonic ballooning and tectonic stress has been numerically modelled and compared to field examples which demonstrates the feasibility of this emplacement mechanism (e.g. Guglielmo (1994)).

Positive distinction between a ballooning or diapiric mechanism remains difficult. However, if one were to take a conceptual approach, all else being equal, it becomes clear that a ballooned pluton is more probable. This is based on the fact that numerous analytical models (discussed above) have shown diapirism is not a mechanically sound mechanism, that most intrusions have a tabular or domed tabular, not bulbous, symmetry (e.g. Arbaret *et al.* (1997); McCaffrey and Petford (1997); Trzebski *et al.* (1997); Vigneresse *et al.* (1999); Petford and Clemens (2000)) and that in only a very small number of examples does the field evidence support a diapiric mechanism yet such evidence is not inconsistent with alternative models.

1.4.3 Intrusion into Active Shear Zones

As already discussed, the spatial and temporal relationship between plutonic activity and kinematic deformation within major crustal structures has been recognised for some time and with it, the suggestion that such structures control the emplacement of igneous intrusions (Figs. 1.6 & 1.9). A structural analysis of granitoid bodies may determine whether intrusion was in fact syn-kinematic and achieved along shear zones or other crustal anisotropies (Hutton 1988b; Hutton 1997). This may be achieved by mapping the distribution of strain within a pluton via meso-scale silicate fabric analysis (Hutton 1982), crystal lattice preferred orientation (Müller *et al.* 2011), anisotropy of magnetic susceptibility (Bouchez 1997), enclave orientation (Paterson *et al.* 2004) or by shear zone distribution and orientation studies (Archanjo *et al.* 2008). Microstructural analysis of plutonic facies may also be used in conjunction with relative or absolute chronological studies to establish the temporal relationship between fabric development and tectonic activity (e.g. Vahid *et al.* (2011)).

Hutton (1996) suggested that a syn-tectonic emplacement may by recognised by: 1) a consistency between magmatic state plutonic fabrics and host rock fabric, 2) minor granitoid veins extending into the host should show pre-solidus deformation structures relating to that of the surrounding strata and 3) any thermal metamorphic aureole should be synchronous with deformation.

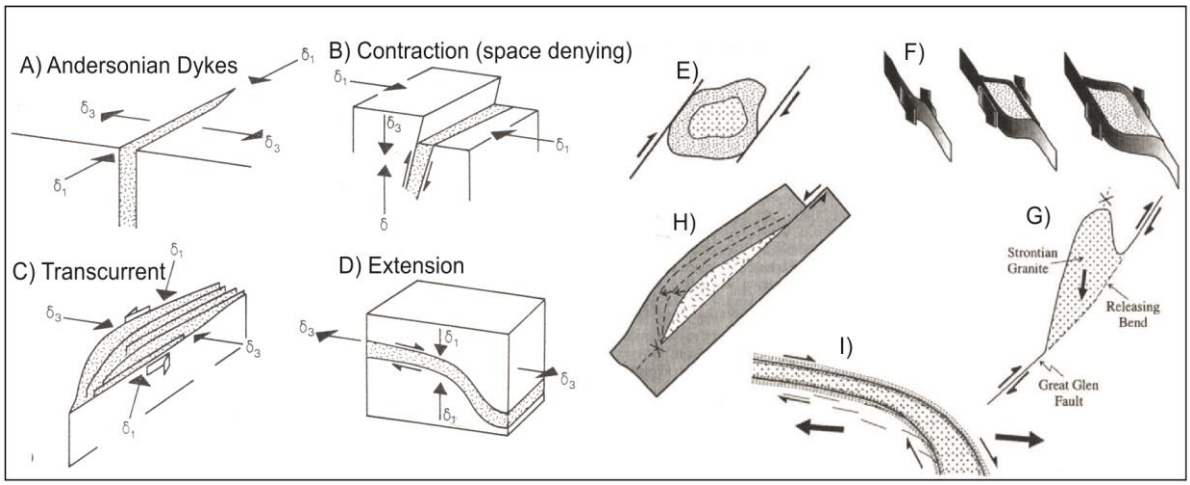


Fig. 1.9 Emplacement can be achieved in contractional, transcurrent and extensional structures highly oblique to the regional stress field (A-D), therefore σ_i must differ from σ_L. Contrasting styles of emplacement (Hutton 1996); E) The Rehamma Granite, Morocco intruded into a transtensional pull apart along a wrench fault (Lagarde *et al.* 1990); F) The Galway Granite, Ireland, intruded into a dilatational jog (Leake 2006); G) the Strontian Granite, Scotland intruded the active Great Glen Fault (Hutton 1988a); H) the Main Donegal Granite, Ireland, intruded at a shear zone termination and I) the Quernetoq Pluton intruded into an active tensional setting (Hutton *et al.* 1990).

The fundamental concept drawn from the occurrence of plutons forming in active shear zones was that the existence of such features must facilitate discrete dilation zones in the host rock (e.g. Hutton (1988b); Vauchez *et al.* (1997)). However, emplacement may occur into a broad range of active tectonic structures including "space denying" systems. Space for granitoid bodies (1000's km^3) is not created by crustal anisotropies rather that they serve to manipulate local stress (ambient tectonic and EMP) at the time of intrusions which leads to large scale dilation.

1.4.4 Laccoliths

In a report on the Henry Mountain in Utah, U.S.A., Gilbert (1877) gave the first detailed accounts of the geometry and nature of laccoliths. The traditional laccolith (in the sense of Gilbert (1877) and Daly (1933)) has a sub-horizontal lensoidal symmetry, a well-defined flat base, domed roof and a dyke fed ascent conduit that is apparently distinct from the laccolith emplacement structure. Laccoliths form by the initial intrusion of a subhorizontal sill which subsequently undergoes vertical thickening during the incremental forceful emplacement of magma (Daly 1933; Corry 1988; Cruden 1998).

Five criteria are used to define laccoliths:

1. Forcefully emplaced (senso Hutton (1988a))
2. Magma is supplied from a subvertical conduit
3. Initial intrusion along a subhorizontal plane
4. Space creation by uplift of overburden (during subsequent laccolith inflation)
5. Contacts are concordant with some bounding sub horizontal structural feature.

Corry (1988) established four stages for laccolith formation, vertical movement of magma through the lithosphere (ascent), reorientation of magma from ascent to lateral spreading (transition to and early emplacement), cessation of lateral spreading and initiation of vertical thickening (continued emplacement), uplift of overburden resulting from laccolith inflation.

Tabular intrusions emplaced through ductile deformation of the country rock are referred to as Christmas-tree (Corry 1988) or compound (Gilbert 1877) laccoliths is one which emplaces via ductile deformation of the host rock, no brittle shear occurs at the margins (Fig. 1.10). Typically, this term implies a suite of laccolithic bodies tapering away from a central ascent conduit at various crustal levels to form a christmas tree like profile (Bates and Jackson 1980). Grount (1918) identified a type of laccolith which exhibited an flat roof but sagging base, i.e. a lopolith which requires uplift of overlying strata during intrusion followed by floor subsidence/sagging and depression of the upper bounding country rock (Wager 1967; Bridgwater *et al.* 1974). Corry (1988) described the formation of a laccolith by the brittle failure of the bounding country rock, i.e. a punched laccolith where inflation is facilitated by radial brittle failure of country rock and direct uplift of the overlying detached roof resulting in a disk shaped intrusion bound by steep faults with a flat top and base (Fig. 1.10).

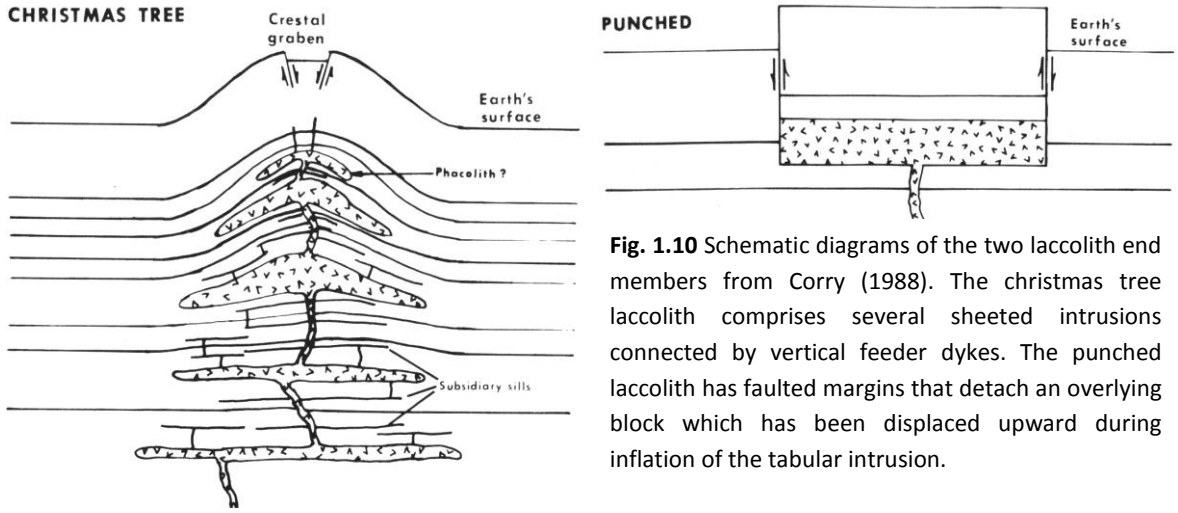


Fig. 1.10 Schematic diagrams of the two laccolith end members from Corry (1988). The christmas tree laccolith comprises several sheeted intrusions connected by vertical feeder dykes. The punched laccolith has faulted margins that detach an overlying block which has been displaced upward during inflation of the tabular intrusion.

Of the several hundred tabular and laccolithic intrusions documented around the world (e.g. see Corry (1988) with additions from McCaffrey and Petford (1997) & Cruden (1998)) relatively few show well exposed floors and roofs. Vigneresse (1990) highlights the time, cost and sensitivity benefits of geophysical investigation in cases where field relationships are unclear (see also Parslow and Randall (1973); Whitcombe and Maguire (1981); Evans *et al.* (1994); Siebel *et al.* (1997); Trzebski *et al.* (1997); Améglio and Vigneresse (1999). The Rosses Complex, Donegal, Ireland, is an interesting example of where geophysical evidence and field relationships conflict. Stevenson (2009) interpreted silicate and magnetic fabrics from this intrusion as representing lateral emplacement of a laccolith however Young (1974) identified a negative gravity anomaly over this granite implies a stock like sub-surface symmetry.

The concept of tabular plutons automatically addresses a large part of the space problem as it invokes only a fraction of the volume of magma that a diapiric model requires. This was demonstrated by McCaffrey and Petford (1997), based on a data set of 156 plutons (135 case studies published in Corry (1988) and a further 21 examples) through the use of the simple equation;

$$T = cL^{a}$$

where, T is unit thickness, L is unit length, c is a constant and a is the power-law exponent. From this application of the power law, McCaffrey and Petford (1997) showed that both tabular and laccolithic intrusions are scale invariant and argued that both tabular and laccolithic granites were intruded in a similar manner, i.e. lateral spreading followed by inflation. Reverting to Hutton (1996), one may expect that extensively inflated tabular bodies would progress to ballooned

plutons in the mid crust, where increased pressure-temperature conditions facilitate ductile deformation of the host rock, an example of which may be the Ardara pluton (Hutton and Siegesmund 2001) which is arguably the end result of an extensively ballooned laccolith.

1.4.5 Cauldron Subsidence

The cauldron subsidence model describes the emplacement of two types of intrusion, inward dipping cone sheets and outward dipping ring dykes plus associated overlying sub-lateral sill-like bodies which they feed (Fig. 1.11). The model invokes the displacement of magma by the subduction of a large crustal block into an underlying magma chamber (Clough *et al.* 1909; Richey 1928; Anderson 1936). Inflation of an epizonal magma chamber forces the uplift of the roof which develops concentric inward dipping fractures and sheeted intrusions (i.e. cone sheets) in response. As the chamber evacuates pressure drops, the roof subsides and sinks forming outward dipping fractures which fill with magma as the roof collapses into the underlying chamber (i.e. ring dykes). These may feed an overlying sub-lateral series of sheets which complete a bell jar ring dyke geometry (Roche *et al.* 2000).

The association between cauldron subsidence and the emplacement of igneous rocks was first noted by Clough *et al.* (1909) in reference to a "subterranean caldera" in Glen Coe, Scotland. Richey (1928) identified this as an emplacement mechanism and suggested the Mourne Granites intruded along steeply inclined ring dykes before emplacing laterally into the space created during the collapse of (initially) overlying host strata. The cauldron subsidence model was further constrained and applied to many British Paleogene igneous complexes including the Ardnamurchan intrusive complex (Richey and Thomas 1930) and the Slieve Gullion ring-complex (Richey 1932; Anderson 1936) and also to several other tectonic settings worldwide (e.g. Kingsley (1931); Pitcher (1953); Stevens (1958); Pitcher *et al.* (1985)) and even, however unlikely, on the moon (Hon 1972).

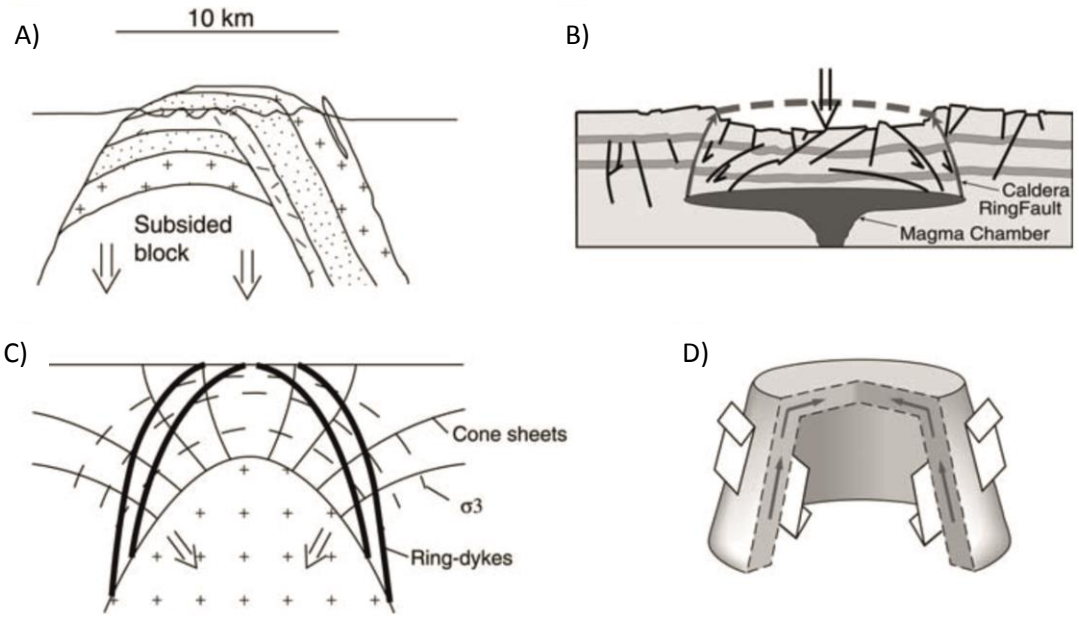


Fig. 1.11 A) The cauldron subsidence model for the Eastern Mourne Granites (Stevenson *et al.* 2008b). B) The emplacement of ring dykes (O'Driscoll *et al.* 2006). C) Cone sheets (Bailey *et al.* 1924). D) Shear sense and magma flow direction within ring dykes (O'Driscoll *et al.* 2006).

Anderson (1936) highlighted that this mechanism does not solve the "space problem". Due to the requirement of a pre-cursor shallow level magma chamber, space is not created so much as it is relocated. A second issue is that, with the exception of a few cases (e.g. Walker and Leedal (1954); Bussel (1985)), the subsided block is rarely identified and so it is simply postulated that its collapse drove magma into ring dyke and cone sheet structures.

Fitting the cauldron subsidence model to any particular intrusion is normally based on the recognition of inward and/or outward dipping concentric dykes, the recognition of a discordant plutonic structure with steeply outward dipping contacts and a lack of host rock emplacement related deformation. These characteristics are just as applicable to other mechanisms e.g. punched laccoliths. In recent years classic examples of ring dyke and cone sheet intrusions have been brought into question. This included data pertaining to the Mourne Granite cauldron subsidence model (Richey (1928) c.f. Meighan (1976); Meighan *et al.* (1984); Stevenson *et al.* (2007b); Stevenson and Bennett (2011)), the Ardnamurchan ring dyke and cone sheet complex (Wager and Brown (1968); Woodcock and Strachan (2000); Bell and Williamson (2002) c.f. O'Driscoll *et al.* (2006) Magee (2011)) and the Slieve Gullion Ring Complex (Richey (1932); Reynolds (1951); Bailey and McCallien (1956); Reynolds (1956); Emeleus *et al.* (2012) cf. Stevenson *et al.* (2008b))

To conclude, the cauldron subsidence model seems to be a viable but unproven even in classic type localities.

1.4.6 Role of Stoping

A stoped block is a block of country rock which has become detached from a pluton's host strata and incorporated into the intrusive body during magma ingress (Fig. 1.12). A volume of magma, equal to the volume of the stoped block, is displaced upwards as the block descends (density permitting). Paterson and Fowler (1993) consider this to be an important Material Transfer Process (MTP) in agreement with other authors who consider it a valid emplacement mechanism (e.g. Marsh (1982); Elena *et al.* (2003); Leake (2011); Burchardt *et al.* (2012)).

Recently, stoping has been cited as a major process during the emplacement of the Carna Pluton, Connemara, Co. Galway (Leake 2011). Leake (2011) suggested that several stoped blocks present around margins of the pluton show that emplacement was achieved essentially exclusively via the stoping process despite the fact that no country rock xenoliths are found within the plutons interior. See Compton (1955); Snowden and Snowden (1981); Burchardt *et al.* (2009) and Burchardt *et al.* (2012) for other examples.

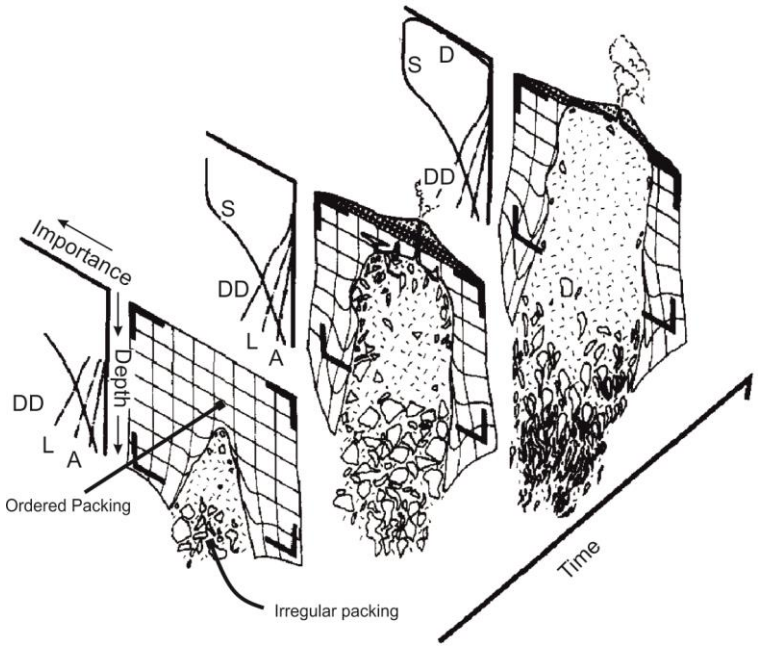


Fig. 1.12 Schematic diagram of a pluton ascending that heavily relies on the stoping mechanism (modified from Paterson and Fowler (1993)). The material transfer process at work varies from assimilation (A), rigid translation of wall-rock (L) and ductile shortening (DD) dominated at depth to stoping (S) and vertical displacement of overburden (D) in the brittle crust. Note that stoping re-deposits material in an inefficient fashion at the base of the diapir, this would ultimately cause arrest of magma ascent.

Fundamental problems are associated with stoping as an emplacement process (see Hutton (1996) & Glazner and Bartley (2006) but also Glazner and Bartley (2008); Paterson *et al.* (2008); Yoshinobu and Barnes (2008)). Among these are heat transfer issues due to an increase in country rock - magma surface area exposure (Hutton 1996; Brown 1928), lack of evidence for large masses of stoped blocks at the base of magma chambers (Buddington 1959; Marsh 1982), lack of large scale assimilation of country rock into granitic melts where stoping is sited (Pitcher 1987; Ague

and Brimhall 1988; Miller *et al.* 1988). Most notably is the space problem i.e. detachment of ordered blocks and random deposition of these at the base of a magma chamber will ultimately stall upward migration of a pluton as magma is left to infill interstitial space between detached blocks. Therefore an initial magma chamber several orders of magnitude larger than the final plutonic body would be required in order to achieve upper crust emplacement. Finally, stoping is most often proposed as an emplacement process for diapiric ascent, a process which is currently highly debatable.

Here, stoping is not considered to be an emplacement mechanism but merely a localised process that occurs as a consequence of the intrusion of magma, which is mechanically achieved by some emplacement mechanism (tectonically assisted, cauldron subsidence, laccolithic intrusion or ballooning).

1.5 Conclusions

The ascent and emplacement of magma in the earth's crust is a dynamic process which is controlled by the local tectonic stress (and by extension ultimately the regional stress field), excess magma pressure and local structural anisotropies. Universally, the transition from ascent to emplacement, the geometry of the emplaced body and its internal architecture will be dictated by the local stress field, and more specifically the orientation of $\sigma 3_i$, i.e. the net effect of the above forces and not by any individual one. Once in place, a crystallising granitoid will undergo strain in reaction to the applied stress field which may be the result of subsequent magma ingress, sub-magmatic shearing along a trans-plutonic fault concurrent with crystallisation, post crystallisation ductile or brittle deformation etc.

The generation of granitoids is inherently related to orogenic processes which are known to dramatically evolve within 5-10Ma periods (McKerrow *et al.* 2000; Dewey and Strachan 2003; Soper and Woodcock 2003; Dewey 2005). Owing to the temporal and volumetric scale at which plutonic and batholithic construction occurs, it is reasonable to consider that the genesis of an entire intrusive complex is dictated by a single kinematic stress field. This concept has been recognised for some time (Compton 1955) and is particularly well exemplified in the Rosses Complex, Donegal (Stevenson 2009), the Ardara Pluton, Donegal (Molyneux and Hutton 2000; Hutton and Siegesmund 2001; Stevenson 2008) and more recently in the Slaufrudalur Pluton, southeast Iceland (Burchardt *et al.* 2012).

Any realistic attempt to relate the controls on pluton construction to regional kinematic models must consider all of the above factors. The current work seeks to evaluate the internal architecture of several Siluro-Devonian granites in Connemara, Co. Galway, western Ireland which were emplaced over ~ 40Ma throughout the latter part of the Caledonian Orogeny and the Acadian Orogeny. It is envisaged that by evaluating the inherent structure of these plutons relative to that of the host rock individual plutons may be temporally and kinematically associated to each other and, by extension, to regional stress field fluctuations. As such it is first necessary to identify regional scale kinematic parameters, local scale structural features and the existing data base on the intrusions which will be studied. This is the focus of the following four chapters, the analytical work carried out on the plutons under investigation is detailed in Chapter 6-9 and the conclusions drawn from these is presented in Chapter 10.

Chapter 2:

The Caledonian and Acadian Orogenies

2.1 Introduction

In this study, the Siluro - Devonian kinematic evolution of the Connemara Metamorphic Complex, western Ireland (CMC, Leake and Tanner (1994)) is assessed through the examination of the temporal and structural relationships between pluton architecture and local host rock structure in this area. The plutons studied (reviewed in Chapter 5) were emplaced concurrently with late Caledonian and Acadian orogenesis. The host rocks into which these granitoids were emplaced also owe their genesis and complex structure to Caledonian processes. Therefore, a review of the current literature on the Caledonian and Acadian orogenies, as they apply to the current work, is necessary.

Section 2.2 establishes the current definition of the term "Caledonian Orogeny" and summarises the literature on the opening of the Iapetus Ocean. Section 2.3 introduces the Dalradian Supergroup which was deposited on the Laurentian margin during the opening of Iapetus and was deformed and intruded by Caledonian Granites later in the Orogeny. Section 2.4 discusses the closure of Iapetus. The Caledonian Orogeny had several discrete orogenic phases, works relating to earlier orogenic phases are briefly outlined for context. Later orogenic phases are reviewed in more detail as these are understood to have driven melting and magma production between ~ 447-380Ma (Atherton and Ghani 2002; Brown *et al.* 2008; Neilson *et al.* 2009; Goodenough *et al.* 2011) and so played a fundamental role in late Caledonian granite petrogenesis. Section 2.5 summarises the literature relating to the Acadian Orogeny which is an entirely separate and later tectonic event. This chapter concludes by highlighting the temporal relationship shared between these orogenic events relative to the timing of emplacement of the late Caledonian Granites of Britain and Ireland.

2.2 Definition of the Caledonian Orogeny

The "Caledonian Orogeny" traditionally refers to a Palaeozoic mountain building event that had its final culmination during the late Silurian closure of the ancient Iapetan Ocean. This closure amalgamated the continents of Laurentia, Baltica and Avalonia along a continental triple junction that formed the Caledonides of Britain and Ireland (Soper *et al.* 1992; Trench and Torsvik 1992).

The term "Caledonian Orogeny" literally translates to "Scottish mountain building event". The word Caledonian has its origins in the Latin word for Scotland and was first used in a geological context by Suess in 1885 (Suess 1906) who used the term in reference to pre-Devonian mountain belts across Norway, Scotland, Ireland and Wales (McKerrow *et al.* 2000). French geologist E. Haug identified four major orogenic events, the Huronina, Caledonian, Hercynian and Alpine Orogeny, at the end of the 19th century in his paper "Les geosynclinaus et les aires continentals". Although subsequent work has greatly modified these original definitions, this was the first published work to specifically identify and constrain the Caledonian Orogeny. Interestingly, the term Caledonian Orogeny was not used as a popular term until the late 1920's, after Stille (1924) proposed that the Caledonian was a short lived, world-wide, deformation event. This paper gained much publicity among British geologists and subsequently the term Caledonian Orogeny became a widely accepted term in geological literature. Retrospectively, this accomplishment is ironic, Stille (1924) successfully promoted the term Caledonian Orogeny through an infeasible concept of a short lived global orogenic event at the end of the Silurian (demonstrated to be inaccurate in several British geological sections that show conformity through the late Silurian and early Devonian (McKerrow 1962; Cocks *et al.* 1971; Hurst *et al.* 1978)). Haug (1900) actually defined the term in a more accurate manner two decades earlier, but his work was generally ignored by his English peers presumably because the script was written in French.

In modern literature, the Caledonian Orogeny is a collective name given to all Palaeozoic tectonic events, that occurred on the margins of Laurentia, Baltica and Avalonia and were associated with the opening and closure of the Iapetus Ocean (McKerrow *et al.* 2000). The geographical extent of the Caledonian Orogeny includes the Neo-Proterozoic and Palaeozoic areas of the British Isles, Ireland, Scandinavia, Svalbard, Greenland, Norway and the northern Appalachians (Soper *et al.* 1992; Torsvik *et al.* 1996; McKerrow *et al.* 2000; Dewey and Strachan 2003). By this definition, the Caledonian Orogeny is a collective term for all tectonic processes which were responsible for the rifting event which opened the Iapetus Ocean and the series of orogenic phases which occurred during its closure, a process that lasted some 200Ma (Scotese and McKerrow 1990).

Evidence for the Acadian Orogeny across Britain and Ireland implies that this was a much shorter event between ~ 400-390Ma, (Meere and Mulchrone 2006; Woodcock 2006). A period of transtension linking the end of Caledonian and start of the Acadian compression defines transition between these two events (McClay *et al.* 1986).

2.3 Summary of Opening the Iapetus Ocean

2.3.1 Initiation of the Iapetus Ocean

In the past, some debate surrounds the relative orientation of Baltica prior to the opening of the Iapetus ocean i.e. was it inverted (Hartz and Torsvik 2002) or not (Hoffman 1991; Dalziel 1992; Torsvik *et al.* 1996; Cawood *et al.* 2003; Pisarevsky *et al.* 2003). Ambiguity surrounding the potential inversion of Baltica arose from the fact that palaeomagnetic data, which was used to define the positions of Proterozoic and Palaeozoic continents, is poorly constrained. It is a rarity to have more than one or two reliable data points which accurately reflect the position of a continent for a stated time interval ((e.g. AWP paths for Laurentia and East Gondwana were interpolated between 720-600Ma in a reconstruction proposed by (Torsvik *et al.* 1996)).

Subsequently palaeomagnetic results are routinely supplemented with other geological information such as geochronological, provenance, palaeontological and sedimentological data. However, the use of such data to build continental drift models must be used only as circumstantial evidence as none of these techniques can definitively place a land mass in a geographical space at a point in time. Regarding the debate over the inversion of Baltica, this is exemplified numerous times (e.g. Cawood *et al.* (2001); Hartz and Torsvik (2002); Cawood *et al.* (2003)). In one example, the traditional model argues for a correlation between late Mesoproterozoic - early Neoproterozoic metasediments in East Greenland and Russian Baltica, both of which are intruded by anorogenic granites at *c.*1-0.93Ma (Khain 1985; Maslov *et al.* 1997; Watt and Thrane 2001). Hartz and Torsvik (2002) dismiss this evidence and argue for a correlation between the Eleonore Bay Supergroup in east Greenland and the sedimentary successions of the Karatau Group in the southern peri-Urals of east Baltica (Nikishin *et al.* 1996; Maslov *et al.* 1997).

A consensus now exists and the findings of Cawood and Pisarevsky (2006) are taken as the most up-to-date data set for deciphering the timing and direction of relative plate movements prior to the opening of the Neoproterozoic Iapetus Ocean and Tornquist Sea (Fig. 2.1). Based on these deductions, the reconstruction of Pisarevsky *et al.* (2003) is favoured over other models (Dalziel 1992; Dalziel 1997; Hartz and Torsvik 2002; Cawood *et al.* 2003).

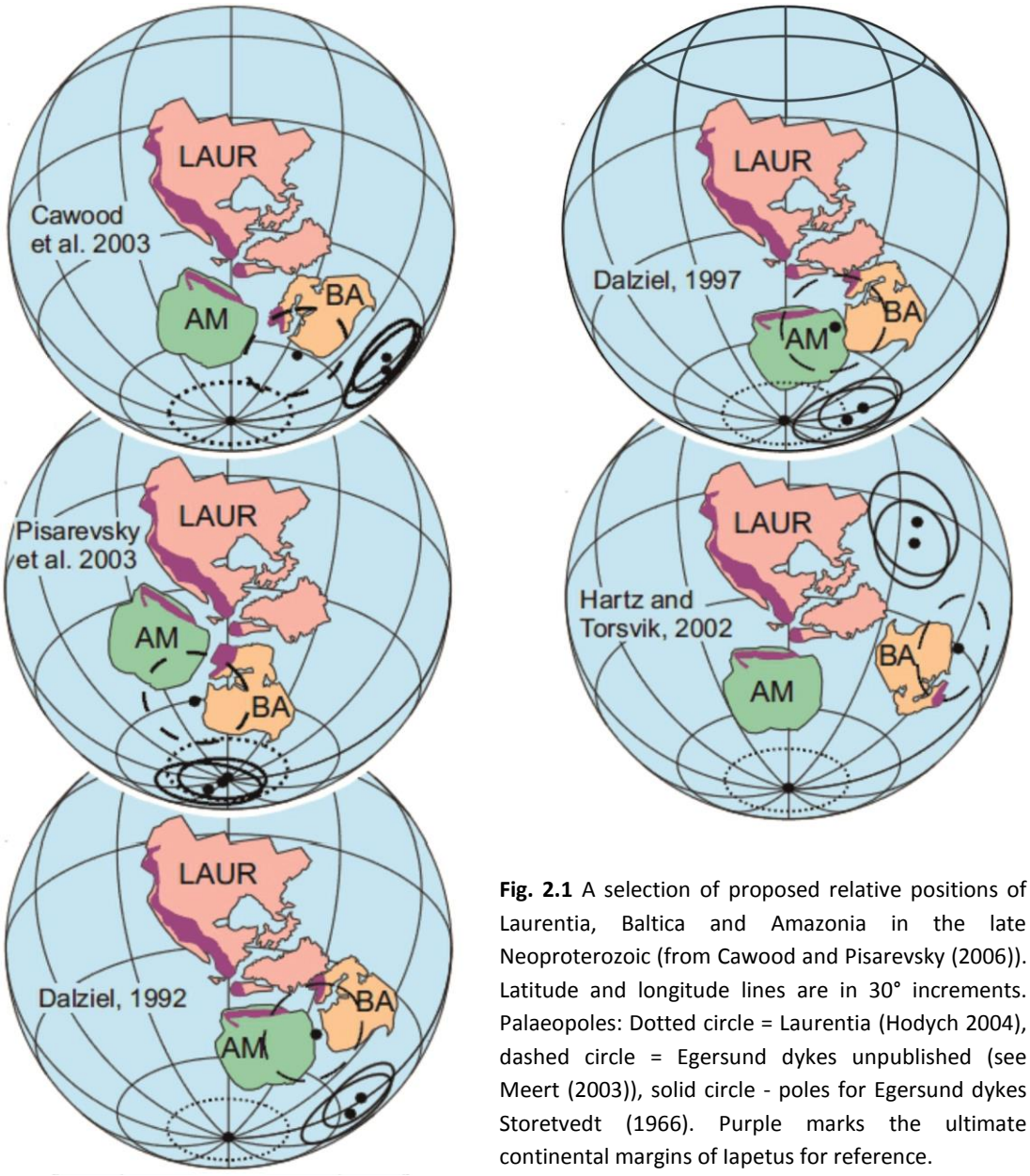


Fig. 2.1 A selection of proposed relative positions of Laurentia, Baltica and Amazonia in the late Neoproterozoic (from Cawood and Pisarevsky (2006)). Latitude and longitude lines are in 30° increments. Palaeopoles: Dotted circle = Laurentia (Hodych 2004), dashed circle = Egersund dykes unpublished (see Meert (2003)), solid circle - poles for Egersund dykes Storetvedt (1966). Purple marks the ultimate continental margins of Iapetus for reference.

Baltica was the right-way-up prior to the 750Ma break up of Rodinia with its Scandinavian margin aligned against Scotland and southeast Greenland. Along the western Baltica margin early Iapetan magmatism is possibly evidenced by the olivine tholeiitic Egersund dyke swarm of south-western Norway (~ 650Ma (Sundvoll 1987; Miller and Barton 1992)), the Ottfjallet dolerite dyke swarm of the Caledonian Sarv Nappe of south-central Sweden (~ 665Ma (Claesson and Roddick 1983; Kumpulainen and Nystuen 1985)), the Troms dolerite dykes of the Corrovarre Nappe in northern Norway (583Ma (Zwaan 1990)) and Keratophyre sheet (595Ma (Halliday *et al.* 1989)). Laurentian margin rift related early magmatism is recorded in the Long Range dykes of south-

eastern Labrador (615Ma (Kamo *et al.* 1989)), the Tayvallich Volcanic Formation felsic tuff (601Ma (Dempster *et al.* 2002)) and the Catoctin basalts of Virginia U.S.A. (600-580Ma (Badger and Sinha 1988; Aleinikoff *et al.* 1995)). Palaeomagnetic data show that Baltica and Laurentia were likely to be in contact up to ~ 620Ma and clearly indicates separation before ~ 580Ma (Torsvik *et al.* 1996). Considering the resolution capabilities of the palaeomagnetic technique, an obvious correlation seems to exist between the geochronological and the palaeomagnetic data from east Laurentia and West Baltica. This allows for the deduction that current day western Baltica rifted from current day eastern Laurentia. Opening of the Tornquist Sea along the south-western margin of Baltica commenced in the late Neoproterozoic evidenced by 560-550Ma magmatism (Compston *et al.* 1995; Nosova 2005) and basin development related to rifting (Poprawa *et al.* 1999).

By early Ordovician times Gondwana, with Avalonia still attached, was close to the south pole, Baltica was positioned to the northeast and experienced a temperate climate while Laurentia was positioned at the equator to the northwest of Iapetus (Cocks (2000) and references therein). The account given by early reconstructions (e.g. Trench and Torsvik (1992)) indicate that the Iapetus extended some 5000km from Laurentia-Avalonia, 3000km from Laurentia to Baltica and 1200-1500km from Baltica to Siberia by the early Ordovician, these data are acceptable as crude dimensions of the maximum extent of the Iapetus Ocean (Fig. 2.2).

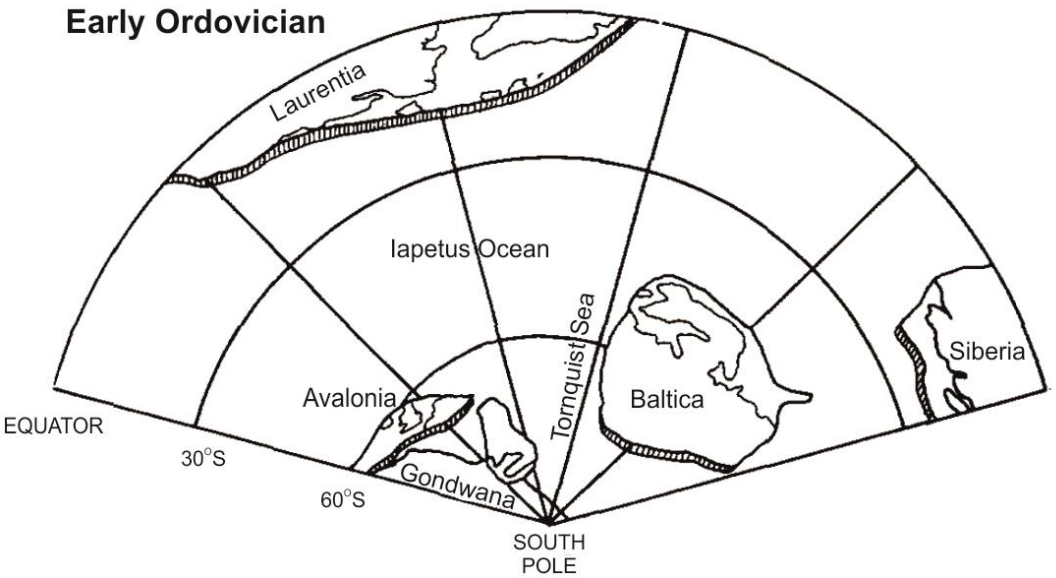


Fig. 2.2 Basic distribution of the continents bordering the Iapetus Ocean in the early Ordovician. Adapted from Trench and Torsvik (1992).

2.3.2 The Dalradian Supergroup

The Dalradian Supergroup hosts several late Caledonian plutons across Britain and Ireland including some of the Siluro-Devonian intrusions in Connemara which are the focus of this study. This sequence of metasediments and mafic volcanics were deposited during the Neoproterozoic and early Cambrian break up of Rodinia (Anderton 1980a; Anderton 1985; Strachan *et al.* 2002; Cawood *et al.* 2003; Cawood *et al.* 2007; Benn 2010). Dalradian stratigraphy is bound, most often, to the northwest by the Great Glen Fault and by the Highland Boundary Fault to the southeast. It is estimated to have an absolute thickness of ~ 25.5km and occupies an area of about 48,000km² (Harris *et al.* 1994). Proterozoic gneisses are tectonically overlain by Dalradian metasediments, these gneisses are taken as Dalradian basement rocks (Kennedy and Menuge 1992). Following deposition, the Dalradian Supergroup was subjected to polyphase regional greenschist-amphibolite grade regional metamorphism during the closure of the Iapetus Ocean (Harris *et al.* 1994; Strachan *et al.* 2002).

The Dalradian Supergroup was, at least in part, deposited into a continuously extending half graben structure on the eastern Laurentian margin which would eventually result in the separation of Laurentia from Baltica and open the Iapetus Ocean (Hoffman 1991; Soper 1994; Dalziel and Soper 2001). Compositionally, these metasediments were originally deposited as a series of carbonate, siliclastic, tillite, conglomerate and mafic volcanic units. These strata were originally correlated with the Lys Supergroup in Newfoundland by Kennedy (1975) who first identified the Appin, Argyll and Southern Highland Subgroups; however subsequent work has brought much of these correlations into question (see Hibbard (1988)). Harris and Pitcher (1976) and Harris (1978) subdivided the Dalradian into the Grampian, Appin, Argyll and Southern Highland Groups. More recently, Tanner and Sutherland (2007) redefined the Southern Highland Group as two Groups i.e. the Southern Highland Group and the overlying Trossachs Group.

Two contrasting hypothesis exist which attempt to account for the tectonic scenario in which the Dalradian Supergroup was deposited (Fig. 2.3) The traditional model suggest the Dalradian represents a period of protracted episodic extension over ~ 300Ma facilitated deposition into a shallow marine ensialic basin which ultimately rifted to form the Iapetus Ocean (Anderton 1982, 1985; Hoffman 1991; Trench and Torsvik 1992; Soper 1994; Soper and England 1995; Torsvik *et al.* 1996). An alternative model suggests that the lower part of the Dalradian was actually deposited

in a convergent regime and extension, ultimately opening the Iapetus Ocean, did not commence until midway through the deposition of the Argyll Group (Prave 1999).

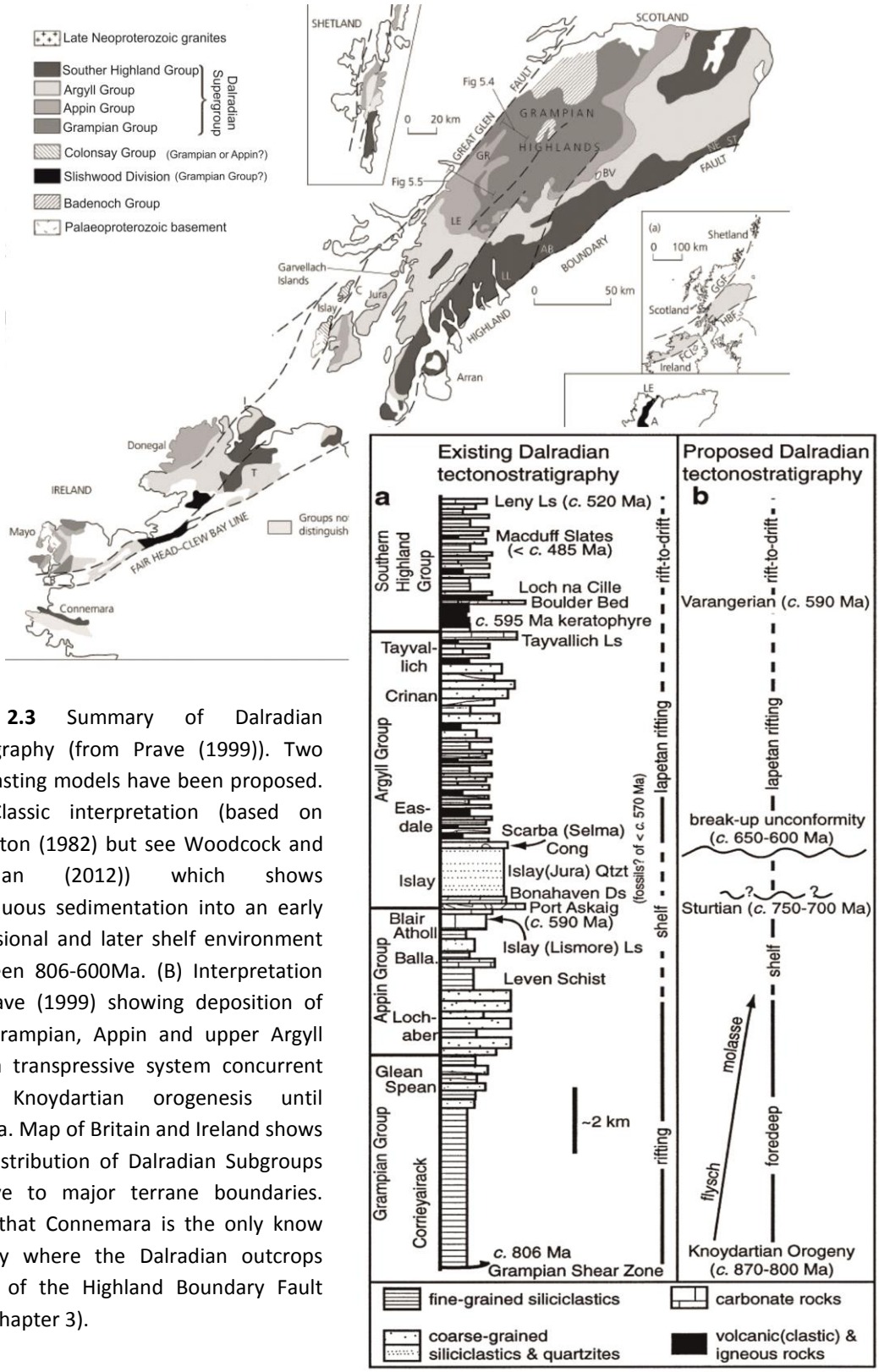


Fig. 2.3 Summary of Dalradian stratigraphy (from Prave (1999)). Two contrasting models have been proposed. (A) Classic interpretation (based on Anderton (1982) but see Woodcock and Strachan (2012)) which shows continuous sedimentation into an early extensional and later shelf environment between 806-600Ma. (B) Interpretation of Prave (1999) showing deposition of the Grampian, Appin and upper Argyll into a transpressive system concurrent with Knoydartian orogenesis until 800Ma. Map of Britain and Ireland shows the distribution of Dalradian Subgroups relative to major terrane boundaries. Note that Connemara is the only know locality where the Dalradian outcrops south of the Highland Boundary Fault (see Chapter 3).

2.3.2.1 Summary of Stratigraphy

Grampian Group

The 806Ma Grampian Shear Zone (U-Pb monazite Noble *et al.* (1996)) represents a tectonic unconformity which separates the ~ 8km thick Grampian Group from upper units of the underlying Moine Supergroup. The Grampian Group has been divided into three lithostratigraphic units these are the Glenshirra, Corrieyairick and Glen Spean Subgroups.

Compositionally, the Grampian Group is reasonably homogenous, dominated by marine quartzo-felspathic psammite and semi-pelite units 100-1000m thick (Glover and Winchester 1989). Minor calc-silicate bands or pods, concordant garnetiferous amphibolite, and well sorted dense mineral layers occur throughout. Readily altered psammite and pelite-semi-pelite bands present in Moine Group sediments are not common in Grampian Group stratigraphy and so aid in distinguishing the upper Moine Supergroup from basal units of the Dalradian Supergroup (Harris *et al.* 1994).

Appin Group

The Appin Group conformably overlies the Grampian Group and is subdivided into the Lochaber, Ballachulish and Blair Atholl Subgroups. The lower units of the Appin Group and the Upper most parts of the Grampian Group exhibit a complex overlapping relationship which clearly indicate that the deposition of sediments from each group occurred in a synchronous manner (Woodcock and Strachan 2012). The consistency this stratigraphy along strike across Britain and Ireland (e.g. Cobbing (1968)), coupled with compositional and primary structural evidence, led Anderton (1985) to the conclusion that this continuous undisturbed sedimentation occurred under stable conditions in the earlier stages of a major rifting event (i.e. the opening of the Iapetus Ocean), a hypothesis challenged by Prave (1999).

Argyll Group

The Argyll Group has been divided into four subgroups, the Islay, Easdale, Crinan and Tayvallich subgroups that reflect rapid basin deepening following short term shallow marine conditions (Anderton 1985). The base of the Islay Subgroup is marked by an obvious glacial tillite horizon, i.e. the Port Askaig Fm. (Anderton 1985; Harris *et al.* 1994). This is attributed to the 590-564Ma Varangerian-Marinoan glaciogenic episodes (Spencer 1971; Anderton 1980a; Hambrey 1983; Fitches *et al.* 1996; Panahi and Young 1997; Saylor *et al.* 1998; Gorokhov *et al.* 2006) but also to the 750Ma end-Sturtian glaciation event (Prave 1999). Most recently Rooney *et al.* (2011)

show units of the Ballachulish Slate to be 659.6 ± 9.6Ma thus proving the Port Askaig Fm. must be younger than this.

The uppermost unit of the Argyll Group is the Tayvallich Subgroup. West of the Cruachan Lineament an extensive suite of high level mafic sills, dykes, pillow lavas and, in the upper most units, felsic tuff deposit (Anderton 1985; Strachan *et al.* 2002) are interbedded with the Tayvallich Limestone i.e. the Tayvallich Volcanic Fm.. This horizon is a product of extreme crustal thinning during a major rifting event at ~ 600Ma (Halliday *et al.* 1989; Dempster *et al.* 2002) which ultimately opens the Iapetus ocean.

The roll of active tectonics during the deposition of the Tayvallich Subgroup is evident in the distribution of sediments and orientation of igneous intrusions. A transtensive strain regime, generated during rifting, created low strain zones along the northwest-southeast Cruachan Lineament and associated minor structures (Woodcock and Strachan 2012). These low strain zones were exploited by upwelling mafic magma and resulted in the emplacement of a swarm of northwest-southeast tholeiitic feeder dykes across the Isle of Jura and eastward as far as the Cruachan Lineament. Synchronous deposition of the Tayvallich Limestone Formation occurred as inter-basaltic horizons into the earlier formed Crinan Grit basins, developed as a product of northwest-southeast transform rift faults, illustrates how the Cruachan, Rothes, Glenlivet, Argyll and Donegal Lineaments played a fundamental roll in generating the Easdale, Crinan and Tayvallich Formations of the Argyll subgroup.

Southern Highland Group

The base of the Southern Highland Group is defined by the Loch Avich Grits which conformably overlie the Tayvallich Subgroup which represent the eroded upper units of the underlying subgroup and form "The Green Beds" (Anderton 1980b; Anderton 1985; Strachan *et al.* 2002). This group is predominantly turbiditic meta-greywackes usually composed of coarse grained poorly sorted graded sandstones interbedded with minor siltstone and limestone beds (Harris and Pitcher 1976; Harris 1978; Anderton 1980a; Anderton 1985). This sequence reflects a continuation of sedimentation in a deep marine environment and marks the final transition from continental rifting to rupture and the birth of the Iapetus Ocean and thermally subsidence of the Laurentian Margin (Anderton 1985).

Trossachs Group

The Trossachs Group consists of dark limestone and slate units and hosts the stratigraphically significant Leny Limestone and Slate Member (Tanner and Sutherland 2007). Overturned

sequences of this member are exposed in the Leny Quarries, near Callander, Scotland, just north of the Highland Boundary Fault. Preserved trilobite species of *Pagetides,* which are known to have populated the *Bonnia-Olenellus* Zone on the outer Laurentian margin, occur in the Leny Limestone at this site and constrain the age of deposition of these rocks, the uppermost Dalradian, to the Lower Cambrian (Pringle 1939; Fletcher and Rushton 2007). There is no evidence or reason to suggest significant volumes of detritus were deposited above the presently exposed Trossachs Group units (Anderton 1985).

2.3.2.2 Temporal Constraints

Some ambiguity surrounds the precise chronostratigraphy of the Dalradian Supergroup. However palynological and paleontological (Pringle 1939; Fletcher and Rushton 2007) and isotopic data (Halliday *et al.* 1989; Noble *et al.* 1996; Highton *et al.* 1999; Dempster *et al.* 2002; Thomas *et al.* 2004; McCay *et al.* 2006; Halverson *et al.* 2007; Prave *et al.* 2009; Sawaki *et al.* 2010); Rooney *et al.* (2011) has provided some insight toward gaining an understand of observed stratigraphic relationships. Key markers have been identified, around which a crude chronological frame work has been constructed. The base of the Dalradian can be taken to be ~ 806Ma (Harris *et al.* 1994; Noble *et al.* 1996; Prave 1999; Woodcock and Strachan 2012), the Grampian and Lower Appin Group sediments were deposited during the following 140Ma. The Ballachulish Slate formation was deposited at ~ 659Ma (Rooney *et al.* 2011) and before the intrusion of the Tayvallich Volcanic Formation at ~ 600Ma (Halliday *et al.* 1989; Dempster *et al.* 2002). The Port Askaig Tillite was deposited at ~ 650Ma (Rooney *et al.* 2011). The Southern Highland Group and the Trossachs Group were both deposited by ~ 540-520Ma over a period of ~ 70Ma (Pringle 1939; Fletcher and Rushton 2007). In total the Dalradian Supergroup deposited over a period of ~ 270Ma, spanning much of the Neo-proterozoic and into the Cambrian.

2.4 Closure of the Iapetus Ocean

The present day three way suture zone across Ireland, Britain and northern Europe represents the final product of the closing of the Iapetus Ocean. Essentially this suture zone was formed by a collision between Laurentia to the northwest, Baltica to the northeast and Avalonia in the south to form the Caledonides of northwest Europe. In total the Caledonian Orogeny lasted 200Ma and

includes all tectonic process involved in the opening and closing of the Iapetus Ocean, between ~ 605Ma-400Ma (McKerrow *et al.* 2000). It is now well documented that the closure of the Iapetus Ocean, involved a series of *Orogenic Phases* which culminated in the final docking of the above mentioned continental blocks. A brief account of the regionally most significant orogenic phases is presented, the regional scale spatial and temporal relationships between these phases are summarised below (Fig. 2.4). This is by no means a comprehensive list, merely a general summary of significant tectonic events which occurred during the closure and final lock up of the Iapetus Ocean.

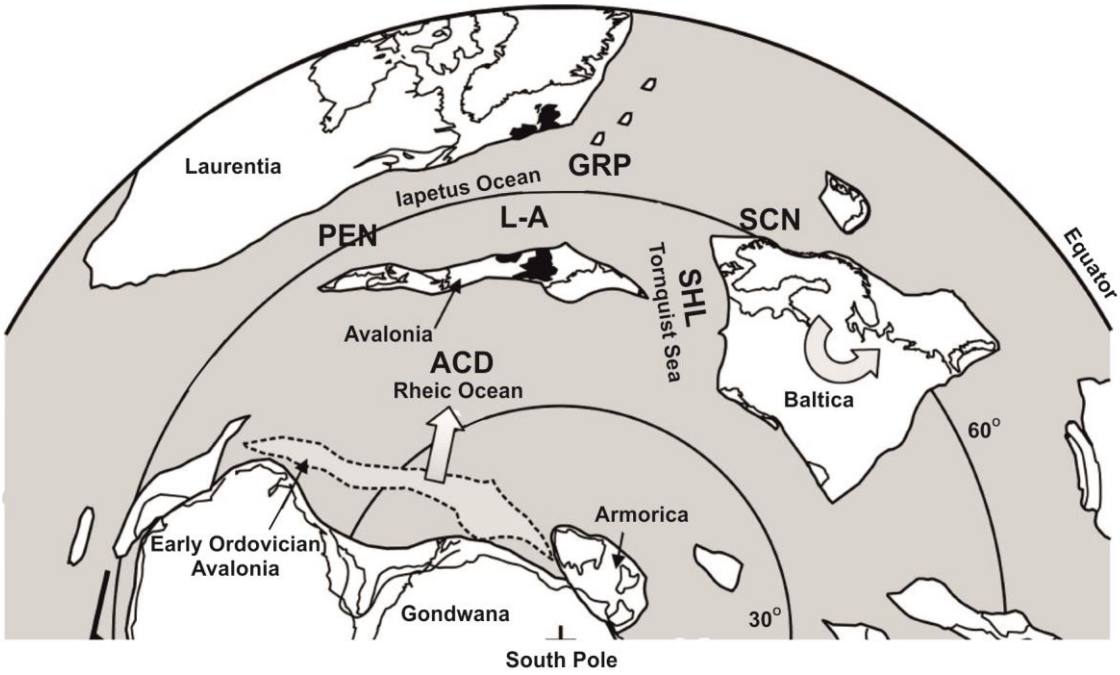


Fig. 2.4 Schematic diagram of the Iapetus Ocean during early closure (~Ordovician) modified from Woodcock and Strachan (2012). Locations of orogenic phases discussed in the text are indicated: PEN = Penobscotian, GRP = Grampian arc system, SHL = Shelveian closure of Tornquist Sea, SCN = Scandian Baltica - Laurentia collision, L-A Laurentian - Avalonian convergence, ACD = Acadian Orogeny closure of the Rheic Ocean. Gray arrows indicate direction of movement of Avalonian and Baltica during closure of Iapetus.

2.4.1 The Penobscotian Orogenic Phase

First recognised by Neuman (1967), the Penobscotian Orogeny is defined by an unconformity between the Grand Pitch Formation (early Cambrian) and Shin Brook Formation (Arenig/Llanvirn) in Maine, New England. It is now recognised from New Brunswick to Newfoundland and also in North Wales and Co. Wexford, Ireland (McKerrow *et al.* 2000). This phase of the Caledonian Orogeny represents a major orogenic event along the north-western margin of the Iapetus Ocean

when the Penobscot Arc (~ 513-486Ma) collided with the Gander-Avalonian continental margin during the early Ordovician (~ 485-474Ma) (van Staal *et al.* 1998; Zagorevski *et al.* 2007).

There are two contrasting, tectonic models for the Penobscotian. The more conventional hypothesis suggests that Penobscotian Ophiolite and arc fragments were obducted onto Ganderia over a northwest directed subduction zone between the late Cambrian and early Ordovician (van Staal *et al.* 1998). This obduction was followed by a subduction polarity reversal and a new phase of back-arc magmatism on the newly composite Gander crust. A second hypothesis suggests that the Penobscotian Arc flanked the Gander margin so that both overlay a SE subduction zone prior to any obduction. This model proposes minor thrusting forced obducted Penobscotian material onto Ganderia and, shortly after, the subduction front migrated southeast away from the continental margin Zagorevski *et al.* (2007). Therefore no subduction flip is required.

2.4.2 The Grampian Orogenic Phase

The Grampian Orogenic phase is the first major event marking significant shortening of the Iapetus Ocean. This orogeny was first defined by Lambert and McKerrow (1977), (following Kennedy (1958) & McKerrow (1962)) as an early Ordovician event generated by the collision of a mid-ocean ridge with southeast Laurentia. Further work carried out through the 1990's (synopsis in Dewey and Mange (1999); Soper *et al.* (1999); Dewey (2005); Woodcock and Strachan (2012)) related the Grampian deformation event, and its accompanying igneous activity, to the accretion of an island arc to the south-eastern Laurentian margin and a subsequent short lived continental magmatic arc. Arc-continent collision was initiated after south-eastern directed subduction of oceanic lithosphere beneath the island arc ultimately caused the collision of the island arc and Laurentia. Continued shortening of Iapetus led to slab break off of the old southward dipping plate and a subduction polarity flip occurred allowing renewed, north-west directed, subduction of Iapetan oceanic lithosphere beneath the newly accreted Laurentian and island arc crust (Fig. 2.5).

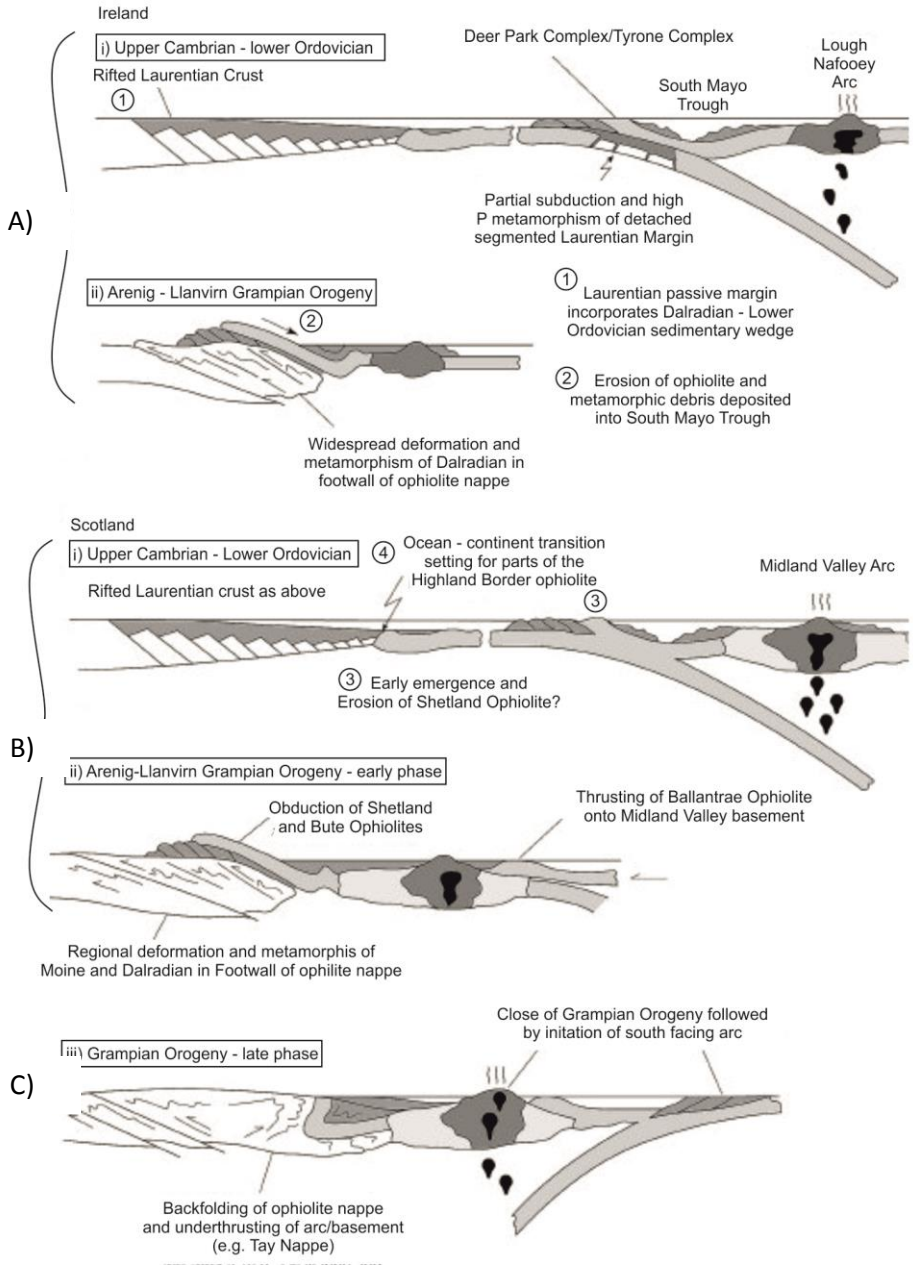


Fig. 2.5 The Grampian orogenic phase of the Caledonian Orogeny (schematic diagram from Woodcock and Strachan (2012) after Ryan and Dewey (1991). (A) and (B) are equivalent examples of Grampian events based on evidence from Ireland and Scotland respectively. In both cases initial southward subduction of ocean crust (i) drives arc magmatism and the formation of the a forearc basin and convergence of the island arc with Laurentia (ii) causes obduction of oceanic crust onto the Laurentian margin. (C/iii) Continued closure of Iapetus causes a new forearc basin to form to the south of the accreted island arc and Laurentia and northward subduction of Iapetan oceanic crust.

Polyphase deformation and metamorphism, as well as extensive igneous activity, is associated with this continental - arc accretion event. Regional D2 & D3 fabrics across the Central Highlands Terrane, located north of the Clew Bay Line in western Ireland and also south of it in Connemara, are generally considered a product of the Grampian Orogeny (e.g. Hyslop and Piasecki (1999);

Soper *et al.* (1999); Tanner and Thomas (2009)). Associated magmatism generated mafic to granitic magmas which were emplaced into the back arc basin, today these intrusions may be observed as amphibolites and orthogneisses in Dalradian group metasediments in Connemara. Regional polyphase metamorphism (typically reaching amphibolite grade), as well as local contact metamorphism, accompanied the emplacement of these intrusions (e.g. Yardley (1976); Yardley (1980); Barber and Yardley (1985); Yardley *et al.* (1987)).

A minimum age for Grampian deformation is unequivocally demonstrated by Upper Llandovery strata which rests unconformably over Dalradian metasediments in Connemara, these sediments have not been subjected to Grampian deformation and so must postdate the event (McKerrow 1960). Amongst the uppermost Dalradian Supergroup units, the Leny Limestone (Tanner and Sutherland 2007) exhibits polyphase Grampian folding and so, these lower Cambrian units (Pringle 1939; Fletcher and Rushton 2007) pre-date the Grampian Orogeny. Some isotopic data suggest some gabbros associated with the Grampian may be up to 490Ma however, these data were acquired from unabraded zircons (Jagger *et al.* 1988) or from unreliable whole rock Rb-Sr specimens (Pankhurst 1970) and are broadly rejected. Work carried out through the 1990's (Cliff *et al.* 1993; Rogers *et al.* 1994; Friedrich *et al.* 1999a; Friedrich *et al.* 1999b) argued that the time period over which the emplacement of Grampian related igneous rocks occurred was between 462-474Ma. This is broadly consistent the findings of Friedrich *et al.* (1999b) and Cliff *et al.* (1996) who reported 460-470Ma late, syn and post D3 pegmatites in Connemara. The rapid nature of this orogeny is highlighted by Dewey (2005) who concluded that the entire orogenic process including initial subduction to post flip shortening of the arc and associated deposition of sediments lasted only 18Ma.

2.4.3 The Shelveian Orogenic Phase

Synchronous with the opening of Iapetus between Baltica and Laurentia a second smaller rift developed between Gondwana and Baltica and progressed to eventually open the Tornquist Sea (Cocks and Fortey 1982; Toghill 1992; Trench and Torsvik 1992). During Arenig-Llanvirn times, a small continent, Avalonia, also rifted from the northern margin of Gondwana and drifted northwards into the Tornquist Sea, this trajectory gradually reduced the expanse of the Tornquist Sea and ultimately its closure when Avalonia docked with southern Baltica in the early Silurian (Trench and Torsvik 1992; Torsvik and Rehnström 2003). The collision of Avalonia with Baltica is referred to as the Shelveian Orogenic Phase and is represented today by the Thor Suture Zone

(TSZ) which remains a composite part of the Trans-European Suture Zone (Pharaoh 1999) and one of three sutures of the British and Irish Caledonides (Fig. 2.6).

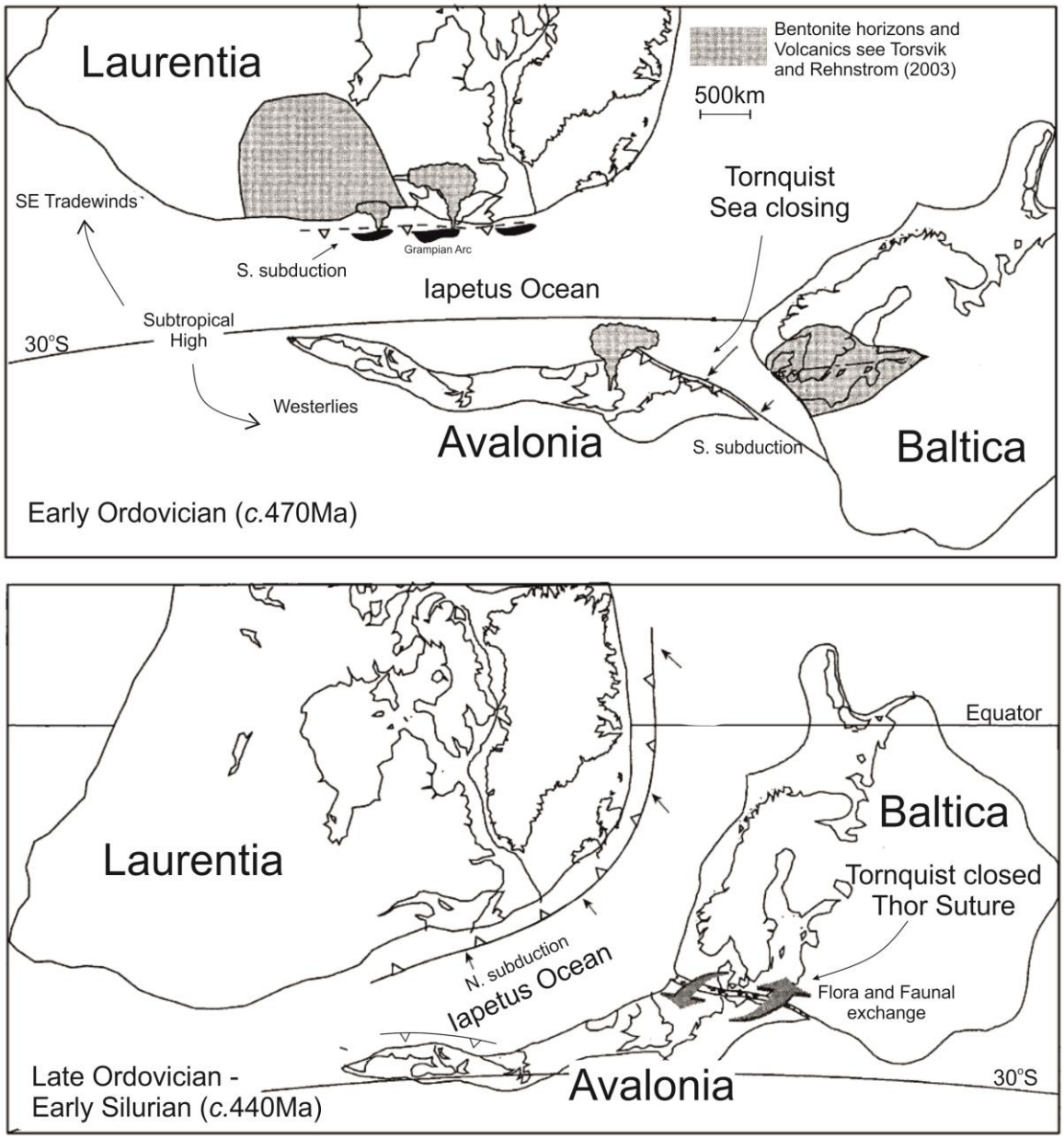


Fig. 2.6 Distribution and relative movements of continents boarding the Iapetus between ~ 470-440Ma during the closure of the Tornquist Sea (adapted from Torsvik and Rehnström (2003)). Volcanism on the Avalonian continent was driven by southward subduction of oceanic crust as Baltica converged on Avalonia and the Tornquist sea closed. Isotopic evidence from this process as well and floral and faunal evidence, places temporal constraints on the timing of this closure. Note Grampian subduction flip on southern Laurentian coast. Note the timing contrast between this model and that in Fig. 2.10.

Although a very important event in the Caledonian Orogeny, there is little immediate evidence for this event. In Britain the occurrence of an unconformity at the base of the Ashgill sequence in Shropshire substantiates the occurrence of the Shelveian Orogeny (Toghill 1992). In addition, research based on the floral and faunal evolution of Baltica and Avalonia which, when coupled with palaeomagnetic, seismic, isotopic and sedimentological studies, show clear correlations between Avalonian and Baltica in the early Silurian (see: Cocks and Fortey (1982); McKerrow (1991); Torsvik *et al.* (1991); Torsvik and Trench (1991b); Torsvik and Trench (1991a); Trench and Torsvik (1992); Cocks *et al.* (1997); Cocks (2000), reviewed in Torsvik *et al.* (1996); Pharaoh (1999); McCann and Krawczyk (2001)) and infer convergence occurred at this stage.

Palaeomagnetic data show that Avalonia rifted from Gondwana in the early Ordovician and by late Ordovician times had an AWP path which overlapped with that of Baltica implying the two continents were in close proximity or merged at this stage (Torsvik *et al.* 1993; Torsvik *et al.* 1996). Micro-palaeontological studies have provided strong evidence that by the Caradoc, benthic faunas from Avalonia had begun to mix with Baltic faunas, and by the Ashgill had similarities at species level (Cocks and Fortey 1982; Cocks and Fortey 1990; McKerrow 1991; Cocks *et al.* 1997; Cocks 2000). Torsvik and Rehnström (2003) sought to constrain these temporal parameters and suggested that the mid Caradoc Kinnekulle K-bentonite (KKb) ash horizon ~ 458 - 455Ma (Min *et al.* 2001), that is present across much of Baltica, was the surface equivalent of late Ordovician calc alkaline intrusions in Britain generated from the subduction of ocean crust beneath Avalonia during the Baltica-Avalonia collision ~ 422-457 (Noble 1993; Pharaoh *et al.* 1993; Torsvik 1998). This data suggests the Shelveian Orogeny would have been underway by the late Ordovician and that the closure of the Tornquist Sea occurred about this time, a hypothesis also suggested by Cocks (2000).

2.4.4 The Scandian Orogenic Phase

First recognised in Scandinavia (Gee 1975) and later identified further south in Scotland (Coward 1990; Dallmeyer *et al.* 2001; Kinny *et al.* 2003) the Scandian Orogeny is today represented by the northward trending extension of the Caledonian Suture Zone triple junction and is one of the most intensively studied phases of the Caledonian Orogeny. This orogenic phase initiated when Baltica collided with, and began to subduct westward beneath, a stationary Laurentia (Torsvik *et al.* 1996) resulting in extensive subduction related magmatism and crustal shortening facilitated by northwest directed thrusting and folding (Fig. 2.7).

The Scandian Orogeny is evidenced by an orogenic belt that extends from East Greenland through Svalbard, Scandinavia and northwest Scotland. In Scotland Scandian deformation is confined to the Northern Highlands Terrane. No influence of Scandian deformation has been documented south of the Great Glen Fault; to the north the Moine Thrust Zone marks the western extent of Caledonian deformation (see Woodcock and Strachan (2012) for synopsis). Within this area, Moine Supergroup metasediments have been thrust over (Coward 1983; Butler 1987; Soper *et al.* 1998), the stratigraphically younger Cambro-Ordovician Laurentian Margin sediments as well as the Torridonian (Stewart 1982; Nicholson 1993; Stewart 2002) and Lewisian Gneiss basement (Park and Tarney 1987; Park *et al.* 2002) via the Moine Thrust Zone.

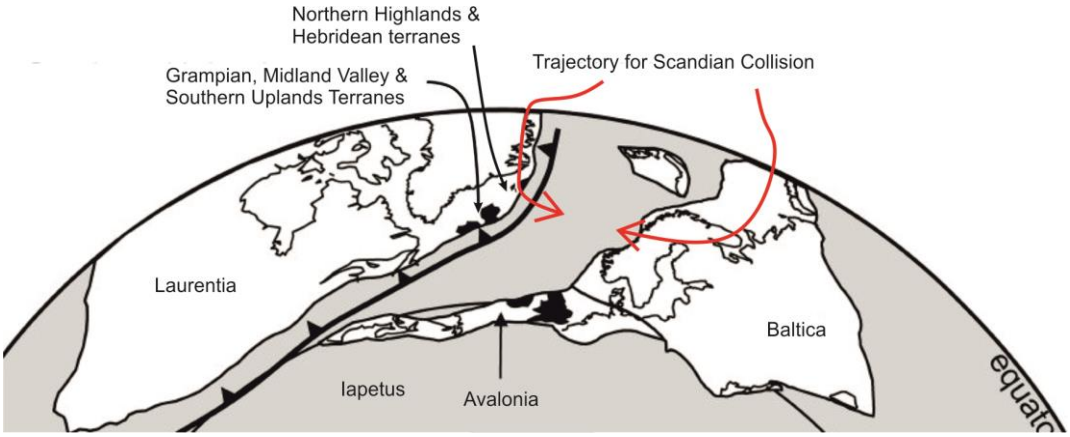


Fig. 2.7 Pre-Scandian (~ 450Ma) distribution of Laurentia, Baltica and Avalonia.

The Moine Thrust Zone (Fig. 2.8) consists of a suite of foreland-propagating thrusts stacked in a piggy-back sequence (Elliott 1980; Coward 1983). Stratigraphic units defining these structures are generally arranged from oldest highest to youngest lowest and exhibit a variety of recumbent folds that developed synchronously with early thrusting in response to the sinistrally oblique nature of the Baltica-Laurentia collision (summary in Woodcock and Strachan (2012)). Underlying the Moine Thrust, a series of faults incorporate Cambro-Ordovician, Torridon Group sediments and Lewisian Gneiss in several minor northwest directed thrusts also related to early Scandian deformation (Elliott 1980; Krabbendam 2010). These northwest directed thrusts, coupled with other structural and palaeomagnetic data indicate that Baltica and eastern Avalonia docked sinistrally oblique to Laurentia (reviewed: Soper *et al.* (1992) & Torsvik *et al.* (1996)). A second phase of folding represents late stage shortening that is most apparent in the North Highland Steep Belt as a series of regional scale tight upright folds (see Strachan and Evans (2008) and references therein). Finally, a sequence of low angle out of sequence faults cross cut the above

described structures, these are believed to be the product of late stage movements, possibly orogenic collapse driven by gravity instability or instantaneous movement along multiple thrust planes contained within one block (see Coward (1982, 1983, 1985); Butler (2004); Holdsworth *et al.* (2006) for discussions).

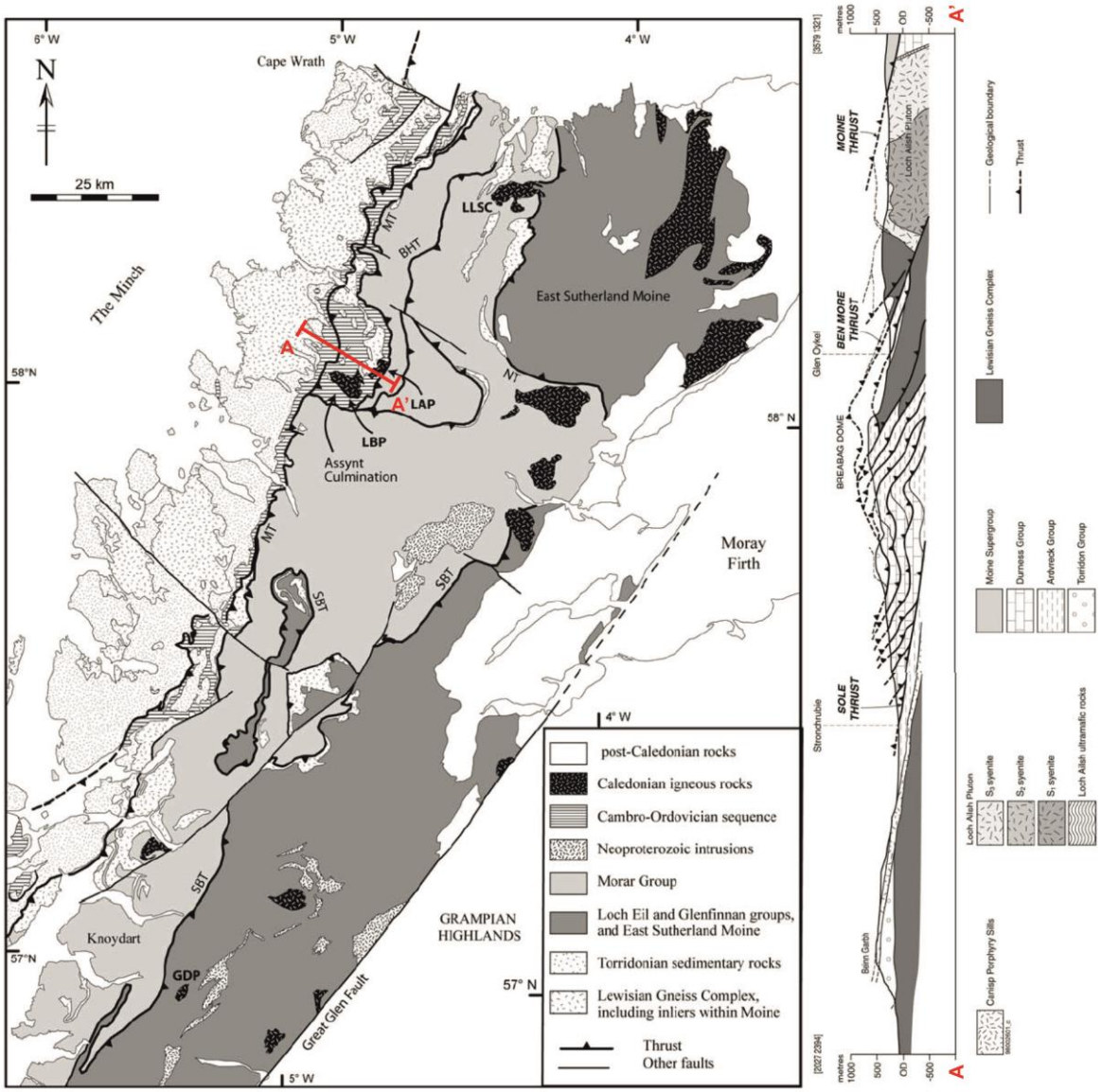


Fig. 2.8 Geological map of the Scottish highlands and more detailed x-section of the classic Assynt area (from Goodenough *et al.* (2011), after BGS (2007)). The Lewisian Gneiss Complex, Torridonian and Cambro-Ordovician strata unconformably overlie each other in that order west to east. The Moine Thrust Zone (MT) overlies and has thrust the early Neoproterozoic Moine Supergroup westward. Several stacked thrusts define the MT, these are uniquely exposed in the Assynt area (x-section). Correlation of thrust sheets with foreland sequences (Lapworth 1883) reveals a piggy-back thrust sequence which propagates toward the foreland (Coward 1985). Thus the structurally highest unit is actually the oldest. BHT, Benn Hope Thrust; NT, Naver Thrust; SBT, Sgurr Beag Thrust; GDP, Glen Dessarry Pluton; LBP, Loch Borralan Pluton; Lap, Loch Ailsh Pluton; LLSC, Loch Loyal Syenite Complex.

Regional metamorphism during the Scandian, which reached amphibolite facies, is concentrated in the west and was synchronous with the crustal shortening (e.g. Roberts *et al.* (1984); Strachan and Holdsworth (1988); Holdsworth (1989); Dallmeyer *et al.* (2001); Kinny *et al.* (2003); Holdsworth *et al.* (2006); Strachan and Evans (2008); Krabbendam *et al.* (2011)). Earlier Grampian related metamorphism was not pervasive here and is best observed in the Sgurr Beag and Naver Nappes to the east (Kinny *et al.* 1999; Rogers *et al.* 2001; Cutts *et al.* 2010).

Subduction of the Baltican crust beneath the Laurentian margin, and related crustal thickening, is associated with Silurian calc-alkaline plutonic bodies across the Scottish Highlands (Dewey 1971; van Breemen and Bluck 1981; Fowler *et al.* 2001; Oliver *et al.* 2008). Extensive high precision U-Pb zircon dating programs have been carried out on Scandian related Northern Highland Terrane plutons (van Breemen *et al.* 1979; Roberts *et al.* 1984; Halliday *et al.* 1987; Holdsworth *et al.* 1999; Goodenough *et al.* 2006). Field, petrographic and geochronological data show that the majority of these were emplaced during the latter stages and after Scandian deformation (~ 430Ma). One confirmed example of early syn-orogenic emplacement is the Glen Dessarry Pluton (447Ma), this is taken as the earliest evidence for Scandian related magmatism (Goodenough *et al.* 2011). Extensive remapping (Goodenough *et al.* 2004; BGS 2007; Krabbendam 2010; Krabbendam *et al.* 2011) demonstrates that movement within the Moine Shear Zone occurred after 447Ma and terminated before 430Ma, hence constraining the Scandian Orogenic event to this time period.

2.4.5 Suturing of Laurentia and Avalonia

As discussed above, the segmented closure of Iapetus between Avalonia and Baltica (closing the Tornquist Sea i.e. Shelveian Orogeny) and Laurentia and Baltica (Scandian) represents the northern and eastern extensions of the Caledonian triple suture of Britain and Ireland. In Britain and Ireland, the third extension is defined by the Solway Line or Iapetus Suture and associated parallel northeast-southwest structures. This major lineament represents the orogenic front along which Avalonia and Laurentia collided, in North America this even is referred to as the Acadian Orogeny (Wilson 1966; Donahoe and Pajari 1973) however in Britain and Ireland this term describes a post Caledonian event (see below). As such, the term Acadian is not applied to the suturing of Laurentia and Avalonia here and only evidence that is observed in Northern Europe for this convergence is summarised here.

The precise timing of convergence initiation is determined from palaeomagnetic data (Torsvik *et al.* 1990; Channell *et al.* 1992; Trench and Torsvik 1992), faunal correlations (McKerrow 1988a; Pickering *et al.* 1988) and basin development and sedimentological studies (Leggett *et al.* 1983; Hutton and Murphy 1987; Soper and Woodcock 1990; Kneller 1991; Kneller *et al.* 1993) that show the eastern part of the Iapetus Ocean, now exposed in Britain and Ireland, closed during the Wenlock.

Northward subduction of Iapetus oceanic lithosphere beneath the Laurentian margin preceded the sinistral soft docking of Avalonia and Laurentia (Fig. 2.9) and developed the southward propagating Southern Uplands accretionary prism (McKerrow *et al.* (1977); Leggett *et al.* (1979) *cf.* Stone *et al.* (1987)). This wedge of clastic sediment exhibits a progressively shallowing facies from the Llandeilo (oceanic Moffat Shale facies) to late Wenlock (termination of shallow turbidites), reflecting progressive shallowing conditions during collision (Floyd 1995).

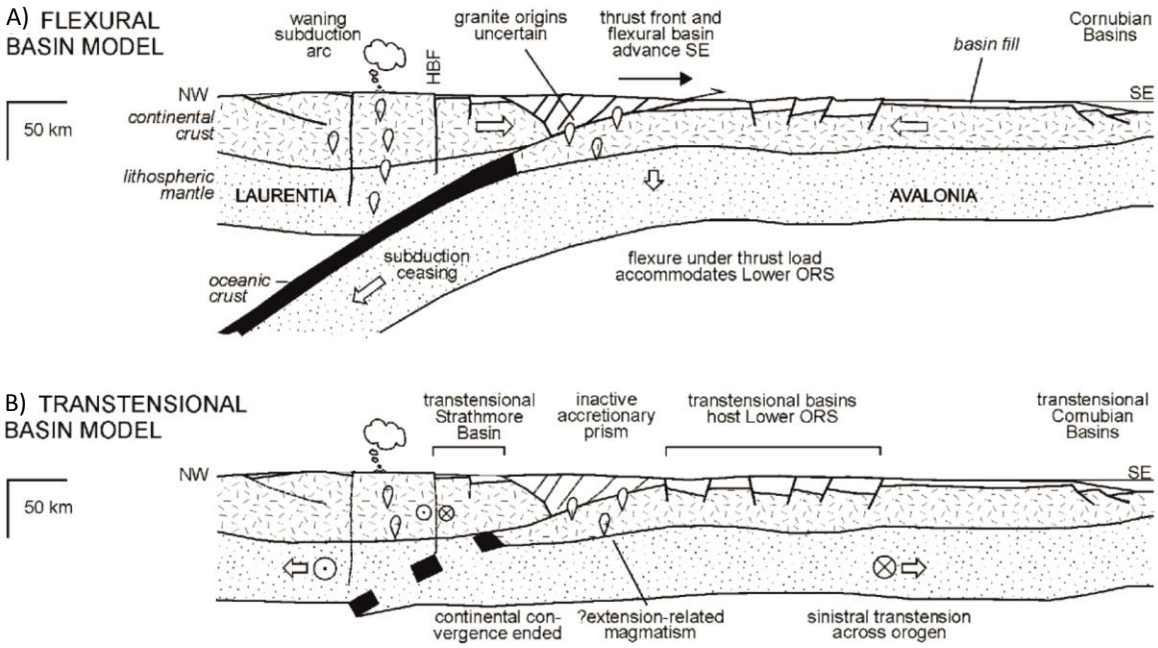


Fig. 2.9 Two contrasting models for the final stages of the soft docking of Laurentia and Avalonia (after Soper and Woodcock (2003)). (A) the classic flexural model proposed that convergence, i.e. transpression, continued after Iapetus closed until 410Ma. (B) Suggests regional transtension (orogenic collapse) initiated by 420Ma soon after closure of Iapetus.

In western Ireland, initially hard sinistral transpressive convergence related deformation is recorded during the Wenlock to early Devonian. Multiple clockwise transecting cleavage sequences in the South Mayo Trough denote polyphase compressive deformation continued post-Wenlock and terminated pre-lower Devonian, as dated by unconformity (Dewey 1997). Hutton

and Murphy (1987) showed that sedimentary detritus was transported across the Iapetus Suture during the Silurian and subsequently deformed during sinistral transpression between the end of the Silurian and early Devonian. This indicates sinistral transpression, and termination of the Caledonian Orogeny in western Ireland occurred at this time i.e. early Devonian (Hutton and Murphy 1987). Both the Corvock and Slieve Gamph Granites were emplaced during transpression but no chronological data is available to place temporal constraints on the crystallisation of these intrusions. Contrasting these results, the Louisburgh Basin, Mayo, western Ireland, is a Pridoli transtensional feature and it has been suggested that this indicates a slightly earlier termination of transpression in this region (Dewey 1997).

Further east in northern Britain Silurian sediments were transported across the Iapetus zone during the late Wenlock (Soper and Woodcock 1990). A late Llandovery deepening episode in the Stockdale Group punctuates foreland basin development along the northwest margin of Avalonia (Kneller 1991; Kneller *et al.* 1993). By comparison to the finds of Hutton and Murphy (1987), the above data indicate that the suturing Avalonia and Baltic occurred in a diachronous manner, being an earlier event in western Ireland. Dewey and Strachan (2003) relate the diachronous nature of this convergence to irregular continental margins. Based on the structural features of Avalonian - Laurentian accretionary prism in England, Stone (1995) suggested that initial orthogonal collision was succeeded by transpression at ~ 430Ma.

2.4.6 Transcurrent Lockup

As demonstrated by palaeomagnetic, provenance and paleontological data, the final sliver of land-locked Iapetus, located between the colliding blocks of Laurentia, Baltica and Avalonia, would have been obliterated by ~ 420Ma (Soper and Hutton 1984; Soper 1988; Torsvik *et al.* 1990; Channell *et al.* 1992; Soper *et al.* 1992; Trench and Torsvik 1992; Stone 1995; Dewey and Strachan 2003; Soper and Woodcock 2003). However, the terrane assemblage that is observed across Britain and Ireland today had not yet taken shape. As discussed, the Grampian event deformed and metamorphosed Moine and Dalradian rocks of the Northern and Central Highlands at a regional scale between ~ 470-460Ma. Succeeding the Grampian, a second episode of deformation (Scandian) is recorded in Moine strata, to the north of the Great Glen Fault which is not present in the Dalradian to the south of this structure. From this it seems apparent that the Northern Highlands Terrane was subjected to Scandian deformation while isolated from the Central Highlands Terrane which evaded Scandian deformation (Coward (1990) and references

there in). This occurred because the Northern Highland Terrane was displaced laterally into its current position by movement along the Great Glen Fault, after undergoing Scandian deformation (Soper and Hutton 1984; Tanner 2008). Thus, the terranes of Britain and Ireland were juxtaposed as a result of sinistral strike slipping along major terrane boundaries which took place during three successive distinctive stress regimes (Fig. 2.10).

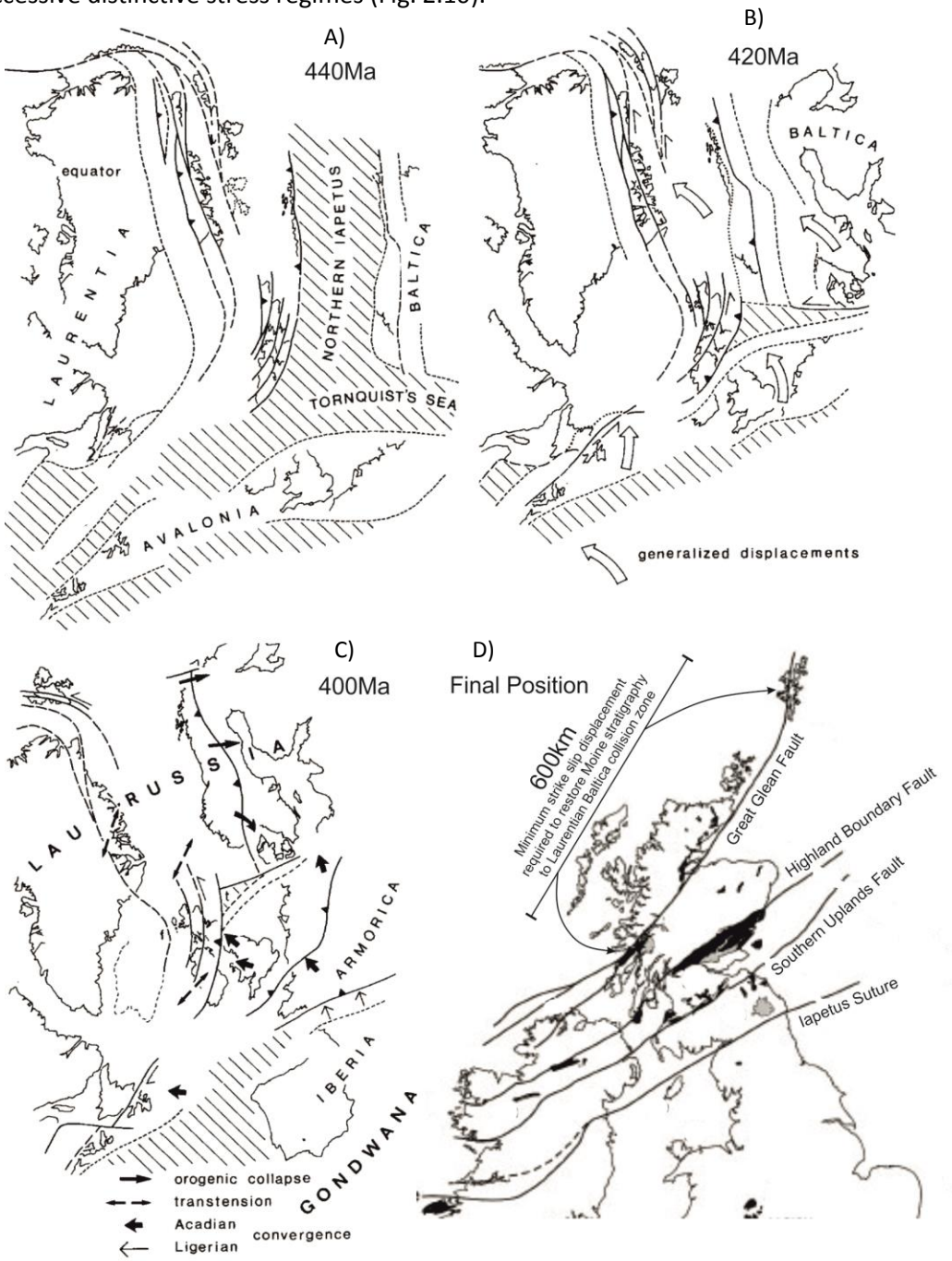


Fig. 2.10 Late Caledonian final closure of Iapetus (after Soper *et al.* (1992)). In this model the Iapetus Ocean is closed by 420Ma (A & B). Regional sinistral strike slipping along major Caledonian faults persist up to 400Ma (C) to juxtapose contrasting terrane blocks in Britain and Ireland (D). This model shows transpression persists after 420Ma and, in contrast to Fig. 2.6 also shows the Tornquist Sea remain open into the mid Silurian.

Quantifying the total amount of displacement along Caledonian lineaments across Scandinavia, Britain and Ireland has proven problematic. Suggestions of less than a hundred kilometres (Mykura 1976), a few hundred (Smith and Watson 1983; Flinn 1985) and over 2000km (Morris 1976; van der Voo and Scotese 1981) have been made. The issue has been complicated further by the recognition of a period of dextral displacement that potentially reactivated some Caledonian structures during the late Devonian through to the Permo-Carboniferous (Ziegler and Kent 1982; Hudson 1985). Considering that Scandian deformed rocks occur as far southwest as the Isle of Mull, that are now juxtaposed against the Avalonian terrane to the south, a displacement of *c.*600km along the Great Glen Fault is required to reposition these rocks adjacent Moine strata identified in Shetland. This is a minimum, it is unlikely that outcrops seen on the Isle of Mull happen to correlate directly to those observed on Shetland and it is likely that the Moine Strata was originally thrust into its current position on the Laurentian continent much further north when the continent originally collided with Baltica. Allowance must also be made for this as well as strain partitioning and sinistral displacement along less prominent parallel Caledonian structures. Movement along the Highland Boundary Fault (~ 200km) and Southern Uplands Fault (*c.*200km) should also be considered. As a consequence of this, an estimate of ≥1200km for total sinistral displacement between *c.*430-400Ma is deemed feasible by some (Dewey and Strachan 2003; Goodenough *et al.* 2011).

Transpression-Transtension Transition

The Laurentian, Baltican and Avalonian margins had converged by ~ 430Ma (summary in Woodcock and Strachan (2012)). Subsequently, a regional sinistral strike-slip regime instigated along the Iapetus suture between Laurentia and the accreted Avalonian-Baltican block, this lasted from about 430Ma to 400Ma (Soper *et al.* 1992; Torsvik *et al.* 1996; Dewey and Strachan 2003; Soper and Woodcock 2003). Regional sinistral transpression initiated first, this was succeeded by sinistral transtension (Fig. 2.11). Although there is consensus on the occurrence this transition, the precise timing of the evolution of the regional stress field remains contentious (Dewey and Strachan 2003; Soper and Woodcock 2003).

Evidence for continued regional transpression up until 410Ma is reviewed in Dewey and Strachan (2003). As discussed above, early Devonian transpressional deformation structures in late Silurian microconglomerrates (Hutton and Murphy 1987), transecting cleavage sequences in the South Mayo Trough and the emplacement of the Corvock and Slieve Gamph Granites in

transpressive pull-aparts structures (Dewey 1997) are consistent with early Devonian transpression in Ireland. In western portions of the Scandinavian Caledonides isotopic data show regional compression continued from 430-410Ma (Dallmeyer 1988) where foreland-propagating thrusting (Fossen and Dallmeyer 1998; Fossen and Dunlap 1998) is temporally associated with high pressure eclogite facies metamorphism (Griffin *et al.* 1985; Smith and Lappin 1989). In east and northeast Greenland, early Devonian transpression is associated with essentially orthogonal (Higgins and Leslie 2000) to oblique (Strachan *et al.* 1992) thrusting within the Laurentian foreland. Similarly, late Silurian and early Devonian sinistral transpression is demonstrated in Svalbard by the presence of subhorizontal tectonic extension lineations along the plane of a steep penetrative foliations that are associated with regional oblique compression (Dewey and Strachan 2003).

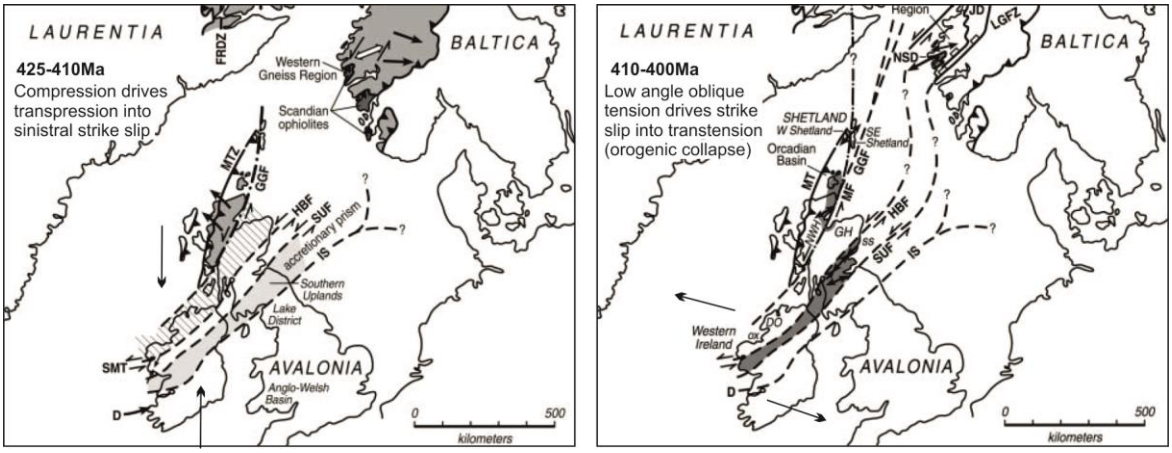


Fig. 2.11 Transition between regional sinistral compression and tension denotes the end of the Caledonian Orogeny (from Dewey and Strachan (2003)).

Across the Scottish Highlands and parts of Ireland and northern England many of the Caledonian "Newer Granites" intruded between 425-410Ma (Brown *et al.* 2008; Neilson *et al.* 2009) into reactivated deep seated lineaments which created local transtensional dilation zones within the ambient regional transpressional stress field (Hutton 1988; Hutton and Reavy 1992; Jacques and Reavy 1994; Brown and Solar 1998; Brown 2007). Models devised on this principal require congruent sinistral movement along the Great Glen, Highland Boundary, Southern Uplands and Iapetan Suture fault zones, this has been shown to be probable (Morris *et al.* 1973; van der Voo and Scotese 1981; Coward 1990; Soper *et al.* 1992). As a consequence of this and the data summarised above, Dewey and Strachan (2003) conclude that regional transpression

initiated at ~ 425Ma and gave way to orogenic collapse and transtension at 410Ma prior to the deposition of Emsian Old Red Sandstone.

Orogenic collapse (sinistral transtension) (McClay *et al.* 1986; Dewey 1988) was underway by ~ 410Ma, continued until ~ 400Ma and was ultimately succeeded by the Acadian Orogenic stress field (Woodcock 2006). However, the timing of the transition from transpression to transtension remains enigmatic (Dewey and Strachan 2003; Soper and Woodcock 2003). Dewey and Strachan (2003) have suggested that transpression was succeeded by transcurrent shear at ~ 420Ma and that orogen oblique extension did not initiate until 410Ma and persisted as late as 395Ma. However, Soper and Woodcock (2003) suggested that this interpretation is only valid for the kinematic dynamic between Laurentian and Baltica; they argue that due to the loose coupling of Baltica and Avalonia the Avalonian-Laurentian and Baltican-Laurentian contacts behaved independently. As a consequence of this, transtension between Avalonia and Laurentia could have initiated earlier at 420Ma and continued until 400Ma (Soper and Woodcock 2003).

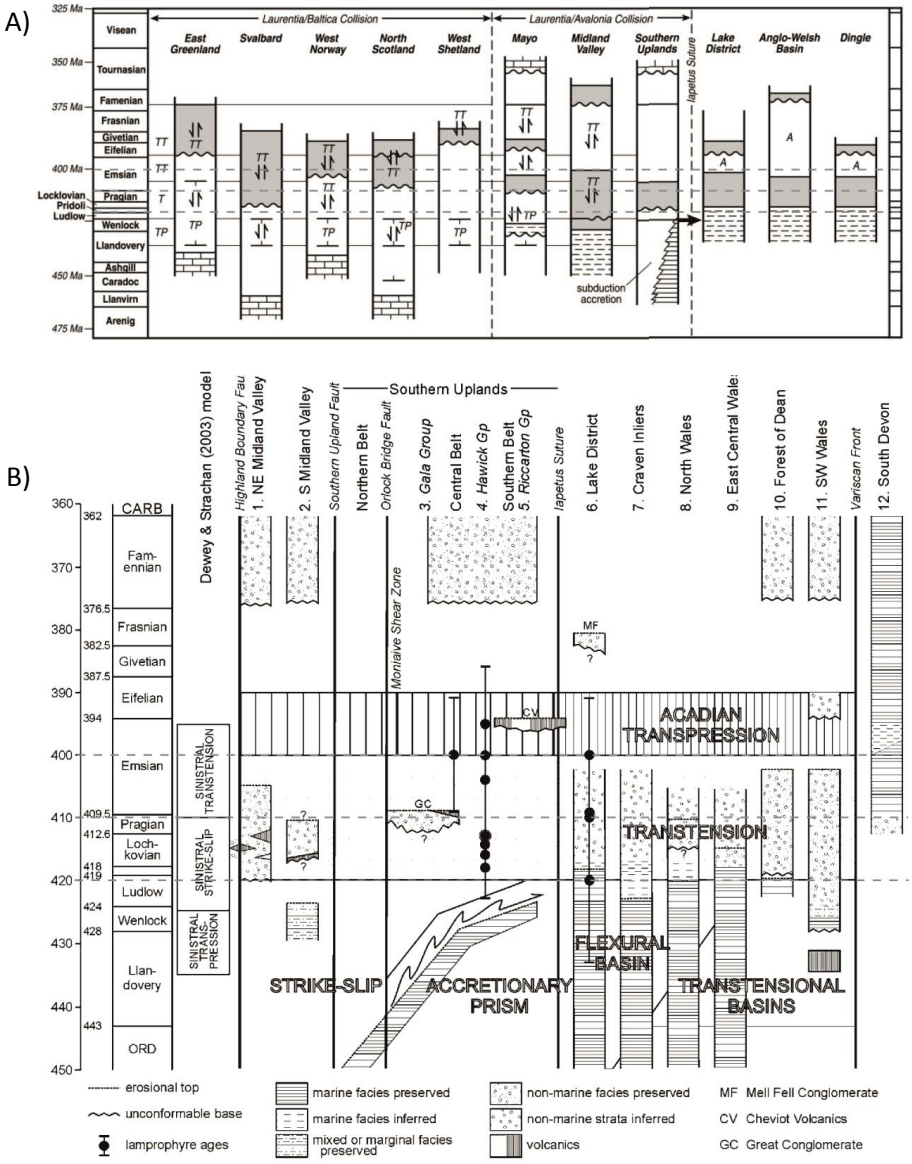


Fig. 2.12 Contrasting tectonostratigraphic columns of Dewey and Strachan (2003) (A) and Soper and Woodcock (2003) (B). (A) TP, transpression; TT, transtension; A, Acadian, shows transtension did not instigate until 410Ma. (B) Shows more uniform relationship across the studied terranes and transtension initiation at 420Ma.

In reality the difference between these models is significant but the supporting evidence is often in conflict along the orogenic belt. For example, Dewey and Strachan (2003) suggest that transpression continued into the early Devonian in East Greenland and Mayo but also show strong evidence that transtension initiated at 420Ma and continued until 380Ma in northwest Norway (Fig. 2.12 A). Soper and Woodcock (2003) present a more internally consistent data set (Fig. 2.12 B) but do not discuss basin development outside of the UK and east Ireland. A large portion of this argument hinges on the termination of growth of the accretionary prism marking termination of convergence (Kemp 1987) and the emplacement of 418-400Ma lamprophyre dykes indicating post 420Ma extension (Rock *et al.* 1986a; Rock *et al.* 1986b; Anderson and Oliver 1996). Neither

of these phenomenon are mutually exclusive of the model proposed by Dewey and Strachan (2003).

Soper and Woodcock (2003) also place emphasis on the opening of late Silurian - early Devonian ORS basins and this is taken as support of an earlier 420Ma transtensional episode. However, basin development can occur in a broad variety of stress regimes (Fig. 2.13) including transpressive systems (Einsele 1992; Nilsen and Sylvester 1999b, 1999a; Allen and Allen 2005). The tectonic orogin of ORS basin development has been variably associated with sinistral transcurrent movements (Vogt 1936; Harland 1985; Dewey 2002) but also orthogonal regional extension (McClay *et al.* 1986; Rogers *et al.* 1989). The fundamental cause of basin development in some cases has been called into question (e.g. Hartz (2000) *c.f.* Dewey and Strachan (2003)). The presence of sedimentary basins does not necessarily infer regional extension, it follows that late Silurian and early Devonian ORS basins are not mutually exclusive of a regional transpressive setting.

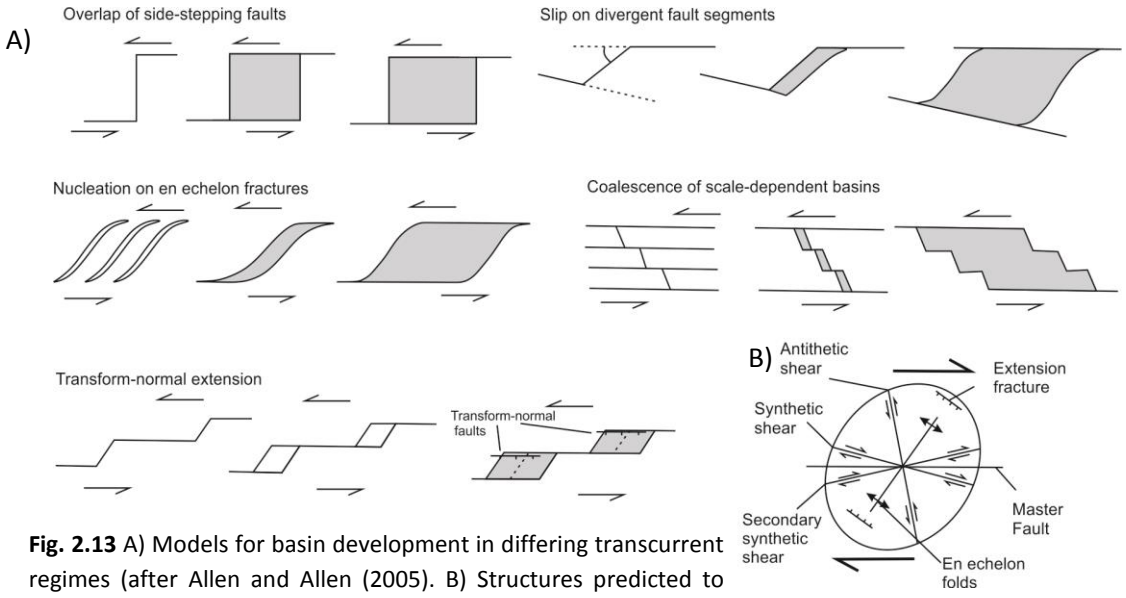


Fig. 2.13 A) Models for basin development in differing transcurrent regimes (after Allen and Allen (2005). B) Structures predicted to form in isotropic medium during dextral shearing (after Wilcox *et al.* (1973)).

The Dingle Basin, in southwest Ireland, provides information critical to the above point and the course of this thesis. The northeast-southwest trending North Kerry Lineament (NKL) and Dingle Bay Lineament (DBL) acted as fundamental controlling structures over basin development from the late Silurian to Carboniferous (Richmond and Williams 1998; Boyd and Sloan 2000; Richmond and Williams 2000; Todd 2000; Meere and Mulchrone 2006). Basin development initiated during convergence of Avalonia and Laurentia and deposition of the lowermost Dunquin Gp., the

overlying Dingle Gp. was deposited during regional transpression (Fig. 2.14). A complex sequence of depositional environments and several unconformities in these strata are consistent with intermittent transcurrent lockup and release, a process with is associated with basin development within transpressional pull apart structures. Sedimentation was coeval with transpression shearing along the DBL (Todd *et al.* 1990), temporal constrains for deposition is provided by the 411 ± 3Ma Cooscraw Tuff Bed (Ballymore Fm.) which was deposited toward to top of the Dingle Gp. (Richmond and Williams 2000). These data place tight temporal constraints on sedimentation and the longevity of sinistral transpression in this area.

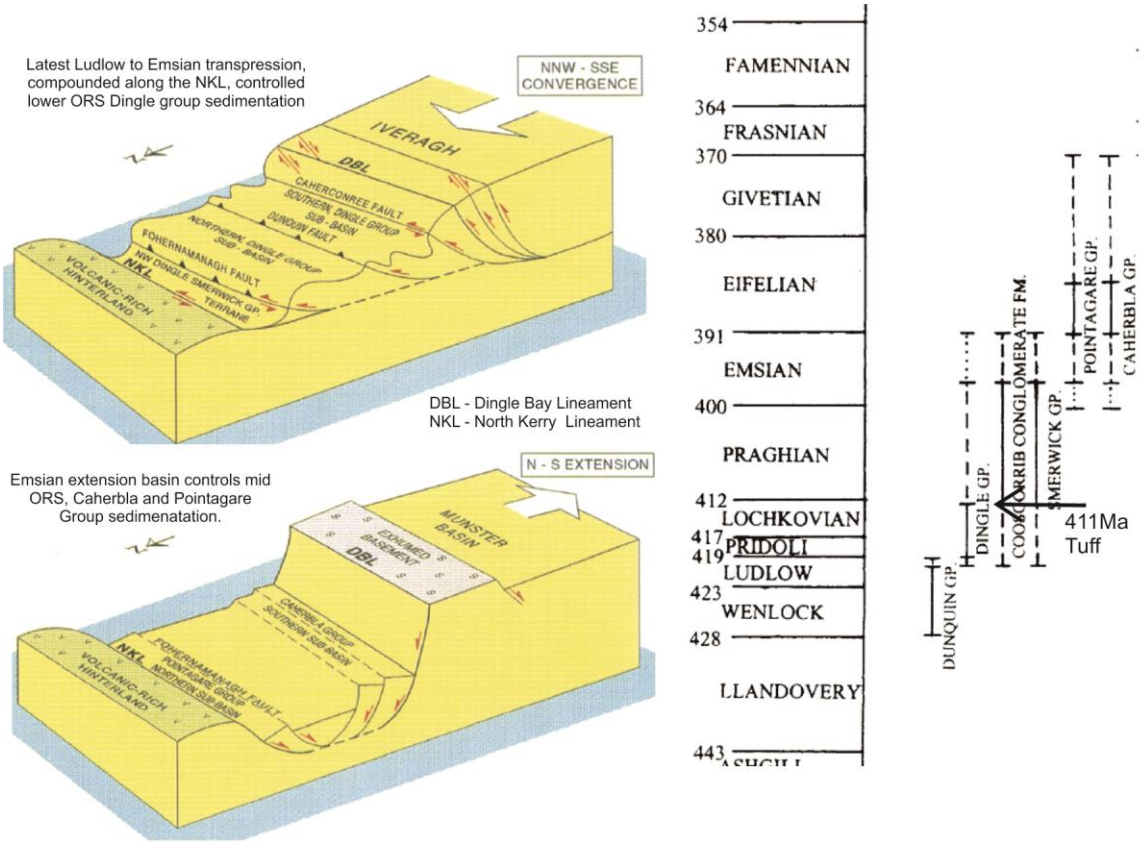


Fig. 2.14 Late Silurian - mid Devonian evolution of the Dingle Basin (from Richmond and Williams (2000)). This work shows regional transpression continued into the early Praghian and this stress field is associated with ORS basin development in this area.

The significance of the Dingle Basin to this study is two-fold. First, it provides solid evidence that late Caledonian transpression was active in this area between the late Silurian and early Devonian, the same period over which many of the intrusions studied in this study were emplaced (Chapter 5). Second it shows that such a stress field was capable of forming significant sedimentary basins, thus casting doubt over the relevance of interpretations which inherently relate the development of ORS basins to transtension (Soper and Woodcock 2003).

The work discussed shows only that the current interpretations of regional kinematics between 430-395Ma along the Caledonian Orogenic belt are debatable. This is largely due to the fact that along strike evidence supporting contrasting regional models is often locally consistent but regionally dubious. The timing of the transition between net compression and extension does vary along strike in a non-systematic way. This may be attributable to misinterpretation of local structures but is more likely associated with the inherent complex nature of a three way suture zone. Thus, the best way of addressing such short falls is to carryout local surveys which seek to independently evaluate the local kinematic parameters based on original data, interpretations may then be expanded to regional scale studies.

2.5 The Acadian Orogeny

Traditionally the Acadian Orogeny was understood to have contributed, in some way, to the suturing of minor terranes to Laurentia. Publications dating back to the early 1990s (e.g. Soper *et al.* (1992); Trench and Torsvik (1992)) suggested that the Acadian Orogeny event post-dated initial docking of eastern Avalonia and Laurentia by several million years. Van Staal *et al.* (1998) suggested that collision of the Maguma Terrane with the western Laurentian margin generated the Acadian Orogeny, Morris (1976) suggested that this event had some role in the amalgamation of east Avalonia and Laurentia during the latest Caledonian Orogeny, while other authors sometimes left the issues open to ambiguity (McKerrow *et al.* 2000). More recently, Woodcock *et al.* (2007) proposed that the Acadian Orogeny was a tectonic event completely separated from the Caledonian Orogeny by an episode of transcurrent shear between 420 and 400Ma (Dewey and Strachan 2003; Soper and Woodcock 2003).

Deformation features, best preserved in Devonian marine and continental sediments across southern Ireland, the Isle of Man, Wales and northwest England, indicate that the Acadian Orogeny was a mid Devonian orogenic event (see Woodcock *et al.* (2007)). In these areas, an Emsian to Frasnian unconformity lies between folded and cleaved early Palaeozoic sediments that unconformably underlie Devonian continental and shelf deposits. This unconformity is understood to have formed during a cessation of sedimentation during the Acadian Orogeny (Woodcock 2006). Deformation of early Palaeozoic rocks in this area is attributed to Acadian deformation; however differentiating fold and cleavage structures which are Acadian from earlier

Caledonian features needs to be carried out in a tentative manner. Definitive evidence of Acadian deformation is best sought in strata which were deposited during the lower Devonian as these clearly postdate Caledonian compression events and predate the lull in sedimentation that occurred during the Acadian Orogeny.

The timing of the Acadian Orogeny across Ireland and Britain is well constrained. Angular unconformities observed on the Dingle Peninsula, southwest Ireland constrain Acadian deformation to between the mid-Emsian and mid-Frasnian (Meere and Mulchrone 2006). Combining this direct field evidence to ages based on absolute dating methods (Merriman *et al.* 1995; Evans 1996; Sherlock *et al.* 2003; Woodcock 2006)) and the tectonostratigraphic and biostratigraphical record (Soper *et al.* 1987; McKerrow 1988b; Woodcock 1990; Verniers *et al.* 2002)) Acadian tectonic activity is constrained to *c.*400-390Ma in Britain and Ireland. Further correlatives of the Acadian can be traced across the Anglo-Brabant Deformation Belt. A 400-390Ma Acadian unconformity is recognised in East Anglia (Pharaoh *et al.* 1987; Woodcock 1991; Woodcock and Pharaoh 1993) and has been correlated with a *c.*415-405Ma (Ar40/Ar39 Dewaele (2002); Debacker (2005)) event in the Barbant Massif, Belgium. From this, Debacker (2005) proposed a episode of prolonged Barbantian style deformation, genetically linked to the Irish and British Acadian but initiated earlier under the influence of the Far Eastern Avalonian block that was sandwiched between eastern Avalonian and Laurentia.

Acadian orogenesis (*c.*400-390Ma) driven by southerly compression originating from subduction of Rheic Ocean lithosphere under the southern Laurassian margin, rather than from Caledonian influences from the north, now seems plausible (Soper *et al.* 1992; Woodcock *et al.* 2007). Continued sedimentation within the Rhenohercynian Zone of southwest England is problematic for this model as is continued extensional magmatism on the Lizard Terrane during *c.*400-390Ma while sediments in northwest Iberia show strong indications of Acadian deformation even thought they are now spatially disassociated from the Acadian belt (Ordóñez Casado *et al.* 2001; Dewey and Strachan 2003; Soper and Woodcock 2003; Gómez Barreiro *et al.* 2006). Woodcock *et al.* (2007) postulate that these issues are neatly addressed via late Acadian or subsequent dextral strike-slip movement, along the Bristol Channel-Bray Fault, which juxtaposed the Rhenohercynian and Lizard terranes against the Acadian belt after deformation.

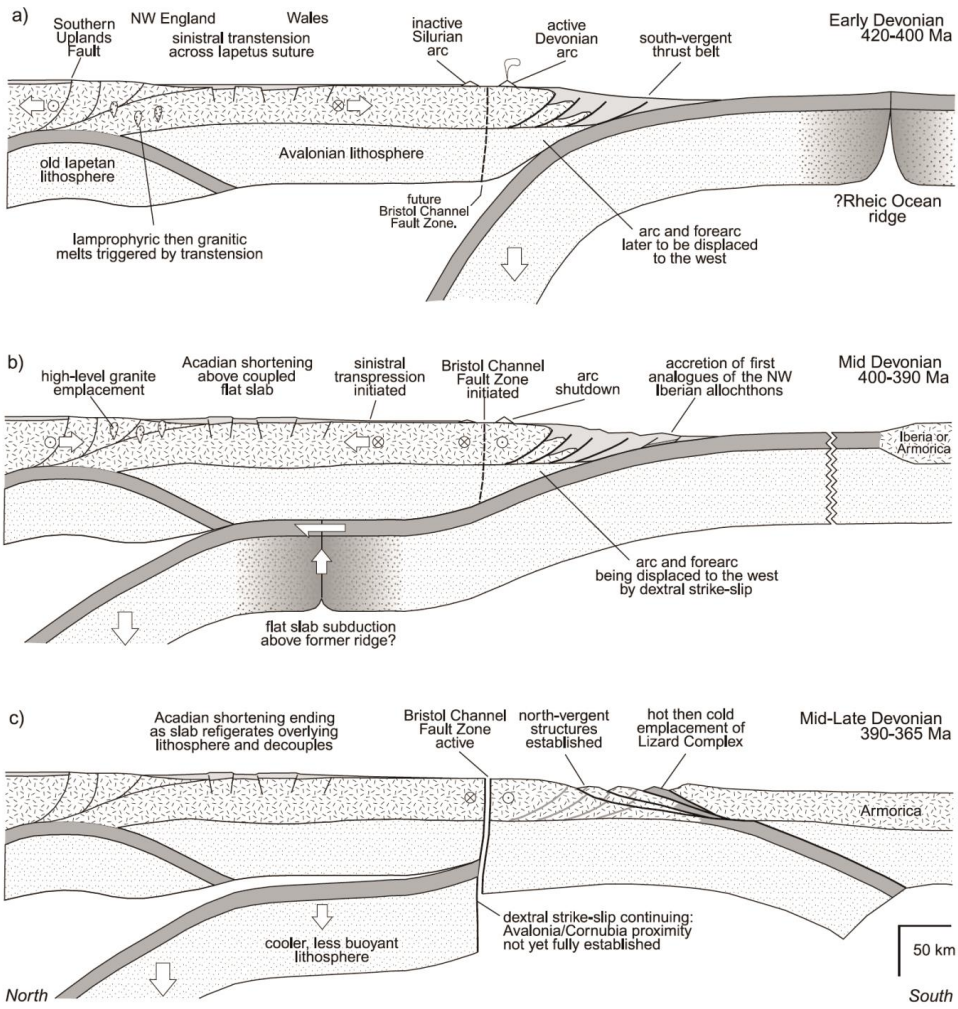


Fig. 2.15 Cross section of the convergence of Armorica with the southern margin of Avalonian during the Devonian (from Woodcock *et al.* (2007) after Soper *et al.* (1992)). The Acadian Orogeny was not an Iapetan margin process and therefore not a part of the Caledonian Orogeny. Following subduction, the Rheic Ocean crust under-plates much of the Caledonian terranes. Such a process would have promoted new melting and magmatism in that same terrane.

The hypothesis that the Acadian event was a product of the closure of the Rheic Ocean and occurred as a proto-Variscan rather than a late Caledonian orogenic event, as depicted by Woodcock *et al.* (2007), is accepted here (Fig. 2.15). It is critical to not that this does not correlate with the Acadian event in North America which was part of the Caledonian Orogeny and an entirely separate tectonic event (van Staal 2004; Wilson 1966; Donahoe and Pajari 1973). According to available data the Acadian Orogeny occurred between 400-390Ma in Ireland and Britain (synchronous with plutonic development across Ireland) and is associated with folding and cleavage development but is most often identified by an early Devonian unconformity. This model recognises that a period of early Devonian transtension marks the end of the Caledonian Orogeny

(Dewey and Strachan 2003; Soper and Woodcock 2003) and that the next compressive event relates to a completely different orogeny, i.e. northwards subduction of the Rheic oceanic crust beneath the Laurasian continent.

The data referred to above unequivocally demonstrate that the Acadian Orogeny occurred at least 20Ma after the closure of the Iapetus Ocean, which had certainly completed by 410Ma.

2.6 Summary of Key Tectonic Parameters

Deposition of the Dalradian Group was largely controlled by the tectonic regime which presided immediately before and during the opening of the Iapetus. These strata were subjected to polyphase regional and local scale metamorphism during several *Orogenic Phases* of the Caledonian Orogeny. The Grampian Orogeny is of particular interest to the current study as it generated large magma bodies which intrude Dalradian strata in Connemara and form the host rock to the granites studied in this thesis (Chapter 3). Introduction of fluids, derived from subducting oceanic slabs, into the overlying mantle wedge, slab break off and late stage decompression associated with orogenic collapse generated granitic magma for the granitoids in Connemara, this is a product of the later phases of the Caledonian Orogeny (Chapter 4).

Silurian and early-mid Devonian stress fields are most pertinent to the current work as continental plate dynamics at this time generated the stress field within which the granitoids studied were emplaced. Plutonism initiated during transpression, continued through transtension and extended into the Acadian and later. The timing of the transition between transpression and transtension remains debatable and probably varies along strike of the orogenic belt. A goal of the current work is to constrain the timing of this transition through the structural and chronological analysis of the Siluro-Devonian Granites of Connemara, western Ireland.

The Acadian Orogeny terminated 10Ma before the last of the Galway Granites crystallised (Feely *et al.* 2003). As this is a tectonic event independent of the Caledonian orogeny and 10Ma younger, it seems unlikely that all of the granites in Connemara may be considered Caledonian. It is plausible that the Acadian Orogeny may have played a significant role in the genesis of the later granitoids in Connemara and possibly further afield. This implies that the intrusions studied were intruded during a number of distinct orogenic stress fields and it follows that analysis of these bodies may return useful data pertaining to these events.

Chapter 3:

Background Geology; The Connemara Metamorphic Complex

3.1 Introduction

Geographical Extent of Connemara

The term "Connemara" originates from an old Irish tribe, the "Conmacne", who fled to the western part of Connacht, west Ireland, during an English invasion in the early 13th century. The Conmacne settled across Co. Galway and Co. Mayo, with one clan opting to take up residence in the western-most part of Co. Galway. As they were surrounded by the sea (to the north by Killary Harbour and to the south and west, by the open Atlantic Ocean) they acquired the name "Conmacne Mara" meaning "Conmacne of the Sea" (muir being Irish for sea). Over time their realm of western Connacht became known as Connemara.

In the strictest sense the geographical extent of Connemara is quite small and is bound by a line extending from Killary Harbour, southeast along the Maam Valley to Maam Cross and then southwest toward Kilkieran Bay (Fig. 3.1). However, it is common place for the entire area of Co. Galway west of Galway city to be referred to as Connemara.



Fig. 3.1 Geographic extent of Connemara and Joyces Country (*pers. comm.* Connemara Heritage Centre). Villages referred to in the text are highlighted. Topographic base sheet modified from the Ordinance Survey Ireland 1:10,000 discovery series.

Geological Layout of Connemara

Geologically, Connemara may be divided into three basic lithological units. The Dalradian Supergroup to the north, the mid-Ordovician Grampian intrusions in central Connemara and the Siluro-Devonian Galway Granites that dominate the south (Fig. 3.2). Together the Dalradian and Grampian rocks of Connemara form the CMC (Connemara Metamorphic Complex, Cruse and Leake (1968); Leake and Tanner (1994)), an area of some 1200km^2.

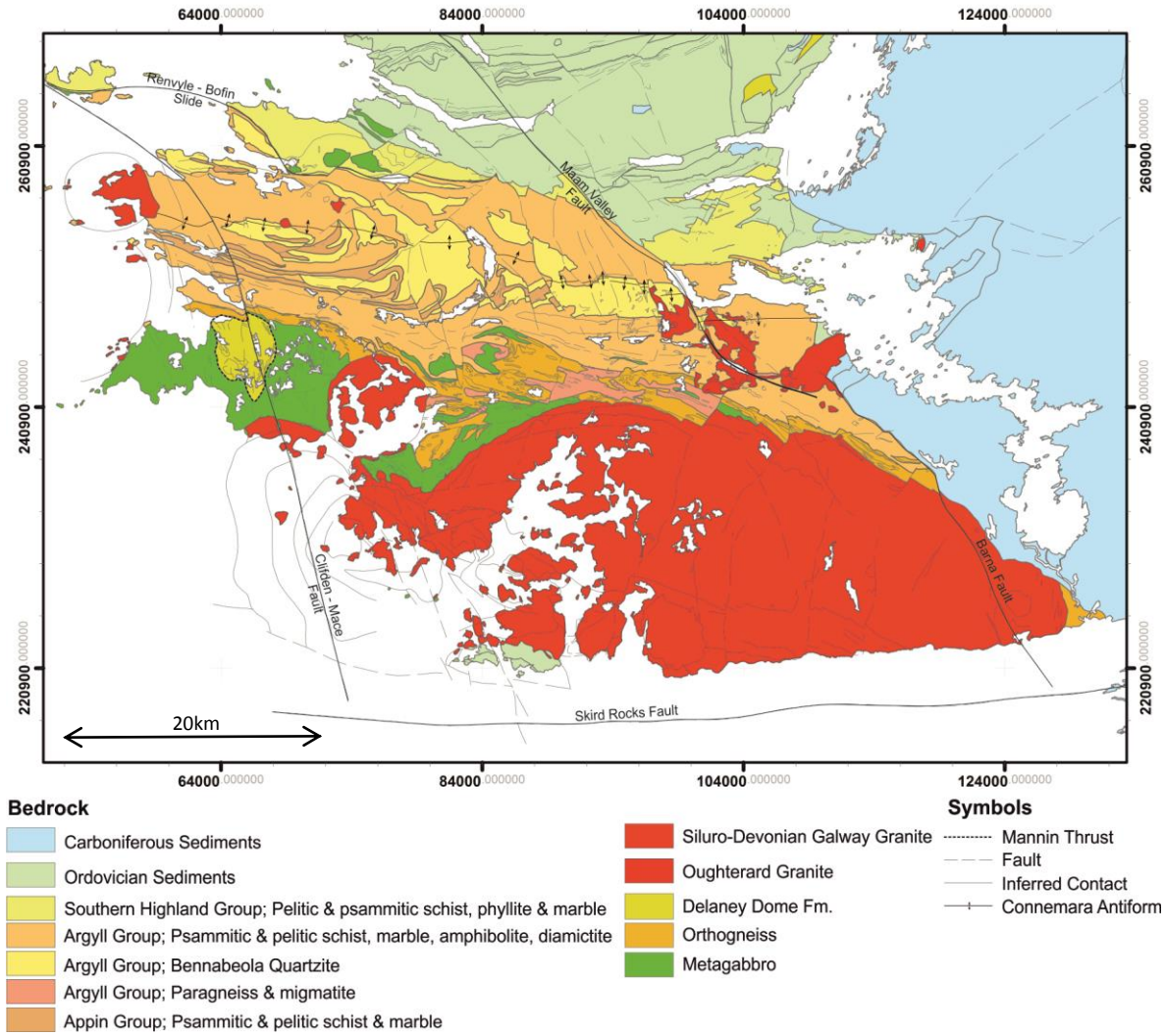


Fig. 3.2 Bedrock geology of Connemara and major structures. The CMC was thrust south along the Mannin Thrust and over the Delaney Dome Fm.. The Oughterard Granite intruded soon after and the Siluro-Devonian granites were emplaced at the end of the Caledonian Orogeny.

Dalradian Supergroup metasediments in Connemara are composed of pelitic and psammitic schists, marbles and quartzites. These strata have been subjected to polyphase metamorphism and deformation, mainly during the Grampian Orogeny and final closure of Iapetus (Tanner 1967;

Cobbing 1968; Leake *et al.* 1981a; Tanner 1981a; Leake 1986; Leake and Singh 1986; Leake and Tanner 1994). The latest major folding event generated the regional ESE-WNW Connemara Antiform that dominates the Dalradian outcrop pattern in this area. The CMC hosts the only known outcrops of Dalradian rocks that are positioned south of the Highland Boundary Fault, this is understood to have been achieved by southward thrusting of the CMC southward along the Mannin Thrust (Badley 1976; Leake *et al.* 1983) after the Grampian Orogeny and during the closure of Iapetus (Tanner and Shackleton 1979; Tanner *et al.* 1989).

A suite of mafic to intermediate intrusive rocks were emplaced into the Dalradian succession as a consequence of the 460-470Ma Grampian Orogeny (Leake *et al.* 1981b; Tanner 1981b; Leake and Tanner 1994; Friedrich *et al.* 1999a; Friedrich *et al.* 1999b; Dewey 2005). Commonly referred to as the "Metagabbro and Orthogneiss Complex" these intrusions form a central strip of bedrock which can be traced east-west across Connemara (Leake and Tanner 1994).

The Oughterard Granite occurs in the east (Fig 3.2). It is spatially and temporally distinct from the Orthogneiss Complex and believed to have been emplaced during the waning stages of D4 and thus pre-dates the late Silurian - early Devonian granitoids in the area (Leake 1988; Tanner *et al.* 1997; Friedrich *et al.* 1999a).

A suite of late Silurian - early Devonian granitoids were emplaced into the CMC following the southward thrusting of this terrane (Leake and Tanner 1994). These are commonly referred to as the Late Caledonian Galway Granites (425-380Ma Feely *et al.* (2010)). Essentially this suite is composed of the "Main Batholith" in the south and four other plutons (Omey, Roundstone, Inish and Letterfrack) in the west and north west. These granitoids are the subject of the current work, pertinent literature is fully reviewed in Chapter 5.

Aims of this Chapter

Local and regional host rock structure plays a leading role in determining the local stress field which in turn dictates the siting and style of emplacement of plutons (Hutton 1988, 1992; Hutton 1997; Vigneresse *et al.* 1999). In order to evaluate the local stress field into which granitoids are emplaced, constraints must be placed on the structural evolution of the country rock.

Literature regarding the structural and metamorphic evolution of the CMC has not been reviewed in the last two decades (Leake and Tanner 1994). Since then much progression has been made in constraining the metamorphic and structural evolution of Connemara (e.g. Cliff *et al.* (1996); Tanner *et al.* (1997); Friedrich *et al.* (1999a); Friedrich *et al.* (1999b); Draut and Clift

(2002); Ryan and Dewey (2004)). To this end, a review of literature relating to the structural and metamorphic evolution of the CMC is deemed essential and is presented below.

3.2 Dalradian Stratigraphy of Connemara

A moderate to high grade metamorphic assemblage of marbles, quartzites and schists was first mapped across northern and central Connemara by the Geological Survey of Ireland in the 1870's (Kinahan *et al.* 1878). These strata were first correlated with the Dalradian rocks of Scotland by Kilburn *et al.* (1965). Following this work, Edmunds and Thomas (1966); Cobbing (1968); Cruse and Leake (1968); Badley (1976) and Tanner and Shackleton (1979) went on to establish a stratigraphical sequence for the Dalradian rocks of Connemara from which the first detailed geological map and cross-sections of the Connemara region were produced (Tanner 1981a; Tanner 1981b).

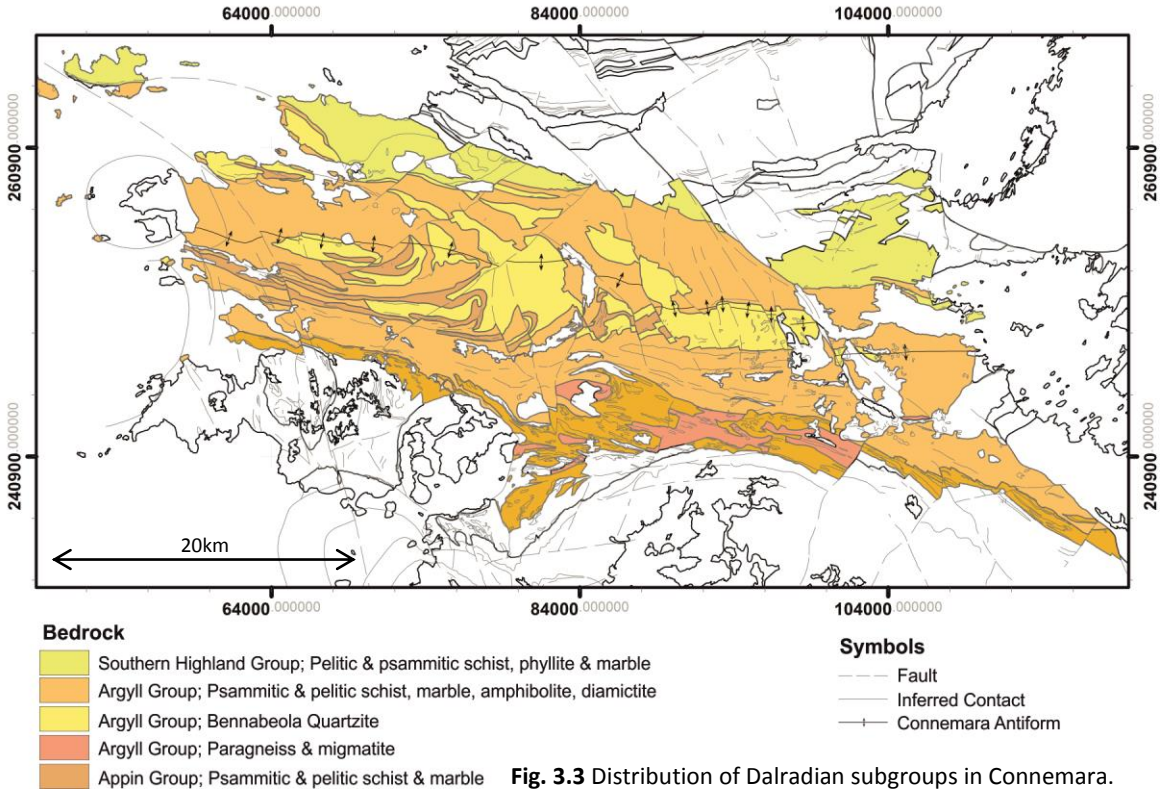


Fig. 3.3 Distribution of Dalradian subgroups in Connemara.

Constituent formations of the Dalradian Supergroup in Connemara belong to the upper part of the Appin Group, the Argyll Group and lower Southern Highland Groups (Fig. 3.3). The Grampian, lower Appin, upper Southern Highland and Trossachs Groups do not outcrop in Connemara (see Leake and Tanner (1994) for a review). In the south, a band of paragneisses are adjacent to the

metagabbro and orthogneiss complex, this is believed to be the Cashel Schist Fm. that was migmatised during the Grampian Orogeny. The three most critical correlations made are that of the Cleggan Boulder Bed Fm. with the Portaskig Tillite Fm., the Bennabeola Quartzite Fm. with the Jura Quartzite Fm. and the Ben Levy Grit Fm. with units of the Southern Highland Group (Cobbing 1968; Tanner and Shackleton 1979). This work has proven critical in establishing the stratigraphic sequence in Connemara (Fig. 3.4).

Group	*Subgroup*	*Formations in Connemara*	*Formations in SW Scotland*
Southern Highland		Lough Kilbride Schist*	
		Ben Levy Grit*	
	Tayvallich	Cornamona Marble*	Tayvallich Limestone
	Crinan	Ballynakill Schist	Ben Lui Schist
			Crinan Grit
Argyll	Easdale	Lakes Marble	(local limestone & quartzite)
		Streamstown Schist	Port Ellen Phyllite
	Islay	Bennabeola Quartzite	Islay Quartzite
			Bonahaven Dolomite
		Cleggan Boulder Bed	Portaskaig Boulder Bed
Appin	Blair Atholl	Barnanoraun Schist	Islay Limestone
		Connemara Marble	Mullach Dubh Phyllite
		Clifden Schist	Ballygrant Limestone

* The stratigraphical position of these three formations is uncertain; they are probably younger than the Ballynakill Schist Formation.

Fig. 3.4 Dalradian stratigraphy of Connemara and possible correlations with Scottish sequences (from Leake and Tanner (1994)).

Little work has been carried out which specifically deals with the stratigraphy of the Dalradian in Connemara in the past two decades. As a consequence of this, the descriptions of Leake and Tanner (1994) is deemed the most current and up to date account of this stratigraphy and the reader is referred to this literature for a synopsis. Formation level descriptions are also available (Cruse 1963; Leake 1963; Kilburn *et al.* 1965; Edmunds and Thomas 1966; Tanner 1967; Cobbing

1968; Cruse and Leake 1968; Leake 1969; Pidgeon 1969; Evans and Leake 1970b; Evans and Leake 1970a; Harris and Pitcher 1975; Leake *et al.* 1975; Badley 1976; Yardley 1976; Treloar 1977; Senior and Leake 1978; Tanner and Shackleton 1979; Leake 1980; Tanner 1981a; Tanner 1981b; Treloar 1982; Anderton 1985; Ferguson and Al-Ameen 1986; Leake 1986; Leake 1989; Leake and Tanner 1994).

3.3 Grampian Magmatism

Early mapping and petrographic work on *Metagabbro and Orthogneisses* in Connemara was carried out by Wager and Andrew (1930); Wager (1932); Ingold (1936); Wager (1939) and Leake (1958). Subsequent mapping, petrographic and geochemical studies have provided an intricate account of the properties and spatial distribution of this suite of rocks ((Morton 1964; Leake 1970; Senior and Leake 1978; Bennett and Gibb 1983; Jagger 1985; Jagger *et al.* 1988; Jenkin 1988) see review in Leake (1989)). Chronological studies show magmatism occurred between ~475-468 (Friedrich *et al.* 1999a; Friedrich *et al.* 1999b), this data coupled with petrographic and geochemical data (e.g. Tanner (1990); Cliff *et al.* (1993); Leake and Tanner (1994); Cliff *et al.* (1996)) show that the Metagabbro and Orthogneiss Complex was generated as a product of the Grampian Orogeny. These are described as two discrete units which are intimately interleaved i.e. the earlier *Metagabbros* and the slightly later *Orthogneisses* (Fig. 3.5).

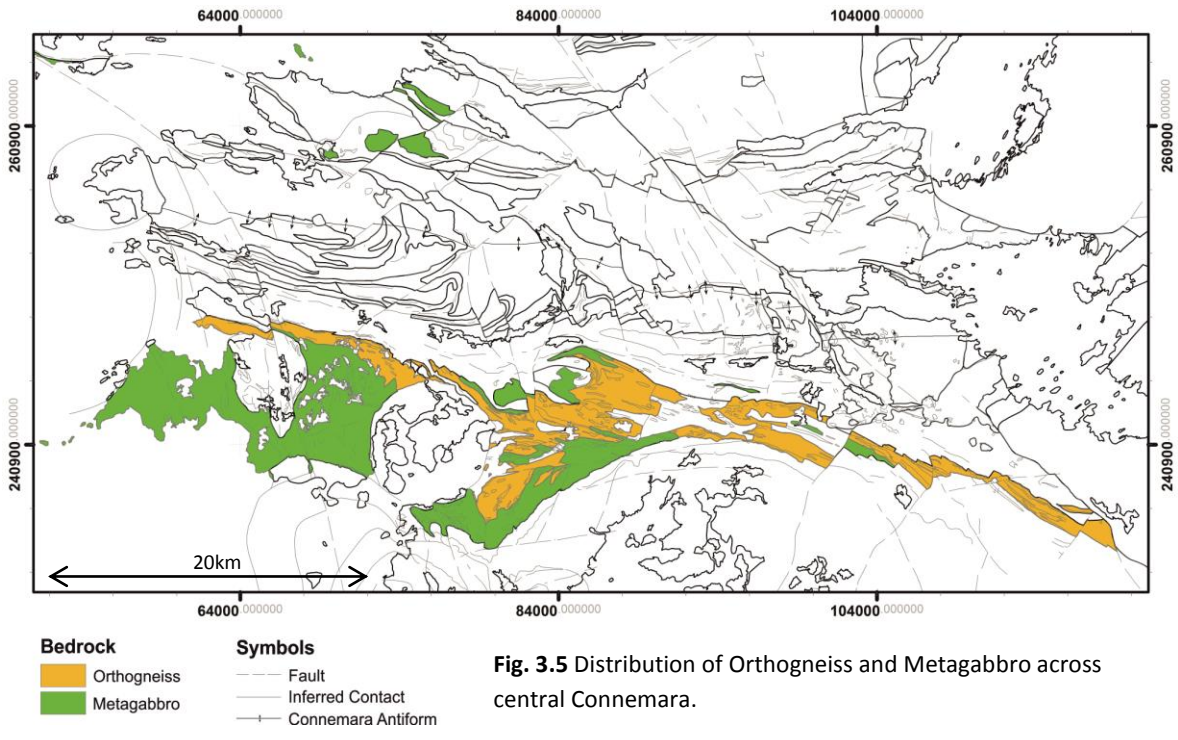


Fig. 3.5 Distribution of Orthogneiss and Metagabbro across central Connemara.

3.3.1 Metagabbros

A diverse assemblage of mafic rocks intruded Dalradian metasediments during the early-mid Grampian Orogeny. In Connemara, this assemblage is dominant by hydrated, hornblende bearing, gabbros and norites that were emplaced into the Dalradian stratigraphy along with a lesser quantities of peridotites and anorthosites (Leake 1969; Evans and Leake 1970b; Bremner *et al.* 1980; Leake 1989). These facies dominate the Grampian bedrock between Slyne Head and Oughterard as well as forming some isolated plutons near Kylemore Abbey (the Dawros-Currywongaun-Doughruagh intrusion and others, see Leake and Tanner (1994)). The distribution of Metagabbro is illustrated below (Fig. 3.5)

Mafic assemblages in Connemara have been subjected to pervasive hydrous metamorphism shortly after intrusion. This is understood to have resulted from the continued intrusion of hydrous melt into the earlier gabbroic bodies. In the field this intrusive relationship is readily demonstrated where meter to kilometre scale metagabbro pods are clearly crosscut and broken up by hornblende bearing gabbro and diorite compositions. A diverse assemblage of amphiboles was produced as a product of associated metamorphism (details in Bremner and Leake (1977) and Keeling (1981), summary in Leake and Tanner (1994)). The growth of metamorphic hornblende, at the expense of clinopyroxene and plagioclase lead to the conversion of much of the gabbros to amphibolites. Metasomatic processes also lead to the crystallisation of quartz at the expense of the primary igneous mineral assemblage (Leake 1969; Angus 1982).

The metagabbros generally exhibit a well defined tectonic foliation at most localities while occasional primary magmatic cumulative layering is sometimes preserved (e.g. south side of Errisbeg Hill, Roundstone (0695, 2396)). Tectonically induced fabrics and inclined or folded primary layering is attributed to D3 Grampian deformation (Tanner 1990; Leake and Tanner 1994) which typically develops folds on a 0.1-1m scale. D3 deformation has completely overturned some gabbroic bodies (e.g. Errismore Gabbro at Slyne Head peninsula) as is demonstrated by inverted cumulate graded bedding (Ingold 1936; Leake 1958; Bremner *et al.* 1980; Leake 1986). Coupling these field observations with palaeomagnetic and thermal demagnetisation data, Morris and Tanner (1977) and Robertson (1988) have demonstrated the Connemara gabbros cooled through their Curie Points (*c.*600°C) after D3 folding and during the earliest stages of D4 folding, hence constraining the timing of both deformation events relative to the rocks' cooling history. These data concur with most subsequent authors (Leake 1989; Tanner 1990; Leake and Tanner 1994; Tanner *et al.* 1997) who suggested that intrusion occurred during the main phases of ductile

deformation, most likely just after D2 and during D3, and that crystallisation was completed by the culmination of D4 which folded the Grampian mafic assemblage (Morris *et al.* 1973) along with the Dalradian assemblage (Leake and Tanner 1994).

Isotopic studies on the Metagabbros aid in establishing the relative timing of the D2-D4 events. Early studies reported ages as old as 504Ma (Pidgeon 1969) and as young as 477Ma (Jagger *et al.* 1988) for D2 and D3 events. High precision $^{207}Pb/^{206}Pb$ zircon analysis was carried out by on abraded zircons from the Lough Wheelaun intrusion (from the same locality as Jagger *et al.* (1988)) and the Currywongaun Gabbro, respective ages of 475.5 ± 1Ma and 470.1 ± 1.4Ma were returned (Friedrich *et al.* 1999a). This work clearly demonstrated that the gabbros intruded and crystallised over a short time period and provided a maximum age for the D3 event.

3.3.2 Orthogneisses

A variety of quartz diorites, tonalites, granodiorites and granites intrude and disarticulate the meta-mafic Grampian plutonic rocks and Dalradian metasediments (Fig. 3.5), these are referred to as the orthogneiss suite (Leake and Tanner 1994). These felsic intrusions form both narrow sheets and composite massive intrusions with gradational or diffuse contacts over 1-10's m, contacts are rarely sharp.

Three basic facies, quartz diorite gneiss, hornblende quartz diorite gneiss and K-feldspar gneiss, are recognised. Compositional variations exist within these subunits and intricate gradational or diffuse contacts are typically observed, as such these terms are used only for convenience to describe the general characteristics of the Orthogneisses.

Quartz diorite is dominantly composed of quartz and plagioclase and also contains some biotite along with smaller quantities of K-feldspar, accessory apatite, sphene, zircon and orthite are also present (Leake 1989). It is generally not closely associated with metagabbro. The hornblende bearing quartz diorite has a primary mineral assemblage of hornblende, plagioclase and quartz as well as minor biotite. This facies is almost always intimately associated with gabbro that obviously promoted the metasomatic growth of hornblende at the expense of augite as relics of the latter can be seen in the former (Leake 1989). The K-feldspar gneiss varies in composition but a minimum of 20% potassium feldspar is used to define this facies; microcline, quartz, andesine and biotite are all present as well as accessory apatite, zircon, magnetite and pyrite (Leake 1989). Generally the Orthogneisses exhibit a ~1cm grain size with .5mm biotite and

hornblende, K-feldspar crystals may be as large as 3cm in granodiorite and granitic assemblages. Similar to the Metagabbro, a strong east-west gneissic fabric is characteristic of the Orthogneisses which wraps around aligned blocks of stoped amphibolite. This is understood to be a syn to post magmatic state fabric formed following emplacement during and immediately after the D3 event (Leake and Tanner 1994). This is direct field evidence for the syn-tectonic intrusion of the orthogneiss suite.

TIMS carried out on zircon separates return 468 ± 2Ma and 467 ± 2Ma respective concordant ages from a hornblende quartz diorite and a granitic pegmatite within the orthogneisses (Friedrich *et al.* 1999b). Both of these samples show only a weak fabric development and so are considered to have been intruded toward the end of or after D3 and prior to the syn-pre-D3 metagabbros thus constraining the timing of the Grampian Orogeny in this area to this time (Morris and Tanner 1977; Robertson 1988; Friedrich *et al.* 1999a; Dewey 2005).

3.4 Oughterard Granite

This granitoid comprises three larger bodies (≤ 6km diameter) which are interconnected via a suite of smaller sheets and granitic pods that extend east and west of the larger plutons (Bradshaw *et al.* 1969; Kennan *et al.* 1987) (Fig. 3.6). The Oughterard Granite is a ~2mm aphyric two mica granite with some myrmekite, sericite, chloritized biotite, and minor oxides (detailed petrography in Dempster *et al.* (1994) and Tanner *et al.* (1997)). Detailed petrographic and geochemical studies have shown that this suite of intrusions are genetically linked and are part of a common intrusive event (Bradshaw *et al.* 1969; Tanner *et al.* 1997).

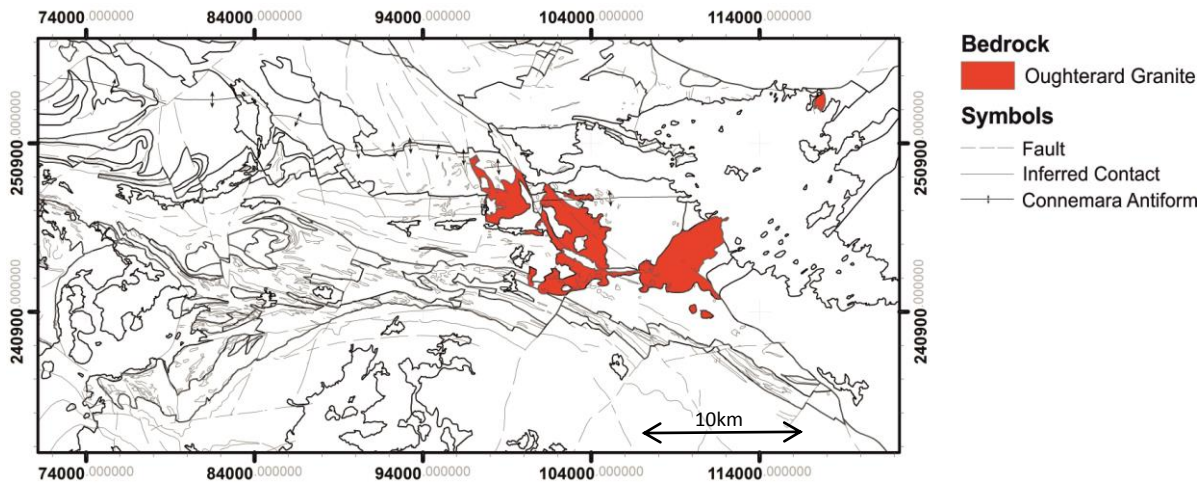


Fig. 3.6 Location of the three main bodies of Oughterard Granite in Connemara.

Weak silicate fabrics are locally apparent but, in contrast to the Grampian metagabbro and orthogneiss further south, no evidence for a pervasive tectonic fabric has been identified in this intrusion (Tanner *et al.* 1997). No contact aureole is documented despite the highly aluminous and calcareous host rocks (Leake and Tanner 1994). Given its likely age of intrusion (discussed below), the lack of contact metamorphism suggests emplacement predated thermal relaxation that followed amphibolite grade metamorphism, associated with Grampian intrusions further south. The Maam Valley Fault cross cuts and brecciates the Oughterard Granite and thus final movement on this post-dates the granite (Leake *et al.* 1981b).

Structural evidence indicate intrusion was achieved during the later stages of D4 deformation, an idea first suggested by Bradshaw *et al.* (1969). It is apparent that the Oughterard Granite post dates D3, as it clearly cross cuts structures related to this event (Bradshaw *et al.* 1969; Leake *et al.* 1981a). Tanner *et al.* (1997) argue that while many small bodies of this granite cross cut D4 folds this is not always the case and point out that several outcrops clearly show Oughterard Granite in disharmonic D4 folds (Fig. 3.7). Tanner *et al.* (1997) concludes that the main body of Oughterard granite intruded shortly after the D4 regional folding event.

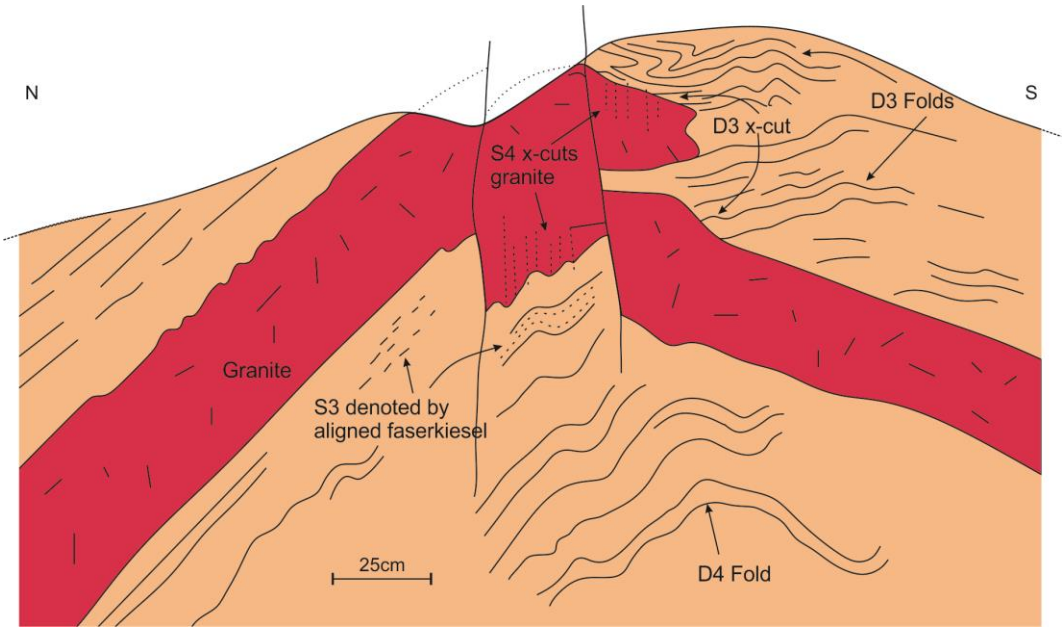


Fig. 3.7 Sketch of the structural relationship between D3 and D4 folding and minor Oughterard Granite sheets (redrawn from Tanner *et al.* (1997)). Granite cross cuts D3 folds and intrudes concordant to D4 folds but exhibits subtle S4 cleavages which show emplacement and folding was concomitant.

Therefore, the Oughterard Granite is useful in that its intrusion marks the end of D4 and predates the intrusion of the later Galway Granites. Various radiometric ages have been put forward (510 ± 35Ma (Leggo *et al.* 1966), 473 ± 9Ma (Elias *et al.* 1988), 466 ± 5Ma (Cliff *et al.*

1996), 473Ma (Tanner *et al.* 1997) and a notably younger 407 ± 23Ma (Kennan *et al.* 1987)). More recent work by Friedrich *et al.* (1999a) returned 462.5 ± 1Ma age of crystallisation, data that is broadly consistent with that of Elias *et al.* (1988) and Cliff *et al.* (1996).

Thus, this granite intruded in the latter stages of D4, prior to thermal relaxation of the country rock following D3, before last movements on the Mannin Thrust and yields an isotopic age of ~ 465Ma. The significance of this is discussed below.

3.5 Regional Metamorphism

A period of high pressure moderate temperature conditions preceded thermal maximum (Yardley *et al.* 1987). The thermal peak of amphibolite grade regional metamorphism is closely associated with the intrusion of Grampian metagabbro and orthogneisses (Charlesworth 1963; Tanner 1967). This resulted in a north (low) to south (high) progression of metamorphic grade from which four zones (Fig. 3.8), the staurolite, sillimanite-muscovite, sillimanite-K-feldspar, migmatite zones, are defined (Badley 1976; Yardley 1980; Leake *et al.* 1981b; Barber and Yardley 1985). The Connemara block was thrust southward during thermal relaxation under low amphibolite grade conditions (Leake *et al.* 1983; Leake *et al.* 1984).

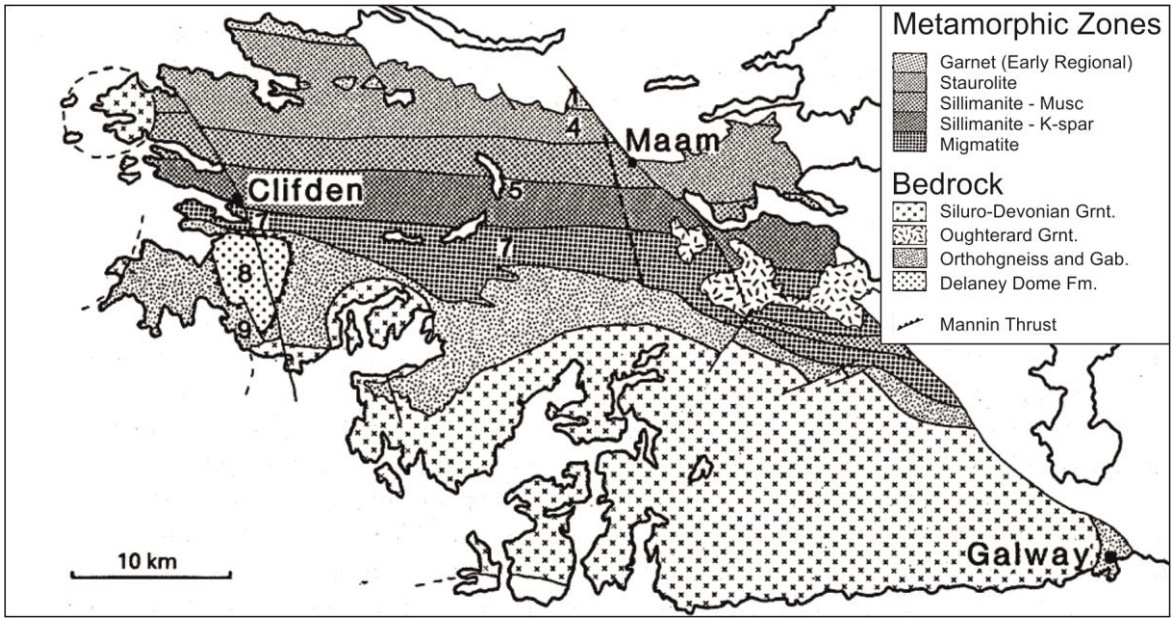


Fig. 3.8 Regional metamorphic zones defined across Connemara (from Yardley (1980)). Early Regional high pressure low temperature garnet bearing M1 is largely overprinted by M2 which show a progression in grade from north to south. Rocks in direct contact with the Gabbro and Orthogneiss Complex are migmatised.

Early Kyanite Facies Metamorphism

Late to post D2 high pressure, lower temperature conditions produced a staurolite, garnet ± kyanite assemblage which is only preserved in rocks to the extreme north and on Inishshark, Inishbofin (Cruse and Leake 1968), and in the east near Maam Cross (Leake and Tanner 1994), and Maam Turk (Ferguson and Harvey 1979). The rare occurrence of early kyanite illustrates that regional metamorphism in this area is not straightforward and that the lower pressure high temperature amphibolite conditions seen in most parts of Connemara were preceded by a low-moderate temperature high pressure regime (Yardley 1980; Yardley *et al.* 1987).

Metamorphic Peak

High temperature - moderate pressure conditions accompanied the intrusion of Grampian plutonic bodies during D3 (peaking at *c.*750°C @ 4.5-6kbar in pelitic gneisses in the migmatite zone (Barber and Yardley 1985)). This was essentially a regional scale contact metamorphic event and the highest grade rocks are always found in close proximity to Grampian intrusions.

The Staurolite zone is the lowest grade assemblage in Connemara. It is defined based on the occurrence of staurolite and the absence of metamorphic sillimanite and cordierite which are present in all other zones (Yardley 1976; Senior and Leake 1978). Spatially this zone is confined to the north and generally restricted to the northern limb of the Connemara Antiform. High grade contact metamorphism is restricted to areas in close proximity to smaller gabbroic bodies (e.g. Dawros in north Connemara (Tanner and Shackleton 1979)).

The sillimanite - muscovite transition zone lies to the south of the staurolite zone (Tanner 1967). The northern margin is defined by the presence of sillimanite which grew at the expense of staurolite. The southern limit of the sillimanite - muscovite transition zone grades into the sillimanite zone and involves the gradual elimination of staurolite. Variable amounts of garnet and white mica are also present.

The sillimanite - K-feldspar zone is distinguished from the sillimanite - muscovite transition zone further north by the presence of K-feldspar (Yardley *et al.* 1987). Leucosome partial melt and K-feldspar abundance increases as one progresses south into a higher grade terrane. Sillimanite is abundant in many pelitic horizons where garnet, cordierite and white mica may be present. Cordierite and rare andalusite are also documented in pelitic units and partial melt in this area (Yardley 1976).

The migmatite zone is in direct contact with Grampian intrusions in the south and is defined by the presence of granitic leucosome, as distinct from leucosome of other compositions that are

present in the sillimanite - K-feldspar zone further north (Yardley *et al.* 1987). This band of paragneiss is likely to belong to the Cashel Schist Fm.. Cordierite, sillimanite and garnet are common (Barber and Yardley 1985). Andalusite is present in east Connemara exclusively in leucosome partial melt denoting a reduction in temperature during thermal relaxation (Barber and Yardley 1985).

Timing peak metamorphic conditions

A relative structural timing of peak thermal conditions is recognised by the nature in which the metamorphic assemblage has not been folded by the D3 event but regional shortening of the thermal isograd, in a north - south direction, has occurred due to folding during D4. This fundamental observation, complimented by other structural data, shows that peak regional metamorphism was synchronous with D3 but complete by D4 (see Leake and Tanner (1994)). This deduction is chronologically confirmed by Friedrich *et al.* (1999a). The absolute timing of plutonic activity during D3 has been constrained to *c.*474-467 (Friedrich *et al.* 1999b) while earliest cooling followed at 468 ± 2Ma (Friedrich *et al.* (1999a) in broad agreement with Cliff *et al.* (1996)).

This sequence of events is consistent with a model suggestive of an early high pressure low temperature regime followed by lower pressure and elevated temperature concurrent with intrusion of gabbro and orthogneisses. Rapid cooling ensued post at ~ 468Ma crystallising andalusite and titanite within leucosome partial melts (Badley 1976; Barber and Yardley 1985; Yardley *et al.* 1987; Cliff *et al.* 1996; Friedrich *et al.* 1999a).

3.6 Structural Evolution of the CMC

Four main deformation episodes (D1-D4, Fig. 3.9) have affected the Dalradian rocks of Connemara. D1-D3 predate the thrusting of Connemara into its current position along the Mannin Thrust, D4 folding is associated with this event (Leake and Tanner 1994). A set of relatively minor folds defined in the Delaney Dome Fm. and a temporally associated suite of conjugate northwest-southeast and northeast-southwest faults represent a fifth deformation event (D5).

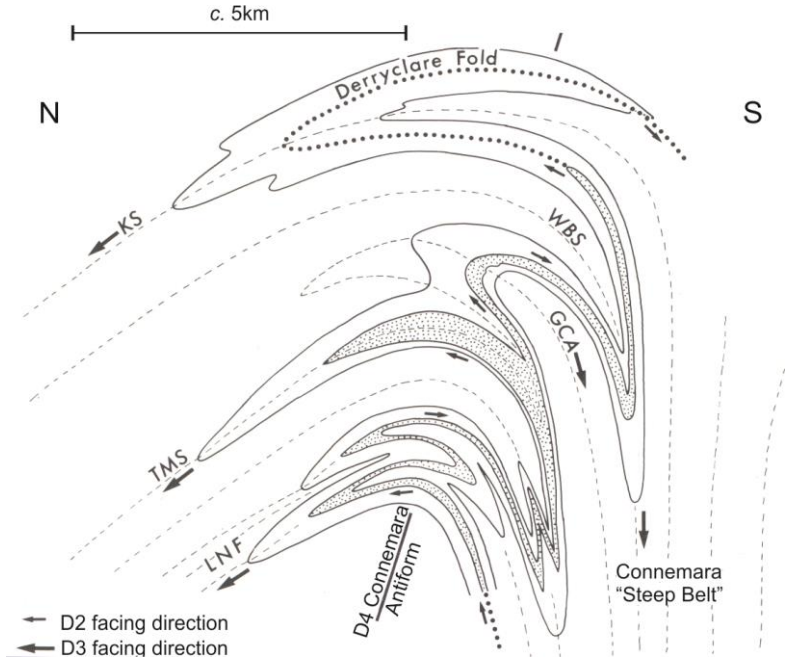


Fig. 3.9 N-S profile across the Connemara Antiform showing the basic symmetrical relationship between folds in Connemara (from Leake and Tanner (1994)). D2 folds control the facing direction of major D3 folds, both D2 and D3 are re-folded by the D4 Connemara Antiform. D2 = Derryclare fold. D3 = Glencoaghan Antiform (GCA); Knockpasheemore Synform (KS); Loch Nahillion Fold (LNF); Tully Mountain Synform (TMS); Waterloo Bridge Synform (WBS).

3.6.1 Deformation Events

D1

Solid evidence for the D1 event is lacking. The existence of this event is based solely on the occurrence of inclusion trails in garnet, and possibly staurolite and plagioclase (Leake and Tanner 1994). These porphyroblasts are always wrapped by a D2 fabric and contain inclusions of a crenulated fabric, the axial planes of which are commonly at 90° to that of the hosts' D2 fabric (Leake 1986). Most authors suggest that no cleavage or fold structures related to D1 survived D2 deformation however, Badley (1976) argued that parts of the Lissoughter Anticline is an D1 fold that became refolded by D2. Subsequent work refutes this claim (Tanner and Shackleton 1979; Leake *et al.* 1981a).

D2

D2 folding is represented by the Derryclare, Lissoughter Anticline and Lissoughter Antiform (Tanner 1967; Badley 1976; Taylor 1980; Yardley *et al.* 1987). These folds cause a repetition of the Bennabeola Quartzite Fm. and Cleggan Boulder Bed Fm. on the eastern flank of the Twelve Bens and across the Maam Turks (Edmunds and Thomas 1966). A crucial observation that identifies these structures as D2 is that they are refolded by the Waterloo Bridge Synform (D3), and again by the Connemara Antiform (D4) (Tanner and Shackleton 1979). At outcrop scale D2 deformation

is recognised by tight to isoclinal folds and in conglomerates larger clasts are commonly rotated into parallelism with the axial line of these folds (especially in the Lakes Marble Fm. and Ballynakill Fm. (Leake and Tanner 1994)). D2 folding within the Connemara "Steep Belt" has not been documented, this is likely due to repetition and truncation of units resulting from intense shortening that occurred in this area.

A syn-D2 age of intrusion was argued for Grampian metagabbros based on suggestions that D2 folds and preferential mineral growth parallel to D2 fold axes were present in some gabbroic bodies (Leake 1964; Leake 1969; Bremner *et al.* 1980). This work was later refuted by the same authors and a post D2 age was later universally accepted (see Tanner (1990) & Leake and Tanner (1994), *c.f.* Boyle and Dawes (1991)).

D3

The main deformation event in Connemara was D3 evidence for which is expressed in all Dalradian and most Grampian Rocks (not the Oughterard Granite). The type example for D3 folding is the Glencoaghan Antiform which clearly refolds the D2 Derryclare Synform and is itself folded by the D4 Connemara Antiform (Tanner and Shackleton 1979), 17 other major D3 folds are documented which exhibit the same structural relationship (Leake and Tanner 1994). D3 fold axes typically plunge ≤ 35° east and exhibit variable axial surface orientations which are controlled by D4 fold symmetry. Across the D4 Connemara Antiform, D3 axial surfaces dip moderately north on the northern limb, shallowly to the east on the fold axis and in the steep belt to the south axial surfaces vary from gentle to subvertical due to the intensive nature of folding in this area. The distinction between D2 and D3 folds is based on fold interference patterns (discussed in Leake and Tanner (1994)).

Grampian metagabbros were intruded prior to the initiation of D3 deformation and continued into the early part of the D3 event as shown by D3 tectonically induced fabrics and D3 folding of cumulate ultramafic layers (e.g. Bennett and Gibb (1983); Robertson (1988); Tanner (1990)). Later, toward the end of D3, the orthogneisses sheeted into the already emplaced gabbro and Dalradian metasediments (Leake 1989; Leake and Tanner 1994). Emplacement was achieved into a high strain regime which imposed a down temperature gneissic fabric on the cooling metagabbros and orthogneisses. Granitic pegmatites, associated with the orthogneiss suite, exhibit weak-no fabric development indicating the end of D3 occurred ~ 467Ma (Friedrich *et al.* 1999b).

D4

The last major deformation event to affect the Connemara Metamorphic Belt was the D4 folding event (Leake *et al.* 1981b, 1981a; Tanner 1981a; Tanner 1981b). The D4 Connemara Antiform, which dominates the outcrop pattern of the Twelve Bens, defines this event (Fig 3.2). The Connemara Synform and Joyce's Antiform are also D4 structures and lie to the east of the Maam Valley Fault. The Connemara Antiform is an asymmetric fold with an ESE-WNW fold axis that plunges 05-15° east, its northern limb dips moderately to the north and its southern limb dips steeply to the south toward the Steep Belt. In the east, Joyce's Antiform to the north and the Connemara Synform to the south form a upright refolded pair with a curvilinear axial line which plunges gently eastwards in the east and westward in the west. On the main Galway - Clifden road spectacular outcrops of the Twelve Bens and Maam Turks clearly show regional scale D4 folds refolding the D2 Derryclare fold. At outcrop scale, fold axes of crenulated earlier cleavages are orientated parallel to the regional trend and plunge of the D4 Connemara Antiform, this can be seen at the western exposure of the Connemara Antiform which outcrops on Barnahallia, adjacent to the Dalradian - Omey Pluton contact.

Intrusion of the metagabbro and orthogneisses had ceased and cooling of the metagabbro had progressed to below 600°C by the instigation of D4 deformation, permitting the rotation of palaeomagnetic poles during folding of the Cashel - Lough Wheelaun gabbro (Leake 1970; Morris and Tanner 1977; Robertson 1988; Leake 1989). Earlier bodies of Oughterard Granite are folded by D4 deformation while the main slightly later (462.5 ± 1Ma Friedrich *et al.* (1999a)) plutonic bodies clearly cross cut the D4 Connemara Antiform (Tanner *et al.* 1997).

D5

D5 is defined by two antiformal and one synformal fold structures in southwest Connemara that deform part of the metagabbro and Delaney Dome rhyolite in this area (Leake and Tanner 1994). Two sets of regional faults (NNW-SSE and NNE-SSW) cross cut the CMC and Siluro-Devonian Granites but are also shown to have been active during the D5 folding event (Leake 1986). These faults are discussed as D5 structures which were re-activated after D5 had terminated.

The N-S trending D5 Dolan and Doohulla Antiforms trend directly north into the southern half of the Delaney Dome Fm. where they cross-cut and buckle the ESE-WNW D4 Mannin Antiform to complete the convex symmetry of the Delaney Dome structure (Fig 3.10). Axial planar cleavage

and brittle fractures associated with this fold pair cross cut D4 Mannin Antiform microstructures which demonstrate the D5 stress field was highly oblique to that of the earlier D4 event (Leake 1986).

A northwest-southeast fault breccia truncates the western limb of the Dolan antiform (Fig. 3.10). Within this breccia, D5 micro folds and crenulations are observed that indicate faulting was concurrent with folding (Leake 1986). This brittle structure shares the same orientation as multiple northwest-southeast structures in the CMC (e.g. Maumahoge, Cur, Recess, Cashel, Derryclare and Bengower Faults) and are oblique to a prominent northeast-southwest fault set (e.g. Barna, Letterfrack, Kylemore-Baunoge and Mauminagh Faults) (Leake and Tanner 1994). Both northwest-southeast and northeast-southwest faults offset D2-D4 fold axes, abut against, or sometimes cross cut, the Galway Granites (Fig 3.2) and are long considered to have complex reactivation histories (Leake *et al.* 1981a; Tanner 1981a; Tanner 1981b; Leake *et al.* 1984). Here, these are considered a regional set of conjugate faults that initiated during D5 folding.

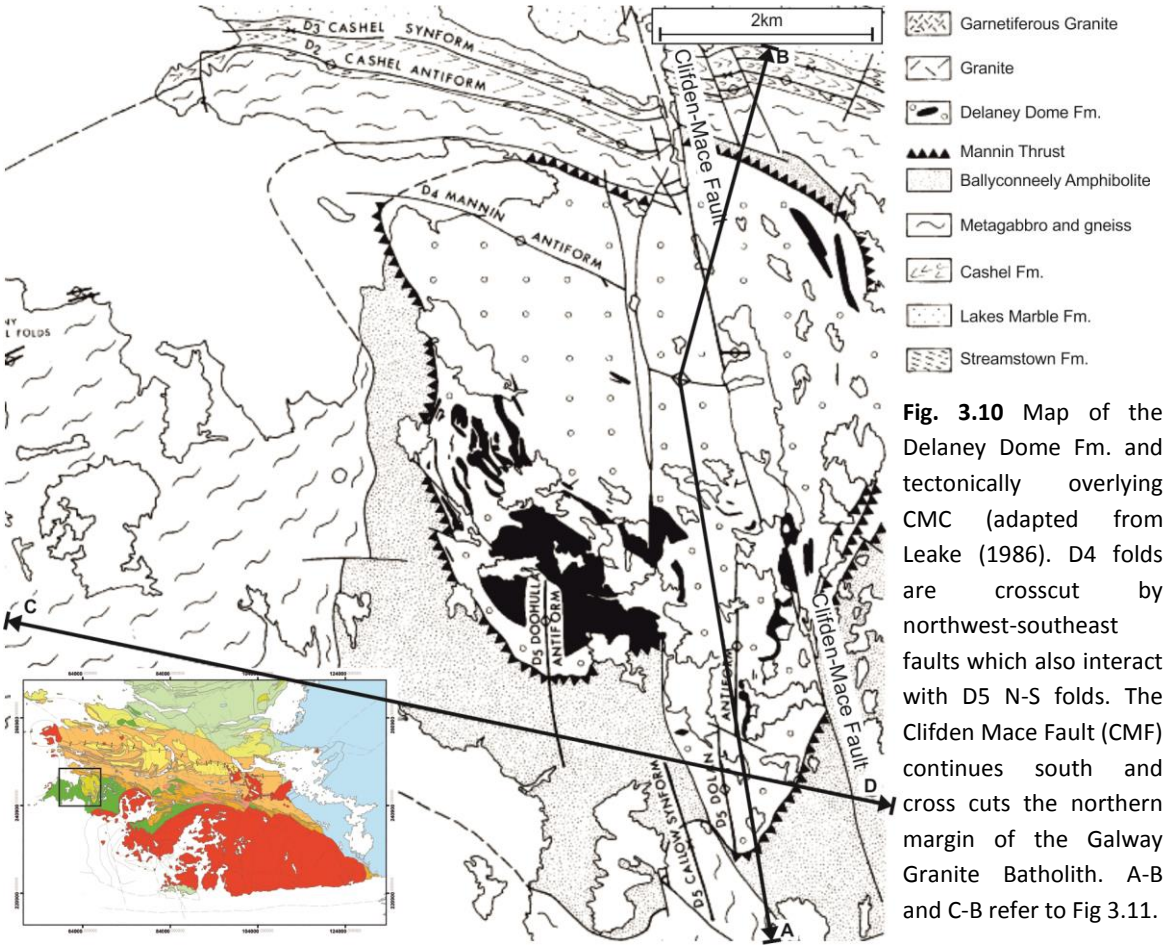


Fig. 3.10 Map of the Delaney Dome Fm. and tectonically overlying CMC (adapted from Leake (1986). D4 folds are crosscut by northwest-southeast faults which also interact with D5 N-S folds. The Clifden Mace Fault (CMF) continues south and cross cuts the northern margin of the Galway Granite Batholith. A-B and C-B refer to Fig 3.11.

Generally speaking NNW-SSE and NNE-SSE show dextral and sinistral strike slip (10-1000m) respectively and minor down throw (Leake and Tanner 1994), but several exceptions do occur. For example, the Clifden-Mace Fault (CMF), the most prominent northwest-southeast structure, shows final left lateral displacement. The degree of offset varies considerably along the CMF from 0.7km (northern margin of the Galway Granite batholith) to 100m (Connemara Steep Belt) (Leake 1986). This further substantiates the deduction that this, as associated structures, were active during the Silurian to mid Devonian period.

Inconsistent lateral displacement may be accounted for by kinematic fluctuations during the final closure of Iapetus and the later Acadian Orogeny (Chapter 2). Bound to the north and south by major Caledonian faults associated with the Highland Boundary Fault (HBF) and Skird Rocks Fault (SRF), the CMC is expected to behave as a large scale deformation zone during sinistral transpression, transtension and later Acadian compression. D5 faults, that are oblique to the bounding faults, would have partitioned strain differentially and reactivated in contrasting ways during these events ~ 430-380Ma. This concept is revisited later.

3.7 Connemara; Ominously South of the Highland Boundary Fault

The Mannin Thrust is a major low angle northward dipping thrust which tectonically places the CMC over the Delany Dome Fm. (Fig. 3.11, Leake *et al.* (1983)). Outcrops indicating this relationship are only found in southwest Connemara on the Errismore peninsula (0640, 2464) where erosion processes have created a tectonic window through the Mannin Thrust (Fig. 3.10). This is understood to be the structure along which the CMC was thrust south of the Highland Boundary Fault (Leake *et al.* 1983; Leake *et al.* 1984), thus repositioning Dalradian stratigraphy this far south. A zone of intense brecciation separates the Ballyconneely amphibolite (HW) from the underlying Delaney Dome Fm. (FW), this is the Mannin Fault which represents the final phases of movement along the Manning Thrust Zone (Leake *et al.* 1983).

The Ballyconneely amphibolite (HW) is a fine grained mafic hornblende schist which exhibits a strong NNW alignment of metamorphic hornblende (Leake *et al.* 1983; Leake 1986). Geochemical analysis have confirmed that this amphibolite is the retrogressed equivalent of the Errismore Gabbro, which forms the bulk of the surrounding bedrock (Leake 1970; Bremner *et al.* 1980; Leake 1980).

The Delaney Dome Fm. (FW) is a strongly foliated, highly siliceous, mylonitised rhyolite (Leake 1986). A pervasive quartz defined NNW fabric is developed in all outcrops and penetrates to a depth of at least 233m (GSI bore hole Chroston and Max (1988)). The degree of fabric anisotropy intensifies and becomes strongly mylonitic in areas adjacent to the brecciated contact with the tectonically overlying Ballyconneely amphibolite.

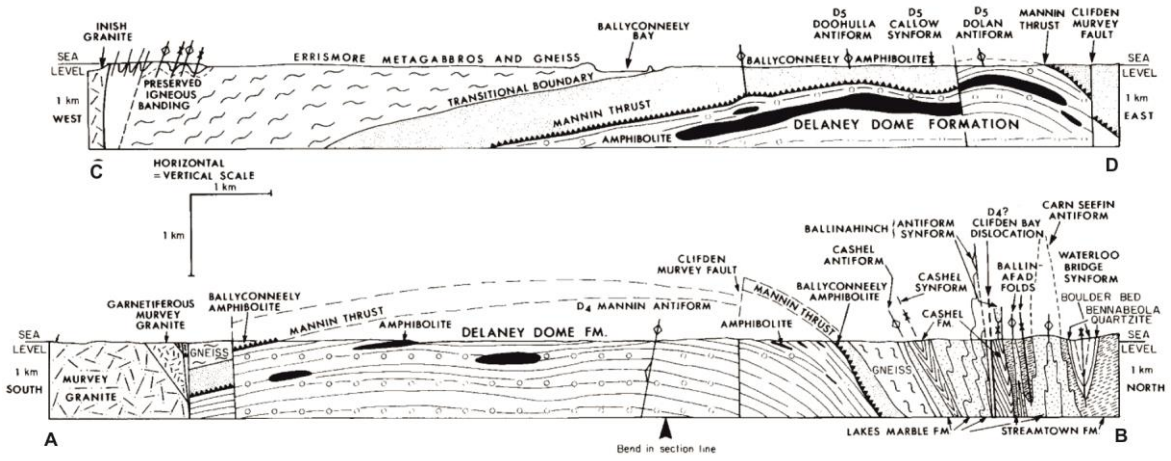


Fig. 3.11 Two cross sections across the Mannin Thrust (from Leake (1986)). Lines of section illustrated in Fig 3.10. X-sections show the Delany Dome Fm. to be a footwall over which the CMC and been thrust via the Mannin Thrust.

Together, chemical, petrographic and microstructural analysis indicate that the Delaney Dome is an extrusive volcanic deposit, containing small amounts of weakly foliated hornblende bearing mafic units (Leake and Singh 1986). Tanner *et al.* (1989) suggested a genetic link between the Tyrone Igneous Complex while Draut and Clift (2002) infer that the Delaney Dome was the extrusive temporal equivalent of the metagabbro and orthogneiss complex in Connemara and also of the volcanic deposits in the South Mayo Trough. Draut and Clift (2002) returned a 474.6 ± 5.5Ma isotopic age for this deposit (within error of all previous work (Leake *et al.* 1983; Cliff *et al.* 1996)).

Timing of Southward Thrusting

The intrusion of quartz diorite and metagabbro occurred prior to D4 and synchronous with D3. In proximity of the Mannin Thrust, D3 fabrics in these intrusions are overprinted by the preferential NNW growth of hornblendes (Ballyconneely amphibolite) and by intense brecciation in many quartz diorite units (Leake 1986; Leake and Singh 1986). The preferential NNW growth of

hornblende show that lower amphibolite temperatures of *c.*500°C persisted toward the latter stages of the thrusting event (Leake 1986; Tanner *et al.* 1989). Leake (1986) shows that part of the tectonic fabric associated with thrusting is folded by the D4 Mannin Anticline and Tanner *et al.* (1997) shows that the Oughterard Granite intruded at the end of D4.

From these field data, it has been shown that the southward thrusting of the CMC occurred shortly after D3 and before the end of D4 folding and that thermal relaxation had not dropped below amphibolite facies at this time.

Attempts to constrain the absolute timing of southward thrusting been made. Leake *et al.* (1983) determined a 460 ± 5Ma age from whole rock analysis of the Delaney Dome Fm. Kennan *et al.* (1987) reinterpreted this date and suggested thrusting may have continued until 426 ± 10Ma. An active shear zone such as this would interact with ascending magma that formed the > 423Ma Omey Pluton (Feely *et al.* 2007), no indication of this is observed. Cliff *et al.* (1996) returned a Rb-Sr muscovite-feldspar isochron age of 457 ± 6Ma from a D4 muscovite bearing quartz vein and suggested that final movement was not excessively later than this age. Based on Rb-Sr isotopic analysis of micas from the Delaney Dome mylonites, Tanner *et al.* (1989) suggested an age of 447 ± 4Ma for final movement and proposed a correlation between tectonic activity in Connemara and that seen in the Midland Valley Grampian and Highland Border terranes at about the same time.

3.8 Conclusions

Assembly of the Connemara Terrane

Southward thrusting of the CMC ceased during D4, shortly after metamorphic grade dropped below lower amphibolite facies (Leake 1986; Tanner *et al.* 1989). The regional thermal maximum occurred between 474.5 ± 1Ma and 467 ± 2Ma during D3 (Friedrich *et al.* 1999a; Friedrich *et al.* 1999b). Thermal modelling shows cooling started by 468 ± 2Ma and proceeded from peak conditions in excess of 700°C to ~ 460°C by ~ 460Ma and from 460°C to 350°C by 450Ma (Friedrich *et al.* (1999b) in broad agreement with Tanner *et al.* (1989)). These data suggests amphibolite grade conditions, and therefore thrusting, had terminated by 450Ma.

The Oughterard Granite had crystallised by 462.5 ± 1Ma (Friedrich *et al.* 1999b) and field data indicate emplacement of the earlier parts of this intrusion was concurrent with latest D4 (Tanner *et al.* 1997). This suggests emplacement occurred largely after southward thrusting had

completed (Tanner *et al.* 1997). Therefore, the isotopic age of the Oughterard Granite should be a viable minimum proxy for final movement on the Mannin Thrust (i.e. 462.5 ± 1Ma)

The existing field, petrographic and isotopic data indicate that southward thrusting was achieved after D3, during latest D4 and terminated prior to thermal relaxation below amphibolite facies, i.e. between ~ 468-462Ma. A more conservative estimate of 468-450Ma is deduced by ignoring the relationship between D4 folding, thrusting and emplacement of the Oughterard Granite. In either case, this compilation shows that the existing data is most consisting with a Darriwillian - Sandbian compressional event was the cause of the southward displacement of the CMC.

Considering this evidence from a broader perspective major perplexing issues arise. Chapter 1 reviews the current knowledge on the timing of Caledonian orogenic phases and shows that the docking of Avalonia and Laurentian occurred during the Wenlock. Based on the data reviewed above, this is a minimum of 20Ma after Connemara was thrust into its current position. In fact only one determination (Kennan *et al.* 1987) returned isotopic data that is consistent with the temporal parameters regarding the docking of Avalonian and Laurentia (this has been widely refuted).

Two explanations are immediately apparent. Either several erroneous deductions have been made from field, isotopic and petrographic observations or the principal deductions are broadly correct but applied incorrectly to regional scale plate tectonic models. It is interesting that data from both the Oughterard Granite and Delaney Dome Fm. indicate a significant tectonic event occurred between the Grampian and docking of Baltica and Avalonia. Such phenomenon could be tentatively used to infer a previously unrecognised arc collision event between 470-450Ma that resulted in the southward thrusting of the CMC along the Mannin Thrust.

3.8.1 Main Structural Features

northwest-southeast lineaments have been identified across Britain and Ireland and are broadly associated with reactivated fault controlled sedimentation (e.g. Graham (1986); Hutton and Alsop (1996a); Hutton and Alsop (1996b)), mineralisation (e.g. Horne (1975b, 1975a) and plutonic activity (e.g. Hutton (1982); Jacques and Reavy (1994); Stevenson *et al.* (2008)) since the Cambrian period (at least). The origin and development of these deep seated repeatedly

reactivated crustal structures has been investigated (e.g. Horne (1975b); Soper (1994); Arrowsmith *et al.* (2005)) but as of yet no satisfactory conclusion has been reached. A structural analysis of the Siluro-Devonian Galway Granites and the inherent structural features of their host rocks offer an opportunity to explore this phenomenon on a local scale.

Several geological features need to be taken into consideration in order to evaluate the dynamic interaction between regional stress and local structure and the implications for this on magma ingress. The Highland Boundary Fault to the north and Skird Rocks Fault (SRF) to the south (an extension of the SUF (Leake 2006) or a southern splay of HBF (Ryan *et al.* 1995)) are the two deep seated crustal lineaments between which Connemara define a deformation zone during sinistral strike slip movement between 430-400Ma (Dewey and Strachan 2003; Soper and Woodcock 2003). The Mannin Thrust is a subhorizontal plane along which the CMC was thrust over the Delaney Dome Fm. (Leake *et al.* 1983; Leake 1986; Leake and Singh 1986).

The Connemara Metamorphic Complex can be summarised as consisting of Dalradian metasediments and early Ordovician intrusions (Grampian). Polyphase deformation introduced planar and fold anisotropies into this system which served to re-orientate local stress fields during the siting of the Siluro-Devonian Galway Granites ~ 425-383Ma (Feely *et al.* 2010). The structural features which are most likely to have interacted with the local stress field during magma emplacement (precluding lithological variations) include the SRF, Mannin Thrust, Connemara Antiform and reactivated D5 (Fig 3.2).

Chapter 4:

Caledonian Granites of Britain and Ireland

4.1 Introduction

Tectonic processes associated with the closure of Iapetus Ocean generated large volumes of magma which ultimately formed the Ordovician-Devonian Caledonian granitoids of Britain and Ireland. The petrogenesis involved has been studied in detail and related to hypothesised, and broadly accepted, tectonic models (Read 1961; Stone *et al.* 1997; Atherton and Ghani 2002; Brown *et al.* 2008; Neilson *et al.* 2009). Such models emphasise the role of subduction zone magmatism (Soper 1986), crustal thickening and anatexis (Dewey 1971; van Breemen and Bluck 1981), slab break-off (Atherton and Ghani 2002; Fowler *et al.* 2008; Baumann *et al.* 2010) or melting of the crust through mantle heat advection (Brown *et al.* 2008; Neilson *et al.* 2009) depending on the timing and tectonic setting of granitoid intrusion.

The Siluro-Devonian Galway Granites do not fit into existing petrogenetic models. This is due to the position of these intrusions relative to major terrane boundaries, their broad age spectrum (*c.*422-380Ma (Feely *et al.* 2003; Feely *et al.* 2010)) and, as of yet, uncertain tectonic origins (e.g. Wright (1963); Claxton (1965); Aucott (1966); Townend (1966); Lawrence (1968); Feely (1982); Crowley (1997); Baxter and Feely (2002)). A recent publication cites all of the above process responsible for magma production and pluton growth in Connemara (Feely *et al.* 2010), this is shown to be unlikely.

The current hypothesises on the subdivisions and petrogenetic origins of the late Caledonian Granites are discussed first. These concepts are then applied to the main examples of Irish Caledonian granitoids.

4.2 Categorising the Caledonian Granites

Caledonian plutonic activity in Britain and Ireland occurred during two main episodes, the 470-460Ma Grampian Orogenic event and the ~ 447-380Ma late Caledonian orogenic phases and Acadian Orogeny. Read (1961) formally named these two independent suites the "Older Granites" and "Newer Granites". Given the succinct nature of the Grampian event no further subdivision of the Older Granites has been required. The Newer Granites were generated over a 67Ma period throughout the terminal phases of the Caledonian Orogeny and also the Acadian Orogeny. Several

subdivisions of the Newer Granites have been proposed which relate groups of plutons based on geological terrane, mineralogy and geochemistry and chronology.

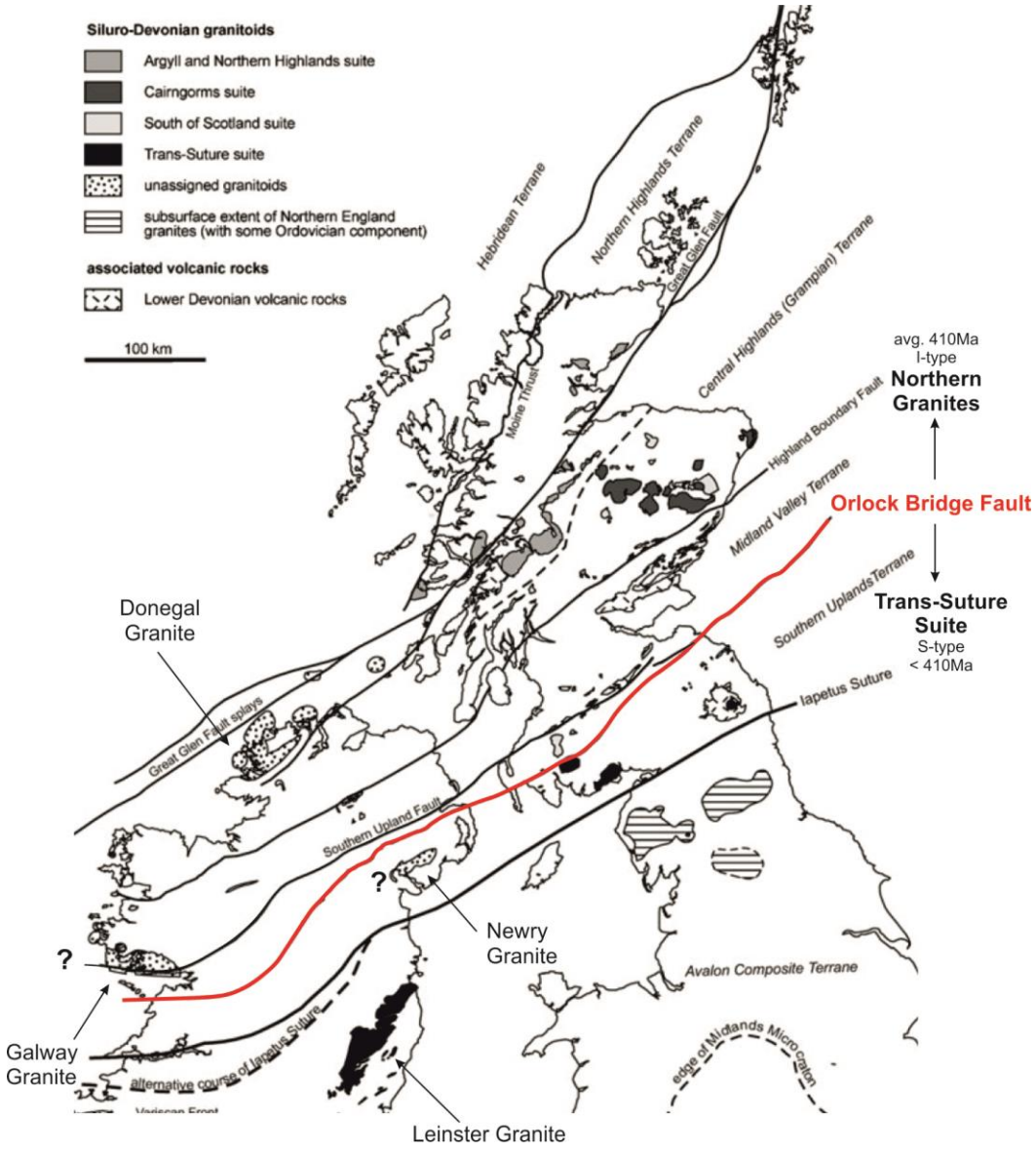


Fig. 4.1 Sub-classifications of the Newer Caledonian Granites and associated volcanics in Britain and Ireland (modified from Brown *et al.* (2008)). Note the position of the I-type Newry Granite south of the OBF and the Galway Granite north of the OBF.

Stephens and Halliday (1984) first distinguished the Argyll, Cairngorm and South of Scotland Suite based on geochemical and petrographic characteristics. Stone *et al.* (1997) noted a fundamental distinction between granites north and south of the Orlock Bridge Fault (Fig. 4.1). South of the Orlock Bridge Fault (OBF) (a.k.a. the Galloway intrusions (Stephens and Highton 1999)) intrusions are all younger than 410Ma and exhibit elevated $^{87}Sr/^{86}Sr$ ratios. North of the OBF granitoids have older crystallisation ages (avg. ~ 410Ma) and exhibit lower $^{87}Sr/^{86}Sr$, Rb/Sr

and La/Y ratios. Stone *et al.* (1997) also emphasised the Pb isotope similarities between granitoids of the Lake District and those in the South of Orlock Bridge Fault Group, an association previously noted by Harmon and Halliday (1980) & Thirlwall *et al.* (1989).

Growing isotopic, geochemical and petrographic data now make it apparent that the granites on either side of the Orlock Bridge Fault have separate petrogenetic origins. Assemblages analogous to I-type granites occur in the north and S-types to the south (of Chappell and White (1974) & Chappell and White (2001)).

From the above, Brown *et al.* (2008) defined the *Trans-Suture Suite* which includes those granitoids which are late Caledonian and sited south of the Orlock Bridge Fault, and the *Northern Granites*, which are those granites believed to be of Caledonian origin and lie north of the Orlock Bridge Fault (Fig 4.1). The petrogenetic models currently attributed to these groups of plutons are investigated below.

4.2.1 The Northern Granites

Mantle wedge melting, during northwest directed subduction of Iapetan Oceanic lithosphere, and anatectic melting, due to crustal thickening associated with the Scandian Orogeny, promoted magmatism and pluton growth north of the Great Glean Fault (Dewey 1971; van Breemen and Bluck 1981; Fowler *et al.* 2001; Oliver *et al.* 2008). The Glen Dessarry Pluton (447 ± 2.9Ma) is the earliest recorded Scandian process currently on record, the Loch Borrolan Pluton (429.2 ± 0.5Ma) marks the end of deformation (Goodenough *et al.* 2011). Regional sinistral strike slipping did not initiated until $\leq$ 430Ma (post Scandian), therefore the *Newer Granites* that are sited north of the Great Glen Fault and are older than ~ 430Ma may be attributed to Scandian process alone.

Together the Argyll, Northern Highland, Cairngorm and the South of Scotland granitoids that are north of the Orlock Bridge Fault define the Northern Granites (Fig. 4.1). These exhibit higher $^{87}Sr/^{86}Sr$ ratios and lower LILE and LREE abundances than those which belong to the Trans-Suture Suite and thus exhibit relative I-type affinities (Thirlwall 1982; Stephens and Halliday 1984; Halliday *et al.* 1986; Thirlwall 1986; Thirlwall *et al.* 1989; Tarney and Jones 1994; Stone *et al.* 1997; Fowler *et al.* 2001). Chronological data reveal that these intrusions have emplacement ages between ~ 390-430Ma. Atherton and Ghani (2002) show a pluton crystallisation age spike from 400-410Ma. Neilson *et al.* (2009) argues for a more protracted period between 420-400Ma.

Additionally, an extensive suite of coeval appinite and lamprophyre dykes have long been associated with the Northern Granites (Rogers and Dunning 1991; Fowler *et al.* 2001; Atherton and Ghani 2002; MacDonald and Fettes 2007).

The association of minor intrusions with granitoids of I-type geochemistry led several authors to suggest that petrogenesis entailed melting of a hydrous mantle that was driven by active subduction of the Iapetus Ocean under the Laurentian margin (e.g. Dewey (1971); Soper (1986); Thirlwall (1988)). However, a sudden increase in plutonic activity between 420-400Ma is not explained by this model, nor continued magmatism into the mid-Devonian.

Atherton and Ghani (2002) proposed a "slab break-off" model (see Davies and von Blanckenburg (1995); Baumann *et al.* (2010)) where the subducted Iapetus lithosphere detached at ~ 420Ma due to the attempted subduction of Avalonian during Caledonian lock up. The detached slab sank causing upwelling of hot asthenosphere that promoted melting of the lower orthotectonic crust. Ultimately, calc-alkaline granite and coeval appinite and lamprophyres were generated in the proceeding 20Ma to form the Northern Granites.

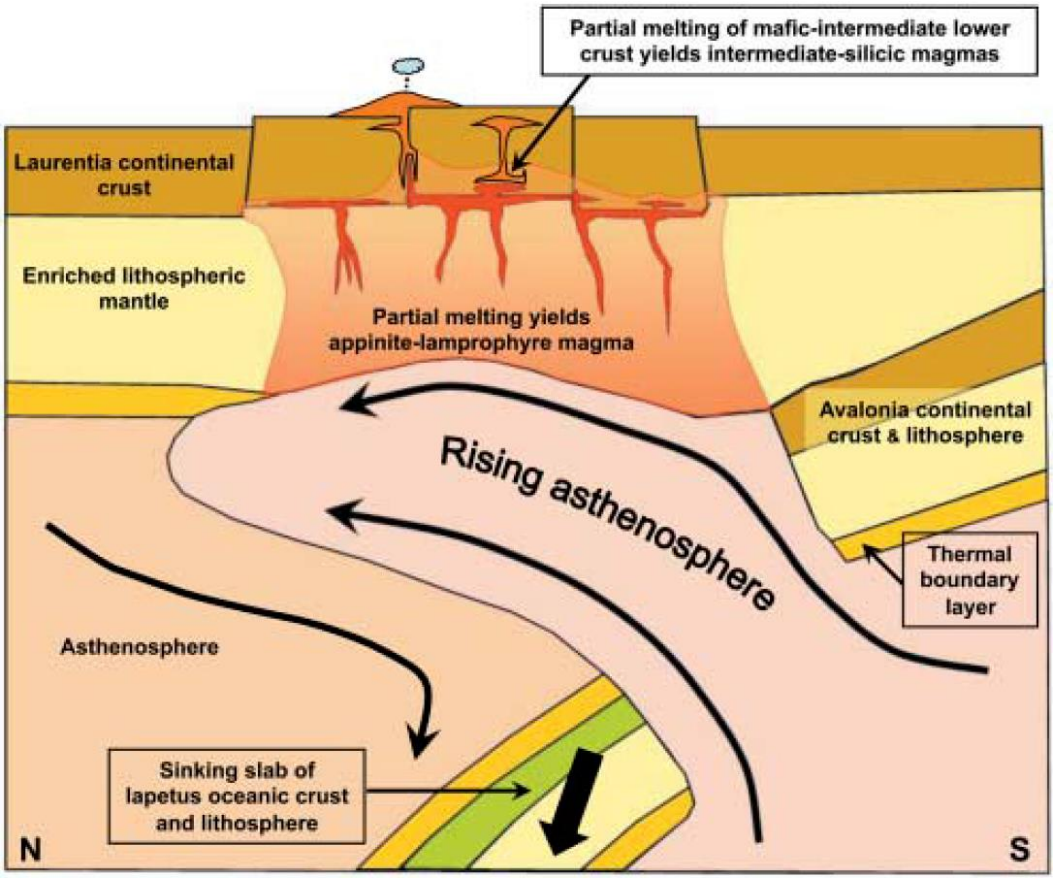


Fig. 4.2 Cartoon diagram of the leading petrogenic model for the Northern Granites (from Neilson *et al.* (2009)). Based off the slab break off model of Atherton and Ghani (2002), this model shows partial melting of enriched lithospheric mantle, new crust generation by intrusion of appinite-lamprophyre sheets and crustal recycling of the lower crust to generate associated plutons and volcanoes.

Neilson *et al.* (2009) re-emphasised (after Pitcher (1982)) that these intrusions are not characteristic Andean I-type granitoids. As magma production peaked after subduction terminated (420-400Ma), they suggest large volumes of intermediate and felsic magma generated at this time were not a consequence of the subduction process. Alternatively, Neilson *et al.* (2009) suggest a slab break-off model (Fig. 4.2) where dry hot asthenosphere triggered melting in the overlying hydrous, enriched lithospheric mantle and suggest no melt was directly sourced from the asthenosphere (Neilson *et al.* 2009). Critically, this model attempts to address protracted voluminous magmatism over 22Ma via under plating and exclusive melting of the lithosphere (crustal recycling) as appose to Atherton and Ghani (2002) who require melt from both sources and show substantial crustal growth.

4.2.2 The Trans-Suture Suite

The Trans-Suture Suite (Fig. 4.1) is inclusive of all granitoids of Caledonian affiliation south of the Orlock Bridge Fault and thus includes the classic S-type Leinster Granite and the Isle of Man granites; the Newry Igneous Complex is an exception and is excluded (Brown *et al.* 2008). Brown *et al.* (2008) characterises the Trans-Suture Suite based an S-type affinities (two mica facies, Sr/Sr ratios from 0.7083 - 0.7061 and εNd_t values between -2 – -4.2) and age ranges between ~ 400-390Ma, all are younger than 410Ma. Brown *et al.* (2008) emphasises that these plutons need not be true S-type granites *sensu stricto* but simply tend towards this end member when compared to granites further north. Many plutons are zoned with I-type outer margins and S-type cores (e.g. the Criffel pluton (Stephens and Halliday 1984; Stephens 1992)).

The Trans-Suture Suite were emplaced on both sides of the Iapetus Suture, during Caledonian transtension (Dewey and Strachan 2003; Soper and Woodcock 2003) and Acadian orogenesis (Woodcock *et al.* 2007). These granitoids are temporally associated with a prominent suite of porphyritic lamprophyre dykes, extending from the Central Belt of the Southern Uplands into Eastern Ireland (Rock *et al.* 1986a; Rock *et al.* 1986b; Vaughan 1996).

Their significantly younger age (~ 20-30Ma after Laurentian-Avalonian convergence), occurrence north and south of the Iapetus Suture, and S-type chemistry must be accounted for in a petrogenetic model. Earlier models (Soper 1986; Brown 1991; Atherton and Ghani 2002)) are incompatible as; (i) subduction of Iapetan and Avalonian lithosphere could not generate magma south of the subduction zone, (ii) Caledonian crustal thickening and anatexis is unlikely as

magmatism continued long after orogenic collapse and (iii) the anomalous age contrast on opposing sides of the Orlock Bridge Fault is not explained by crustal thickening.

Brown *et al.* (2008) proposed that the documented suite of lamprophyre dykes, generated and intruded during 410-400Ma transtension and drove heat advection through the lithosphere. In this model basic magmas charged with volatiles, derived from partial melting of metasomatized sub-continental lithospheric mantle, coincide with Devonian transtensional decompression. Ultimately, melting of the paratectonic crust led to upward migration of magma and crystallisation of hybridised magmas with an overall S-type affinity that also containing relatively primitive mafic components (e.g. the Criffel I-S type zoned pluton with mafic enclaves). Brown *et al.* (2008) concluded that melt generation during 410-400Ma transtension could explain magmatism into the Frasnian.

Woodcock *et al.* (2007) suggested that northward subduction of the Rheic Ocean lithosphere under the accreted Laurassian margin drove the Acadian Orogenic event between 400-390Ma in Ireland and Britain. Studies on the Costelloe Murvey Granite, in Connemara, show this intrusion to be 380.1 ± 5.5 Ma (Feely *et al.* 2003) and new data from the Iapetus Suture Zone return crystallisation ages which range from 395-375Ma (Helen O'Rourke *pers. comm.*). These data show heat was continuously generated into the mid-Devonian. It is difficult to relate such phenomenon to Caledonian processes.

An alternative model, not previously proposed, relates Acadian orogenesis to granitoids which are currently considered late Caledonian. Northward subduction of Rheic Oceanic lithosphere beneath the Laurassian margin could have generated a scenario analogous to that which generated the late Caledonian Granites. Subduction drove melting of the overlying wedge and introduced new hot volatiles into the crust (which was already hot following earlier Caledonian processes) before, during and for a time after the main 400-390Ma event. Generated magma migrated preferentially along existing deep crustal structures such as the Solway Line, Orlock Bridge Fault and Skird Rocks Fault and preferentially distributed magma near such localities (similar to the mechanisms envisaged by Hutton and Reavy (1992) and Jacques and Reavy (1994)).

This basic concept (subducting Rheic Ocean lithosphere promoted melting) seems intuitively acceptable and it is not inconsistent with any existing data. Additionally, it has the obvious advantage of explaining how magmatism was concentrated in the south, and not further north, for so long after the Caledonian Orogeny had ended. However, it is accepted that this explanation is not yet supported and the hypothesis remains untested.

4.3 Regional Petrogenetic Models Applied to Irish Granites

In Ireland no granites are attributed to Scandian orogenic processes. The age, tectonic setting and geochemistry of the Donegal Granites ((Stevenson *et al.* 2008) and references therein) are consistent with the a break-off model (Atherton and Ghani 2002; Neilson *et al.* 2009). The Newry Complex exhibits strong I-type affinities and ages of ~ 420-410Ma (Meighan 2003) but is situated south of the Orlock Bridge Fault. Therefore its anomalous but considered part of the Northern Granites (Brown *et al.* 2008). The Leinster Granite is a classic S-type granite with minor I-type inclusions (Grogan and Reavy 2002), geochemistry and geochronology data for this intrusion characterise a Trans-Suture granitoid.

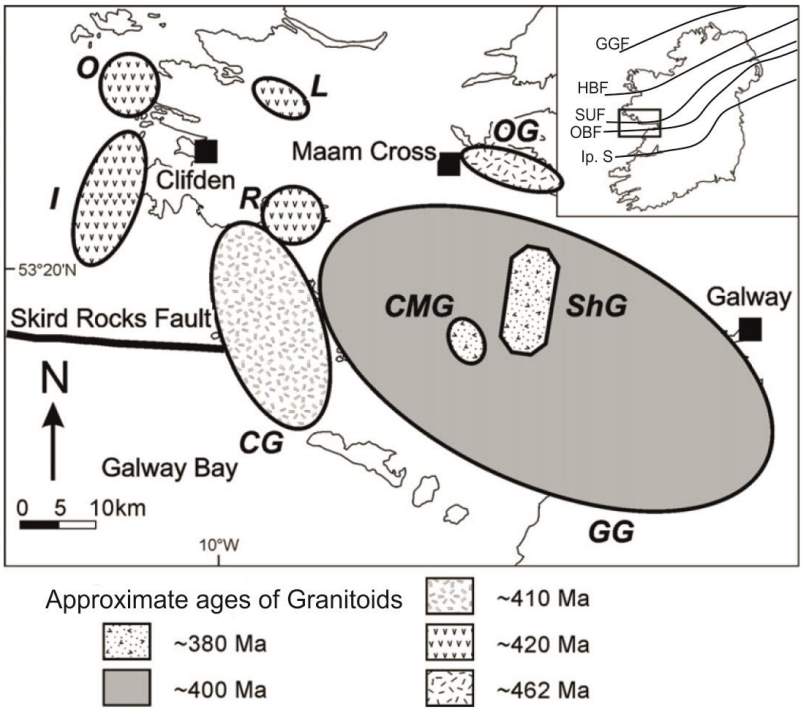


Fig. 4.3 Distribution of Siluro-Devonian plutons in Galway and approximate ages determined (Feely *et al.* 2010). Note that all intrusions are sited north of the Orlock Bridge Fault but a broad range of isotopic age determinations have been reported which are inconsistent with the petrogenetic models discussed in the text.

The Siluro-Devonian Galway Granites (Fig. 4.3) are all cited north of the OBF, the largest intrusion, the Main Batholith, straddles the Skird Rocks Fault (SRF) (an extension of the Southern Uplands Fault (Feely *et al.* 2006; Leake 2006) or southern splay of the Highland Boundary Fault (Ryan *et al.* 1995)). Existing geochemical data is most indicative of an I-type magma (Wright 1963; Claxton 1965; Aucott 1966; Townend 1966; Lawrence 1968; Leake 1974; Feely *et al.* 1991; Gallagher *et al.* 1992; El-Desouky *et al.* 1996; Crowley 1997; Baxter and Feely 2002), no facies with obvious S-type characteristics are present (Feely *et al.* 2006). Geochemical similarities are drawn

between the Siluro-Devonian Galway Granites and the Argyll Suite (Crowley 1997) and, in contrast, the Cairngorm Suite (Leake 2011).

A broad spectrum of crystallisation ages have been determined from these plutons (~ 422 - 380Ma (Buchwaldt 2001; Feely *et al.* 2003; Feely *et al.* 2007). Accepting these dates as correct, magmatism initiated shortly after Laurentian-Avalonian convergence and continued for 10Ma after Acadian orogenesis.

Much of the principal traits of the Galway Granites meet the criteria for classification as part of the Northern Granite suite. They all exhibit I-type affinities and intrude north of OBF and many were emplaced between ~ 425-405Ma (Selby *et al.* 2004; Feely *et al.* 2007). However, the largest volumes of magma intruded between 402-397Ma, the latest facies is 380.1 ± 5.5 (Feely *et al.* 2003). Therefore, the younger intrusions are temporally suited to the Trans-Suture Suite but are tectonically out of place being north of the OBF. The older intrusions (425-405Ma) are consistent with models proposed for the Northern Granites but share a spatial and chemical association with those younger intrusions discussed and are therefore unlikely to be totally petrogenetically distinct.

The late Caledonian Galway Granites are ideally placed in space and time to encapsulate the entirety of the late and post Caledonian tectonic events and represent a current natural enigma that does not conform to existing theoretical models. With the aim of resolving some of these issues, and those raised in the previous two chapters, the focus is now turned to the Silurian to Devonian Galway Granites.

Chapter 5:

The Galway Granite Complex

5.1 Introduction

The Siluro-Devonian Galway Granites are defined by four small older plutons which are sited about a younger batholith which is a composite of several granitoid - diorite intrusions. These granitoids were emplaced into the Connemara Metamorphic Complex (Leake and Tanner 1994) to the north and the South Connemara Group to the south (Ryan and Dewey 2004) between ~ 425-380Ma (Feely *et al.* 2010).

In Section 5.2 the nomenclature used in describing the Siluro-Devonian Galway Granites is revised for clarification purposes. The literature relating to each member of the mid Silurian to mid Devonian Galway granites is then summarised. The chapter concludes by placing the granitoids referred to in a regional context relative to the petrogenetic models discussed here and the regional and local geology discussed in the previous two chapters. From this, corner stone queries are raised which form the basis the current work.

5.2 Clarification of the Nomenclature

The term "late Caledonian Galway Granites" refers to the suite of mid Silurian to mid Devonian granitoids that intrude the Connemara Metamorphic Complex in Co. Galway, western Ireland. These include the "Main Batholith" and associated "Satellite Plutons" i.e. Omey (1), Inis (2) and Letterfrack (3) Roundstone (4) plutons (Fig. 5.1).

The "Main Batholith" is composed of two distinctive parts. An oval shaped NNW-SSE oriented intrusive body, recently described as the "Western Ring Complex of the Galway Granite Batholith" (Leake 2011), forms the western portion. To the east, a larger, younger, ESE-WNW orientated oval intrusion extends from Galway City to 3km NW of Ardmore, this forms the larger portion of the Main Batholith. It is emphasised that the western part of the Main Batholith is both temporally and structurally distinct to that which occurs in the east (as previously implied by Max (1978) and Wright (1963)). The "Main Batholith" is here defined as a composite batholith of two structurally and temporally distinct parts, the earlier "Carna Pluton" (6) in the west and the adjoining "Kilkieran Pluton" (7) to the east (Fig. 5.1).

A misleading phrase used in reference to the Galway Granites is "Satellite Plutons". Satellites must have some larger body to orbit or be associated with. The prefix "satellites" implies that the plutons situated outside of the Main Batholith post date it. This is not the case (Main Batholith 410Ma - 380Ma, the "Satellite" plutons are understood to be ~ 410-425Ma ((Elias *et al.* 1988; Buchwaldt 2001; Feely *et al.* 2007; Leake 2011)). Therefore, the use of the term satellite is incorrect and unnecessarily confusing to those unacquainted with the regions geology. To address this, the author hence forth refers to the Inish, Letterfrack, Omey and Roundstone plutons as the "Earlier Plutons". This term reflects our current level of understanding, i.e. these are stand alone plutonic bodies that predate the Main Batholith, and should be used instead of former term in the future.

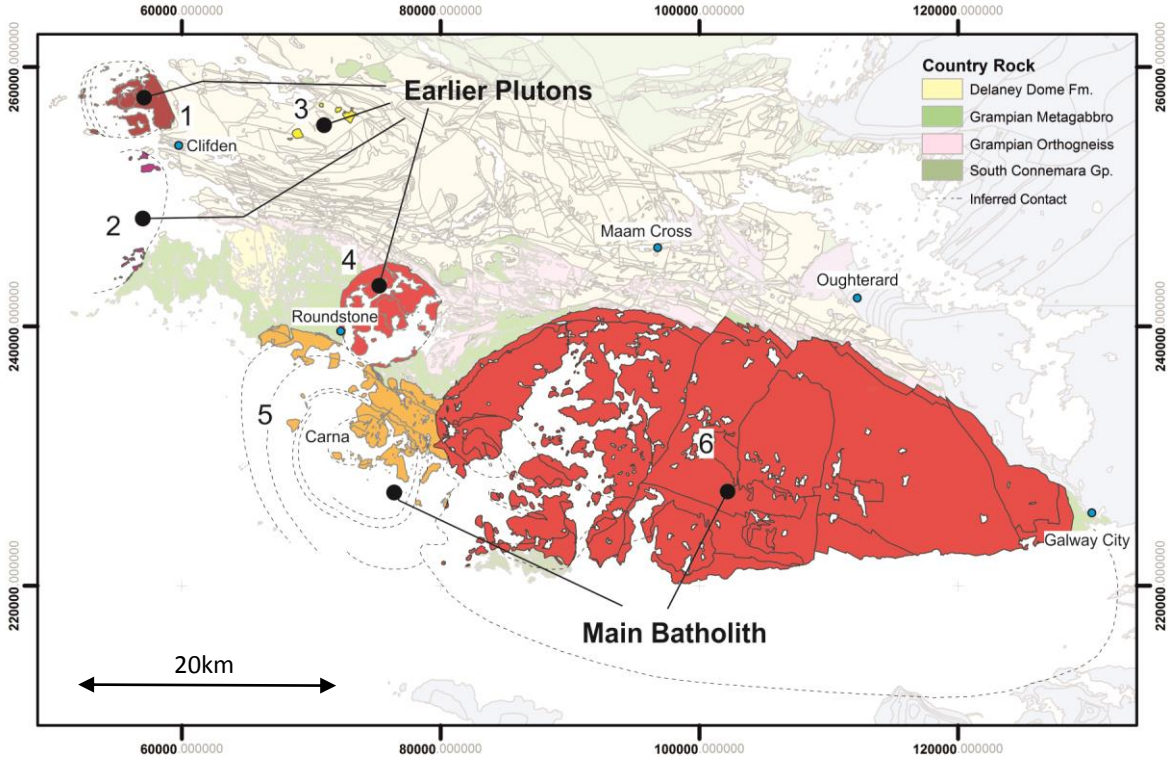


Fig. 5.1 The Siluro-Devonian Galway Granite Complex is comprised of the Earlier Plutons and the Main Batholith both of which comprise of several temporally, structurally and petrographically distinct plutons. Pluton names; 1 = Omey, 2 = Innis, 3 = Letterfrack, 4 = Roundstone, 5 = Carna, 6 = Kilkieran.

Finally, it has been clear for some time now that the Main Batholith and Earlier Plutons intruded over > 40Ma, (422Ma - 380Ma, Feely *et al.* (2010)). Magmatism initiated during the latest stages of the Caledonian Orogeny (Dewey and Strachan 2003; Soper and Woodcock 2003) and continued for 10Ma after the Acadian terminated (Woodcock *et al.* 2007). The entire suite of plutons cannot be attributed to Caledonian processes exclusively, therefore the use of the term "Caledonian Granites" carried unproven connotations regarding the tectonic and petrogenetic

origins of these granites. It suggested that the suite of Silurian to Devonian granites in Connemara be referred to as the "Galway Granite Complex" as oppose to any term which unjustifiably relates these intrusions to a specific orogenic event.

The "Galway Granite Complex" (GGC) is therefore used as an umbrella term to refer to the complex of Siluro-Devonian granitoids which occur in the Connemara region (Fig. 5.1). This suite of granites is comprised of the "Main Batholith", a composite of the "Carna Pluton" in the west and the "Kilkieran Pluton" to the east, and the "Earlier Plutons", which include the Roundstone, Omey, Inish and Letterfrack plutons.

5.3 Constituents of the Galway Granite Complex

Constituent granitoid bodies of the GGC are discussed in best estimated chronological order starting with the Earlier Plutons and concluding with components of the Main Batholith. Relevant petrographic, structural and chronological information is summarised and original descriptions in the literature referred to.

5.3.1 The Earlier Plutons

The Omey, Inish, Letterfrack and Roundstone Plutons are located north and northwest of the Main Batholith and intrude the Connemara Metamorphic Complex, these are the Earlier Plutons (Fig. 5.1). Reconnaissance mapping identified the outline of these bodies and concluded that they were most likely of metamorphic origin (Kinahan 1869; Kinahan *et al.* 1878). Subsequent structural, petrographic and geochemical work concluded a magmatic origin for these bodies (e.g. Wager (1932, 1939); Cobbing (1959); (Leggo *et al.* 1966); Townend (1966)).

Townend (1966) published the only detailed field based analysis of the Omey, Inish and Letterfrack intrusions. Aside from recognisance mapping in the 1800's (above references) the Roundstone Pluton has never been mapped in full but parts of the intrusion have been investigated separately (Morton 1964; Harvey 1967; Leake 1969; Bremner *et al.* 1980; Leake 2011).

5.3.1.1 The Inish Pluton

The Inish Pluton is located ~ 10km SW of Clifden town on the western coast of Connemara (Fig. 5.1). Exposure is extremely limited, mainland outcrops only occur within ≤ 0.5km area on the western end of Errisbeg peninsula. Small islands directly offshore and north of here on the islands of Inishturk and Turbot are almost completely composed of the Inish Pluton.

Townend (1966) documented two facies, the Inishturk Adamellite and the Inish Adamellite. The Inishturk Adamellite forms the bedrock for Inishturk and Turbot and is a medium grained biotite hornblende granite with local chilling near contact margins. The Inish Adamellite outcrops further south on the Errisbeg peninsula, this has less plagioclase than the Inishturk adamellite and no hornblende. A suite of lamprophyre dykes are mapped in the southeast corner of Turbot Island (Townend 1966). Aplitic, pegmatitic and granitic sheets are observed in Dalradian host strata on Inishturk island. Leggo *et al.* (1966) yielded an isochron age of 404 ± 8Ma from this granite, older than the average age the same paper returned for the Main Batholith (385 ± 7Ma).

5.3.1.2 The Letterfrack Pluton

The Letterfrack Pluton is exposed at three localities close to the fold axis on the northern limb of the D4 Connemara Antiform between 4km ESE and 3km SSW of Cleggan Village (Fig. 5.1). Due to limited outcrop the existing data base is minimal.

Two facies of granodiorite are described from this area, the Coarse Letterfrack Granodiorite and Fine Letterfrack Granodiorite. Petrographically these are almost identical and a distinction is made primarily on grain size and a higher abundance of K-feldspar in the latter facies (Townend 1966). The Fine Letterfrack Granodiorite typically outcrops in the cores of exposed intrusions while the coarser variety forms the outer margins. Pluton - country rock contacts dip gently outward and exhibit localised chilled margins and brecciation of the host strata. Townend (1966) concludes the three spatially distinct exposures probably form one plutonic body at depth.

5.3.1.3 The Omey Pluton

The Omey Pluton is situated 11km NW of Clifden Village (Fig. 5.1). This composite intrusion is ~ 7km in diameter and slightly elongate along an WNW-ESE axis. The long axis of the intrusion is

sited on and parallel to the axial trace of the D4 Connemara Antiform which is composed of Lower Appin Group metasediments (Cobbing 1968; Leake and Tanner 1994).

Field & Geochemistry Relationships

Townend (1966) mapped and described two major facies (Fig. 5.2). The Omey Granite is a pink coarse grained (5-10mm) biotite granite with trace amounts of hornblende. Townend (1966) recognised one sub-facies, the Barnahallia Granite, which exhibits a slightly higher modal abundance of hornblende. The Island Granite is a medium-fine grained aphyric pink biotite minor muscovite granite, it is more siliceous and has a lower strontium and higher rubidium concentration than the Omey Granite (Leggo *et al.* 1966).

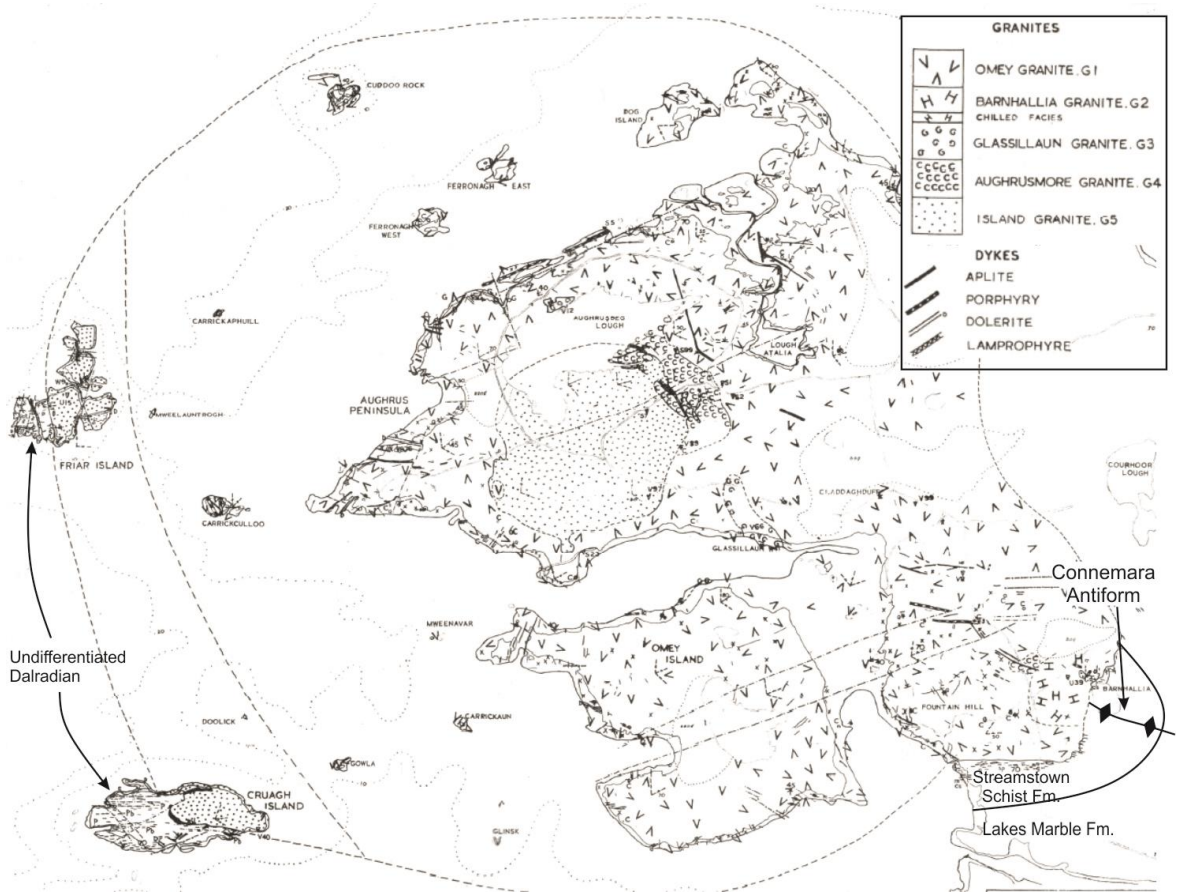


Fig. 5.2 Map of the Omey Pluton after Townend (1966). The longest axis of the pluton is parallel to the D4 Anticline and the Island Granite forms a "central plug".

Two significant subfacies are also recognised. The Aughrus More Adamellite is a pinkish gray medium grained (6mm) biotite hornblende granite. This facies is considered an intermediate between the Island and Omey facies (Townend 1966). The Glassillaun Granodiorite is described by

Townend (1966) as exhibiting a "hypidiomorphic texture which may be equigranular or inequigranular" with light pink K-feldspar tabular phenocrysts in a finer grained groundmass.

The Omey Pluton intrudes the Streamstown Schist Fm. and Lakes Marble Fm. in the east and Dalradian strata (unknown correlation) in the west off shore, contacts are described to be largely subvertical (Townend 1966). Townend (1966) reported that the contact between the Island Granite and the Omey or Aughrus More facies is always sharp and that contacts between other facies are variably sharp or gradational (attitudes not reported). Minor ENE-WSW and NNW-SSE fault sets that cross cut the pluton reported but no further detail provided (Townend 1966)

Chronological and Fluid Inclusion Data

Analysis of the intrusions metamorphic aureole has established that metamorphic conditions were 615 ± 25°C at 2.5 ± 0.25kbar in the pelitic host strata (Ferguson and Harvey 1979; Ferguson and Al-Ameen 1986) and 640 ± 20°C at 3.3 ± 0.3kbar within Lakes Marble skarn deposits adjacent to the Omey Pluton (Ahmed-Said and Leake 1996). Based on new data and that of Gallagher *et al.* (1992), Feely *et al.* (2007) suggested that molybdenite mineralisation within the Omey Pluton occurred at ~ 302-380°C at 2.5 ± 0.25 kbar. Therefore, this is a epizonal granite.

The age of the Omey Pluton was first constrained by Leggo *et al.* (1996) who determined a Rb-Sr whole rock analysis age of 388 ± 17Ma for the Island Granite. Elias *et al.* (1988) obtained K-Ar age from a contact aureole biotite that implied cooling initiated before 412 ± 8Ma. This deduction was supported with U-Pb single zircon data which indicates the Island Granite crystallised ~ 420Ma (Buchwaldt 2001). Most recently fluid inclusion studies and isotopic data from quartz-molybdenite stockwork veins suggest mineralisation occurred at 422.5 ± 1.7Ma, soon after crystallisation of the host granite (Feely *et al.* 2007). These data suggest that Omey is the oldest intrusion in the GGC and magma ingress was temporally coincident with regional transpression (Dewey and Strachan 2003).

5.3.1.4 The Roundstone Pluton

Technically this intrusion is a composite part of the Main Batholith as it shares an intrusive contact with the northeast corner of the Carna Pluton (Fig. 5.1). However, the Roundstone Pluton is considered to predate the all facies of the Main Batholith (Harvey 1967; Feely *et al.* 2006; Feely

et al. 2010; Leake 2011) and has an outcrop pattern totally independent of either the Carna Pluton or the Kilkieran Pluton, it is therefore considered part of the Earlier Plutons.

Field Relationships

Geological maps of the Roundstone Pluton show this to be a circular, fault bound, petrographically homogenous granodiorite (~ 8km diameter) with peripheral concentric fabric development (Harvey 1967; Leake 1969; Leake 2011). One sub-facies (slightly more siliceous and foliated) is mapped within a few hundred meters of the country rock (Leake 1969).

The Carna Pluton is in contact with the Roundstone Pluton in the southwest, in all other areas this granitoid intrudes the Connemara Metamorphic Complex. The attitude of host rock fabric to the pluton varies but a steep faulted or stoped contact is always observed (Morton 1964; Leake 1969; Evans and Leake 1970; Bremner *et al.* 1980; Downs-Rose 1985). Minor garnetiferous aplitic and pegmatitic sheets occur within 300m from the pluton-country rock contact (Leake 1969). A weak contact-parallel subvertical silicate fabric has been recognised around the outer margins (Leake 1969). A series of minor faults and residual melt aplitic sheets as well as late stage plagioclase-phyric porphyry and lamprophyre dykes, that penetrate the host strata, are also documented within the pluton (Harvey 1967; Leake 1969).

Leake (1969) regards brittle deformation of the bounding wall rock and subtle contact parallel silicate fabrics as evidence of "upward movement of the nearly solid magma". Based on the very rare occurrence of stoped blocks within the pluton and small scale granitic sheets within the country rock, Leake (2011) suggests stoping had a significant role to play during emplacement.

Geochronology

Leggo *et al.* (1966) obtained a 395 ± 80Ma age of crystallisation from the Rb-Sr whole rock analysis of the Roundstone Granite. This is the only existing absolute chronological data for this intrusion.

Leake (2011) mapped a high concentration of northwest-southeast aplitic sheets in close proximity to the Carna-Roundstone contact (20m exposed) and argued that southwest-northeast opening, that facilitated emplacement, was caused by the intrusion of the Carna Pluton to the southeast, therefore relatively dating the Roundstone Granodiorite as pre-Carna (410Ma, Selby *et al.* (2004)). However, expansion of the Carna Pluton would cause compression along northwest-

southeast veins not opening. Furthermore, earlier work shows these late stage sheets are not exclusively related to proximity to the Carna Pluton contact (Harvey 1967; Leake 1969).

The relative dating hypothesis of (Leake 2011) is rejected. Due to the large margin of error returned by Leggo *et al.* (1966) the assumption that the Roundstone Pluton predates the Main Batholith and intruded as part of the Earlier Plutons can neither be confirmed nor rejected.

5.3.2 The Main Batholith

The first geological maps of the Main Batholith were published by the Irish Geological Survey following recognisance field work between 1860-1870. These identified the outline of the intrusion and a foliated northern margin (Kinahan 1869; Archer 1980).

The Main Batholith dominates the bedrock geology of the Galway Bay area. The batholith formed during episodic emplacement of mafic and felsic material into the Connemara Metamorphic Complex (Leake and Tanner 1994) in the north and the South Connemara Group (Williams *et al.* 1989; Ryan and Dewey 2004) in the south during the early to mid-Devonian (Pidgeon 1969; Buchwaldt 2001; Feely *et al.* 2003; Selby *et al.* 2004). The batholith is comprised of two distinctive parts, the earlier Carna Pluton in the west and the Kilkieran Pluton to the east (Fig. 5.1). Together these form an ESE-WNW orientated oval batholith (~ 22x27km) that extends south under Galway Bay where it stitches the east-west striking Skird Rocks Fault (Murphy 1952; Max *et al.* 1983) and has an approximate total surface area of 1300km^2.

5.3.2.1 The Carna Pluton

The Carna Pluton is a composite elliptical intrusive body (~ 17x12km) with a NNW orientated long axis that is crudely parallel to the NNW-SSE Clifden - Mace Fault (CMF) which cross cuts the central axis of the intrusion. Approximately 60-70% of the intrusion lies under the Atlantic Ocean, the remaining 30% is reasonably exposed in the Carna-Mace Head area, at Dog's Bay west of Roundstone Village and on the islands which lie several kilometres offshore in Galway Bay (Fig. 5.3).

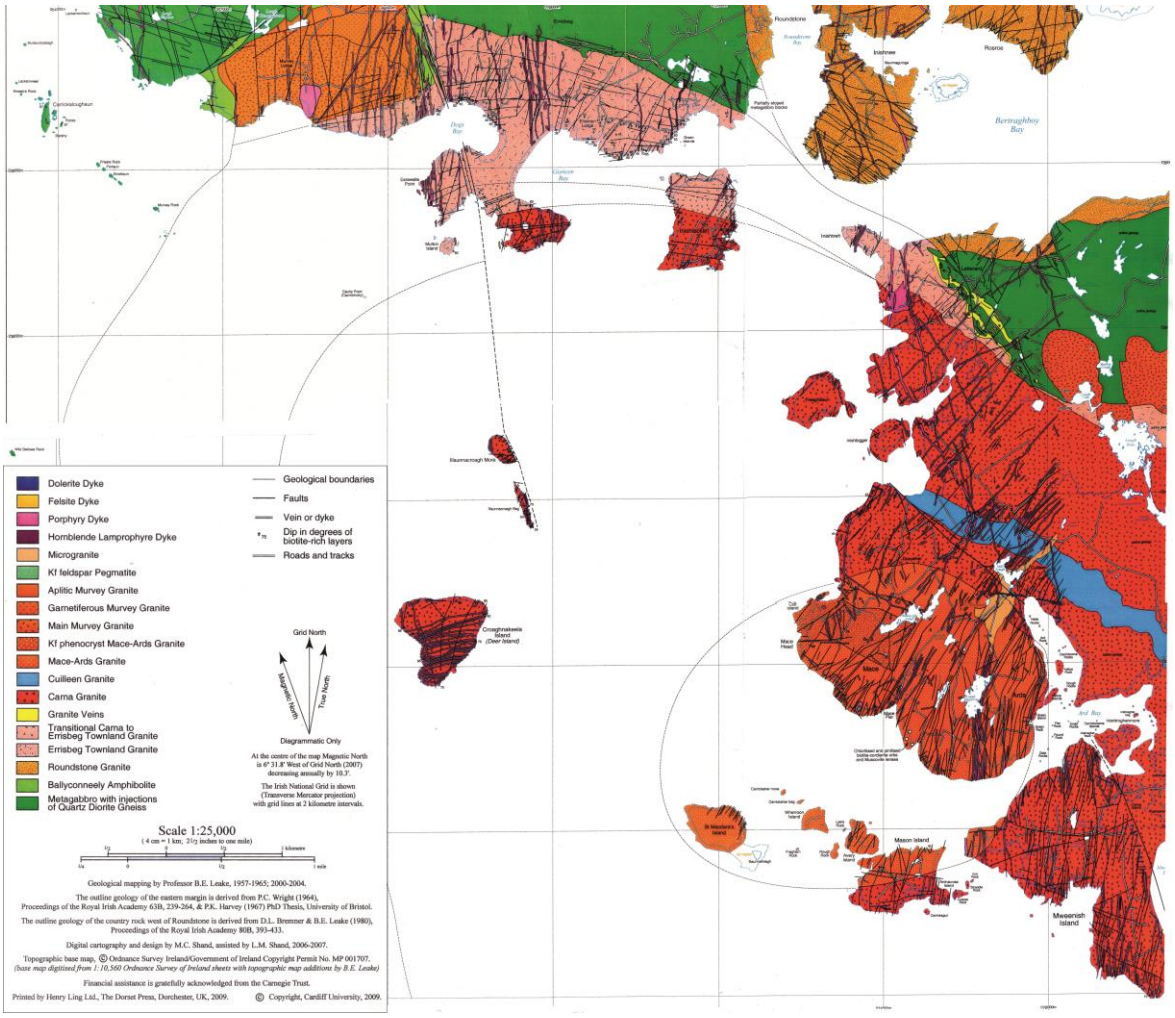


Fig. 5.3 Geological Map of the Carna Pluton (from Leake (2011)). This intrusion is interpreted by Leake (2011) as a central ring complex emplaced via stoping and without the influence of tectonic processes.

Field Relationships

Geological mapping demonstrates that the pluton intrudes metagabbro of the Connemara Metamorphic Complex (CMC) in the north and east (Wager 1932; Wright 1963; Harvery 1967; Leake 1969; Evans and Leake 1970; Bremner *et al.* 1980) and the Roundstone Pluton in the northeast. The contact between the Carna and the Kilkieran pluton is very poorly exposed and no definitive contacts between these have been recognised as of yet (Wright 1963; Leake 1974a; Leake 2011). This is largely due to the similarities between the outer facies of both intrusions in this area (both K-feldspar megacrystic granites both called Errisbeg Townland Granite, distinguishable on texture). The southeast margin of the Carna Pluton is extrapolated by extending the mapped country rock contact southeast parallel to internal facies contacts and northwest-southeast oriented faults which propagate from the country rock and cross cut the Main Batholith in this area (Figs. 5.1 & 5.3).

Early work focused on the petrology of the intrusion (Wager 1932; Wright 1963; Leake 1974b). Leake (2011) defined five facies, the Errisbeg Townland Granite, Carna Granite, Cuilleen Granite and two varieties of Mace-Ards Granite (porphyritic and non-porphyritic). All major facies are biotite hornblende granites which are distinguished based on minor mineral abundances and texture (full descriptions in Leake (2011)).

In addition the Roundstone Murvey Granite (Wright 1963) outcrops on the north of the pluton and the K-feldspar Breccia and several minor late stage microgranite facies are mapped in the core of the intrusion (Derham and Feely 1988). The Roundstone Murvey Granite is a 3mm aphyric biotite hornblende leucogranite with two subfacies, aplitic granite and garnetiferous granite (full descriptions in Leake (2011).

A concentric pattern is defined by facies distribution, this is concordant to the intrusion's bounding margin which dips moderately outwards from the core of the pluton (Leake 2011). Facies contacts are generally gradational, usually over 5-20m, and are orientated parallel to external contacts (Feely *et al.* 2006; Leake 2011). Late stage minor facies exhibit sharp contacts as does the Murvey and Errisbeg Townland Granite contact.

Contact parallel faults in the metagabbro country rock on the southern flank of Errisbeg Hill are associated with continued inflation of the pluton (Leake and Tanner 1994), unfortunately no shear sense indicators (e.g. Hutton (1988)) have been recovered from these. Leake (2011) recorded several examples of stoped blocks along the northern and eastern pluton margins.

A subtle contact parallel foliation is noted in very close proximity to the external contact (Leake 2011). Coeval Micro-granular mafic enclaves in the Murvey Granite occur in close proximity, and are parallel to the pluton-concentric ETG contact (Wright 1963). Wright (1963) first documented a suite of biotite fractionation layers within the ETG and Carna Granite facies which are orientated parallel to the pluton's external contact and dip moderately to steeply outwards. Thus, while little detailed examinations have been made it seems apparent that a sub-magmatic concentric foliation is present which parallels both internal and external contacts.

The Clifden-Murvey Fault cross cuts and sinistrally offsets the northern margin of the Carna Pluton by ~ 650m (Fig. 5.3). This structure pre-dates the Carna Pluton and is related to several NNW-SSE faults which cross cut the contact between the Carna Pluton and Kilkieran Pluton and extend into the country rock to the north (D5 faults Chapter 3).

Quartz stockwork veining hosts Mo-Cu chalcopyrite-pyrite-pyrrhotite mineralisation at Mace Head, this is associated with several late stage microgranite and K-feldspar intrusions (Derham

and Feely 1988; Feely and Högelsberger 1991; Selby *et al.* 2004). This mineralisation is located at the core of the intrusion, close the predicted intersection of the Skird Rocks Faults and numerous NNW-SSE D5 faults (Bluck *et al.* 1992; Long and McConnell 1995a; Ryan *et al.* 1995).

Geochronology and Fluid Inclusions

Direct dating of facies within this pluton is limited to the work of Pidgeon (1969) who suggested a 420 ± 20Ma age of crystallisation for the entire pluton. This is within statistical error of the averaged whole rock Rb/Sr age published for the entire batholith by Leggo *et al.* (1966) (407 ± 5Ma). While a crude correlation may exist, such methodologies are unsuitable for distinguishing the temporal relationships between inter-plutonic facies in this case (Leggo *et al.* 1966).

Selby *et al.* (2004) obtained four Re/Os molybdenite ages from the Carna Pluton, two from disseminated mineralisation in the Roundstone Murvey Granite (410.8 ± 1.4Ma, 410.5 ± 1.5Ma) and two from stockwork mineralisation at Mace Head (407.3 ± 1.5Ma, 407.3 ± 1.5Ma). Feely and Högelsberger (1991) show that mineralisation at Mace Head occurred during initial cooling of the host granite at pressures between 1.2-2kb and between 360-450°C (Gallagher *et al.* 1992). This data is the most accurate proxy for the crystallisation of the Carna Pluton.

Existing Models

The gradational nature and subtle modal variations that are characteristic of this pluton implies facies emplacement occurred in close succession (Wright 1963; Leake 2011). Chronological data support this but reflects the secondary process of mineralisation and not, directly, the crystallisation of magma.

Consistently outward dipping, contact parallel biotite layers may suggest that a ballooning or diapiric emplacement model may be applicable. A geometrical and spatial relationship between the D5 northwest-southeast faults and the orientation of the Carna Pluton is also apparent but has remained un-investigated by previous workers. Furthermore, the pluton is also centred over the intersection of the Skird Rocks Fault and Clifden Mace Fault.

The occurrence of stoped blocks reflect a material transfer process that occurred during emplacement (Paterson and Fowler 1993) and not a space generating or emplacement mechanism for intrusion (Hutton 1996). Despite this, Leake (2011) suggests emplacement was controlled by magmatic processes alone and that local structures and tectonic stress had no role (Leake 2011). The lack of data pertaining to the internal architecture of the pluton and its relationship to the surrounding terrane impedes further development of this hypothesis.

5.3.2.2 The Kilkieran Pluton

Max *et al.* (1978) published the first synopsis of early work on the Main Batholith and referred to the current area as the "Kilkieran East Pluton". Here this term is abbreviated to "Kilkieran Pluton".

The long axis of the oval shaped Kilkieran Pluton strikes 110° and extends from Galway City to the eastern margin of the Carna Pluton in the west (Fig. 5.1). At least half of the intrusion is exposed along the northern shores of Galway Bay, the remaining portion is completely unexposed under the bay and is identified via geophysical means (Murphy 1952; Max *et al.* 1983; Madden 1987).

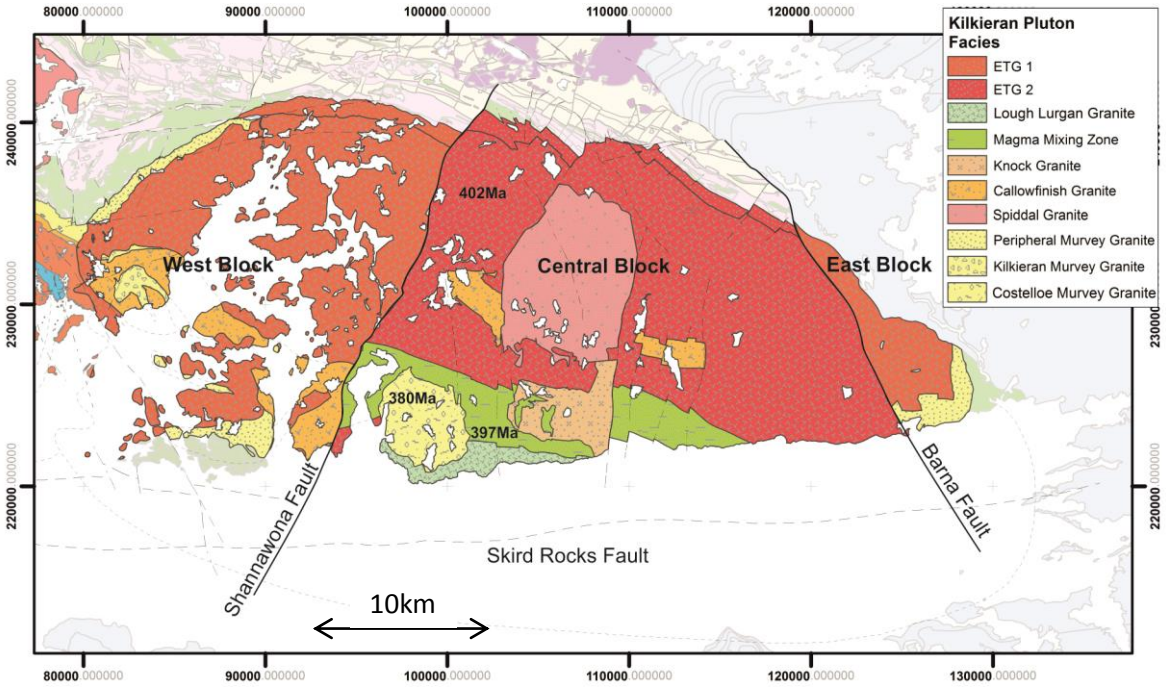


Fig. 5.4 Map of the Kilkieran pluton illustrating the fundamental structure and cross cutting relationships established by the authors referred to in the text. Map redrawn based on Long and McConnell (1995b) and the work referred to in the text. Geochronology shows oldest and youngest constituents of the Kilkieran Pluton as well and the age of the MMZ (from Feely *et al.* (2003)).

The Kilkieran Pluton (Fig. 5.4) is subdivided into the Western, Central and Eastern Blocks separated by the southwest-northeast Shannawona Fault Zone (SFZ) and the northwest-southeast Barna Fault (BF) in the west and east respectively (Max *et al.* 1978). These major faults are understood to be a result of the upward displacement of the central block relative to the east and western blocks during construction of the pluton (Plant 1968; Leake 1978; Leake and Said 1994). Geobarometry studies and detailed field mapping (Callaghan 1999, 2005) show that the central

block is ~ 3.5km thinner and crystallised at a greater depth (1kb deeper) than equivalent granite on opposite sides of the SFZ and BFZ and thus support the hypothesis that the central block has been up-faulted. As such a broader spectrum of facies heterogeneity is observed in the Central Block (diorite through granite to alkali feldspar granite, see Plant (1968); Feely (1982); McGloin (1988); El-Desouky (1992); Crowley (1997); Callaghan (1999); Baxter (2000); Leake (2006)) than in the Western and Eastern Blocks (granite to alkali feldspar granite see Wager (1932); Leggo (1963); Wright (1963); Claxton (1965); Aucott (1966); Wilson (1969); Coats and Wilson (1971)) as this reflects a deeper level in the intrusion.

Field Relationships

Owing to the detail in which this area has been studied a large number of facies and sub-facies are documented (see above references). For simplicity the Kilkieran Pluton can be summarised as having 7 facies; Errisbeg Townland Granite (ETG), Magma Mixing Zone (MMZ), Callowfinish Granite (CWG), Shannapheasteen Granite (SPG), Lough Lurgan Granite (LLG), Knock Granite (KKG) and Murvey type granite (descriptions in Wager (1932); Feely *et al.* (1991); El-Desouky *et al.* (1996); Crowley and Feely (1997) and Baxter and Feely (2002)).

ETG forms the bulk of the Kilkieran Pluton and is petrographically identical to the ETG of the Carna Pluton except that it contains larger K-feldspar phenocrysts. The MMZ (or banded zone (Max *et al.* 1978)) forms the central axis of the pluton and constitutes hybridised sheets of shear out diorite-tonalite-granodiorite facies. This is broadly accepted to represent the zone which directly overlies the conduit along which magma ascended to form this pluton i.e. the Skird Rocks Fault (Leake 1974a; El-Desouky *et al.* 1996; Crowley and Feely 1997; Baxter *et al.* 2005; Leake 2006).

The Murvey type granite is recognised at several locations around the Main Batholith. The *Roundstone Murvey Granite* (RMG), of the Carna Pluton, was first recognised by Wager (1932). Subsequently a narrow strip of Murvey type Granite was mapped along the northern (Aucott 1966) and eastern (Coats and Wilson 1971) margins, and the *Kilkieran Murvey Granite* (KMG) along the southern margins (Lawrence 1968; Giles 1980), of the Kilkieran Pluton. The *Costelloe Murvey Granite* (CMG) is the largest body of Murvey type granite and forms a standalone pluton which sharply cross cuts the MMZ and LLG in the Central Block (petrographic and REE data in Feely *et al.* (1991)). Isotopic analysis demonstrates these to be temporally distinct magmas, for example the KMG is at least 10Ma older than the CMG (Feely *et al.* 2003; Feely *et al.* 2010). Buchwaldt (2001) considers the CMG a magma completely distinct to that of other facies of the GGC and suggested it to be a product of re-melting of earlier facies by ascending mantle material.

A strong 120° subvertical gneissic fabric is present in the metagabbro and quartz diorite country rock on the northern and eastern margins of the Kilkieran Pluton. This fabric is related to Grampian orogenic processes (Leake 1989; Leake and Tanner 1994), no significant ductile deformation recorded in this host strata is associated with the emplacement of the Kilkieran Pluton. A suite of contact parallel small scale brittle faults are noted within 10km north of the batholith, these are attributed to magma emplacement (Leake and Tanner 1994). Several stoped blocks have been mapped along the northern and western margin however very few examples are reported in the batholiths interior (Leake 2006).

Hybridised elongate mafic enclaves are noted throughout the pluton, these parallel magmatic to submagmatic fabrics in the host granite and show an increase in anisotropy and axis ratios toward the northern margin of the pluton (e.g. Claxton (1965); Wilson (1969); Leake (2006)). No shear sense is determined and fabrics are moderate-steeply inclined outwards and are contact parallel. Baxter *et al.* (2005) showed that this co-axial fabric development was a product of continued plutonic inflation during episodic injection of magma i.e. ballooning.

A strong WNW-ESE oblate fabric is pronounced throughout the MMZ, this foliation parallels the 110° strike of these intrusions, the long axis of the pluton and the pre-solidus fabric of the ETG immediately to the north (Baxter 2000; Baxter *et al.* 2002; Baxter *et al.* 2005). These are interpreted as magmatic state fabrics which record less strain with increasing proximity from the MMZ central axis. El-Desouky *et al.* (1996) identified a west directed laminar flow within these composite sheets and inferred emplacement of magma progressed in a westward direction across the Main Batholith.

Geochronology

Crowley and Feely (1997) established a temporal relationship between the main facies of this Pluton and proposed the following sequence of emplacement; ETG was followed by the MMZ which was x-cut by LLG, CFG and LFG which were followed by the KKG and finally the CMG which was emplaced at 380.1 ± 5.5Ma (Feely *et al.* 2003).

These deductions are supported by U-Pb zircon data (some data on Fig. 5.4) which demonstrates crystallisation of the ETG = 394.4 ± 2.2Ma - 402Ma; MMZ between 397.1±1.1Ma - 399.5 ± 0.8Ma; CMG at 380.1 ± 5.5Ma (Feely *et al.* 2003). More recently Re/Os molybdenite data indicates that the LLG (399.5 ± 1.7Ma) may have been intruded prior to the MMZ (383 ± 1.1) (Feely *et al.* 2010). These data ultimately show that the vast majority of the Kilkieran Pluton was

emplaced and crystallised between ~ 402-396Ma and that the latest phase, the CMG, intruded some 15Ma later Feely *et al.* (2010).

Existing models

The Skird Rocks Fault has long been considered a controlling structure to the Kilkieran Pluton (Leake 1974a; Max *et al.* 1978; Madden 1987). Following a geophysical investigation Ryan *et al.* (1995) proposed that siting of the pluton was facilitated by an extensional duplex structure along the Skird Rocks Fault (SRF) bound to the east and west by northwest-southeast conjugate Reidel shears. El-Desouky *et al.* (1996) argued that any feasible model must provide for some form of mantle driven magmatism and account for the structural deformation observed within the batholith and devised a crustal pull apart model bound by a northwest-southeast dextral shear couple i.e. the Maam Valley and Clifden Faults (Fig. 5.5).

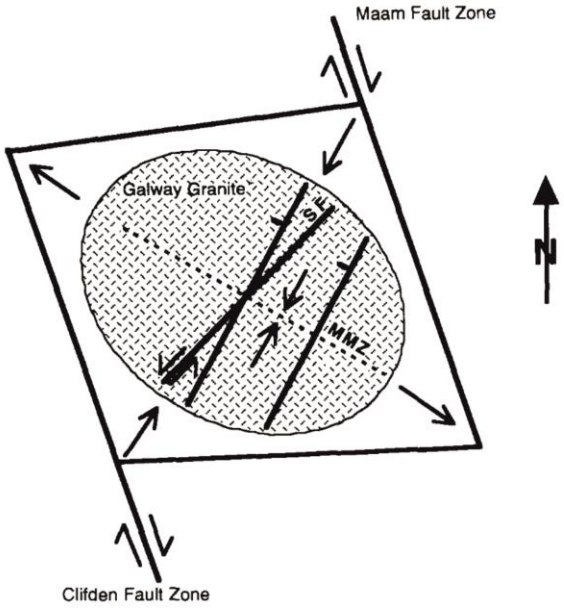


Fig. 5.5 Schematic model for the emplacement of the Main Batholith (Kilkieran Pluton and Carna Pluton) as proposed by El-Desouky *et al.* (1996). In this model, space for magma ingress was created by dextral shearing along the Clifden Fault and Maam Fault which acted as bounding translation faults to a crustal pull apart. El-Desouky *et al.* (1996) suggested that the MMZ intruded parallel to the compressive axis of the batholith and the Shannawona Fault (SF) cross cut the core of the pluton as a left lateral dip slip release structure.

This interpretation was widely accepted, Crowley and Feely (1997) added that late stage intrusions (LLG, CMG et*c.*) ascended along the SRF and were then emplaced via stoping of the previously emplaced MMZ and ETG and ballooning. Baxter *et al.* (2005) assessed silicate, enclave and magnetic (Baxter 2000) fabrics and also concluded in favour of El-Desouky *et al.* (1996) however, contrary to the former author, Baxter *et al.* (2005) suggested that ascent was achieved at the intersection of the SRF and Clifden-Mace Fault (CMF) to the west (despite returning co-axial fabrics). Such an interpretation fails to recognise that the Carna Pluton is an independent intrusive body distinct from the Kilkieran Pluton (Max *et al.* 1978).

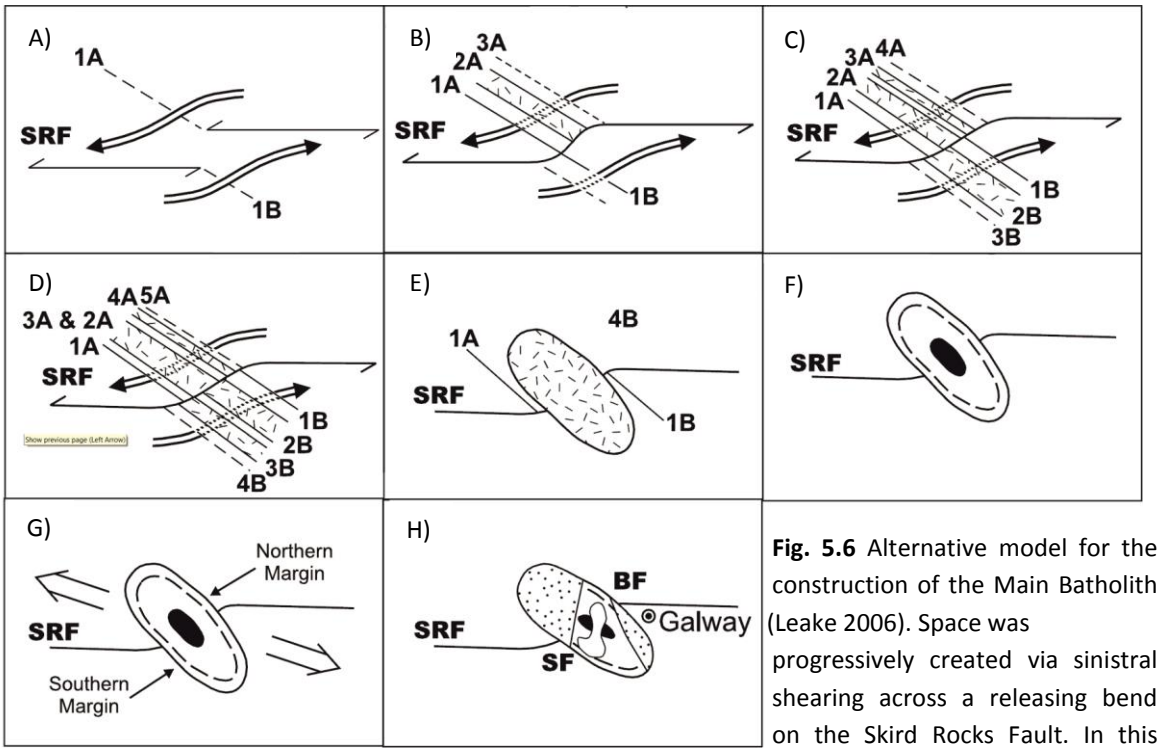


Fig. 5.6 Alternative model for the construction of the Main Batholith (Leake 2006). Space was progressively created via sinistral shearing across a releasing bend on the Skird Rocks Fault. In this model, a jog on the SRF partitions stress preferentially onto the 120° host rock fabric which ultimately opens a series of WNW-ESE dilation zones into which magma intrudes (A-D). Shearing along the SRF terminates at (E) but magma ingress continues forcing a marginal concentric oblate fabric to develop (F). Sinistral transtension facilitates late stage aplite dykes to emplace (G) and finally the cover is eroded to the current exposure level (H).

Leake (2006) rejected a crustal pull apart model (El-Desouky *et al.* 1996) as neither of the cited structures show sufficient displacement of the country rock strata required for such a model. Leake (2006) suggests opening of ESE-WNW extensional fractures resulted from bifurcation of the SRF along an orogenic releasing bend during regional sinistral transtension (Fig. 5.6) Emplacement was controlled by the stoping parallel to the 110° strike of the metagabbro and orthogneiss country rock and upward displacement of the central block by buoyancy of under plating highly siliceous magma (Leake 2006).

5.4 Summary and Objectives

Large scale petrogenetic models discussed above are readily applicable to most Newer Granites in Britain and Ireland. The Galway Granite Complex comprises a suite of granitoids which intruded throughout the final convergence of Avalonia and Laurentia, regional strike slipping and the Acadian Orogeny. No similarly distinguishable suite of intrusions in Britain and Ireland emplaced over such a protracted period within a single tectonic terrane (Brown *et al.* 2008;

Neilson *et al.* 2009). By this qualification the GGC is unique and offers the opportunity to assess the evolution of magmatism through the late-Silurian to mid-Devonian.

As discussed much of the principal traits of the Galway Granites indicate this to be part of the Northern Granite suite however much of the Kilkieran Pluton intruded quite late and the Costelloe Murvey Granite is temporally incompatible with petrogenetic models associated with the Northern Granites. Conversely, the entire complex is located too far north to be associated with the Trans-Suture Suite. More stringent controls are required over the inherent structural and geochemical characteristics of the GGC before they may be associated with and contribute to regional scale kinematic and petrogenetic models. The current work focuses on the structural characteristics of the GGC and attempts to identify a temporally consistent internal evolution which may be related to the regional scale kinematic evolution of the Caledonides from 425-380Ma.

A substantial data base has been compiled on the structural, geochemical and temporal characteristics of the Kilkieran Pluton but very little on the Carna Pluton. The most recent work that reports on the structural features of the Earlier Plutons was carried out between three and five decades ago. It follows that there is a stark contrast between data pertaining to different members of the GGC. Several tectonic models have been devised for the Kilkieran Pluton but only a single hypothesis has been suggested for the Carna Pluton and no author has assessed the structural controls over any of the Earlier Plutons.

The mechanical factors which controlled the development of the constituents of the Earlier Plutons are unconstrained and so the structural relationship between these and the Main Batholith is not understood. As a consequence, the unique tectonic position of the GGC is underutilised as a regional kinematic indicator. The GGC offers an opportunity to assess the evolution of the local stress field dynamic during late Caledonian lockup and the Acadian Orogeny. Such an assessment has the potential to provide new information on the regional scale kinematic evolution throughout the period over which these granites were intruded and thus contribute in a meaningful way to the study of orogenic kinematic evolution. The current work seeks to address this issue.

5.4.1 Key Questions

The first objective of the current work is to obtain and assess data from the Omey, Roundstone and Carna Plutons to evaluate the internal architecture of these intrusions. This will represent the first detailed structural analysis of these granitoids and specifically aim to relate the structure of these plutons to established mechanisms of ascent and emplacement. The plutons have been selected as they are better exposed relative to the other Earlier Plutons and limited information is currently available that pertain to the structure of these bodies relative to the Kilkieran Pluton. Therefore these intrusive offer an opportunity to carry out innovative investigative work.

A second objective is to determine if a structural relationship exists between the Earlier Plutons and the Main Batholith and, if so, whether a temporally consistent continuum exists between magma conduits, pluton architecture and local structure in the Connemara region. An adequate volume of data exists for the Kilkieran Pluton and it is envisaged that sufficient data will be generated from the Omey, Roundstone and Carna Plutons to facilitate such a comparison.

The final objective and ultimate goal of this project is to determine if local controls over the siting and emplacement of plutons can be related to far field regional stress fluctuations. Regional differential stress is manipulated and re-orientated on a local scale by anisotropies in the crust which in turn react to the applied stress. At the same time, magma in the crust tends to exploit pre-existing anisotropies as conduits during migration and will preferentially exploit those structures suitably orientated within the local stress field. If follows that with reorientation of a regional stress field local magma conduits may no longer be preferably orientated and new structures may open to facilitate ascent and emplacement along different trajectories. In this way granitoid bodies may be used to evaluate the kinematic evolution of regional stress field during orogenesis. The protracted period of magmatism recorded in Connemara during Caledonian lockup and Acadian Orogenesis facilitates such an undertaking.

Chapter 6:

A Review of Applied Theory

6.1 Introduction

This project assesses the temporal relationship between fabric development in granitoid bodies and regional stress fields. Field mapping, petrographic and anisotropy of magnetic susceptibility (AMS) fabric analysis and rock magnetic experiments are employed as the main sources of data. Geochronological data has also been obtained to supplement and evaluate the existing chronological data base on the Galway Granite Complex (GGC).

Geochronological procedures are detailed in Section 6.2. Section 6.3 deals with rheology and the microstructural investigation of granitoids. Section 6.4 discusses traditional methods for strain evaluation. Section 6.5 summarises the main concepts surrounding the AMS. Section 6.6 introduces the rock magnetic experiments used in this thesis to evaluate the magnetic mineralogy of AMS samples. Supplementary information on rock magnetic principals is provided in Appendix D. Analytical procedures for all rock magnetic experiments are provided in Appendix B. Notes on and copies of open source software used are contained in Appendix F.

6.2 Geochronology

Absolute age determinations of facies from the Roundstone and Carna Plutons are presented as part of this thesis. Compiled with data from earlier authors (Feely *et al.* 2010), these data place the studied plutons in context relative to the other members of the GGC and also to that of the broader Siluro-Devonian kinematic framework.

U-Pb dating of accessory zircon was targeted as the chosen chronometer in order to obtain the age of crystallisation of selected granitoid samples. The U-Th-Pb system was selected owing to the slow diffusion rates exhibited by parent and daughter isotopes (Dickin 2005). The tendency for U to become concentrated and Pb to be excluded during the crystallisation of zircon makes this an ideal target mineral for U-Pb work (Dickin 2005).

A range of U-Pb techniques are now available including thermal ionisation mass spectrometry (TIMS), laser ablation inductively coupled plasma mass spectrometry (LA-ICP-MS), secondary high resolution ion-microprobe (SHRIMP), electron microprobe, conventional isotope dilution and single zircon grain evaporation (methods reviewed in de Laeter (1998); Becker (2005); Ireland (2013)). Thermal ionisation mass spectrometry (TIMS) was chosen as a first choice analytical method owing to the superior precision and accuracy offered by this technique

relative to other methods for the age range expected from samples examined in the current study (Roddick *et al.* 1987; Heumann *et al.* 1995). However, a preliminary study, carried out in the National Centre for Isotope Geochemistry at UCD, returned anomalous results among standard samples. This was attributed to calibration issues with the mass spectrometer which rendered further work using this method infeasible at this time.

Inductively coupled-plasma mass spectrometry (ICP-MS) (Houk 1986) facilitates the measurement of parent - daughter isotope ratios by ionising a sample from solution to produce a stable and consistent ion beam which can then be fed through a magnetic sector (Burgoyne and Hieftje 1996) or quadrupole (Paul and Steinwedel 1953; Douglas 2009) mass spectrometer in a reproducible manner (Lee and Halliday 1995; Blichert-Toft *et al.* 1997). Linear quadrupole mass spectrometers lack stability relative to magnetic sector spectrometers. However, the U-Pb system exhibits a large natural range in isotope compositions and so this less precise quadrupole mechanism of analysis may still be utilized in U-Pb dating (Ireland 2013).

The process of dissolving a sample may be bypassed and in situ analysis of zircon can be carried out from a polished sample or resin mounted separated zircons (to avoid contamination) by mating a laser ablation source to an ICP-MS apparatus (Arrowsmith 1987). A simplified plan of the apparatus used is presented below (Fig. 6.1). During laser-ablation inductively coupled-plasma mass spectrometry (LA-ICP-MS), a portion of a targeted sample is ablated using a laser and the dissociated sample is transported by a carrier gas (noble gas) from the sample site. The gas is then converted to a plasma which ionises the sample which is then fed through the ICP-MS apparatus for analysis (Koch and Gunther 2011). A major advantage of this system is that targeted sections of the individual mineral can be sampled, thus obtaining information from parts of a crystal to avoid inherited cores, disrupted margins or metamictic zones within, for example, an individual zircon. The first lasers were 1064nm (Feng *et al.* 1993), these required larger sample areas and were also associated with undesirable fracturing and thermal modification to the host crystal. It is desirable to use lasers with shorter wavelengths and smaller better defined spots to achieve ablation via bond-breaking within the targeted mineral to avoid thermal issues that lead to fracturing and melting of the sample (Eggins *et al.* 1998). Spot diameters currently available is on a scale of ~ 5-30nm, these achieve better resolution data to be collected from individual grains (Koch and Gunther 2011).

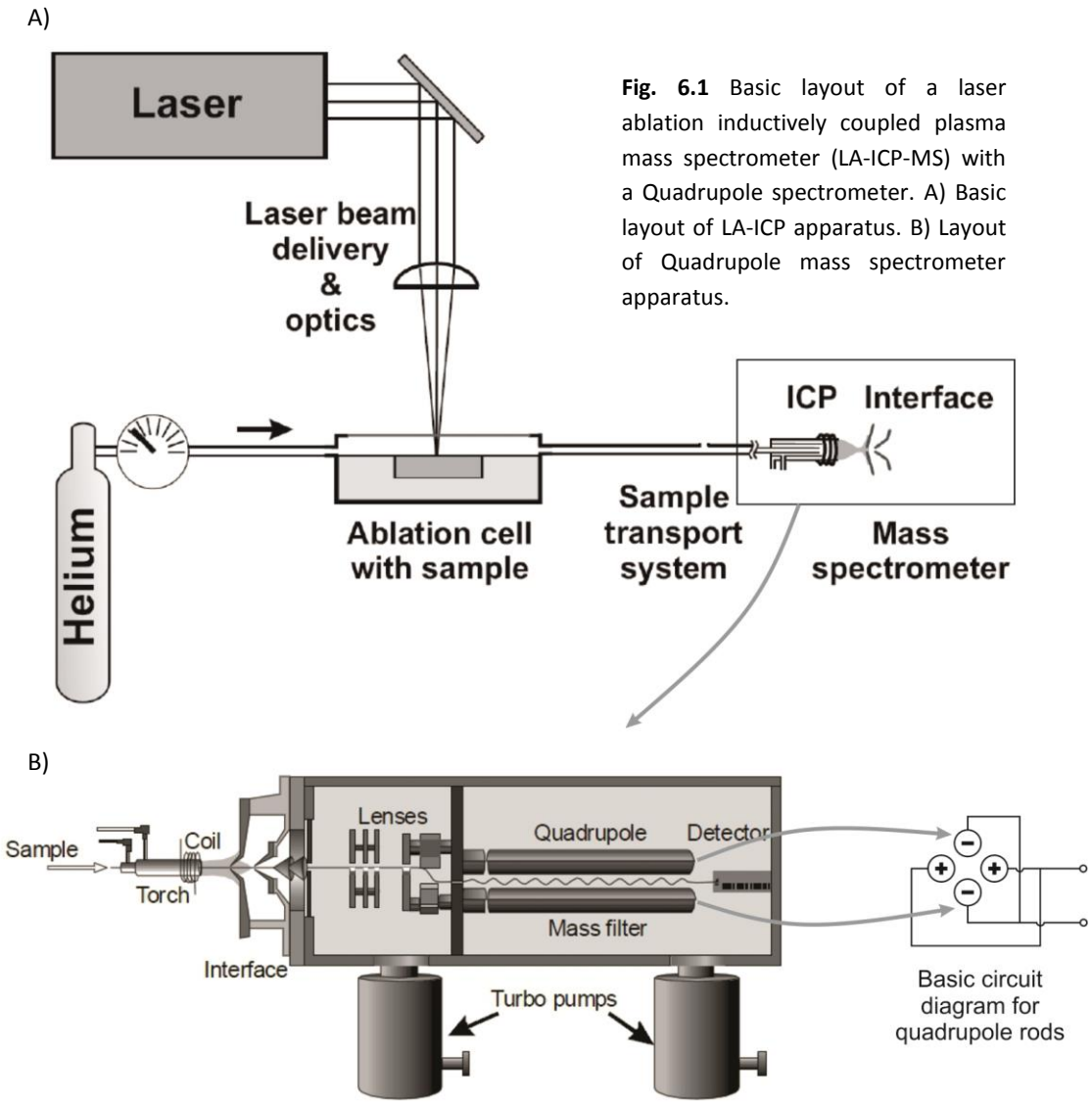


Fig. 6.1 Basic layout of a laser ablation inductively coupled plasma mass spectrometer (LA-ICP-MS) with a Quadrupole spectrometer. A) Basic layout of LA-ICP apparatus. B) Layout of Quadrupole mass spectrometer apparatus.

LA-ICP-MS is broadly applied to U-Pb geochronology owing to improvements regarding the accuracy and precision of this method as well and the potential to obtain multiple data points which traverse a single crystal (Guillong 2004; Jackson *et al.* 2004; Ding *et al.* 2006; Koch and Gunther 2011). In this study U-Pb zircon LA-ICP-MS is carried out in order to determine the age of crystallisation of various granitoids. Here, it is important to avoid potentially inherited cores, metamictic zones in crystals and late stage modified zones of the crystal due to deuteric or mineralisation processes in the granite where possible. This method facilitates this type of analysis in a timely and economically efficient manner relative to other methods such as SHRIMP or SIMS and provides both the accuracy and precision required. As such this technique is determined to be an ideal method to obtain U-Pb isotope age determinations from accessory zircons.

6.2.1 Analytical Process

Samples preparation and analysis procedures are detailed below. Sample preparation was carried out by the author while processing through the LA-ICP-MS apparatus and data manipulation was carried out by Prof. Q. Crowley of Trinity College Dublin. Final age determinations were made by both parties in the context of field relationships and magnetic data complied during the current work. All separation and analytical work was carried out in Trinity College Dublin.

Block samples (20-25kg) were thoroughly washed to avoid contamination from loose sediments. Samples were crushed and the grain size progressively reduced to a maximum of 5mm via successive reduction of the aperture between pulsating crushing plates in a Retsch BB200WC rock crusher. Samples were sieved to 250µm, the <250µm fraction was processed for zircon separation.

Heavy mineral separation was first performed on a gravity separation table (Gemeni Mk 2 Model 60). Magnetic grains were then separated from the dense fraction using a Nd hand magnet and automated magnetic separator (Frantz Magnetic Barrier Laboratory Separator (LB1)). Zircon was further concentrated from the least magnetic fraction (non-magnetic at 1.5A) via heavy liquids separation using methylene iodide ($\rho = 3.3\ gcm^{-3}$).

The zircon separate from each sample was chemically abraded (modified from Mattinson (2005)) to reduce contamination from Pb/U released as a product of metamictic or post crystallisation processes. A bulk zircon fraction from each sample was annealed in quartz glass beakers at 850^{o}C for 60 hours and subsequently leached in concentrated HF and HNO_3 acids in an oven at 180^{o}C overnight in modified Teflon micro-centrifuge tubes placed in a 125 ml Parr bomb (Parr Instrument Company acid digestion bomb 4748). After cooling, the bulk annealed and leached zircon fractions were rinsed several times alternating with purified water (18.2 MΩ resistance) and dilute HCl on a hotplate at ~ 60^{o}C. Acicular tubule-bearing fine grained zircons (most likely to be representative of final crystallisation), were handpicked in ethanol alcohol with surgical steel tweezers under a binocular microscope and mounted in epoxy resin (Struers EpoFix) which was cured overnight at 40^{o}C.

Laser ablation analysis was conducted using a Thermo SCIENTIFIC iCAP Quadrupole inductively-coupled-plasma mass spectrometer coupled to a Photon Machines Analyte Excite 193nm Excimer UV-laser. The laser was configured to deliver 28% power, with a 30 µm spot

diameter at a 4 Hz repetition rate. 85 second sample ablations were conducted, using helium as the carrier gas. The 91500 zircon (Wiedenbeck *et al.* 2004) was used as the primary standard and the Temora-2 zircon (416.75 ± 0.24 Ma; Woodhead et al 2004) used as the secondary standard. No more than 10 unknowns were analysed between standards. Single laser ablations were made from the rim of zircons and a minimum of 22 maximum of 31 analysis of separate zircons were take per block sample.

U-Pb data were reduced offline using the VizualAge data reduction scheme (Petrus and Kamber 2012) in Iolite (Hellstrom *et al.* 2008; Woodhead 2008; Paton *et al.* 2011). Quoted errors (Chapter 9) include uncertainties associated with the reproducibility of the standard.

6.3 Rheology; Magmatic, Sub-magmatic and Solid State Fabrics

The rheological state under which a rock was deformed may be determined based on careful investigation of the host microstructure and grain scale deformation features. Such analysis can prove invaluable when investigating the deformation history of granites as the temporal relationship between strain and crystallisation history may be determined.

6.3.1 Rheology

In geology, rheology is the study of the quantitative response of rock to an applied stress (Passchier and Trouw 2005). A Newtonian fluid is characterised by a single coefficient of viscosity at a given temperature, the viscosity of such a material is not affected by flow or strain rate, conversely, non-Newtonian fluids exhibit strain rate and flow rate dependencies (Schümmer 1979). Therefore, a material which exhibits a linear relationship between stress and strain is said to exhibit Newtonian flow where as an exponential increase in strain with stress defines a non-Newtonian/power law flow (Batchelor 2000).

Siliceous melt is commonly considered a Newtonian fluid (Herbert *et al.* 1980; Román-Berdiel *et al.* 2000; Petford 2003), however granitic magma consists of solid, liquid and gaseous matter. The relative proportions of these phases will fluctuate during the crystallisation process and ultimately alter the mechanical behaviour of the crystal mush (e.g. Clemens and Petford (1999)). As such, the mechanical behaviour of granite is very difficult to predict and viscosity is generally

considered to be variable on a logarithmic scale (Baker 1996; Scaillet *et al.* 1996; Dingwell 1999). Several authors have quantitatively constrained the rheological properties of molten and partially molten samples under laboratory conditions using numerical and analytical models (Arzi 1978; Rushmer 1995; Vigneresse *et al.* 1996; Bagdassarov and Dorfman 1998; Vigneresse and Tikoff 1999; Takeda and Obata 2003). Such work shows that viscosity values are generally lower for mafic melt (~ 10^1-10^2 Pa·s) and higher for granitic melt (~ 10^4-10^8 Pa·s crystal free) (see Petford (1996) & references therein).

Following fundamental theoretical work of Roscoe (1952) and based on preliminary experiments on partially molten granite, Arzi (1978) demonstrated that during melting, the melt fraction reaches a critical point where an abrupt decrease in rock strength occurs, this was called the Rheological Critical Melt Percentage (RCMP). This concept was supported by Van der Molen and Paterson (1979) (using a different terminology the "critical melt fraction" (CMF)) who concluded that a CMF of ~ 30-35% was typical in granitic material. The RCMP hypothesis was originally drawn from the results of melting experiments and not crystallisation. Rheologically, these are not reversible processes (Vigneresse *et al.* 1996) and so the applicability of RCMP to the crystallisation process could be questioned. However, the RCMP model was formulated based on Roscoe (1952) who recognised viscosity fluctuations resulting from the locking of rigid particles i.e. crystals within a magma and so many consider this system valid for the analysis of crystallising magma (Van der Molen and Paterson 1979; Lejeune and Richet 1995; Takeda and Obata 2003; Passchier and Trouw 2005).

RCMP is defined as the point of maximum rate of decrease in strength (Arzi 1978). Takeda and Obata (2003) questioned the validity of the RCMP/CMF theory and argued that when plotted on a linear scale (as appose to logarithmic scale used by Arzi (1978) and Van der Molen and Paterson (1979)) data from melting experiments showed a linear relationship between rock strength and melt fraction, hence the RCMP is 0%. Directly contradicting the former authors, Rosenberg and Handy (2005) showed that the relationship between rock strength and melt percentage was in fact non-linear and defined a new point along the melting curve, the "melt connectivity transition" (MCT). The MCT is the point at which melt interconnectivity causes a rapid reduction in the rocks strength (between solidus and 0.07%). Rosenberg and Handy (2005) argue that this occurs prior to, and is much more significant than, the final breakdown of the crystalline frame work, i.e. the "solid-to-liquid transition" (SLT) that corresponds to the RCMP.

Differing environmental conditions will control the melting and crystallisation process and so the rheological properties of a magma will vary during ascent and emplacement. Pressure plays a lesser role while temperature and composition are more influential (Petford 1996). A generally acceptable frame work from which the rheological properties of crystallising melt may be based is that granitic magma will behave as a Newtonian fluid at about ~80-90% melt fraction, below ~ 70% Bingham plastic behaviour is expected, the CMF or RCMP is reached at 30-35% melt fraction and full crystal lock up occurs at 25-30% melt fraction and MCT is at 0.07% (Arzi 1978; Van der Molen and Paterson 1979; Vigneresse *et al.* 1996; Rosenberg and Handy 2005).

6.3.2 Microstructural Analysis of Granite

Microstructural analysis may be used to evaluate subtle textures and grain scale deformation features that can be used to determine whether the measured magnetic anisotropy relates to pre-solidus or post-solidus deformation (e.g. Cruden *et al.* (1999); López de Luchi *et al.* (2004); Esmaeily *et al.* (2007)). Microstructural analysis has been applied to plutonic emplacement investigations (e.g. Steenken *et al.* (2000); Archanjo and Fetter (2004); Vegas *et al.* (2008)) and in conjunction with structural mapping may be used to examine the relationship between granitoids and the regional tectonic regime (e.g. Davis and Henderson (1999); Barros *et al.* (2001); Mamtani and Greiling (2005)). In the current work, this principle is applied to the Galway Granite Complex.

6.3.2.1 Microstructures of Common Granitic Minerals

Different mineral phases have distinct physical properties, within a cooling granitoid a variety of deformation and recovery mechanisms will be in affect in each mineral phase. Characterisation and cross referencing deformation characteristics of several mineral phases may be used to constrain the rheological conditions under which a fabric developed (Passchier and Trouw 2005); thus crystallisation and subsequent deformation history of a granitoid can be evaluated.

Bulging (BLG), subgrain rotation (SGR) and grain boundary migration (GBM) are the three mechanisms of dynamic recrystallisation (Passchier and Trouw 2005). In essence, BLG is the most important recrystallisation mechanism at low temperature and high strain rate, GBM is most important at high temperature and lower strain rates and SGR is an intermediate recovery

mechanism that occurs under moderate temperature and strain conditions (Fig. 6.2). For a full explanation of rock microstructure the reader is referred to Vernon (2004); Passchier and Trouw (2005) and (Blenkinsop 2000).

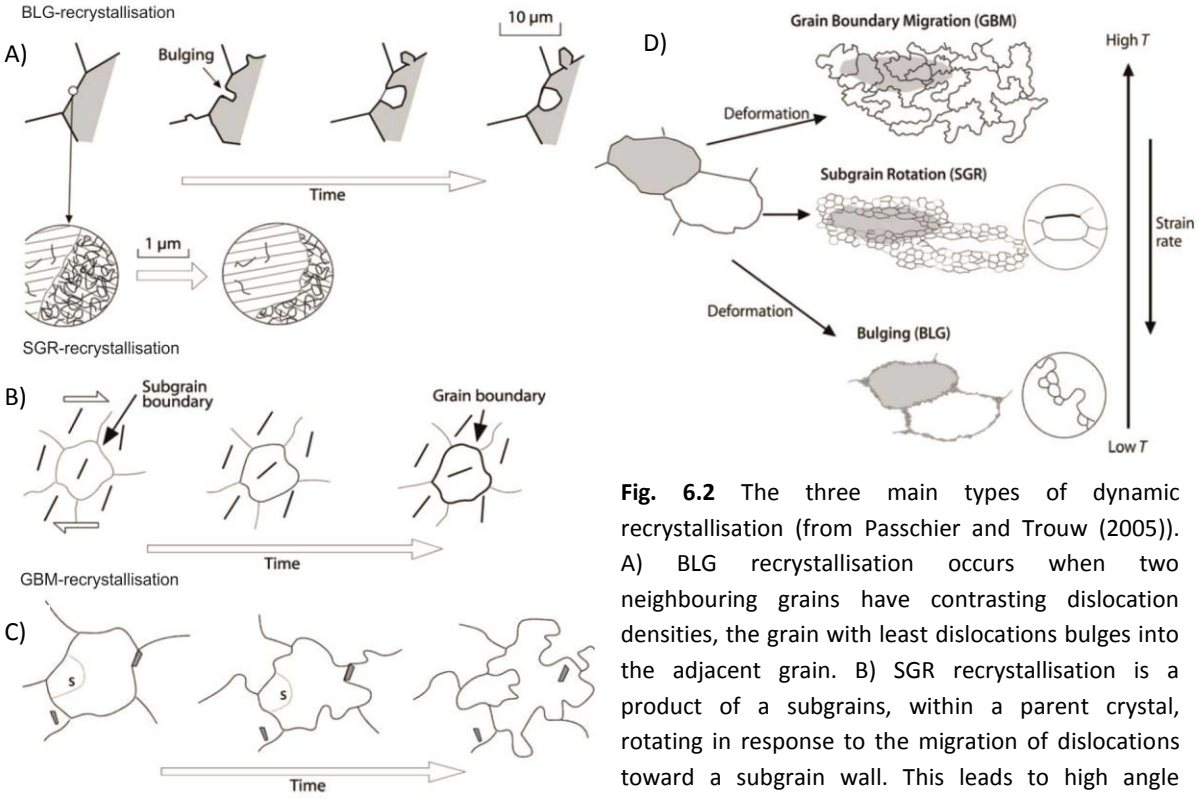


Fig. 6.2 The three main types of dynamic recrystallisation (from Passchier and Trouw (2005)). A) BLG recrystallisation occurs when two neighbouring grains have contrasting dislocation densities, the grain with least dislocations bulges into the adjacent grain. B) SGR recrystallisation is a product of a subgrains, within a parent crystal, rotating in response to the migration of dislocations toward a subgrain wall. This leads to high angle subgrain boundaries and ultimately the formation of new grains. C) GBM is a high temperature process. Grain boundaries are highly mobile and can sweep across crystals in any direction, this removes dislocations and produces amoeboid grain boundaries. D) The dominance of GBM, SGR and BLG in a system is controlled by temperature and strain rate.

Quartz

The mechanism of deformation is highly dependent on water content within the crystal lattice and pore fluid pressure (Kekulawala *et al.* 1981; Doukhan 1995). Temperature variation is an important parameter but strain rate and differential stress are major contributors as the activation of differing slip systems is subject to these influences (see Hobbs (1985)). As such, the mechanical behaviour of quartz under strain is not completely understood and the characteristics presented are given as guides.

Brittle fracturing and pressure solution are the dominant deformation mechanism below 300°C, these processes form grain fractures, undulose extinction, kink bands and fracture infill from reprecipitation of quartz following dissolution in higher strain zones (see Stipp *et al.* (2002)).

BLG recrystallisation is dominant from 300-400°C but may occur at lower temperatures under high differential stress conditions (Hirth and Tullis 1992; Stipp *et al.* 2002; Passchier and Trouw 2005). Patchy progressing to sweeping extinction, deformation lamellae and mechanical "Dauphine" twinning occur under low temperature conditions (e.g. Lloyd and Knipe (1992); Lloyd (2004)). Recovery is accommodated by grain boundary migration as apposed to dislocation climb (Hirth and Tullis 1992). This is characteristic of Regime 1 (Hirth and Tullis 1992).

SGR recrystallisation is dominant between 400-500°C as dislocation creep becomes the most energetically favourable mechanism by which defects are eliminated from and concentrated within the crystal lattice (Passchier and Trouw 2005). Old crystals show obvious signs of ductile deformation (highly undulose) and are surrounded by new fresh crystals; relative grain-subgrain lattice orientations become increasingly high angle and new crystals are highly oblique to their parents' lattice orientation (Hirth and Tullis 1992; Stipp *et al.* 2002). The orientation of both old and new grains become increasingly aligned orthogonal to the principal stress direction. Ultimately all grains will have approximately even dislocation densities and a strong crystal preferred orientation (Hirth and Tullis 1992). This is characteristic of Regime 2 (Hirth and Tullis 1992).

GBM recrystallisation is the primary dynamic recrystallisation mechanism between 500-700°C. Grain boundaries form via SGR but are immediately highly mobile (Passchier and Trouw 2005). In lower temperature ranges lobate grain-grain boundaries and core and mantle structures are seen via optical microscopy, TEM imaging will show low dislocation densities as pining of dislocations can still occur (Hirth and Tullis 1992). At ~700°C+ recrystallisation is rapid and grains appear strain free, chessboard extinction or chessboard subgrains is diagnostic (Kruhl 1996; Stipp *et al.* 2002). This is characteristic of Regime 3 (Hirth and Tullis 1992).

Quartz ribbons are common strain features in granites that have become strained (e.g. Culshaw and Fyson (1984); Baxter *et al.* (2005)) and several authors have investigated their genesis via crystal plastic deformation (Ramsay and Huber 1983; Ghosh 1994). Manual *et al.* (1997) highlight another mechanism of quartz ribbon development through plastic deformation of the original grain. In this case stretching of an original quartz grain into short monocrystalline ribbons is achieved plastically and progressively into long polycrystalline ribbons. Conditions for

this style of deformation are highly pressure and temperature dependent (*c.* 5-6kb at 900°C) and are comparable to Regime 2 of Hirth and Tullis (1992) (Manual *et al.* 1997).

Feldspar

As well as temperature and strain rate (Fig. 6.3), the mechanisms through which feldspars deform are subject to compositional variations that occur during metamorphism (Tullis and Yund 1991; Rosenberg and Stünitz 2003; Rosenberg and Handy 2005). Modelled behaviour of feldspar under differing strain and temperature conditions assume chemical equilibrium during recrystallisation, this is often not the case (e.g. Na segregation in the production of albite flecks in K-feldspar phenocrysts). As such the mechanical properties of feldspar will evolve during a progressive deformation process (Stunitz 1998).

Below 400°C feldspar deforms by brittle mechanisms. Breccia fragments, derived from fracturing and cataclastic flow, typically exhibit internal deformation features such as patchy undulose extinction, poorly defined subgrain boundaries, grain scale faulting and evidence of very low temperature ductile deformation such as bent cleavage planes and mechanical twins (Tullis and Yund 1987; Kanaori *et al.* 1991; Passchier and Trouw 2005).

Low temperature ductile deformation becomes more apparent and accompanies brittle processes between 400-500°C. Within this temperature range, dislocation glide gives rise to abrupt kink and deformation bands, undulose extinction, and mechanical twinning (Tullis and Yund 1987; Passchier and Trouw 2005). Grain scale bookshelf fracturing (fracturing across the long axis of a grain to produce a "stacked book shelf" set of subgrains) is typical of lower temperature conditions (Passchier 1982). BLG recrystallisation may take place but is not of major significance. Flame perthite emanates from high strain zones and can be used to evaluate the orientation of the principal stress axis (Pryer and Robin 1995). Larger feldspars are sufficiently ductile to augen but core-and-mantle structures will not form (Shigematsu 1999).

Dynamic recrystallisation processes become active, and dislocation climb energetically feasible, from ~ 450°C. Brittle deformation is less apparent but grain scale fracturing can occur as a product of strain hardening (Altenberger and Wilhelm 2000). Fine-grained fresh aggregates about older deformed cores, i.e. core-and-mantle structures, and intercrystalline micro-shear zones punctuated by fine grained bands of recrystallised parent crystal are formed by BLG recrystallisation (Passchier 1982). Mechanical twinning is apparent. Grain size homogeneity among recrystallised mineralogically heterogeneous aggregate, that exhibit a lack of LPO are definite indicators of deformation of feldspar grains between 450-600°C (Passchier and Trouw

2005). Closer to 600°C mechanical twinning becomes less important and myrmekite and flame perthite become increasingly prominent (Simpson 1985; Pryer 1993; Pryer and Robin 1995).

Above 600°C SGR and BLG recrystallisation can occur. Core and mantle structures exhibit increasingly gradational transitions between the old grain cores and associated new grain-subgrains, this is a product of increased rates of recovery and subgrain boundary mobility (Pryer 1993; Kruse and Stünitz 1999). Myrmekite is abundant along foliation planes. Grain scale fracturing, kink bands, undulose extinction, flame perthite and SGR and BLG recrystallisation are present under very high pressure conditions, under lower pressure flame perthite is absent, rare microcracks occur and grains are relatively strain free (Kruse *et al.* 2001; Rosenberg and Stünitz 2003; Vernon 2004).

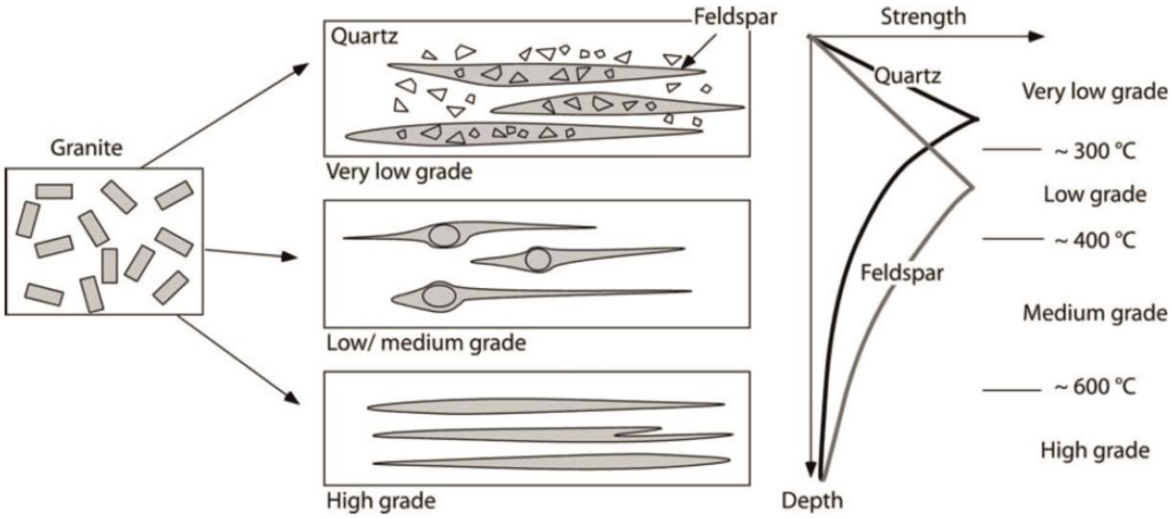


Fig. 6.3 Contrasting deformation behaviour of quartz and feldspar (from Passchier and Trouw (2005)). At low temperature quartz is more competent. Quartz begins to deform in a ductile fashion at lower temperature than feldspar and becomes less competent under moderate temperature conditions. At higher temperatures both minerals have similar strength properties.

Micas

Below 250°C biotite will deform in a brittle manner and exhibit kinks and cleavage parallel slip forming "mica fish" (Kanaori *et al.* 1991). Above this temperature ductile deformation may ensue, folding of the outer crystal and kinking of the inner portions is typical as strain most often exploits the planar weaknesses along the well defined basal cleavage plane (Vernon 2004). GBM can become active at medium and high grade conditions (Bell 1998). Pressure solution, fracturing and undulose extinction are all commonly concentrated along cleavage planes and crystal margins. In

general muscovite is less susceptible to ductile deformation and will deform in a brittle fashion where biotite is ductile (Passchier and Trouw 2005).

Amphibole

Amphibole behaves in a brittle fashion at relatively high temperatures (up to c.700°C) when compared to many other silicate minerals (Passchier and Trouw (2005) and references therein). Under such conditions strain is also accommodated by twinning and slip along cleavage planes and kinking along basal cleavages. Aggregates of small needles of amphibole are associated with fracturing of a larger crystal rather than recrystallisation processes (Imon *et al.* 2002; Imon *et al.* 2004), core-and-mantle structures may be formed in the same manner or via chemical disequilibrium rather than BLG recrystallisation (Fitz Gerald and Stünitz 1993; Stünitz and Gerald 1993).

At high temperature several slip systems become active and crystal plastic deformation may instigate. Product subgrains are typically elongate parallel to the c-axis, further detail of slip system activation and associated reference can be found in Passchier and Trouw (2005) pp. 61.

6.3.3 Classification of Rheological State Based on Microstructure

Magma is typically emplaced as a crystal poor liquid with ≥50% melt fraction (Petford 2003). Due to low population density of crystals, early mineral phases are free to rotate unimpeded by neighbouring crystals. Deviatoric stress applied at this stage will promote alignment of any suspended rigid particles. As crystallisation progresses, grain-grain interaction and crystal plastic strain will become necessary for crystal rotation. In the latest stages of crystallisation brittle and low temperature ductile deformation mechanisms will accommodate strain. Obviously, it is useful to temporally relate the fabric development with the rheological state of a medium during deformation (e.g. Hutton (1982); Brun *et al.* (1990); McCaffrey (1992); Archanjo and Fetter (2004).

Several authors have proposed schemes which attribute deformation characteristics of minerals and their microstructures to the rheological state under which deformation occurred. Hutton (1988a) used the broadly defined terms "pre-full crystallisation" and "crystal plastic strain" to describe fabric development before and after full crystallisation of a host. Paterson *et al.* (1989) was far more precise and defined five classes of magma state based on micro-structural analysis;

magmatic flow, sub-magmatic flow, high temperature solid-state and low temperature solid-state deformation and solid state deformation. Tribe and D'Lemos (1996) argued that both sets of nomenclature carried ambiguities and pointed out that the terms "magmatic" and "pre-full crystallisation" could both be used to describe fabric development up until a magma had completely crystallised. Instead Tribe and D'Lemos (1996) describe rheological state and fabric development relative to the rheological critical melt percentage (RCMP) (Arzi 1978).

The terms *Magmatic flow*, *sub-magmatic flow* and *solid state* (as defined by (Passchier and Trouw 2005) after Paterson *et al.* (1989)) are used here as well established terms which effectively describe the three fundamental rheological states of magma (Blenkinsop 2000; Vernon 2000, 2004; Passchier and Trouw 2005). Blenkinsop (2000) used "non-magmatic" in place of "solid-state" which is technically more correct as some fluid will always be present.

6.3.3.1 Magmatic Flow

Magmatic flow is the displacement of magma in response to applied stress with consequent rotation of constituent mineral phases without sufficient grain-grain interference to cause crystal plastic deformation of those rigid particles (Paterson *et al.* 1989; Passchier and Trouw 2005). In the magmatic state strain is very easily over printed, as such fabrics that reflect magmatic flow are likely to represent differential stress applied during the later stages of plutonic development. Magmatic flow fabrics may well reflect primary emplacement flow patterns (Stevenson *et al.* 2007) as well as other processes such as plutonic ballooning (Baxter *et al.* 2005), as such it is best practice to examine of textural evidence in conjunction with other structural evidence.

Classic evidence for magmatic flow is the preferential alignment of undeformed euhedral early mineral phases, commonly K-feldspar phenocrysts and biotite in granitic rocks. Flow fabrics may be distinguished from phase layering based on compositional heterogeneity, inequant crystal size distributions and a characteristically isotropic interstitial groundmass found in flow fabrics (Vernon 2004). Wright (1963) and Leake (2011) discuss some examples of modal layering, schlieren bands and flow fabrics, all defined by biotite rich horizons, from the Carna Pluton, Connemara. A shape preferred orientation among included xenoliths and enclaves (see Paterson *et al.* (2004) for exceptions and considerations) may also be used to diagnose magmatic state flow as long as no evidence for plastic deformation is associated with these inclusions. The presence of "tiled" or imbrication of euhedral phenocryst phases can be used as an indicator of magmatic flow direction (e.g. Mulchrone *et al.* (2005)). The isotropic distribution of minerals, presence of

undistorted growth twins and oscillatory zones within phenocryst phases and a lack of deformation fabric features in plutonic rocks indicate no strain occurred subsequent to the magmatic state (Vernon 2000, 2004; Passchier and Trouw 2005). Minor ductile deformation features are not exclusive of magmatic flow deformation regimes (Passchier and Trouw 2005).

6.3.3.2 Sub-magmatic Deformation

Sub-magmatic deformation/flow is the displacement of melt and crystals facilitated by the crystal plastic deformation of rigid particles (Paterson *et al.* 1989; Passchier and Trouw 2005). Submagmatic flow will initiate once the crystal population density reaches a critical level, i.e. the RCMP of Arzi (1978), CMF of Van der Molen and Paterson (1979), or the SLT of Rosenberg and Handy (2005). This is the rheological state that bridges the transition between liquid magma and solid rock, as such a broad spectrum of increasingly intensive crystal-plastic to brittle deformation features are observed (reviewed in Vernon (2000, 2004)). Grain scale crystal plastic deformation, strain partitioning of melt rich zones, melt enhanced embrittlement, diffuse mass transfer, contact melting assisted grain boundary migration and melt assisted grain boundary sliding are processes that facilitate submagmatic flow (Paterson *et al.* 1998).

A shape preferred orientation of constituent minerals achieved via crystal-plastic deformation of solid particles during rigid body rotation is strong evidence for deformation in the submagmatic state. Fabric development via recrystallisation or brittle deformation may also be generated in the submagmatic state but evidence for the presence of liquid magma is required (Paterson *et al.* 1989; Vernon 2000). Evidence of ductile deformation within the crystal lattice (undulose extinction, mechanical twinning, bent twins, smearing of biotite) may aid in determining the rheological state and temperature at which submagmatic deformation occurred (e.g. Tribe and D'Lemos (1996); Cruden *et al.* (1999); Baxter *et al.* (2005)); again evidence for the presence of melt is critical. Pockets of late stage melt in pressure shadows around large phenocrysts or even xenoliths suggest very late stage submagmatic flow (Bouchez *et al.* 1992). Several accounts detail the presence of micro fractures with melt infill (Karlstrom *et al.* 1993; Blenkinsop 2000). Bouchez *et al.* (1992) provides an illustrated summary of contrasting brittle fracture - melt infill microstructural features.

As granitoids are associated with orogenic processes, it is often the case that emplacement is achieved into a dynamic stress regime and a continuum of down temperature fabric development may be expected. This however is not always the case and a hiatus often occurs between high

temperature submagmatic and solid state deformation (Tribe and D'Lemos 1996). In the scenario where the principal stress directions become re-orientated during crystallisation, distinct deformation episodes may be detected by cross cutting crystalline anisotropies (e.g. Neves *et al.* (2003)). Progressive inflation of plutonic bodies often produce a submagmatic fabric parallel to earlier magmatic state fabrics, in such a scenario distinction between the two is best made by field and petrographic microstructural investigation (e.g. Baxter *et al.* (2005)).

6.3.3.3 Solid State Deformation

Solid state deformation refers to deformation in the absence to liquid magma, other fluids (metamorphic, meteoric etc.) may be present. Strong undulose extinction, subgrain formation and recrystallisation and cataclastic flow are common grain scale solid-state deformation features if the evidence shows such features developed in the absence of melt (Vernon 2004). In deformed granite, quartz and biotite will become stretched out, typically forming polycrystalline ribbons or smears, *wings* or *tails* are useful shear sense indicators (e.g. Baxter *et al.* (2005)). Boudins of larger phenocryst phases and mechanically strong minerals such as hornblende and feldspar may be present, again these are useful shear sense indicators. Myrmekite may also develop (Vernon 2000) in the solid state (as distinct from magmatic state myrmekite (Paterson *et al.* 1989)). Myrmekite forms at sites of high strain while that which crystallised from the magmatic state will grow in dilation sites round phenocrysts. In a porphyritic rock, the matrix will anatomise around larger minerals. Through prism slip, the c-axis of quartz grains will tend towards alignment with the stretching direction (e.g. Law (1990); Graham (1997)).

6.4 The Strain Record in Granite

The ascent and emplacement process is controlled by the orientation of the local stress field at the time of intrusion (Chapter 1). It follows that the stress regime that controls plutonic development is different from that which was responsible for transporting magma to the site of emplacement. The anisotropic distribution and alignment of minerals within a granitoid is often dictated by the stress regime that presided over the crystallisation process. However, fabrics, particularly weak fabrics formed in the magmatic state, are easily overprinted by latter deformation events or changes to the ambient stress field during the crystallisation process.

Therefore, the observed strain record is a product of the stress and rheological history of the magma but may not reflect earlier deformation events such as that which controlled the ascent process, or, in the case of granitoids deformed in the solid state, the emplacement process.

The Shape Preferred Orientation (SPO) of a crystalline matrix reflects the total stress history to which a material was exposed. Several authors have demonstrated that the relationship between SPO and the stress history is not simple (e.g. Owens (1973); Ildefonse and Fernandez (1988)). Numerical modelling shows that a cyclic pattern exists during pure shear deformation where by an increasingly well defined oblate coaxial fabric will form in response to greater strain while in simple shear regimes fabric intensity is generally weaker and forms by asymptotic rotation of the fabric forming minerals toward the shear plane (Ildefonse *et al.* 1992). This demonstrates that while the SPO is a direct reflection of the stress field, quantification of that stress through analysis of a fabric is a complicated process and in all cases the calculated value can be taken as a minimum estimate only. Within plane strain monoclinic flow regimes Piazolo *et al.* (2002) demonstrated that deformation is concentrated about high strain simple shear zones that are bound by zones of low strain with higher rigid body populations (i.e. a high strain gradient is associated with the formation of high strain and low strain zones). This shows that strain distribution and rigid particle interaction is influential on the SPO and that the role of matrix rheology in forming a SPO is dependent to some degree on particle aspect ratio. More recently Wright and Weinberg (2009) illustrated that the affects of strain localisation on the rheological properties of shallow level magma is sufficient to alter numerically modelled behaviour on natural samples. This work demonstrates that the complex interaction of the stress field and strain record can create a feedback loop where energy may be dissipated more effectively in localised high stress zones promoting melt fragmentation.

A definite relationship exists between deviatoric stress and the strain record but in no circumstance is this a simple one. The impact of this on the study of granitoids is twofold. First and foremost, strain observed in an outcrop reflects the stress history but a quantitative measurement of finite strain is not realistically possible, at best a minimum estimate may be possible. Second, an observed fabric is likely to have been over printed several times by a progressively evolving stress field, even if only a single magmatic state fabric is now visible. Hence in attributing a fabric to a particular process (ascent, emplacement, ballooning, deformation) a multitude of parameters must be taken into consideration (e.g. pluton architecture, microstructure, country rock structure, stress fields etc.).

6.4.1 Quantifying Strain

A simple set of nomenclature was devised by Flinn (1985) (Fig. 6.4) to describe fabric and inclusion anisotropy in the context of the shape of the strain ellipsoid (K value). In this system the geometry of the finite strain ellipse is qualitatively related to inclusion or matrix anisotropy by three terms; "L" which represents prolate/ linear fabrics, "S" which represents oblate or planar fabrics and "L-S" which indicates both a planar and linear fabric are detected ("F", foliation, may be used in place of "S", schistosity). Several quantitative methods have now been devised (summarised Tarling and Hrouda (1993) pp. 18) to quantify the strain ellipse based on the dimensions of the three principal strain axes (i.e. XY, XZ, ZY). The most widely applied method is that of Ramsay and Huber (1983) who calculated the Harmonic mean axial ration (H);

$$H = n/(Rf1^{-1} + Rf2^{-1} + Rfn^{-1})$$

which can accurately quantify true tectonic strain to within in few percent.

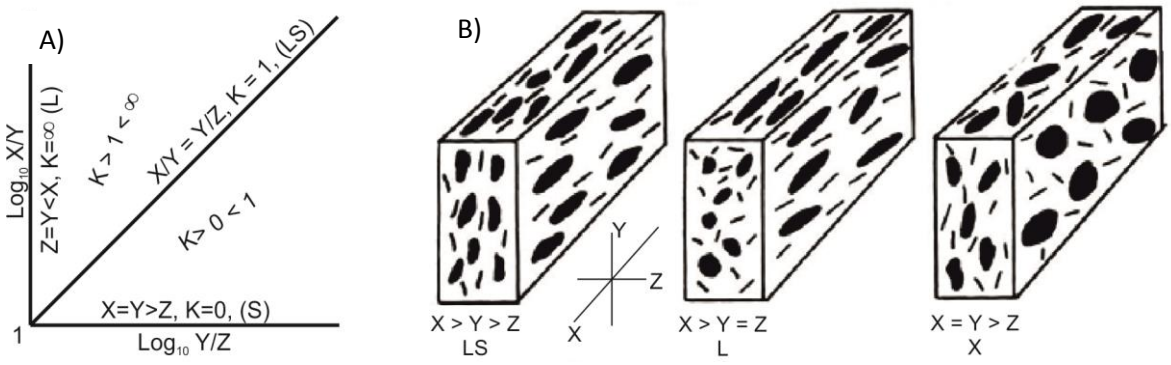


Fig. 6.4 Graphical representation of the possible symmetry of the strain ellipsoid based on the Flinn diagram (A) and associated rock fabrics (B) (from Hutton (1988a)). X, Y and Z are the max, intermediate and minimum strain axes of a strain marker, L= prolate fabric, S = oblate fabric, LS = triaxial ellipsoid or fabric with both lineation and foliation. A higher H value (Ramsay and Huber 1983) is equivalent to greater distance from the origin (1) on the Flinn plot.

The distribution of strain in a pluton may be determined in a semi-quantitative manner through a broad spectrum of analytical techniques (some discussed below). The main challenge when interpreting the strain record in igneous rocks is to determine what the measured anisotropy reflects, i.e. a single or composite magmatic, submagmatic or solid state fabric related to the intrusion process or some tectonic stress.

6.4.2 Field Based Fabric Analysis

In magmatic state fabrics, anisotropy is best identified among the earliest crystallised phases (biotite, hornblende, K-feldspar) as such minerals are likely to exhibit more pronounced euhedral shapes with larger aspect ratios (Atherton 1995). As crystallisation progresses, strain is accommodated by grain scale ductile flow (dislocation glide/creep, dissolution precipitation, twinning and kinking); as the solidus is approached brittle deformation and cataclastic flow will take over (see Passchier and Trouw (2005)). In down temperature regimes the SPO will be defined by minerals that are more susceptible to dynamic recrystallisation processes. For example, quartz will crystallise as anhedral interstitial fill between aligned K-feldspars and biotite as a product of magmatic state deformation but inflated plutons exhibit marginal fabrics defined by elongate quartz ribbons and smeared out biotite between brecciated K-feldspars (e.g. Baxter *et al.* (2005)).

In either case, if a granitoid has a well defined SPO both the K value and strain intensity can be extrapolated in a semi-quantitative manner. The long axis of K-feldspar phenocrysts indicate the lineation direction while the plane that is defined by the alignment of multiple crystals orthogonal to the lineation is the foliation. In the case of euhedral platy biotite, the foliation is defined by the plane orthogonal to the c-axis (001 face) while a lineation may be defined by the statistical alignment of the "zone axis" (Bouchez 1997). Quartz may or may not be useful depending on the temporal relationship between strain and fabric development. The simplest technique requires the measurement of the long and short axis of individual crystals on three planes that correspond to the principal strain axis. Hutton (1988a) recommends a minimum of thirty shape ratios (for ductile inclusions) the mean of which may be considered a representation of the strain ratio of a particular plane while strains determined from any two planes may be combined to determine the K value.

6.4.3 Inclusions as Strain Markers

Two basic types of inclusion occur, enclaves (typically relatively mafic and cognate hybrid magma, (Fig. 6.5)) and country rock xenoliths. Regardless of inclusion type, a rheological contrast between host and inclusion will be present. The time at which an inclusion is incorporated into a magma is usually unconstrained. These problems are accentuated in host rock xenoliths which are considered poor indicators of strain. Hence determining the relevance of strain associated with a

xenolith to that of the magma must be carried out in a tentative manner (see Ramsay and Huber (1983) and Paterson *et al.* (2004) for best practices).

Magmatic enclaves are coeval with the intruding granite (Pitcher 1997) and provide a strain record that is more objectively relevant. Studies which use the SPO of enclaves as strain markers assume that the enclave was introduced as a roughly unstrained spherical inclusion and recorded strain passively during the crystallisation process.

The validity of enclaves as viable strain markers has been disputed as some consider the dynamic between inclusion and host poorly understood (Paterson and Vernon 1995; Paterson *et al.* 1998). The fundamental problems regarding the use of enclaves as strain markers have been highlighted by Paterson *et al.* (2004). These issues pivot about rheological and strain history conflicts such as the initial shape and timing of enclave introduction (relative strain history), rheological contrasts between the two materials and the effect of enclave population density on the SPO of the matrix and inclusions. Theoretical and analytical models (e.g. Williams and Tobisch (1994); Scaillet *et al.* (2000); Piazolo *et al.* (2002); Wright and Weinberg (2009)) have shown that the use of enclaves as strain markers is limited and subject to influences that may not be accounted for from field based projects.

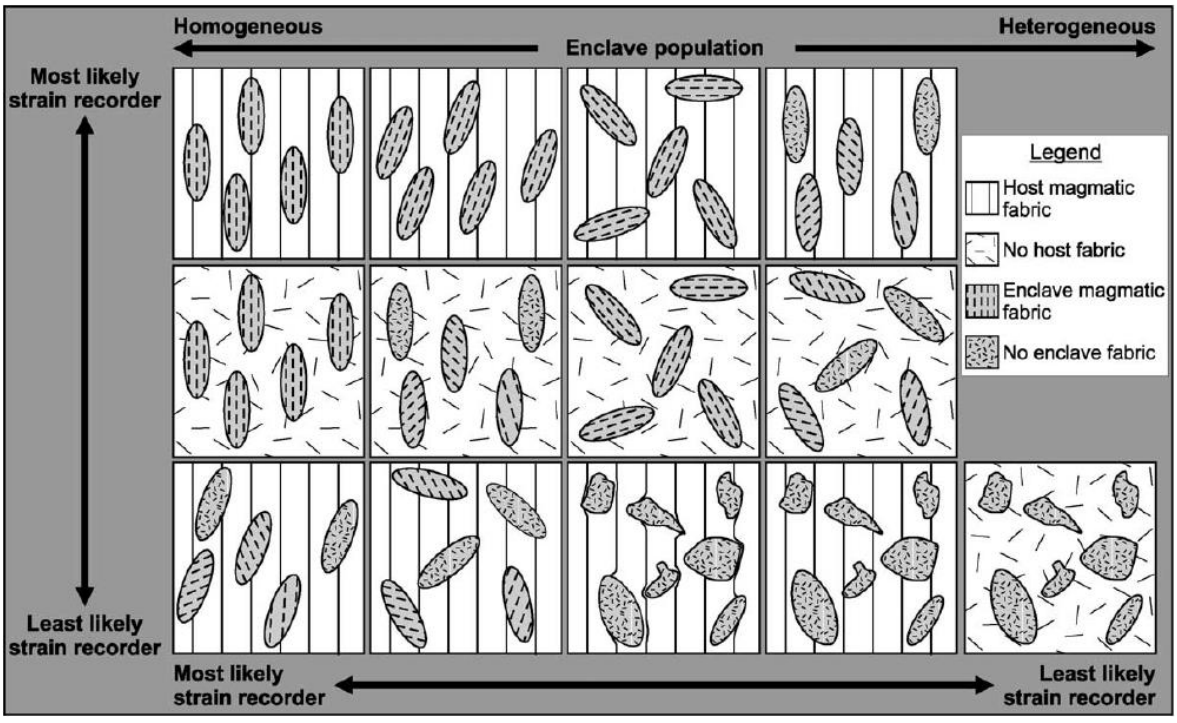


Fig. 6.5 Schematic diagram of the relationship between strain in granite as recorded in mafic inclusion and the host magma (from Paterson *et al.* (2004)). The most likely enclave strain markers exhibit an internal fabric and long axis that is parallel to the observed fabric in the host rock.

Taking account of these issues, SPO analysis of enclaves is still considered a valuable tool in detecting strain distribution and intensity if the data are combined with suitable host fabric analysis (Holder 1979; Hutton 1988b; Molyneux and Hutton 2000; Vassallo and Wilson 2002; Paterson *et al.* 2004)). Rheological contrasts may be estimated by observing the nature of fabric development within host and enclave. Divergent or convergent host fabrics around or through an inclusion suggest a relatively higher or lower enclave viscosity, in the case where both enclave and host have similar rheological properties no fabric deflection is noted (Fig. 6.5). It is emphasised that if enclave SPO is used as a strain proxy a multitude of considerations must be made (see Paterson *et al.* (2004)).

6.4.4 Shear Sense Indicators

Anisotropy forms in reaction to some applied deviatoric stress yet the relationship between principal stress axis and SPO orientation may not be simple (e.g. Ildefonse *et al.* (1992); Wright and Weinberg (2009)). The recognition of S-C fabrics (Berthe *et al.* 1979) in the field illustrates this well. Two types of S-C fabrics are recognised; (i) a compressional crenulation cleavage (C) that forms in response to compression and occurs at high angles (45°-90°) to an existing foliation and (ii) a shear band cleavage (C') forms oblique to the bulk shortening direction and the bounding shear band and develops due to some extension at a low angle (<45°) to an existing foliation which is normal to the shear band (Passchier and Trouw 2005) (Fig. 6.6). The symmetrical relationship between the S and C components is variable, the angle of repose between the two fabrics will decrease in rocks that exhibit higher strain intensities, in very low strain regimes conjugate C planes may form (Hutton 1982). Descriptions of other contrasting obliquity fabrics and sub-fabrics (S-S', S-L, S'-L' etc.) are given in Platt and Vissers (1980); Blumenfeld and Bouchez (1988) and Passchier and Trouw (2005).

Elongation and ribboning of quartz, smearing of biotite and feldspar augens are examples of useful post-magmatic and solid state shear sense indicators (discussed above). At outcrop scale imbrications of early crystal phases can be used as evidence for magmatic state simple shear flow (Vernon 2004). In the absence of stacked tabular phenocrysts, shear sense may be determined by studying the relationship between a phenocryst and the attitude of the groundmass fabric which may exhibit fold closure toward the direction of phenocryst rotation (Vernon 1987). Submagmatic

micro-fractures have been used to affectively determine shear sense and temperature of fabric development (Bouchez *et al.* 1992; Hippertt 1993).

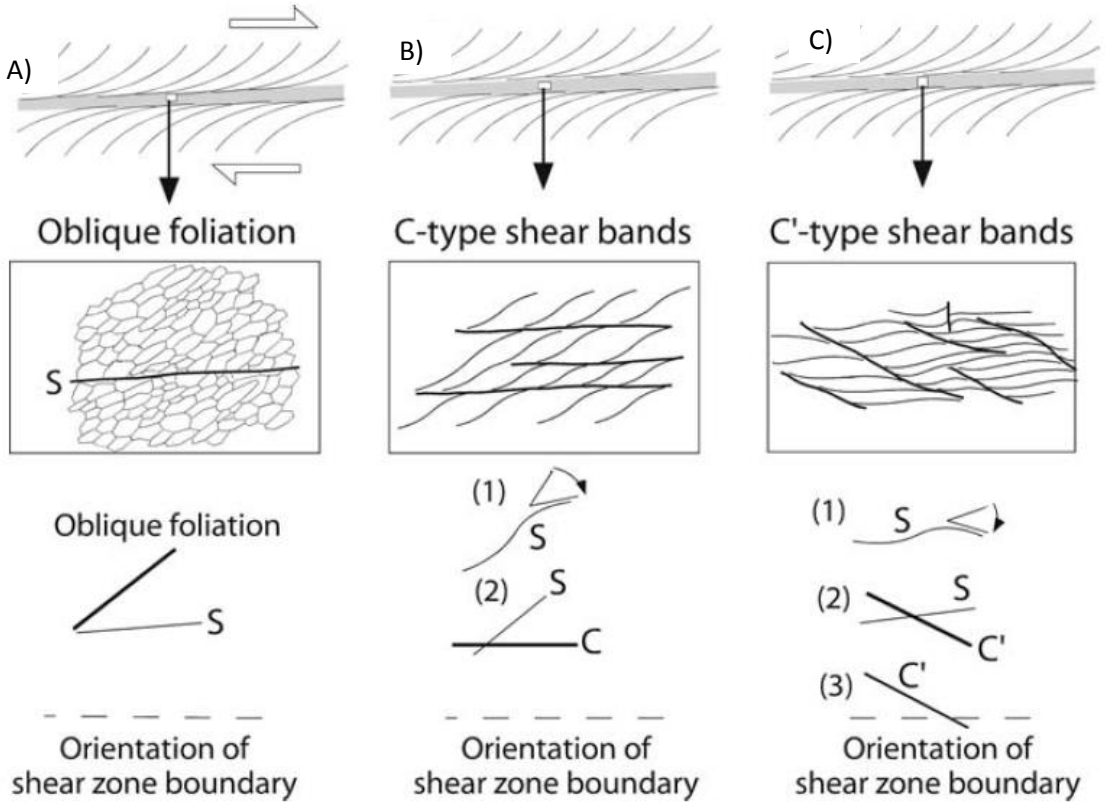


Fig. 6.6 Development of S,C and C' fabrics within shear zones (from Passchier and Trouw (2005)). A) A S-type fabric. B) C-type S-C fabric due to compression, the C-plane is parallel to the shear zone boundary and laterally continuous. C) C' type S-C fabric due to extension, the C-plane is oblique to the shear zone boundary and is laterally discontinuous.

6.4.5 Deformation of the Country Rock

The intrusion process requires the transfer of crustal material in order to facilitate the growth of a new plutonic body (Paterson and Fowler 1993). It is not possible to achieve this without causing some degree of strain and therefore all host rocks will undergo emplacement related deformation. In some cases an intrusion may appear isotropic and information relating to syn-emplacement strain must be recorded from the host rock (e.g. Droop and Treloar (1981); Stevenson (2008)). Structures which bound an intrusion may reflect information about the kinematic regime that presided over the emplacement process or pre-existing anisotropies in the host strata that may have acted and conduits for magma flow (e.g. Hutton (1988b); Grocott *et al.* (2009)). In the cases where intrusion initiated after or finished before regional deformation a knowledge of the structural history or the country rock may aid in relatively dating emplacement

(e.g. (Tanner *et al.* 1997)), conversely, knowing the age of the granite may aid establishing the timing of deformation (e.g. Hutton and McErlean (1991); Stewart *et al.* (2001) but see Paterson *et al.* (1988)).

On map scale, structural features in the country rock can characterise divergent, compressive, simple (Ramsay 1967) or orogenic oblique (Sanderson and Marchini 1984; Dewey *et al.* 1998) stress regimes. Structures formed as a product of these distinct stress fields are often exploited by intruding magma (Hutton 1988a, 1992) and may define the bounding margins of a pluton. The distribution of strain within a pluton relative to host rock structure can therefore be used to relate regional strain to local structures; therefore kinematic process may be related to the ascent and emplacement of igneous rocks (Hutton 1982; El-Desouky *et al.* 1996; Baxter *et al.* 2005; Leake 2006; Stevenson 2009). A knowledge of the kinematic regime that presided during the ascent and emplacement process and of host rock structure on a regional scale can be used to synthesise regional scale conduit models, as in Jacques and Reavy (1994). Finally, analysis of the metamorphic aureole can provide information about the timing of emplacement relative to host deformation history, a well studied example of this would be the Omey Pluton, Galway (Ferguson and Harvey 1979; Elias *et al.* 1988; Ahmed-Said and Leake 1996).

6.5 Anisotropy of Magnetic Susceptibility

A low field magnetic susceptibility may be induced by lowering a specimen (cube or cylinder) into an induction coil assemblage charged with a weak AC current. The applied current induces a magnetization in the specimen and a neighbouring sensory coil measures the change in ambient magnetic field. By this means the induced magnetisation or magnetic susceptibility is generated by the interaction between the samples mineral assemblage and the applied AC field is quantified. This provides the bulk susceptibility of that sample along the axis parallel to the applied field only.

As individual minerals of the assemblage, as well as the sample itself, are texturally and magnetically anisotropic (e.g. Owens and Bamford (1976); Tarling and Hrouda (1993); Bouchez (1997)) the magnetic susceptibility will differ if measured along different axes. In order to measure the *Anisotropy of Magnetic Susceptibility* (AMS) of the same sample, it is necessary to measure susceptibility on three orthogonal axes to calculate the susceptibility tensor.

As with any statistical work, the more measurements made the better (Girdler 1961; Jelinek 1977; Borradaile and Stupavsky 1995; Jelínek and Pokorný 1997; Tauxe 1998; Trindade *et al.* 2001; Kelso *et al.* 2002). The convention of Jelinek (1977) has been applied by several authors in

examining the structural evolution of igneous bodies (e.g. O'Driscoll *et al.* (2008); Stevenson (2009); Stevenson and Bennett (2011); Magee *et al.* (2012)) and is deemed acceptable for this project.

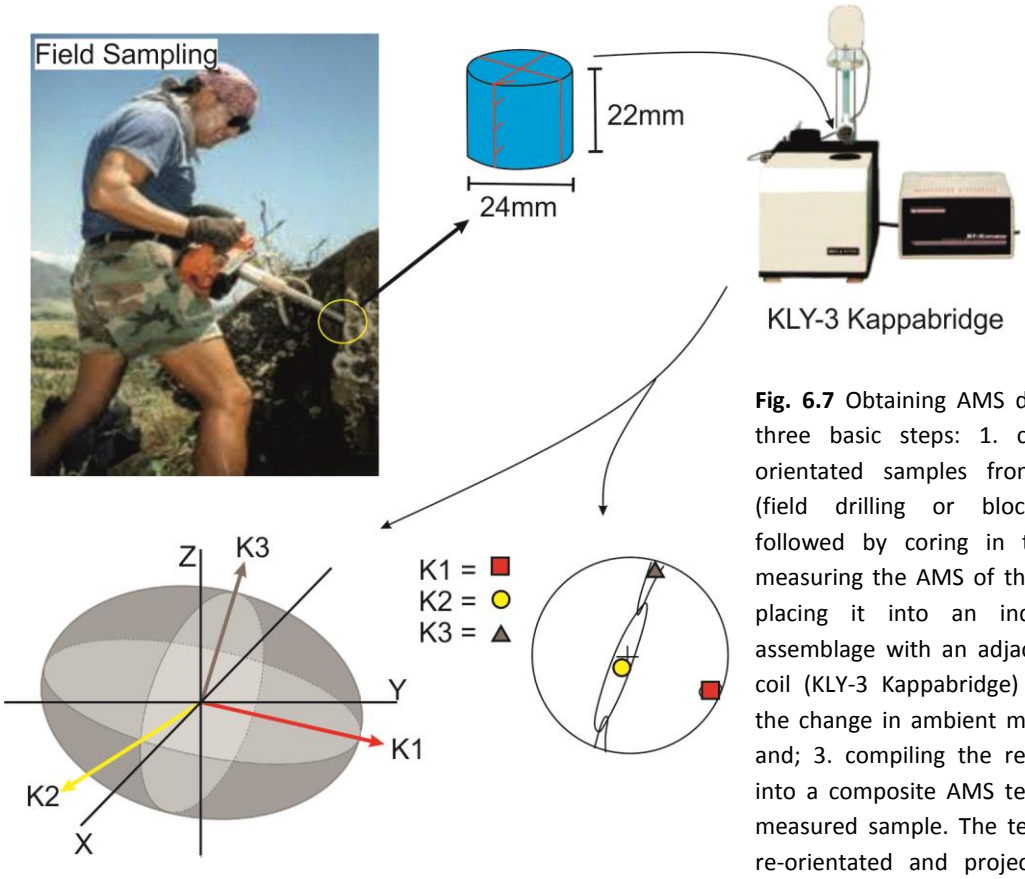


Fig. 6.7 Obtaining AMS data involves three basic steps: 1. collection of orientated samples from the field (field drilling or block sampling followed by coring in the lab); 2. measuring the AMS of the sample by placing it into an induction coil assemblage with an adjacent sensory coil (KLY-3 Kappabridge) to measure the change in ambient magnetic field and; 3. compiling the recorded data into a composite AMS tensor for the measured sample. The tensor can be re-orientated and projected onto a southern hemisphere projection stereonet for interpretation.

Once recorded, susceptibility data can then be applied to a choice of matrix equations (see Girdler (1961); Jelinek (1977); Owens (2000b); Borradaile (2003)) designed to solve the 6 independent elements of the second-rank susceptibility tensor to define the AMS of a given specimen. The second-rank susceptibility tensor may be projected as a magnitude ellipsoid (Nye 1957) defined by the intensity and orientation of the K_1, K_2 and K_3 axes which reflect the maximum, intermediate and minimum magnetic susceptibility axes, respectively, of the specimen.

The shape and intensity of a specimen's magnetic susceptibly ellipsoid often reflects the preferred orientation of the magnetic minerals within a sample, thus it can be related in orientation, but not directly in terms of magnitude, to the principal axes of the finite strain ellipsoid (e.g. Borradaile (1987); Tarling and Hrouda (1993); Borradaile and Henry (1997); Bouchez (1997); Borradaile and Jackson (2004, 2010)). It is important to note that the principal axes of the AMS ellipsoid may not always coincide with crystallographic long, short and intermediate axes of

the magnetic mineral phase(s) present (e.g. Potter and Stephenson (1988); Rochette (1988); Hargraves *et al.* (1991); František (1992); Housen *et al.* (1993); Stephenson (1994); Archanjo *et al.* (1995); Grégoire *et al.* (1995); Parés and van der Pluijm (2002c); Parés (2004)) and further scrutiny of data is essential in order to correctly attribute AMS to the shape preferred orientation of silicate minerals, this is discussed further below. This may be due to the net AMS tensor reflecting crystalline anisotropy, shape anisotropy, distribution anisotropy or composite fabrics (see Appendix D for full review).

AMS is an indirect means of measuring the material tensor. Just as measurement of quartz c-axes, reduction spots, enclaves, pebbles, and fossils may be used to partially quantify finite strain but not finite stress, so too can AMS. However, the critical difference between the AMS ellipsoid and the finite strain ellipsoid is that the AMS ellipsoid varies in both shape and magnitude while the strain ellipsoid may only vary in shape. Therefore, data derived from traditional methods of strain analysis may be directly compared from outcrop to outcrop while AMS data may not and the relative magnitude of each ellipse must also be considered as this is controlled partially by crystalline anisotropy but also by the susceptibility properties of constituent minerals.

6.5.1 AMS Parameters and Data Manipulation

AMS analysis will yield three principal susceptibility vectors, K_1, K_2 and K_3. Regardless of the approach taken all subsequent interpretation is derived from these data.

An averaged mean susceptibility value, (K_{mean}), is always calculated;

$$K_{mean} = \frac{K_1 + K_2 + K_3}{3}$$

this provides the bulk value for the integral of the susceptibly of the ferromagnetic, paramagnetic, and diamagnetic mineral phases present in the specimen (Nagata 1961). It may be used to indicate the quantity and species of the dominant magnetic mineralogy within the specimen (Tarling and Hrouda 1993) and also to normalise the susceptibility tensor to aid in distinguishing composite fabrics (Owens 2000a; Borradaile 2003).

Quite a broad variety of equations have been derived which attempt to characterise the shape and magnitude of the susceptibility ellipsoid (see Tarling and Hrouda (1993) pp.18). For example, the parameters include;

$$L = K_1/K_2 \qquad F = K_2/K_3 \qquad P = K_1/K_3$$

where L = lineation (Balsley and Buddington 1960), F = foliation (Stacey 1960) and P = the anisotropy degree (Nagata 1961) are generally accepted as the most commonly used to constrain fabrics in granites. A sample may be strongly prolate or oblate or have both a L and F component. The relationship between these values may be determined by plotting L vs. F on the Flinn Plot (Flinn 1965). This is an attractive system as it allows for very rapid "first glance" data evaluation. However, these parameters alone are insufficient for dealing with particularly low degrees of anisotropy, as is typically the case in AMS studies in granites (e.g. Khan (1962); Hrouda *et al.* (1971); Owens (1974); Jelínek (1981)).

Shape Factor and Corrected Anisotropy Degree

The ratios between the principal susceptibility axes are of more interest in AMS studies and not necessarily their absolute value (when determining AMS as opposed to mineralogy). Jelinek (1981) proposed a suite of new parameters that are calculated using the natural logarithms of K_1, K_2 & K_3;

$$n_1 = \text{Log}_e K_1 \qquad n_2 = \text{Log}_e K_2 \qquad n_3 = \text{Log}_e K_3$$

and

$$n = n_1 + n_2 + n_3$$

Through this adoption Jelinek (1981) calculated a new parameter, the *corrected anisotropy degree*;

$$P' = \exp \sqrt{\{ 2 [(n_1 - n)^2 + (n_2 - n)^2 + (n_3 - n)^2]}$$

to describe the scatter of the natural logarithms of the principal susceptibility axes. This parameter is commonly referred to as Pj. Evaluating the natural logarithm values n_1, n_2, & n_3 relative to the principal quadratic elongations axes of Ramsay (1967), Jelinek (1981) also calculated the *shape factor* (T);

$$T = \frac{2n_2 - n_1 - n_3}{n_1 - n_3}$$

to describe the overall shape of the ellipsoid. T will always return a value between -1 and 1. This parameter is commonly referred to as Tj. When $-1 < T < 0$ the shape anisotropy is prolate and when $0 < T < 1$ the shape anisotropy is oblate, if $T = 0$ the magnetic susceptibility is isotropic.

If P' and T are plotted on a simple Cartesian graph a poor representation of the actual fabric shape and degree of anisotropy is returned. As such, Borradaile and Jackson (2004) conclude that in order to obtain an unbiased distribution a polar plot is the preferred method of data projection, particularly when dealing with small P' values.

The advantage of this system is that with two parameters one may concisely describe any ellipsoid shape based on an interpretation derived from all available data on a scale that suits the nature of the raw data (i.e. subtle degrees of anisotropy). Parameter P' allows one to efficiently determine the intensity or quantity of anisotropy, a spherical tensor will return P' = P. The shape of two ellipsoids may be readily compared completely autonomously of P'. In this way one may compare and contrast neighbouring data points in terms of fabric quality and shape independently.

Anisotropy Shape and Total Anisotropy

Another useful set of parameters are the Lineation (L) and Foliation (F) of Khan (1962) and the percent of total anisotropy (H) and the anisotropy shape (μ) of Owens (1974), these are defined as;

$$L = \frac{K_1 - K_2}{K_{mean}} \qquad F = \frac{K_2 - K_3}{K_{mean}} \qquad H = \frac{K_1 - K_3}{K_{mean}} \qquad \mu = \tan^{-1} L_1/F_1$$

These parameters normalise all product values to K_{mean} and so the problems relating to susceptibility contrasts with L, F and P are avoided. H represents the total anisotropy degree and is often quoted as a percentage (i.e. H x 100). The anisotropy shape μ ranges from 0°-90°, if $0 < \mu < 45°$ the fabric sits in the oblate field while if $45° < \mu < 90°$ a prolate fabric is present, and thus may be plotted on the Flinn diagram as is standard strain data.

Stereographic projection of Normalised vs. Un-normalised tensor data

In order to obtain a statistically significant AMS ellipsoid, it is good practice to analyse between 10-20 sub-samples per site where possible (depending on grain size see Tarling and Hrouda (1993)). These data are incorporated into the statistics above in order to determine the magnitude and shape of the susceptibility ellipsoid. It is also useful to project the orientation of K_1, K_2 & K_3 onto a lower hemisphere equal area projection.

On a stereonet, the pole of the magnetic foliation is defined by K_3 while the best fit great circle between K_1 & K_2 denotes the magnetic foliation plane. A prolate fabric is defined by the orientation of K_1. Depending on the distribution of data points one may determine whether an L, S or L-S fabric is present. If K_3 has a tight confidence ellipse and K_1 & K_2 overlap an oblate fabric may be interpreted, a prolate fabric is determined in the reverse case where K_2 & K_3 overlap and K_1 is well constrained. Where K_1, K_2 & K_3 are well constrained a L-S fabric may be interpreted.

Data are typically projected stereographically in one of three formats, individual point data with a K_1, K_2 & K_3 for each sub-sample from a single block, un-normalised (six-fold tensor) point data represented by a 95% confidence ellipse for each K_1, K_2 or K_3 axis, or as data normalised by the mean of its trace elements (five-fold tensor) and represented by a 95% confidence ellipse for each K_1, K_2 and K_3 axis (Fig. 6.8).

Using two contrasting samples, Owens (2000a) demonstrated the benefits of inspecting both normalised and unnormalised data. In his example, the stereographic projection from one sample exhibits almost identical normalised and un-normalised distributions while data from a second sample shows a significant discrepancy between the size and shape of normalised and unnormalised confidence ellipses (Fig. 6.8). If inconsistencies are observed between the normalised and un-normalised stereographic projections, it is not advisable to represent the principal susceptability data by a single mean as it is likely that more than one fabric is present

that has produced a composite AMS fabric. In such cases further investigation using more sophisticated magnetic analysis methods is advised (e.g. Hrouda (1992); Housen *et al.* (1993); (Martin-Hernandez and Ferre 2006)).

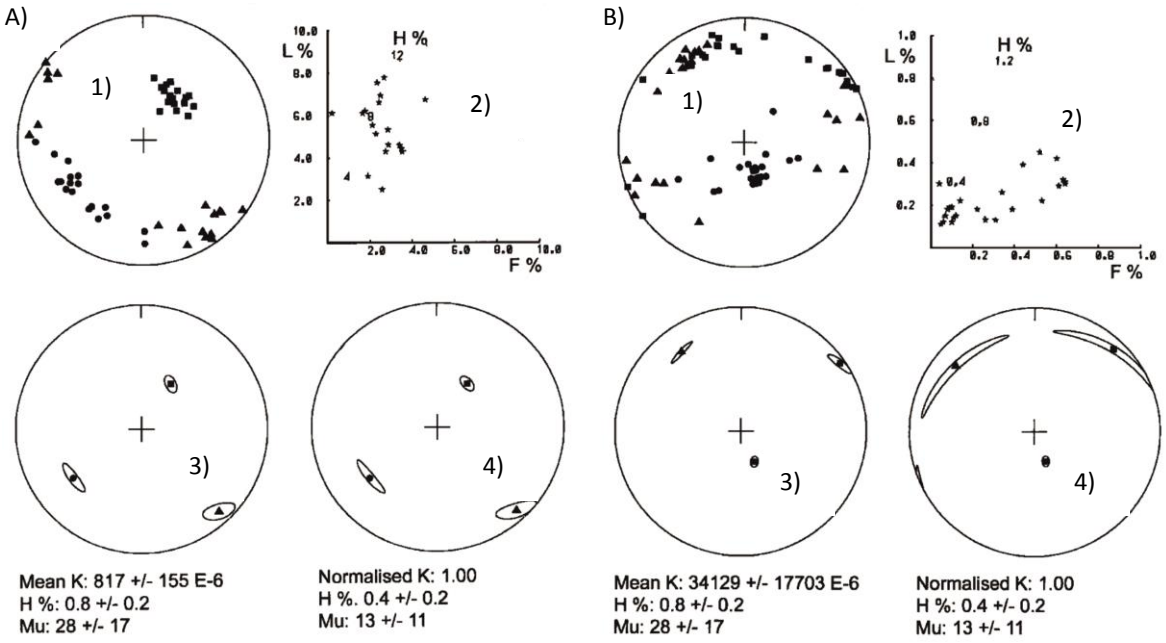


Fig. 6.8 A & B) AMS data from two independent samples (from Owens (2000a)). In both cases (1) shows principal axis directions for all sub-samples. 2) is a Flinn plot of the same data. 3) shows the un-normalised mean principal susceptibility axes for the compiled data with a 95% confidence ellipse. 4) is the normalised mean principal susceptibility axes for the compiled data with a 95% confidence ellipse. Note in sample (A) normalised and un-normalised projections are essentially identical but in (B) they differ. This shows the averaged AMS tensor in (B) is complex and many contain a sub-fabric and that of (A) is relatively straight forward.

6.5.2 AMS of some Minerals

The relationship between the orientation of the AMS ellipsoid and bulk susceptibility of individual minerals vary according to stoichiometry, impurity, and inclusion content. Therefore, while shape and crystalline anisotropy values are constrained for many mineral type examples of minerals (particularly Fe-Ti oxides), specific parameters of individual minerals in a natural specimen may vary considerably and cannot be take for granted. Published values (e.g. Rochette *et al.* (1992); Tarling and Hrouda (1993); Dunlop and Ozdemir (1997)) act as guides but not absolute values which characterise susceptibility in any particular mineral. For a detailed account of AMS associated with particular minerals, the reader is referred to Nagata (1961); O'Reilly

(1984); Thompson and Oldfield (1986); Tarling and Hrouda (1993) and Dunlop and Ozdemir (1997).

Rocks exclusively composed of diamagnetic minerals, such as quartz, calcite, and dolomite, carry a weak negative susceptibility that is controlled by the predominant diamagnetic mineral (Friedman and Higgs 1981). However, due to extremely low susceptibility values exhibited by these minerals, a presence of only 0.001% of ferromagnetic or less than 10% of paramagnetic minerals is sufficient to generate a bulk positive susceptibility value and control the low field AMS of a sample (Tarling and Hrouda 1993).

Iron bearing paramagnetic silicate minerals are important contributors to the AMS ellipsoid especially in samples with low ferromagnetic abundances (~ 1-2% (Tarling and Hrouda 1993)). In the absence of ferromagnetic minerals, paramagnetic phases will almost always dominate over diamagnetic phases owing to the high susceptibility values of the paramagnetic mineral phase(s) (see Tarling and Hrouda (1993) pp. 30-32). Crystalline structure dictates the magnetic anisotropy of these minerals as demagnetising fields and magnetisation values are extremely low (Dunlop and Ozdemir 1997). Amphibole, pyroxene, and olivine all return principal susceptibility axes approximately parallel to the long axis of the grain with attributing crystal dimensions and thus conveniently relate petrofabrics to the AMS ellipsoids (Borradaile and Jackson 2004). However, tourmaline and cordierite may return inverse tensors (see below).

Owing to their higher intrinsic susceptibility values, ferromagnetic grains will most often be significant contributors to the AMS tensor if present. The iron oxide titanomagnetite (ulvospinel - magnetite) and ilmenohematite (ilmenite - hematite) series are the most important ferromagnetic group and in this study are present in 99% of all specimens. As a general proxy, if a sample contains ~ 10% paramagnetic minerals and $K_{mean} > 5x\ 10^{-3}$ (SI) the tensor is likely controlled by a ferrimagnetic (*sensu lato*) fraction, if K_{mean} is $< 5 \times 10^{-4}$ the paramagnetic fraction is likely to be the dominant magnetic phase and between these values a dual paramagnetic-ferromagnetic control is implied (Tarling and Hrouda 1993). Grain size is an important parameter in the ulvospinel-magnetite series as this is proxy for domain state. In essence, if magnetite is very fine grained it is more likely to contain a single magnetic domain which, among other attributes, may generate a net inverse bulk AMS tensor due to self demagnetisation fields; although this effect is poorly understood (see Dunlop and Ozdemir (1997)).

Summary illustrations of the magnetic shape anisotropy, strength of anisotropy and bulk susceptibly values of important diamagnetic, paramagnetic and ferromagnetic minerals are

presented below (Fig. 6.9). More specific properties may be found in Dunlop and Ozdemir (1997) and Tarling and Hrouda (1993).

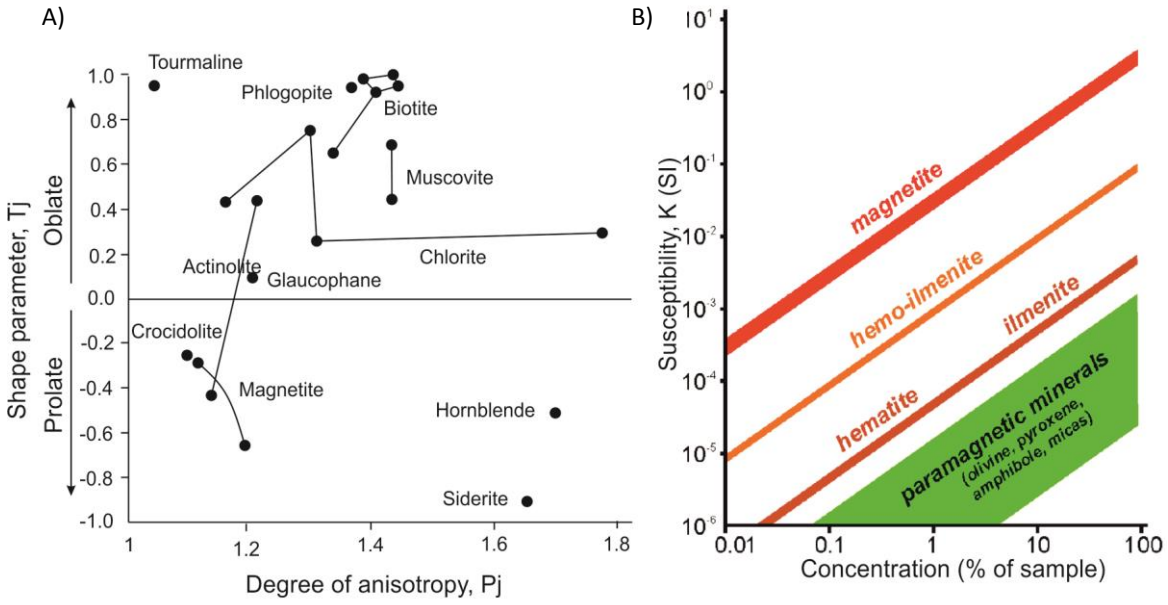


Fig. 6.9 A) Low field magnetic susceptibility shape anisotropy and degree an anisotropy parameters of some minerals (from (Tarling and Hrouda 1993)). Shape anisotropy values in many paramagnetic minerals are much higher and more consistent that those associated with magnetite. B) The contribution of different mineral phases to the bulk magnetic susceptibility of a rock depends on the minerals intrinsic susceptibility and concentration (after Hrouda and Kahan (1991)). For example, <0.5% modal abundance of magnetite will generate a higher susceptibility than a >50% modal abundance of biotite.

Ising (1942) first used AMS in a geological context to examine stratified sediments, later Graham (1954) emphasised the usefulness of this technique in geological investigations on a much broader sense. AMS is now a widely accepted method of indirect non-destructive petrofabric and strain analysis and has a broad variety of applications in structural geology (Jackson and Tauxe 1991; Tarling and Hrouda 1993; Borradaile and Henry 1997; Borradaile and Jackson 2004, 2010).

An elementary application of AMS in the investigation of granitic bodies relates the magnetic susceptibility ellipsoid to a petrofabric thus providing information on the rocks strain and emplacement history. Bouchez (1997) highlighted the fact that the crystalline matrix of granite is never isotropic although granitoids often 'appear' visually isotropic due to extremely low degrees of anisotropy.

In the same manner as traditional fabrics, AMS fabrics may be used to identify planar and linear petrofabric elements (e.g. King (1966); Callot *et al.* (2004); Fanjat *et al.* (2012)) and

distinguish their relative significance (e.g. K1 does not automatically reflect a flow direction). More dynamic AMS fabrics have been interpreted to determine flow direction and shear sense (e.g. Callot and Guichet (2003); Stevenson *et al.* (2007); Stevenson and Bennett (2011); Magee *et al.* (2012)). Such interpretations are extremely convincing when coupled with supporting evidence from traditional flow and shear sense indicators (e.g. Femenias *et al.* (2004); O'Driscoll *et al.* (2008); Ono *et al.* (2010); Valley *et al.* (2011)). It is common practice to use microstructural investigation to determine the rheological state of a host rock during fabric development (e.g. Bouchez *et al.* (1990); Cruden *et al.* (1999); Archanjo and Launeau (2004); Mamtani and Greiling (2005); Esmaeily *et al.* (2007)). The above examples clarify that in a great many cases the internal architecture of plutonic rocks may be described in detail using a combination of AMS, meso, micro, and map scale structural analysis.

6.5.3 Caveats of AMS

Due to the sensitivity of the AMS technique, materials which are visually isotropic often return anisotropic AMS tensors. Interpretation of AMS data under such circumstances should be carried out in a scrupulous manner. This is due the simple fact that the relationship between a samples AMS ellipsoid and petrofabric cannot be assumed to be related in a simple way as the possibility exists of a measured fabric may represent a tectonic or magmatic flow fabric or a combination of both (e.g. Rochette (1988); Rochette and Fillion (1988); Borradaile and Puumala (1989); Ferré (2002); Debacker *et al.* (2004); Fanjat *et al.* (2012)). To evaluate the relationship between the AMS tensor and any possible petrofabric (or petrofabrics) one must consider the following potential caveats;

1. Possibility of inverse, normal or intermediate fabrics
2. The mineralogy and dominant magnetic minerals in an assemblage
3. Magnetic interaction between ferromagnetic grains
4. Relationship between silicate lattice and ferromagnetic grains
5. Presence of multiple petrofabrics

The terms normal, inverse, and intermediate fabric are used in AMS studies to describe the directional relationship between the orientation of the long, intermediate and short dimensions of a grain (X, Y, Z) to the principal susceptibility axes of the AMS tensor (K1, K2, K3). In the

straightforward case, a *normal* AMS ellipsoid has K1, K2, and K3 orientated respectively parallel to the X, Y & Z. If the magnetic fabric is inverted relative to the dimensional axes of a grain, positioning K1 parallel to the Z axis and K3 parallel to the X axis, the AMS fabric is said to be inverse. If a mixture of both normal and inverse components are detected, the AMS fabric is said to be intermediate (Ferré 2002). Inverse and intermediate fabric may be generated due to a structural modification of an original anisotropy or due to the presence of, or concentration of, particular mineral species in a host rock.

Structurally defined intermediate fabrics are generated when a single fabric is partially overprinted/cross cut by a second fabric. The net AMS tensor is a composite ellipse which reflects elements of both fabrics and does not accurately depict a single deformation event. A sub-fabric may be generated in two ways, either by successive tectonic overprints e.g. a bedding-cleavage intersection which defines a prolate tensor parallel to the intersection lineation (Parés and van der Pluijm 2002a; Parés 2004) or by episodic mineral growth, e.g. secondary magnetite due to hydrothermal alteration (Usui *et al.* 2006; Petronis *et al.* 2011). The presence of a sub-fabric may be detected and in some case two fabrics resolved through the statistical analysis of the AMS data (discussed above) and the comparison of this to field data. Several more complex analytical means of isolating magnetic sub-fabrics exist (Vincenz 1965; Bathal 1971; Daly and Zinsser 1973; Edwards 1984; Rochette and Fillion 1988; Ellwood *et al.* 1993; Launeau and Robin 1996; Cagnoli and Tarling 1997; Lüneburg *et al.* 1999; Robion *et al.* 1999; Lagroix and Borradaile 2000; Aubourg and Robion 2002; Hrouda 2002; Parés and van der Pluijm 2002b; Robin 2002; Launeau and Robin 2005; Martin-Hernandez and Ferre 2006; Usui *et al.* 2006) but all require specialised equipment and in most cases sub-fabrics can be identified and dealt with through correct handling of AMS parameters and field data (Tarling and Hrouda 1993; Borradaile and Jackson 2004).

Hydrothermal alteration may also generate an intermediate AMS tensor due to either the breakdown of paramagnetic or ferromagnetic phases into new minerals that yield different susceptibility attributes, or through the precipitation of completely new mineral phases (Kelso *et al.* 1991; Trindade *et al.* 2001; Just *et al.* 2003; Just *et al.* 2004; Petronis *et al.* 2011). Petronis *et al.* (2012) distinguished hydrothermal late stage oxide growth from primary titanomagnetite associated with upwelling deuteric fluids in the Western Granite, Isle of Rum, NW Scotland and associated this process with an increase the magnetite grain size. Just *et al.* (2004) associated progressive deformation of primary magmatic fabrics with a tectonic deformation fabric and associated mineralization in a granite in the Upper Rhine Graben, Germany. In both cases, careful analysis of AMS and field data used in conjunction with petrographic and rock magnetic

experiments (discussed below) aided the distinction of sub-fabrics from the composite AMS tensor detected.

Inverse and intermediate AMS fabrics may also be generated due to the presence of, or particular concentration of, specific minerals in a study sample. Calcite, tourmaline, and single domain magnetite all generate magnetic fabrics that oppose the direction of the applied field (Owens and Rutter 1978; Ellwood *et al.* 1986; Potter and Stephenson 1988; Rochette 1988; Rochette and Fillion 1988; Borradaile and Puumala 1989; Ellwood *et al.* 1989; Rochette *et al.* 1992; Rochette *et al.* 1999; Ferré 2002; Hamilton *et al.* 2004; Chadima *et al.* 2009). If any one of these minerals magnetically dominate a sample, the net tensor generated will be oblique or orthogonal to the true crystallographically defined anisotropy. If a mixture of inverse and normal minerals is present, an intermediate tensor is often generated. If only small quantities are present, or those present are magnetically negligible, an essentially normal tensor is produced. Samples with both normal and inverse components yielded lower anisotropy values, a minimum of a 20% inverse component is required before an intermediate fabric will form (Ferré 2002).

Ferromagnetic minerals (*senso lato*) have the ability to generate a textural anisotropy via grain-grain interaction (Fuller 1963; Wolff *et al.* 1989; Hargraves *et al.* 1991; Stephenson 1994; Archanjo *et al.* 1995; Grégoire *et al.* 1995; Grégoire *et al.* 1998). Cañón-Tapia (1996) argued that whenever magnetic interaction takes place, AMS is dominated by the distribution of grains (textural anisotropy), not by the preferential orientation of those grains, and further stipulated that the combined effects of these two factors may produce a hybrid magnetic fabric which does not simply relate to petrofabric nor textural anisotropy. However, Archanjo *et al.* (1995) demonstrated a strong relationship between petrofabric (biotite, feldspar, enclave), MD magnetite shape fabrics and AMS using examples from the Gameleiras pluton, Brazil. Numerous other authors also report a positive relationship between AMS and silicate fabric (e.g. Borradaile and Henry (1997); Bouchez (1997); Neves *et al.* (2003); López de Luchi *et al.* (2004); Esmaeily *et al.* (2007); Ono *et al.* (2010); Petronis *et al.* (2011)) suggesting cases which exhibit no relationship, or a weak relationship, are anomalous rather than typical (e.g. Fanjat *et al.* (2012)). It is now established that grain-grain interaction is only a factor when the distance between ferromagnetic grains is less than the mean ferromagnetic grain size (Gaillot *et al.* 2006), which is extremely rare.

6.6 Characterising the Magnetic Properties of a Specimen

A specimen's mineral assemblage and the relative abundance of individual phases, their typical chemical composition and grain size are factors that influence that specimens bulk AMS (Tarling and Hrouda 1993; Dunlop and Ozdemir 1997). Intermediate and inverse tensors may be a product of structural or hydrothermal overprinting or a product of a mixture or dominance of minerals which have inverse magnetic susceptibility tensors (discussed above). Careful statistical and qualitative analysis of field, petrographic and AMS data can identify structural overprints in most cases (Borradaile and Jackson 2010). If the degree of anisotropy is extremely low, the origin of intermediate or inverse fabrics may be difficult to recognize. In such cases, it is desirable to characterise the magnetic mineralogy of a specimen to determine if ambiguous or anomalous AMS data reflect a true petrofabric, textural anisotropy, or are due to the presence of some inverse minerals such as single domain magnetite.

Rock magnetic experiments are also useful in distinguishing subtle differences in mineralogy within a single facies. For example, identifying a systematic fluctuation in ferromagnetic grain size across an intrusion can be carried out efficiently using a range of rock magnetic experiments and has applications in determining the cooling or hydrothermal history of a host rock (e.g. Kelso *et al.* (1991); Petronis *et al.* (2011); Just and Kontny (2012)).

In this study, a suite of rock magnetic experiments were employed to characterise the mineral assemblage of each facies studied in each pluton. The primary aim was to determine if anomalous magnetic fabrics, which were oblique to observed field fabrics, were a product of structural overprinting or the presence of some inverse minerals. In addition, the experiments returned data that show the degree of heterogeneity of the ferromagnetic and paramagnetic assemblage across the intrusions studied; this aids with the interpretation of AMS as local contrasts in susceptibility parameters are better understood. Finally, in some instances, detailed rock magnetic investigation returns data that show that some specimens underwent unique cooling or hydrothermal histories, this is related to field and petrographic observations to constrain the relative timing of causative events.

6.6.1 Rock Magnetic Experiments

The rock magnetic experiments used to evaluate the magnetic mineralogy of rock sample in this study are discussed below.

6.6.1.1 Temperature vs. Low Field Susceptibility (T vs. K)

The most straightforward means by which one can evaluate a mineral assemblage from a magnetic point of view is by measuring low-field susceptibility versus temperature under a constant applied field. This experiment involves exposing a sample to a constant weak magnetic field (200 A/m @ 976 Hz) as ambient temperature is progressively increased. The experiment is conducted within an inert Ar atmosphere to limit oxidation during heating. The fluctuation in low-field susceptibility as temperature increases (following the Curie-Weiss Law and Curies Law (Appendix D) is measured at short regular intervals.

Monitoring susceptibility fluctuation with temperature from room temperature to ~ 700°C allows one to evaluate the magnetic composition of a given sample (example Fig. 6.10A). The Curie point, the temperature at which super exchange and exchange forces are no longer effective and ferromagnetic materials behave paramagnetically (Getzlaff 2007), may be estimated based on the Hopkinson peak method (Moskowitz 1981) or the inflection point method (Tauxe 1998). From this the Ti content of titanomagnetite can be inferred (Akimoto 1962; Lattard *et al.* 2006). The shape of the Hopkinson peak, if present, may be used as a crude proxy for grain size and domain state as SD grains are more likely to exhibit a sharp peek over a shorter temperature range relative to MD grains (Dunlop and Ozdemir 1997).

Cryogenic experiments were also carried out (example Fig. 6.10B). This involved cooling samples in liquid nitrogen to -198°C and monitoring the change in susceptibility on heating to room temperature. Inspection of the shape of the progressive heating curve vs. low-temperature susceptibility can reveal other less obvious magnetic contributors which have T_C/T_N at lower temperatures and contribute less to the bulk susceptibility at room temperature (Hrouda *et al.* 2006). Abrupt fluctuations in susceptibility during heating can be used to identify phase transitions associated with particular minerals, for example the magnetite Verwey Transition (-153°C) (Verwey 1939; Verwey and Haayman 1941), and the hematite Morin Transition (-13°C) (Morin 1950).

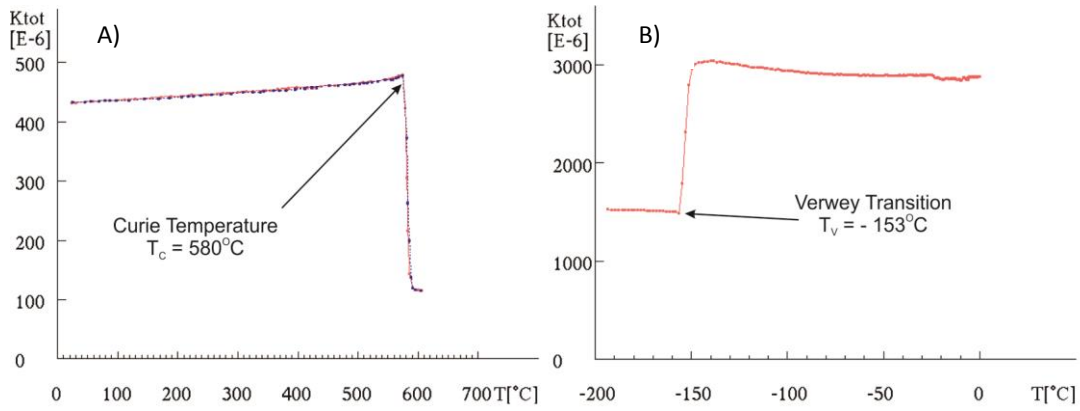


Fig. 6.10 Schematic graph of the variation of susceptibility in pure magnetite with temperature. A) The susceptibility of magnetite increases with temperature up to the Curie Temperature where the mineral undergoes a transition from a ferrimagnetic to paramagnetic state, this is associated with a major decrease in susceptibility. B) At low temperature magnetite undergoes a transition from cubic to orthorhombic symmetry, this is indicated by an abrupt decrease in susceptibility and is termed the Verwey Transition.

6.6.1.2 The Lowrie - Fuller Test

Experimental results show that normalised data returned from two cycles of AF-(Alternating Field) demagnetisation on the same sample, first targeting an imposed ARM (anhysteretic remanent magnetisation) and the second an IRM (isothermal remanent magnetisation), will return different relationships depending on whether SD or MD grain size dominates the grain size of the sample (Lowrie and Fuller 1971). This work proposes that for larger grains ARM is removed by weaker AF-demagnetising fields than that which is required for demagnetisation of SIRM. Thus, by carrying out two progressive demagnetisation experiments Lowrie and Fuller (1971) were able to propose a means through which one may evaluate grain size. Two examples of data from this test, along with demagnetisation of NRM, is presented as an example below (Fig. 6.11).

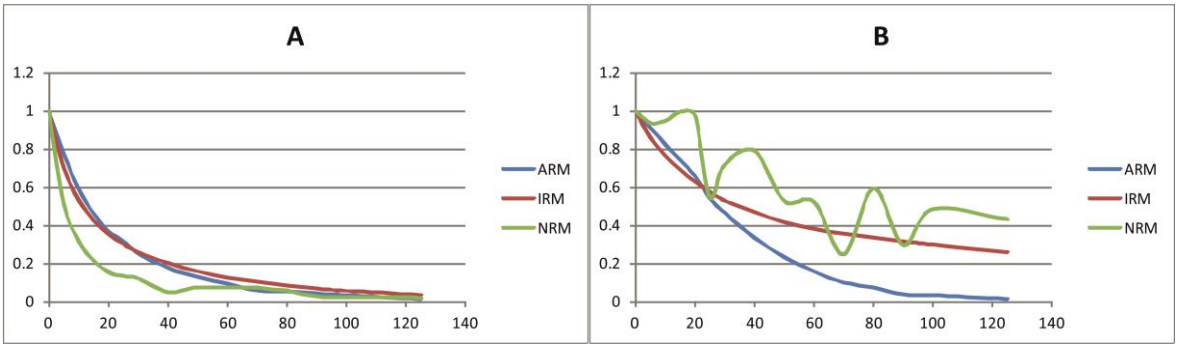


Fig. 6.11 Examples of data from the Lowrie-Fuller test carried out on two contrasting samples. In sample "A" rapid demagnetisation of ARM, IRM and NRM is consistent with the presence of magnetically soft minerals such as multidomain magnetite. Sample "B" demagnetises at a much slower rate. IRM is much more stable than ARM and the NRM demagnetisation curve contains several peaks and troughs. This is consistent with the presence of magnetically hard minerals such as haematite or single domain magnetite.

to hydrothermal affects which are believed to have played a pivotal role in the generation of the subject MD magnetite grains (Xu and Dunlop 1995).

Ultimately, the Lowrie-Fuller test is considered useful in evaluating magnetic properties of a sample when combined with other rock magnetic experiments. Comparing the shape of ARM and SIRM demagnetising curves reflects the coercivity spectrum as opposed to domain state and grain size directly (Dunlop and Ozdemir 1997). Thus, this test can be used as an indirect means through which one may evaluate the former parameters but best practice will seek to compliment this technique with further work.

6.6.1.3 IRM Acquisition Curves

IRM acquisition is achieved by applying a progressively larger magnetic field along a single axis of a previously AF-demagnetised sample. Remanent magnetisation is measured after each applied field. IRM Field intensity is gradually increased until magnetic remanence plateaus as it reaches saturation, i.e. saturation isothermal remanent magnetisation (SIRM) is reached (Fig. 6.12). The magnetic field is then reversed along the same axes to generate a back-field IRM (BIRM). BIRM demagnetisation measurements record the reverse field required to return M_r (magnetic remanence) to a value of zero (coercivity of remanence H_{CR}) from M_s (saturation magnetisation) (Fig. 6.12). This is a non-destructive method (not magnetically but in terms of sample integrity) for investigating the coercivity spectrum of a sample (Dunlop and Ozdemir 1997) and results are comparable to those generated from full hysteresis measurements.

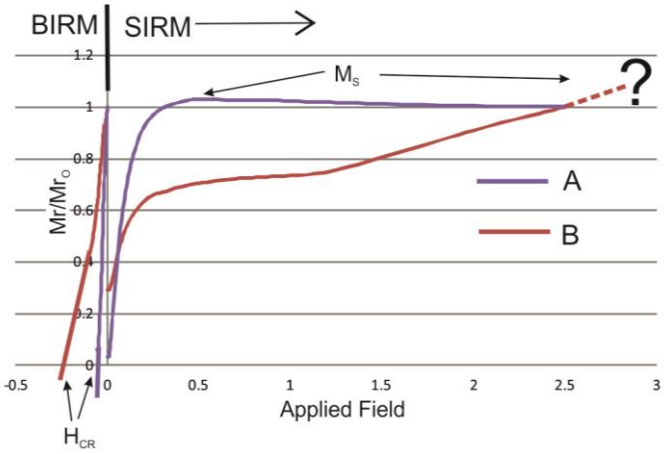


Fig. 6.12 SIRM and BIRM acquisition and demagnetisation curves for samples "A" and "B" (same as those used in Fig. 6.11) Rapid acquisition of remanence and demagnetisation of "A" shows low coercivity minerals dominate. Sample "B" never reaches saturation and carries much higher H_{CR} value. This is consistent with the presence of higher coercivity minerals in B relative to A and is consistent with the data shown in Fig. 6.11.

Resulting data characteristically show rapid acquisition in MD grains relative to SD grains of the same mineral species. It follows that for progressively smaller grain sizes, and simpler domain structures, M_s is reach in progressively elevated fields (e.g. Day *et al.* (1977); Argyle and Dunlop (1990)). Furthermore, as coercivity contrasts between distinct ferromagnetic minerals exist, and M_s is reached under differing fields, analysis of both SIRM and BIRM curves can be used to aid in evaluating the presence of mineral species as well as domain state (Lowrie and Heller 1982; O'Reilly 1984). Thus, the presence of more than one phase may be identified by stepwise increases in the inducing SIRM field (Butler 1982) and grain size/domain state may be indicated by the relationship between the SIRM and BIRM curves (Dunlop and Ozdemir 1997).

6.6.1.4 Thermomagnetic Analysis of Three-Component IRM

As minerals of the same species and similar grain size exhibit characteristic coercivity spectra and demagnetisation properties, these features may be used to evaluate the type of magnetic minerals present by combining IRM acquisition with thermal demagnetisation (Dunlop 1972). However, many ferromagnetic minerals have coercivity characteristics that overlap which impedes the identification of dominant phases if a single IRM acquisition curve is used.

Thermomagnetic analysis of three-component IRM (Lowrie 1990) is executed by applying magnetic fields of variable intensity along three orthogonal axes (X, Y, Z) of a previously AF-demagnetised sample. The three inducing fields are selected based on prior knowledge of suspected magnetic contributors established from IRM acquisition data. In the original experiment (Lowrie 1990), fields of 1.2T, 0.4T and 0.12T were applied to test for the presence of goethite, pyrrhotite hematite, maghemite, and magnetite. Magnetic remanence is then measured before, and episodically during, stepwise thermal demagnetisation, usually from 0°C to 700°C as the unblocking temperature of hematite is *c.*675°C (O'Reilly 1984). The magnitude of M_r along each axis during each demagnetisation interval, and the temperature required to fully remove M_r are used to interpret the mineral species present and their relative proportions (Fig. 6.13). This can help to evaluate the origin of anomalous bulk susceptibility or AMS data (for example, by revealing a hydrothermal overprint) and also has various application in palaeomagnetic studies (see Dunlop and Ozdemir (1997)).

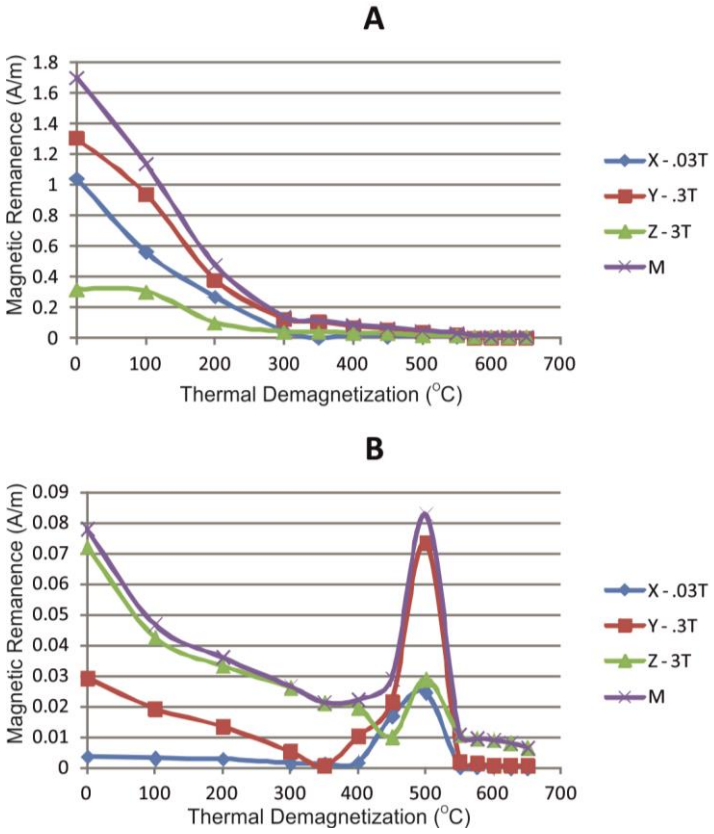


Fig. 6.13 Thermomagnetic Analysis of three-component IRM data from samples A & B (same samples as used above). Sample "A" has a large proportion of the modulus magnetic vector (M) dominated by low (X - 0.03T) and moderate (Y - 0.3T) coercivity minerals, high coercivity minerals are not abundant (Z - 3T). The modulus vector of sample "B" is dominated by high coercivity minerals (Z - 3T) and low coercivity minerals are negligible. These data are consistent with the results shown above and indicate that sample "B" has a magnetic assemblage distinct from sample "A". This contrast in mineral modal abundance means that the AMS of each sample is not directly comparable as it is controlled by entirely different magnetic parameters that are inherent to each mineral assemblage.

6.7 Summary

Owing to the high degree of accuracy, sensitivity and efficiency, rock magnetic analysis, and AMS in particular, are invaluable to the investigation of plutonic rocks. In the past two decades technological progress has improved functionality, accuracy and efficiency (Bouchez 1997; Borradaile and Jackson 2010) and a more detailed understanding of the mineralogical controls over AMS has been obtained (Tarling and Hrouda 1993; Dunlop and Ozdemir 1997; Borradaile 2001, 2003; Borradaile and Jackson 2004; Martin-Hernandez and Ferre 2006; Borradaile and Jackson 2010). This makes AMS an ideal supplement for traditional methods employed in this thesis.

It is crucial to understand the magnetic mineralogy of specimens examined. This may be partially achieved by transmitted and reflected light microscopy which must be supplemented by some form of rock magnetic analysis. As a minimum, bulk susceptibility measurements may sometimes suffice but can only give a very vague indication of the grain scale contributors to the bulk AMS ellipsoid (Tarling and Hrouda 1993). In order to satisfy the critical evaluation of AMS

data some rock magnetic experiments should be employed. Such work is desirable in all cases but is critical in scenarios in which magnetic fabrics contradict field or petrographic relationships.

6.7.1 The use of Rock Magnetic in this Thesis

In the current work, field work was supplemented with petrographic and rock magnetic data. All data collected were considered in a relative context during interpretation. Orientated block samples were collected according to a predefined grid pattern across each intrusion regardless of the presence or absence of meso-scale matrix fabrics however defined shear zones were avoided. Where necessary, multiple samples (for redundancy) were collected from areas in close proximity and within shear zones. Similarly, in areas of particular interest extra samples were collected to test for localised strain patterns. On average, for every ten samples collected a duplicate sample was taken for standardisation purposes.

All block samples (total of 432) underwent AMS analysis. Approximately 13-18 sub-specimens were cored and prepared from each block following the methodology detailed in Owens (1994). AMS analytical work was carried out on a KLY-3S Kappabridge susceptibility meter (operating at 300 A/m @ 875 Hz) at the magnetics lab in the Geology and Geography Department, University of Birmingham U.K..

Susceptibility values were compiled and initial parameters were calculated using in-house software designed by Dr. W. H. Owens at the University of Birmingham U.K. (open source software in Appendix F) after Jelinek (1977). GPS co-ordinates, field fabric measurements and principal susceptibility data (orientation and magnitude) were compiled on Microsoft Excel and the parameter used were calculated (primarily Pj, Tj and K_{mean} but also L, F, H, M, Mu, LnPj and Uj).

Data reflecting mean susceptibility, fabric shape, and orientation were projected onto base maps using Arc GIS 10.1 (licensed software) for comparative and processing purposes. Contour and DEM maps of K_{mean}, Pj, Tj and H were constructed using Arc GIS 10.1 and Arc Scene 10.1. Scalar data was graphically evaluated using Golden Software Surfer8 (licensed software) and Golden Software Grapher6 (licensed software).

Rock magnetic experiments were carried out on select AMS cored specimens based on preliminary susceptibility experiments, facies, spatial distribution and unique characteristics such

as hydrothermal overprinting or proximity to brittle structures. Experiments included varying temperature *vs.* low field susceptibility, the Lowrie-Fuller test, IRM acquisition and demagnetisation experiments and thermomagnetic analysis of three component IRM as described above.

All rock magnetic experiments were carried out at the Paleomagnetic-Rock Magnetism Laboratory at New Mexico Highlands University, New Mexico, U.S.A.. Susceptibility experiments were carried out using an AGICO MFK1-A multifunction Kappabridge with a CS4 attachment for thermal experiments. Remanence measurements were made using a AGICO JR-6A dual speed Spinner magnetometer. An in-house built DC impulse electromagnetic coil, constructed by M_r. Bob Macy (University of New Mexico, U.S.A.), was used to induce IRM. ARM magnetisation and demagnetisation was carried out using a D-tech D-2000 AF-demagnetizer with ARM/PARM capabilities. Thermal demagnetisation was carried out in an ASC TD48 thermal demagnetiser in zero field. All specimens were protected from background magnetic fields between experiments in magnetic shields and all remanence measurements were carried out in a faraday cage with ambient magnetic fields of trace and 0.963μT respectively.

Remanence measurements were first evaluated using Agico Remasoft (open software, see Appendix F), compiled in Microsoft excel and finally projected using Golden Software Grapher6 (licensed software). Temperature *vs.* susceptibility measurements were analysed in Agico Cureval8 (open software, see Appendix F) compiled in Microsoft Excel and projected using licensed Golden Software Grapher6.

Chapter 7:

The Omey Pluton;
A Discordant Phacolith

7.1 Introduction

The Omey Pluton is located *c.*11 km northwest of Clifden Village in northwest Connemara, Co. Galway. First mapped by Cobbing (1959), this granite intrudes the Argyll Group of the Dalradian Supergroup along the hinge of the Connemara Antiform (Cobbing 1968; Leake and Tanner 1994). Contact metamorphism has generated a marked 300m thermal aureole in adjacent calcic and schistose country rock which over prints regional metamorphism (Ferguson and Harvey 1979; Ferguson and Al-Ameen 1985; Ahmed-Said and Leake 1996). Townend (1966) mapped the interior in detail and described a normally zoned forcefully emplaced granite with a central acidic plug derived from the concentration of volatiles during cooling.

Several authors have attempted to constrain the timing of emplacement of the Omey Pluton. Early attempts had unacceptable margins of error (Leggo *et al.* 1966) or did not directly measure the age of crystallisation (Elias *et al.* 1988). More recently Buchwaldt (2001) calculated a 420Ma U-Pb zircon age and Feely *et al.* (2007) 422.5 ± 1.7Ma Re-Os age from stock work molybdenite bearing quartz veins hosted within the granite. A consensus now stands that this is the oldest member of the Galway Granite Complex (GGC) (Feely *et al.* 2010) and that emplacement was concurrent with the onset of late Caledonian regional transpression (Dewey and Strachan 2003).

Accepting this as the oldest member of the GGC, the Omey Pluton is an ideal starting point in unravelling the magmatic-tectonic late Silurian to mid-Devonian history of Connemara. The mechanisms of ascent, emplacement and deformation of this granite and how they relate to other members of the GGC or regional kinematics is currently poorly understood. The present work re-examines specific field relationships within the pluton and country rock with an aim to describe its internal architecture. Rock magnetic data, including Anisotropy of Magnetic Susceptibility (AMS) measurements are used in conjunction with field and petrographic data in order to constrain the structural and kinematic controls on the siting of the Omey Pluton.

7.2 Geological Background

The bedrock geology of Connemara is summarised in Figure 7.1. The Dalradian Supergroup was subjected to five major deformation events (D1-D5) during the earlier stages of the Caledonian Orogeny prior to the intrusion of the Omey Pluton (discussed in Chapter 3). D4 compression formed a regional scale asymmetric WNW-ESE trending fold known as the Connemara Antiform

which plunges gently east (~ 5-10°) (Leake and Tanner 1994). The Omey Pluton is nestled between the steeply (~ 70-80°) southward dipping and moderately northward dipping (~ 55°) limbs of this fold, the centre of the intrusion sits astride the fold axis. In map view the pluton defines a tear drop shape (Ø = 7.5km) along a WNW-ESE axis pinching out to the east (Cobbing 1968).

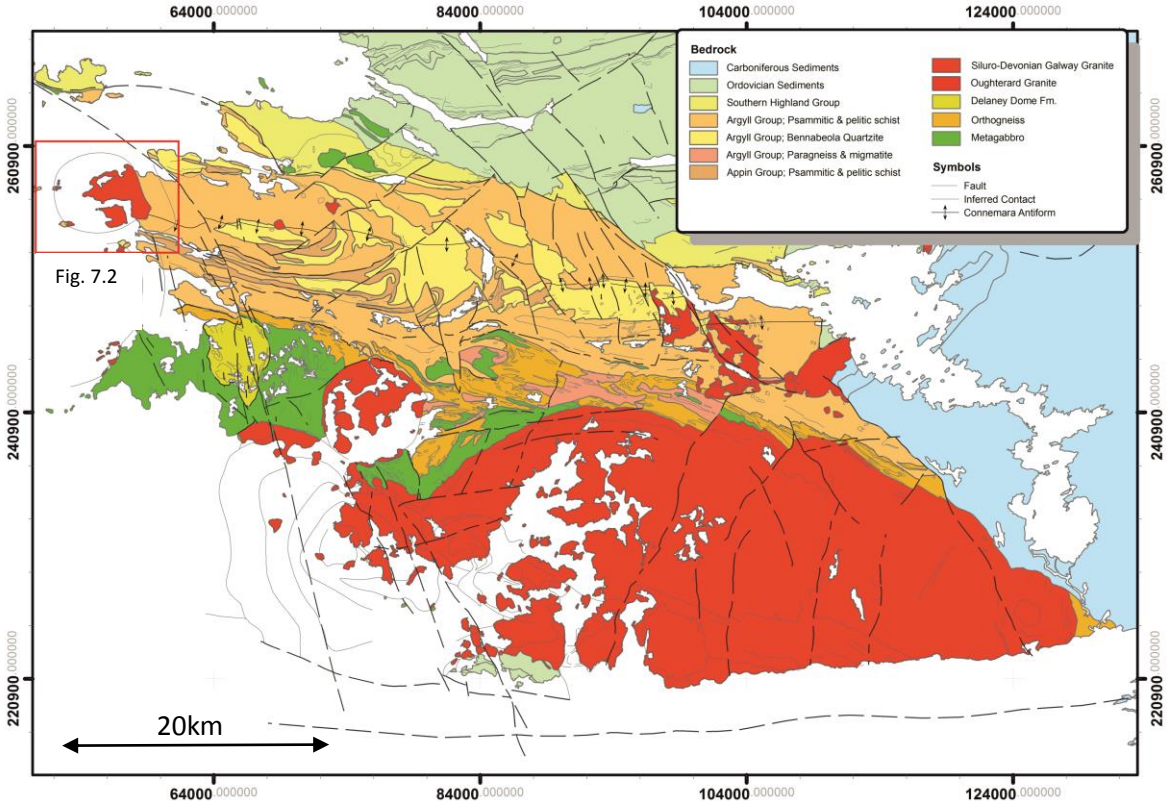


Fig. 7.1 Summarised geology of Connemara. D4 Connemara Antiform axis trends ESE-WNW across the region and is cross cut by the Omey Pluton in the west. Several northwest-southeast and southwest-northeast D5 faults cross cut the Connemara Metamorphic Complex and some members of the Galway Granite Complex.

The final tectonic event recorded prior to the emplacement of the GGC is represented by a suite of northwest-southeast and southwest-northeast conjugate faults that cross cut the Connemara Metamorphic Complex (Leake and Tanner 1994). It has been established that these structures were active during the late Silurian and early Devonian (Chapter 3). Figure 7.1 shows these to be regionally significant fault systems, several of which are located within 4km of the Omey Pluton. Here activity along these structures in the late Silurian is associated with the late Caledonian sinistral transcurrent regime (Dewey and Strachan 2003; Soper and Woodcock 2003).

The Streamstown Schist Fm. and the Lakes Marble Fm. (Badley 1976; Treloar 1977, 1982; Leake 1986; Leake and Tanner 1994) are in contact with the granite in the southeast and

northeast respectively (Fig. 7.2A attached map). The eastern most outcrops of the pluton, at Barnahallia Lough (059300, 255700), are in contact with gently eastward inclined (10-20°) fold axis of the D4 Connemara Antiform. The northern, southern and much of the western margin of the intrusion's external contact is off shore and cannot be observed. Two islands, Friar Isl. (052230, 257730) and Cruagh Isl. (052970, 254980), expose the granite country rock contact at the western extremity of the pluton. The country rock here is currently unassigned stratigraphically (Leake and Tanner 1994; Long and McConnell 1995) and is dominated by well bedded pelites and psammites. Townend (1966) described the presence of a narrow quartzite unit and several quartz pebble bed horizons on Cruagh Isl., an observation supported here. Similarities between the quartz conglomerate units observed here and observations made by Kilburn *et al.* (1965) at Cleggan Head (059600, 259900), suggest that the stratigraphic units on these Islands can be correlated with the Cleggan Boulder Bed Fm..

The attitude of bedding on Cruagh Isl. and Friar Isl. correlate with outcrops along strike on the mainland. On Cruagh Isl. bedded horizons dip steeply south (~ 70°) and strike WNW-ESE while on Friar Isl., bedding dips between 10-25° east and strikes NNE-SSW. Thus Cruagh Isl. and Friar Isl. are the off shore representations of the southern limb and fold hinge of the Connemara Antiform respectively, although Friar Isl. probably sits slightly south of the actual fold hinge.

Thus, the Omey Pluton is bound by distinctive formations of the Argyll Group which progressively young from west to East. These are the Cleggan Boulder Bed Fm. off shore to the west and the stratigraphically higher Streamstown Schist Fm. and overlying Lakes Marble Fm. to the southeast and northeast respectively.

7.3 Petrographic and Field Descriptions

Townend (1966) described the internal facies of the Omey pluton and its basic structural features. Here, a new geological map of the Omey Pluton is presented (Fig. 7.2A attached map) following detailed remapping of the intrusion. This work substantiates much of the previous author's work however considerable modifications have been made to the original map regarding facies definition, distribution and contact relationships.

7.3.1 Facies Descriptions and Distribution

The Omey Pluton is a composite intrusion consisting of three main facies, G1, G2 and G3 previously termed the Omey Adamellite, the Aughrus More Adamellite and the Island Adamellite respectively (Townend 1966). This nomenclature is applied as an effective means of identifying individual facies of a pluton and the suggested order of intrusion (Richey 1928). The existence of the Glassillaun Granodiorite (Townend 1966) as a sub-facies of the Omey Pluton; a suite of ESE-WNW trending granodiorite dykes that cross cut the pluton are recognised in place of the Glassillaun Granodiorite.

G1 is a medium grained (8mm) equigranular biotite hornblende monzogranite with rare 2cm tabular phenocrysts of pink K-feldspar. Typically, subhedral K-feldspar occurs as 10mm crystals amongst slightly finer quartz and biotite. Prismatic titanite and zircon along with apatite and rutile are common accessory minerals. The modal abundance of constituent minerals is: 30% alkali feldspar, 34% oligoclase-andesine, 30% quartz, 3% biotite, >2% hornblende and 1% accessories. Overall this facies contains 72% SiO_2 (Leggo *et al.* 1966). Dark green prismatic (3mm) hornblende is most abundant in the east where a sub-facies G1A (previously the Barnahallia Granite (Townend 1966)) is defined based on this slightly higher (~ 2%) modal abundance of hornblende.

G2 is a medium grained biotite hornblende monzogranite and is very similar to G1. As distinct from G1, G2 is finer grained (~ 6mm), contains a lower abundance of hornblende (0-1%) and exhibits very rare large phenocrysts of tabular K-feldspar up to 4cm long. Quartz commonly occurs as rounded 6-8mm grains or as slightly elongate lobes which define a subtle foliation if present, into which biotite is also incorporated. Andesine (An 30-40 (Townend 1966)) is the dominant feldspar. The modal abundance of constituent minerals is; 29% alkali feldspar, 33% plagioclase, 34% quartz, 3% biotite and 1% accessories.

G3 is a medium to fine grained (~ 2-6mm) pink quartz-phyric monzogranite. Biotite is far less abundant, muscovite is present but rare and hornblende is absent, oligoclase (An 20, (Townend 1966)) is the dominant feldspar. Magnetite is present in lower abundances than that observed in earlier facies and a higher proportion of hematite is present. Accessory minerals include zircon, apatite, rutile and fluorite. Modal abundances are as follows; 30% K-feldspar, 33% oligoclase, 35%

quartz, 2% biotite, >1% muscovite and >1% accessories. Overall this facies contains 75% SiO_2 (Leggo *et al.* 1966).

All facies of the Omey Pluton plot just to the bottom right of the monzogranite field. A subtle trend is noted whereby facies become progressively siliceous, finer grained and modally less mafic from G1 to G3. Figure 7.3 depicts characteristic petrographic features of facies G1 and G2. G1 and G2 are texturally and petrographically quite similar and are best distinguished by the presence of larger K-feldspars (Fig. 7.3E) and rounded quartz in G2 (Fig. 7.3G, H) and a higher abundance of hornblende in G1. In both cases, prismatic green hornblende (~ 2-4mm) is typically fresh while biotite (2-6mm) is almost always euhedral (outside of shear zones) and extensively chloritised. Feldspars are partially altered and commonly extensively replaced by sericite (Fig. 7.3B, C). Larger K-feldspars are poikilitic exhibiting 0.5-2mm quartz, euhedral feldspar and oxides that accreted to or nucleated on the once outer margins of the phenocrysts crystal lattice (Fig. 7.3D, E). A broad variety of zoning textures are noted in both sodic and potassium rich feldspars including oscillatory, normal and rarely boxy zoning. Calcic spikes are most obvious as these are more extensively sericitized (Fig. 7.3A, B). K-feldspar regularly exhibits dramatic microperthite texture with thin exsolution lamellae of albite flames which may be parallel or irregularly orientated (Fig. 7.3E). Although rare, the conversion of orthoclase to microcline is present and spatially associated with minor wedged twins in plagioclase, kinking and smearing of biotite and more prominent undulose extinction in quartz and some feldspars. These features are associated with syn-post emplacement strain, a topic discussed further below.

The G3 facies characteristically exhibits a porphyritic texture defined by ≤ 15mm tabular plagioclase and orthoclase (Fig. 7.4A-E) and ≤ 12mm studs of anhedral or rounded quartz (Fig. 7.4F) set in a 2-5mm monzogranite groundmass. This facies has a slightly higher SiO_2 content and less mafic minerals than G1 and G2. It is thus very distinct from other facies and represents a more evolved, acidic magma. Quartz phenocrysts exhibit minor undulose extinction and are approximately circular. Both plagioclase and orthoclase phenocrysts show normal and oscillatory zonation with sericitization concentrated along calcic rich cores or spiked concentric rims (Fig. 7.4A, B). As in G1 and G2, biotite is almost always extensively chloritised. Fluorite associated with biotite layering on Cruagh Island is associated with concentration of late stage residual fluids rich in incompatible elements near the upper portions of the intrusion (Townend 1966).

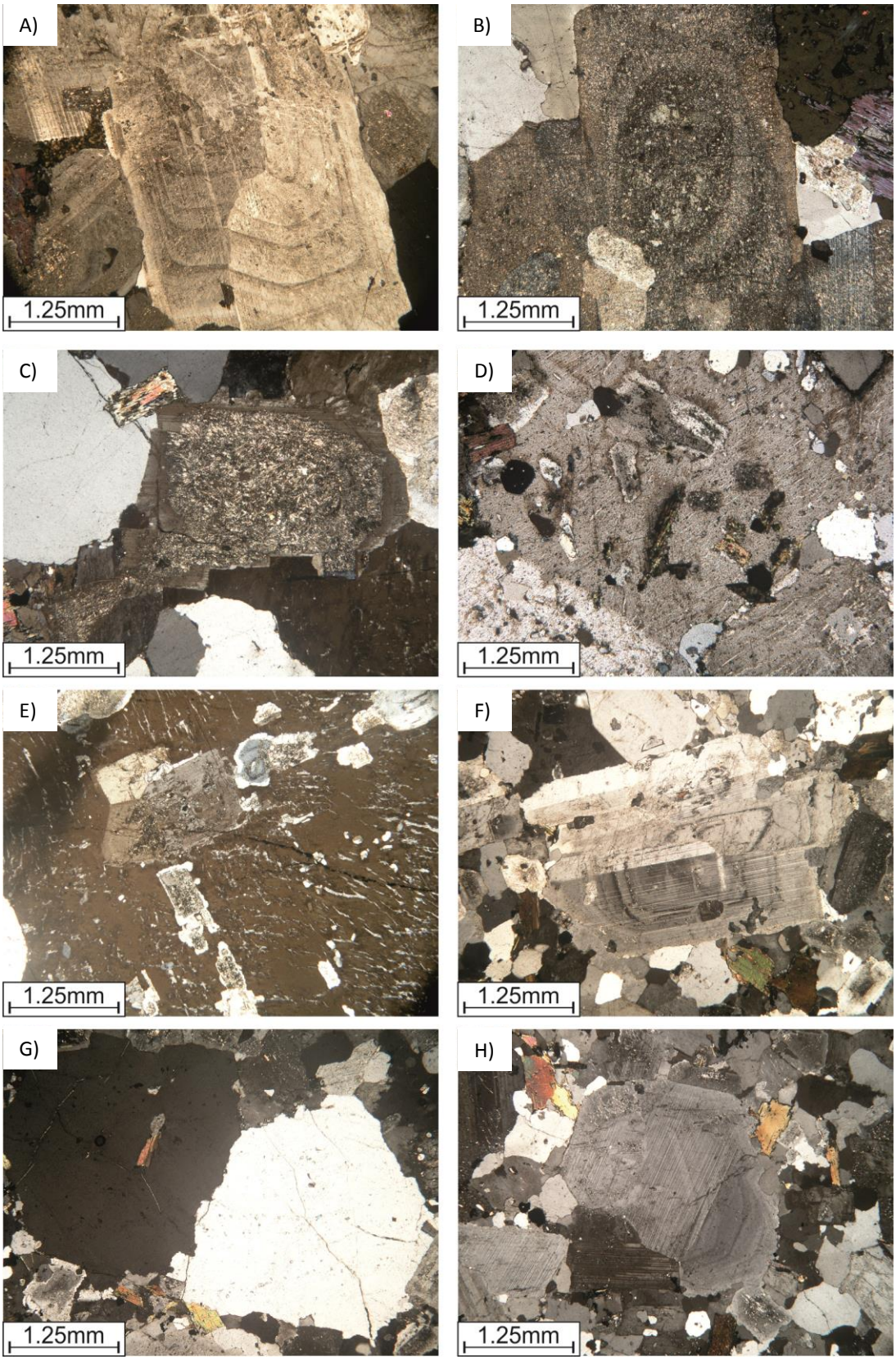


Fig. 7.3 Characteristic petrographic features of facies G1 and G2. Calcic spikes are extensively sericitized (A, B). Feldspars are partially altered and commonly extensively replaced by sericite (B, C). Poikilitic K-feldspars exhibit 0.5-2mm quartz, euhedral feldspar and oxides that accreted to or nucleated on the once outer margins of the phenocrysts crystal lattice (D, E). Microperthite texture with thin exsolution lamellae of albite flames in K-feldspar (E). G2 is distinguished from G1 by the presence of larger K-feldspars (E) and rounded quartz (G, H).

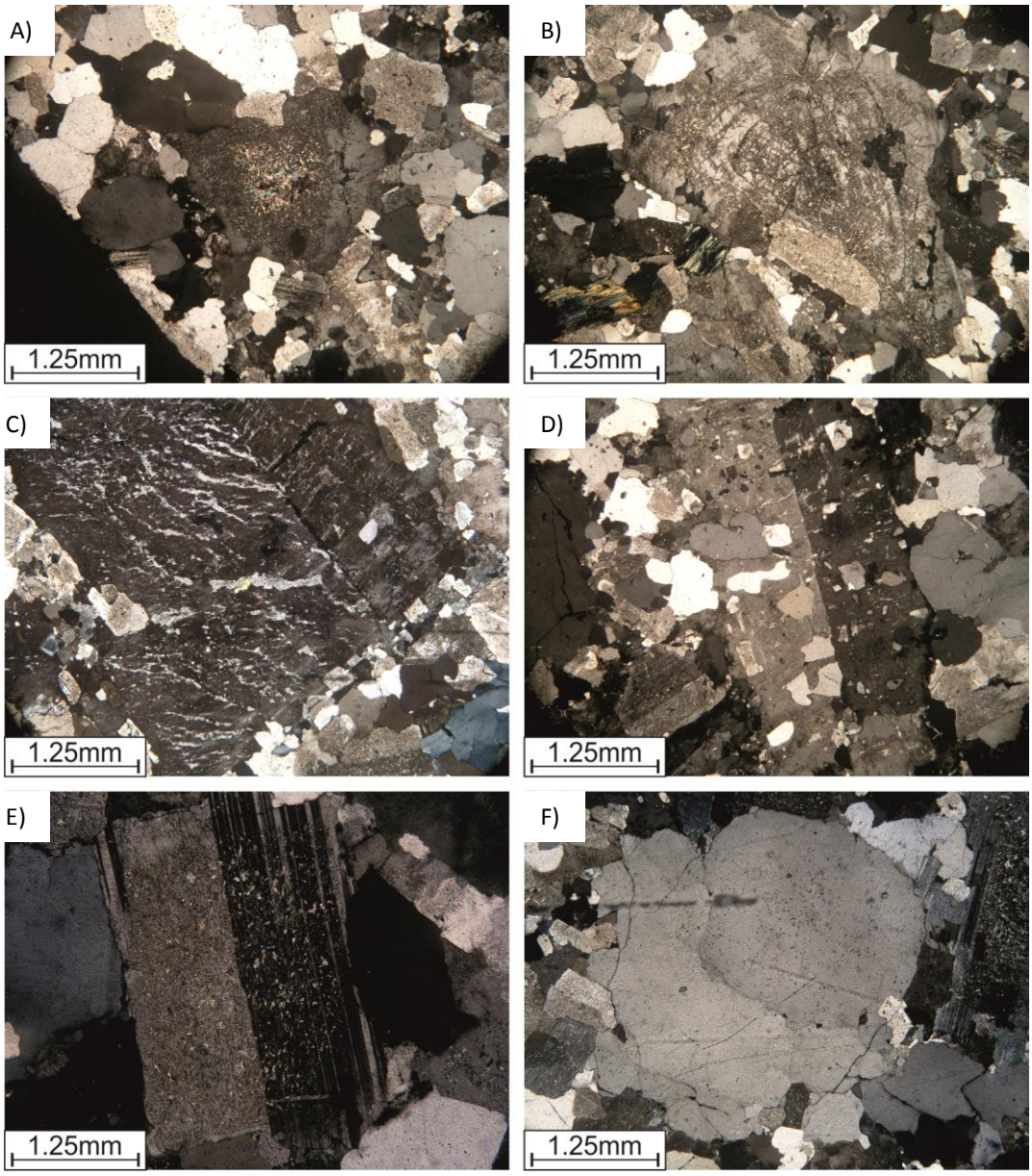


Fig. 7.4 Charactoristic petrographic features of G3. Sericitization of plagioclase and orthoclase is concentrated along calcic rich cores or spiked concentric rims (A, B). Porphyritic texture defined by ≤ 15mm tabular plagioclase and orthoclase (A-E) and ≤ 12mm studs of anhedral or rounded quartz (F).

Hand sample and reflective light microscopy observations indicate the presence of magnetite, pyrite and hematite in all facies of the Omey Pluton. Iron oxide phases (magnetite & rare hematite) typically occur as elongate aggregates or cubic crystals which adhere to the lattice and cleavage planes of silicate minerals (Fig. 7.5A) or as secondary alteration products of titanite (Fig. 7.5B, D) and biotite that pseudomorph the primary mineral's crystal habit (Fig. 7.5C). Magnetite exhibits marginal alteration to maghemite along fracture and crystal peripheries (Fig. 7.5C), this is generally more extensive in G3 than G1 or G2. Aggregates of fine to medium grained

disseminations of molybdenite, pyrrhotite and pyrite occur very locally in all facies but are most common in G2 and G3 as secondary deposits within brittle structures (see Feely *et al.* (2007)).

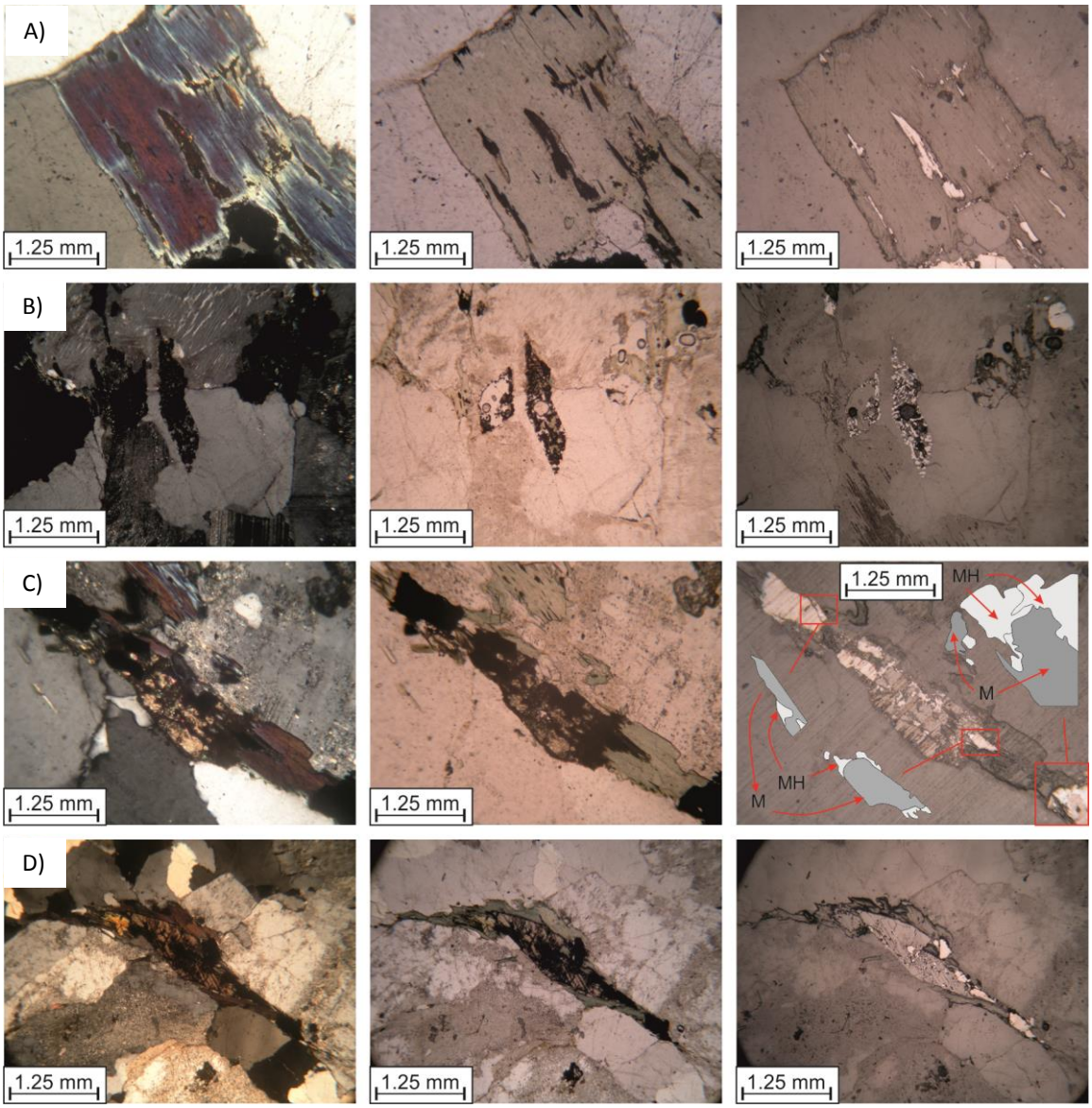


Fig. 7.5 Left to right, XPL, PPL and RL images of representative samples that show the relationship between iron oxide phases and silicate minerals. A; Elongate aggregates of magnetite along cleavage planes within biotite. B; Alteration of titanite with product magnetite psudomorphing the original mineral. C; RL image shows three blow-ups of magnetite crystals (dark gray) that have been undergone maghemitization along fracture and crystal margins (light gray). D; . Altered biotite pseudomorphed by secondary magnetite.

Summary of facies distribution

Omey Island and a large proportion of the Aughrus Peninsula are composed of the G1 facies which makes up a dominant portion the pluton. An array of small rocky sea stumps and islands lie 100-1000km off shore to the west and north, the majority of these are also composed of G1. In the east, near Barnahallia Lough, G1A is denoted by a notable increase in abundance of prismatic

dark green hornblende. South of Aughrusbeg Lough (055770, 258230) and north of Tonashindilla Pier (055790, 256650), a circular body of G3 (Ø = 1.2km) forms the core of the Aughrus Peninsula and the highest point within the pluton, Aughrus More (056475, 257626). In the west, Cruagh Isl. and Friar Isl. are composed predominantly of G3. G2 is only found between the G1 and G3. The largest exposures of G2 skirt around the northwest and north east perimeter of the large G3 sheet in the centre of the Aughrus Peninsula. The G2 facies is also present on the eastern tip of both Friar Isl. and Cruagh Isl. and also immediately north of Tonashindilla Pier.

7.3.2 Contact Relationships

7.3.2.1 External Contact Relationships

The axial trace of the Connemara Antiform separates the Omey Pluton into zones along which the orientation of the granite contact varies systematically according to country rock structure (Fig. 7.2). South of this line, from Barnahallia southwest to Fountainhill Beach (058293, 255265) and on Cruagh Isl., granite is in contact with the steeply inclined (~ 80°) southward dipping limb. North of the fold hinge, from Barnahallia northwest to Rossadillask Beach (058064, 259035) the granite is in contact with the moderately inclined (~ 55°) northward dipping limb of the D4 anticline. Within the proximity of the fold hinge, at Barnahallia in the east and on Friar Isl. in the west, the granite is in contact with the gently eastward plunging (~ 10°) fold hinge.

Southern Limb

The granite contact extends along an east-west trajectory from Fountain Hill beach (058260, 255260) to Grallaghan (059060, 255270) before swinging north toward Barnahallia (Fig. 7.2).

Between Fountain Hill beach and Grallaghan, a well defined steeply dipping contact parallels the southward dipping southern limb of the Connemara Antiform. Several sheets which extend from the pluton are traced up to 50m into the host rock exploiting structural discontinuities and ultimately define sheets which are concordant to bedding (Fig. 7.6). Detailed mapping and aerial photography reveal that abrupt undulations in the granite-country rock contact in this area occur parallel to regional joint sets (NNW-SSE, WNW-ESE) and illustrate that localised discordant emplacement of magma was facilitated by pre-existing joint planes. The most prominent example (058450, 255270) adjusts the position of the contact by ~ 35m along a NNE-SSW line. These features are associated with the broken bridges concept (Hutton 2009; Schofield *et al.* 2012)

where magma wedging preferentially exploits a vulnerable plane of weakness (bedding) and periodically sheets discordantly along a second pre-existing anisotropy (joints) (Fig. 7.6 F). However, no example is found where the level of exposure is sufficient to properly interpret a direction of magma migration.

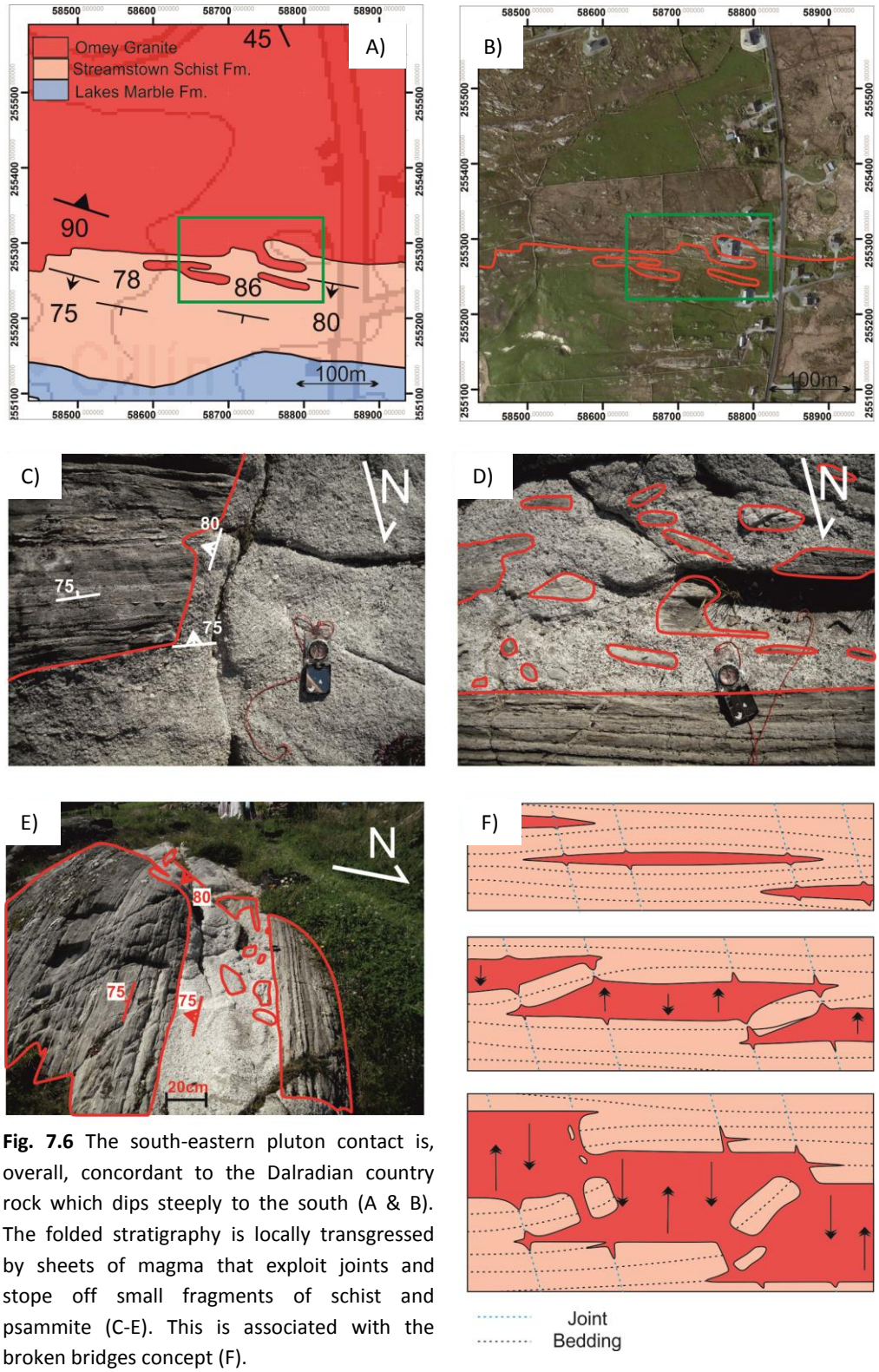


Fig. 7.6 The south-eastern pluton contact is, overall, concordant to the Dalradian country rock which dips steeply to the south (A & B). The folded stratigraphy is locally transgressed by sheets of magma that exploit joints and stope off small fragments of schist and psammite (C-E). This is associated with the broken bridges concept (F).

Between Grallaghan and Barnahallia, closer to the core of the D4 antiform, the granite contact swings north into the Barnahallia area (Fig. 7.2). In total only two locations were observed which expose the granite contact. Sheets share the same geometrical relationship to the host strata as observed on Fountain Hill beach. In close proximity to the fold hinge, the inclination of the country rock progressively decreases northwards from ~ 70° to less than 30° closer to Barnahallia Lough.

Owing to better topographic relief and exposure, the sheeted nature of the granite contact is best observed in 3D on Cruagh Isl.. This island forms part of the southern limb of the Connemara Antiform, steeply dipping (70-60 S°) units of the Cleggan Boulder Bed Fm. are intruded by concordant sheets of G3 which penetrate into the country rock up to 50m past the defined contact zone. Some large (1-5m) detached blocks are present and local grain size reduction is noted from east to west toward the pluton contact.

The Northern Limb

The granite contact along the north eastern margin is exposed at two localities only. At the eastern end of Rossadillask beach (058060, 259000), G1 shares a sharp contact with the northward dipping limb of the of the Connemara Antiform (Figs. 7.7, 7.2). As observed further south, in this area granite sheets parallel or discordantly cross cut bedding. In instances where the contact is discordant, both flat and steeply inclined contacts are observed which parallel regional joint sets (NNW-SSE, WNW-ESE). Sheets which are concordant with bedding extend from the pluton up to 30m into the country rock and taper into progressively narrower sheets (50cm-1m thick). A minor reduction in grain size over a few centimetres is occasionally accompanied by extremely subtle contact parallel foliations.

Much of the remainder of the north-eastern contact lies under bog cover and is thus not exposed. The only exception is at (059240, 256450) northwest of Barnahallia and southeast of Claddaghduff. Exposure here is very limited but G1 is again observed intruding the Lakes Marble Fm. concordant with northward dipping bedding planes and along joint sets.

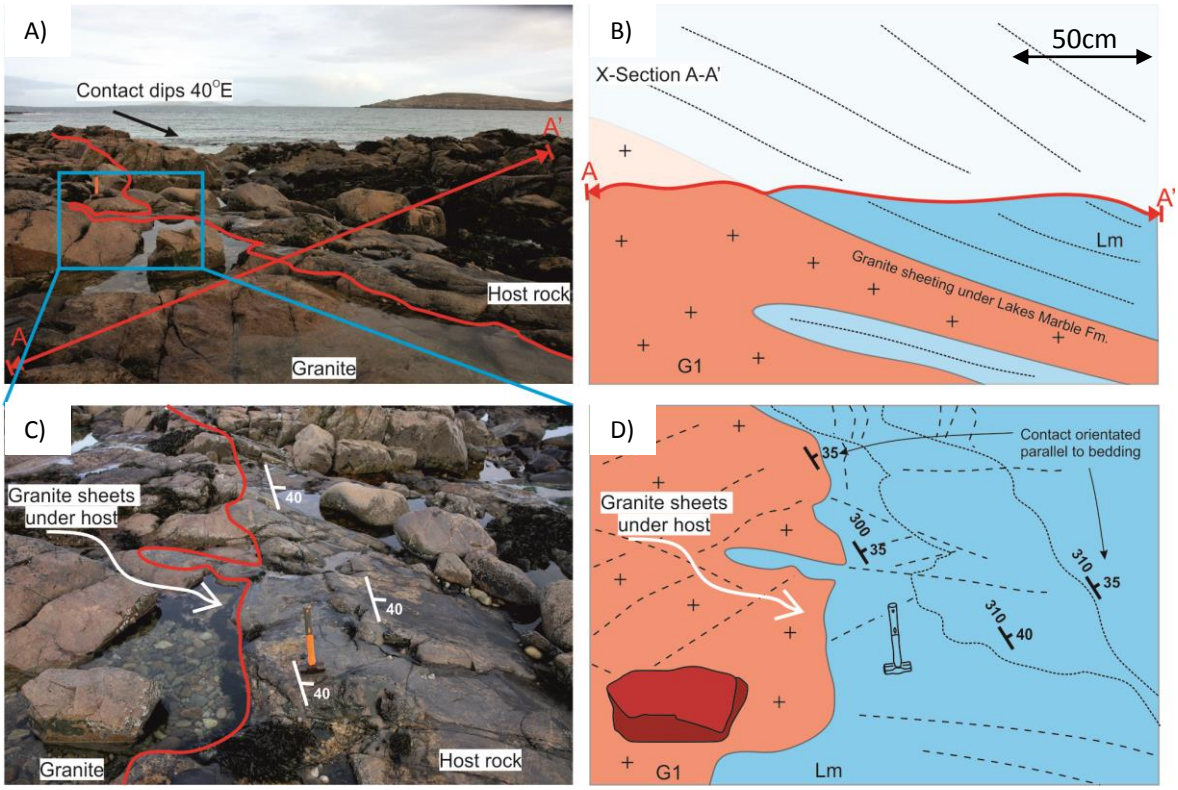


Fig. 7.7 A) The northern contact on Rossadillask beach (looking north), the granite contact dips to the east concordant to host rock bedding (Lakes Marble Fm., Lm). B) Cross section along A-A' of the sheeted contact. C) Blow-up area highlighted in blue in (A). D) A sketch of the Blown-up area in (C). Granite has emplaced into the Lakes Marble Fm. concordantly with the northward dipping limb of the Connemara Antiform.

Along the Fold Hinge

Between Barnahallia Lough and outcrops located at (059240, 256450) the lower units of the Lakes Marble Fm. meet the upper units of the Streamstown Schist Fm., the contact is not exposed. At Barnahallia Lough the Streamstown Schist Fm. lies in direct contact with the Omey Pluton while to the northwest at (059240, 256450) the same can be said for the Lakes Marble Fm. (Fig. 7.2). It is therefore clear that intruding granite cross cut the Streamstown Schist Fm. at map scale.

At the southeast granite contact, the axis of the Connemara Antiform is located just north of Barnahallia Lough. At this locality, the inclination of country rock bedding is slightly steeper than that observed further east along the fold hinge (10-20° vs. 5-10°). This implies that bedding has been vertically displaced at this locality, probably as a result of bifurcation during granite emplacement.

Townend (1966) described the granite contact in this area as generally steep. In 2D plan view, much of the contact does appear to be discordant to bedding approximately following regional

joint sets. Thus, the initial observations of Townend (1966) are supported. However, 3D exposures show that a series of granite sheets were emplaced sub-horizontally, parallel to bedding under the Streamstown Schist Fm. and Lakes Marble Fm. (Fig. 7.8). These sheets range from several centimetres to over 1m and dip gently to the SSW (~ 5-25°). As observed on Rossadillask Beach, sheets often deviate from bedding and exploit pre-existing joint structures, along which they may terminate leaving an apparent vertical contact when viewed in map rather than profile view.

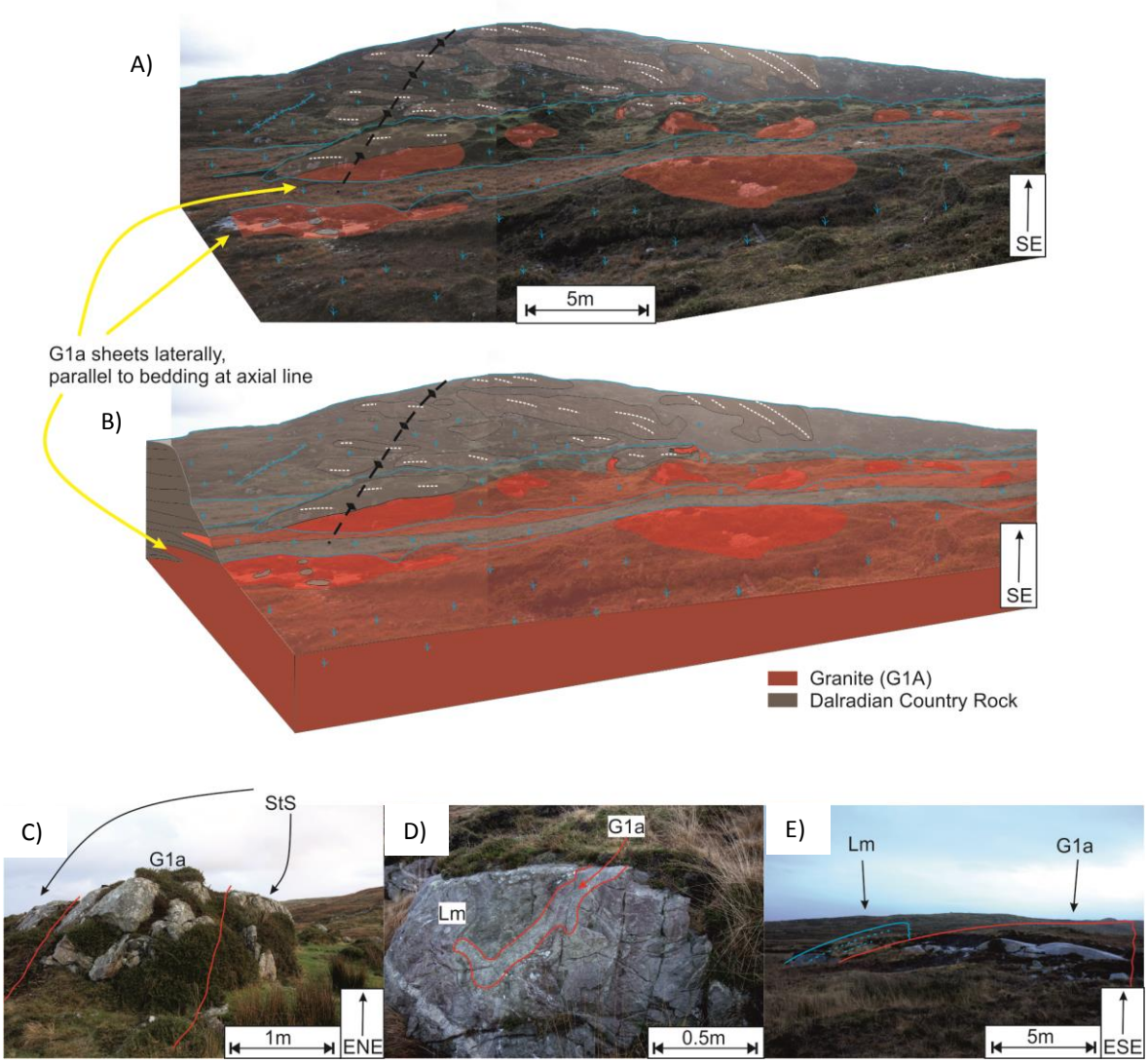


Fig. 7.8 The nature of the granite-country rock contact at the hinge of the Connemara Antiform in the east of the pluton near Barnahallia. A) Photograph (looking ESE) of the granite contact at the fold hinge, outcrops of granite are shaded red and the host rock is shaded brown, white dashed lines indicate orientation of bedding planes, the antiform fold hinge is denoted in black. B) Interpretation of contact relationships; this projection shows concordant sheets of granite intruding parallel to the folded host strata which dips gently to the east. At outcrop scale, sheets of G1a are observed cross cutting the Streamstown Schist Fm. (StS) (C) and several examples of granite sheets intruding meter scale (D) and 10's m scale parasitic folds are present (E).

Due to abrupt topographic relief and high degrees of exposure, the attitude between country rock and granite near the fold hinge of the Connemara Antiform is best observed on Friar Isl. (Fig. 7.9). The majority of the granite bedrock is G3 however a small proportion of the eastern bedrock belongs to the G2 facies, the topographic high point (27m) in the east is G3. The contact between G2 and G3 on Friar Isl. is gradational. An overall east to west reduction in grain size occurs toward the country rock contact along with increasing numbers of small (usually cm - m scale) stoped blocks. No visible fabric is present in the granite. In the western extremity of the island, the Clifden Boulder Bed Fm. dips gently (~ 10°) to the east and strikes NNE-SSW. As observed at Barnahallia Lough in the east, the inclination of the country rock bedding increases slightly (~ 15-20°) eastwards toward the granite contact. At the contact, sheets of granite, some over four meters thick, are plainly observed intruding into and above units of the Cleggan Boulder Bed Fm. and along inclined joints (Fig. 7.9C, D). A schematic vertical profile looking east shows bedded schists, overlain by a thick granite sill, then a three meter sequence of schists which is again overlain by a granite sheet (Fig. 7.9B). This suggests vertical displacement of the gently inclined country rock was achieved in order to accommodate granite emplacement.

In light of these new observations, it seems apparent that sheets of magma have propagated into and beneath the Streamstown Schist Fm. at Barnahallia and into and above the Cleggan Boulder Bed Fm. on Friar Island. Thus, where the granite is in contact with the hinge of the Connemara Antiform in the east, the Lakes Marble Fm. in the northeast and the Streamstown Schist Fm. in the southeast form the bounding roof of the intrusion. Off shore to the west, the Cleggan Boulder Bed Fm. forms the floor for the intrusion at the hinge of the same fold.

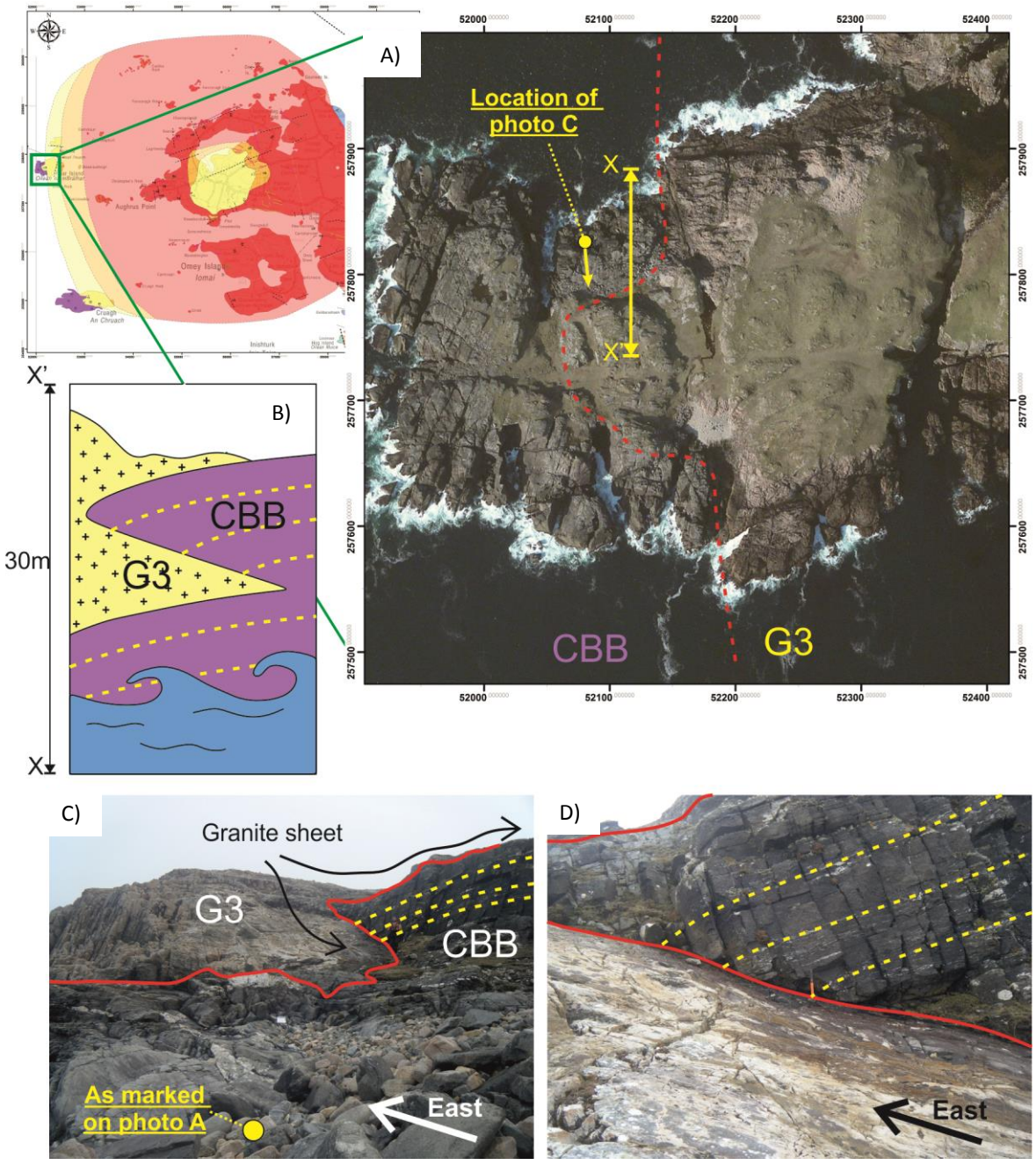


Fig. 7.9 Pluton contact relationships on Friar Isl. A) The eastern and central part of the island is dominantly composed of G3 that sheets into and over the gently dipping (10°-20° E) bedded strata of the Cleggan Boulder Bed Fm. in the west. B) A schematic section, (looking south) from sea level (X) to the topographic high point on the island (X'), shows that the granite intruded concordant to bedding but also cross cuts bedding along joint planes. This relationship is illustrated in (C) and (D) where the granite has cross cut bedding along a large joint but also sheets parallel to bedding on the cliff top.

7.3.2.2 Internal Contacts

Internal contact relationships between G1, G2 and G3 are reasonably straightforward and all facies outcrop as part of spatially cohesive units. Overall, contacts observed in the field are

gradational with the exception of some rare examples on the Aughrus Peninsula. As such, the orientation of these cannot be directly measured in the field. Instead the attitude of gradational contacts have been determined by comparing mapped facies boundaries to elevation contours. For this reason, the orientation of contacts is discussed following a general description of the nature of the inter-plutonic contacts.

No clear boundary is defined between G1 and G1A but a gradational zone in which hornblende modal abundance slowly decreases is identified over ~ 100m, in broad agreement with Townend (1966).

The contact between G1 and G2 is best observed on the north-eastern flank of Aughrus More (Fig. 7.2). Here a completely gradational contact over 15m is observed. The transition is best defined based on the occurrence of rounded quartz grains, a higher proportion of biotite and a more common occurrence of tabular K-feldspar crystals than that observed in G1. The contact between G1 and G2 is estimated in the area southwest of Aughrusbeg Lough as it is completely unexposed. A more abrupt transition (~ 4m) is observed north of Tonashindilla Pier where G1 and G2 respectively form the base and top of a local topographic high. This outcrop demonstrates that here G2 overlies G1 and does not intrude vertically through the earlier facies. These observations suggest that the G1 and G2 emplaced as independent sheets in quick succession.

The G1-G3 contact can be observed at Gannoughs, toward the western end of the Aughrus Peninsula at two localities (055236, 257021 and 055193, 257203). At the first location, a single flat outcrop exhibits a sharp contact orientated NNW-SSE, true dip and strike could not be measured owing to lack of 3D exposure. At the second locality, a local depression exposes a gradational contact over 1m which when traced out dips gently toward the west (<5°). Critically, G3 lies on top of G1 suggesting that G3 was emplaced sub-horizontally over G1 at this locality. No chilled margin or textural anisotropy is apparent in either facies near this contact.

The contact between G2 and G3 is observed on Cruagh Isl., Friar Isl. and also at several outcrops east and northeast of the summit of Aughrus More. In contrast to the findings of Townend (1966), a gradational rather than sharp contact is observed. An exception to this occurs to the immediate northeast of the summit of Aughrus More where minor G3 sheets cross cut G2. In all other areas the contact between G2 and G3 is gradational most often over a distance of less than a 4m.

Attitude of Internal Contacts

Comparing the attitude of the mapped geological boundaries to topographic contour lines (Fig. 7.10), some information regarding the attitude of internal contacts can be inferred.

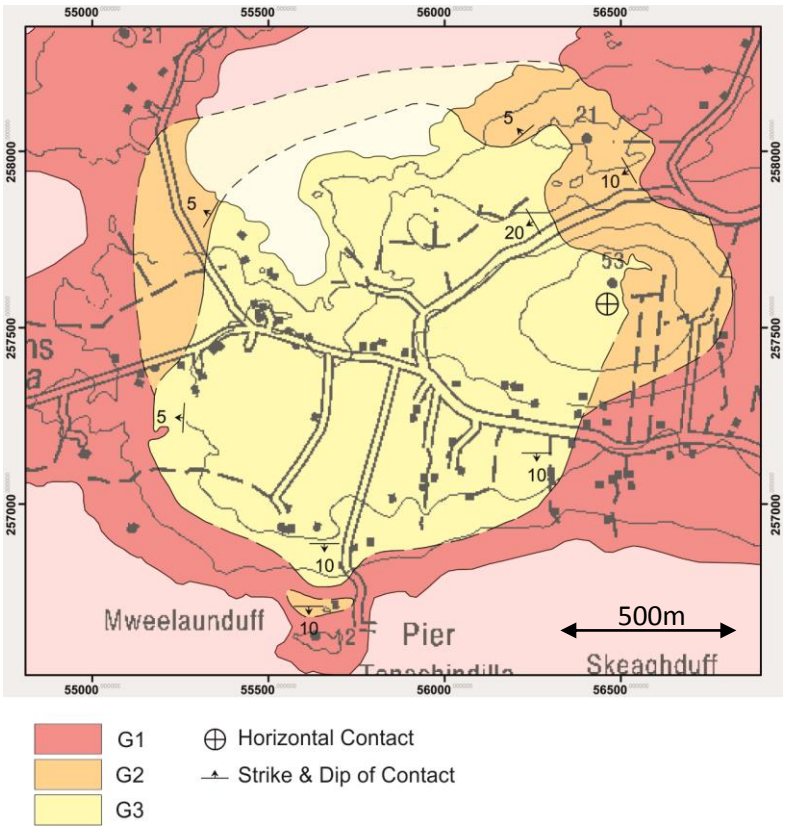


Fig. 7.10 A map of the central portion of the Omey pluton. Contacts between G1, G2 and G3 are almost exclusively gradational and thus the orientation cannot be directly measured. Mapped contacts east of Aughrus Hill and north of Mweelaunduff are approximately contour parallel and therefore likely to be subhorizontal. A very gently inclined sharp G1-G3 contact is observed in the west. Contours mapped in the north east and southern part of the map cross cut topographic contours and thus must be inclined.

Close to the summit of Aughrus More the mapped G1-G2 contact is approximately contour parallel, as is the G2-G3 contact, and so is likely to be flat lying. Further north the contact cross cuts topography, particularly along a local depression that strikes ENE-WSW half way between Aughrus More and Aughrusbeg Lough, indicating moderately inclined westerly dipping G1-G2/G2-G3 contacts in this area. The relationship between contact and contour shows that south of Aughrus More contacts dip gently south and further north, near Aughrus Lough, contacts dip gently north.

On the western side of the Aughrusbeg Lough, the estimated G1-G2 contact dips gently northwest. A contour parallel G1-G3 contact 700m to the south suggests an essentially flat lying contact consistent with subhorizontal west dipping contacts observed at this locality. Assuming that G2 intruded as a single pulse of magma, the topographic position of G2 at Tonashindilla Pier suggests the G1-G2 contact dips gently to the south in this area.

In summary, both external and internal contacts dip to the north and south in the north and south of the pluton and gently to the east along a central ESE-WNW axis. Thus, the symmetry of the Omey Pluton broadly reflects that of the Connemara Antiform into which it was emplaced. However, several examples of highly discordant external contacts have been observed which follow steep and horizontal joint sets in the country rock. Based on these observations the Omey Pluton appears to partially pseudomorph the symmetry of the D4 Antiform and is also observed to be partially discordant. Therefore, this intrusion is best described as a partially discordant phacolithic (Fig. 7.2C).

7.3.3 Late Stage Minor Intrusions

Aplitic Dykes

Late stage aplitic dykes are common throughout the Omey Pluton. These are usually between 10-50cm thick and can be traced for up to 200m in well exposed coastal areas. Contacts are typically sharp and unchilled and may cross cut foliations observed in the host granite. Dykes contain quartz, K-feldspar and plagioclase, exhibit a saccharoidal texture and may contain porphyritic idiomorphic albite up to 5mm in diameter. Biotite is rare and always fine grained (>1mm). Internal contacts parallel textural anisotropies defined by grain size fluctuations indicating that some aplitic dykes are composites and a product of sequential opening of fractures during cooling. Pegmatitic zones contain euhedral quartz and feldspars up to 2-3cm and 1cm rosettes of epidote and biotite. Trace quantities of oxides, interpreted to be magnetite based on rock magnetic analysis (see below) are also observed. These are considered the final product of residual crystallising melt (Wright 1961; Townend 1966).

Late Silurian Porphyritic Dykes

Three varieties of porphyritic dykes are noted across the pluton. All cross cut the G3 facies and associated late stage aplitic dykes. Townend (1966) has described the petrology and nature of lamprophyre and hornblende plagioclase porphyritic dykes. A third variety, a suite of porphyritic microgranite dykes, are recognised and described here for the first time. The orientation and relative timing of intrusion of these dykes is deemed to be of significance to the structural evolution of the pluton as they propagated along lines of weakness parallel to ESE-WNW striking zones of shear that cross cut the pluton.

The Glassillaun granodiorite has previously been described from a series of isolated outcrops that are best exposed along a northwest-southeast trajectory between the south-eastern flank of Aughrus More to Omey Beach (Townend 1966). Figure 7.2 illustrates that a suite of broadly east-west trending microgranite dykes outcrop in this area and are hosted in G1 granite and this rock is not a sub-facies. The best example of such an intrusion is 3m thick and has been traced for over 500m striking parallel to the east-west striking southern shore of the Aughrus Peninsula.

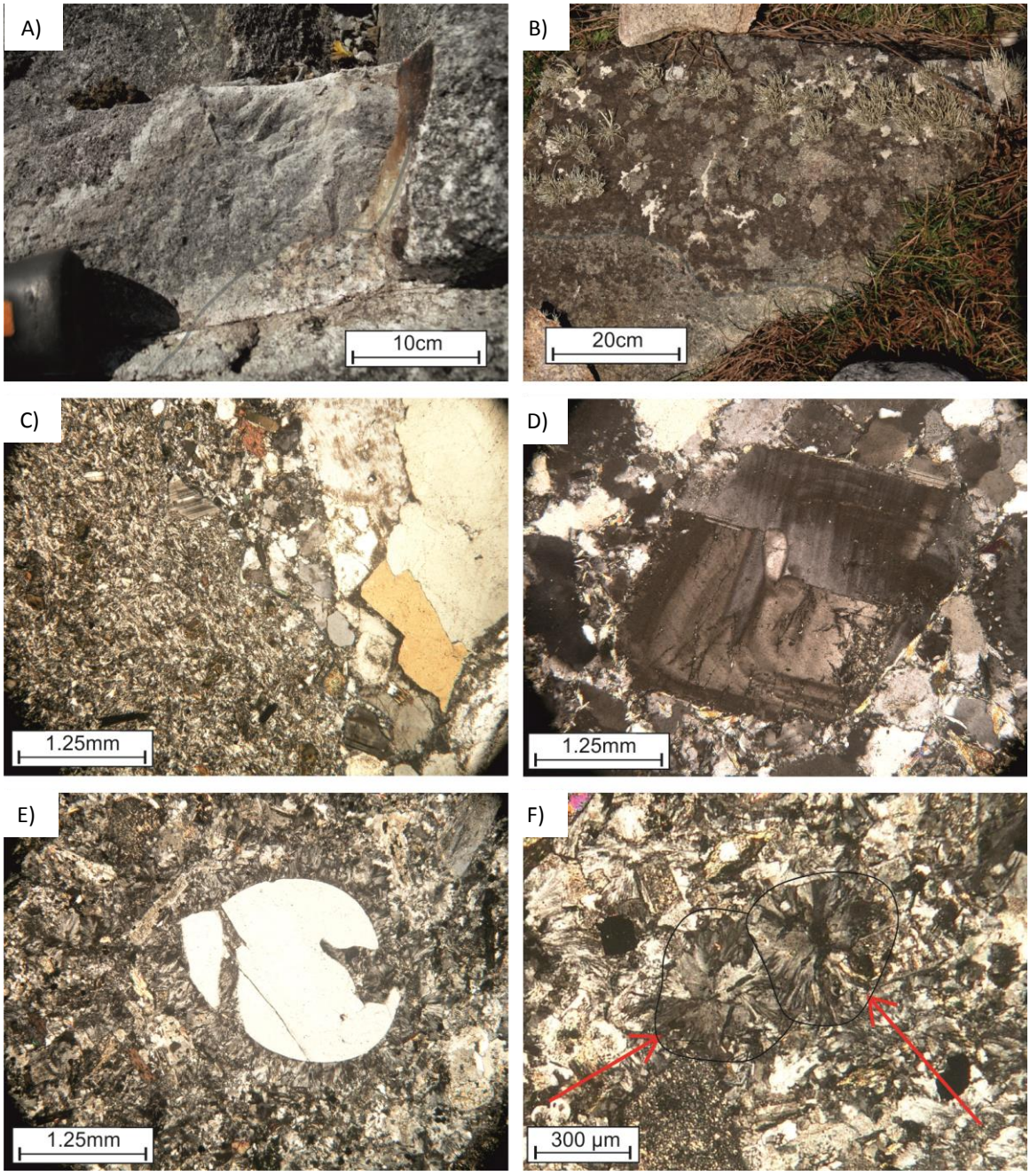


Fig. 7.11 Late porphyritic dykes exhibit narrow gradational (A) or sharp lobate contacts (B) with only minor chilled margins (C) (if present). D) Part of a tabular plagioclase with dramatic zoneation and pericline twins. E) Rounded quartz with peripheral spherulitic quartz. F) Spherulitic quartz aggregates.

Dykes are typically between 30-100cm thick and broadly trend east-west and dip sub-vertically. Where visible, these dykes exhibit lobate or straight contacts with the host granite (Fig. 7.11A, B), weak or no chilled margins (Fig. 7.11C) and have an granular texture punctuated with tabular feldspar phenocrysts and studs of rounded quartz (~ 5mm) and rare euhedral hornblende. Plagioclase feldspars show complex oscillatory zoning and carlsbad, multiple and pericline twinning (Fig. 7.11D). Rounded quartz grains exhibit radial fibrous growth of secondary quartz fringes which have nucleated around the primary grain (Fig. 7.11E, F). Spherulitic aggregates similar to this have been interpreted as a product of secondary crystal growth from a homogenous magma (Vernon 2004). Biotite is usually chloritised, hornblende was not found in thin section but is present in some dykes as 1-2mm euhedral crystals.

Based on the observations above, the existence of the Glassillaun granodiorite as a sub-facies of the Omey Pluton is questioned. Instead a suite of quartz-feldspar porphyritic dykes which trend ESE-WNW and have a similar petrography as that described for the Glassillaun Granodiorite (Townend 1966) are found to cross cut the G1.

The Barnahallia Breccia

Adjacent to the roof of the pluton, in the Barnahallia area, a high concentration of minor porphyritic dykes are closely associated with three well defined zones exhibiting spectacularly brecciated metasedimentary and igneous rocks hosted in a fine grained granitic matrix (Fig. 7.2). Each of the three breccia pods have a surface area of less than 2,500m^2 and all lie within a 20,000m^2 area, an example of a typical outcrop is presented in (Fig. 7.12A). A sharp irregular unchilled contact is identified between the surrounding G1A facies and the microgranite, which hosts the breccia clasts (Fig. 7.12C, D). Granite clasts are clearly of G1 or G1A composition. Metasedimentary clasts contain well defined small scale folds and crenulation cleavages. Extensive replacement and alteration of garnet porphyroblasts and micas is evident in pelitic clasts. The metasedimentary breccia clasts are a likely derivative of the Streamstown Schist Fm.. It is envisaged that a block of country rock became detached by intruding G1A granite and later engulfed and disarticulated by melt associated with the quartz-feldspar porphyritic microgranite suite of dykes, which the groundmass most closely resembles. This is a striking feature of the Omey Pluton which in itself deems further study, unfortunately this lies outside the remit of the current work.

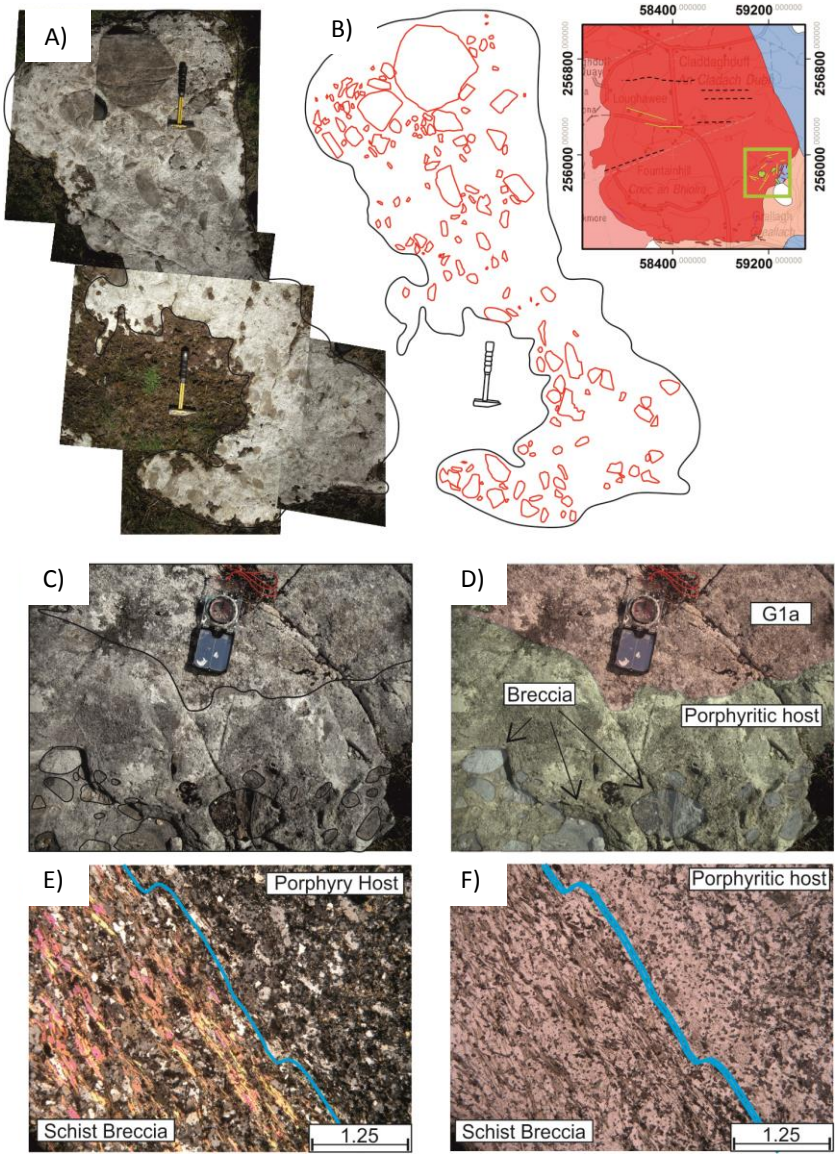


Fig. 7.12 A) Representative images of the Barnahallia Breccia. B) Outline of breccia clasts shows a crude NNW-SSE preferred orientation, breccia clasts are not completely randomly orientated. This breccia is not hosted directly in the G1a but instead is suspended within a porphyritic microgranite which exhibits sharp contact with the surrounding G1a (C & D). E & F) XPL and PPL images of a contact between the fine grained porphyritic microgranite host and a breccia clast (in this case a schist. It can be concluded from this preliminary work that this not an "*explosion breccia*" hosted within the G1 facies.

Carboniferous Dykes

Several dolerite dykes cross cut the Omey Pluton that clearly post date late Silurian magmatism. These are usually between 30cm-2m, always exhibit chilled margins and are occasionally vesicular (Fig. 7.13), full description in Townend (1966)). Here, these are attributed to Carboniferous magmatism. Sixteen olivine dolerite dykes are documented by Townend (1966) who detailed that of this number eleven are oriented between ENE-WSW and ESE-WNW and that these intrude pre-existing brittle structures in the pluton. Two of the largest Carboniferous dolerite dykes cross cut the headland by Tonashindilla Pier along an ENE trajectory.

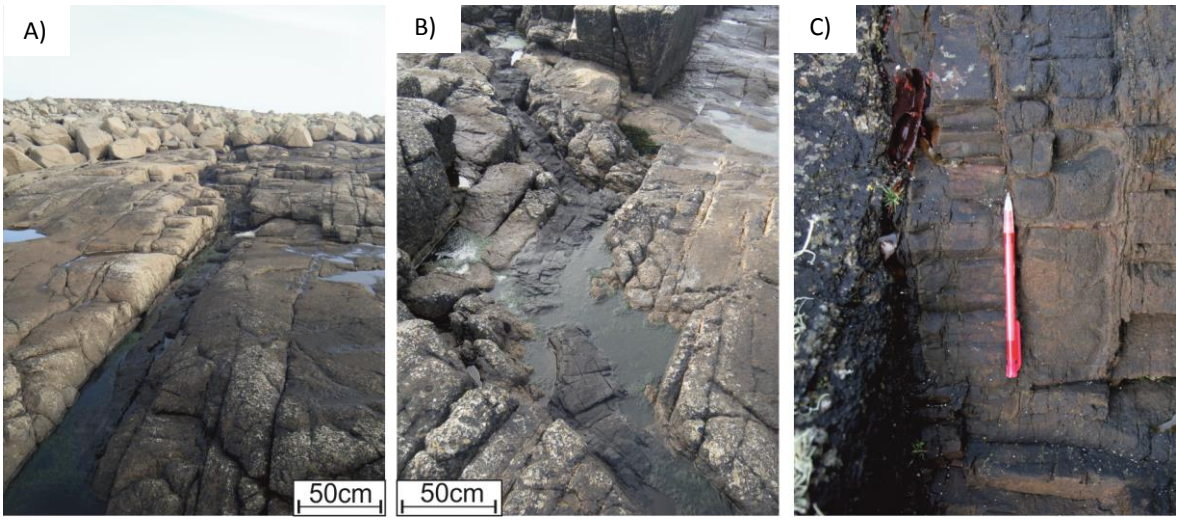


Fig. 7.13 Typical examples of Carboniferous dolerite dykes in the Omey Pluton. These typically zig-zag through the granite as they follow joint sets (A & B). All exhibit chilled margins (C).

7.3.4 Fabrics in the Omey Pluton

Visible foliations in the Omey Pluton are characteristically weak or absent outside of minor well defined zones that exhibit submagmatic deformation features. Below, features which relate to the process of emplacement are first described follow by the field evidence for post emplacement deformation.

Emplacement Related fabrics

A marked lack of visible fabrics typifies this intrusion. Those present are laterally discontinuous and cannot be traced very far along strike. When observed, weak foliations are defined by subtle alignments of undeformed K-feldspar, euhedral platy biotite and fresh interstitial quartz which may be slightly elongate parallel to the fabric observed (Fig. 7.14). Foliations such as this are recorded sporadically across Omey Isl., across the Claddaghduff area and northwest along the north side of the Aughrus Peninsula and overall define a broadly concentric pattern (Fig. 7.2). Most outcrops are either not exposed in 3D or display a weak anisotropy from which a dip direction cannot be determined. A point to note is that while fabrics are observed in G1 and G2, no visible textural anisotropy is observed in G3 at any field location.

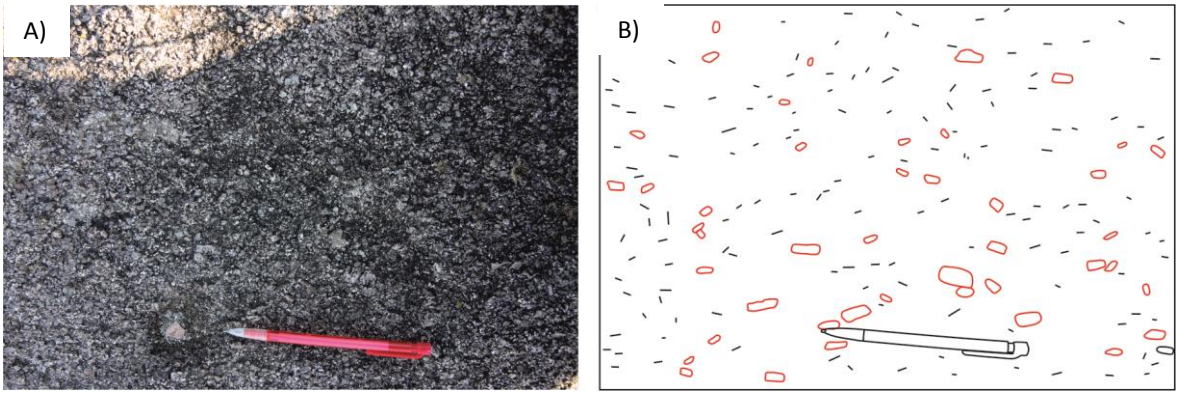


Fig. 7.14 A) An example of a typical magmatic foliation observed in the Fountainhill area. B) A trace of the same image demonstrates the presence of a foliation predominantly defined by K-feldspar and biotite.

Localities which exhibit weak silicate fabrics were block sampled and sectioned for petrographic microstructural evaluation. It was found that quartz is typically fresh, anhedral and only exhibits weak undulose extinction (essentially undeformed). Chloritised biotite is euhedral, platy and has only minor undulose extinction along grain-grain contacts. Feldspars are idiomorphic and essentially unstrained, twinning in plagioclase is straight and associated with post crystallisation strain. These features characterise a dominantly magmatic to higher temperature weak sub-magmatic deformation (Vernon 2004; Passchier and Trouw 2005) and indicate that any strain recorded was imparted before and during the crystallisation of granite. As such, weak fabrics observed in these localities are attributed to forces associated with the emplacement of granite.

Distinctive biotite layers are observed on the south-western shores of Omey Isl. and Cruagh Isl. (Fig. 7.15). These have sharp bases defined by high concentration of fresh and equigranular (~ 5mm) biotite which grade upwards into a quartz-feldspar rich composition depleted in mafic minerals. A continuous gradation is seen from a biotite rich base to an upper horizon rich in tabular feldspar and anhedral interstitial quartz. Occasional poikilitic K-feldspar phenocrysts protrude through the biotite layers illustrating the contemporary nature of these schlieren and the primary crystallisation process. Horizons are 20cm thick, laterally discontinuous and can be traced for no more than 10m. On Cruagh Isl. multiple biotite layers strike east west and dip sub-vertically approximately parallel to the country rock contact. In similar fashion, two screens identified on the western shore of Omey island (055810, 255719 and 056000, 255488) strike WNW-ESE and dip moderately (60°) south, crudely parallel to the attitude of the down dipping limb of the D4 anticline. Townend (1966) described moderately dipping (40°) schlieren that also consistently dip toward the country rock contact, however these were not found during the

current work. Townend (1966) (after Harry (1960)) suggested that these layers are a product of crystal settling and, on Cruagh Isl., an accumulation of heavier minerals that were segregated from a melt rich in fluid and volatiles close the roof of the intrusion.



Fig. 7.15 Biotite layers in the Omey Pluton on the western coast of Omey Island. Note that these dip steeply to the south, essentially parallel to the southward dipping limb of the Connemara Antiform further along strike.

Townend (1966) has described the petrology of mafic enclaves found in the Omey Pluton. Paterson *et al.* (2004) detailed the benefits and pitfalls of using such features as strain markers. Coeval basic to intermediate enclaves typically have 10-150cm long axes and exhibit variable aspect ratios from 1:1 to 1:5. Localised swarms of hybridised mafic enclaves are found on the north-western shore of Omey Island hosted in G1. Measurements taken from this site and elsewhere around the intrusion show that the shape anisotropy and orientation of these enclaves is random (Fig. 7.16) and shares no affinity with other strain features noted in the granite to date.

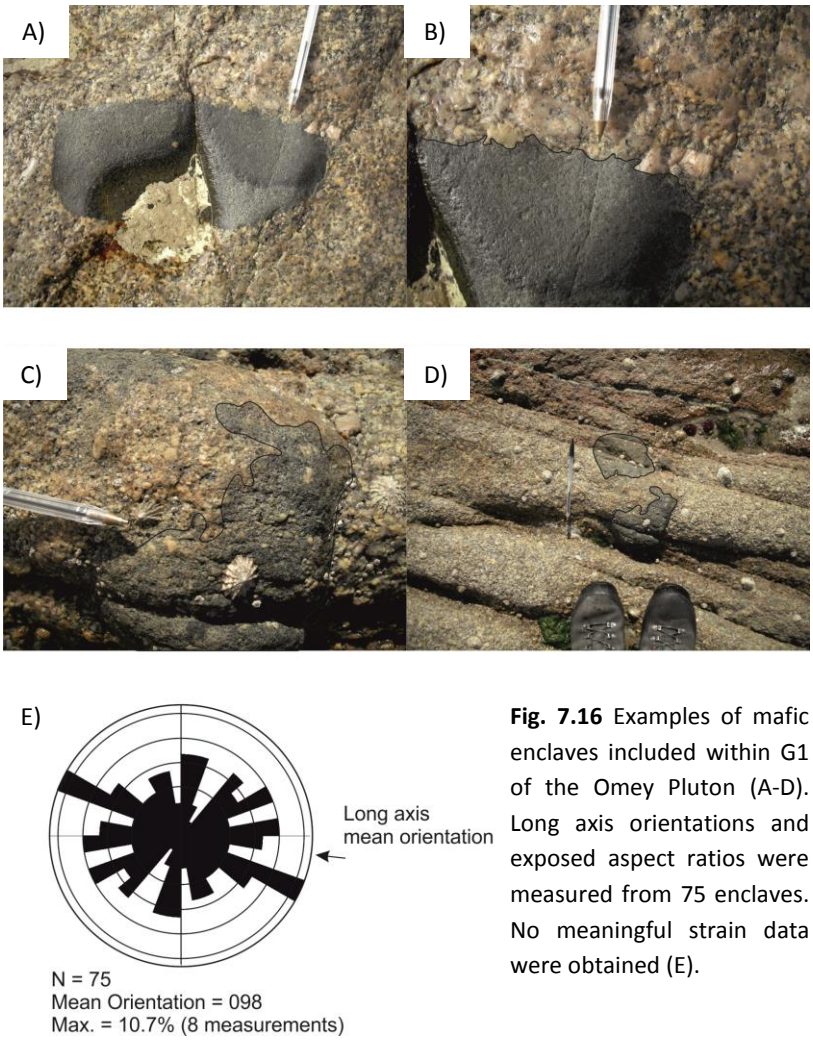


Fig. 7.16 Examples of mafic enclaves included within G1 of the Omey Pluton (A-D). Long axis orientations and exposed aspect ratios were measured from 75 enclaves. No meaningful strain data were obtained (E).

Post Emplacement Fabrics

The Omey Pluton does not exhibit any strong fabrics that are considered diagnostic of significant syn-magmatic tectonic deformation (such as those described by Hutton (1988)). However, Townend (1966) identified two distinctive fault sets (NNW-SSE and east-west) that cross cut all facies of the pluton but did not elaborate on the origin of these structures. Small degrees of offset were reported by Townend without a reference to local or overall shear sense. These fabrics are discordant to pluton contact and thus may represent significant post emplacement structural overprints. A descriptive account is given below and a geometrical relationship between these and regional D5 brittle structures is identified.

Several prominent NNW-SSE and east-west to northeast-southwest abrupt topographic lows are observed across the Omey Pluton on both topography maps and aerial photographs (Fig. 7.17). These define small valleys and scarps which cut through Aughrus More, Omey Island and

define the shape of the coastline which surrounds these land masses. On the ground, these features are most often observed as zones of fine scale intense micro-fracturing which are 2-10m across. A marginal moderate to weak crystallographically defined foliation is sometimes present along the periphery. Fracture density may increase gradually or abruptly and in several instances late stage porphyritic dykes and Carboniferous dykes intrude parallel to or within these zones. Owing to limited exposure, no consistent sense of shear is observed across these structures.

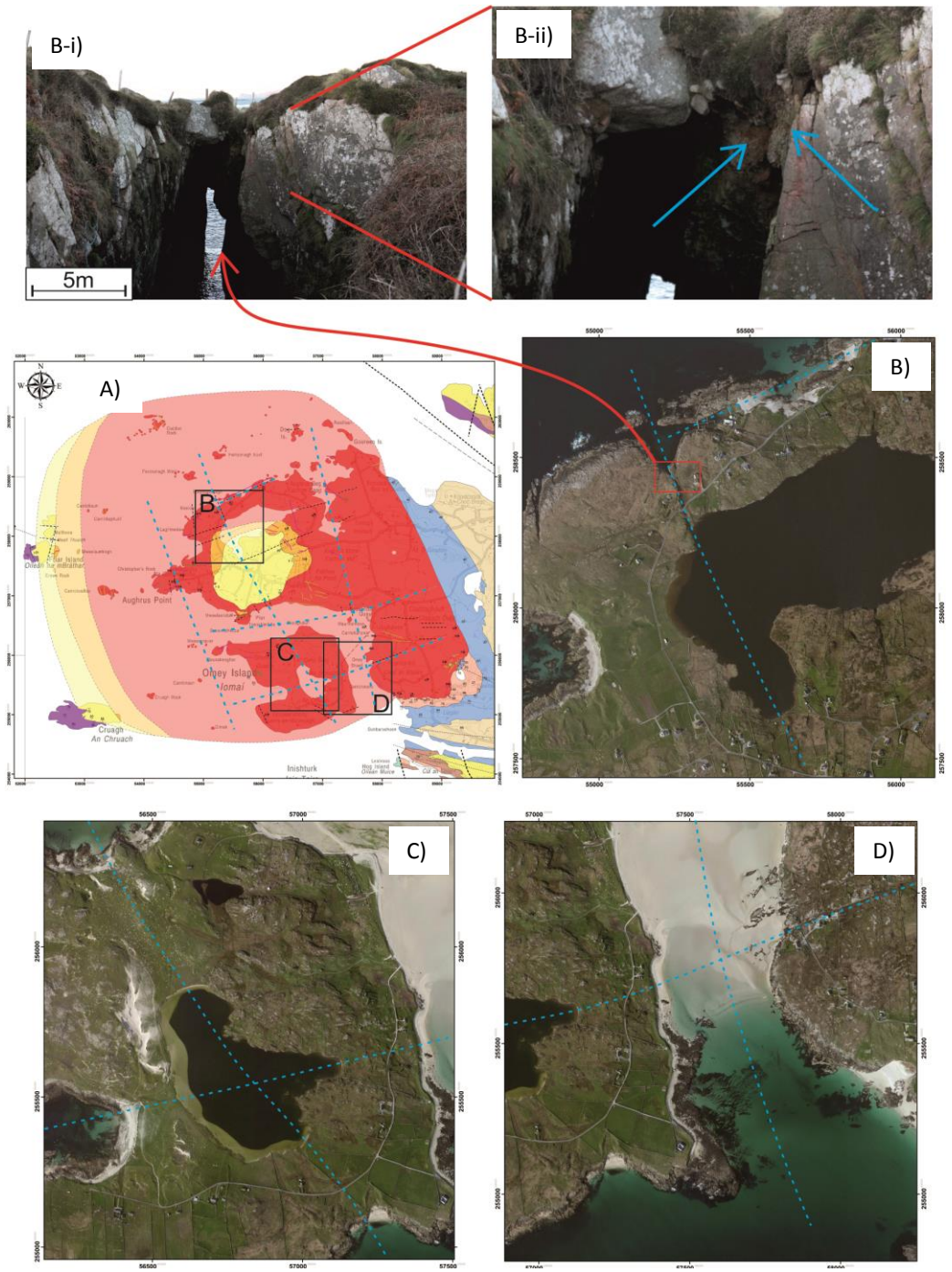


Fig. 7.17 Abrupt topographic lows cross cut the Omey pluton (A). These lows are associated with scarps (B), caves (B-i), lakes (C) and bays (D). In some cases minor brecciation is observed (B-ii).

Outcrops at Aughrus Point (054550, 257250) best illustrate the nature of these shear zones (Fig. 7.18). Traversing from undeformed granite in the east into the shear zone in the west, visual fabric anisotropy becomes increasingly obvious. The flank of the shear zone is denoted by a weak to moderate NNW-SSE subvertical foliation defined by elongate quartz, aligned or smeared biotite and partially aligned feldspars and fractured feldspars. At the core of the shear zone, fabric development gives way to a grain scale pervasive micro-fracturing which defines a NNW-SSE textural anisotropy (as opposed to a crystallographic foliation).

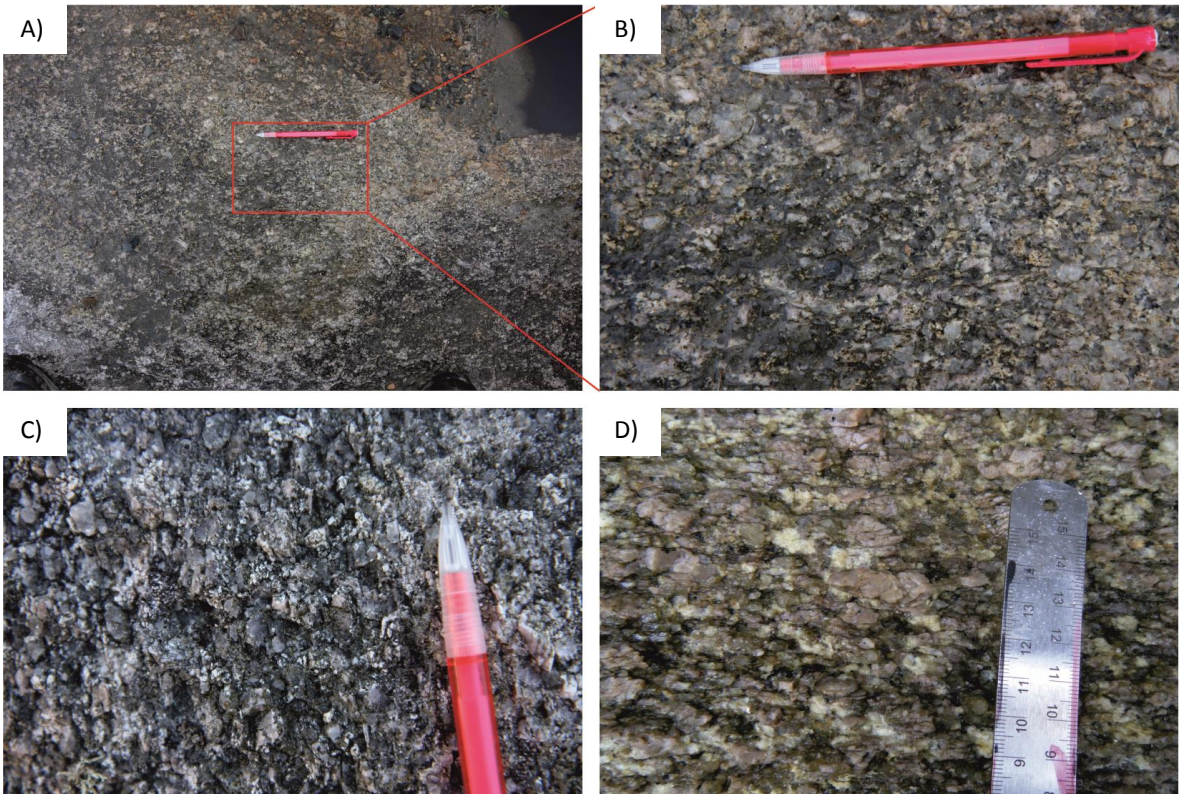


Fig. 7.18 Fabric development within a NNW-SSE shear zones mapped at Aughrus Point. A & B) On the periphery of the shear zone a definite petrographic fabric is observed, this is defined by elongate quartz and smeared biotite. An apparently strong foliation is observed within the shear zone (C). Close inspection reveals a moderate petrographic foliation that parallels fine scale micro fracturing which give rise to a strong textural anisotropy (D).

Petrographic analysis reveal the rheological state under which fabric development occurred at shear zone localities (Fig. 7.19). Quartz is often elongate and composed of multiple subgrains which often exhibit moderate undulose extinction and define quartz ribbons (Fig. 7.19A). Biotite is variably kinked and often smeared around euhedral feldspar phenocrysts (Fig. 7.19A & B). Fractures through some feldspars are infilled with primary magmatic quartz (Fig. 7.19D), this is also, very rarely, observed in biotite (Fig. 7.19C). Feldspars are sometimes incorporated into the foliation, in such as case it typically exhibits weak to moderate undulose extinction and shows

marginal cataclastic flow or low temperature dynamic recrystallisation (Fig. 7.19E & F). Orthoclase is sometimes partially converted to microcline. Such features are characteristics of submagmatic to solid state deformation (Vernon 2004).

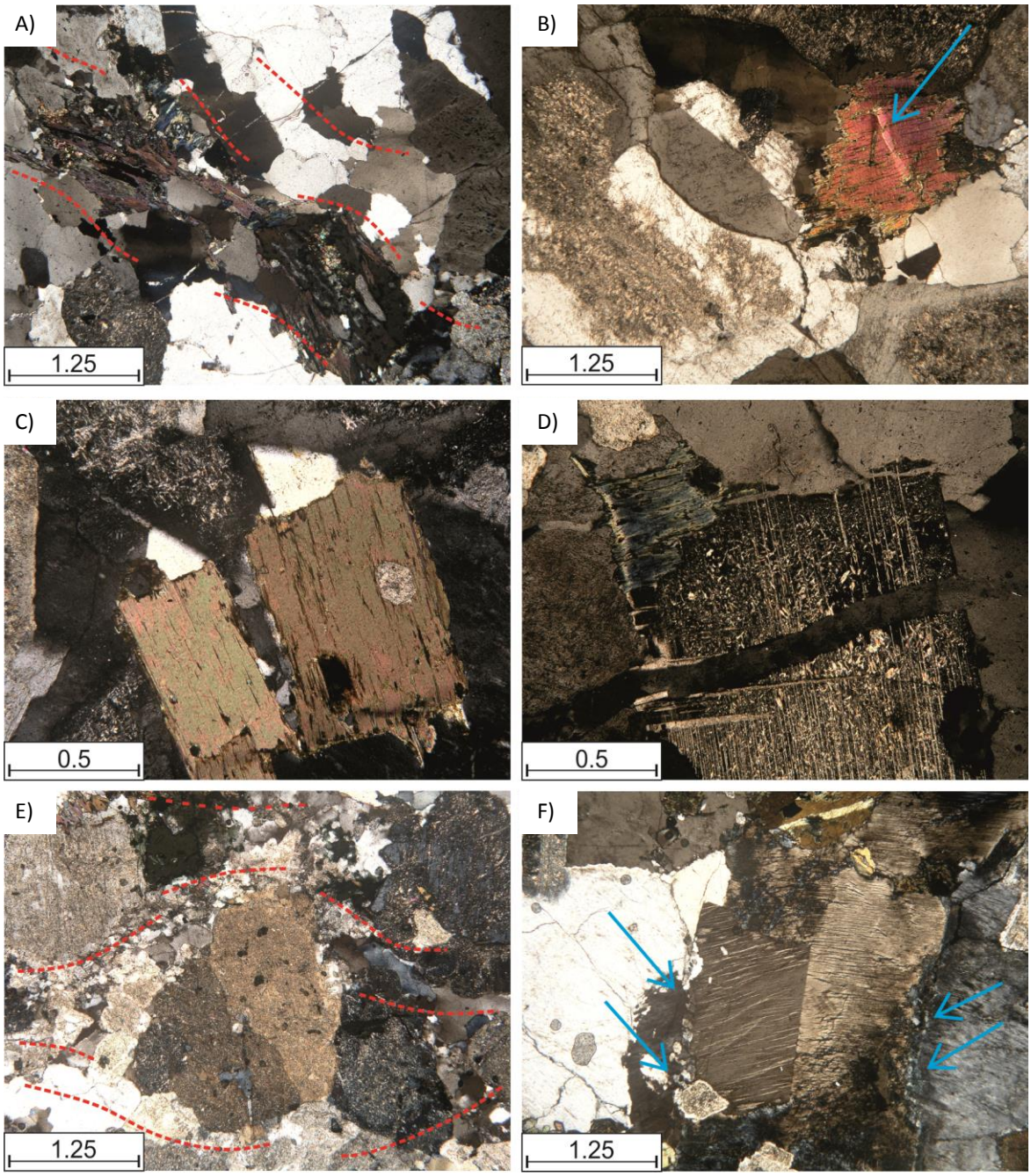


Fig. 7.19 XPL images of microstructural observed within a NNW-SSE shear zone on Aughrus Point. A) Quartz ribbons and smeared biotite. B) Minor kink in biotite, undulose extinction in quartz. C) Fracture along biotite cleavage plane and (D) fracture through plagioclase both with primary magmatic quartz infill shows submagmatic deformation occurred. E & F) Marginal dynamic recrystallisation of plagioclase into the foliation plane.

SSE of Aughrus Point, weak NNW-SSE foliations are observed on the west coast of Omey Island. Several outcrops to the east of Omey Strand (057760, 256370) exhibit similar NNW-SSE foliations and again along strike between Lough Atalia (057100, 258140) and Garranraheen (056920, 259100) the same fabric is detected.

Despite detailed fieldwork and thin section analysis, no overall shear sense is determinable from these (at best) moderate foliations. In many areas these structures are pronounced as zones of pervasive grain scale micro-fracturing. These are still considered to be of significance owing to two factors;

1. They are pervasive, observed as several discrete structures across the pluton and in many cases exhibit a true petrographic foliation which is related to submagmatic strain.
2. These structures are parallel to NNW-SSE D5 brittle structures that cross cut the country rock, predate granite emplacement and are known to have accommodated shearing after emplacement (Chapter 3).

These observations imply a concurrent relationship between fault reactivation and pluton construction.

7.3.5 Summary of Field Observations

The architecture of the Omey Pluton appears to be dictated by the pre-existing host rock structure, namely the Connemara Antiform and associated regional joint sets. The overall symmetry of the intrusion is envisaged as a highly discordant phacolith (Harker 1909; Corry 1988) (Fig. 7.2). The Cleggan Boulder Bed Fm. acts as the base of this sheeted intrusion and the Streamstown Schist Fm. in the southeast and the stratigraphically higher Lakes Marble Fm. in the north form the discordant roof. Internal contacts dip gently to the south in the southern and to the north in the northern portions of the pluton and sub-horizontally to the west along the WNW-ESE trending central axis. Thus the internal architecture also reflects the symmetry of the Connemara Antiform, be it to a more subdued degree.

The distribution of emplacement related strain within the pluton is largely unconstrained due to extremely low degrees of visible anisotropy. A very crude concentric foliation is defined by

magmatic state fabrics at some localities however an overall lack of fabric development inhibits the development of an emplacement model.

A common trend is shared between zones of elevated strain that are identified in the granite (NNW-SSE and ENE-WSW) and dykes which intruded both soon after the granite crystallised and several million years later. Porphyritic dykes share a spatial and temporal relationship with subtle deformation structures observed in the granite as they lie parallel to identified shear zones and also exhibit un-chilled or weakly chilled margins (discussed below). Submagmatic and cross cutting contact relationships clearly indicate emplacement closely followed construction of the Omey Pluton. Townend (1966) noted that all lamprophyre dykes in the area strike parallel to NNW-SSE faults while the vast majority of Carboniferous dykes strike east-west parallel to, if not within, east-west deformation features in the granite.

In addition, there is a striking consistency between the orientation of NNW-SSE shear zones within the granite and those D5 NNW-SSE faults observed in the country rock. This is most obvious in a comparison drawn between the Clifden-Murvey Fault and those noted within the Omey Pluton.

It is postulated that these structures may have played an active role in facilitating magma ascent from this location however the temporal relationship between faulting and magma ascent and emplacement cannot be constrained based on field evidence. In order to test this hypothesis a rock magnetic analysis study was undertaken to obtain further data relating to the structural evolution of this pluton and elucidate upon the magmatic and tectonic process involved in its genesis.

7.4 Rock Magnetic Analysis

In many instances the structural evaluation of plutonic rocks is impeded due to extremely weak or subtle mineral alignment fabrics (i.e. visual anisotropy). In such cases, AMS provides a efficient means through which extremely weak fabrics may be detected and evaluated in 3D, even when the outcrop has no obvious visible fabric (Bouchez 1997). The benefits of AMS in examining intrusive rocks are now clear and this is considered a standard means investigation (e.g. Bouchez (1997); Cruden *et al.* (1999); Bolle *et al.* (2003); Femenias *et al.* (2004); Vigneresse (2005); Pressler *et al.* (2007); Stevenson *et al.* (2007); Borradaile and Jackson (2010); Ono *et al.* (2010); Petronis *et al.* (2012).

However, there are several factors that adversely affect the way in which AMS relates to specimen petrofabric (Fuller 1963; Borradaile 1987; Rochette 1987; Potter and Stephenson 1988; Rochette 1988; Wolff *et al.* 1989; Jackson 1991; Borradaile and Dehls 1993; Housen *et al.* 1993; Callot and Guichet 2003; Bouchez *et al.* 2006; Gaillot *et al.* 2006; Fanjat *et al.* 2012). These caveats must be considered when making any interpretation. In every case, the phenomenon referred to (discussed in Chapter 6) will cause the AMS tensor to deviate from the true petrofabric to some degree. The significance of these influences can be assessed by comparing AMS interpretations with observations made in the field, by applying standard statistical checks to AMS data (Balsley and Buddington 1960; Nagata 1961; Khan 1962; Owens 1974; Jelinek 1977, 1981; Owens 2000a) and through the application of rock magnetic experiments (Lowrie and Fuller 1971; Bailey and Dunlop 1983; Dunlop 1986; Argyle and Dunlop 1990; Lowrie 1990; Heider *et al.* 1992; Argyle *et al.* 1994; Xu and Dunlop 1995; Dunlop and Ozdemir 1997) designed to identify and determine relative contributions made by constituent minerals (Chapter 6).

The Omey Pluton is a prime example of an intrusion in which only weak foliations have been detected and the majority of outcrops exhibit no obvious visible fabric.

7.4.1 Sampling

A total of 113 orientated block samples were collected from across the intrusion in an approximately even distribution. Extra attention was afforded to areas of specific interest near contacts zones or areas of high strain identified during field work. On average, 1/20 samples were duplicated for quality control purposes. Between 7 - 22 (average 15) 21x25mm cylindrical sub-specimens were cored from each block using a non-magnetic abrasive diamond tip drill following the parameters set by Owens (1994).

Based on preliminary AMS data, thin section analysis and field observations, several representative and anomalous specimens were selected for further rock magnetic analysis.

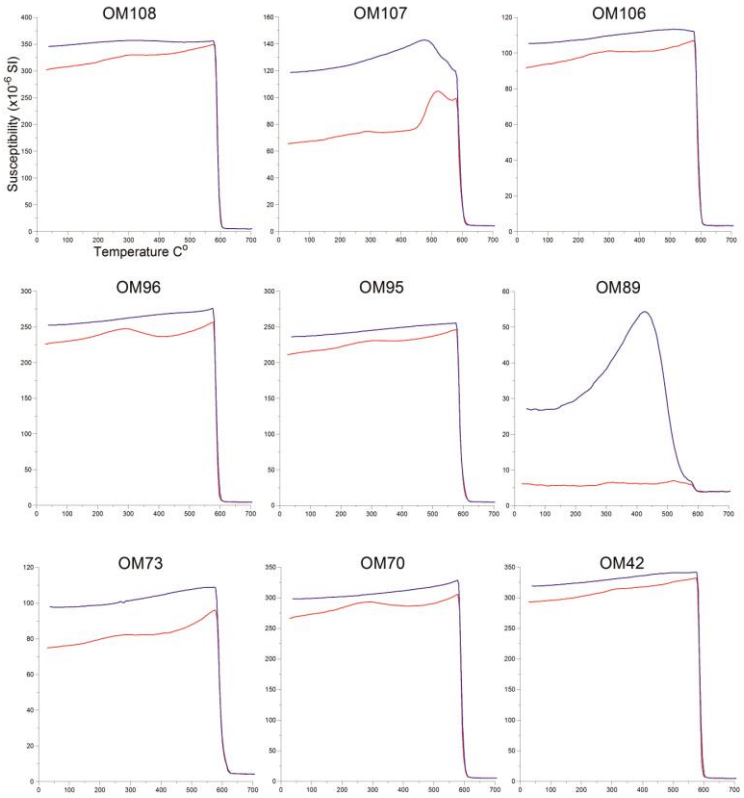
7.4.2 Results of Rock Magnetic Experiments

In order to characterise magnetic mineralogy, selected specimens were subjected to a series of rock magnetic experiments at the paleomagnetic laboratory, New Mexico Highlands University.

The purposes and benefits of each experiment is discussed in Chapter 6. The applied analytical procedures are included in Appendix B, original data files are included in Appendix E.

Variation of Susceptibility with Temperature

Continuous measurement of low field susceptibility during step wise heating and cooling of powdered samples was performed in order to estimate the Curie point (T_C) for each selected sample (representative graphs and summarised results in Fig. 7.20). Using either the Hopkinson Peak or the inflection point methods (Moskowitz 1981; Tauxe 1998), eight of nine samples return an inferred T_C between 577-580°C. OM89 is the exception and returned a susceptibility values on the heating curve, relatively high susceptibility values on the cooling curve and a $T_C \sim 590$.



	HEATING		COOLING	
SAMPLE	TC	Ti (x)	TC	Ti (x)
OM106	577	0.01	578.1	0.01
OM107	580	0.00	579.1	0.01
OM108	579.1	0.01	577.3	0.01
OM42	576.2	0.01	577.5	0.01
OM70	579.1	0.01	579.1	0.01
OM73	579.7	0.00	579	0.01
OM89	590.2	-0.01	496	0.14
OM95	578.8	0.01	576.9	0.01
OM96	578.9	0.01	577.1	0.01

Fig. 7.20 Representative Curie Point data and Summarised table of results. All samples show an increase in susceptibility on the cooling curve and all but OM89 exhibit clearly defined Hopkinson's peaks. Some exhibit minor 300°C "bumps" on the heating curve, these are always absent on the cooling curve which indicates some mineralogical change occurred during the experiment. Ti content is low in all samples.

The shape of the Hopkinson Peak may also be used to infer domain state of constituent grains (Orlický 1990). A tighter more abrupt peak is indicative of single domain (SD) grains, broader peaks indicate a dominant multi domain grains (MD) (Dunlop and Ozdemir 1997). Eight samples have well defined Hopkinson Peaks with minor increases in susceptibility immediately prior to T_C. The scale of the increase in susceptibility prior to T_C is not diagnostic of but is consistent with a pseudo-single domain (PSD) grain size (Dunlop and Ozdemir 1997).

The Curie Point for pure magnetite reduces from 580°C with increasing Ti content and increases as O is incorporated into the Fe-Ti cubic phase (Readman and O'Reilly 1970, 1972). Thus, T_C may be use as a proxy for Ti content (Akimoto 1962; Lattard *et al.* 2006), however T_C is also subject to oxidisation levels. Susceptibility parameters returned in this study indicate a low Ti (≤0.1%) titanomagnetite as the dominant phase.

All samples are essentially irreversible on the heating-cooling thermomagnetic curve and exhibit elevated susceptibility after cooling from 700°C. All samples also show a minor 5-15% increase in susceptibility between 200-400°C. Hrouda (2003) relates such fluctuations to homogenization Fe-Ti oxides during heating. This process exsolves a Ti enriched phase (usually ilmenite following oxidisation of ulvospinel) and a near pure magnetite phase from an original oxidised Ti-Fe cubic or rhombohedral phase. Maghemitization is a low temperature oxidisation process that initiates at temperatures below 250°C and converts Fe_3O_2 to Fe_3O_4 to form maghemite (Dunlop and Ozdemir 1997). Maghemite is metastable above 300°C and inverts to magnetite. Thus the inversion of the oxidised portion of magnetite grains (maghemite) to magnetite causes a peak in susceptibility at 300°C and a net increase in susceptibility after cooling (Hrouda 2003; Hrouda *et al.* 2006). Subtle bumps noted in the heating curves of the current data set are considered a product of this process.

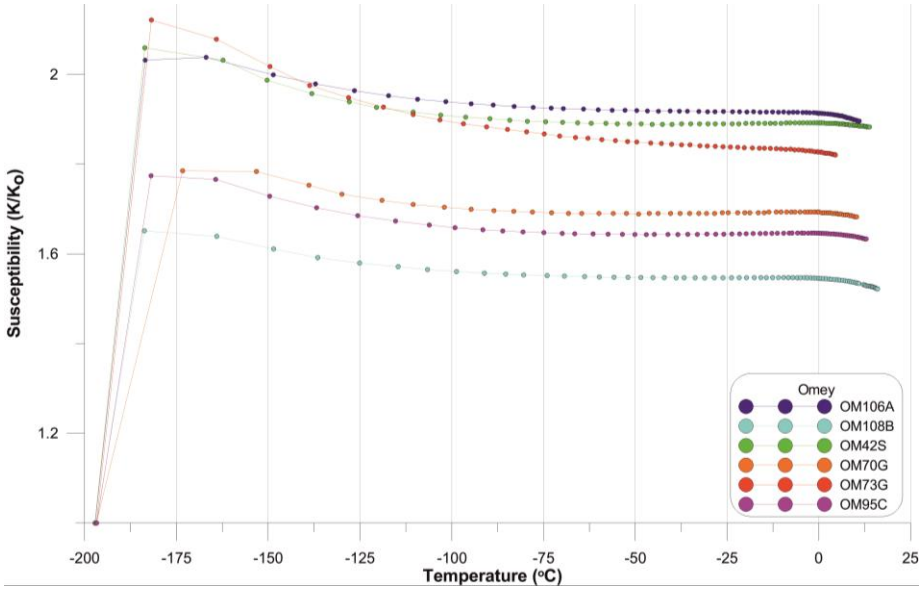


Fig. 7.21 Results of cryogenic experiments show little variation among the sample population. All exhibit a rapid increase in susceptibility between -198°C and -170°C (at T_V) followed by a gradual decline up to room temperature.

On increasing temperature from -198°C to 12°C, susceptibility of all specimens behaved in a similar fashion (Fig. 7.21). A rapid increase in susceptibility is noted between 75-90K followed by a

moderate decline between 90-190K. Between 190-285K no significant change in susceptibility is noted. On cooling magnetite below 122°C it is forced to modify its crystallographic structure from inverse spinel to normal spinel, this is known as the Verwey Transition (T_V) (Verwey 1939). The actual temperature at which this transition occurs is dependent on stoichiometry (Dunlop and Ozdemir 1997). The rapid increase in susceptibility between 75K and 90K is attributed to T_V and is typical with that of fairly pure magnetite. The lack of susceptibility variation at freezing temperatures over T_V indicate that titanomagnetite is the dominant phase but does not totally exclude potential paramagnetic other ferromagnetic (senso lato) influences.

Lowrie - Fuller Test

The stepwise AF demagnetisation of natural remanent magnetisation (NRM), anhysteretic remanent magnetisation (ARM) and isothermal remanent magnetisation (IRM) was carried out to constrain the coercivity parameters of constituent minerals (Lowrie and Fuller 1971).

Both the shape of the demagnetisation curve and the relative demagnetising fields at which the median destructive field (MDF) is reached provide information on the domain state of constituent ferromagnetic minerals. Rapid demagnetisation at low field intensities and exponential demagnetisation curves are associated with unstable remanent magnetisation, conversely a concave up curve reflects stability. These features are indicative of MD and SD grains respectively (Dunlop and Ozdemir 1997). Lowrie and Fuller (1971) proposed that grain size can be predicted based on the stability of weak-field (here ARM is used) versus strong-field (here IRM is used) induced magnetisation. If IRM reaches the median destructive field at lower demagnetising fields than ARM, a SD grain size is predicted. However, this is not always the case (Dunlop *et al.* 1973; Heider *et al.* 1992). Xu and Dunlop (1995) have demonstrated stability of ARM and IRM is actually dependent on grain size and dislocation density, and refer to L-type and H-type results to depict samples which exhibit increased stability in ARM and IRM respectively rather than infer information regarding grain domain state. Thus the Lowrie-Fuller test is not exclusively dependent on grain size alone and other parameters such as the demagnetising fields and the relationship between NRM, IRM and ARM should be considered.

NRM MDF values below 25mT are characteristic of low-coercivity phases while values between 25-70mT characterise higher coercivity minerals (Dunlop and Ozdemir 1997). In the current data set (Fig. 7.22), the NRM MDF is reached in fields ≤10mT for all samples. The NRM demagnetisation curve exhibits an initial rapid decrease in remanence with subsequent undulations. This is related to ongoing exchanges between dominant NRM vectors as

progressively stable elements of the net vector are removed. Both IRM and ARM demagnetisation curves are initially steep followed by a more gradual decline in remanence. A smooth profile is always observed, this is attributed to earlier removal of NRM and over printing by IRM and ARM fields which drown out trace NRM. ARM is always more stable than IRM and reaches the median destructive field (MDF) between 0mT and 25mT.

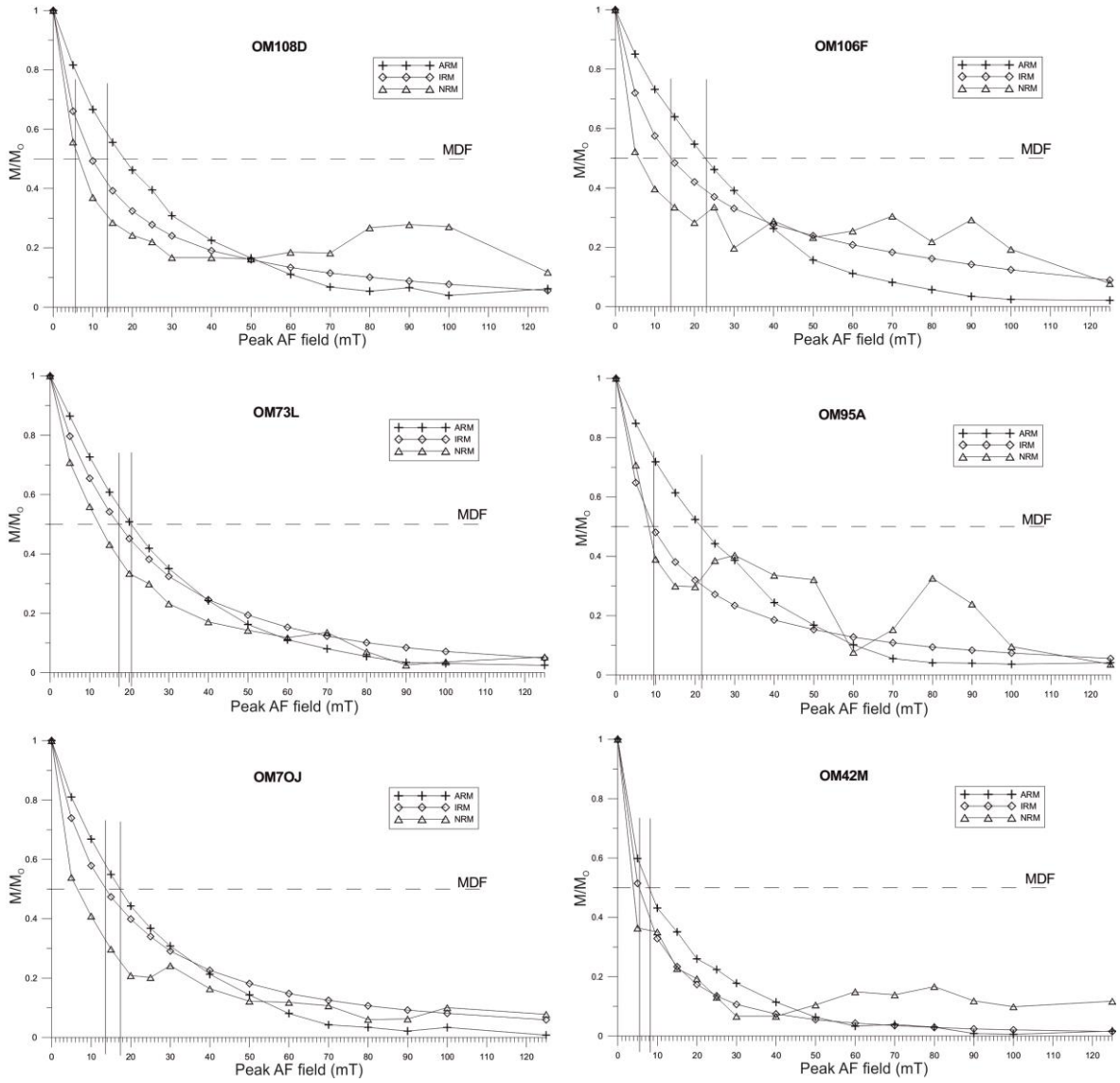


Fig. 7.22 Results of Lowrie-Fuller test as discussed in the text.

All results return a SD Lowrie-Fuller test or a L-type result (Xu and Dunlop 1995). The abrupt rate of demagnetisation (in all cases <25mT) coupled with the MDF value for ARM demagnetisation suggests a PSD to MD grain size (Argyle and Dunlop 1990), more precise dimensions cannot be extrapolated owing to unconstrained stoichiometric parameters. IRM

acquisition data shows that a low coercivity phase such as titanomagnetite is the likely dominant magnetic mineral.

A relationship is observed between G3 (OM108, OM106, Om73) and G1/G2 (OM95, OM70, OM42) samples. G3 carry higher MDF values across board (ARM = G1~18-23mT vs. G1/G2~3-21mT) and also show a slower rate of remanence decay. This suggests a larger proportion of relatively high coercivity phases are present in the G3 facies.

SIRM Acquisition and BIRM

Acquisition of saturation isothermal remanent magnetisation (IRM) and back-field isothermal remanent magnetisation (BIRM) are used here to determine magnetic mineralogy and grain size.

IRM acquisition curves show steep acquisition for all samples at low inducing fields. All samples reach 95% saturation between 0.12T and 0.3T, complete saturation is reached between 0.3T and 0.7T. Beyond 0.7T no significant increase in magnetic remanence is observed (Fig. 7.23A). These observations are supported by back-field data which also show rapid decline in magnetic remanence between 0.01T to 0.03T. Coercivity of remanence (H_{CR}) is achieved in fields between 0.03 - 0.68mT (Fig. 7.23B). A decline in the rate of decay is observed from 0.03T to H_{CR}, this is most obvious in G3 samples.

A clear distinction exists between G3 (OM73, OM106, OM108) and G1/G2 (OM95C, OM70J, OM42) samples. G3 samples exhibit higher coercivity values, reaching H_{CR} between -0.068 and -0.046 while G2/G1 samples reach H_{CR} between 0.055T and 0.031T. Similarly, G3 samples require greater inducing fields in order to reach full saturation by comparison to sample for the two associated facies (0.4-0.7 versus 0.3-0.5).

The rapid acquisition of saturation to 95% by 0.3T is consistent with multidomain titanomagnetite as the primary ferromagnetic mineral in all samples. The continued minor acquisition of remanence in fields greater the 0.3T is indicative of the presence of a minor contribution from a higher coercivity mineral. These observations show that G3 samples contain a minor contribution from some higher coercivity mineral phase, possibly some amount of maghemite or hematite.

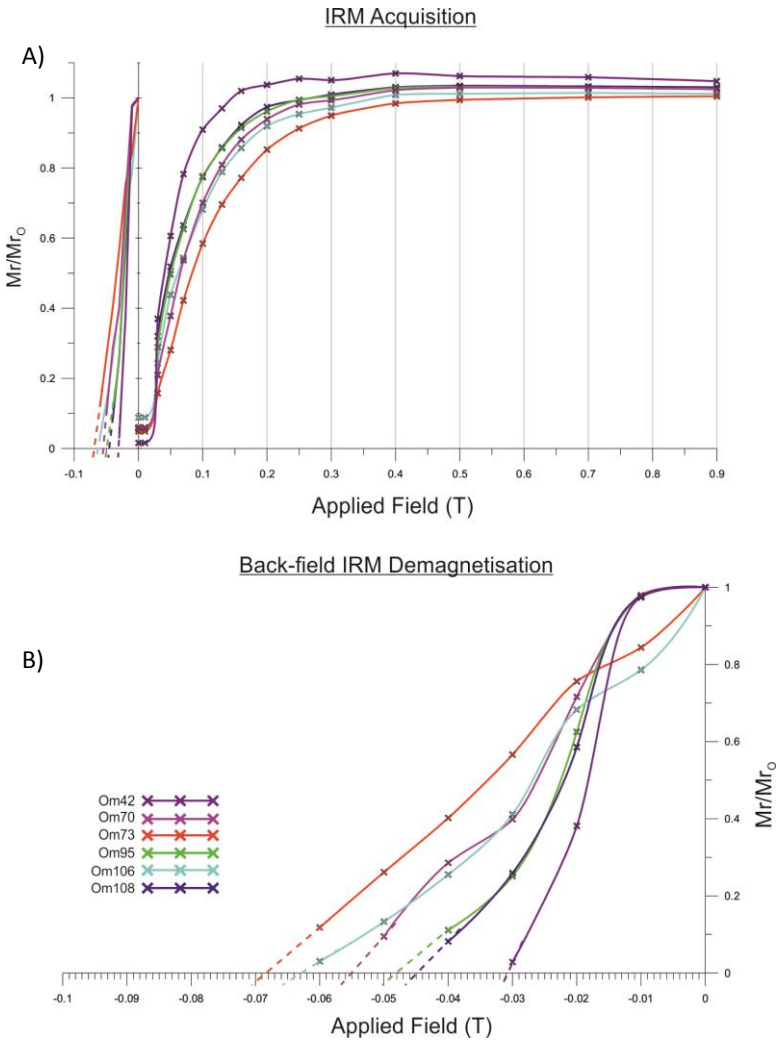


Fig. 7.23 A) results of SIRM acquisition experiments. B) Results of BIRM demagnetisation experiments. All samples exhibit exponential demagnetisation curves and are saturated in less than 0.3T (exception of OM73). Those samples which the highest coercivity values (OM73 & OM106) also required higher AF - demagnetising fields in the Lowrie - Fuller test.

Three-Component IRM Demagnetisation

The response of five samples to thermal demagnetisation of three contrasting IRM intensities imposed along orthogonal axes of each sample (Lowrie 1990) was measured and results are presented below (Fig. 7.24) . Inducing fields of 3T, 0.3T and 0.03T were selected in order to determine the relative contribution to bulk remanence made by low, moderate and high coercivity minerals within this spectrum.

The shape of the modulus demagnetisation curve shows that G1 and G2 samples rapidly demagnetise to <20% by 300°C while G3 samples demagnetise at a slower more progressive rate (Fig. 7.24). In all cases the moderate coercivity axis (y-axis, 0.3T) return the highest remanence values. G1 samples consistently contain a higher proportion of moderate coercivity minerals than counterpart G2 and G3 samples. G3 samples consistently show high coercivity minerals (z-axis, 3T) are the second most significant contributor, conversely in G1 the z-axis component is consistently the least significant. In G2, the relative contribution made by x-axis and z-axis to the modulus are

approximately equal. Modulus value of G3 samples all show a rapid decrease in intensity up to 200°C and are fully demagnetised by 580-600°C. In all G3 samples, the z-axis demagnetisation curve illustrates that this initial decline is attributed to minerals within the higher coercivity spectra with unblocking temperatures ~200°C.

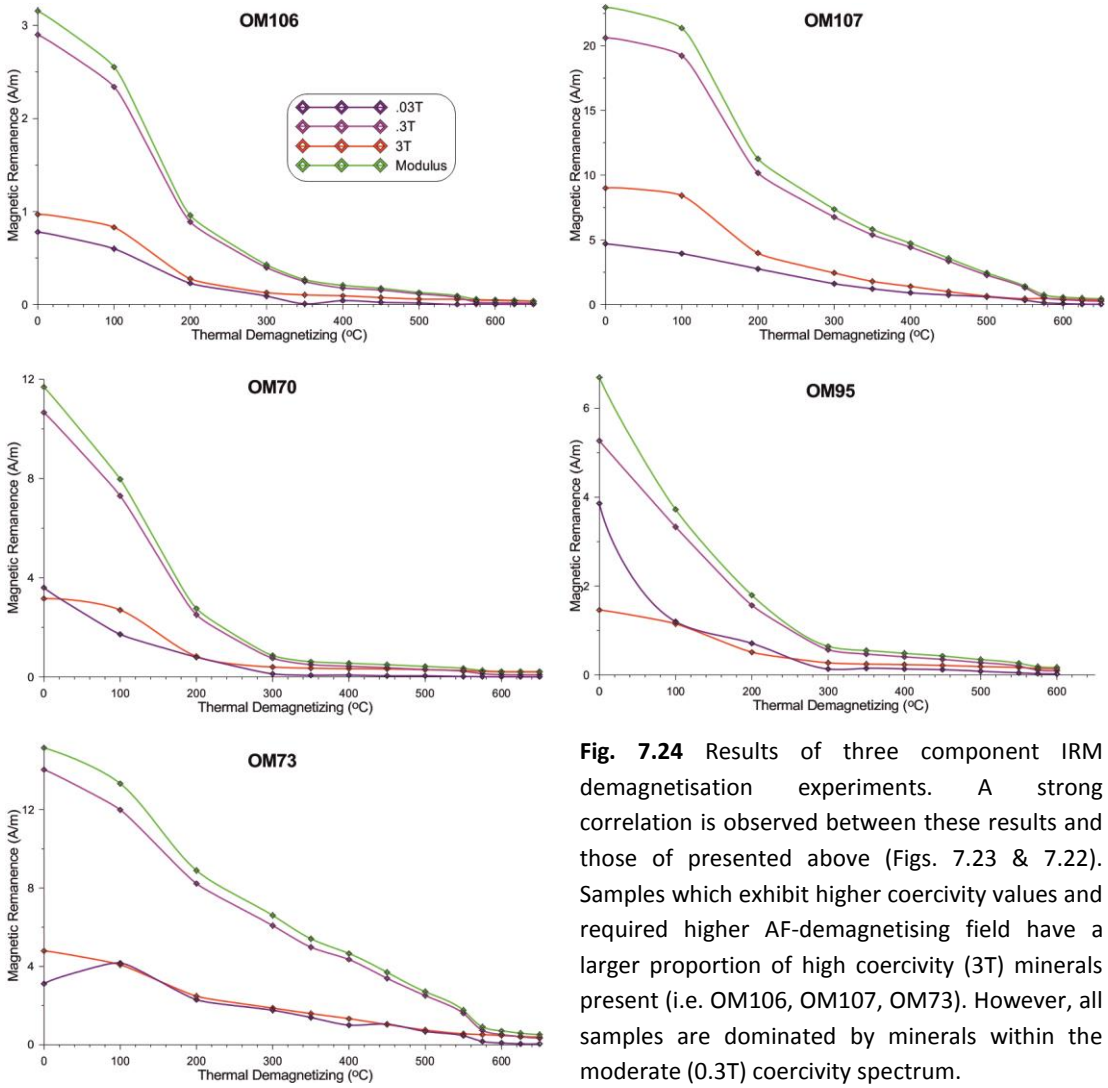


Fig. 7.24 Results of three component IRM demagnetisation experiments. A strong correlation is observed between these results and those of presented above (Figs. 7.23 & 7.22). Samples which exhibit higher coercivity values and required higher AF-demagnetising field have a larger proportion of high coercivity (3T) minerals present (i.e. OM106, OM107, OM73). However, all samples are dominated by minerals within the moderate (0.3T) coercivity spectrum.

Three component demagnetisation data show a clear contrast in ferromagnetic mineralogy between facies G1 and G3. G1 is relatively straight forward and contains a very large proportion of low and moderate coercivity minerals which demagnetise rapidly prior to 300°C and are essentially fully demagnetised by 580°C. This is consistent with a low-Ti titanomagnetite dominant phase. Again, a low-Ti titanomagnetite is the likely major ferromagnetic contributor in G3, however a greater proportion of higher coercivity minerals are present relative to G1 and G2. This may reflect a greater proportion of oxidised Fe-Ti phases are present in this facies such. Hematite

is unlikely to be present in significant quantities as all samples are fully demagnetised by about 600°C. This observation suggests that maghemitization or deuteric oxidisation may have promoted advance oxidisation of primary magnetite in G3, a feature which is not prominent in G1 or G2.

7.4.3 Anisotropy of Magnetic Susceptibility Results

Anisotropy of Magnetic Susceptibility (AMS) was measured from all 113 sampled sites. A summary of AMS data is presented in Table 7.1. An overview of the data collected is presented in Appendix C, full data files are contained in Appendix E.

All Sites					
Parameter	Tj	Pj	lnPj	H (%)	K x 10^{-6}(SI)
Min	-0.71	1.01	0.007	1.17	166
Max	0.95	1.07	0.064	10.12	17819
Mean	0.2	1.04	0.03	5.33	9688
Std. Dev	0.42	0.013	0.012	1.83	4938

G2					
Parameter	Tj	Pj	lnPj	H (%)	K x 10^{-6}(SI)
Min	-0.29	1.01	0.007	1.17	166
Max	0.84	1.06	0.058	7.63	13975
Mean	0.32	1.04	0.0345	5.32	9285
Std. Dev	0.34	0.014	0.0138	1.94	4746

G1					
Min	-0.71	1.01	0.007	1.28	1119
Max	0.95	1.066	0.064	10.12	17819
Mean	0.14	1.03	0.034	5.3	10934
Std. Dev	0.43	0.0125	0.012	1.84	4138

G3					
Min	0.002	1.01	0.01	1.55	244
Max	0.016	1.06	0.06	8.76	5082
Mean	0.011	1.03	0.036	5.58	1941
Std. Dev	0.004	0.01	0.011	1.68	1472

Table 7.1 Summary of compiled AMS data from all sites and for each facies.

Susceptibility and Anisotropy

Mean susceptibility (K_{mean}) values vary from 166 x 10^{-6} to 178.19 x 10^{-4} (SI units) across the pluton (average 9.688 x 10^{-3} ± 4.938 x 10^{-3}). A sharp contrast in average K_{mean} values is noted between facies (G1 = 109.34 x 10^{-4}, G2 = 92.85 x 10^{-4}, G3 = 19.41 x 10^{-4}) that clearly indicates a higher concentration of ferromagnetic minerals in earlier facies. This indicates the AMS tensor in G3 samples may be influenced to a greater extent by paramagnetic minerals (biotite) than samples taken from G1 or G2.

The corrected degree of anisotropy (Pj) varies between 1.01 and 1.07 with a mean value of 1.04 ± 0.013. A maximum variance between mean Pj values calculated from each facies is 0.01 and the overall degree of anisotropy H is 5.3%. These values reflect an even distribution of the strength of anisotropy which seemingly ignores facies boundaries. Shape factor (Tj) values range

between well defined oblate (-0.71), to tri-axial to strongly prolate (0.95) (Table 7.1). G1 and G2 samples exhibit a full spectrum of AMS ellipsoid shapes but G3 return only weak to moderate oblate ellipsoids (Tj min = 0.0024, max = 0.016) and no prolate ellipsoids.

These results indicate that while susceptibly is drastically influenced by compositional contrasts between facies, Tj and Pj are not.

7.5 General Discussion of Magnetic Data

7.5.1 Rock Magnetic Properties

Curie point estimates clearly indicate the presence of a low Ti titanomagnetite phase in all samples. All samples reach 95% saturation in IRM fields of magnitude ≤ 0.3T and the coercivity of remanence is achieved in BIRM fields < 0.07T. Demagnetisation of NRM, IRM and NRM during the Lowrie - Fuller test (Lowrie and Fuller 1971) return exponential curves and an L-type result is observed between IRM and ARM curves (Xu and Dunlop 1995). These results are consistent with a MD to PSD titanomagnetite phase which is the dominant carrier of remanence and susceptibility in all samples (Argyle *et al.* 1994; Dunlop and Ozdemir 1997).

Rock magnetic data makes a clear distinction between G1 and G3 facies. This is most evident in SIRM, BIRM and three component demagnetisation graphs where G3 samples (OM107, OM106 and OM73) show initial rapid decay followed by a gradual reduction in remanence or progression to saturation in fields greater than those required for G1 samples (Figs. 7.23 & 7.24). It is therefore clear that G3 contains a significant proportion of higher coercivity minerals as distinct from G1 which does not. Three component demagnetisation curves indicate at least one significant high coercivity phase is a significant feature in G3 and to a lesser extent in G2. Unblocking temperatures of ~ 300°C and ~ 600°C indicate pyrrhotite and maghemite respectively but as maghemite is unstable over 300°C this mineral normally does not reach T_C or the unblocking temperature (Bina and Daly 1994; Dunlop and Ozdemir 1997).

Field and petrographic observations from this and other studies (Townend 1966; Feely *et al.* 2007) have identified a higher (but still minor) modal abundance of hematite (identified as maghemite here) and coarse sulphides in the later G2 and G3 facies. G2 (OM70) contains an elevated proportion of sulphides and higher coercivity minerals relative to G1 but less than what is indicated in G3. As such G2 acts (magnetically) as a transitional zone across G1 and G3. In this

case the rock magnetic data are interpreted as reflecting the presence of some maghemite and to a lesser extent iron sulphide phase which is most abundant in G3.

The species and structure of ferromagnetic minerals formed from crystallising magma is dependent on chemistry and cooling rate of a magma (Lindsley 1991). A slower rate of cooling encourages exsolution of Fe rich and Ti rich cubic phases which, once formed, will be sensitive to evolving oxidising conditions which increase as crystallisation progresses (Tarling and Hrouda 1993). Generally, prolonged cooling rates or reheating of previously cooled magma, and the circulation of hydrothermal fluids promotes oxidisation and growth of maghemite from magnetite (Tarling and Hrouda 1993).

It is proposed that a reduced rate of cooling in the upper, latest, facies (G3) facilitated prolonged oxidisation and the tendency for cubic Fe-Ti oxides to tend toward the maghemite end member of the TiO_2-FeO-Fe_2O_3 ternary diagram (Lindsley 1976, 1991). The process converted significant proportions of magnetite to maghemite which resulted in accentuated irreversible low field susceptibility thermomagnetic curves and elevated coercivity parameters in G3 samples and to a lesser extent G2 samples. This deduction is consistent with the concept that G1 intruded earlier into relatively cool country rock and G3 followed and cooled slower due to elevated ambient temperatures. Thus we observe progressive higher oxidisation levels in from G1 through to G3.

7.5.2 Controls over AMS Vectors

A lack of accentuated Hopkinson Peaks (Fig. 7.20), exponential demagnetisation curves (Fig 7.22) and low IRM fields required to reach saturation (Fig. 7.23) indicate a PSD to MD titanomagnetite phase is the dominant magnetic mineral in all samples. These data show that the affect from any SD magnetite (or any other ferromagnetic or paramagnetic minerals with inverse tendencies) will be overwhelmed by PSD to MD titanomagnetite. Mean susceptibly values across the intrusion are consistent with this finding. Titanomagnetite is several orders of magnitude more susceptible than paramagnetic minerals at room temperature in low fields (Hrouda 1982; Tarling and Hrouda 1993; Archanjo *et al.* 1995) and so is expected to dominate the AMS tensor (Rochette 1987).

A contour map of K_{mean} reveals a low magnetic anomaly over the Aughrus Peninsula, Friar Isl. and Cruagh Isl. (Fig. 7.25) that coincides with the mapped extent of the G3 facies. There is a similar although less apparent anomaly defined by the extent of the G2 facies which also has a lower mean susceptibly value than G1. These data illustrate a strong dependence of susceptibility on mineralogy, show G3 is depleted in ferromagnetic contributors and that a greater contribution from paramagnetic minerals to AMS is likely in this facies. However, no significant paramagnetic influences on susceptibility were noted during cryogenic experiments (Fig. 7.21).

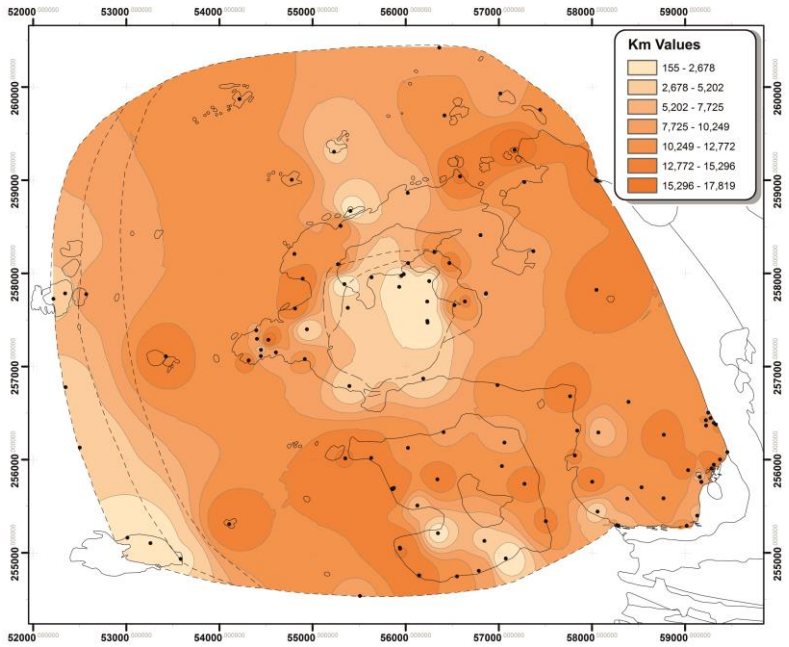


Fig. 7.25 A contour map of K_{mean} susceptibility values in the Omey Pluton. A low magnetic susceptibility anomaly is centred over the localities where G3 is mapped. Negligible differences are detected between G1 and G2.

Comparing contour maps of H (Fig. 7.26) and Tj (Fig. 7.27), no abrupt change in the shape or strength of the AMS tensor is noted in samples collected from neighbouring sites across facies contacts. It may be significant that only weakly oblate ellipsoids are returned from G3 sample sites, however adjacent G2 and G1 sites also return similar shape parameter and strength of anisotropy parameters. In rocks which lack ferromagnetic minerals, any iron bearing paramagnetic silicates will become increasingly important contributors to the AMS ellipsoid (Borradaile and Jackson 2010). It has been shown that trace ferromagnetic grains are often included within the paramagnetic crystal lattice typically along cleavage planes (Rochette *et al.* 1992; Borradaile and Werner 1994; Borradaile and Lagroix 2001). This results in elevated susceptibly values (relative to pure paramagnetic samples) and accentuation of the AMS tensor which is primarily controlled by the host crystals' magnetic anisotropy. Based on the rock magnetic data and petrographic observations described above, the resultant AMS tensors

returned from G3 are a product of interactions between biotite grains with interstitial and included trace quantities of titanomagnetite. In contrast, G2 and G3 samples show much higher K_{mean} values which suggests that their AMS signal is controlled by a PSD to MD titanomagnetite that essentially masks the contribution from lower susceptibility mineral phases

Therefore, a minimal contribution to AMS is made from paramagnetic phases. However owing to the overall reduction in abundance of titanomagnetite and the oblate grain scale anisotropy of biotite, an oblate bias may still be imparted on the resultant magnetic tensor from sites with particularly low mean susceptibility values ($x10^{-6}$ SI).

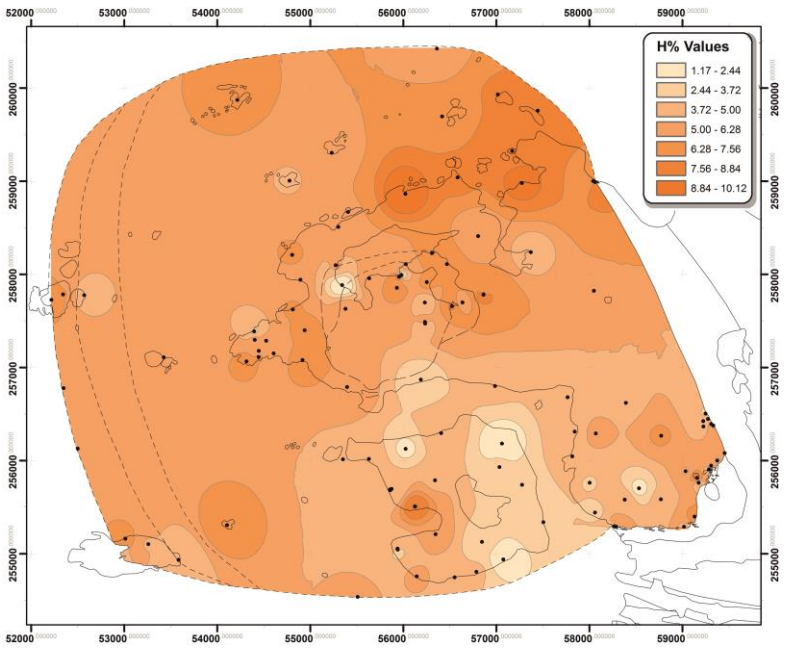


Fig. 7.26 A contour map of determined H values. No definite pattern is observed which can be correlated with facies distribution.

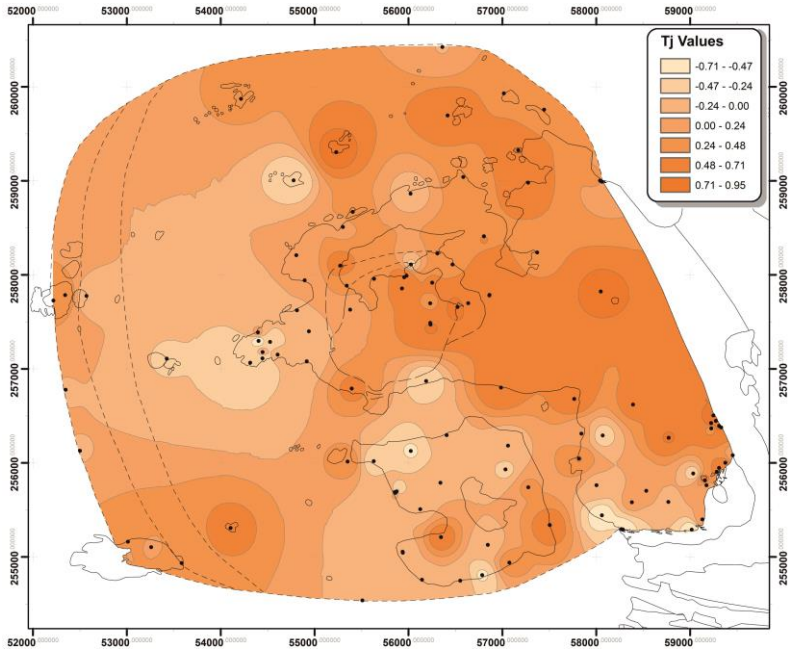


Fig. 7.27 A contour map of determined Tj values. No definite pattern is observed which can be correlated with facies distribution. A concentration of prolate shape anisotropy values is detected where submagmatic shear zones were mapped.

Finally, it has been demonstrated using a combination of image analysis and AMS that crystallising oxide phases commonly use the silicate crystal framework as nucleation sites and become incorporated along crystallographically defined planes in a host rocks constituent minerals (Archanjo *et al.* 1995; Launeau and Cruden 1998). Petrographic observations from the current study show elongate aggregates, and euhedral cubic magnetite hosted within the cleavage planes of biotite crystals and among interstices of plagioclase (Fig. 7.5). A final test comparing the AMS fabric to those observed in the field (where available) reveals a strong consistency between magnetic anisotropy and silicate fabrics observed in the field (Fig. 7.28).

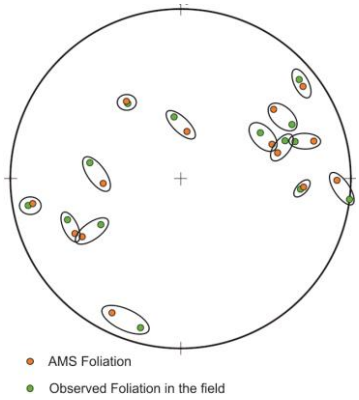


Fig. 7.28 The poles of foliations that are observed in the field correlate well with the orientation of the AMS K3 vector determined from blocks sampled from the same site. This indicates that AMS data is a valid petrofabric proxy.

These observations suggest the orientation of oxide phases are controlled by the preferred orientation of silicate minerals and that a normal relationship exists between the principal geometrical and principal susceptibility axes of the dominant magnetic grains. Thus the net AMS tensor will ultimately reflect the crystal preferred orientation of constituent silicate minerals. As such, the AMS tensor can be expected to reflect *normal* crystallographic preferred orientations.

7.5.3 Symmetry and Attitude of Magnetic Fabrics

Tj is used to distinguish dominantly oblate from dominantly prolate fabrics (Jelinek 1981) (see also Owens (1974); Jelinek (1977); Owens (2000a, 2000b) for comparative parameters). In fabrics which are purely oblate, the shape of the AMS ellipsoid may be visualised as 'flattened' in the K1-K2 plane and samples from within a single sample site return consistent K3 axes orientations (pole of plane) while K1-K2 axes are distributed along the plane of flattening. Thus, strongly prolate AMS ellipsoids are interpreted, and a lineation inferred, when K1 axes cluster and K2 and K3 axes confidence ellipses overlap (Fig. 7.29A). The converse is true for oblate fabrics, if K3 is well constrained and confidence ellipses for K1 and K2 axes overlap, a foliation is inferred (Fig. 7.29B). An L-S fabric may be determined where K1, K2 and K3 axes are all well constrained (Fig. 7.29C).

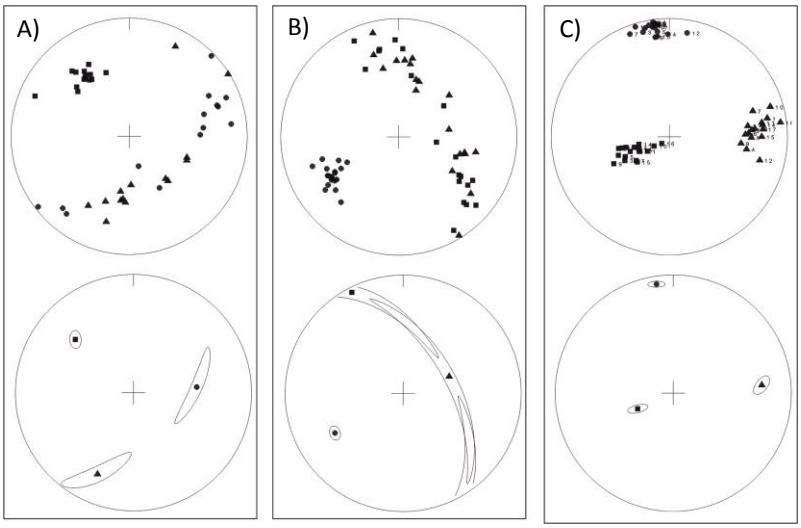


Fig. 7.29 Examples of different AMS tensor shapes depicted on southern hemisphere stereonets (individual sub-specimen susceptibility axes plotted above, mean susceptibility axes with 95% confidence ellipses below; square = K1, circle = K3, triangle = K2). A) A prolate fabric is defined when K1 is well constrained and K2 and K3 define a girdle. B) An oblate fabric is defined when K3 is well constrained and K2 and K1 define a girdle. C) Both a foliation and lineation may be determined when all axes are well constrained.

Deciphering whether an ellipsoid reflects an L, S or LS fabric, or whether it is a composite of two or more sub-fabrics may be determined in part by examination of the distribution of sub specimen principle susceptibility axes (Owens 1974, 2000b, 2000a; Ferré 2002; Chadima *et al.* 2009). In addition more complex methods can be applied to determine the presence, significance and genesis of sub-fabrics (see Appendix D). K1 is often interpreted to reflect the direction of magma flow (Stevenson *et al.* 2007; Stevenson and Bennett 2011; Magee *et al.* 2012). However there are many caveats surrounding the interpretation of prolate AMS fabrics and such an interpretation cannot be taken for granted. When dealing with igneous rocks, such fabrics may reflect primary emplacement flow fabric (Cruden *et al.* 1999; Parés and van der Pluijm 2002a; Callot *et al.* 2004), tectonic fabrics (Ono *et al.* 2010; Valley *et al.* 2011), post solidus hydrothermal alteration (Just *et al.* 2004; Lau *et al.* 2007) or any combination of the above. As such, any interpretation of the significance of the shape of the AMS tensor must be complimented by field and petrographic observations.

In Figure 7.30 (attached map) lineations are plotted when the AMS tensor is dominantly prolate ($Tj < 0$) and foliations are plotted where the tensor is dominantly oblate ($Tj > 0$). Figure 7.31 (attached map) is a summary of the sites sampled and plots lineations, foliations or both lineations and foliations were respective L, S or L-S fabrics are interpreted from each AMS tensor. Figure 7.32 (attached map) is an overlay for Figures 7.30 or 7.31, and depicts the stereographic

projections (95% confidence ellipse) of the AMS ellipsoids which were used in conjunction with the statistical analysis of Jelinek (1981) and Owens (2000a) during interpretation.

Of the 113 sites sampled, 40 yield prolate and 73 yield oblate AMS ellipsoids. Figure 7.30 illustrates that fabrics which are dominantly prolate are largely confined to the southern and western portion of the intrusion while oblate fabrics are more dominant in the central and eastern portion. From this it is apparent that a spatial relationship among fabric symmetry is present in the pluton but it is not dependent on facies distribution. A polar plot of Tj vs. Pj accurately depicts the relationship between the strength of the magnetic fabric and shape anisotropy (Fig. 7.31B) and again shows that no significant correlation is made between fluctuation in shape anisotropy and granite facies. Figure 7.30, used in conjunction with Figure 7.32, reveals that for a majority of sites both K1 and K3 axes show confidence ellipses which allow both a lineation and foliation to be determined. This is further supported by comparing normalised and un-normalised stereographic projections of the AMS tensor from each site. A very strong alignment of K1 axes trending consistently NNW-SSE with drastically fluctuating plunge (subhorizontal to near vertical) is immediately apparent (Fig. 7.31C). By extending the averaged trend of well defined lineations a parallel relationship emerges between shear zones identified in the field and magnetic lineations.

Planar components (K1-K2 plane) identified from AMS tensors exhibit a less obvious geometrical relationship. From these two distinct foliation patterns are determined.

At the core of the intrusion moderately inclined outward dipping fabrics define a strong concentric fabric pattern. The orientation and dip of foliation planes is consistent across contact boundaries and generally decreases outwards. This is best demonstrated along a traverse from Aughrus More, where dips average ~ 65° northwards, to islands offshore, where foliation inclination eventually reaches 36°. In close proximity to the external plutonic contacts, magnetic foliations are also, most often, contact parallel. In the east, where the granite is in contact with the Lakes Marble Fm. and Streamstown Schist Fm., foliations strike approximately parallel and dip within 10° of the host strata that pseudomorph the symmetry of the bounding D4 fold. Off shore on Cruagh Isl. AMS foliations are not parallel to the steeply inclined east-west striking host rock strata but are, in whole, contact parallel and strike northwest-southeast. This is in contrast with field observations which clearly indicate that magma sheeted into the country rock along pre-existing planes of weakness i.e. subvertical southern limbs of the D4 Connemara Antiform. On

Friar Isl. AMS foliations strike parallel to the country rock strata and dip moderately west within 10° of the inclination of the Cleggan Boulder Bed Fm..

A large number of sites return magnetic and visual foliations which are discordant to the concentric pattern described above. These are most prevalent on the east and west of Omey Beach (057700, 257000), to the north between Aughrus Beg and Rossadillask (057100, 258200) and, very obviously, at Aughrus Point (054400, 257200). In these areas foliations most often strike parallel to NNW-SSE magnetic lineations and dip moderately to the west. A stereographic projection of poles of AMS foliation planes that occur within 250m of these zones clearly illustrates this anomaly (Fig. 7.33B).

Finally, several examples of magnetic fabrics which bear no immediate relationship to either the concentric pattern identified earlier or the consistent NNW-SSE suite of lineations which discordantly cross cut the former, are noted on Omey Island and immediately east in the Fountain Hill area. These most likely reflect structurally intermediate fabrics (Owens 2000a; Ferré 2002; Parés and van der Pluijm 2002b; Debacker *et al.* 2004) (as oppose to intermediate fabrics brought about by anisotropy properties of constituent minerals (Potter and Stephenson 1988; Rochette 1988)).

7.5.4 Summary of AMS Fabrics

In summary, two distinct sets of fabrics have been detected. A distinct outward dipping suite of foliations is present. This is evenly distributed about the intrusion and is concentric. These foliations lie parallel to the folded host rock strata within a margin of error. Distinct from this are NNW-SSE lineations which are discordant to internal and external pluton contacts. The most prolate fabrics are located within mapped shear zones. Spatially associated magnetic foliations are parallel to the strike of the shear zone or are intermediate between the concentric and cross cutting NNW-SSE fabrics described.

7.6 The Emplacement and Tectonic History of the Omey Pluton

Here, the significance of magnetic fabric data and their genesis is discussed, with reference to the field, petrographic and rock magnetic data already described, in order to elucidate the

structural evolution of the Omey Pluton and its relationship with the regional kinematic regime during the mid Silurian.

7.6.1 Tectonic Overprint of an Emplacement Foliation

The temporal relationship between fabric development and crystallisation state is critical in deciphering the mechanisms responsible for driving the development of textural anisotropies in igneous rocks. There are two fabric end members, those which form due to the alignment of crystals in an essentially molten magma and those which develop as a product of plastic deformation and recrystallisation processes in a solid rock. Fabrics formed in a low viscosity passive medium (i.e. magma) imply the recorded strain reflects either the magma flow direction or syn-emplacement tectonic strain. Conversely fabrics formed in a fully crystallised rock reflect strain attributable to post emplacement processes or ongoing inflation of a plutonic body (e.g. Baxter *et al.* (2005)). A continuous down temperature spectrum of fabric development has been documented and numerous classification schemes have been proposed (Arzi 1978; Van der Molen and Paterson 1979; Hutton 1988; Tribe and D'Lemos 1996; Takeda and Obata 2003; Rosenberg and Handy 2005). Here the terms magmatic or magmatic flow, sub-magmatic flow and solid state are used to indicate fabric development in a passive medium, in a state between a truly passive medium and final crystal lock up and in a essentially solid rock (Passchier and Trouw 2005). Vernon (2004) and Passchier and Trouw (2005) summarise microstructural features which can be used to distinguish magmatic, sub-magmatic and solid state deformation. Just as visible fabrics defined by silicate minerals may reflect primary flow, tectonic or composite fabrics, so too can AMS fabrics (Rochette and Fillion 1988; Rochette *et al.* 1992; Bouchez 1997; Rochette *et al.* 1999; Borradaile and Jackson 2004, 2010). AMS data alone carries no indication of the root cause of fabric genesis and so must be coupled with the techniques outlined above (Chapter 6). However basic statistical checks comparing normalised and un-normalised projections of AMS polar plots (Owens 2000a) and comparison of the shape factor (Tj) and the difference shape factor (U) can be used to identify net AMS tensors which possibly reflect multiple sub-fabrics. Thus, inferences may be made regarding the genetic origins of AMS fabrics.

In the current study area two discrete sets of fabrics are identified. Those which are concentric and those which are orientated NNW-SSE and cross cut the intrusion (Fig. 7.33). Below it is argued that the set of outward dipping concentric fabrics reflect the latest phases of the emplacement

process while prolate and oblate NNW-SSE fabrics are a tectonic overprint and are related to extremely subtle syn-magmatic to post solidus shearing. Fabrics which are not immediately recognisable as part of either of the two groups discussed above are considered intermediate and have been frozen in the process of recording tectonic strain over emplacement related fabrics.

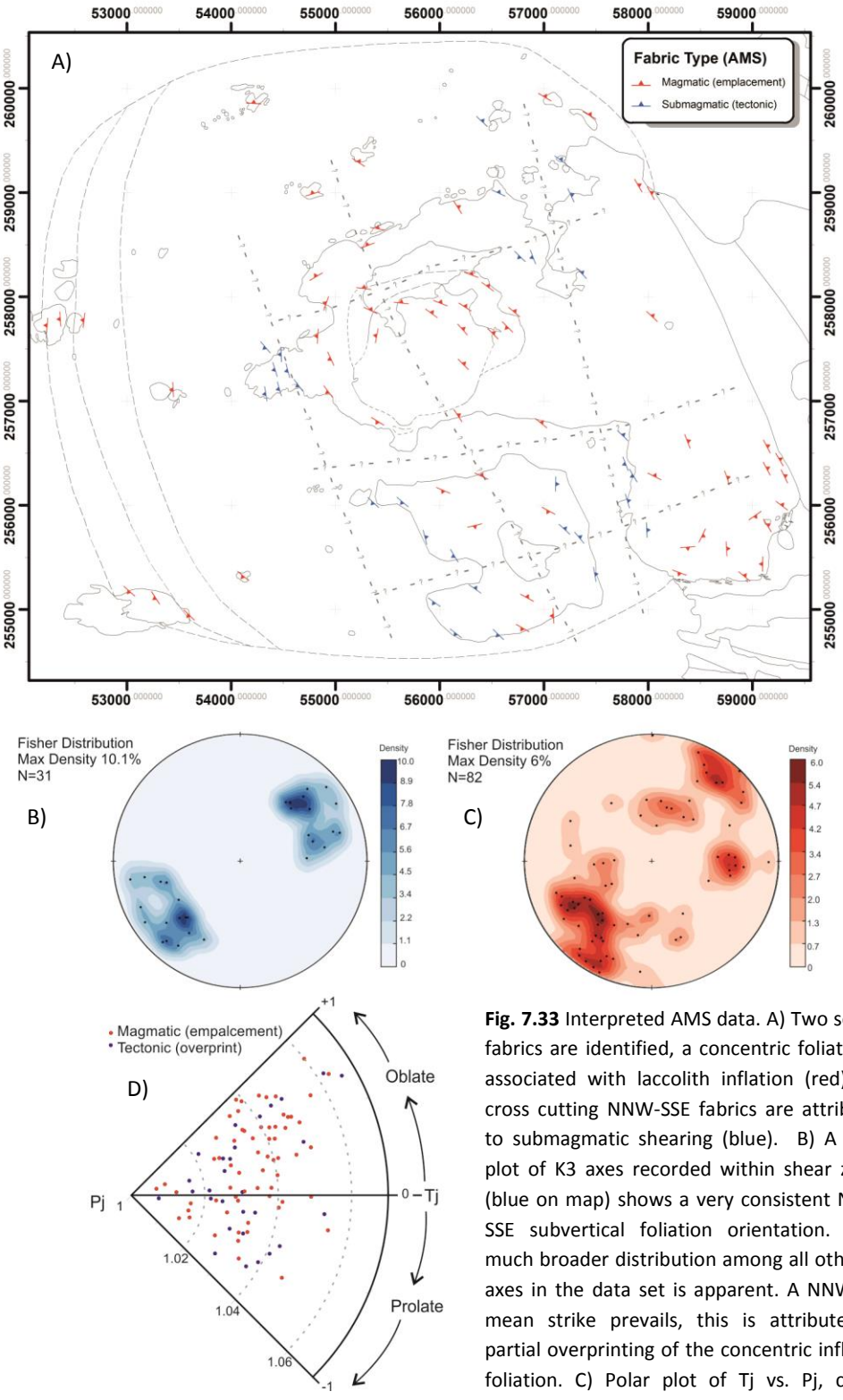


Fig. 7.33 Interpreted AMS data. A) Two sets of fabrics are identified, a concentric foliation is associated with laccolith inflation (red) and cross cutting NNW-SSE fabrics are attributed to submagmatic shearing (blue). B) A polar plot of K3 axes recorded within shear zones (blue on map) shows a very consistent NNW-SSE subvertical foliation orientation. C) A much broader distribution among all other K3 axes in the data set is apparent. A NNW-SSE mean strike prevails, this is attributed to partial overprinting of the concentric inflation foliation. C) Polar plot of Tj vs. Pj, colour coding correlates to that in (A). A broad spectrum of tensors are detected.

Concentric Magmatic AMS Fabrics

In the field, evidence for emplacement related processes are lacking. However, AMS data clearly shows a well defined concentric foliation pattern about the inner and outer part of the Pluton (Fig. 7.33). Thin sections derived from these AMS blocks show that biotite and feldspars are typically totally undeformed and quartz occurs as anhedral interstitial grains occasionally exhibiting weak to very weak undulose extinction. These observations show that fabric anisotropies reflected in AMS data were imparted in the magmatic to high temperature sub-magmatic state.

Foliations are orientated parallel to the outer pluton contacts and typically lie approximately parallel to the bedded nature of the country rock. However on Cruagh Isl., where the granite locally sheets parallel to bedding, AMS foliations are parallel to the overall discordant contact and maintain an overall concentric symmetry at map scale (Fig. 7.33). The degree of dip declines from moderate-steep to moderate-shallow from the core of the pluton towards the granite perimeter and defines a dome like symmetry. Thus, concentric AMS fabrics were formed by strain imparted in the magmatic or high temperature post magmatic state and thus must reflect processes temporally related to emplacement.

Submagmatic to Post Solidus Shearing

AMS data from shear zone localities, used in conjunction with field data, provides critical information regarding the timing of shearing relative to magma crystallisation. Fabric development at Aughrus Point is used as a characteristic example (Fig. 7.34).

Field mapping identified distinctive NNW-SSE foliations at this locality. Within shear zones, the planar component of AMS fabrics are orientated NNW-SSE, parallel to those observed in the field (Fig 7.34A, blue). Moving away from the core of shear zones, oblate fabrics deviate from a NNW-SSE strike and eventually become concentric (Fig 7.34A, red). Several fabrics are interpreted to be intermediate between magmatic inflation and tectonic shear zone fabrics (Fig. 7.34A green). These data indicate that tectonic strain has overprinted the earlier ballooning fabric but does not provide any temporal constraints on deformation.

Microstructural features from samples that are spatially disassociated from these deformation zones show no sub-magmatic deformation features (Fig. 7.34B). Traversing toward the centre of the shear zones, kinking of biotite leads way to smearing (Fig. 7.34C, E), brittle deformation of feldspars with magmatic infill becomes more common (Fig. 7.34D), and pervasive quartz ribbons are also observed (Fig. 7.34E). Based on these observations these fabrics are considered to reflect weak degrees of strain imparted in the sub to post magmatic state.

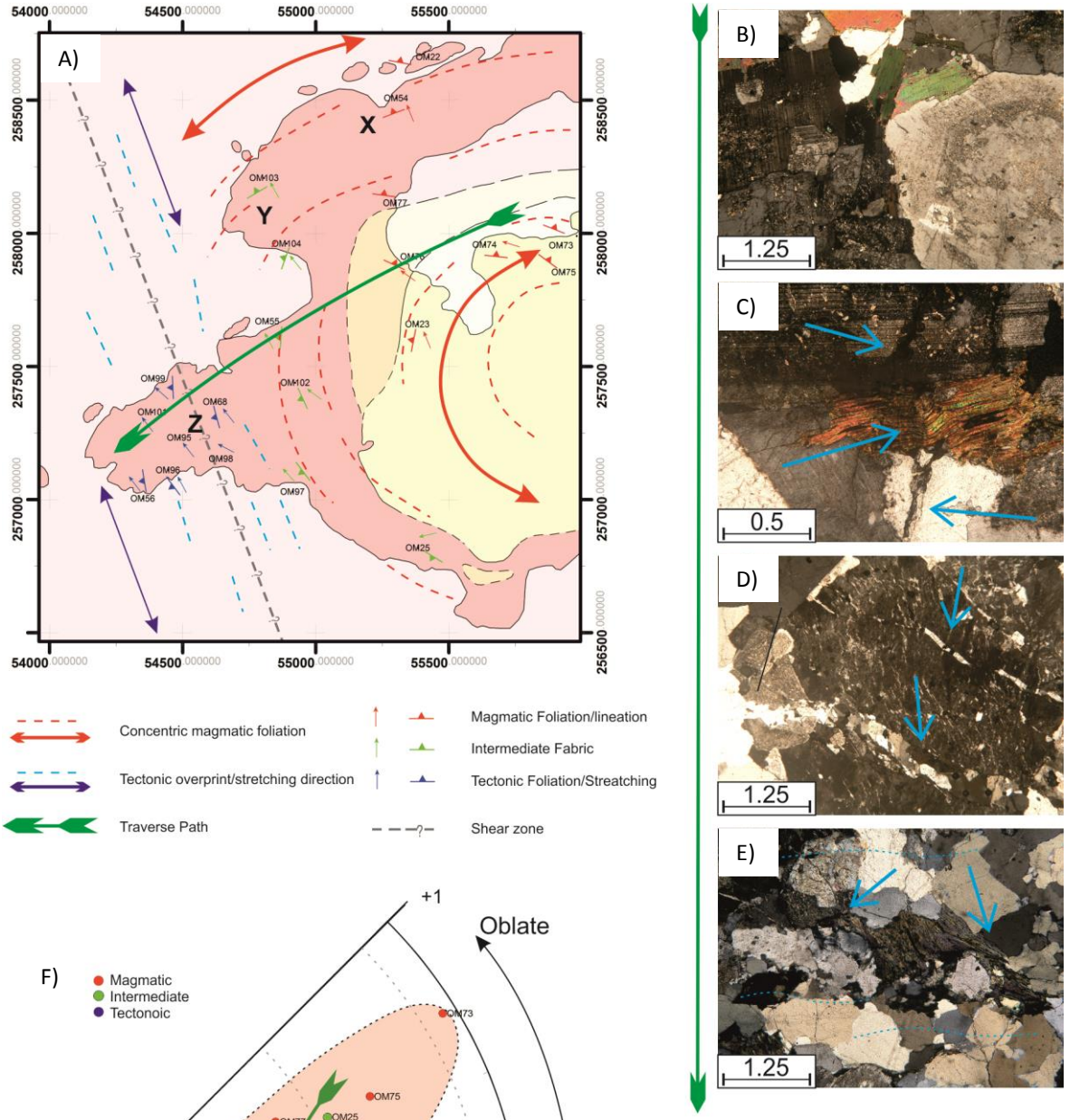


Fig. 7.34 Influence of submagmatic shear zone deformation on host microstructure and AMS shape anisotropy. In all images, green arrow denotes traverse towards shear zone, red, green and blue reflect primary emplacement, intermediate and tectonic fabrics respectively. A) Traversing toward the shear zone (along the green arrow) concentric fabrics become overprinted by the NNW-SSE tectonic fabric. B-E) Low temperature submagmatic deformation becomes increasingly intense towards the shear zone. F) Shape anisotropy evolves from oblate (red) to triaxial (green) to prolate (blue) along the traverse line toward the shear zone.

The shape of AMS tensors also show a very consistent pattern along a traverse across the shear zones identified (Fig. 7.34A, F). Outside of the shear zones AMS tensors are oblate (Fig. 7.34F red), traversing toward the shear zone shape anisotropy tends toward the prolate field (Fig. 7.34F green), these are intermediate fabrics. Samples taken from the centre of NNW-SSE shear zones return dominantly prolate strain ellipsoids (Fig 7.34F blue). These are always orientated NNW-SSE (parallel to observed foliations) and carry moderate anisotropy parameters (mean Tj = -0.3, Pj = 1.04, H = 6.1%). This is a typical of progressive tectonic overprinting of a primary fabric where the tensor is progressively stretched into a oblate shape (Parés and van der Pluijm 2002a).

The azimuth of AMS K1 vectors is strikingly consistent between data collected from within and outside of shear zones that are observed in the field (Fig. 7.31A, C). Thus, both samples which exhibit magmatic state concentric oblate fabrics, and no signs of down temperature deformation, and those which exhibit submagmatic-solid state microstructures all return ~ NNW-SSE K1 vectors. These are typically discordant to internal contacts and the bounding country rock structure. At individual localities the plunge of K1 is sometimes reasonably consistent especially within shear zones, however across the pluton the plunge of the K1 axis are very inconsistent (Fig. 7.31A, C).

AMS lineations may reflect primary magmatic flow (Callot *et al.* 2004; Hacker *et al.* 2007), the intersection of two planar fabrics (Borradaile and Tarling 1981; Housen *et al.* 1993) or tectonic stretching directions (Ferré and Améglio 2000; Hirt *et al.* 2000). Parés and van der Pluijm (2002a) clearly illustrate that the magnitude and orientation of the AMS tensor prior to deformation strongly influences the post deformation net AMS ellipsoid. In the case of the Omey Pluton the emplacement ballooning fabric is only detectable via AMS analysis and is thus highly sensitive to overprinting by the tectonic stretching direction.

There is an overall tendency for lineations to plunge south in the south and north in the north. This may reflect the original magma transport direction as field evidence suggest intruding magma followed the trend of the Connemara Antiform structure prior to vertically thickening, however such a claim is difficult to substantiate with the current data set.

An alternative interpretation, which is preferred here, relates observed K1 axis orientations to shearing. It is highlighted that, on average, K1 vectors not only lie parallel to NNW-SSE shear zones identified in the granite but are also parallel to regional D5 NNW-SSE faults in the host rock. The lack of uniformity in lineation plunge across the pluton is also consistent with an overprinting stretching lineation imparted upon an earlier subtle emplacement fabric (Ferré and Améglio 2000; Hirt *et al.* 2000; Parés and van der Pluijm 2002a). On this basis NNW-SSE magnetic lineations

observed are interpreted as a tectonic stretching lineation imparted by shearing along a pre-existing basement structure during and after the emplacement of the pluton.

7.6.2 Controls on the Emplacement of the Omey Pluton

Many analytical and numerical modelling studies have investigated the role played by magma buoyancy, internal magma pressure, viscosity and hydrostatic pressure in the ascent and emplacement of granite (e.g. Weertman (1971); Ramberg (1981); Cruden (1988); Emerman and Marrett (1990); Barnichon *et al.* (1999); Ablay *et al.* (2008)). Magma conduits propagate when a locally tensional regime is achieved and fracture mediated intrusion occurs orthogonal to local σ3 (Anderson 1951). A feasible reactivation envelope describes this process when propagation is facilitated by, and occurs parallel to, a pre-existing planar discontinuity (Magee *et al.* 2012). Hutton (1988) recognised that crustal anisotropies serve to concentrate strain (and therefore causative strain) and ultimately facilitate emplacement of magma into seemingly counter intuitive compressive regimes (e.g. Hutton (1992); Hutton and Ingram (1992)). The interplay between excess magma pressure (EMP), crustal anisotropies and the local stress field is considered and modelled by Vigneresse *et al.* (1999) who concludes that the interaction of these factors control the orientation of σ3 during the ascent and emplacement process and therefore pluton geometry. As EMP is an inherent feature of magma, it plays a fundamental role in juvenile fracture propagation (Ablay *et al.* 2008) and must also interact with the stress field into which it intrudes to promote a localised tensile stress field during magma transport.

Fundamentally, the orientation of σ3 at the time of magma ingress controls conduit orientation and symmetry. This is most often at variance to regional σ3 as the local stress field is subject to heterogeneity in the crust. The influence of excess magma pressure from intruding magma further alters the local stress field at that time. These parameters are modified as magma moves through the crust and this ultimately promotes the transition from ascent to emplacement (Chapter 1).

The Omey Pluton was emplaced *c.*422.5Ma (Feely *et al.* 2007). Regional sinistral transpression initiated at 425Ma and lasted until 420Ma (Soper and Woodcock 2003) or 410Ma (Dewey and Strachan 2003). Therefore the Omey Pluton intruded concurrently with this transpressive stress regime. Field observations show that the pluton has a sheet like morphology and is cross cut by several NNW-SSE and ENE-WSW shear zones that pre-date the intrusion. Local σ3 must have been subvertical at the time and level of emplacement, a local ascent conduit is required for magma

transport to the site of emplacement and the influence of trans-plutonic shear zones, that were active concurrently with magma crystallisation, must be considered.

It is proposed that a dynamic interplay between the suite of D5 conjugate faults, the D4 Connemara Antiform and regional transpression facilitated the ascent, emplacement and subsequent deformation of the Omey Pluton. Differential northwest-southeast compressive stress between the Skird Rocks Fault to the south and the Highland Boundary Fault (Ryan *et al.* 1995) to the north instigated regional sinistral transpression. Bound by these regional structures, the Connemara block acted as a passive large scale fault block within which northwest-southeast and northeast-southwest D5 faults re-activated and forming several discrete fault blocks across the Connemara terrane. Dextral and sinistral displacements along northwest-southeast and northeast-southwest respective faults lead to progressive anticlockwise rotation of individual fault bound blocks. Similar to the block rotation model of Jacques and Reavy (1994), it is proposed that where NNW-SSE and ENE-WSW lineaments intersected, localised subvertical zones of low strain were formed. These were exploited by over pressured magma as magma ascent conduits during the construction of the pluton.

Field observations show a clear relationship between the symmetry of the Omey Pluton and that of the bounding country rock. The intrusion assumes a discordant phacolithic geometry that reflects the D4 Connemara Antiform. It is suggested that as magma ascended to this crustal level, due to reduced isostatic pressure and a significant rigidity contrast between differing members of the Dalradian host strata (underlying schist vs. overlying psammite), σ3 was rotated to a subvertical plane that is orthogonal to the axial plane of the Connemara Antiform. This provided a new path of least resistance for ascending pressurised magma and facilitated the transition from ascent along a fracture conduit, to emplacement guided by the folded host strata that acted as a strain barrier.

Concentric emplacement related strain distributed about an intrusion may be explained by two hypothesis; diapirism or ballooning. In the diapirism model, a single dominant direction of movement (pluton up) is expected while the ballooning model should return uniform oblate fabrics throughout the pluton and a lack of evidence of vertical ascent of the entire pluton (Hutton 1997). AMS fabrics returned from the Omey Pluton are concentric, dip outwards and progressively steepen toward the core of the intrusion. The pluton has a defined floor and roof, as demonstrated by the presence of gently eastward inclined country rock contacts in the east and west of the intrusion. Submagmatic shear zones observed in the country rock are laterally continuous across the intrusion which indicates the intrusion is a thin sheet and not a massive,

cross cutting, ascending magma body. These observations are most consistent with progressive inflation and ballooning (Corry 1988; Hutton 1997; Hutton *et al.* 2000; Molyneux and Hutton 2000). The fold hinge of the D4 Connemara Antiform plunges between 15-20° near the margins of the Omey Pluton (Barnahallia Hill and Friar Isl.), regionally the hinge line plunges sub horizontally (5-10°) to the east (Leake and Tanner 1994). This infers the floor and roof of the pluton were displaced along a vertical axis during emplacement of the pluton.

In the west G3 is in direct contact with the floor of the pluton, at Aughrus More G3 overlies G1 and in the east G1 is in direct contact with the roof of the pluton. This seemingly paradoxical situation is easily addressed by considering the initial dominantly eastward emplacement of G1 followed by the westward emplacement of the latest G3 facies. Thus, the pluton is stacked in the core but in the western and eastern extent is dominated by a single temporally distinct facies, G3 and G1 respectively (Fig. 7.2B).

Following the philosophy of Corry (1988), the emplacement of the Omey Pluton is envisaged to have occurred largely as a series of laterally emplaced and vertically thickened sheets. G1 magma emanated from a central ascent site and was emplaced sub-laterally eastwards to form thin sheets which preferentially propagated along the hinge of the D4 fold and, to some degree, down the fold limbs and along pre-existing joints in the country rock. Corry (1988) suggested a transition between lateral spreading and vertical thickening occur once sheets are ~30m thick. G2 magma was emplaced soon after G1 and so is recognised as a distinct facies with a gradational contact. Finally, G3 was emplaced over the central ascent site and then preferentially westwards, presumably due to the earlier stitching of the roof and floor by G1 and G2. Progressive inflation ultimately led to the overprinting of the emplacement flow fabric with a concentric inflation fabric.

The consistent NNW-SSE AMS K1 vector is here attributed with tectonic stretching that overprints weak primary fabrics. Local D5 NNW-SSE structures were active throughout the construction of the Omey Pluton. Small displacements along these structures imparted a subtle stretching lineation on the granite in the magmatic state throughout lateral emplacement and vertical inflation. Strain partitioning became an increasingly significant process as viscosity increased during cooling. This concentrated strain directly over underlying basement structures and led to the formation of subtle fabric development and zones of intense micro-fracturing that are observed in the field and are discordant to the concentric inflation fabric.

7.7 Conclusion

The Omey Pluton is a composite intrusion of facies G1, G2 and G3. It is concluded that zones of elevated strain and shear within the granite, that were later exploited by minor intrusions, are the surface expression of deep seated basement structures. It is proposed that magma ascent was achieved along a central ascent conduit formed by dilation between deep seated D5 shear zones, which underlie the intrusion, during regional sinistral transpression. The site of ascent is stipulated to underlie the Aughrus More Peninsula. This prediction is based on the increase the G1-G2 and G2-G3 contact dip to the north of Aughrus More (~ 25-45° west), which may reflect the neck of the ascent site.

The folded bedding planes of the Cleggan Boulder Bed Fm. the Streamstown Schist Fm. and the Lakes Marble Fm. acted to modify the local stress regime and facilitate a transition from ascent to emplacement. Magma overpressure, focused along folded bedding planes promoted fracturing, magma wedging and ultimately sheeting of melt sub-laterally into the country rock. Magma was emplaced as a series of batches into the Connemara Antiform preferentially along the regional fold hinge. G1 was emplaced first as a narrow sheet bound by the bedded country rock closely followed by G2 and later G3. Initial lateral emplacement was succeeded by vertical thickening which ultimately vertically displaced and buckled the hinge of the D4 Connemara Antiform during inflation. Locally, joints in the country rock acted to redirect strain diverting granite sheets oblique to bedding and ultimately define a partially discordant phacolith geometry.

Continued shearing along underlying deep seated NNW-SSE faults progressively partitioned strain into increasingly defined shear zones. As a result, subtle NNW-SSE lineations were imparted throughout the intrusion in the magmatic state and discrete shear zones several meters wide are observed in the field.

The current work clearly shows that the influence and timing of regional stress can be examined through detailed structural analysis. It follows that a change in this regional stress may be detected and dated by studying a suite of plutonic bodies which intruded during a shift in the regional tectonic regime. It also emphasises the importance of careful examination of AMS data in order to correctly diagnose the source of magnetic lineations, particularly the distinction between fabrics derived from magmatic versus tectonic processes.

Feely *et al.* (2010) constrained the chronological link between the Omey Pluton and many other members of the Galway Granite Complex (GGC). As of yet no comparison may be drawn between

the kinematic controls over this and other granites associated with the GGC. It remains to be seen whether common structures control all members of the GGC or if the continuously evolving regional stress field between 420-380Ma modified the style and symmetry of magma transport conduits and the emplacement structures. In order to critique and correlate existing regional scale tectonic models between the mid Silurian to mid-Devonian it is essential to gain a understand of the tectonic evolution at a local scale. Such studies are essential as the time period in question hosts a major kinematic transition from Caledonian to Acadian dominated tectonic regimes. This work provides a base template for further investigations on the kinematic controls over plutonism in Connemara and its relationship with regimes further north in Scotland, Norway and northeast North America.

Chapter 8:

The Roundstone Pluton; A Punched Laccolith

8.1 Introduction

Reconnaissance mapping by the GSI (Kinahan 1869; Kinahan *et al.* 1878) identified the Roundstone Pluton as a slightly oval shaped granodiorite body (7.5 x 8km elongate along ~ N-S axis) that's western contact is located at Roundstone Village, Connemara. A series of detailed mapping, mineralogical and geochemical studies (Leake and Leggo 1963; Harvey 1967; Benjamin 1968b; Leake 1969; Evans and Leake 1970b; Bremner *et al.* 1980) documented the metamorphic and structural features of the surrounding orthogneiss, metagabbro and paragneiss host strata.

Harvey (1967); Leake (1969); Evans and Leake (1970b) and Bremner *et al.* (1980) detailed that the Roundstone Pluton cross cuts and shares a subvertical faulted contact, in the south, east and north, and stoped contact, in the west, with the country rock. In the south east the Roundstone Pluton shares an intrusive contact with the (presumed) later Carna Pluton. The above mentioned authors also identified a subtle foliation within a few hundred meters of the unchilled country rock contact that is concentric and contact parallel. Stoped blocks are rarely noted within the granodiorite body and several small scale felsic sheets (1-4m thick) are observed about the perimeter of the intrusion. Leake (2011) draws on these features as evidence for emplacement by upwards movement of magma driven by density contrast which progressed as stoped blocks sunk into a deep underlying magma chamber.

The age of crystallisation of this intrusion remains largely unconstrained. Leggo *et al.* (1966) returned an isochron of 395 ± 80Ma ($^{87}Sr/^{86}Sr$) for aplites hosted within the granite. These aplites are derived from late stage residual fluids concentrated during the cooling of the Roundstone Pluton. However, owing to the poor quality of this data, Leggo *et al.* (1966) dismisses its use as a proxy for determining the relative ages of this and neighbouring members of the Galway Granite Complex (GGC). Subsequent authors (Harvey 1967; Feely *et al.* 2006; Feely *et al.* 2010), most recently Leake (2011), consider this to be an early member of the GGC which predates all constituents of the Main Batholith however there is a complete lack of data to support such a hypothesis (*c.f.* Leake (2011)).

The structure and metamorphic history of the host strata is well constrained and need not be investigated further here (Chapter 3). In contrast, the internal architecture of the Roundstone Pluton is essentially unknown. No work has been carried out on the core of the intrusion and no study has yet examined the pluton as a whole.

Using a combination of field observations, rock magnetic analysis and petrographic observations the internal structural features of the Roundstone Pluton are investigated here. It is

shown that such work can be used to determine the nature of granite emplacement and relate the ascent and emplacement of spatially isolated intrusions to each other in a regional kinematic context.

8.2 Geological Setting

The Connemara Metamorphic Complex (CMC) (Leake and Tanner 1994) was thrust southward over the Delaney Dome Fm. along the Mannin Thrust (Leake *et al.* 1983; Leake *et al.* 1984; Leake 1986; Leake and Singh 1986; Tanner *et al.* 1989) between ~468-450Ma (Chapter 3). Thus, orthogneiss, metagabbro and paragneiss rocks that are in contact with the Roundstone Pluton, at the current level of exposure, are constituents of a large hanging wall under which the Delaney Dome Fm. (Leake and Singh 1986; Draut and Clift 2002) lies as the corresponding footwall on a major regional scale thrust. As a consequence of this, an appreciable structural discontinuity exists between the footwall (rhyolite) and hanging wall (metagabbro, orthogneiss, metasediments) which is defined by the gently northward inclined thrust plane (Fig. 8.1).

Following the southward thrusting of the Connemara Metamorphic Complex, a suite of conjugate northwest-southeast and northeast - southwest strike slip faults cross cut the Connemara terrane (Leake and Tanner 1994). As discussed earlier (Chapter 3), continued reactivation of these faults throughout the late Caledonian transcurrent regime is evidenced by off-sets observed across all geological units in the area. Several of these are observed to cross cut the country rock immediately to the north and south of the Roundstone pluton and several abut or offset the margins of this intrusion (Figs. 3.2 & 8.1).

The Roundstone Pluton intruded after the CMC was thrust south along the Mannin Fault. D5 faults were established prior to intrusion of the Roundstone Pluton and were reactivated after the granite had crystallised

8.3 Field Relationships

The host rocks to the Roundstone Pluton and the margins of the intrusion itself have been described in detailed by several previous authors. New observations made during this project are incorporated with these earlier works with an emphasis placed on their relevance to the internal architecture of the subject intrusion.

8.3.1 External Contact Relationships

A series of D3 ESE-WNW trending asymmetrical close to isoclinal folds within the Dalradian host strata (i.e. the Connemara Steep Belt) are cross cut by the northern portion of the Roundstone Pluton, several D3 folds also appear to deflect to the north and south (Fig. 8.1) (Leake 1969; Evans and Leake 1970a). The western and south-eastern margin of the intrusion is in direct contact with the Grampian Metagabbro and Orthogneiss of the CMC (Morton 1964; Harvey 1967; Benjamin 1968a). The attitude of the host rock foliation to the contact of the Roundstone Pluton is variable from highly oblique to, rarely, contact parallel.

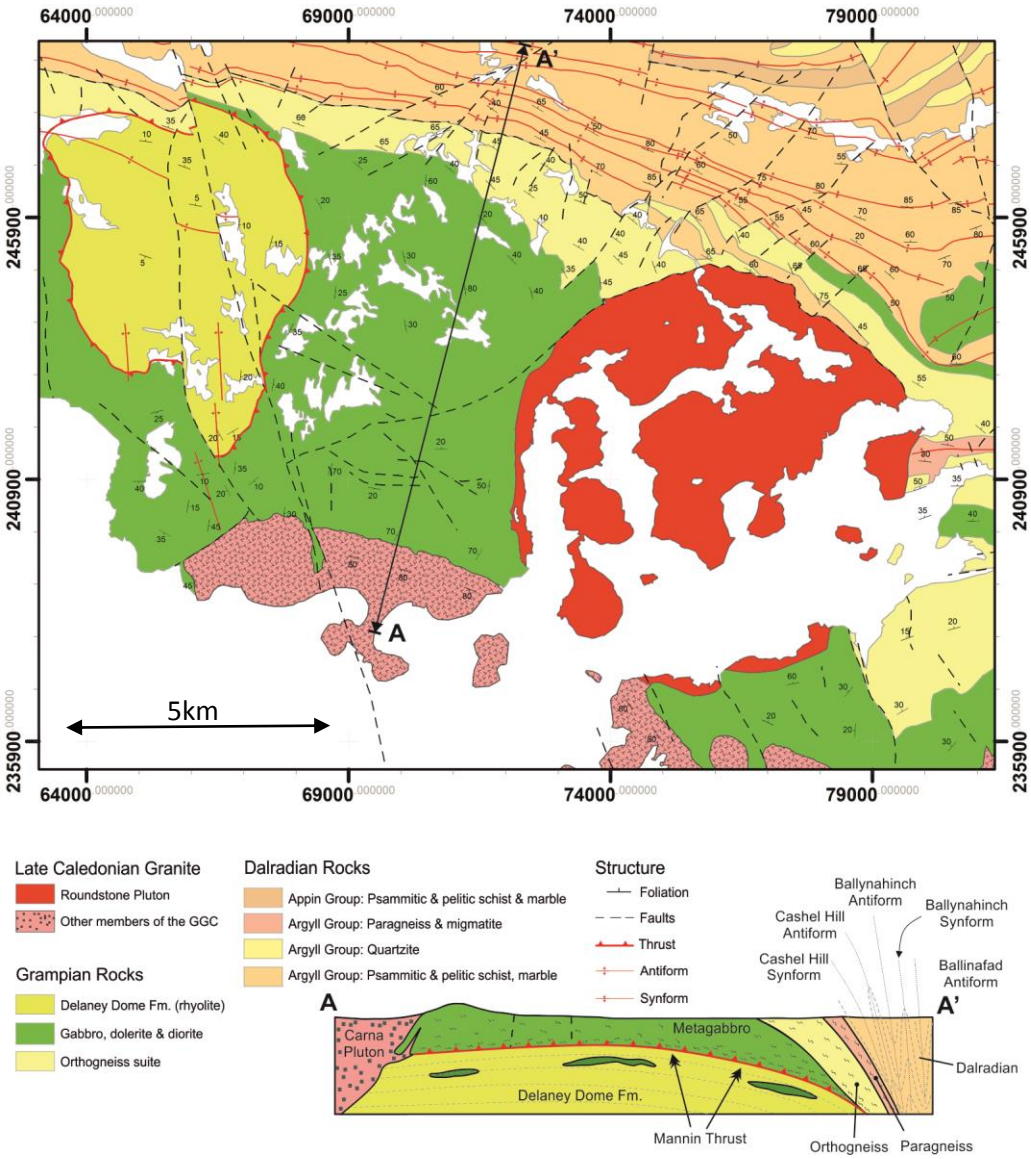


Fig. 8.1 Summary geological map of the study area (modified after Leake and Tanner (1994)) and cross section (modified after Leake (1986)). The Connemara Metamorphic Complex in intruded by the Roundstone Pluton at the current exposure level. The CMC is a hanging wall to the Mannin Thrust which is exposed ≈5km to the west of the pluton. The Roundstone Pluton cross cuts the host rocks WNW-ESE foliation and is cross cut by reactivated D5 faults.

The nature of the country rock - granodiorite contact has been described previously (Leake 1969; Evans and Leake 1970a) and is either faulted or stoped. Exposed eastern, northern and southern contacts are defined by subvertical or steeply outward dipping faults. This is best observed on Lehanagh South Peninsula (079685, 240648) due to enhanced topographic relief (Fig. 8.2). In this area a well defined host rock tectonic foliation (~110 - 80°N) is truncated without significant distortion by the subvertical easterly dipping pluton contact.

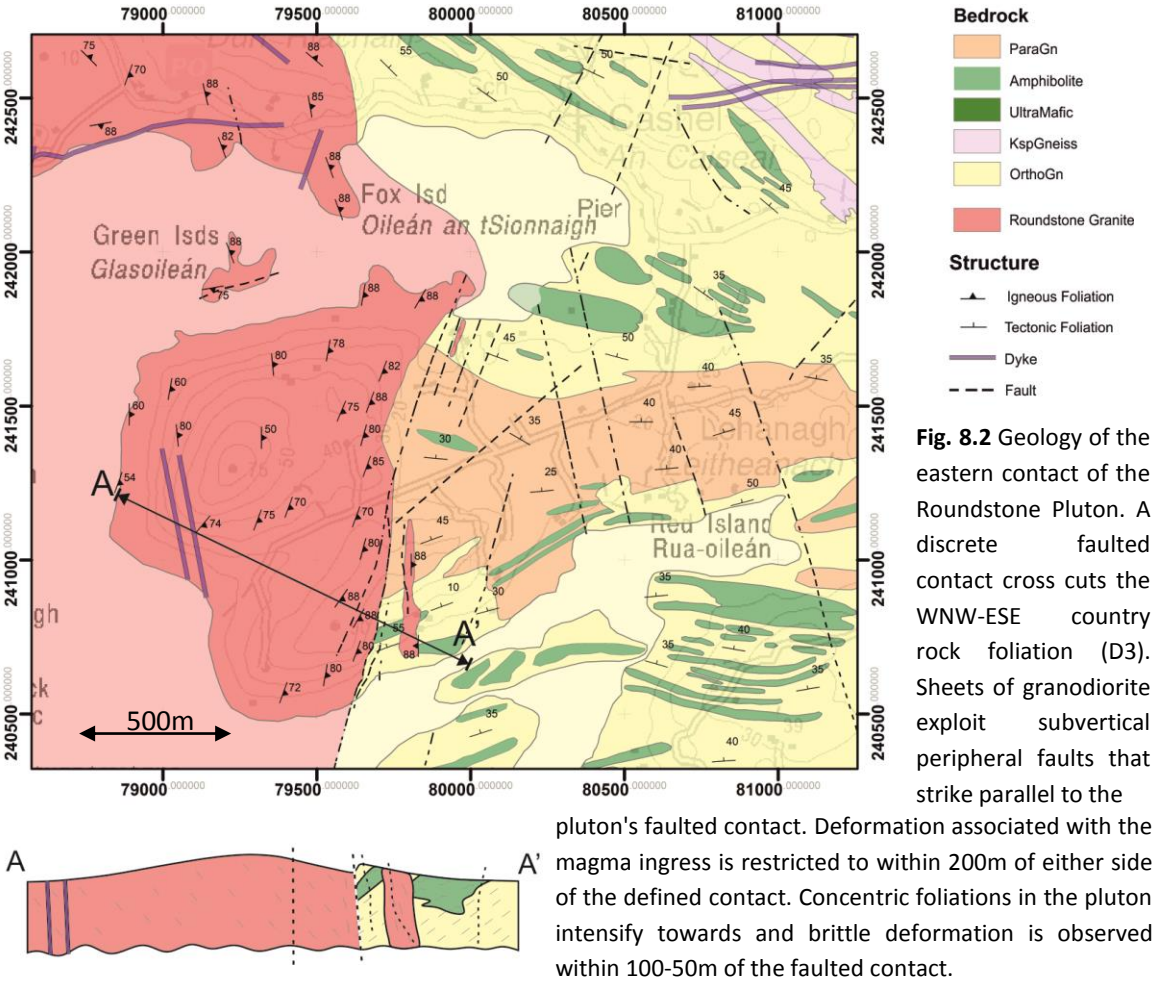


Fig. 8.2 Geology of the eastern contact of the Roundstone Pluton. A discrete faulted contact cross cuts the WNW-ESE country rock foliation (D3). Sheets of granodiorite exploit subvertical peripheral faults that strike parallel to the pluton's faulted contact. Deformation associated with the magma ingress is restricted to within 200m of either side of the defined contact. Concentric foliations in the pluton intensify towards and brittle deformation is observed within 100-50m of the faulted contact.

Faulted contacts are defined by moderate contact parallel foliations up to 100m from the fault and a cataclastic texture of brecciated, hydrothermally altered granodiorite that is cross cut by 5-40mm stockwork quartz veins within 20m of the contact (Fig. 8.3). Deformation of the country rock is limited to within 50m of the contact and is defined by progressively intense brecciation as the contact is approached.

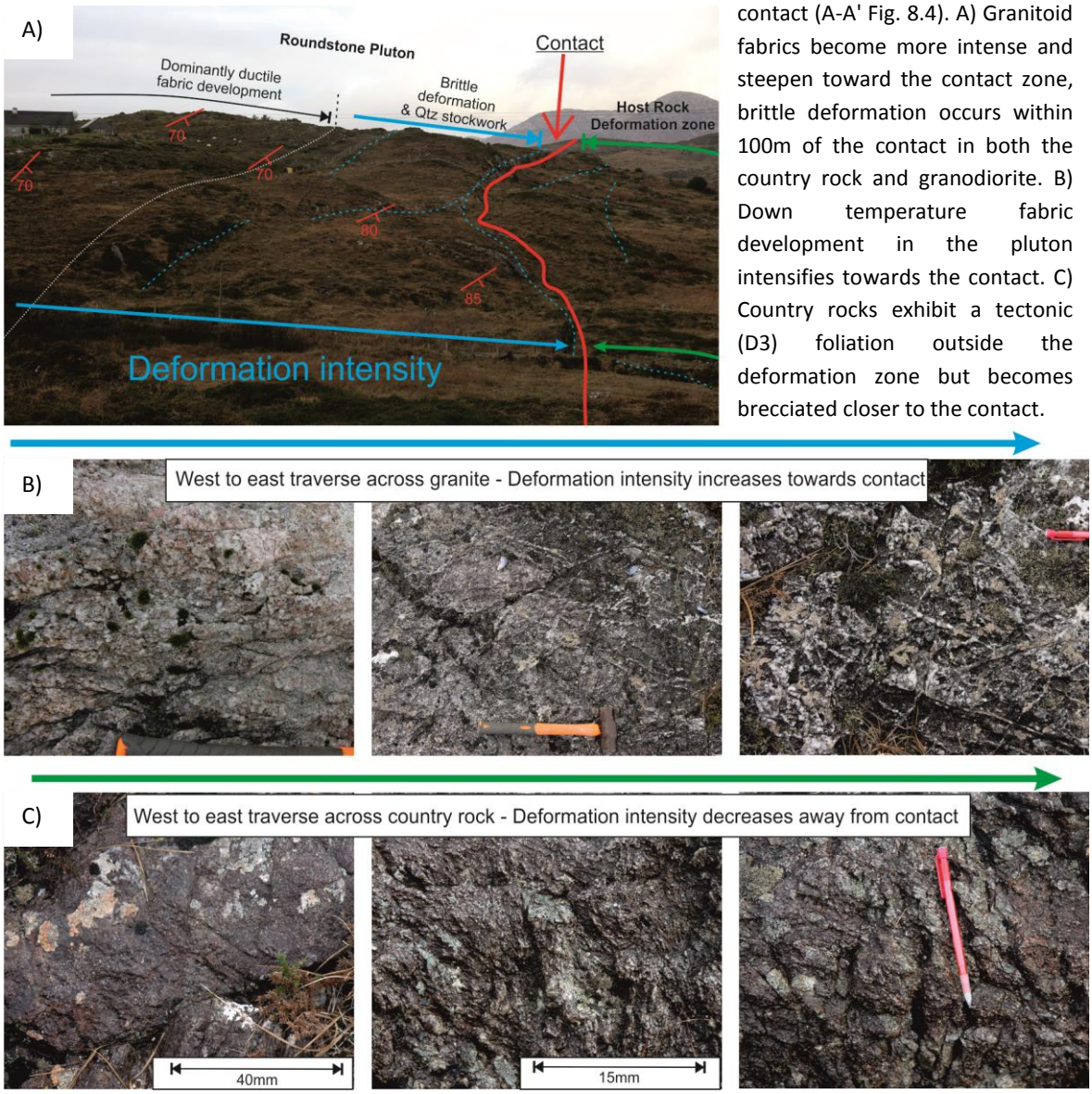


Fig. 8.3 Traverse across faulted contact (A-A' Fig. 8.4). A) Granitoid fabrics become more intense and steepen toward the contact zone, brittle deformation occurs within 100m of the contact in both the country rock and granodiorite. B) Down temperature fabric development in the pluton intensifies towards the contact. C) Country rocks exhibit a tectonic (D3) foliation outside the deformation zone but becomes brecciated closer to the contact.

Subvertical, sharp, unchilled stoped contacts are also observed most often in the east but occasionally also in the south. These are comprised of angular or sub-angular fragments of local country rock that are suspended in or are in the process of becoming surrounded by intruding magma. Sheets associated with stoping rarely extend more than 100m from the main intrusive body, are < 2m wide, strike parallel to the mapped contacts and usually aplite or pegmatite (Evans and Leake 1970a). These are discordant overall but exploit foliation planes and folds in the host rock at outcrop scale where disarticulated splinters of host strata are incorporated into the intruding granodiorite (Fig. 8.4). Within the pluton xenoliths are rare and most often less than a few meters along the long axis. Two significantly larger mafic xenoliths are noted, one immediately west of Roundstone Village (072287, 240201) and a second on the southern end of

Tawnrawer Cartron (073558, 237882). These were most likely detached from the nearby country rock as a product of magma ingress during the emplacement process.

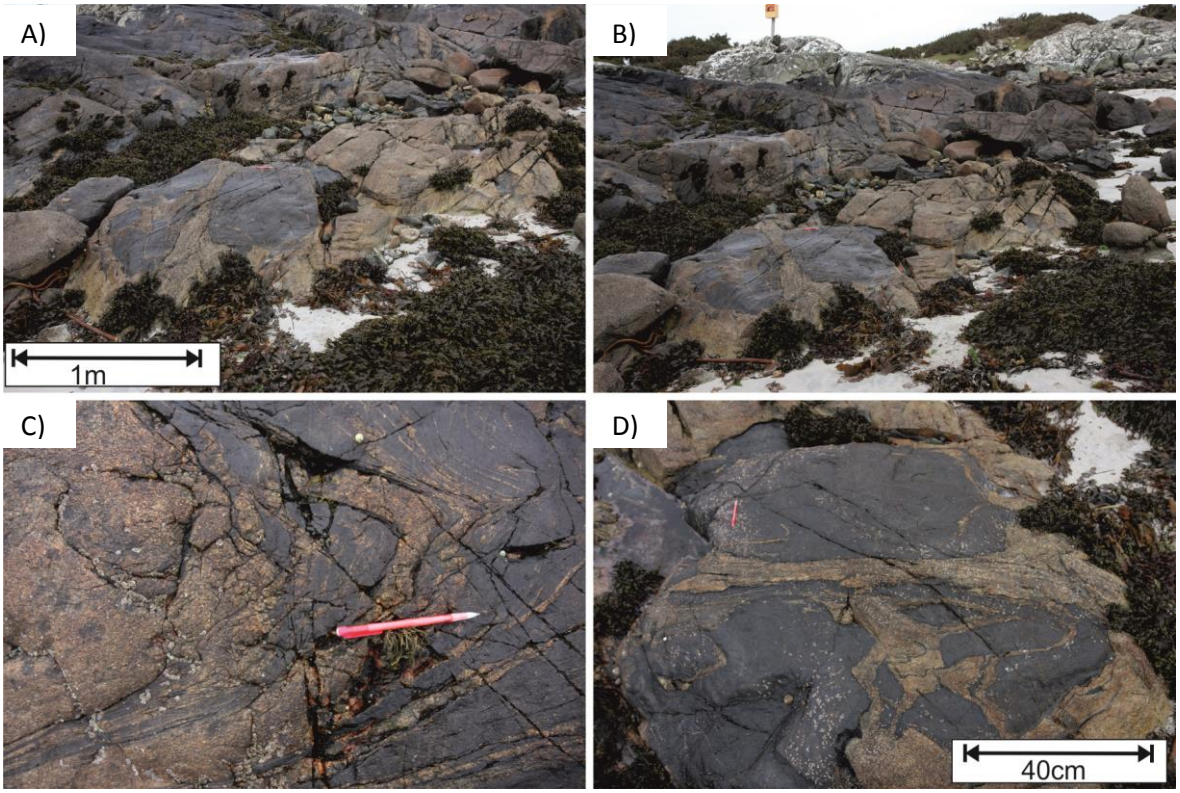


Fig. 8.4 Examples of stoped blocks and the relationship shared between country rock structure and the intruding granodiorite. Overall, the pluton is discordant relative to host rock structure (A & B) but locally intrudes along the tectonic fabric associated with D3 folding in the CMC (C & D).

The is no obvious relationship between inherent host rock structure and the structure which bounds the Roundstone Pluton. Subvertical faulted contacts typically cross cut country rock foliations and folds. Granodiorite sheets in the country rock are generally contact parallel and define a circular pattern about the pluton. Thus, the field relationships show this to be a discordant pluton with minimal distortion to the host rock outside of the 100m peripheral host rock deformation zone.

8.3.2 Facies Distribution

The Roundstone Pluton was previously recognised as an essentially homogenous granodiorite body with a single minor subfacies mapped in the north west corner of the pluton (Leake 1969). Several sets of crosscutting dykes, not directly associated with the main body, are also

documented (Leake 1969; Evans and Leake 1970a; Leake 2011). The current work demonstrates, for the first time, that the Roundstone Pluton is in fact composed of two granodiorite facies, G1 and G2, which are mineralogically and texturally distinct. G1 forms the outer portion of the intrusion while G2 occurs as a extensive network of sheets that cross cut G1 in the core of the intrusion (Fig. 8.5). Both of these facies predate late porphyritic and mafic dykes.

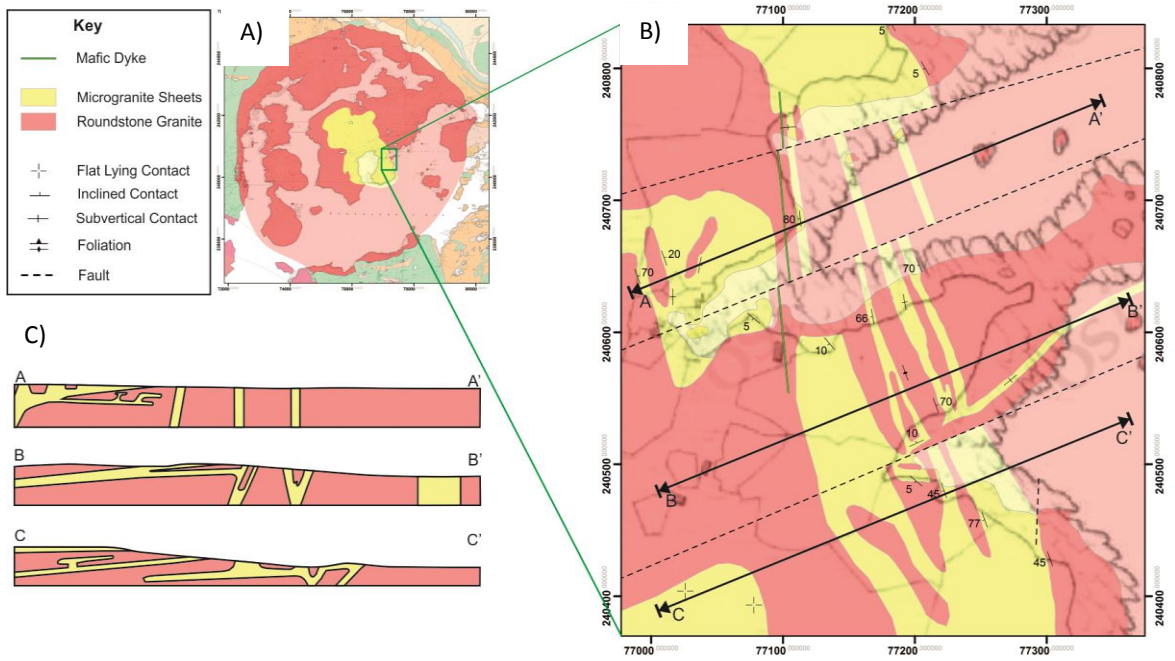


Fig. 8.5 Distribution of G1 and G2 facies in the Roundstone Pluton. G2 constitutes porphyritic granodiorite coeval sheets which cross cut G1. The pluton scale map (A) reflects localities where G2 sheets are found. Subvertical G2 intrusions most often strike NNW-SSE and feed subhorizontal sheets (≈1-5m) thick in the Canower area (B & C).

G1 is a phanerocrystalline equigranular biotite, hornblende granodiorite (2-5mm) with euhedral to subhedral plagioclase and K-feldspar. The modal abundance of constituent minerals is 46.6% plagioclase, 23.4% quartz, 21% alkali feldspar, 7% biotite, 1% hornblende and 1% accessory titanite, apatite, magnetite, rutile and zircon. Examples of typical G1 textures are illustrated below (Fig. 8.6). Plagioclase is sometimes zoned, occasionally most often normally zoned, sometimes strongly, giving rise to selectively seritised calcic-rich cores (Fig. 8.6A, C, D). Orthoclase contains obvious micro-perthitic intergrowths and is the predominant alkali feldspar, when present larger phenocrysts often contain numerous inclusions of quartz, feldspar and biotite (Fig. 8.6B). Microcline is rare. Outside of zones which exhibit strain (discussed below) quartz is anhedral and biotite is usually fresh or partially chloritised. Rutile and cubic magnetite are often clustered around biotite (Figs. 8.6E, F), included along cleavage planes or occur as interstitial aggregates between the lattice of neighbouring crystals (Fig. 8.6G, H).

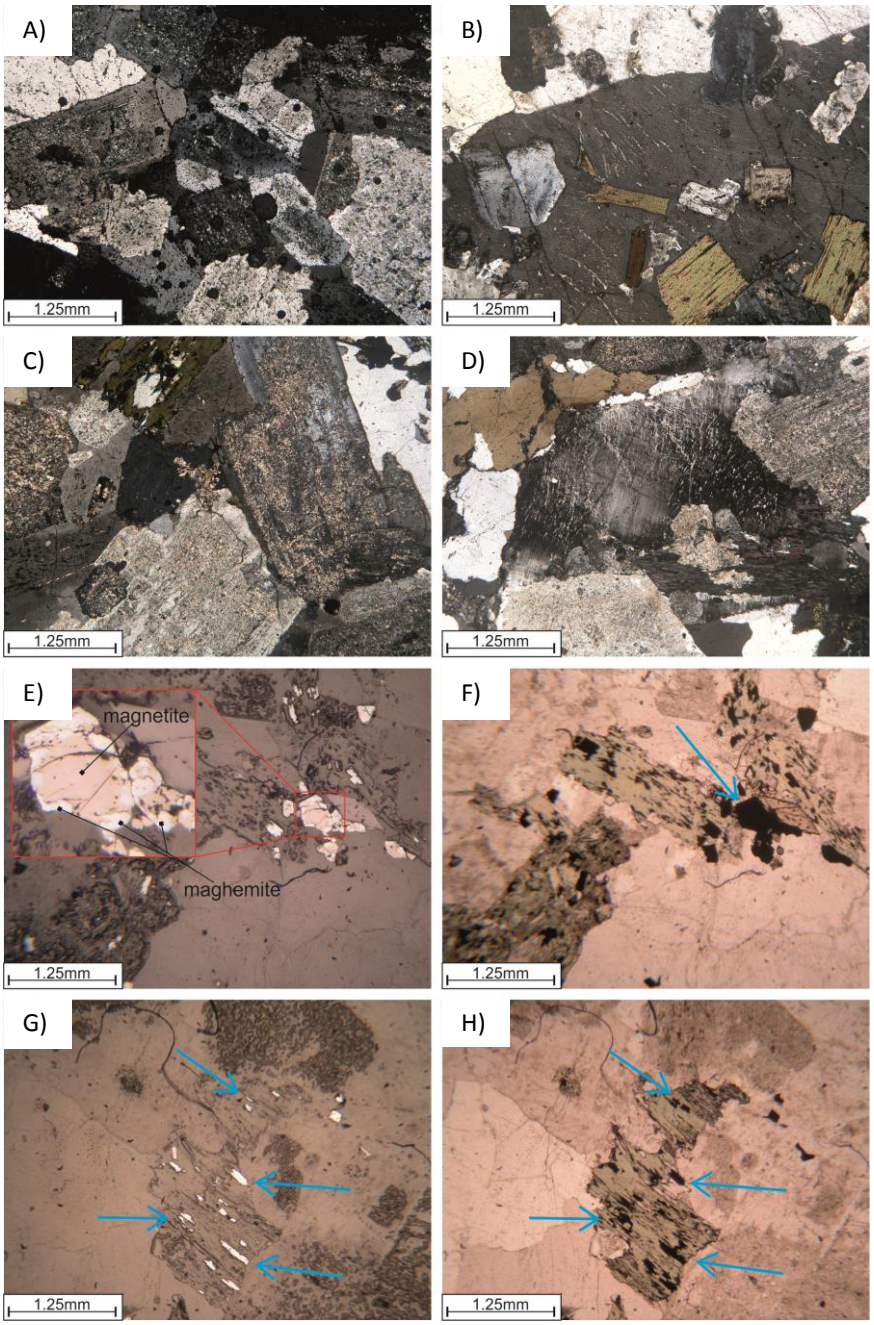


Fig. 8.6 Typical petrography of G1. Medium grained granodiorite, occasional perthitic K-feldspar with included feldspar and biotite (A & B), euhedral weakly normally zoned feldspars with calcic cores and anhedral quartz (C & D). Reflected light and PPL views (E-H) of biotite that hosts a disproportionate amount of magnetite. This can be associated with incorporation of magnetite into the biotite cleavage during crystallisation and deuteric alteration of biotite Dunlop and Ozdemir (1997). E) Periphery of maghemite oxidised to maghemite.

Leake (1969) recognised and described a quartz rich orthoclase poor subfacies along the northeast margin of the intrusion (Fig. 8.22 attached map). This shares a completely gradational contact with G1 over ~ 10m and is mineralogically quite similar to G1 apart from being slightly more siliceous and having a small grain size reduction. As such it is considered a subfacies of G1 and is referred to here as G1a for simplicity.

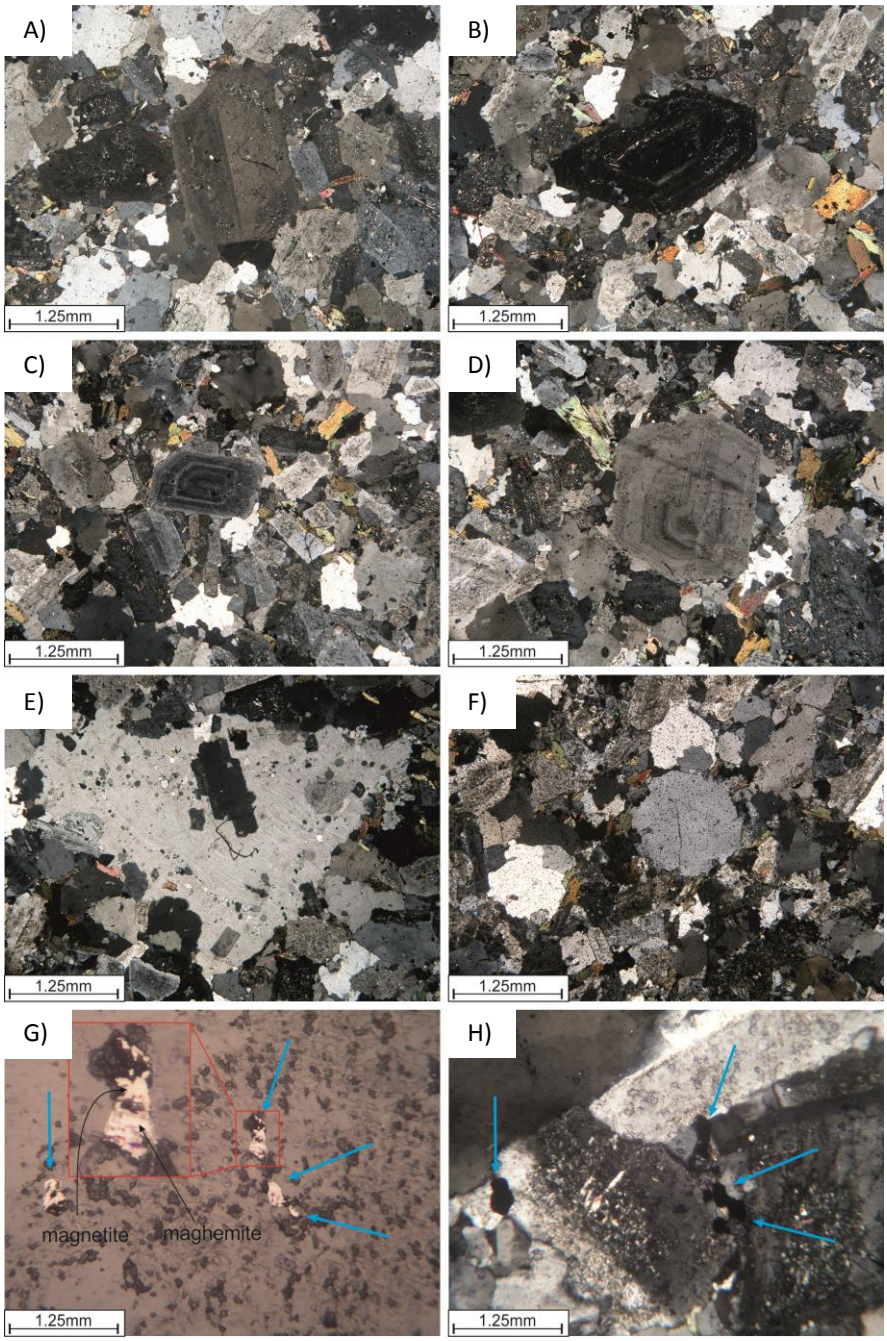


Fig. 8.7 Characteristic petrography of G2. G2 exhibits a finer grained ground mass, strongly complexly zoned euhedral xenocrysts of plagioclase with distinctive calcic spikes (A-D) and rounded quartz (F). Some K-feldspar phenocrysts contain relic crystal margins with agglutinated matrix mineral inclusions (E). Coarse magnetite is typically interstitial and partially oxidised to maghemite along grain boundaries (G & H).

G2 (Fig. 8.7) is typically a fine grained (0.5-2mm) equigranular biotite granodiorite which contains 3-5mm xenocrysts of strongly zoned plagioclase feldspar and rounded quartz. Averaged modal abundances are as follows; 42.7% plagioclase, 40.5% quartz, 13.7% alkali feldspar, 6% biotite and trace epidote, hornblende, magnetite, zircon and rutile. Thus, G2 sits on the opposite side of the granodiorite field adjacent to the tonalite field while G1, having a greater proportion of K-feldspar and less quartz, represents a granodiorite approaching the monzogranite field.

Plagioclase shows strong polysynthetic and Carlsbad twinning. Some feldspars, more often plagioclase, are strongly normally zoned (Fig. 8.7A-D); this feature is not as prevalent in G1. The presence of rounded quartz and strongly zoned feldspar xenocrysts is interpreted as reflecting a more dynamic mixing history in G2 relative to G1. Groundmass quartz is typically anhedral with indented grain boundaries between equigranular neighbouring orthoclase, plagioclase and quartz grains (Fig. 8.7A-F). This reflects mutual interference between grains which passed through the solidus contemporaneously (Vernon 2004). Biotite is euhedral, partially chloritised and spatially associated with accessory oxide phases and rutile. Chlorite forms after biotite.

The G2 facies occurs as an plexus of sheeted intrusions that protrude through G1 in the centre of the pluton. Extensive bog cover across most of the Rosroe Townland (0760, 2410) and boulders amongst thick seaweed and lichen along the surrounding coastline hamper efforts to map the inner part of the Roundstone Pluton in any detail, thus a detailed map of the precise orientation and distribution of these sheets remains poorly constrained. Despite this, plotting the distribution of outcrops where this facies is found alone, or cross cutting G1, reveals an overall distribution along a NNW-SSE axis across the core of the pluton (Fig. 8.5A).

The best exposure is found in the Canower area (077100, 240500, Fig. 8.5B) where some detail of the contact relationships can be seen. Here both vertical and subhorizontal meter scale G2 sheets are observed cross cutting G1 (Fig. 8.8A, B). The contact between G1 and G2 pass from sharp (Fig. 8.8C, D) to lobate (Fig. 8.8C, D, E) to gradational (Fig. 8.8F, G) along strike. On Canower Hill (076991 240279) a large sheet of G2 cross cuts G1 can be traced contour parallel and thus defines a subhorizontal sill (Fig. 8.4B). In contrast, 200m to the northeast, several narrow (1-3m) subvertical sheets are traced along a NNW-SSE trend for up to 150m across the headland until they are eventually truncated by a late ENE-WSW dextral fault (Fig. 8.5B). A dip slip component is presumed on these brittle structures as drastically different sill symmetries (sills vs. dykes) are noted on opposing sides.

Many G2 sheets exhibit a sharp contact with G1 and also exhibit several sharp internal contacts that are parallel to the G1-G2 contact. Internal contacts within G2 sheets are defined by abrupt changes in grain size without a change in mineral modal abundance, several of these may be observed in a single dyke or sill. Thus, G2 sheets are composite nature which indicates these structures formed during sequential opening.

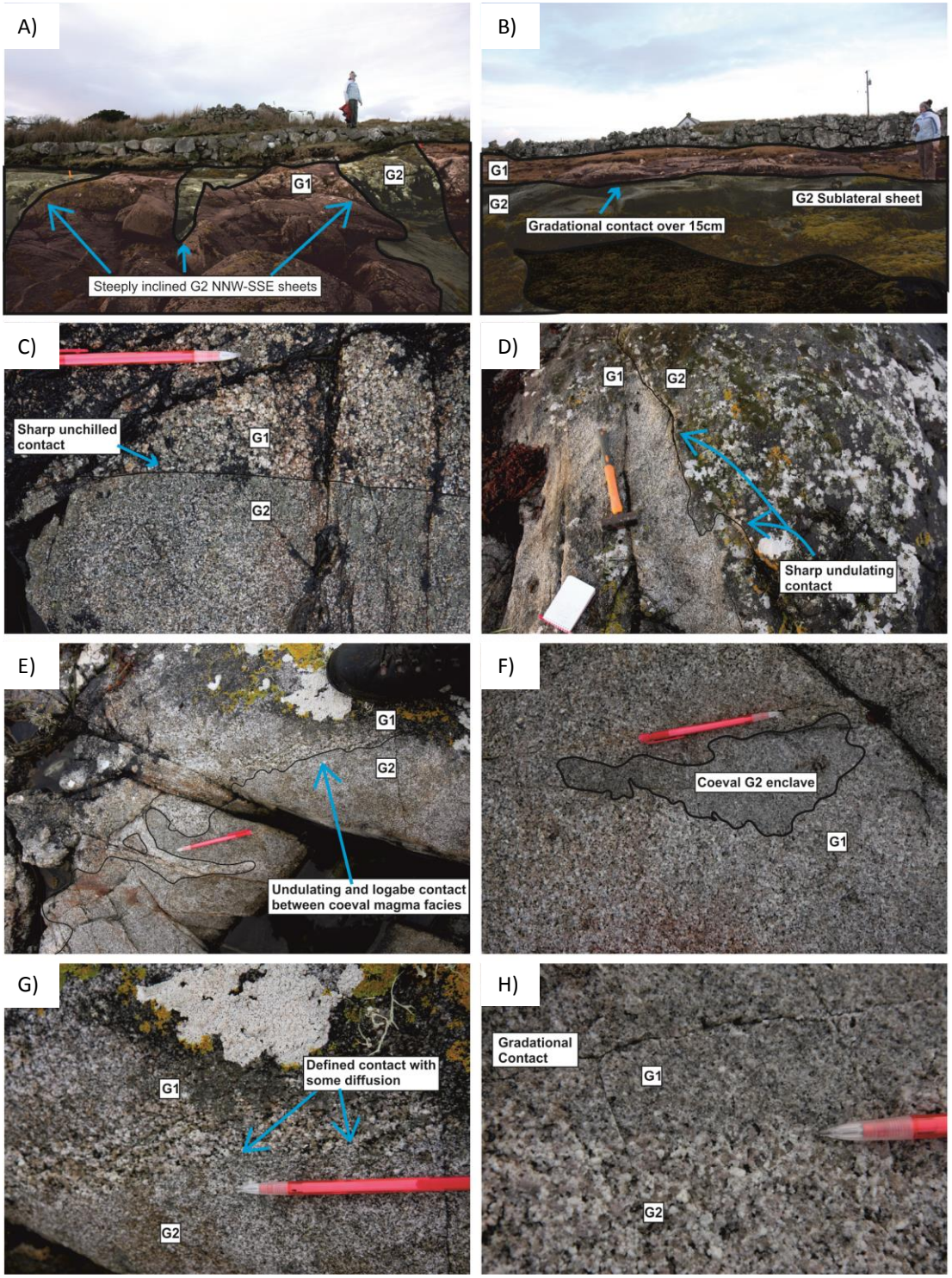


Fig. 8.8 A variety of gradational, highly lobate and sharp G1-G2 contacts show G1 was cooling as G2 continued to intrude (A-H). Enclave of G2 with lobate contacts hosted in G1 (F).

Examination of LiDAR data (courtesy of the Geological Survey of Ireland) demonstrates a relationship between D5 faults in the country rock and those observed within the Roundstone Pluton (Fig. 8.9). This image clearly shows prominent submarine scarps cross cut the pluton parallel to D5 NNW-SSE faults mapped in the host strata to the north and south. It is emphasised

here that these structures lie parallel to the general trend of G2 granodiorite sheets mapped in the core of the pluton and the overall trend of the G2 facies distribution (Fig. 8.5) as well as post magmatic microgranite porphyritic, felsite and dolerite dykes in the area previously noted by Leake (1969) and Evans and Leake (1970a).

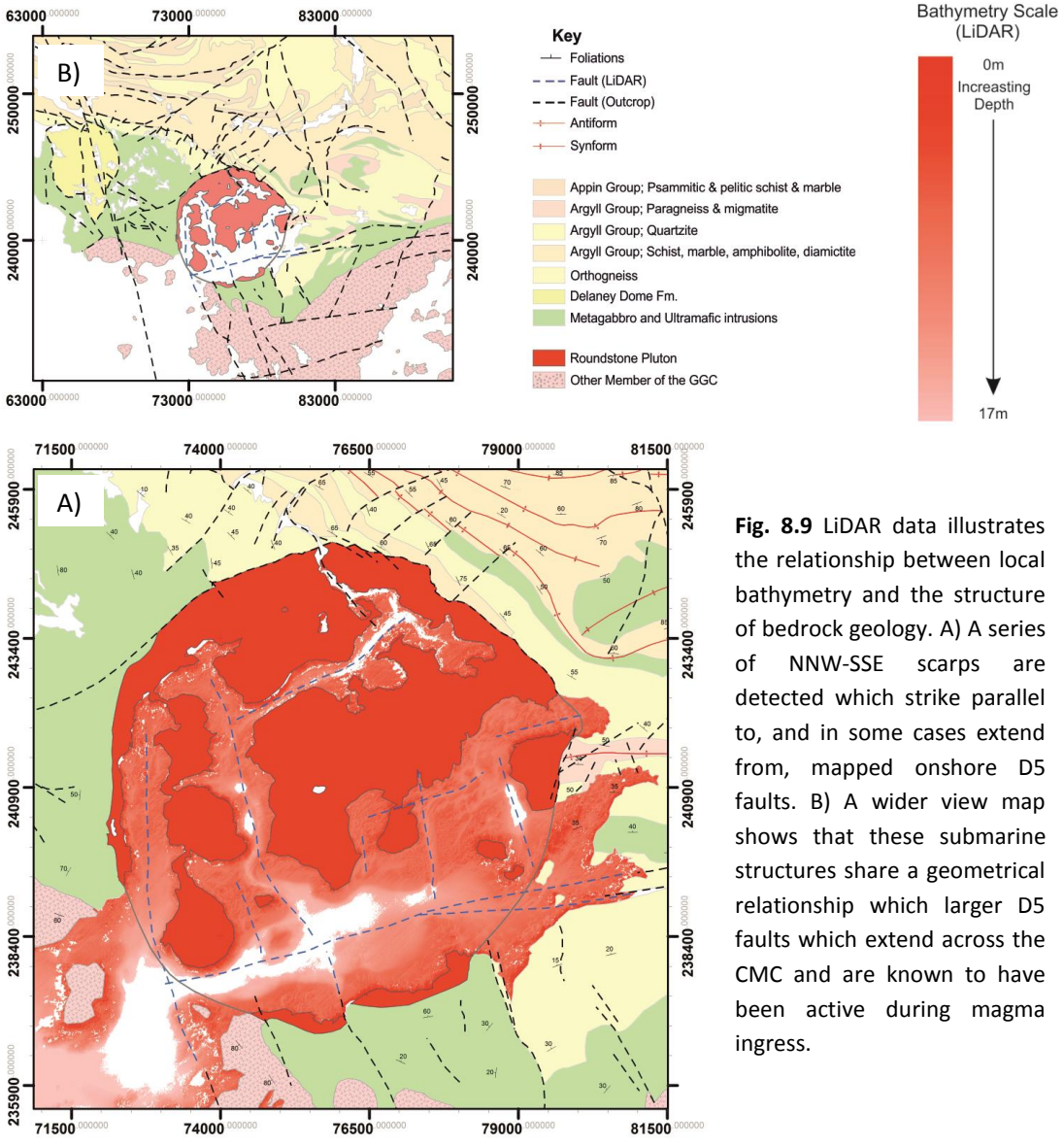


Fig. 8.9 LiDAR data illustrates the relationship between local bathymetry and the structure of bedrock geology. A) A series of NNW-SSE scarps are detected which strike parallel to, and in some cases extend from, mapped onshore D5 faults. B) A wider view map shows that these submarine structures share a geometrical relationship which larger D5 faults which extend across the CMC and are known to have been active during magma ingress.

8.3.3 Fabric Development

The circular outline of the Roundstone pluton is paralleled by a concentric foliation which occurs about the circumference of the intrusion (Fig. 8.10). This marginal fabric is generally weak in the north and south and particularly well defined in G1a (Leake 1969) and along the western

contact near Roundstone village. Marginal foliations are vertical to subvertical, always contact parallel and best defined within 100m of the country rock contact.

A second distinct zone of strain approximately 1km wide is also present between 1-2km from the pluton's external contact, again this foliation is subvertical and broadly contact parallel. This strain is not homogenously distributed and is most intense along two arcs on opposite sides of the intrusion that are centred along an approximately east - west axis (Fig. 8.10). At these locations, a moderate foliation is defined by elongate quartz (axial ratio ~ 3:1) and partially aligned feldspars and biotite. Traversing north and south from these localities fabric intensity fades and eventually dies out completely or becomes indistinguishable from/amalgamated with the concentric marginal fabric described above.

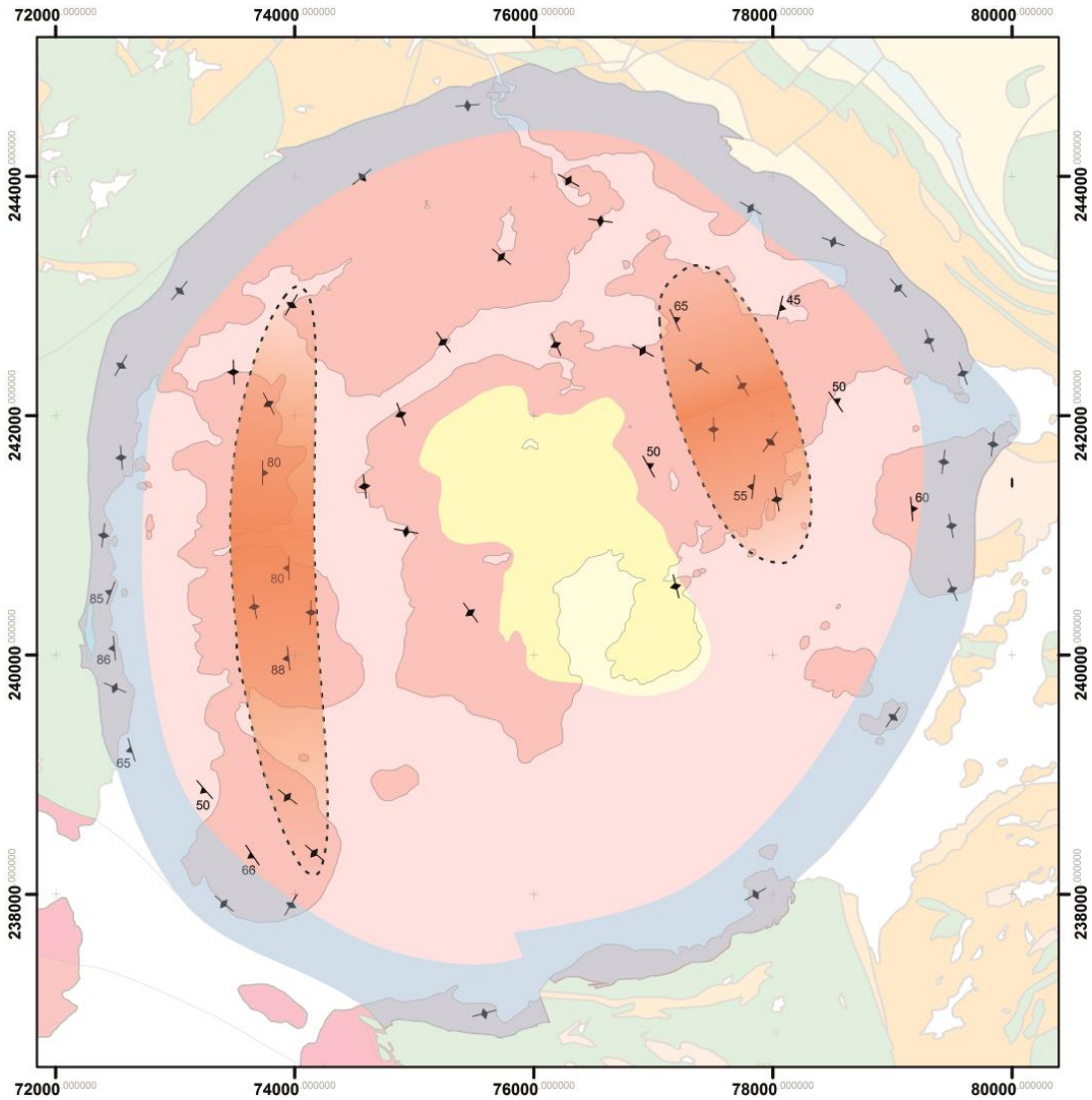


Fig. 8.10 Summary map of the distribution and orientation of fabrics observed in the field. The degree of fabric anisotropy increase towards the pluton contact, an overall concentric ballooning foliation is observed (blue). Fabric intensity decreases toward the centre of the pluton, fabrics are extremely rare in the core and north and south of the intrusion. Two zones of anomalous foliations are observed in the east and west of the pluton 3km from the pluton margin (red).

In the field, elongate quartz grains (axial ratio ~ 2:1), poorly aligned biotite and occasionally tabular feldspars define the outer fabric (Fig. 8.11A, B). In thin section, subhedral to euhedral biotite shows minor kinks and smearing (Fig. 8.11C, D). Quartz occurs as 3-6mm elongate primary grains which contain multiple equant well defined subgrains which reflect a large orientation difference between subgrain lattices (Fig. 8.11C). Larger feldspars show some marginal recrystallisation and weak undulose extinction (Fig. 8.11E). Brittle fractures in larger feldspars are occasionally infilled with primary quartz and feldspar that also exhibiting weak grain scale plastic deformation (Fig. 8.11E, F). These features are consistent with low temperature submagmatic fabric genesis (Bouchez *et al.* 1992; Hirth and Tullis 1992; Vernon 2004; Passchier and Trouw 2005).

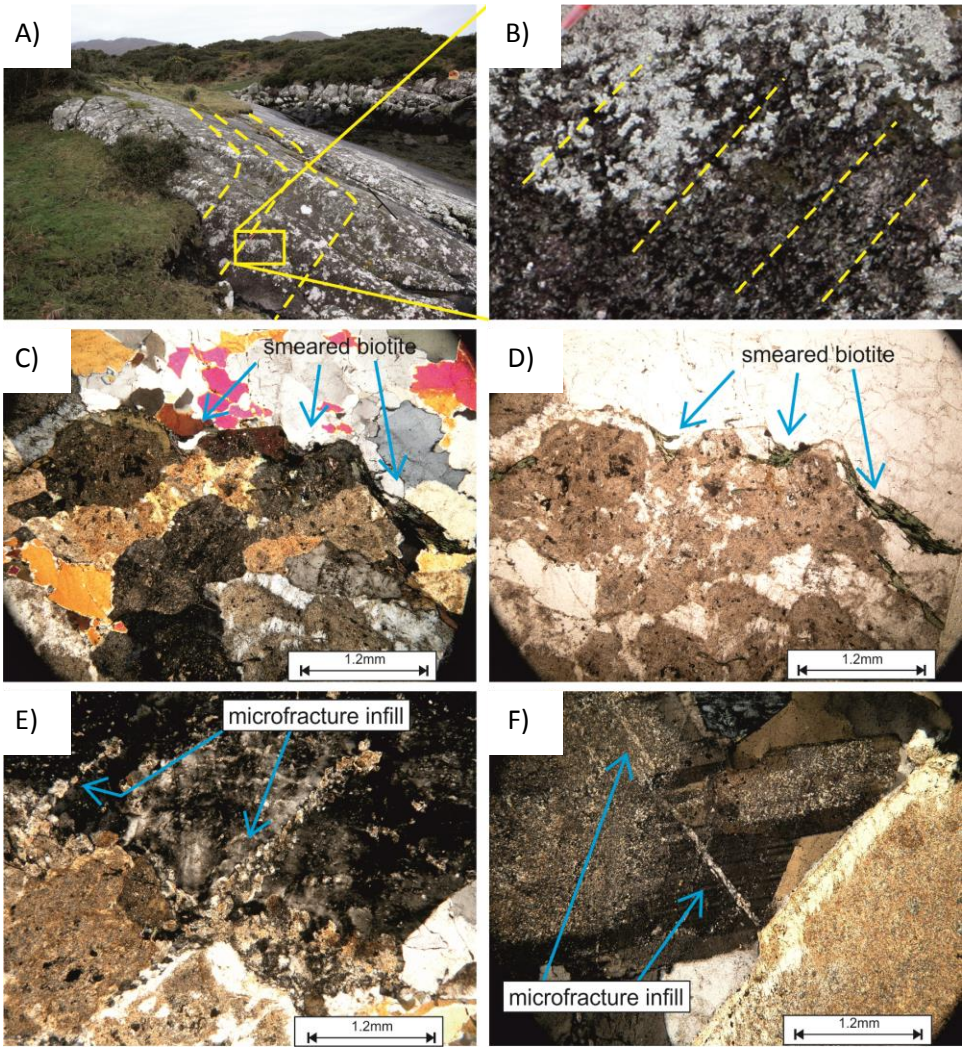


Fig. 8.11 A & B; Typical examples of low temperature marginal fabrics at outcrop scale (blue in Fig. 8.10). C & D; Smearing of biotite (C & D) and fracturing of feldspars infilled with quartz and feldspars indicate deformation occurred under low temperature conditions

The inner foliation zone is micro-structurally distinct (Fig. 8.12). Quartz grains are elongate and aligned with occasional tabular feldspars at outcrop scale (Fig. 8.12A, B). Most large quartz grains

have been extensively recrystallised, primarily by subgrain rotation (SGR), and define quartz ribbons that wrap around more competent partially aligned feldspar crystals (Fig. 8.12C, D). Recrystallisation via the bulging mechanism (BLG) is also apparent in many quartz and feldspar crystals (Fig. 8.12D, E). Microcline, inverted from orthoclase, as well as examples of wedged structural twins in plagioclase are common, flame perthite is rare but present (Fig. 8.12F). The above features are compounded in larger grains. Not all crystals exhibit extensive deformation features. Partially chloritised biotite is rarely smeared and instead wraps around more competent feldspars forming broad cleavage folds. Furthermore, pressure shadows between larger grains contain essentially undeformed quartz, feldspar and biotite aggregates. Quartz-plagioclase myrmekite is also present but rare.

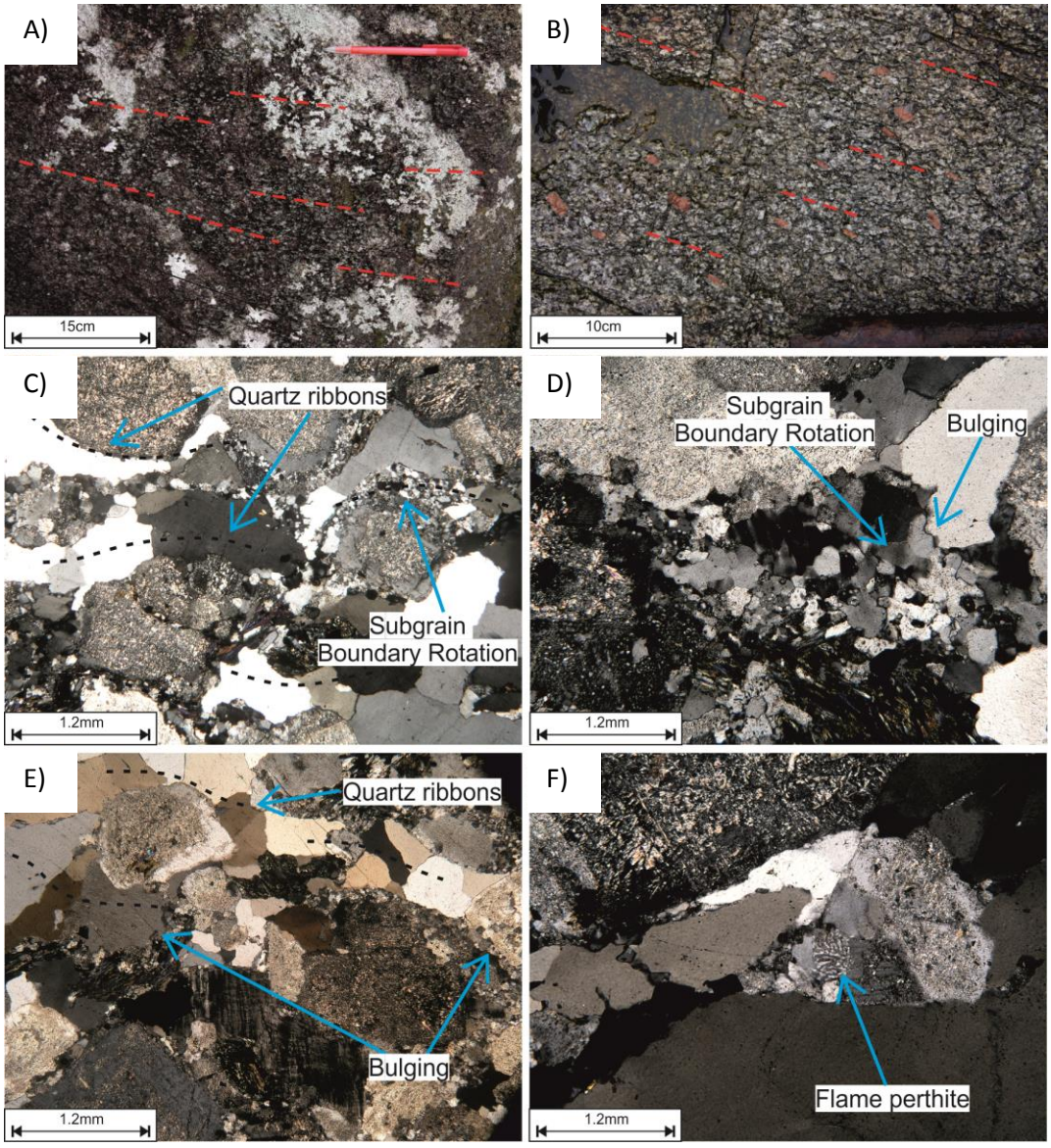


Fig. 8.12 Microstructures associated with the inner foliation zone (red in Fig. 8.19). A; Fabric observed at outcrop scale. B; Observed aligned tabular K-feldspars indicating the fabric formed in the submagmatic state. C, D & E; microstructural analysis shows deformation was achieved through bulging and subgrain boundary rotation indicating deformation occurred in the submagmatic state. F; Flame perthite is rare but

8.3.4 Summary of Field Data

The Roundstone Pluton is composed of two main facies, G1 forms the majority of the intrusion and G2 occurs as a plexus of steep and gently inclined sheets that cross cut G1 at the core of the intrusion. Lobate and gradational contacts between G1 and G2 coupled with a complete lack of chilled margins unequivocally demonstrate these facies intruded in close succession. G2 is slightly more siliceous and evolved but otherwise compositionally very similar to G1 which further supports the temporal and genetic link between these magmas. Other sets of dykes in the area, which do exhibit chilled margins, are unrelated although many share a broadly common trend (north - south). This may be related to the reactivation of common structural conduits.

New interpretations based on LiDAR data clearly show a suite of NNW-SSE scarps below sea level within the Roundstone Pluton. They parallel the general trend of G2 sheets as well as NNW-SSE D5 fault sets in the country rock which abut against and penetrate into the southern margin of the granite and extend north across Connemara. These faults were active prior to 420Ma and later than 410Ma (Chapter 3) concurrently with the stipulated timing of emplacement of the Roundstone Pluton (Leake 2011). Thus, the above observations infer, but cannot confirm, some interaction between this fault set and the emplacement of G2, and possibly G1.

Concentric foliations around the periphery of the intrusion exhibit moderate to low temperature submagmatic microstructures. The attitude and nature of these foliations are consistent with a progressive inflation and ballooning model similar to that proposed for the Ardara Pluton, Donegal (Molyneux and Hutton 2000; Hutton and Siegesmund 2001). However, owing to their subtle nature and lack of marginal syn-magmatic shear sense indicators, the current data set does not preclude other models such as the diapiric model which was suggested for the Ardara Pluton (Vernon and Paterson 1993; Paterson and Vernon 1995). Adding further complexity to the issue is the presence of the internal zone of (relatively) higher strain which is clearly concentrated in the east and west and is absent in the north and south. Again the current data set is inadequate to draw any form of robust conclusion. To address this short coming, an extensive AMS study has been undertaken to further evaluate the distribution of strain in the Roundstone Pluton.

8.4 Rock Magnetic Investigation

8.4.1 Sampling

In total, 177 orientated block samples were collected from the Roundstone Pluton along an evenly distributed grid. Of these, four were collected as duplicates to check for consistency, further duplicate samples were deemed unnecessary due to the detailed nature of the sample grid (neighbouring sites were always between 100-300m apart).

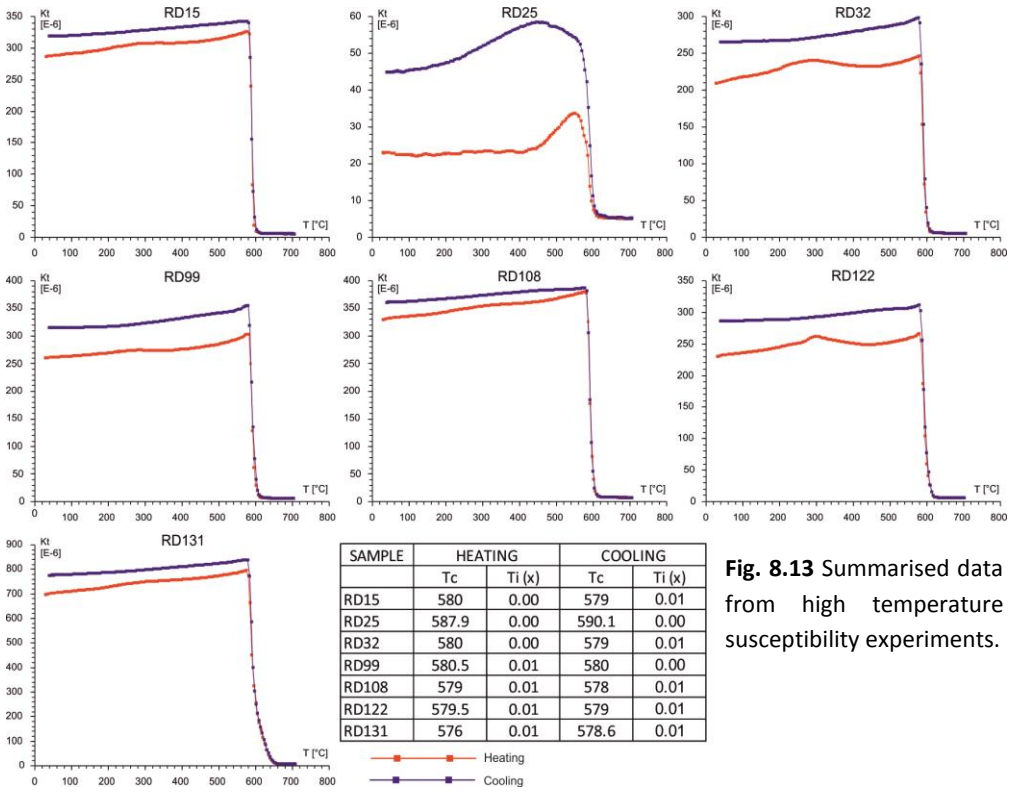
On average, 15 21x25mm cylindrical sub-specimens were cored from each sample block using a non-magnetic abrasive diamond tip drill bit following the parameters set by Owens (1994). Sub-specimens from all 172 blocks underwent AMS analysis. Based on preliminary field, petrographic observations and preliminary AMS data, several specimens were selected for detailed rock magnetic analysis to constrain what the calculated AMS tensor from each site actually reflects and to identify or eliminate the possible presence of complicating features (e.g. Potter and Stephenson (1988); Rochette (1988); Wolff *et al.* (1989); Hargraves *et al.* (1991); Stephenson (1994); Cañón-Tapia (1996, 2001); Aubourg and Robion (2002); Bouchez *et al.* (2006); Gaillot *et al.* (2006); Chadima *et al.* (2009); Almqvist *et al.* (2010); Fanjat *et al.* (2012)). Specimens selected for detailed magnetic experiments were representative for each facies, those which returned particularly high or low susceptibility values were also targeted during sample selection. Full data tables and original data files may be found in Appendix E.

8.4.2 Results of Rock Magnetic Experiments

Below, the results of a suite of standardised rock magnetic experiments are presented. Six samples, four from G1 (RD15, RD25, RD32, RD99) and 2 from G2 (RD108, RD122), were selected. In addition, the thermal demagnetisation behaviour of three component IRM (modified from Lowrie (1990)) of two samples was measured. All experiments were carried out in the palaeomagnetic laboratory in Highlands University New Mexico following the procedures detailed in Appendix B.

Fluctuation of Susceptibility with Temperature

Curie Point estimates (T_C) were determined by measuring continuous low field susceptibility during stepwise heating and cooling of powdered samples between room temperature and 700°C in an argon atmosphere (Fig. 8.13).



SAMPLE	HEATING		COOLING	
	Tc	Ti (x)	Tc	Ti (x)
RD15	580	0.00	579	0.01
RD25	587.9	0.00	590.1	0.00
RD32	580	0.00	579	0.01
RD99	580.5	0.01	580	0.00
RD108	579	0.01	578	0.01
RD122	579.5	0.01	579	0.01
RD131	576	0.01	578.6	0.01

Fig. 8.13 Summarised data from high temperature susceptibility experiments.

Five out of six samples exhibit a well defined peak in susceptibility which, using either the inflection point method or the Hopkinson Peak Method (Moskowitz 1981; Tauxe 1998), return T_C values between 578-580°C. Using T_C as a proxy for Ti content in magnetite (Akimoto 1962; Lattard *et al.* 2006), these data indicate a dominance of near stoichiometric magnetite (<0.1%) in the majority of samples. The shape of the susceptibility curve may also be used as an indicator of magnetic domain state through the presence or absence of a distinct abrupt Hopkinson Peak (Orlický 1990). In all cases a defined maximum is recognised prior to T_C which is followed by a rapid drop off in susceptibility however a clear single domain Hopkinson Peak is never recorded.

All specimens are irreversible on the cooling curve and show an increase in susceptibility (10-50%) when cooled after reaching 700°C. Distinct bumps are also noted during heating between 270-340°C which are not present on the cooling curve (also identified in samples from the Omey Pluton). Moreover, samples which exhibit a more pronounced bump show a greater increase in susceptibility on cooling, suggesting a relationship between these two observations.

These features may be related to breakdown of a single Ti-Fe oxide phase into two minerals that leads to an overall increase in susceptibility (Hrouda 2003; Hrouda *et al.* 2006). Titanomaghemite is unstable and will invert to magnetite and ilmenite at ~ 300°C in oxidising conditions (Dunlop and Ozdemir 1997). This reaction may be facilitated by the presence of oxygen

liberated from crystal cleavage planes and introduced to the argon atmosphere during the heating process. Such a phase change causes a net increase in bulk susceptibility owing to the formation of magnetite (and ilmenite) from less susceptible titanomaghemite which causes a shift in the cooling curve relative to that of the heating curve (see discussion in Petronis *et al.* (2011)). Thus the increase in susceptibility during cooling is deemed a product of exsolution of Ti-poor magnetite and Ti-rich ilmenite from titanomaghemite during the heating process.

Measuring fluctuation of susceptibility with increasing temperature from -197°C to 10°C (room temperature) is a useful means of determining the relative importance of paramagnetic contributors as the masking effect of any ferromagnetic components is reduced at extremely low temperatures. This test can also be used to further constrain the composition of ferromagnetic contributors as stoichiometric variations cause the crystallographic structure of a mineral to modify under cryogenic condition at differing temperatures. This is detectable and is reflected in contrasting thermo-magnetic heating curves (Verwey 1939; Verwey and Haayman 1941; Özdemir *et al.* 1993; Muxworthy 1999; Jackson *et al.* 2011).

Results show good correlation between all samples tested with initial rapid increases in susceptibility between -197°C and -175°C followed by a very slow decline during gradual heating (Fig. 8.14). The initial increase is associated with the Verwey Transition (T_V), the temperature range at which this occurred is characteristic of magnetite. A lack of dramatic fluctuation in susceptibility between -175°C and 10°C shows that paramagnetic minerals have a negligible contribution to bulk susceptibility under these conditions.

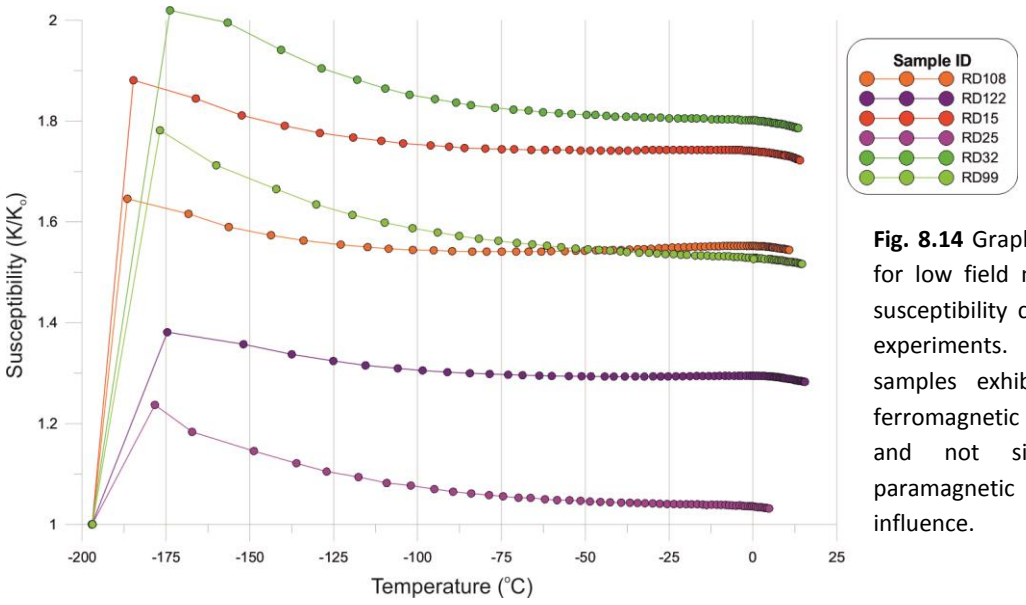


Fig. 8.14 Graphed data for low field magnetic susceptibility cryogenic experiments. All samples exhibit clear ferromagnetic controls and not significant paramagnetic influence.

Lowrie - Fuller Test

A modified Lowrie - Fuller test (Lowrie and Fuller 1971) was carried out to constrain the coercivity parameters of constituent minerals in each sample. With the exception of RD25, the current data set show very consistent demagnetisation behaviour between all samples (Fig. 8.15). NRM MDF is reached in fields of less than 15mT and is followed by a gently undulating demagnetisation curve which reflects the stripping of increasingly stable NRM vectors. In similar fashion, ARM and IRM demagnetisation curves show an initial rapid decrease in remanent magnetisation followed by a gradual decline to almost full demagnetisation (≤95%) in fields of 125mT. In five out of six cases ARM is more stable than IRM during AF-demagnetisation however in all cases the difference between MDF values for ARM and IRM demagnetisation curves is very small (<4mT).

Strictly speaking, the relative stability of ARM over IRM in the majority of samples suggests a predominance of SD magnetite (Lowrie and Fuller 1971). However it has been proven that this is not a hard and fast rule (Dunlop *et al.* 1973; Bailey and Dunlop 1983; Heider *et al.* 1992) and that ARM-IRM stability is determined as a function of dislocation density and domain-wall width (Xu and Dunlop 1995). In the current work all samples return L-type results with the exception of RD99 which returns a H-type result (Xu and Dunlop 1995). Rapid demagnetisation of IRM and ARM infers the dominance of a very low coercivity ferromagnetic and NRM MDF values ≤25mT characterise this (Dunlop and Ozdemir 1997). As ARM is used here in place of weak field TRM, ARM MDF values may be used as a proxy for magnetic grain domain state (Argyle and Dunlop 1990) which suggests all specimens carry coarse PSD to MD magnetite.

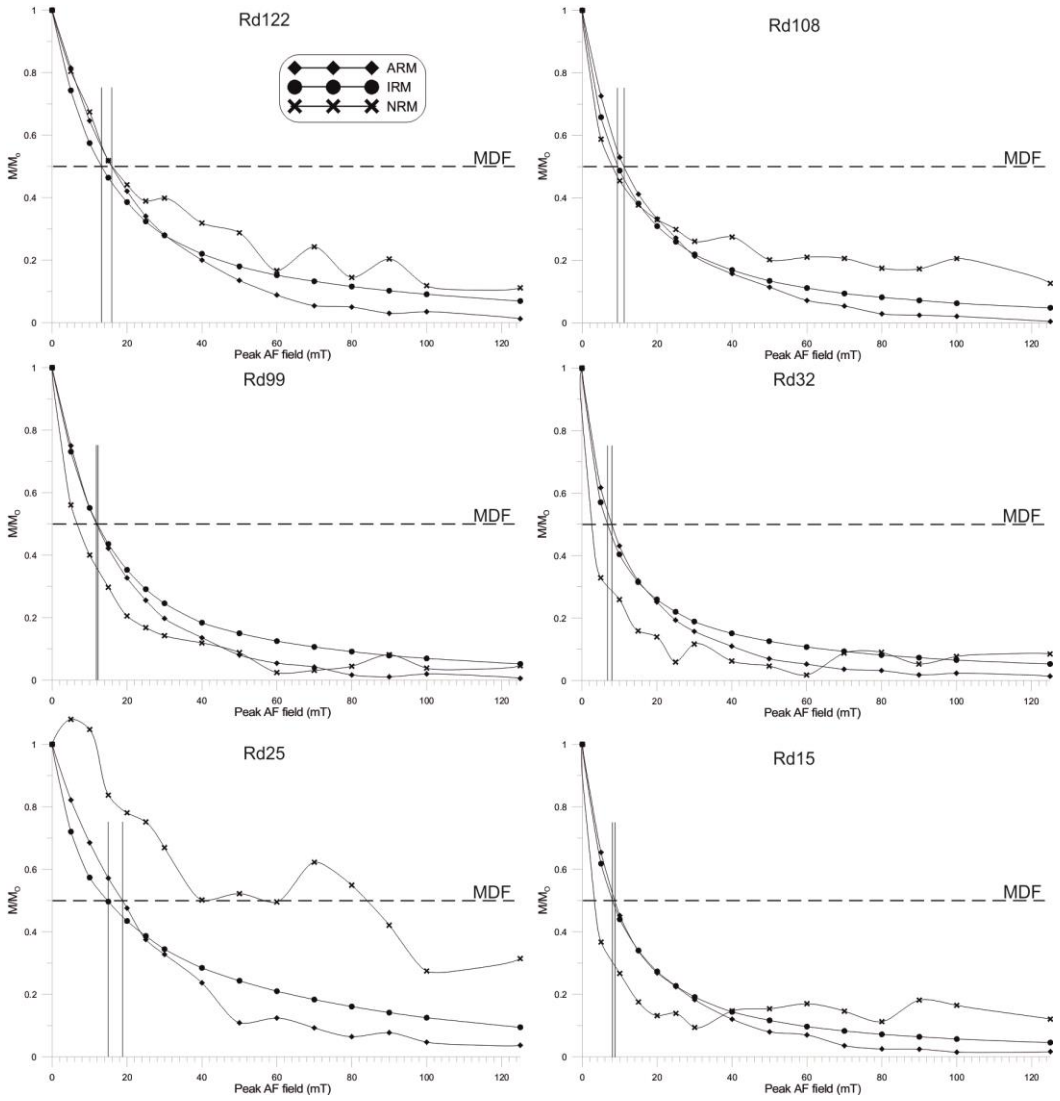


Fig. 8.15 Graphed data from the modified Lowrie-Fuller test. Irregular demagnetisation of NRM in RD25 may reflect TRM or NRM interference due to heat or fluid convection during emplacement of the Carna Pluton.

SIRM Acquisition and BIRM

Measuring the acquisition of saturation isothermal remanent magnetisation (SIRM) and back-field isothermal remanent magnetisation (BIRM) aids in determining magnetic mineralogy and grain size (Dunlop and Ozdemir 1997).

SIRM acquisition curves (Fig. 8.16) show a rapid increase in remanence in low inducing fields that reach 95% saturation between 0.13 - 0.25T, complete saturation (M_S) is always reached prior to 0.4T. No significant increase is noted between 0.4T and 2.5T. The coercivity of remanence (H_{CR}), extrapolated from BIRM curves (Fig. 8.16), is reached in fields between 0.035 - 0.062T for all samples. A sound level of consistency is noted between BIRM and SIRM curves in that samples requiring higher SIRM fields also require higher BIRM fields to reach H_{CR}.

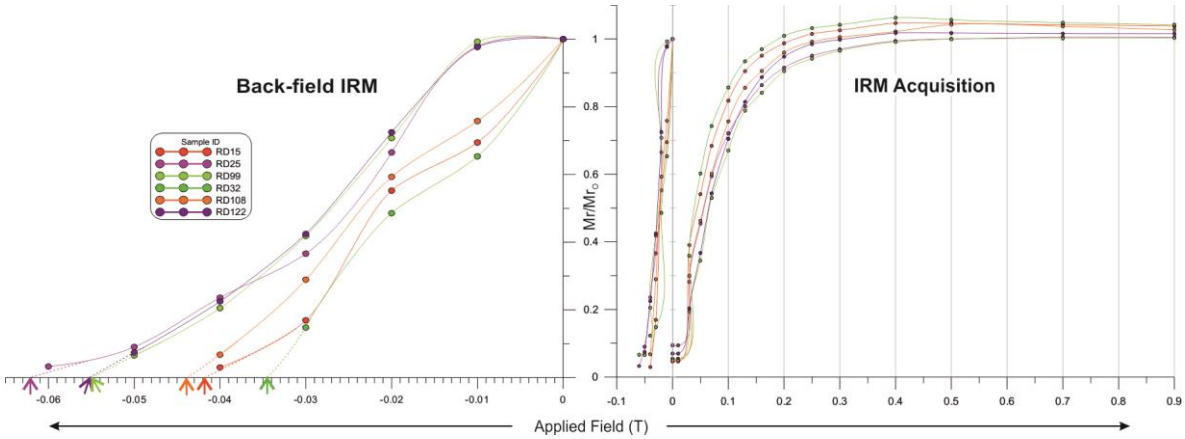


Fig. 8.16 Results of IRM acquisition and back-field IRM demagnetisation. All samples show a narrow spectrum of responses and most are essentially saturated in fields below 0.3T. RD25 and RD122 are significantly H_{CR} & M_s values

Three-Component IRM Demagnetisation

The above results suggest that only very subtle variations in magnetic mineralogy exist across the pluton. The aim of this test is to determine the relative contribution made by minerals within specified coercivity spectra to a sample's total magnetic remanence. Two specimens, one from each facies (G1 (RD25) & G2 (RD122)), were subject to three component IRM demagnetisation (modified after Lowrie (1990)) to determine if the ferromagnetic constituents of G1 and G2 are essentially identical, as implied from the results above, or if the net remanence and coercivity values measured reflect the net interaction of several distinct contributors. Inducing fields of 0.03, 0.3T and 3.0T were selected and results are illustrated in Figure 8.17.

The modulus thermal demagnetisation curve shows that both samples demagnetise at approximately equal rates. However, by observing the three independent demagnetisation curves of the 0.03T, 0.3T and 3.0T axes it is apparent that minerals of differing coercivity spectra do not contribute equally to produce the net vector value.

Both samples are dominated by minerals which are saturated in field between 0.03T - 0.3T. The 0.3T demagnetisation curve declines rapidly between 0-250°C (M_r < 20%) and proceeds to full demagnetisation at a more gradual rate by about 580°C. This is consistent with the occurrence of a low Ti titanomagnetite as the dominant ferromagnetic mineral in both granodiorite facies.

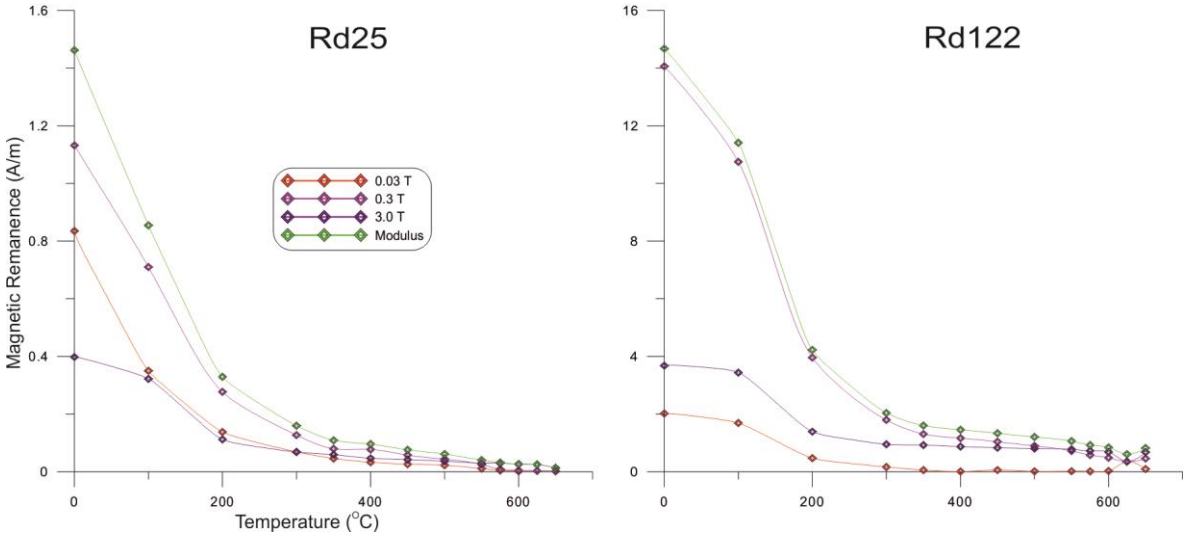


Fig. 8.17 Results of three component IRM thermal demagnetisation. A comparison of the data shows both samples are dominated by moderate coercivity mineral (0.3T) and the overall mineralogy are comparable. However, low coercivity minerals (3.0T) are much more abundant in RD25 and the higher coercivity fraction is more stable relative to that in RD122. This may be indicative of a distinctive deuteric regime or post crystallisation hydrothermal history.

A distinction is noted between samples based on the relative importance of high coercivity (3.0T) and low coercivity (0.03T) minerals. Low coercivity minerals (0.03T) are, initially, a major carrier of remanence in RD25, full demagnetisation is reached by 580°C. In the same sample, the high coercivity minerals (3.0T) make the smallest contribution to the modulus initially but demagnetise at a slower rate and thus contribute to a greater portion of the modulus than the 0.03T curve between 300-600°C. In contrast, demagnetisation curves from RD122 show that high coercivity minerals contribute twice as much as low coercivity minerals to the overall modulus vector prior to demagnetisation. This is brought about by a much lower contribution from the 0.03T curve rather than an increase in the relative magnitude of the 3.0T curve. This may indicate that both samples have roughly equal proportions of magnetically "hard" minerals but RD122 has a much smaller proportion of magnetically "soft" minerals relative to RD25.

In both samples similar demagnetisation behaviour is observed along the respective 3.0T and 0.03T curves. The 0.03T curve demagnetises rapidly between 0-200°C and full demagnetisation is reached between 400-550°C. This behaviour is indicative of a moderate to high Ti magnetite component (Dunlop and Ozdemir 1997). The 3.0T curve again decays rapidly between 0-250°C and stabilises until remanence is abruptly fully removed between ~600-650°C. This indicates that a minor contribution is made to both samples bulk remanence by two high coercivity minerals that require unblocking temperatures of ~250°C and in excess of 600°C, these may correspond to the presence of pyrrhotite and titanomaghemite/maghemite respectively (Dunlop and Ozdemir 1997).

8.4.3 Anisotropy of Magnetic Susceptibility Results

The results of AMS analysis are summarised in Table 8.1, a full data table and full data files are attached in Appendix E. Of the 177 blocked samples, 5 were discarded due to losses incurred during sample preparation.

All Sites					
Parameter	Tj	Pj	lnPj	H%	K_m x 10^{-6} (SI)
Min	-0.714	1.02	0.023	3.96	1206.73
Max	0.973	1.25	0.226	33.83	24083.99
Mean	0.411	1.09	0.089	13.28	14448.03
Std. Dev	0.347	0.05	0.048	6.81	4133.89

G1					
Min	-0.334	1.03	0.025	4.19	1206.72
Max	0.973	1.25	0.226	33.83	24083.99
Mean	0.474	1.1	0.096	14.18	14549.37
Std. Dev	0.295	0.055	0.049	6.85	4387.62

G2					
Min	-0.714	1.02	0.023	3.96	9442.8
Max	0.573	1.08	0.078	12.81	19816.72
Mean	0.026	1.05	0.048	7.73	13827.33
Std. Dev	0.388	0.016	0.016	2.51	2951.55

Table 8.1 Summary of AMS results and determined parameters. These data demonstrate that no large fluctuation in susceptibility data is directly attributable to either facies as mean parameters determined are comparable. It is therefore probably that determined AMS parameters are controlled by essentially indistinct petrographic assemblages.

Susceptibility and Anisotropy

Mean susceptibility (K_{mean}) values across the pluton range from 1206-24083 x 10^{-6} (SI units). Of the 172 analysis made, an average of 14448 x 10^{-6} ± 4387 x 10^{-6} was calculated. No significant fluctuation in mean susceptibility values was recorded between G1 and G2 (Table 8.1). A contour map of K_{mean} across the intrusion illustrates a lack of anomalous K_{mean} susceptibility values in the pluton (Fig. 8.18).

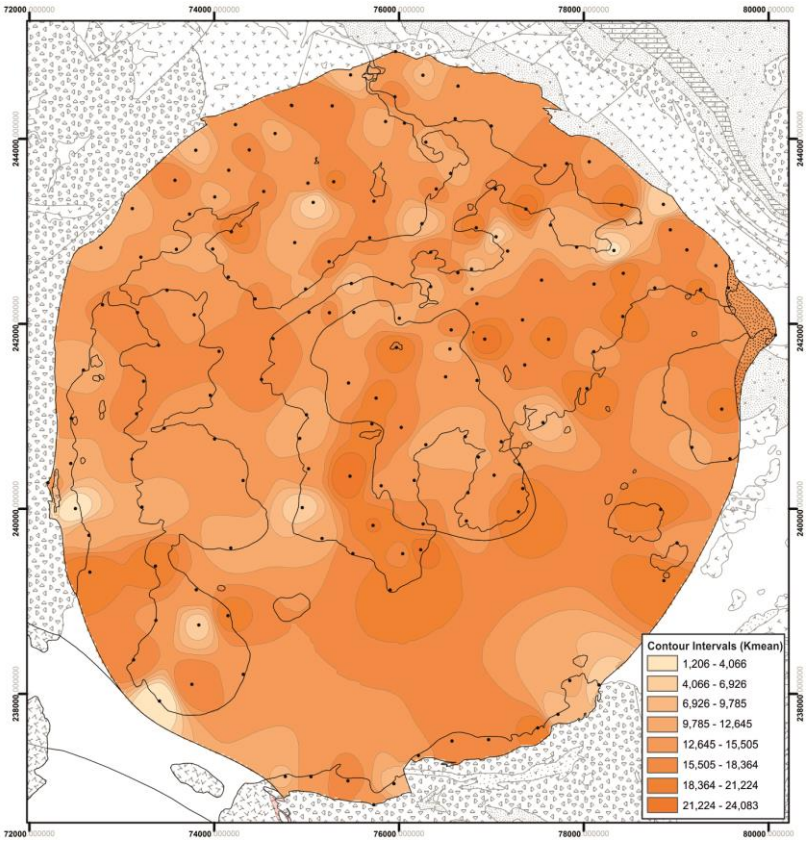


Fig. 8.18 Contour map of K_{mean} values. No major fluctuation is observed indicating a reasonably homogenous assemblage.

The corrected degree of anisotropy (Pj) varies from 1.02-1.25 and the average degree of anisotropy is 13% ± 6.8%. A contour map of H across the pluton shows a systematic distribution of anisotropy (Fig. 8.19) where weak H values (~ 4-12%) are recorded in the core and much higher H values (~ 18-34%) are recorded around the periphery of the pluton. Additionally, along the margin of the intrusion elevated H/Pj values are concentrated in the ENE and WSW that contrasts low H/Pj values in the NNW and SSE contact.

Shape factor values (Tj) vary between -0.71 and 0.97, this reflects tensor symmetries which range from strongly prolate to strongly oblate. Of 172 AMS ellipsoids measured, 20 were dominantly prolate (Tj < 0 > 1) and 152 were dominantly oblate. A contour map of the compiled data shows a very systematic distribution of Tj values (Fig. 8.20). A suite of prolate to triaxial tensors (Tj < 0.3 > -0.7) extend along a NNW-SSE axis and define a zone distinct from those areas to the east and west. Predictably, the marginal areas of the pluton are dominated by oblate magnetic fabrics which are most pronounced in the east and west and weakest in the NNW and SSE. Finally, two zones with anomalously oblate Tj values are recorded in the east and west 2km from the country rock contact. These define NNW-SSE oriented arcs defined by Tj values between

0.54-0.97 (Average = 0.7) which is significantly higher than the average Tj value recorded for tensors about the periphery (0.45).

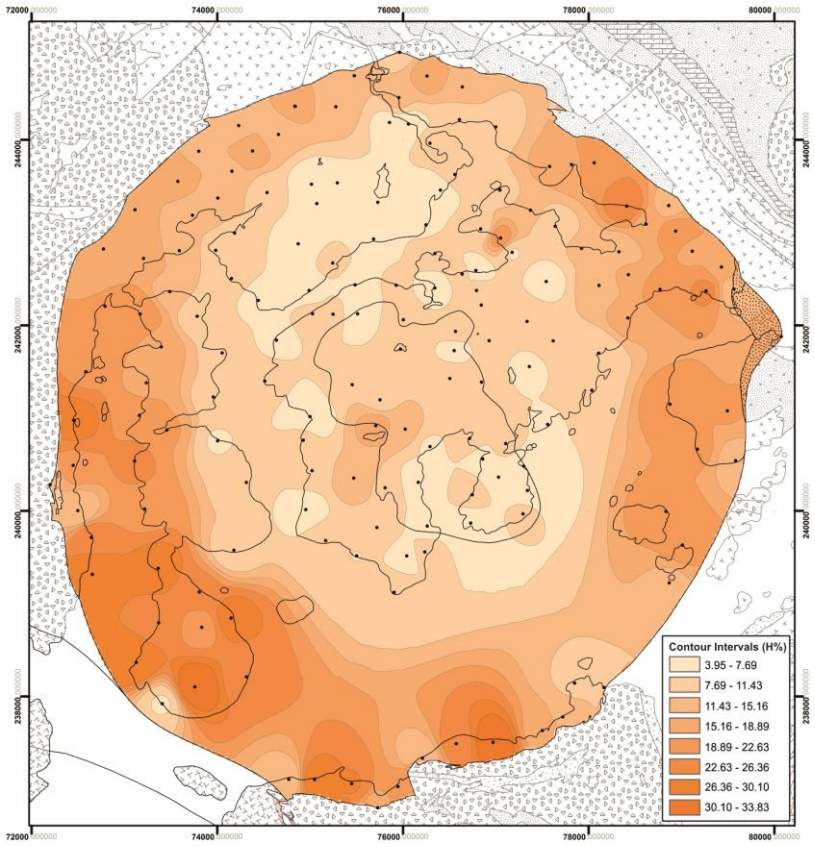


Fig. 8.19 Contour map of H values determined from AMS analysis. A low degree of anisotropy is associated with the core and NNW-SSE axis of the intrusion. The highest H values are in the west and east. Note that peak values are not always associated with the margins of the intrusion and are concentrated in the ENE and WSW, this is inconsistent with a straightforward ballooning scenario.

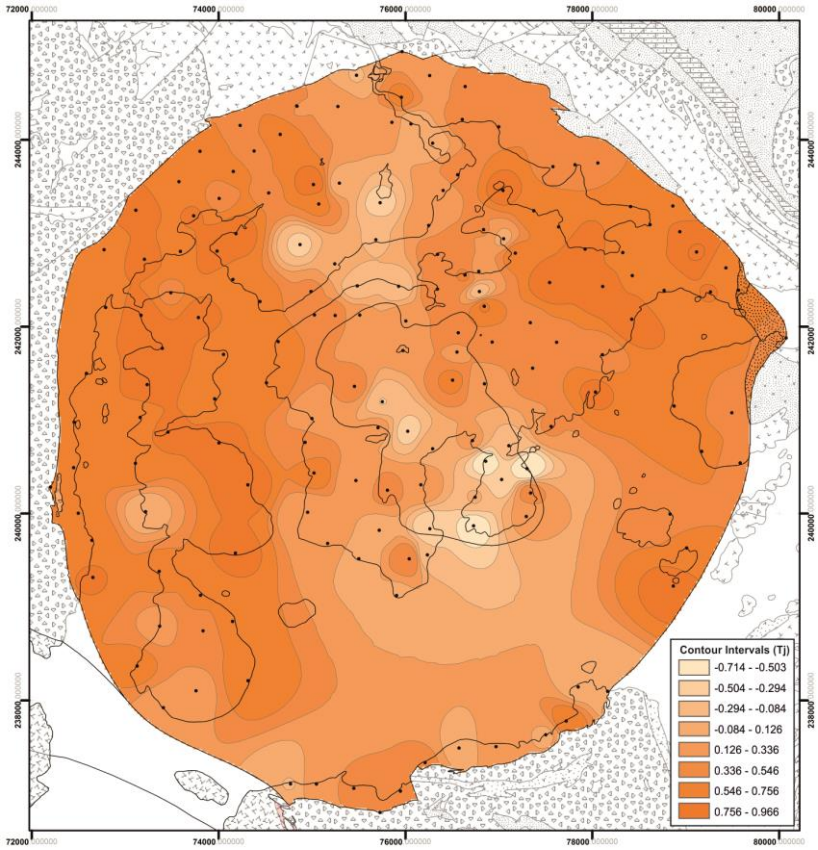


Fig. 8.20 Contour map of Tj values determined from AMS analysis. Again an anomaly is observed along the central NNW-SSE axis where prolate (≤ 0 ≥ -1) tensors are detected. The highest shape anisotropies are oblate and are located in the east and west but peak values are associated with the inner strain zone and not the pluton's marginal fabric.

Attitude and distribution of Magnetic Fabrics

Figure 8.21 (attached map) illustrates the attitude and distribution of AMS tensors based on the shape factor (Tj) value calculated from each sample. Calculated ellipsoids which are dominantly prolate are depicted as lineations (parallel to K1, axis of maximum susceptibility) and those which are dominantly oblate are represented with a foliation symbol (the pole to which is K3, axis of minimum susceptibility). Representative stereographic projections are included which summarise the general character of the AMS ellipsoids in respective localities. Figure 8.22 (attached map) is a summary of interpreted results which plots lineations, foliations or both where L-S fabrics are extrapolated from AMS data based on statistical evaluation (Hext 1963; Owens 1974; Jelinek 1977, 1981; Owens 2000a, 2000b; Borradaile 2001).

Stereographic projections of AMS data (95% confidence ellipse) reveal that, for the majority of samples, determined K1, K2 and K3 axes are extremely well constrained in the centre and margins of the intrusion. Dominantly prolate ellipsoids are concentrated in the centre of the intrusion, these are consistently orientated NNW-SSE and plunge moderately to the south. Lineations which are identified as part of L-S fabrics generally radiate outward from the core of the intrusion and plunge at moderate to steep angles. Lineations identified at the periphery of the intrusion plunge moderately to steeply down dip of concentric outward dipping foliations.

Foliations dip consistently outwards at moderate to steep angles and are concentric. Two distinct zones are identified in the east and west along which only oblate foliations are recognised, corresponding stereographic projections characteristically exhibit tight K3 axes and girdles defined by K1 and K2 axes (Fig. 8.21). In these zones steep foliations define a crude ellipsoid symmetry elongate along a NNW-SSE axis which is anomalous when compared to nearby marginal foliations which are essentially perfectly contact parallel.

In summary, both lineations and foliations may be determined from most AMS tensors. These define steep outward dipping concentric foliations and lineations that either radiate from the centre of the intrusion or are parallel to the faulted and stoped country rock contact.

Dominantly prolate fabrics are clustered in the centre of the pluton and trend NNW-SSE parallel to internal facies contacts and mapped faults in both country rock and pluton.

A oval shaped zone of accentuated strongly oblate foliations is noted the long axis of which is also orientated NNW-SSE.

8.5 Discussion

The results of the magnetic analytical experiments are discussed below in light of the petrographic, field and regional geological data presented above.

8.5.1 Characterising Magnetic Mineralogy

Rock magnetic data are consistent with the predominance of a ferromagnetic phase, most likely magnetite with an extremely low Ti content, as the main contributor to magnetic remanence in the Roundstone Pluton. Results from the Lowrie - Fuller test show exponential demagnetisation of, and overall minor stability contrasts between, ARM and IRM that yield dominantly L-type results (Xu and Dunlop 1995). AF demagnetisation of NRM in RD25 returned an extremely irregular demagnetisation curve. This may reflect a ChRM or TRM superimposed upon the primary NRM in particularly low coercivity ferromagnetic grains that were detected in this sample only, an observation supported by Curie temperature and three component thermal demagnetisation data.

IRM acquisition curves are characteristic of low coercivity minerals and typical of PSD to MD magnetite (Dunlop 1986). M_S (95%) is always reached in fields below 250mT, very minor increases in remanence between 300mT and 2.5T suggesting only trace amount of higher coercivity minerals are present. A clear relationship is observed between SIRM and BIRM results in that those which return elevated H_{CR} values require higher magnetising fields and vice versa as would be expected. Inducing fields required to reach the coercivity of remanence during the BIRM experiment are characteristic of a magnetically soft titanomagnetite as the dominant ferromagnetic mineral in all samples.

Three component thermal demagnetisation tests show the dominant ferromagnetic mineral is a moderate coercivity mineral which is fully demagnetised prior to reaching 580°C, this is indicative of magnetite and is consistent with Curie temperature estimates which suggest almost stoichiometric magnetite is present. These experiments also show a minor contribution from some higher coercivity minerals which corroborates with residual increases along the SIRM curve in fields over 0.3T. These are interpreted to be titanomaghemite, a product of deuteric superficial oxidisation of coarse grained titanomagnetite, based on unblocking temperatures and coercivity spectra (Dunlop and Ozdemir 1997).

Cryogenic susceptibility experiments compliment T_C values of 578-580°C and show that magnetite is the dominant magnetic mineral and that paramagnetic minerals have negligible influence on susceptibility. A typical Ti content in magnetite is calculated to x=.01 ($Fe_{3-x}Ti_xO_4$) after Akimoto (1962).

RD25 is anomalous in all rock magnetic tests as it carries a much greater proportion of low coercivity minerals and also exhibits a low K_{mean}. This may be attributed to the growth of secondary magnetite from biotite as a product of hydrothermal alteration associated with the intrusion of the Carna Pluton 200m to the south (Tarling and Hrouda 1993). It may also reflect a slower cooling rate of this sample relative to others in the pluton which could also be attributed to the emplacement of the Carna Pluton if it occurred during the crystallisation of the Roundstone Pluton, thus slowing the rate of cooling an promoting the incorporation of Ti into the ferromagnetic lattice (Tarling and Hrouda 1993). The current data set does not facilitate a conclusive interpretation but does suggest that the southwest portion of the Roundstone Pluton was subjected to elevated temperatures independent of the rest of the pluton. This is consistent with the currently accepted but untested hypothesis that the Carna Pluton intruded shortly after the Roundstone Pluton.

K_{mean} values are reasonably consistent across the intrusion. There is no correlation between the distribution of shape factor values, the degree of anisotropy values or the G1 - G2 contact and mean susceptibility values. The average K_{mean} value ($14448 \times 10^{-6} \pm 4133 \times 10^{-6}$) suggests that ferromagnetic contributors control the AMS tensor and the contribution from paramagnetic minerals will, in general, be negligible (Tarling and Hrouda 1993), this is consistent with cryogenic data. However it is noted that the distribution and orientation of magnetite is controlled by the orientation of the crystal lattice of silicate minerals (Figs. 8.6, 8.7). It has been shown that in cases where primary magnetite is included in the crystal lattice or where secondary magnetite grows along cleavage planes (often the case in biotite), or in interstitial pore spaces, and mimics the symmetry of surrounding minerals, magnetic anisotropy reflects the crystal preferred orientation of the silicate crystals (Hrouda *et al.* 1971; Heller 1973). Thus while the AMS tensor is dictated by the degree of anisotropy of titanomagnetite the preferred orientation of this mineral is most often controlled by the preferred orientation of silica minerals and it is thus a good proxy for the CPO of silicate minerals.

The influence of high coercivity minerals on AMS is predicted to be negligible owing to the relatively low abundance and low susceptibility values of these minerals (Dunlop and Ozdemir 1997). Differences in magnetic properties between samples are very subtle and cause only minute contrasts in susceptibility behaviourisms.

8.5.2 Comparison of Field and Magnetic Data

A relationship between host rock structure and the orientation of facies contacts is obvious when LiDAR data is compared to the orientation of mapped G2 sheets in the core of the pluton. Identified submarine NNW-SSE faults have been traced into the country rock to the south of the pluton where it is revealed these are trans-plutonic extensions of previously mapped faults (Harvey 1967). Here, these are considered part of the D5 suite that cross cut the Connemara terrane. Similar relationships are noted to the north of the pluton but are not as prevalent owing to the lack of good exposure. A concomitant relationship between these faults and ascent of the G2 facies is implied as G2 sheets have preferentially emplaced parallel to these structures. This suggests D5 faults acted as conduits for magma transport during the ascent process. Contact relationships between G1 and G2 prove the near coeval nature of the two facies and by extension show that D5 faults were active prior to the crystallisation of G1, thus indicating these may have also facilitated transport of G1 magma.

Fabric data collected in the field concur with AMS results. Both sets of data show a moderate concentric marginal foliation which is steeply inclined parallel to the intrusion's faulted and stoped contact. No stretching direction is discerned in the field from outcrops in close proximity to the pluton's contact however well defined K1 axes of AMS mean tensors are well constrained and are consistently steeply inclined and parallel to both faulted and stoped contacts. Owens (2000b) discussed the identification of composite AMS fabrics based on the comparison of 6-rank and normalised 6-rank tensors. In these areas the K1 axis is typically well constrained in both normalised and un-normalised stereographic projections of AMS data. An evaluation of microstructures in this area show the strain continued into the low temperature submagmatic field but did not continue into the solid state or become brittle. These data indicate that the marginal concentric foliation, and accompanying steeply inclined maximum susceptibility vector, is not the product of post solidus overprinting and is related to submagmatic stress applied during the construction of the pluton. This is interpreted as a ballooning or inflation fabric.

A broad inner zone of elevated strain recognised during field recognisance mapping is constrained through the application of AMS analysis. A digital elevation model (Fig. 8.23), using Tj as the z-axis, best depicts an elliptical inner zone of strain orientated along a NNW-SSE axis that is parallel to submarine brittle structures and G1-G2 intrusive contacts discussed above. Fabrics in this zone are highly oblate, steep to subvertical and strike parallel to the defined oval shape (Fig. 8.24) as depicted by well constrained K3 axis and girdle distribution of K1 and K2 axes in associated AMS stereographic projections (Fig. 8.21). It is noted that the foliations are most oblate along an ENE-WSW axis which coincide with localities that show the most intense high to moderate temperature sub-magmatic microstructures. No change in mineral modal abundance, rock texture or magnetic properties is noted across this area. Therefore, this fabric anomaly is interpreted to reflect the preferential distribution of strain during crystallisation rather than a subtle intrusive contact or the preferential distribution of ferromagnetic minerals.

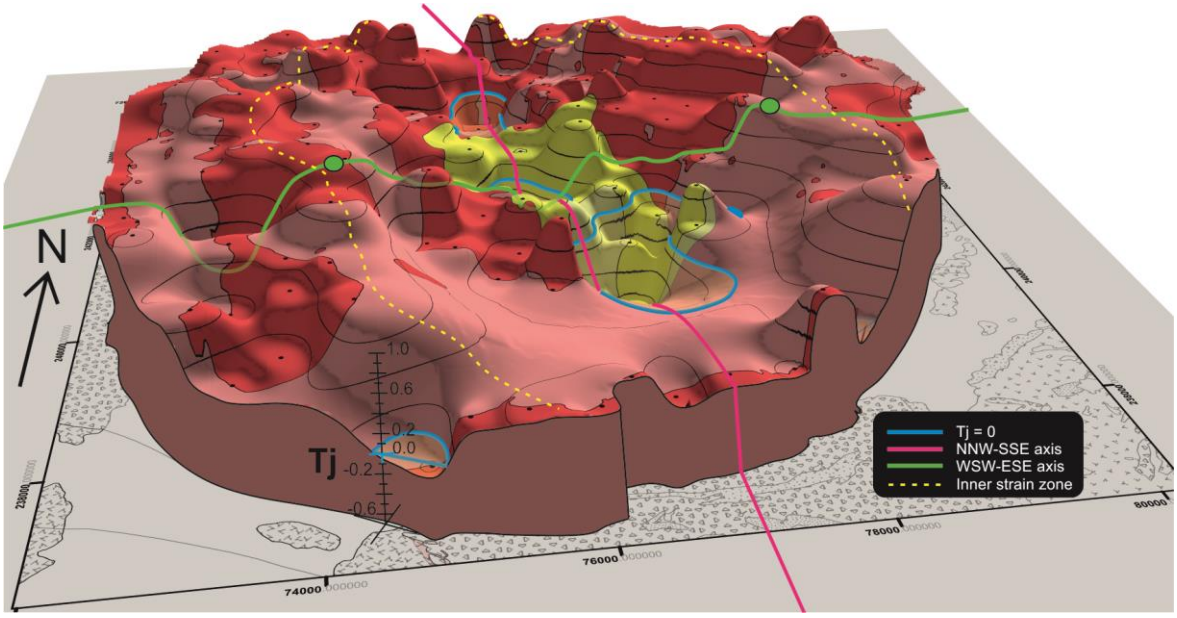


Fig. 8.23 Digital elevation model using Tj as the z-axis parameter draped with basic facies map of the pluton. Note that the highest Tj values (highly oblate) occur along two arcs marked in dashed yellow which define an oval elongate along a NNW-SSE axis. Green dots mark the localities with the highest Tj values, these define a line orthogonal to that defined by the lowest Tj and H values.

The interior of the pluton appears isotropic in the field and AMS analysis return H values between 4-12% which reflect an overall low degree of anisotropy. AMS ellipsoids are dominantly oblate, concentric and have maximum susceptibility axes orientated away from the centre of the intrusion at a moderate to steep angle. In thin section, magmatic textures are characteristic and no evidence for submagmatic deformation is apparent.

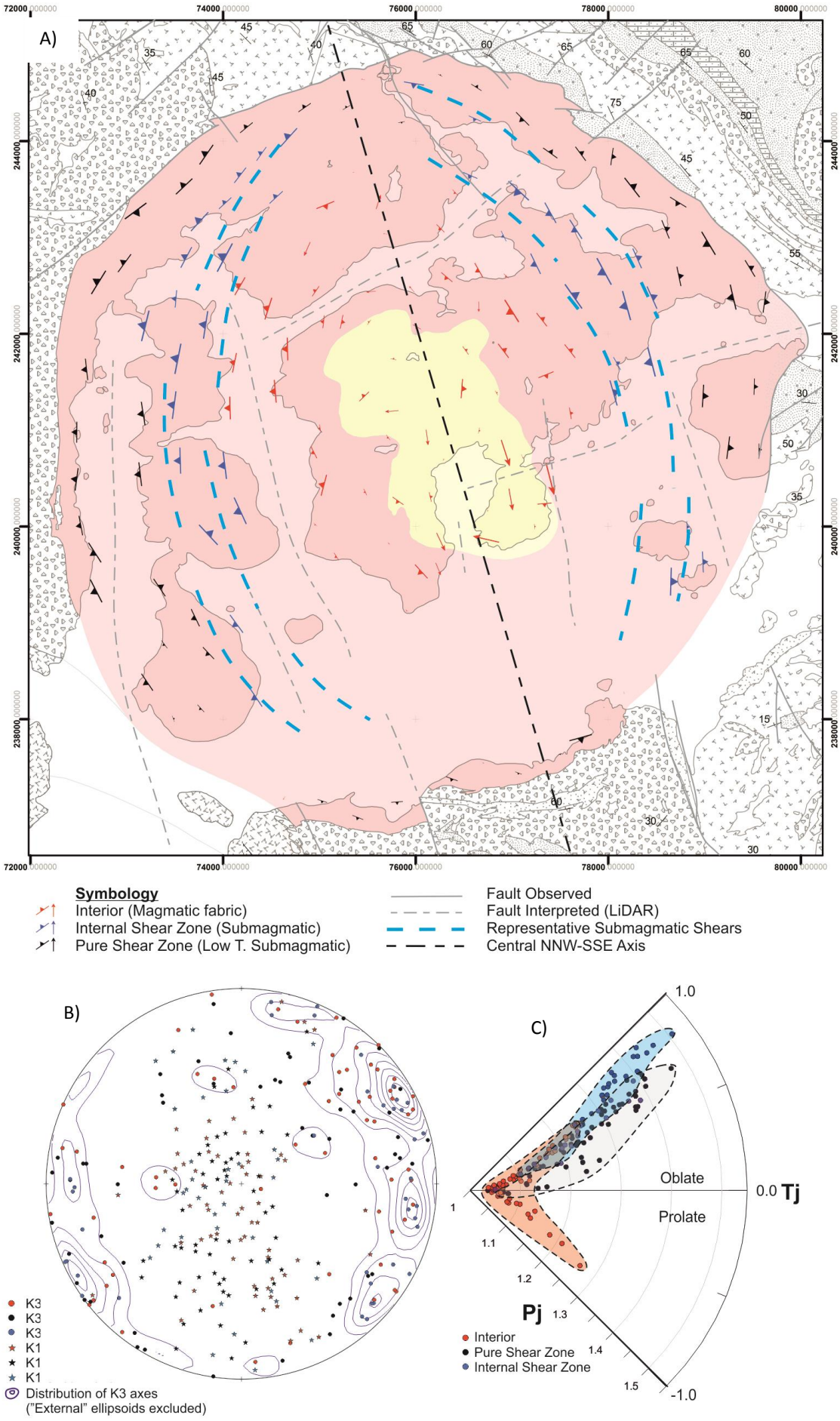


Fig. 8.24 (A) Summary map of AMS data (figure caption continued over page).

Fig. 8.24 (A) Summary map of AMS and field data with interpreted structures. Fabric symbols are weighted based on Tj. Prolate tensors only occur in the centre of the pluton with other tri-axial or slightly oblate tensors (Red). A pure shear flattening fabric occurs close to the pluton margin (black). The strongest fabrics are oblate and occur along the inner strain zone (blue). B) Stereographic projection of AMS fabrics shows a preferential orientation of K1 axes along a NNW-SSE axis and K3 axes are concentrated in the ENE-WNW as depicted in strain distribution contour maps. C) The pure shear flattening, internal strain and interior strain zones identified defined clusters on a poplar plot of AMS data in support of (A).

This data compilation show that a definite relationship exists between fabric symmetry and distribution, G2 sheet and D5 fault orientations, submarine scarps and the occurrence of a low strain zone across the core of the pluton and a high strain zone in the WNW and ESE. This reflects the structural and kinematic factors which controlled pluton construction.

Significantly, the majority of specimens that return prolate ellipsoids were sampled from the central part of the pluton (Fig. 8.21). In these cases, the K1 axis was orientated NNW-SSE and dipped moderately or steeply to the SSE. K1 axes determined from ellipsoids which were not dominantly prolate are most often subvertical or moderately inclined and preferentially orientated along a NNW-SSE axis. Owing to the lack of sub-magmatic microstructures and consistency between normalised and un-normalised AMS ellipsoids, these are considered magmatic lineations which reflect magma transport directions, which is a product of stress imparted in the magmatic state (Vigneresse *et al.* 1999; Passchier and Trouw 2005; Ablay *et al.* 2008). Comparing this data to field and LiDAR data reinforces this interpretation in that the lineations identified lie parallel to mapped G2 sheets and D5 faults. This indicates that these prolate fabrics reflect the transport of magma which was permitted along D5 structures during the ascent of the G1 and G2 facies.

8.6 An Emplacement Model for the Roundstone Pluton

The Roundstone Pluton is believed to have been emplaced sometime between 422-410Ma (Feely *et al.* 2010). Although no direct evidence for a depth of emplacement is available, a comparison of data from the Omey Pluton and the Carna Pluton indicate that the Roundstone Pluton was emplaced into the epizone between 4-10km (Ferguson and Harvey 1979; Ferguson and Al-Ameen 1986; Gallagher *et al.* 1992; Ahmed-Said and Leake 1996). Leake (1969) suggests that marginal foliations formed as a result of "upward movement of nearly solid magma". More recently Leake (2011) argues that stoping, driven exclusively by a buoyancy contrast between the intruding granodiorite and country rock, provided space and was the main emplacement mechanism.

Stoping as a mechanism of emplacement is refuted at a principle level for reasons already discussed (Chapter 1) and is considered an effect of, rather than the mechanism of, magma ingress. In addition, stoping as a mechanism does not explain the occurrence of key features of this pluton which include a severe lack of country rock xenoliths, a steep circular faulted contact, a NNW-SSE orientated submagmatic elliptical zone of oblate fabrics, the nature of vertical and horizontal G2 sheets or the near perfect circular foot print of the intrusion (stoping should exploit pre-existing ESE-WNW grain of the country rock). An argument for buoyancy driven ascent is also redundant as the foot wall of the Mannin Thrust, through which granodioritic magma must have ascended, is rhyolitic (Leake and Singh 1986; Draut and Clift 2002) and therefore less dense.

Corry (1988) describes a punched laccolith as one which has a defined flat base and roof, is bound by steep or vertical peripheral faults and assumes a crude cylindrical shape. Characteristic traits include a brittle bounding margin, minimal distortion to the host rock close to the faulted contact, occasional small scale laterally discontinuous dykes parallel to the contact, a close to circular outline and a shallow level of emplacement (epizone) (Gilbert 1877; Hunt 1958; Koch *et al.* 1981; Cruden 2008). Goulty and Schofield (2008) argue that sub-circular saucer shaped intrusions, similar to the outline of the Roundstone Pluton, are fed by steeply inclined dykes that lie directly below the observed intrusion and strike parallel to their long axis and numerically predict marginal faulting to be a product of radial distribution of tensile strain in the roof.

Taking the above points into account a punched laccolith model is found to be most consistent with the field, magnetic and geophysical data discussed above.

8.6.1 Interaction between Regional Transpression and Local Structures

Leake and Tanner (1994) show that the majority of D5 NNW-SSE faults in the hanging wall of the Connemara Metamorphic Complex (CMC) (Leake 1986) exhibit a dextral shear sense. These structures were active during the latest southward thrusting of the CMC and continued to be reactivated into the Devonian period (Chapter 3).

In the foot wall of this thrust complex (i.e. Delaney Dome Fm.), and lower parts of the hanging wall (i.e. Metagabbro, orthogneiss, metasedimentary sequence) the Clifden - Mace Fault (CMF) is defined by several brittle structures and a broad fault zone (Leake *et al.* 1983; Leake 1986; Leake and Singh 1986). In contrast, higher in the stratigraphic sequence to the north this fault is a much more discrete structure. This implies D5 NNW-SSE faults are inherent to the footwall block and

propagated upwards through the Mannin Thrust and into the overlying hanging wall during Siluro-Devonian deformation.

It is argued that the Mannin Thrust acted as a significant planar discontinuity against which underlying basement structures abutted and penetrated into the overlying hanging wall where they are now expressed as discrete, relatively minor, faults (Fig. 8.25). Following the southward thrusting of Connemara, the onset of sinistral regional transpression (Dewey and Strachan 2003) was the causative force behind dextral reactivation of NNW-SSE faults and the clockwise rotation of competent blocks within the accretion zone between converging Laurentia and Avalonia. The Mannin Thrust provided a structural break between hanging wall and footwall that subdued the upwards propagation of D5 faults into the hanging wall.

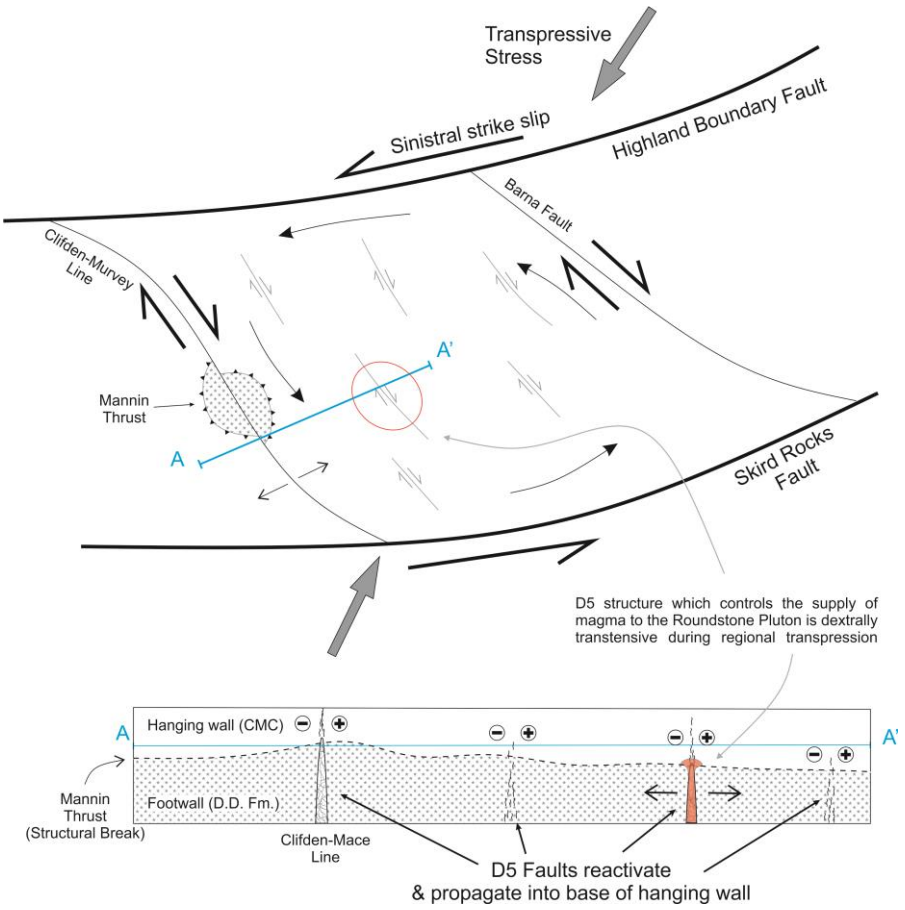


Fig. 8.25 Schematic model of the relationship between regional stress, local structure and magma transport. The terrane bound by the Skird Rocks Fault and Highland Boundary Fault acted as a large scale deformation zone. Anticlockwise rotation of blocks bound by NNW-SSE faults generated localised dextral transtension long these shear zones. These faults provided vertical ascent conduits for ascending magma which was capped by the Mannin Thrust stress barrier at the site of emplacement.

8.6.2 Controls on Ascent and Emplacement

Structurally Controlled Sheet Ascent

The current data are consistent with the presence of a significant NNW-SSE brittle structure beneath the Roundstone Pluton. This is evidenced by the presence of superficial NNW-SSE faults, that have propagated through the Mannin Thrust discontinuity into the hanging wall, around the northern and southern margins of the Pluton and those identified within the intrusion itself from field, LiDAR and AMS data.

Physical barriers, such as a defined parting surface, coupled with the reduced affects of lithostatic pressure at shallow depth, are shown to be capable of "capping" ascent conduits and forcing lateral emplacement of magma (Mudge 1968). Layered host strata of contrasting competencies act as stress barriers under differential stress and can exceed vertical excess magma pressure at shallow levels (Engelder and Sbar 1984). Similarly, the intersection of a horizontal structural dislocation with a propagating vertical ascent conduit may serve to re-orientate the local stress field and promote a transition from ascent to emplacement (Weertman 1980; Engelder and Sbar 1984).

The Mannin Thrust is a local major subhorizontal dislocation which separates extrusive felsic footwall rock from intrusive metaigneous and paragneiss hanging wall rock. It is proposed that ascent conduits intersected and were truncated by the overlying Mannin Thrust. Significant competency contrasts between hanging wall and footwall materials and the inherent weakness of this lateral decollement acted as a stress barrier to form an approximately axi-symmetric stress field at the time of intrusion where σ3 is rotated to the vertical plane and $\sigma 1 > 2\sigma \sim 3\sigma$.

Mechanism of Emplacement

A single NNW-SSE fault zone provided a plane of weakness which abutted against the subhorizontal Mannin Trust (Fig. 8.26A). Along this structure, excess magma pressure and the ambient stress field rotated local σ3 to the vertical plane during ascent of batches of magma before a combination of reduced hydrostatic pressure allowed the Mannin thrust to act as a stress barrier and promote lateral emplacement of magma (Fig. 8.26B).

Lateral emplacement of magma initially occurred as a thin sheet that extended to the full diameter of the intrusion to form a disk shape prior to vertical inflation (Pollard and Johnson 1973; Corry 1988). Early emplacement was driven by excess magma pressure and facilitated by ductile vertical deflection of the bounding roof that caused inflation and up doming of the roof (Fig. 8.26B). Internal lateral emplacement fabrics became overprinted by progressively inclined

oblate strain tensors as magma became packed into the site of emplacement (Fig. 7.26C). Progressive inflation increased radial tensile strain in the roof which caused brittle failure around the periphery to form a cylindrical fault bound intrusion under a block of vertically displaced country rock (Fig. 7.26D). Inflation continued until hydrostatic pressure from the overlying block equalled the force exerted by upwelling magma.

Stoped contacts observed in the field represent localities where magma was permitted to intrude into the peripheral fault and incorporate blocks of country rock into the granodiorite body, larger xenoliths such as that observed on Inishnee may represent roof pendants. The final phase of pluton construction involved the ascent of a plexus of G2 sheets via NNW-SSE conduits and the lateral emplacement of this magma into the still crystallising G1 facies (Fig. 7.26D). Post failure relaxation of the country rock generated a subtle pluton-up shear sense expressed as a contact parallel stretching direction in AMS data close the contact.

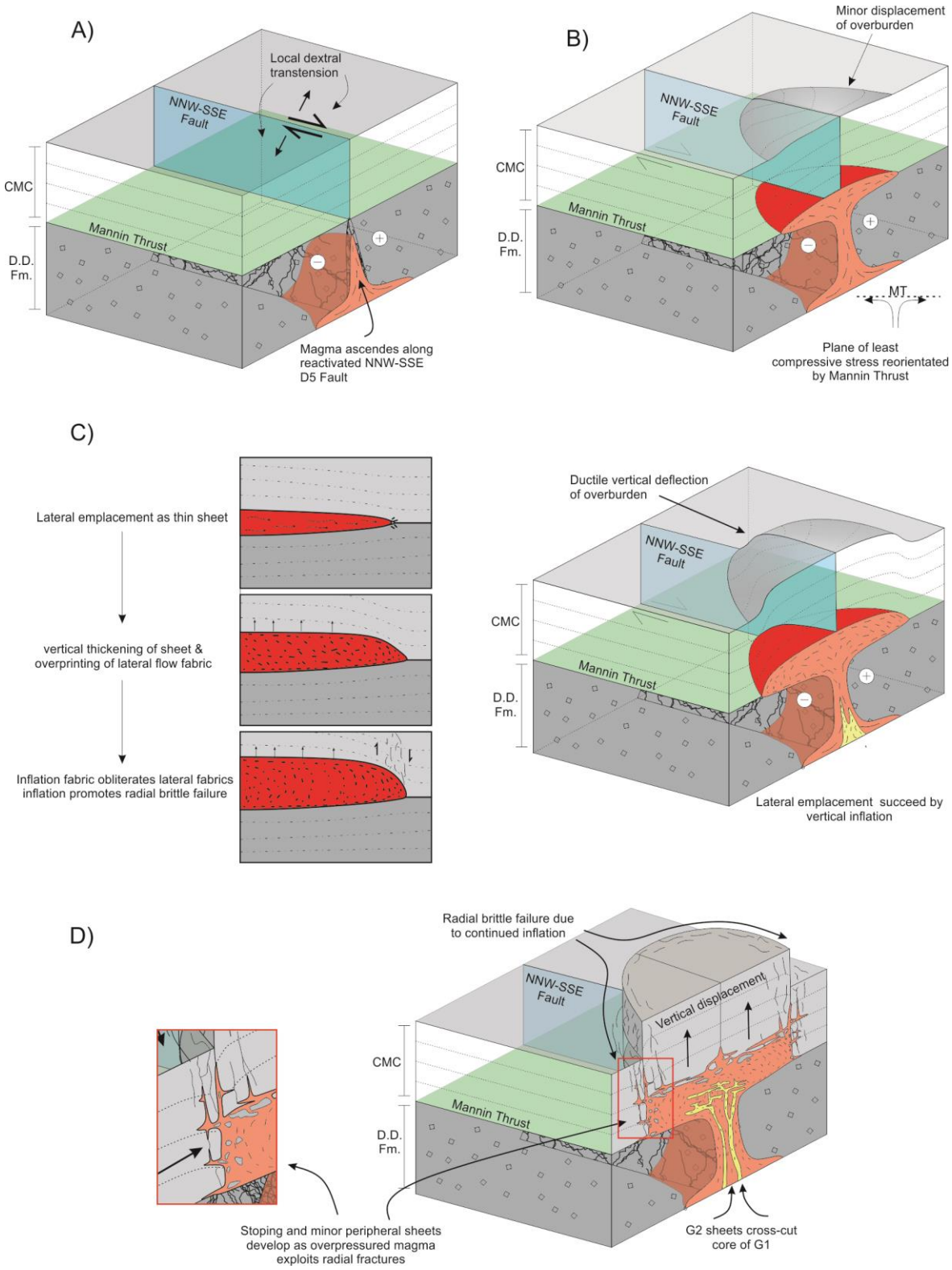


Fig. 8.26 Punched Laccolith model for the Roundstone Pluton as discussed in the text. A) Siting of the pluton is controlled by reactivated D5 faults during regional sinistral transpression. B) Lateral emplacement is controlled by the subhorizontal Mannin Thrust which rotates the plane of opening from vertical to horizontal . C) Thickening of the pluton is achieved by ductile deformation and displacement of overburden and lateral emplacement fabrics are overprinted. D) Tensile strength of overlying strata is exceeded, roof is up-faulted and magma intrudes radial faults and localised stoping occurs as a consequence of this.

Interaction between Regional Stress and Inflation

The inner elliptical zone of accentuated oblate submagmatic fabrics (Figs. 8.23 & 8.24) is significant. It is emphasised that the long axis of this ellipse lies parallel to NNW-SSE minor faults that displace the northern and southern margins of the pluton and are responsible for the sheeted ascent of magma. It is proposed that the above structural, magnetic and petrographic data show this anomaly to be a product of the stress field generated as a consequence of the interaction between regional transpressive force and concurrent magma ingress, rather an internal subtle facies contact.

Continued ascent and emplacement of magma promoted lateral migration of magma away from the central NNW-SSE ascent conduit. Ongoing regional sinistral transpression promoted dextral transtension along the now established NNW-SSE conduit (Fig. 8.25). Shear stress across the central NNW-SSE axis of the pluton interacted with excess magma pressure during inflation of the pluton; this generated a zone of reduced strain parallel to the underlying shear zone and elevated strain orthogonal to this. As a result a distinct elliptical zone of strain was imparted across the pluton. This is expressed as a zone of strongly oblate submagmatic foliations across the WSW-ENE central axis where flattening was greatest and, orthogonal to this, a NNW-SSE zone of characteristically weak triaxial fabrics.

An alternative hypothesis attributes the nature of this elliptical strain zone to processes exclusively associated with magma emplacement. Here the architecture of the Roundstone Pluton is equated to the symmetry of an elliptical saucer shaped sill where an inner sill, i.e. interior of the intrusion, is flat and the outer margin an arcuate inclined sheet with a ragged outer contact (as in Thomson and Hutton (2004)). In such a case an inner zone may be bound by peripheral oblate foliations which depict the transition zone between a flat internal and inclined external sill. The orientation of the feeder dykes, depth of emplacement and excess magma pressure control the shape and size of the inner and outer sill (Goulty and Schofield 2008). However the earlier model is preferred as the latter is not supported by AMS data outside the zone of elliptical strain where Tj values again decrease or by the presence of prominent submagmatic foliations within the zone of strain.

8.7 Conclusions

The Roundstone Pluton is a punched laccolith. Deep seated NNW-SSE D5 faults are prominent features of the footwall of the Mannin Thrust that became reactivated during regional sinistral transpression between the late Silurian and early Devonian. Ascent was gained through the basement via preferential juvenile fracture propagation along these reactivated structures. The propagating conduit abutted against the gently inclined Mannin Thrust in the epizone where lateral emplacement of magma progressed to inflation and eventual radial failure of the roof rock to form a sub-circular laccolith elongate parallel to the NNW-SSE feeder conduit.

Rock magmatic data do imply, but do not prove, that this intrusion is older than the Carna Pluton. Further testing of this interpretation is required.

A structural relationship is now evident between the Omey and Roundstone Plutons. NNW-SSE structures are identified in both intrusions, the magnetic and microstructural data presented indicate that these structures were active concurrently with the emplacement of magma and in both cases these are sited as probable ascent conduits. In addition, it is postulated that both plutons intruded between 425 - 410Ma, concurrently with regional transpression and thus the local scale fabric analysis. Therefore, local structural and regional kinematic controls over the construction of Omey and Roundstone plutons are shown to be related (assuming the postulated age for the Roundstone Pluton is correct.

The manner in which the Omey and Roundstone plutons relate to the Carna Pluton or the later constituents of the Main Batholith remains unconstrained from a kinematic point of view. The only published model for the Carna Pluton argues that emplacement was achieved entirely independently of the ambient regional stress field and local structural features (Leake 2011). All evidence from the Main Batholith indicate an east-west structure, probably the Skird Rocks Fault, was highly influential in siting this part the intrusion (El-Desouky *et al.* 1996; Crowley and Feely 1997; Baxter *et al.* 2005; Feely *et al.* 2006; Leake 2006). Thus there is a break down in the sequence of kinematic events that took place during and facilitated the siting of older plutons (Omey and Roundstone) and the later part of the Main Batholith. This issue is elucidated upon in the next chapter.

Chapter 9:

The Carna Pluton; Evidence for a Regional Kinematic Transition

9.1 Introduction

Previous chapters demonstrate that D5 NNW-SSE faults were preferably orientated during regional transpression to facilitate ascent and emplacement of magma that formed the Earlier Plutons of Omey and Roundstone between ~ 425-410Ma. The 402-380Ma (Feely *et al.* 2003; Feely *et al.* 2010) Kilkieran Pluton has been the subject of a multitude of mapping, structural, geochemical and chronological studies (see Chapter 5). Arising emplacement models differ in terms of precise magma transport mechanisms (Leake 1974; Ryan *et al.* 1995; El-Desouky *et al.* 1996; Baxter *et al.* 2005; Leake 2006) but a consensus has formed that emplacement was achieved along the ESE-WNW Skird Rocks Fault (SRF). This structure is understood to have been in extension at the time of magma ingress as a product of regional sinistral transtension. The above work shows that the siting and emplacement of the Earlier Plutons and the Kilkieran Pluton is fundamentally controlled by the net interaction between regional stress, local structure and excess magma pressure inherent to ascending granitoids.

Based on post-emplacement Re-Os Molybdenum data, the Carna Pluton, which forms the western end of the Main Batholith, is believed to have been emplaced between 410-407Ma (Selby *et al.* 2004). The existing emplacement model for this intrusion suggests the pluton was constructed by "general upward movement of the magma" via buoyancy and progressive stoping of the host rock, without any significant tectonic influences (Leake 2011). Therefore, existing data implies that the Carna Pluton emplaced syn-kinematically at the transtension-transpression transition (Dewey and Strachan 2003) or during transtension (Soper and Woodcock 2003). It is difficult to resolve the model of Leake (2011) with that for other members of the Galway Granite Complex (GGC) discussed above in the context of the regional stress field.

Chronological data from the Carna Pluton (Selby *et al.* 2004) hinge on the process of secondary mineralisation, not primary crystallisation of magma. Better constraints on the timing of emplacement of the Carna Pluton are required in order to temporally relate emplacement of this intrusion to other members of the GGC and to regional kinematics. Data compiled on the internal architecture of the Carna Pluton are presented by Leake (2011). This work represents the only published structural information on the intrusion and focuses on the distribution of late stage faults and weak foliations and biotite layers which are concordant to the pluton's margins. The contact between the Kilkieran and Roundstone plutons is not defined on existing geological maps (Leake and Tanner 1994; Long and McConnell 1995; Leake 2011) and the outer facies of both

intrusions is termed the Errisbeg Townland Granite (ETG) which may infer to some that these are part of the same magma body. Temporal relationships between faulting in the pluton and magma ingress remains unconstrained as does the origin of trans-plutonic NNW-SSE submagmatic foliations (King 1966).

Here, the temporal development of fabrics and faults in the Carna Pluton relative to its crystallisation history is assessed. Structural data (AMS and field based) was compiled to evaluate the internal architecture of the pluton and relate this to host rock structure. Laser Ablation Inductively Coupled Plasma Mass Spectrometry (LA-ICP-MS) determinations are presented for several facies of the Carna Pluton and G1 of the Roundstone Pluton. Coupled with earlier work (summarised in Feely *et al.* (2010)) these new data facilitate the critical evaluation of existing Rb-Sr molybdenite data and also allow comparison of crystallisation ages between all major members of the GGC for the first time. A new data driven model for the emplacement of the Carna Pluton is presented and which carries implication for the proposed regional kinematic models for late Caledonian lockup.

9.2 Field Data

Essential features of the Carna Pluton have recently been described by Leake (2011) and the reader is referred to this text for elegant petrographic descriptions of each facies, accounts of external and internal contact relationships and the currently available geochemical data. Data discussed here pertain to host rock structure and field based structural relationships.

Facies definition and Pluton Contacts

The distribution of facies within the pluton is illustrated in Figure 9.1 (attached map). Leake (2011) describes several monzogranite facies of the Carna Pluton (in brackets below). Here these are referred to as G1a (Murvey), G1b (Garnetiferous/Aplitic Murvey), G2 (Errisbeg Townland), G3a (Carna), G3b (Cuilleen), G4a (Mace-Ards), G4b (Kf porphyritic Mace-Ards) and G5 (minor late intrusions). This system conveniently distinguishes each facies efficiently to the unacquainted reader (Richey 1928). In contrast to the reckoning of Leake (2011), here G1 (Murvey Granite) is identified as the earliest member of the Carna Pluton following the work of Selby *et al.* (2004). Here, G5 is used as an inclusive term for all minor late facies including the Mace Pier Granite, the

K-feldspar breccia pegmatite and the late granite porphyritic intrusion at Murvey (details in Leake (2011).

The geological map presented (Fig. 9.1, modified from Wright (1963); Leake (1974); Leake (2011)) illustrates the concentric symmetry of this intrusion that is replicated by the internal facies distribution and emplacement related fabrics. The pluton is elliptical, elongate along a NNW-SSE axis, intrudes Ordovician metaigneous rocks in the north and north-east (Leake 1974; Friedrich *et al.* 1999a; Friedrich *et al.* 1999b) and is cross cut by the ETG of the Kilkieran Pluton in the southeast (Wright 1963; Max *et al.* 1978). The Carna G2 and Kilkieran ETG facies are petrographically akin making the contact between the two plutons challenging to identify (both termed the ETG). Accurate mapping of this contact has not yet been undertaken however the concentric foliation within the Kilkieran Pluton (Kinahan 1869) contrasts that which parallels the margin of the Carna Pluton (Fig. 9.1). In the Carna Area (south east of the Carna Pluton at the Kilkieran Pluton contact) this marginal fabric is accentuated and the contact masked by several later NNW-SSE faults which cross cut the contact zone. These mutually divergent concentric foliations show the Carna Pluton was emplaced, and inflated, prior to intrusion of the later Kilkieran Pluton. This interpretation is supported by new chronological data presented below.

External contacts are locally faulted but most often stoped and exhibit laterally continuous sheets of granite that have been traced for ~ 100m into the amphibolite country rock in the north and north east (described in Leake (2011)). Internal contacts are characteristically gradational (~ 5-30m). Those observed between G1 or G5 and neighbouring facies are often sharp (Leake 2011) indicating a more substantial temporal break between these magma pulses. External and internal sharp contacts dip moderately or steeply outwards, chilled margins are rare.

Emplacement Fabrics and Structures

Dramatic biotite layering is observed at several localities around the pluton. These are 2-15cm thick and primarily composed of 2-8mm fresh primary biotite crystals as well as small proportions of feldspar and quartz; titanite, apatite, zircon and magnetite are accessories. Graded bedding, cross-bedding, rupture and flame structures and large biotite crystals (Fig. 9.2) indicate these to be primary horizons derived from initial crystallisation of magma and not a product of shearing or late stage fluid remobilisation. Layers typically exhibit sharp bases and grade upwards into horizons enriched in euhedral K-feldspar and plagioclase. The orientation of these horizons fluctuate but are, overall, contact parallel and inclined moderately (20-70°) to the north at Dogs Bay, moderate-steeply (40-70°) to the east in the east at Carna, to the south in the south on the

series of island offshore south of Carna and to the west on Croaghnakeela Isl. in Galway Bay. This defines an overall radial symmetry dipping away from the centre of the intrusion. Leake (2011) interpreted this as evidence for the upward movement of the whole "ring complex" through the G2 (ETG) facies that ultimately produced concentrically outward dipping horizons. It is emphasised that such features are consistent with that model but are not exclusive of others (e.g. Molyneux and Hutton 2000; Hutton and Siegesmund 2001).

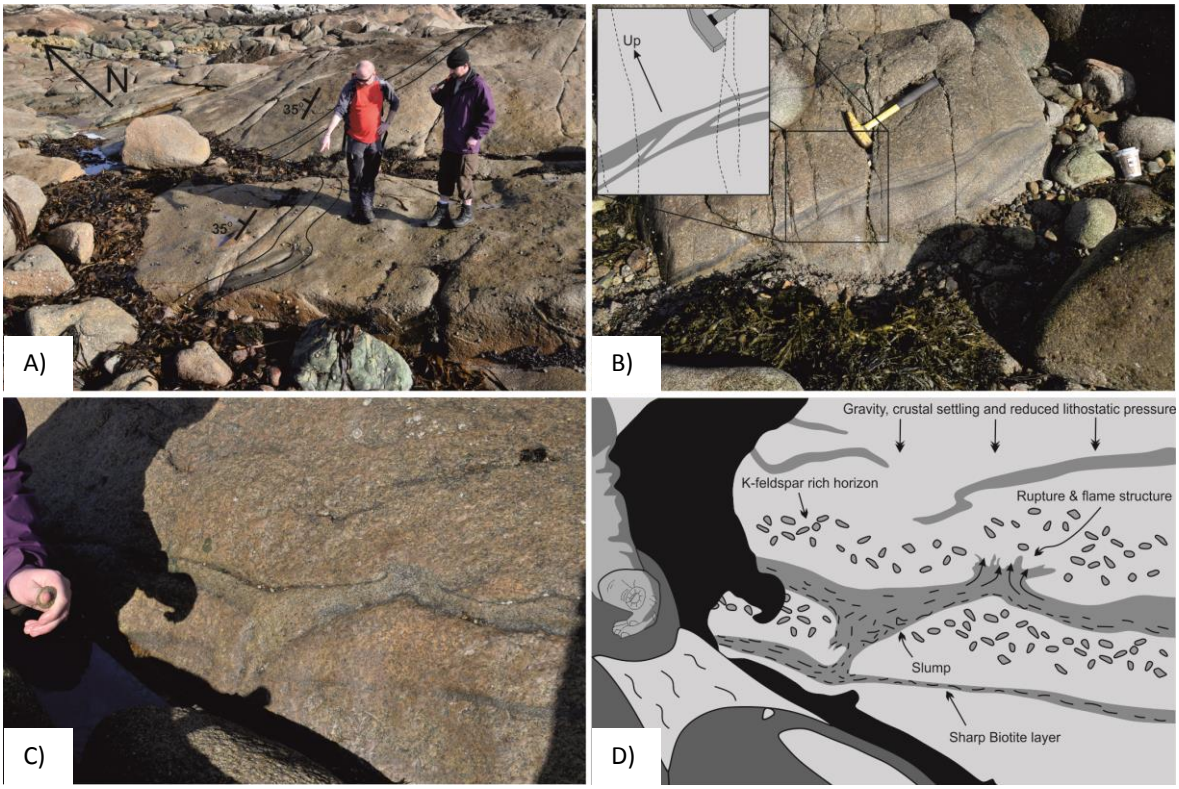


Fig. 9.2 A) Northward dipping biotite layers at Dogs Bay. B) Cross bedding identified in fractionated biotite layers. C & D) Biotite and K-feldspar modal layering disrupted by slumping and flame structures.

Magmatic to submagmatic emplacement related foliations are best preserved around the periphery of the pluton. These are concentric, contact parallel and defined by the alignment of biotite and tabular K-feldspars which are hosted in a groundmass of anhedral to subhedral partially aligned quartz (Fig. 9.3). In close proximity to external contacts (1000-500m) foliations are more pervasive and dip moderately - steeply outwards parallel to neighbouring biotite layers. Owing to the subtle nature of detectable fabrics in the centre of the intrusion inclination is rarely determined but weak foliations strike consistently parallel to internal facies contacts.

Petrographic analysis of biotite rich layers and concentric foliations indicate these fabrics formed prior to full crystallisation of magma. Away from fault zones, quartz is fresh, anhedral and shows only weak undulose extinction. K-feldspar is often euhedral in G2 but sub-euhedral in other

facies yet does not, characteristically, show signs of brittle deformation or plastic deformation. Biotite is fresh or partially chloritised and euhedral. Within 500m of the country rock moderate undulose extinction and rare subgrain boundary rotation is observed in quartz and biotite may be euhedral or partially smeared about feldspars which become increasingly aligned with proximity to the host rock.

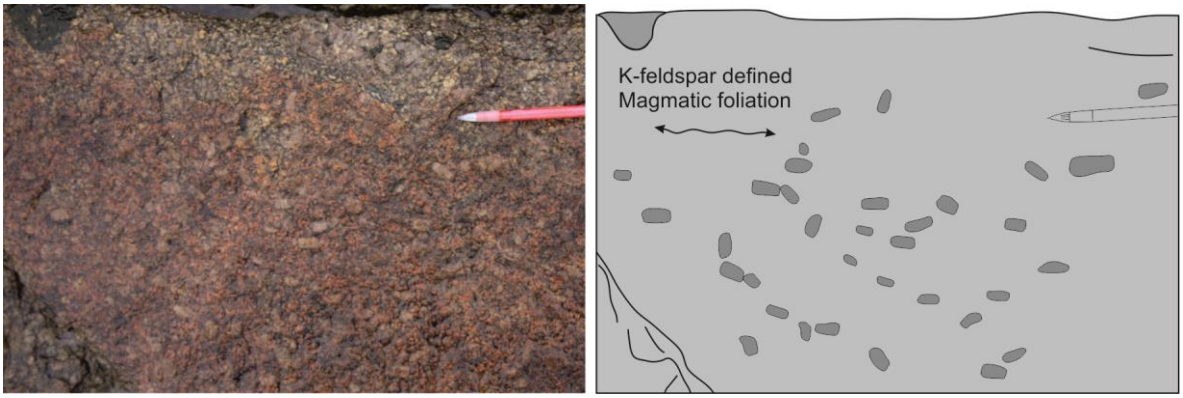


Fig. 9.3 Concentric foliation formed in the magmatic state defined by aligned tabular K-feldspar (North of Gorteen).

The observations above are consistent with fabric development in the magmatic to upper sub-magmatic state (Vernon 2004; Passchier and Trouw 2005). The features described are typical of those associated with down temperature deformation which occurs concurrently with laccolith inflation (e.g. Brun *et al.* (1990); Brown and McClelland (2000); Baxter *et al.* (2005)), and are here considered a product of this process.

Tectonic Strain

Prominent evidence for tectonic overprinting of magmatic emplacement related fabrics is found in the north of the pluton in the Dogs Bay area and on the southern flank of Errisbeg Hill and is best defined by NNW-SSE and NNE-SSW fault sets (Fig. 9.1). A large D5 fault, the Clifden-Mace Fault (CMF), cross cuts the northern margin of the pluton in this area and is associated with several other minor NNW-SSE faults some of which host minor late stage felsite or porphyritic dykes (Fig. 9.4).

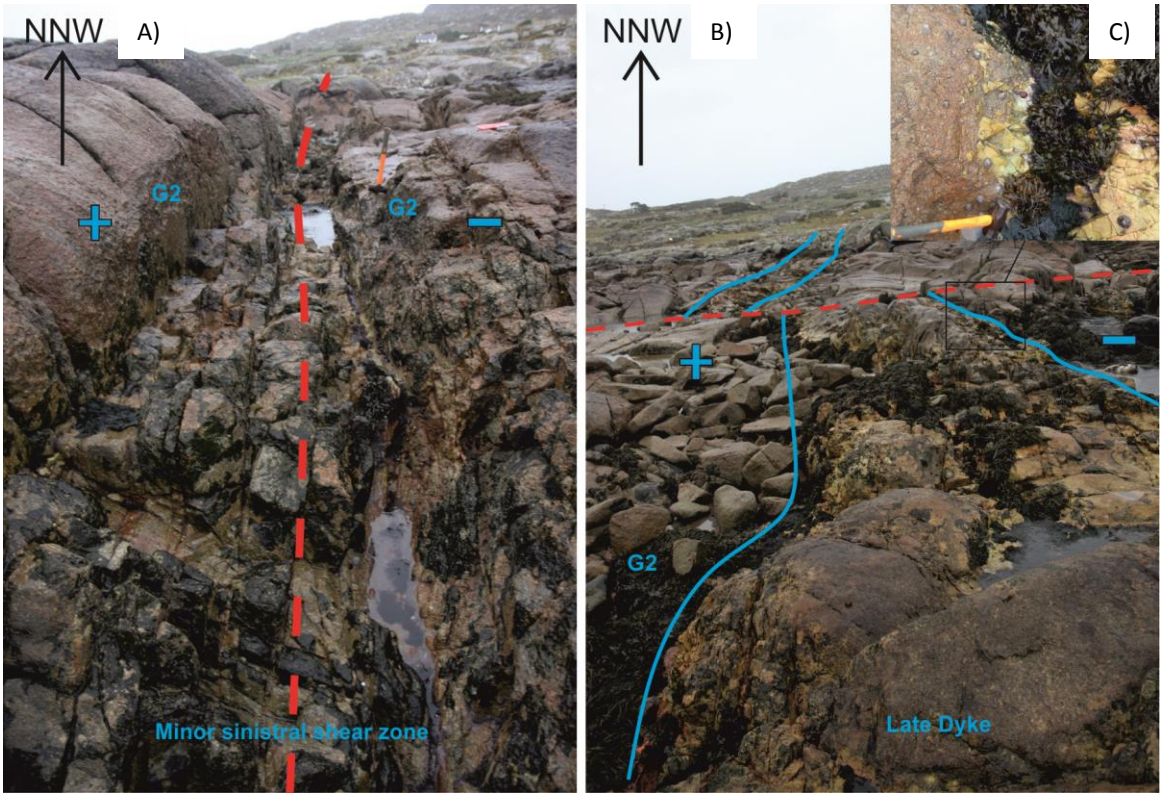


Fig. 9.4 A & B) Examples of NNW-SSE brittle shear zones which strike parallel to the Clifden - Mace Fault . In both cases late stage quartz/feldspar-phyric dykes have been emplaced into these faults. B) These dykes are cross cut by minor WNW-WSW faults after full crystallisation. C) Faulted margins are brecciated and angular fragments of the intruding rhyolitic dykes are included within the granite host.

The CMF is defined by a 15-30m wide zone of heavily brecciated, chloritised G2 that is cross cut by stockwork quartz veins (Fig. 9.5). A 750m top to the left displacement of the granite contact is noted across this fault, this shear sense is repeated in most large (meter scale) NNW-SSE brittle structures. Despite this, at outcrop scale shear sense across NNW-SSE ductile structures are markedly inconsistent as both sinistral and dextral S-C fabrics are observed (Fig. 9.5 B-F). This observation is supported at other localities further to the northeast where again a limited number of dextral shear zones are observed. S-C fabrics or discrete shear planes are most often submagmatic or solid state as they are defined by extensive quartz ribboning, smearing of biotite (now chloritised) and pervasive brittle deformation and rotation of feldspars (Fig. 9.5 C, D & F). Rare examples are also found where shear sense is defined by relatively undeformed tabular feldspars, moderately defined quartz ribbons and biotite which is aligned and/or smeared (Fig. 9.5 E), features which indicate deformation in the magmatic to submagmatic state.

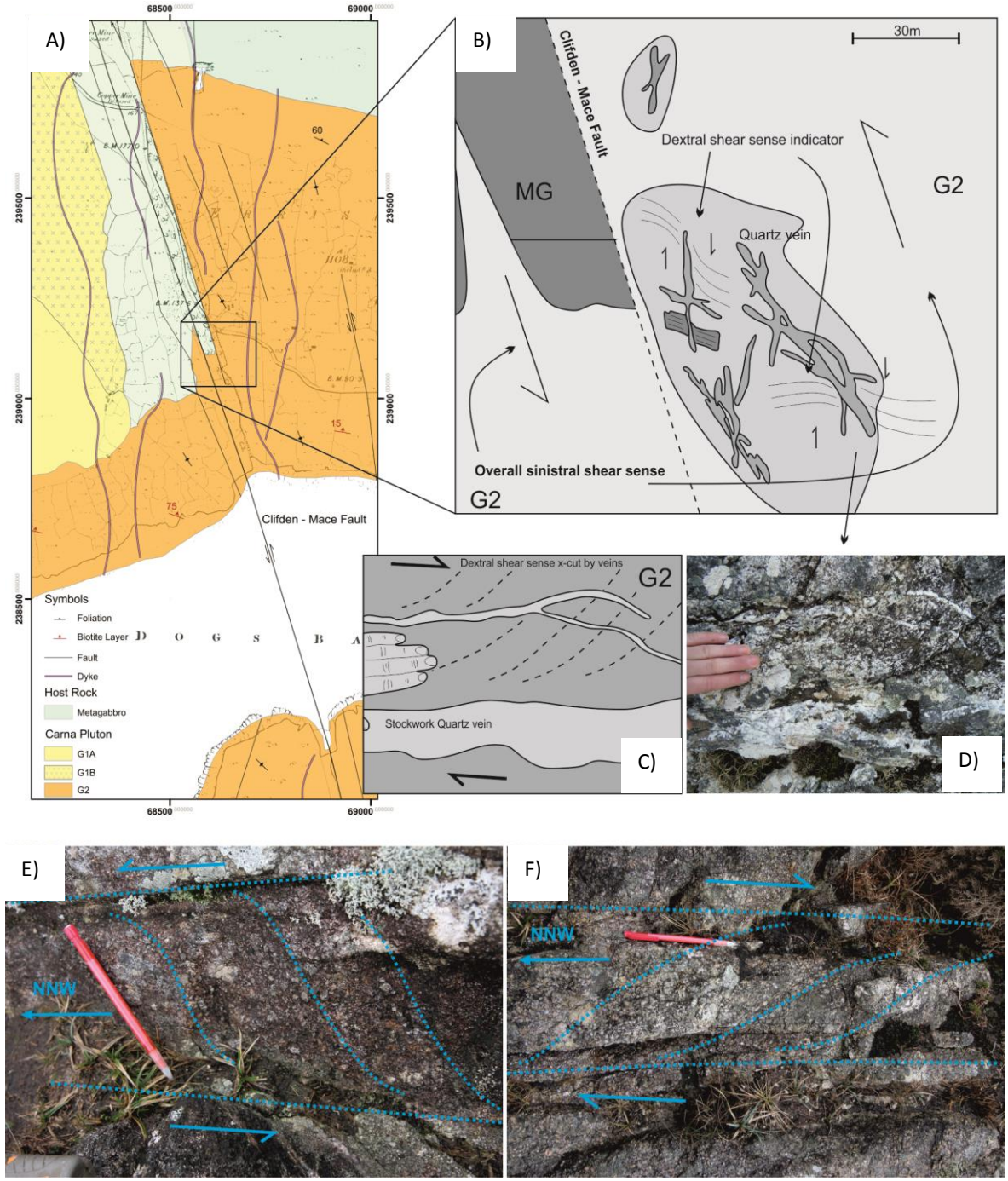


Fig. 9.5 Shear sense indicators along NNW-SSE faults in the Dogs Bay area. A) Overall 700m sinistral shear sense across the Clifden - Mace Fault. B) Sketch of outcrop adjacent to Clifden-Mace Fault, extensive stockwork quartz veins and brecciation is associated with faulting, several examples of dextral shear sense is noted within this zone (C & D). Further to the northeast on the southern side of Errisbeg several ductile NNW-SSE shear zones are noted, both dextral and sinistral shear sense indicators are present, lack of brittle deformation and in some cases aligned tabular feldspars indicate shearing was active in the submagmatic state (E & F).

Several kilometres east of the CMF zone, to the north of Gorteen Bay, a subtle NNW-SSE tectonic fabric overprints a weak concentric foliation. The tectonic foliation is subvertical and defined by elongate quartz grains and partially aligned biotite that cross cuts a K-feldspar-defined

contact parallel inflation foliation (Fig. 9.6). Similar observations were reported from the Cuilleen Townland area (075550, 233120) based on magnetic data by King (1966) and observational field data by Leake (2011) who described a quartz/feldspar/biotite-defined submagmatic foliation trending 120-140° in this area. This foliation cross cuts the G2/G3 contact and is associated with a topographic low (Fig. 9.1). Leake (2011) cites this as evidence for minor compression arising from the upwelling of magma during the emplacement of the G3-G4 facies as a central ring structure. However, the fact that these foliations are not concordant with internal contacts but are sub-parallel to prominent NNW-SSE faults in the area suggest these relate to tectonic rather than magmatic processes and are therefore attributed to submagmatic shearing along the CMF during granite crystallisation.

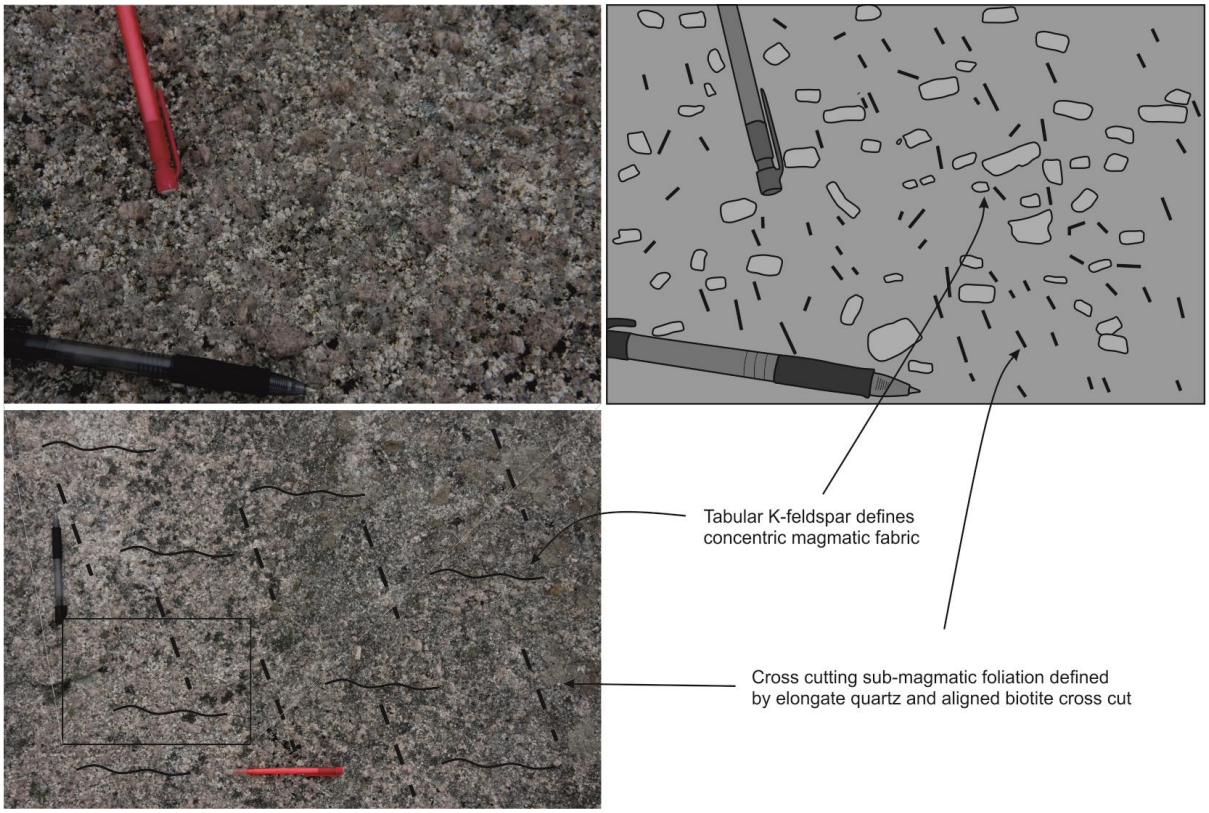


Fig. 9.6 Concentric K-feldspar defined inflation fabric cross-cut by NNW-SSE tectonic foliation associated with submagmatic shearing along the Clifden - Mace Fault (North of Gorteen Bay).

Summary

The Carna Pluton is a composite intrusion with a moderately outward dipping magmatic-submagmatic concentric fabric that is here associated with the process of inflation. The intrusion is elliptical in shape and elongate along a NNW-SSE axis which is sub-parallel to the strike of the CMF that cross cuts close to the core of the intrusion. A suite of NNW-SSE subvertical foliations

are also identified that lie parallel to the CMF and cross cut the concentric inflation foliation. Here, these fabrics are attributed to fault activity prior to full crystallisation of the granite.

Final displacement along the CMF is sinistral however several examples of sub-magmatic dextral NNW-SSE shears have also been identified. This indicates that the observed sinistral displacement of the northern margin is the net product of multiple opposing reactivations and that this activity was concurrent with, and continued after, crystallisation of the granite. These observations are consistent with regional studies which conclude that shearing along D5 faults was active throughout the Silurian to mid-Devonian (discussed in chapter 3).

9.3 Geochronology

A targeted U-Pb LA-MC-ICP-MS study was carried out which sought to constrain the temporal relationship between the Roundstone and Carna Plutons relative to each other and other members of the GGC. These new data represent the first accurate age determinations from both intrusions that directly constrain the timing of emplacement and crystallisation.

9.3.1 Sampling and Methodology

A total of four block samples were collected for analysis (see Table 9.1, Fig. 9.8 for localities). Three blocks were sampled from the Carna Pluton, CN2 was sampled from G4B, CN3 from G5 (Mace Pier Granite) and CN4 from G5 (K-feldspar Breccia near Mace Pier). One block was sampled from the Roundstone Pluton (RD1). All rock crushing, mineral separation, zircon picking and U-Pb dating was conducted at the Department of Geology, Trinity College Dublin. Methods used are detailed in Chapter 6, full data tables are provided in Appendix E.

9.3.2 Results

Between 17 and 31 zircons were analysed per block sample from which discordant and statistical outliers were rejected before final mean or ZircTuff (Ludwig and Mundil 2002) age determinations were calculated (see discussion). Summary results are presented in Table 9.1. Concordia plots and statistical parameters are presented in Figure 9.7.

Sample	East	North	Facies	Analysed	Accepted	Age
RD1	074998	244472	Roundstone G1 (Hornblende Granodiorite)	31	21	423.8 ± 3.2Ma
CN2	073354	232543	Carna G4b (K-feldspar-phyric monzogranite)	29	15	412.8 ± 2.4 Ma
CN3	074147	231547	Carna G5 (Mace pier granite, Cu-Py-Mo-Qtz minor stockwork veins)	29	29	409.8 ± 7.2 Ma
CN4	073727	231525	Carna G5 (Megacrystic K-feldspar Breccia, Cu-Py-Mo-Qtz minor stockwork veins)	23	21	409.6 ± 3.6 Ma

Table 9.1 Summary of Zircon U-Pb age determinations

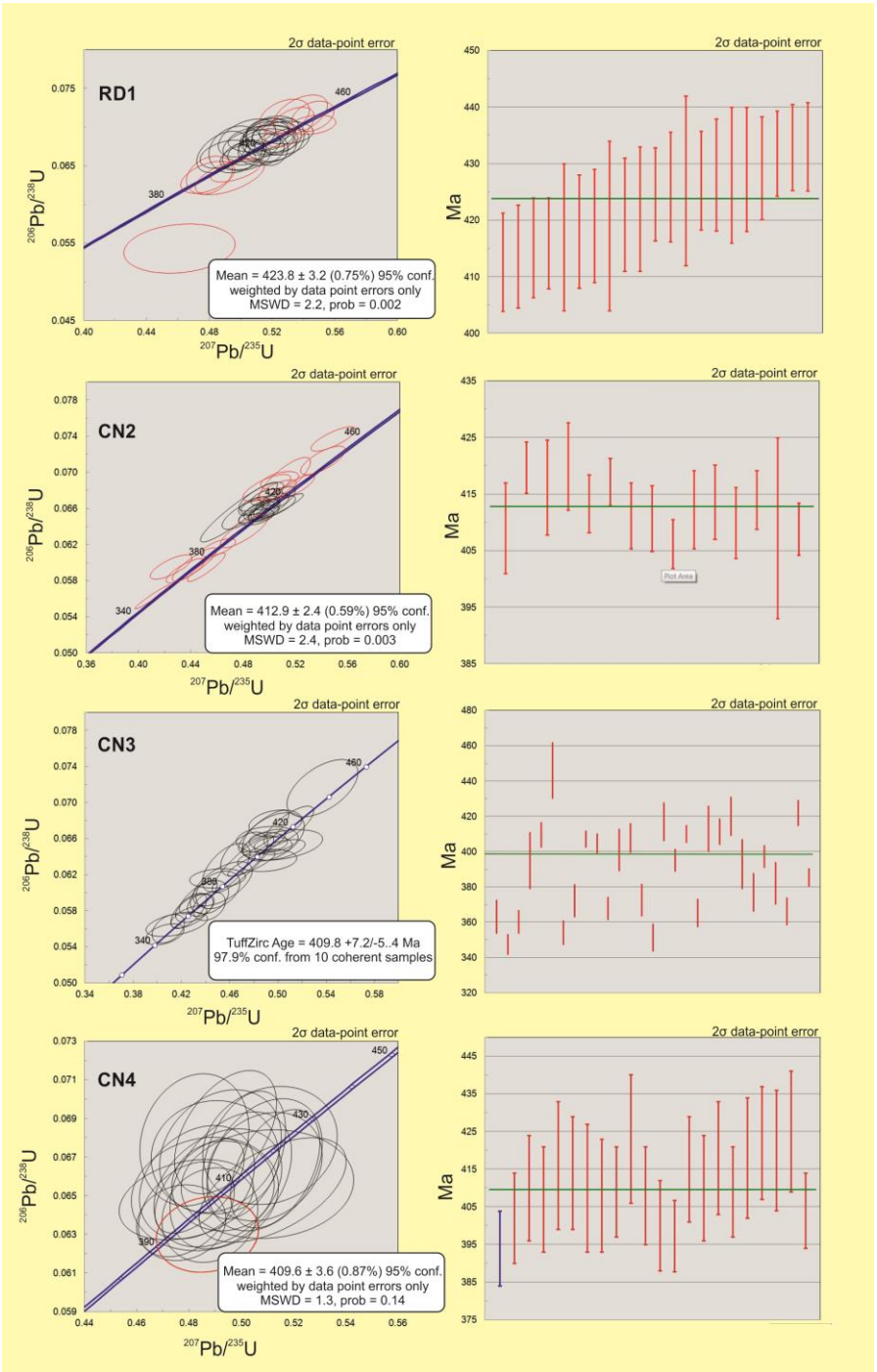


Fig. 9.7 Graphed Zircon U-Pb data. Red circles on isochron plots indicate rejected data points. All red points on bar charts were counted in calculated determined age.

9.3.3 Discussion

Several zircons analysed from three of the four bulk samples (CN2, CN3 & CN4) return apparently younger ages that other analysis carried out on respective block samples. This is most apparent in CN3 which was sampled from strata known to have suffered significant post crystallisation hydrothermal alteration (Derham and Feely 1988; Feely and Högelsberger 1991). CN2 and CN4 were also sampled from strata which exhibit signs consistent with some degree of hydrothermal mineralisation, as is demonstrated from the rock magnetic data below. Standards ran during the analytical procedure do not show a similar data spread thus indicating the observed results are real and reflect inherent features of the zircons analysed. In contrast to this, RD1 returned only one analysis which was highly discordant and all other data points cluster on the concordia and show little evidence for inheritance or post crystallisation disruption to the U-Pb chronometer.

Data which return discordant or anomalously young ages on the concordia in samples CN2 and CN4 are attributed with Pb-loss during post crystallisation hydrothermal alteration and these are rejected. Several data points in RD1 and CN2 exhibit unrealistically older results which are considered to be a product of inheritance and thus are also rejected. From the remaining data mean age determinations have been calculated as follows; RD1 = 423.8 ± 3.2Ma, CN2 = 412.8 ± 2.4Ma and CN4 = 409.6 ± 3.6Ma.

Data from sample CN3 are treated separately owing to the degree of disruption to the U-Pb system. Again, younger and older data points are considered a product of hydrothermal disruption leading to Pb-loss and zircon inheritance respectively. The mean age calculated from a reduced data set returned a U-Pb age of 405 ± 3.8Ma (0.95% error) from a set of 13 analysis. Although this determination is appealing due to a low margin of error, it omits a large portion of the data set, appears excessively low and is inconsistent with previous work (Selby *et al.* 2004). Through the application of "TuffZirc" statistical analysis of the entire data, an alternative determination was calculated (409.8 +7.2/-5.4Ma). This function implements the TuffZirc algorithm of Ludwig and Mundil (2002) for extracting reliable ages and age-errors from suites of $^{206}Pb/^{238}U$ dates on complex single zircon or domains within single zircons. If the TuffZirc algorithm can find a coherent (i.e. statistically within analytical error) group of at least five analyses (or 0.3 × total number of analyses, whichever is larger), the age and uncertainty of the median of the coherent group is calculated. This function can tolerate up to 70% of the data being non-cogenetic within eruption / emplacement age, (i.e. xenocrystic, non-zero magma-residence time, or suffered Pb-loss). The algorithm produces an asymmetrical uncertainty expanded in the

direction of most complexity and will at best produce an error comparable to that of the most precise analysis used in the calculation (*pers. comm.* Quentin Crowley). Despite the increased margin of error, the TuffZirc determination is accepted as the most accurate age of crystallisation as it utilises the entire data set and returns a value which is consistent with field and existing isotopic data and at the same time realistically reflects the degree of uncertainty.

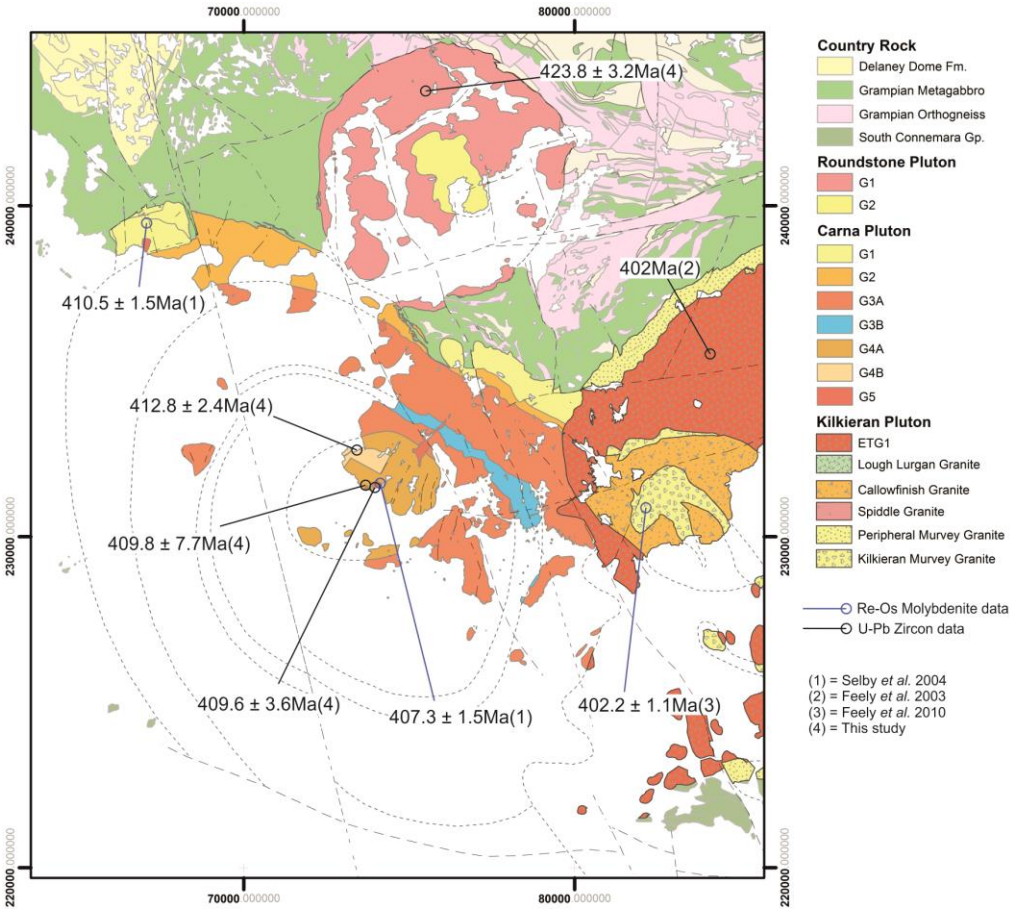


Fig. 9.8 Compilation of old and new chronological data for the Carna and Roundstone plutons (Leggo *et al.* (1966) and Pidgeon (1969) omitted).

This work shows that the youngest facies of the Carna pluton (G5) intruded at ~ 409Ma and the latest main facies (G4a), for which isotopic data are available, intruded at 412.8 ± 2.4Ma (Fig. 9.8). Field relationships show it is most probable that G3, G2 and G1 are all older than the determined age for G4a but no data are available to substantiate this claim at this time. Current age determinations compliment Re-Os chronological data which indicate secondary mineralisation (stockwork quartz-molybdenite-chalcopyrite-pyrite) at Mace Head occurred due to hydrothermal alteration at 407.3 ± 1.5Ma (Selby *et al.* 2004). Data from RD1 shows that G1 had crystallised by 423.8 ± 3.2Ma and thus predates the Carna Pluton by a substantial amount (*c.f.* Leake (2011)). Therefore, the Roundstone Pluton is the oldest confirmed member of the GGC

however it is probably that the Omey Pluton is older as existing Re-Os data show secondary mineralisation occurred at 422.5 ± 1.7Ma and thus the Omey Pluton had been intruded prior to this time.

9.4 Rock Magnetic Analysis

A series of rock magnetic tests were carried out to elucidate the internal structure of the Carna Pluton chiefly through AMS analysis. Rock magnetic experiments were conducted to determine each facies' magnetic mineralogy to verify interpretation of AMS data (Chapter 6).

9.4.1 Sampling

In total, 134 orientated block samples were collected, of these 15 were duplicates. Samples were collected at 400-700m intervals, a higher sample density was collected from the Dogs Bay area to investigate the relationship between faulting and emplacement fabrics in this area. On average, 13 21x25mm cylindrical sub-specimens were cored from each block sample using a non-magnetic diamond coring drill bit following the parameters set out by Owens (1994). AMS analysis was carried out at Birmingham University.

The Carna Pluton underwent post emplacement hydrothermal alteration and mineralisation (Feely and Högelsberger 1991; Suzuki *et al.* 2001; Selby *et al.* 2004). This could drastically affect ferromagnetic and paramagnetic mineralogy, and hence the AMS tensor, and potentially invalidate AMS as a proxy for anisotropy relating to emplacement/early post-emplacement deformation. To address this possible source of error a suite of rock magnetic experiments was applied to 31 representative core samples to characterise magnetic mineralogy (Table 9.2). Rock magnetic experiments were carried out in New Mexico Highlands University (procedures in Appendix B, full data in Appendix E).

Facies	AMS	Curie Point Estimates	Cryogenic Susceptibility	Lowrie-Fuller Test	SIRM-Acquisition and BIRM	3 Component Demagnetisation
G1	20	4	4	4	4	3
G2	51	15	8	10	10	3
G3	40	5	1	2	2	1
G4	20	5	4	5	5	4
G5	3	2	1	2	2	1
Total	134	31	18	23	23	12

Table 9.2 Summary of number of samples which underwent different rock magnetic experiments.

9.4.2 Results of Rock Magnetic Experiments

Fluctuation of Susceptibility with Temperature

Low field magnetic susceptibility of powered samples was measured continuously during stepwise heating and cooling between room temperature and 700°C. A representative sample of data collected is presented in Figure 9.9 and a summary of all data in Table 9.3. Reasonably well defined Hopkinson's peaks are identified for most samples, the Curie Temperature (T_C) was most often reached between 573-582°C (approximated after Moskowitz (1981) or (Tauxe 1998)). An increase in susceptibility on cooling is the norm and this varies from 5-20% up to 1000% in one sample (G2.42). As observed from samples from Omey and Roundstone, distinctive "bumps" are noted on the heating curves of some samples which are absent from the associated cooling curves, these samples exhibit a greater increase in susceptibility during cooling.

Several outliers are noted including those with reduced T_C values (e.g. G1.15 T_C = 546°C) and those with T_C values higher than that of stoichiometric magnetite (e.g. G5.1 G5.2 G1.17). Some samples did not yield a clear T_C. Of particular interest are samples G1.19, G4.5 and G4.15 which return only very weak susceptibility values on heating and cooling, this indicates an absence of or extremely low modal abundance of ferromagnetic minerals in the original sample. Sample G1.15 also returns very low susceptibly values on heating but two very distinctive peaks at 320°C and 520°C which confirm some minor amount of ferromagnetic material must be present.

Subsequently, the low temperature susceptibility characteristics of 18 selected samples was recorded during progressive heating from -198°C to 12°C (Fig. 9.10). The majority of samples pass through the Verwey Transition (T_V) before reaching -175°C (Verwey 1939). These results are in

agreement with T_C estimates and indicate the presence of low Ti titanomagnetite (Özdemir *et al.* 1993; Petrovský *et al.* 2006; Jackson *et al.* 2011).

No distinctive spike in susceptibility is observed in three samples (G1.15, G1.19 and G4.5) and instead a gradual decrease in susceptibility from -180°C to room temperature is recorded. These samples correspond to those which returned diamagnetic-paramagnetic curves between room temperature and 700°C and very low K_{mean} values during AMS analysis (see below). Such behaviour is consistent with the absence of significant amounts of ferromagnetic minerals and the predominance of paramagnetic silicate minerals over the AMS tensor (Tarling and Hrouda 1993; Dunlop and Ozdemir 1997).

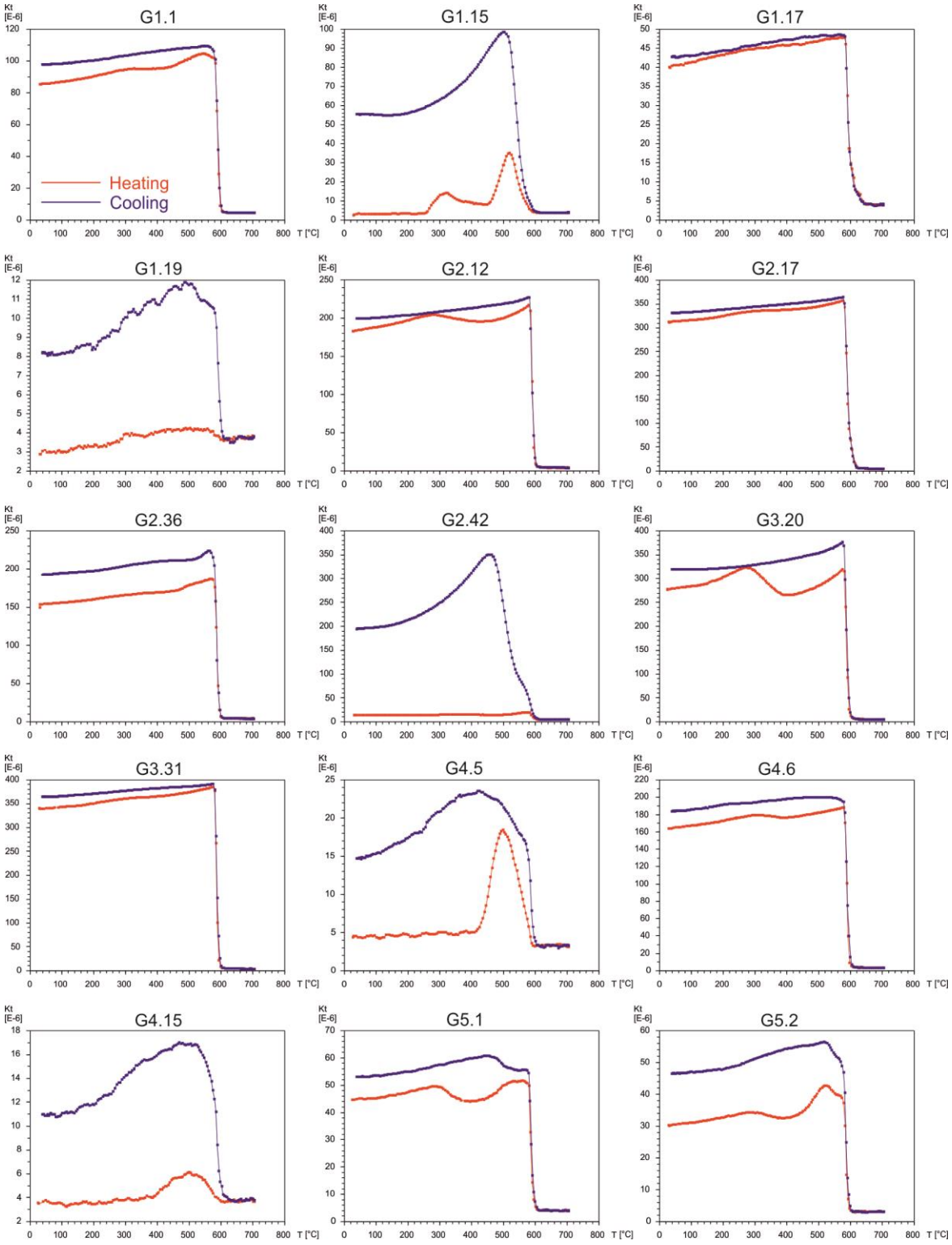


Fig. 9.9 Graphed data from high temperature low field susceptibility experiments, blue = cooling, red = heating. Note several samples exhibit distinct "bumps" at 300°C which are not present on the corresponding cooling curves.

SAMPLE	HEATING		COOLING		SAMPLE	HEATING		COOLING	
	T_C	Ti (x)	T_C	Ti (x)		T_C	Ti (x)	T_C	Ti (x)
G1.1	580	0.00	578	0.01	G2.45	579	0.01	579	0.01
G1.15	546	0.06	576	0.01	G2.46	577	0.01	579	0.01
G1.17	582	0.00	580	0.00	G2.47	577	0.01	576	0.01
G1.19	NA	NA	582	0.00	G2.50	578	0.01	578	0.01
G2.12	580	0.00	582	0.00	G3.20	580	0.00	579	0.01
G2.17	578	0.01	577	0.01	G3.26	551	0.05	284	0.47
G2.18	580	0.00	580	0.00	G3.29	580	0.00	580	0.00
G2.19	578	0.01	577	0.01	G3.31	576	0.01	576	0.01
G2.20	579	0.01	579	-0.01	G3.36	579	0.01	577	0.01
G2.29	579	0.01	583	0.00	G4.15	NA	NA	591	0.00
G2.36	576	0.01	578	0.01	G4.16	577	0.01	580	0.00
G2.36	579	0.01	573	0.02	G4.2	577	0.01	577	0.01
G2.38	573	0.02	576	0.01	G4.5	NA	NA	580	0.00
G2.42	580	0.00	531	0.08	G4.6	579	0.01	578	0.01
G2.43	577	0.01	578	0.01	G5.1	581	0.00	580	0.00
G2.44	579	0.01	577	0.01	G5.2	587	0.00	587	0.00

Table 9.3 Summary of high temperature susceptibility experiments (Curie point estimates).

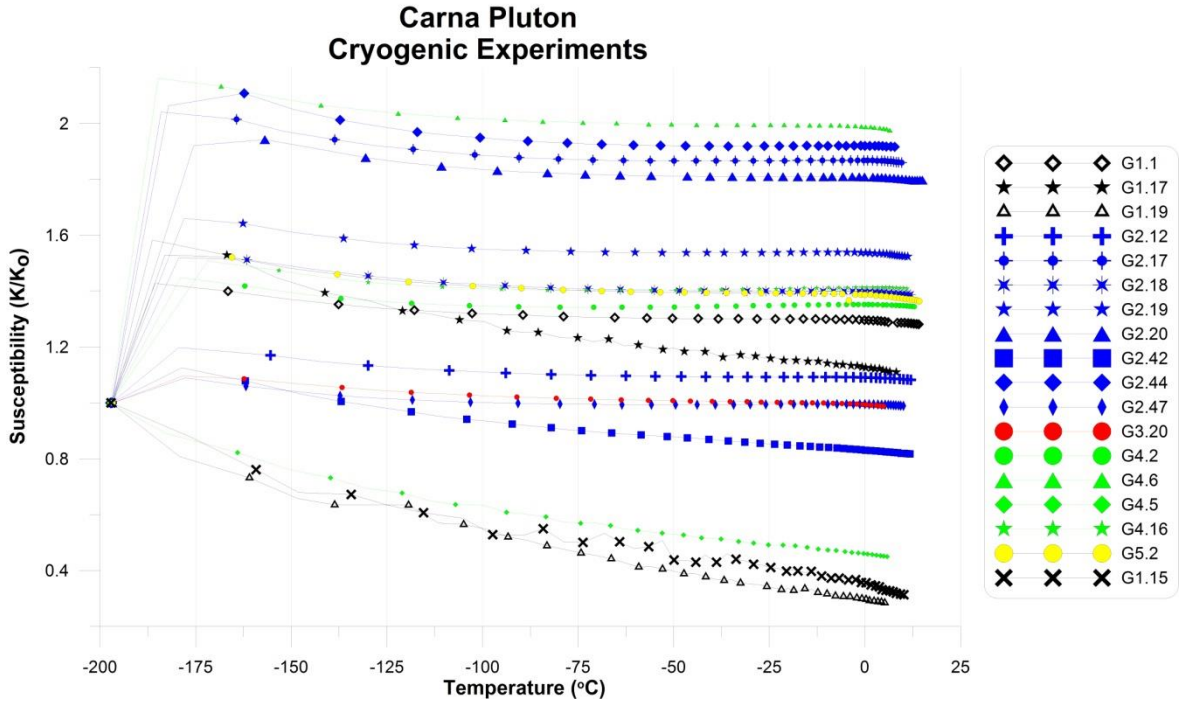


Fig. 9.10 Graphed results of cryogenic low field susceptibility experiments. Only three samples do not show a defined Verwey Transition (G1.15, G1.19 and G4.5) which indicate the paramagnetic fraction may heavily influence the AMS tensor.

Progressive heating Experiments

During heating from 0-700°C, both G3.20 and G1.15 show a "bump" on the heating curve at ~ 250-350°C as well as a net increase in susceptibility at the end of the experiment (G1.15 30 → 480 (SI), G3.20 300 → 360 (SI)). As the T vs. K curve is not reversible a change in magnetic mineralogy is indicated.

To investigate the origin of the ~ 300°C "bump", G3.20 and G1.15 were selected for progressive stepwise heating experiments. Modified from Hrouda (2003), the variation of susceptibility of powdered samples was measured over progressively higher temperature intervals to determine the conditions under which significant variations in susceptibility occur. These variations are diagnostic of the presence of various silicate, sulphide and Fe-Ti oxide phases as the susceptibility response to phase breakdown, inversion or oxidisation to form single or multiphase constituents is reasonably well constrained (Dunlop and Ozdemir 1997).

This experiment was executed in an argon atmosphere to impede oxidisation, however adverse affects of intercrystalline O_2 could not be totally eliminated (discussed in Petronis *et al.* (2011)). Heating intervals were tailored to each specimen according to the behaviour of each specimen in earlier experiments (i.e. temperatures at which phases changes were indicated). For G1.15, intervals of 20°C were selected between 240-450°C and 50°C between 450-600°C and finally 100°C between 600-700°C. G3.30 required a higher resolution of data at higher temperatures and thus 25°C temperature increments were applied between 220-620°C and finally 80°C between 620-700°C.

In both cases minimal change is observed below 250°C after which point each sample behaves in a distinct manner.

G1.15 shows an abrupt increase along the cooling curve once the 250°C threshold is broken, this relative increase remains constant up to 400°C, a second abrupt change in susceptibly along the cooling curve is noted at 400°C and becomes more punctuated as samples are exposed for longer periods to higher temperatures (Fig. 9.11). Based on these results two distinct phase changes are interpreted, the first at 250°C and the second continuously between 400-700°C.

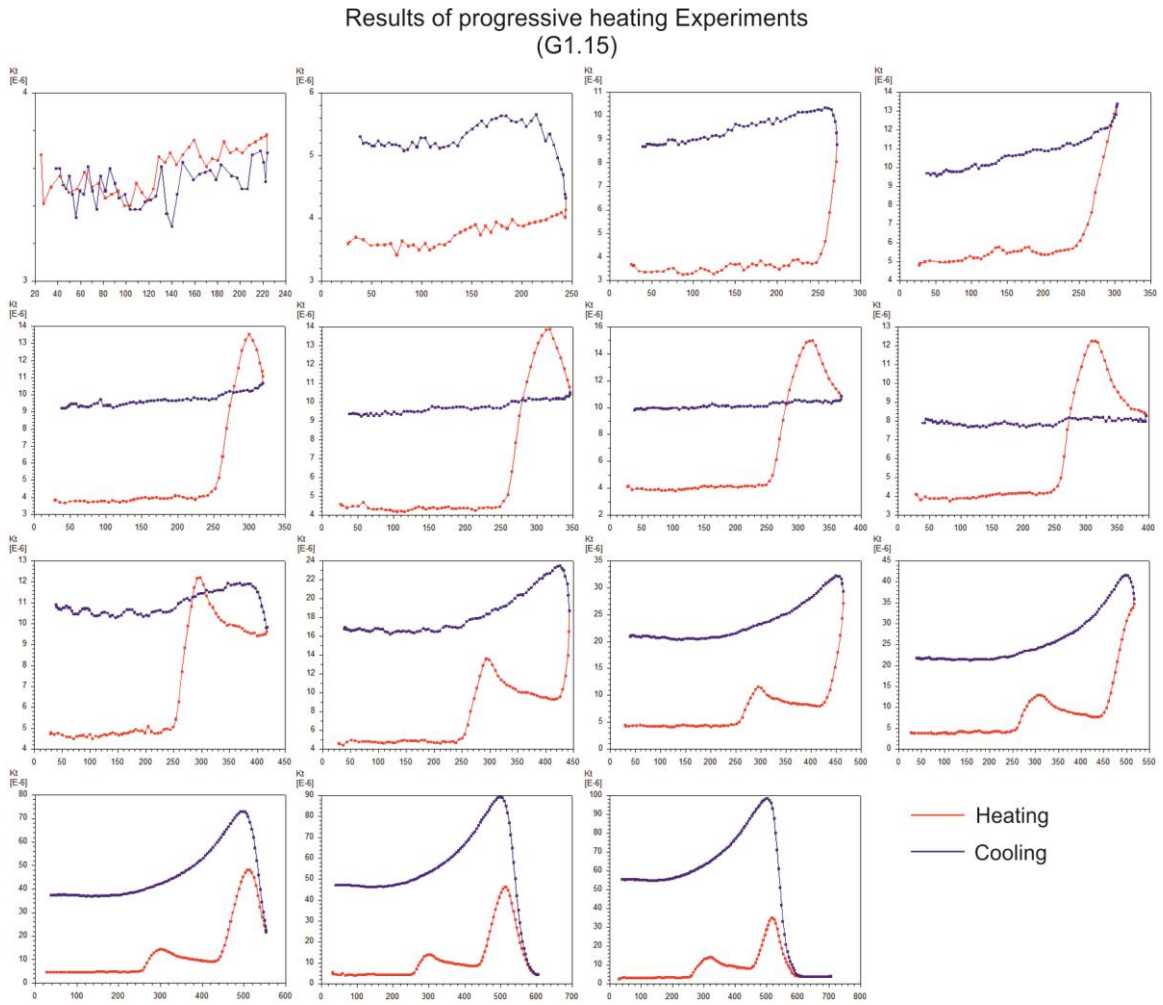


Fig. 9.11 Progressive stepwise heating of G1.15 shows no net change in susceptibility occurs prior to 250°C, over this temperature a net increase is observed on the cooling curve which stabilises up to 400°C. From 400-600°C a second increase in susceptibility is recorded, over this temperature range the relative magnitude on the cooling curve progressively increases as the sample is exposed to higher temperatures over longer time intervals. The heating curve "bump" is fully erased from the cooling curve by 325°C.

G3.20 is distinct in that the 250-350°C "bump" is followed by a net decrease in susceptibility on the heating curve at intervals between 330-450°C (Fig. 9.12). In contrast to G1.15 a net decrease in susceptibility (relative to pre-heating K) also accompanies removal of the "bump" along the cooling curve between these temperature intervals. Furthermore, between 450-520°C a very pronounced increase on the heating curve (T_C) is followed by a distinct increase in susceptibility along the cooling curve which stabilises and does not show any further relative increase when samples are exposed to temperatures in excess of 520°C. Based on these results a breakdown of some ferromagnetic phase (*senso lato*) is interpreted to have occurred at 280-330°C that was replaced by a mineral of lower susceptibility at temperatures below 450°C. Between 450-520°C a second new ferromagnetic phase is crystallised.

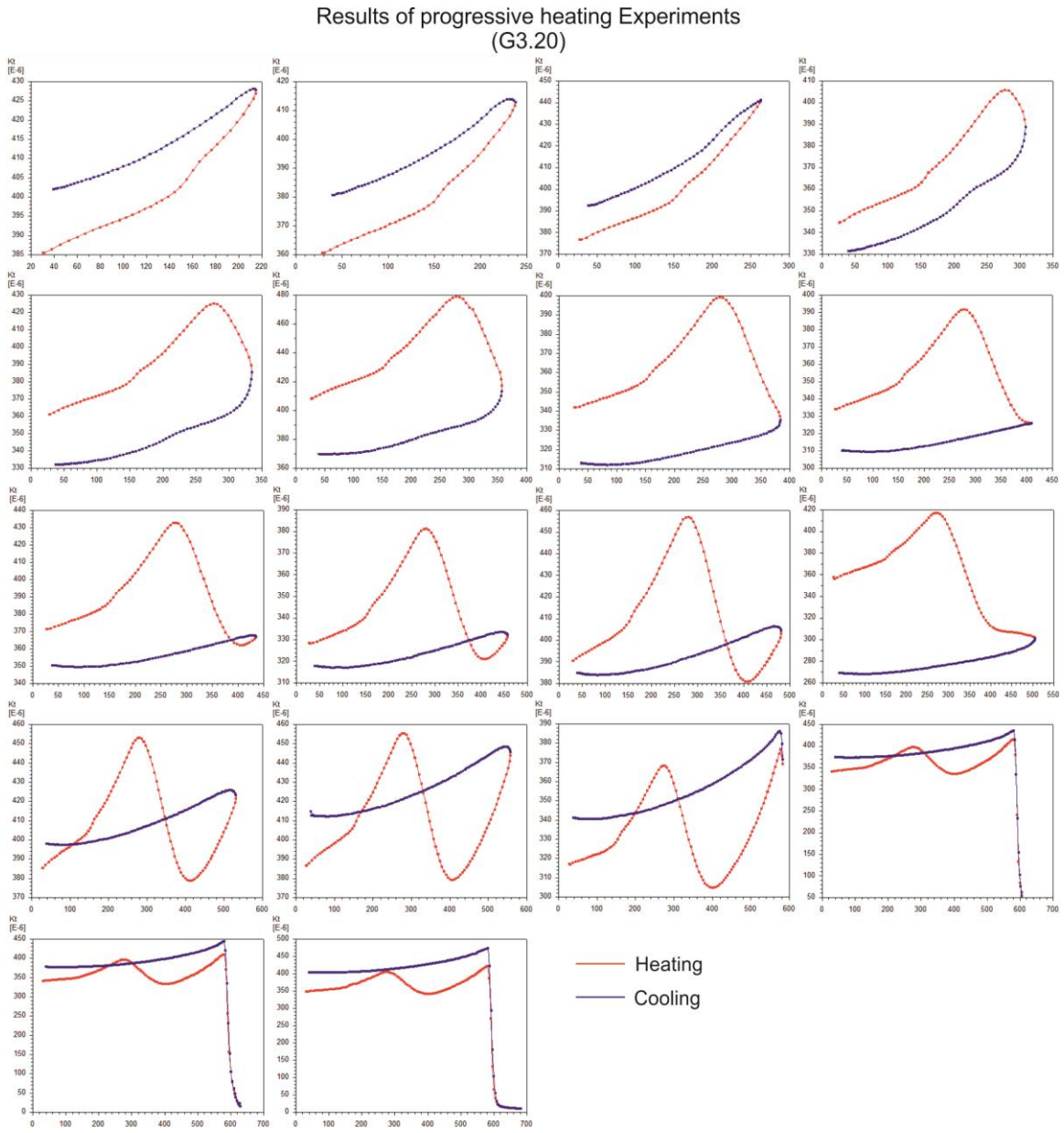


Fig. 9.12 Progressive stepwise heating of G3.20 shows defined "bump" between 250-350°C. No net change in susceptibility occurs prior to 250°C. Between 250-450°C a net decrease in susceptibility is noted on the cooling curve and the "bump" is erased. From 450-520°C an abrupt increase on the heating curve is accompanied by a net increase on the cooling curve. This sharply contrasts the results of G1.15 as susceptibility on the cooling curve initially decreases at lower temperatures and then increases at a much more abrupt rate over 450°C.

Lowrie - Fuller Test

The Lowrie - Fuller test (Lowrie and Fuller 1971) was carried out on 23 samples in order to evaluate the coercivity parameters of dominant magnetic minerals at each sample site (Fig. 9. 13). The majority of samples show exponential demagnetisation of NRM, ARM and IRM in low AF demagnetising fields, the MDF is typically reached prior to 25mT. ARM is more stable in 19 of 23 cases and thus the majority of specimens return an L type result (Xu and Dunlop 1995). These data are consistent with the presence of a coarse grained titanomagnetite phase as the dominant

ferromagnetic mineral in these samples despite returning S-type Lowrie - Fuller results (Dunlop and Ozdemir 1997).

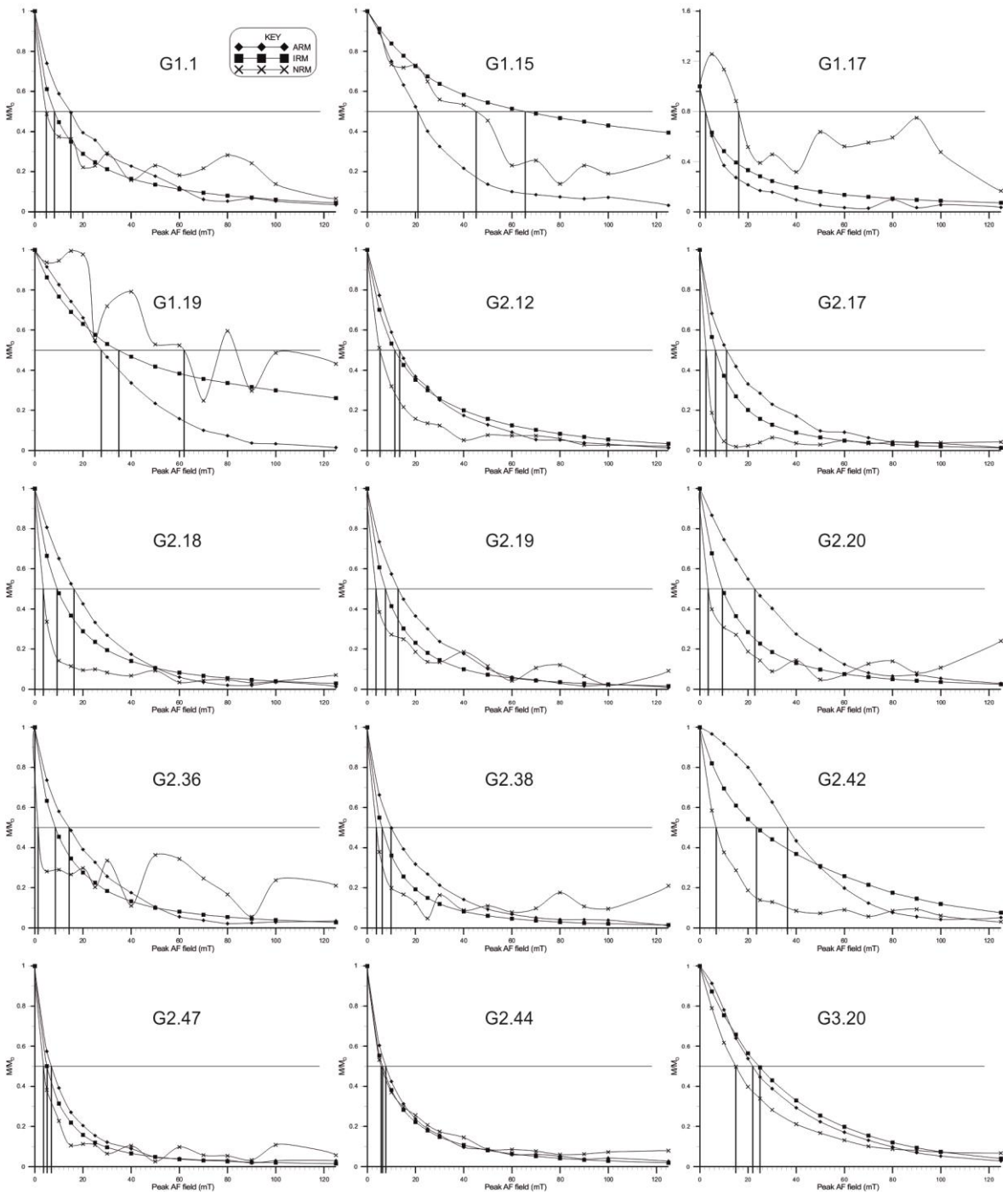


Fig. 9.13 Graphed results of Lowrie-Fuller test (continued below).

The rate of demagnetisation of weak field remanent magnetisation (ARM) can be used to approximate grain size, and hence domain state, for samples with a prominent magnetite

component (Argyle and Dunlop 1990; Dunlop and Ozdemir 1997). The results above indicate a crude grain size of between 200-1µm in most samples, those with steeper ARM demagnetisation curves containing the coarsest grains.

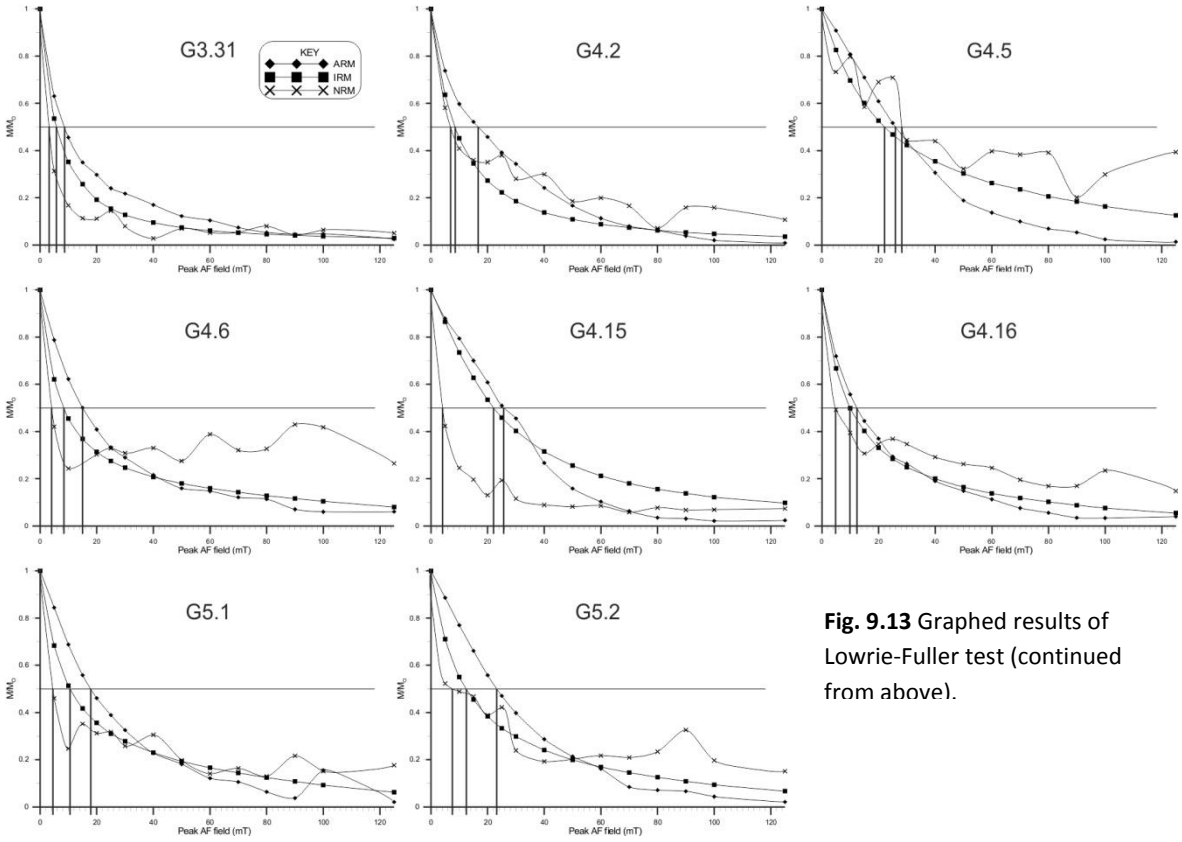


Fig. 9.13 Graphed results of Lowrie-Fuller test (continued from above).

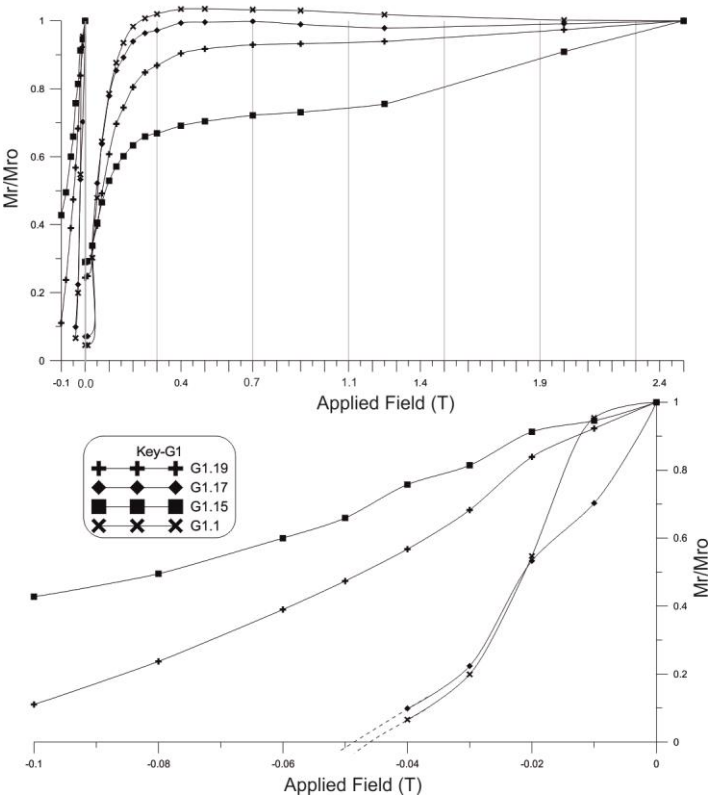
Samples G3.20, G1.15, and G1.19 returned clear H type results (Xu and Dunlop 1995) and require demagnetising fields between of 20-30mT and 25-70mT to reach the MDF for induced ARM and IRM fields respectively. This reflects a more gradual rate of decay under AF demagnetisation. These data are consistent with the presence of fine grained titanomagnetite, moderately oxidised titanomagnetite (i.e. titanomaghemite) or some other high coercivity mineral such as impure hematite.

SIRM and BIRM Properties

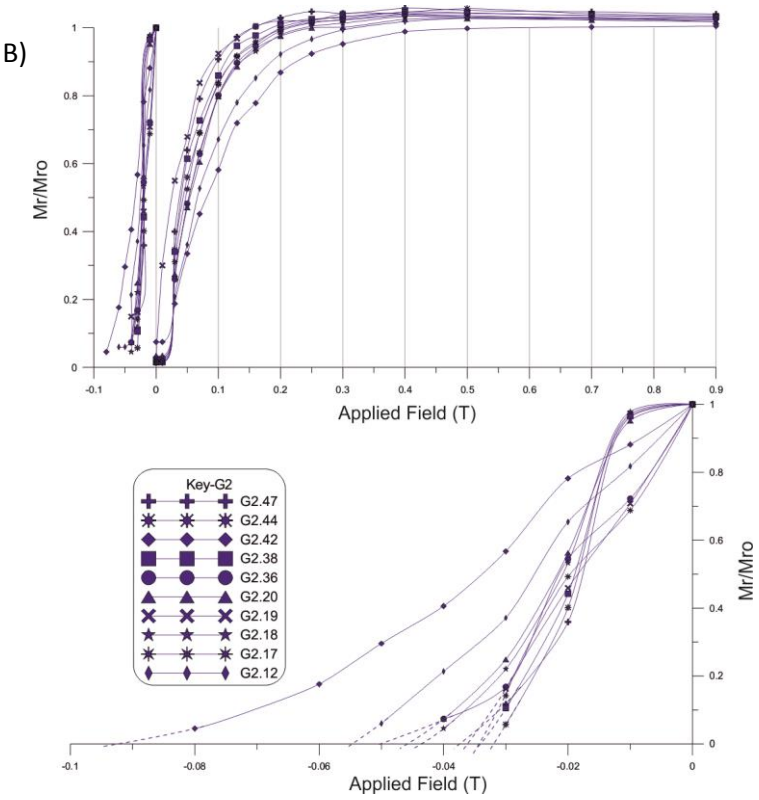
The acquisition and removal of SIRM was measured to constrain the respective coercivity spectra of 23 select samples (Fig. 9.14). Typically, samples reach magnetic saturation (M_S, i.e. 95% saturation) in IRM fields of less than 0.3T and approximated coercivity of remanence (H_{CR}) values are between 0.03-0.06T in the majority of samples across all facies. The most prominent outliers are G1.15, G1.19, G2.42, G3.20, G4.5 and G4.15, which require fields ≥ 0.3T to reach M_S. Of

particular note, G1.19 requires an IRM of 1.5T to reach M_S and G1.15 does not reach full saturation at 2.5T.

A)



B)



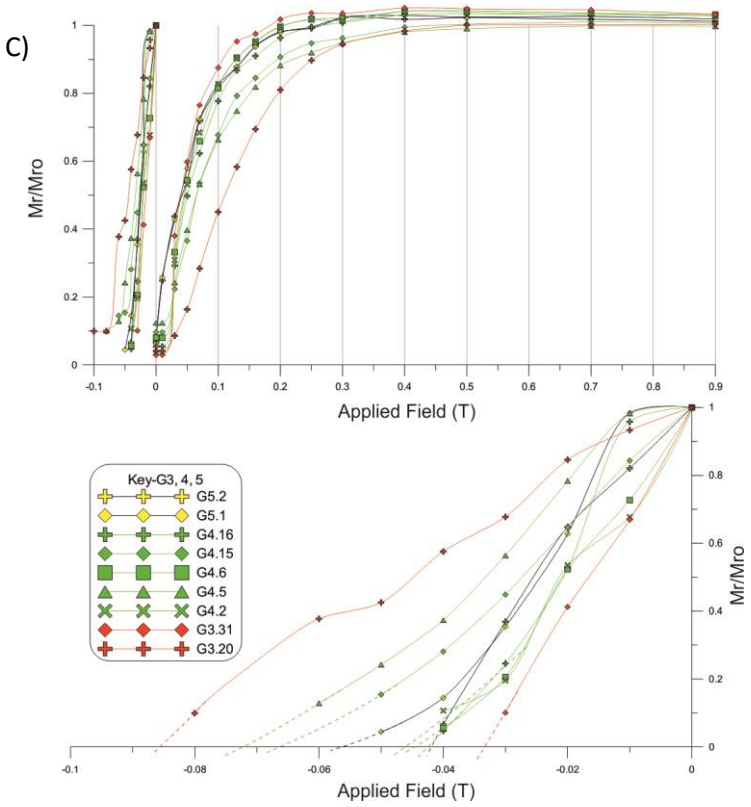


Fig. 9.14 Graphed results of SIRM and BIRM experiments. A) G1 facies return higher coercivity values than G2 (B) or G3, G4 and G5 samples (C).

BIRM estimates for H_{cr} correlate well with SIRM data. These data indicate G1.19 and G1.15 contain larger proportions of a high coercivity phase. Samples G2.42, G3.20, G4.5 and G4.15 contain ferromagnetic minerals of lower coercivity spectra than the G1 samples mentioned but are significantly harder than "typical" specimens of the Carna Pluton, this is consistent with either a finer grain size or significant partial oxidisation of a dominant titanomagnetite phase.

Three-Component IRM Demagnetisation

A total of 12 samples were selected for progressive thermal demagnetisation of three component IRM (Lowrie 1990). IRM fields of 0.03T, 0.3T and 3T were selected in order to constrain the relative contribution made to each samples net magnetic vector by minerals of certain coercivity spectra and unblocking temperature. Emphasis was placed on evaluating the degree of homogeneity between "typical" samples in the pluton and determining the relative importance of high and low coercivity minerals in atypical specimens such as G1.19 and G1.15.

The results of three-component IRM demagnetisation are plotted in Fig. 9.15. The modulus vector in most samples decays at a rapid rate to about 30% of M_S between 200-400°C followed by a more gradual rate of demagnetisation to 95% between 500-600°C. Samples which returned M_S

values between 0.01-0.3T in SIRM experiments are dominated by minerals within the 0.03-0.3T coercivity spectrum. The relative importance of the high and low coercivity contributors varies but a slight bias toward the 3T axes is observed indicating that for a small majority of "typical" samples high coercivity minerals such as titanomaghemite/hematite are more important than very low coercivity minerals such as coarse grained titanomagnetite.

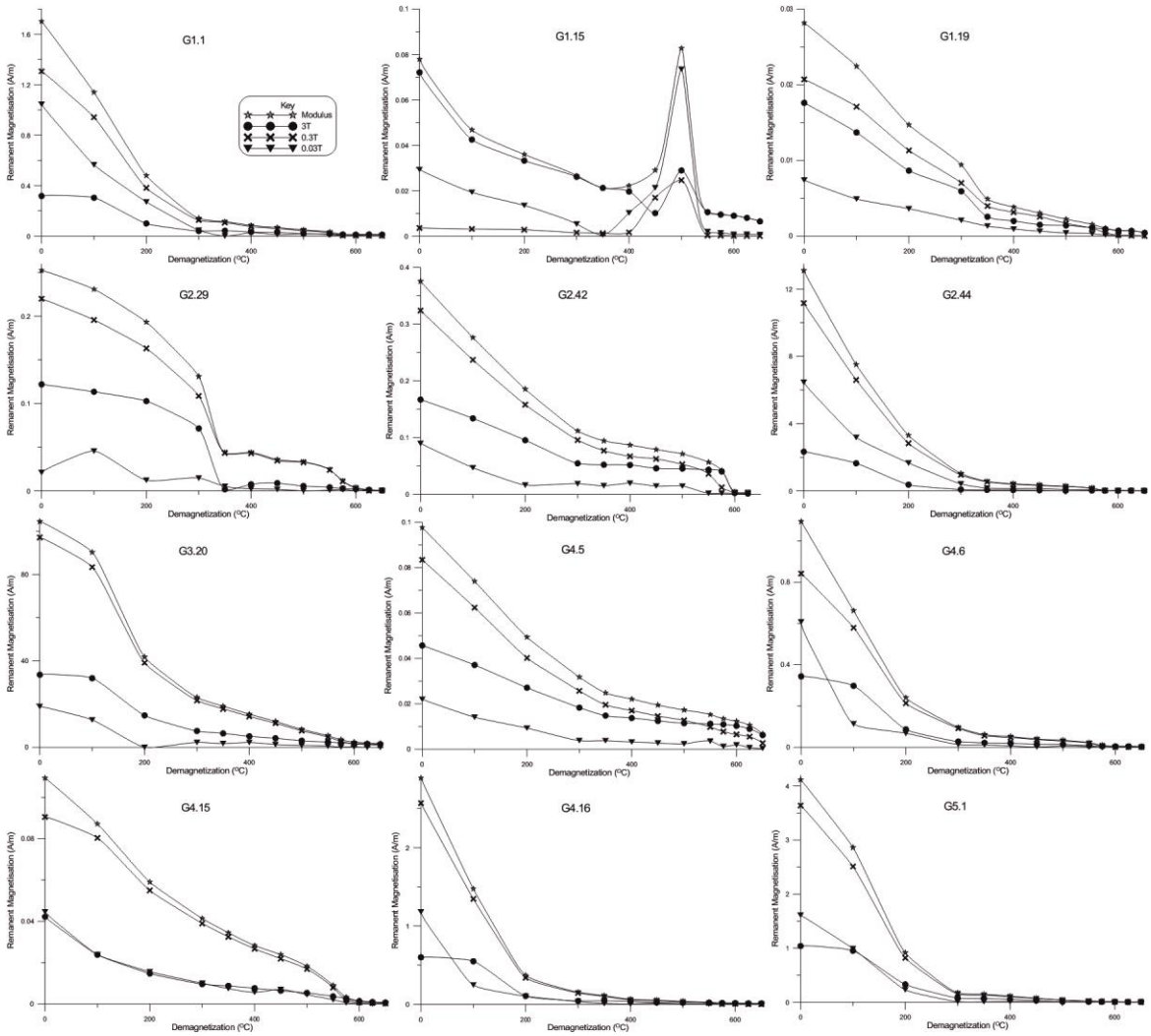


Fig. 9.15 Graphed results of 3 component demagnetisation. The majority of samples are dominated by moderate coercivity minerals (0.3T). G1 samples are atypical and exhibit a large high coercivity fraction.

Predictably, G1.15 is the only sample in which the majority of M_r is carried by high coercivity minerals. Remanence values are extremely low and gradual rate of demagnetisation is recorded between 0-700°C which is consistent with the predominance of maghemite/hematite. A large contribution of M_r in G1.19 is also carried by high coercivity minerals although those within the 0.3T spectrum are slightly more important.

Atypical demagnetisation trends are noted in two samples in particular. G4.5 continues to demagnetise post 600°C and G2.29 is reasonably stable up to 300°C but then rapidly demagnetising to > 30% at 350°C. These features is discussed below relative to other anomalous results returned from the respective sample sites.

9.4.3 Anisotropy of Magnetic Susceptibility Results

AMS data from 134 sample sites are compiled and summarised in Table 9.4. Averaged K_{mean} values for G2, G3, G4 and G5 are significantly greater than the average K_{mean} value for G1. This is directly attributable to the leucocratic G1b and G1c facies which consistently return the lowest susceptibility values in the pluton (~ 30-500 x 10^{-6}).

All Sites					
Parameter	Tj	Pj	lnPj	H%	K x10^{-6}(SI)
Min	-0.63	1.01	0.01	1.1	27
Max	0.94	1.26	0.14	22.6	25384
Mean	0.22	1.08	0.05	7.1	11026
Std. Dev	0.36	0.05	0.03	4.1	7177

G3					
Parameter	Tj	Pj	lnPj	H%	K x10^{-6}(SI)
Min	-0.52	1.01	0.02	3.2	302
Max	0.90	1.15	0.14	22.6	25385
Mean	0.32	1.06	0.06	9.4	16702
Std. Dev	0.32	0.03	0.03	4.7	5799

G1					
Min	-0.50	1.01	0.01	1.3	27
Max	0.88	1.12	0.11	15.9	8359
Mean	0.24	1.04	0.04	6.1	2137
Std. Dev	0.33	0.026	0.03	3.8	2191

G4					
Min	-0.40	1.01	0.01	1.1	54
Max	0.85	1.12	0.12	16.9	20955
Mean	0.37	1.05	0.05	7.1	9186
Std. Dev	0.34	0.0267	0.03	3.8	6059

G2					
Min	-0.63	1.01	0.01	1.4	116
Max	0.94	1.13	0.12	20.8	21764
Mean	0.07	1.04	0.04	5.9	11291
Std. Dev	0.36	0.019	0.02	3.1	5527

G5					
Min	0.01	1.01	0.01	1.9	801
Max	0.84	1.04	0.04	5.6	4089
Mean	0.34	1.03	0.03	4.3	2381
Std. Dev	0.36	0.0125	0.01	1.7	1345

Table 9.4 Summary of AMS data for all sites and for each facies.

The corrected degree of anisotropy (Pj, Jelinek (1981)) fluctuates from 1.01-1.26 and has a standard deviation of 0.05, the maximum degree of variance between each facies' mean Pj value is 0.02.Tj varies from highly oblate to triaxial to moderately/strong prolate in all facies. A total of 36 tensors returned a dominantly prolate symmetry, the remaining 98 were dominantly oblate.

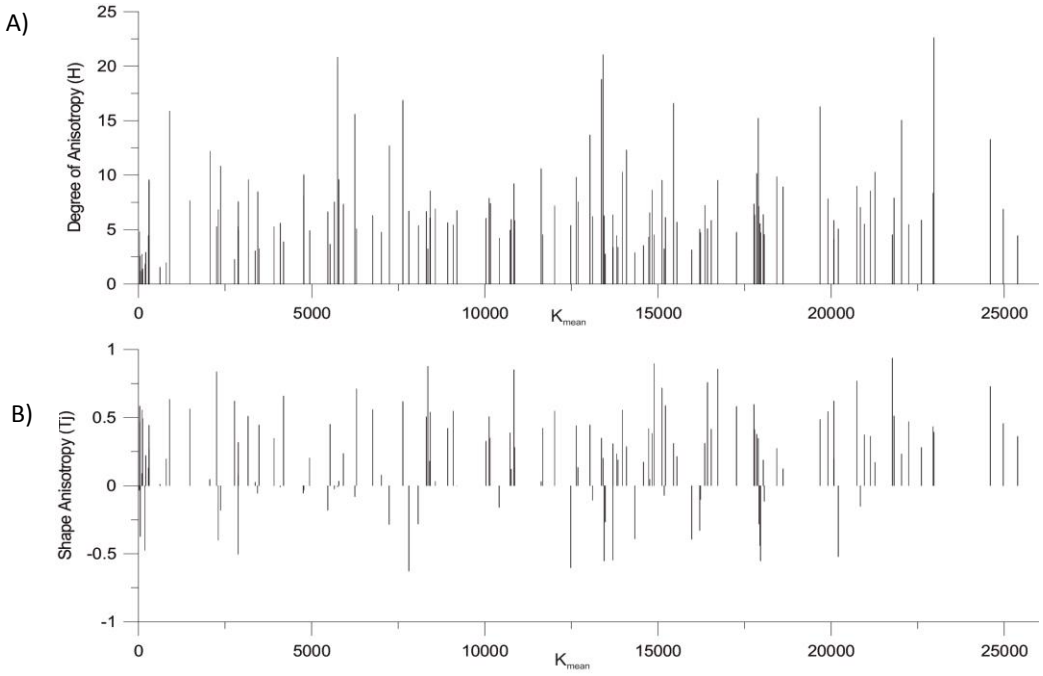


Fig. 9.16 A bar chart of the degree of anisotropy vs. K_{mean} (A) and shape anisotropy vs. K_{mean} (B) shows that even though a broad spectrum of susceptibility values are detected in different facies there is no systematic relationship between H or Tj and K_{mean}.

A bar chart of K_{mean} vs. Tj and K_{mean} vs. H depicts the relationship between the distribution of anisotropy and magnetic susceptibility (Fig. 9.16). These graphs show that no correlation between tensor shape or degree of anisotropy and mean susceptibility is detected. Thus, despite a large variation in K_{mean} values (Table 9.4, most notable between G1 and G2-G5), these data show anisotropy parameters are comparable across all facies. Therefore, while K_{mean} values vary across G1-G5, the shape anisotropy and degree of anisotropy from each facies can still be compared because these values reflect the preferred alignment of dominant magnetic minerals and do not fluctuate significantly with K_{mean} in this data set.

9.5 Discussion of Magnetic Data

The majority of samples return remanence, demagnetisation and susceptibility characteristics which are indicative of the presence of low Ti weakly maghematized titanomagnetite. Samples with anomalously low K_{mean} values are unique to these observations and are discussed separately. An increase in maghemitization and the presence of ferromagnetic iron sulphides in some samples characterises a low temperature post emplacement hydrothermal alteration assemblage which is distinct from the weakly hematized diuretic Fe-Ti oxide ferromagnetic assemblage.

9.5.1 Magnetic Assemblage

Mean susceptibility values are in the order of 20 - 5 x 10^{-3}(SI) for the majority of samples. This is consistent with the presence of magnetite in sufficient quantities to dominate the AMS ellipsoid (Tarling and Hrouda 1993). Cryogenic and high temperature low field susceptibility data exhibit well defined Verwey transitions (< -175°C) and Curie points (~ 570-582°C). These data support the above generalised interpretation but indicate that a low Ti titanomaghematite dominates rather than straight forward Fe_3O_4 as T_C values fall both just below and above that of stoichiometric magnetite (Readman and O'Reilly 1972; O'Reilly 1976). A typical Ti component of X < 0.1 and oxidisation parameter of Z < 0.02 is predicted (Akimoto 1962; Readman and O'Reilly 1972; Nishitani and Kono 1983; Moskowitz 1987; Petrovský *et al.* 2006).

If magnetite/titanomagnetite predominantly occur as multidomain (MD) and/or pseudo-single domain (PSD) grains a normal AMS fabric is generated however single domain (SD) grains are characterised by inverse AMS fabrics (Potter and Stephenson 1988; Tarling and Hrouda 1993; Borradaile and Jackson 2010). Grain size can be approximated from the shape of the Curie Point on heating as abrupt well defined peaks are indicative of progressively finer grains which approach SD state (Orlický 1990). The current data set show a majority of heating curves do not posses SD like Hopkinson's peaks. This is consistent with results of the Lowrie - Fuller test which show exponential AF demagnetisation of NRM and artificial weak and strong field remanence. Despite returning SD type results (Lowrie and Fuller 1971), these curves are interpreted to reflect the presence of magnetically soft spinel Fe-Ti oxide phase (Xu and Dunlop 1995) with a limited range of grain sizes within the PSD and MD field (Argyle and Dunlop 1990). This interpretation concurs with hysteresis parameters (also dependent on Ti composition (Day *et al.* 1977) and the level of maghemitization (Hauptraan 1974; Nishitani and Kono 1983)) determined from SIRM and BIRM data which show M_S and H_{cr} is reached in fields characteristic of samples dominated by a soft MD-PSD weakly oxidised Ti magnetite phase (Dunlop and Ozdemir 1997). Three component demagnetisation data show M_r is dominated by strongly magnetic minerals which are saturated in fields between 0.03-0.3T, again this is consistent with the dominance of a MD titanomaghematite phase. These data also show the bulk remanence vector has both high and low coercivity contributors minerals which probably reflect slight contrasts in maghemitization and Ti content of titanomagnetite phases respectively.

The above points highlight that in almost every case M_r is controlled by a composite of several phases including magnetite-titanomaghemite, hematite and possibly some pyrrhotite. A low Ti weakly oxidised titanomaghemite is the most abundant and considering this minerals mass

susceptibility, relative to that of other constituents (magnetite - maghemite = 578 - 500 x 10^{-8} Si/kg vs. hematite = 25 Si/kg; pyrrhotite = 0.1-20 Si/kg (Dunlop and Ozdemir 1997)), is also the most important contributor to the AMS tensor.

Several samples exhibit very low K_{mean} values, of these G1.15, G1.19, G4.5 G4.15 and G3.20 are particularly anomalous. T vs. K data demonstrate that, with the exception of G1.19, all of these samples test positive for the presence of some quantity of ferromagnetic minerals. G1.19 shows a paramagnetic heating curve and a strong MD magnetite Curie Point on the cooling curve which probably reflects the exsolution of magnetite from constituent biotite at high temperature (Wones and Eugster 1965; Czamanske and Mihalik 1972; Whalen and Chappell 1988). Cryogenic susceptibility data support these findings but clearly indicate minimal quantities of ferromagnetic minerals are present in G1.15 and G4.5. A strong correlation is noted across the data set where those samples which return low susceptibility values exhibit low M_r and higher coercivity values. This is interpreted to relate to the relative portions of ferromagnetic minerals present rather than the overall quantity of minerals of contrasting coercivity spectra present in a sample (i.e. samples with low susceptibility have less cubic Fe-Ti oxides rather than more rhombohedral Fe-Ti oxides).

The AMS tensor in samples with K_{mean} values of less than $5x10^{-4}$ are likely to be controlled by ferromagnetic (senso lato) and paramagnetic constituent minerals (Borradaile 1987; Rochette 1987; Hrouda and Jelínek 1990; Tarling and Hrouda 1993). Three component demagnetisation data show that, in this case, samples with very low K_{mean} values do contain moderate-low coercivity minerals (0.3-0.03T) but that high coercivity constituents are always very significant contributors to bulk remanence. Petrographic observations clearly show that all facies contain some biotite and often hornblende (details in Leake (2011)). No tourmaline is present, thus complexities relating to its inverse magnetic anisotropy (Tarling and Hrouda 1993; Bouchez *et al.* 2006) is avoided. Despite the presence of some ferromagnetic minerals, it is concluded from this data that the AMS tensor in low susceptibility samples is likely dominated by paramagnetic phases with a minor ferromagnetic contribution.

These data proves that drastically different assemblages (dominantly paramagnetic vs. dominantly ferromagnetic) generate the AMS of some neighbouring samples. However it is plain to see that, despite differing mineralogical controls, neighbouring samples return AMS tensors with very similar shape parameters even though the relative magnitude of these tensors is quite different. This infers a common causative force behind anisotropy (flow or deformation of crystals) and proves that, here, only the magnitude of the tensor is dependent on the mineralogy.

9.5.2 Genesis of Ferromagnetic Assemblage

If cooled rapidly from high temperature, titanomagnetite will crystallise as a fine grained homogenous single phase mineral with a relatively high Ti composition (Dunlop and Ozdemir 1997). At moderate-high temperatures (< 600°C), under oxidising conditions, iron-rich single phase silicates and oxides exsolve toward end members of the ulvospinel-magnetite or ilmenite-hematite solid solution series to form a dual or multiphase Fe-Ti oxide during deuteric oxidation (Buddington and Lindsley 1964; Wones and Eugster 1965; Czamanske and Mihalik 1972; Whalen and Chappell 1988; Tarling and Hrouda 1993). This process is known to lead to a predominance of deuteric, near stoichiometric, magnetite (Ti and O poor) in cooling granitic rocks (Haggerty 1976). It is interpreted that the "primary" (i.e. immediately after crystallisation of the silicate groundmass, pre-hydrothermal alteration) ferromagnetic assemblage in the Carna Pluton formed via the slow cooling of magma through a combination of the above exsolution processes. Subsequently the process of maghemitization caused minor oxidisation about the periphery of the coarse grained primary titanomagnetite.

Distinct from this are data which indicate a post crystallisation modification of the Fe-Ti oxide assemblage. Some results of high temperature low field susceptibility experiments return strongly irreversible heating-cooling thermo-magnetic curves. This is characterised by the presence of a small increase, or "bump", in susceptibility between 250-400°C during heating and a net increase in susceptibility on the cooling curve. In several specimens, disseminated iron sulphides have been observed, these are documented in Derham and Feely (1988); Feely and Högelsberger (1991) and Selby *et al.* (2004). These features and data indicate an inhomogeneous ferromagnetic assemblage is present, as well as some S^{2-} phases, in some samples and that homogenisation occurred during heating experiments.

Numerous studies have documented the process of oxidation under differing temperature - oxidisation regimes (Buddington and Lindsley 1964; Ade-Hall *et al.* 1971; Haggerty 1976; Torsvik *et al.* 1983; Lapointe *et al.* 1986; Trindade *et al.* 1999; Just *et al.* 2004; Petronis *et al.* 2011; Just and Kontny 2012). In relation to the current study the literature referred to may be summarised by stating that:

1. The composition and textural features of a Fe-Ti assemblage is sensitive to the chemical and temperature conditions during and after cooling of a magma (Lindsley 1991).

2. Where present, a cubic Fe-Ti oxide phase or phases will most often control the AMS tensor (Tarling and Hrouda 1993).

Susceptibility and coercivity values may be determined by the oxidation state of Fe-Ti oxides alone and be independent of modal abundances and grain size (Lapointe *et al.* 1986). It follows that these assemblages may provide an opportunity to assess and distinguish post emplacement hydrothermal events (Torsvik *et al.* 1983; Just *et al.* 2004; Petronis *et al.* 2011). Interpretation of magnetic parameters should be carried out tentatively as hydrothermal processes can obscure primary relationships. For examples, extensive hydrothermal alteration at divergent plate boundaries on the sea floor may impart an undesirable ChRM that impedes the retrieval of a stable NRM (i.e. TRM) (Irving 1970; Ryall and Ade-Hall 1975; Johnson and Atwater 1977). In an example from Upper Rhine Graben, Germany, Just *et al.* (2004) demonstrated that progressive deformation of a primary magmatic fabric to a tectonic fabric accompanied hydrothermal alteration within a granite pluton. This was attributed to both brittle deformation of the host rock and the growth of new oxide phases which geometrically pseudomorphed "primary" phases but also grew along micro-cracks (Just *et al.* 2004).

Samples G1.15 and G3.20 were selected for progressive reheating experiments. G3.20 exhibits a more prominent "bump" which is followed by a net reduction in susceptibility (less than initial K) while G1.15 did not exhibit the same pronounced trough (Figs. 9.11 & 9.12). Therefore G3.20 is typical of one type of "bump" which was repeated in G5.1 and G5.2 while G1.15 shares more in common with G1.1, G2.12.

Results show a mineralogical change in G1.15 initiated and completed under different temperature conditions which occurred in G3.20. In the latter case a reduction in susceptibility on the cooling curve was noted between 280-330°C. This was followed by a defined net increase in susceptibility along the cooling curve which increased in magnitude between 450-520°C. This indicates the removal of some ferromagnetic phase ~ 300°C and the growth of a new phase initiated at ~ 450-500°C. In the case of G1.15, two phases of mineral growth are inferred by the increase in susceptibility over two temperature intervals, (250-400°C and 400-700°C).

Maghemitization is a low temperature topotactic oxidation process which involves the diffusion and oxidisation of Fe^{2} from magnetite ($Fe^{2+}Fe^{3+}{}_2O_4$) to convert to Fe_3O_4 to Fe_20_3 (details in Dunlop and Ozdemir (1997)). This process initiates at low temperatures (>250°C) and is accentuated by fine grain size and hydrating conditions (abundance of OH^-) such as those created

during hydrothermal alteration of plutonic bodies or on the sea floor and (Nishitani and Kono 1983; O'Reilly 1984; Worm and Banerjee 1984; Kelso *et al.* 1991; Dunlop and Ozdemir 1997). The product (titano)maghemite is metastable at ~ T > 300°C and will invert into a two phase cubic - rhombohedra Fe-Ti oxide intergrowth of magnetite or hematite (depending on oxidising conditions) and ilmenite (Readman and O'Reilly 1970; Marshall and Cox 1972; Readman and O'Reilly 1972) under laboratory conditions. This results in an irreversible heating-cooling curve and is consistent with the presence of titanomaghemite in the original assemblage (Hrouda 2003; Hrouda *et al.* 2006).

The presence of iron sulphides may also cause an irreversible heating-cooling curve. Pyrrhotite has a Curie temperature of 320°C and breaks down at 500°C to form new magnetite (Bina and Daly 1994). This process would cause an decline in susceptibility during heating as pyrrhotite broke down, final susceptibility values would remain low until temperatures were high enough (~ 500°C) to start crystallising new magnetite in place of pyrrhotite.

The current data sets show properties of both inversion of titanomaghemite to magnetite-ilmenite (G1.15) and breakdown of pyrrhotite and subsequent growth of magnetite (G3.20). The relative increase that is observed in G1.15 between 400-700°C is interpreted as oxidisation of minor portions of magnetite from constituent biotite which was exsolved at high temperature (Wones and Eugster 1965). This feature was also noted in G1.19 but not in other samples, probably owing to the relatively high proportions of magnetite already present in the rock sample.

In the cases of G1.15, G1.1 and G2.2, low temperature (< 250°C) oxidisation (maghemitization) promoted the growth of minor quantities of titanomaghemite around the periphery of some titanomagnetite grains. This may have occurred in conjunction with hydrothermal (i.e. mineralisation) activity but not necessarily as maghemitization often occurs as part of routine crystallisation processes and can even occur at the surface (Dunlop and Ozdemir 1997).

Results from G3.20, G5.1 and G5.2 indicate the presence of pyrrhotite. This is not a common feature of plutonic granitic rocks and in this case is believed to be directly associated with the post emplacement Mo-Cu stockwork mineralisation that is associated with localised small scale hydrothermal alteration of the core of the Carna Pluton (Derham and Feely 1988; Feely and Högelsberger 1991; Gallagher *et al.* 1992; Selby *et al.* 2004).

Summary

The above parameters indicate MD, low Ti, weakly oxidised, titanomagnetite (partially oxidised to titanomaghemite) is the dominant ferromagnetic mineral. The grain size, shape and distribution of this mineral is expected to control the AMS tensor in most samples and is expected to be a *normal fabric* (Chapter 6). Paramagnetic minerals dictate the AMS tensor in low K_{mean} samples however attributed anisotropy parameters are still comparable with other samples.

Just *et al.* (2004) demonstrated the possible effects of hydrothermal alteration on the AMS tensor and the issues associated with using affected data as a proxy for magmatic flow/syn-emplacement strain. The current data set show some samples have been hydrothermally altered and return tensors which are highly irregular. This applies for samples G3.20, G5.1, G5.2, G2.46, G2.45 and G3.20. These data are included in results but are not considered a true magmatic or tectonic fabric in the context of pluton construction. Those samples which return elevated levels of maghemitization return tensors which are comparable to those from neighbouring sites and are accepted as valid petrofabric proxies.

9.5.3 Overview of AMS Data

Based on the parameters of Jelinek (1981) the attitude and distribution of dominant AMS vectors are presented in Figure. 9.17 (attached map) where dominantly oblate or prolate fabrics are plotted as foliations or lineations respectively. Sample stereographic projects (95% confidence ellipse) of AMS data are also included. The same data are interpreted as L, S or L-S petrographic fabrics following a comparative analysis of field fabric data, magnetic remanence and the statistical evaluation of AMS data (Hext 1963; Owens 1974; Jelinek 1977, 1981; Owens 2000a, 2000b; Borradaile 2001) and projected in Figure 9.18 (attached map).

AMS stereographic projections are a useful proxy for the degree of fabric homogeneity within a sample site. Viewing the current data set in this way (Fig. 9.17) shows that samples taken from the north of the pluton return broad 95% confidence ellipses. These fabrics vary between oblate and prolate and are most often orientated NNW-SSE. The opposite is characteristic for samples taken from the central, east and northeast of the intrusion. In these areas K1, K2 and K3 are usually well constrained and, typically, the tensor is dominantly oblate and contact parallel.

Graphic illustrations of quantitative comparative analysis (Fig. 9.18) reinforces the above observations and three sets of fabrics are identified. Consistent with results from magnetic experiments, the data show that a sample's shape anisotropy or degree of anisotropy is not

dependent on facies (Fig. 9.16) but does vary systematically based on locality and proximity to local faults (Fig. 9.18A). A stereographic polar plot of all AMS data (Fig. 9.18C) illustrates that the mean K3 axes are scattered but K1 axes are orientated predominantly along a NNW-SSE axis parallel to the long axis of the intrusion and parallel to the Clifden Mace Fault. Within this data set, a dominantly oblate, contact parallel, concentric fabric that dips moderately to steeply outwards has been identified (Fig. 9.18A, D). This is most obvious in the centre and about the periphery of the intrusion. In addition, two sets of fabrics that are highly discordant to the pluton's contacts were also identified (Fig. 9.18A, E, F). These are orientated NNE-SSW and NNW-SSE and associated with shear zones described above.

9.6 Interpretation

The data presented above are combined and interpreted below, relative to the emplacement and deformation history of the Carna Pluton.

9.6.1 Syn to Post Emplacement Shearing

A moderately inclined outward dipping concentric foliation is typical of strain imparted during the inflation of laccolithic bodies (Gilbert 1877; Pollard and Johnson 1973; Corry 1988; Molyneux and Hutton 2000; Hutton and Siegesmund 2001) and is interpreted as such in this case. A more complex fabric relationship is also noted whereby a suite of NNW-SSE and NNE-SSW faults cross cut this emplacement fabric and, in places, the granite contact (Fig. 9.18A). This is recognised in the field via the S-C fabrics which show that simple shearing occurred in both directions during crystallisation of magma. The NNW-SSE fabric first identified by King (1966) in the Cuilleen area is also interpreted as a tectonic and not emplacement related fabric (Leake 2011) due to its discordant relationship to internal contacts. This is substantiated by AMS data which show magnetic lineations plunge between 5°-57° and strike NNW-SSE in this area (Fig. 9.18A), this is not consistent with a vertical magma flow conduit (*c.f.* Leake (2011)) but is consistent with intermediate anisotropies formed via submagmatic simple shear.

Normalised and un-normalised stereographic projections weight the contribution of sub-specimens to the averaged tensor differently. The 95% confidence ellipse will differ to a greater extent if a sub-fabric is present (Owens 2000b). Two samples from the current data set are

presented (Fig. 9.19) which illustrate this principle and reveal that some AMS tensors represent a composite of two sub-fabrics. In these samples, sub specimen susceptibility axes are scattered and broad 95% confidence ellipses defined for un-normalised (2) and normalised (3) stereographic projections. Un-normalised and normalised confidence ellipses substantially differ, e.g. the un-normalised projection for G1.17 depicts a gently inclined prolate fabric trending north but the normalised projection depicts a subvertical north-south foliation. This indicates the tensor is a composite of two fabrics, in this case a NNW-SSE tectonic foliation superimposed upon a contact parallel emplacement fabric.

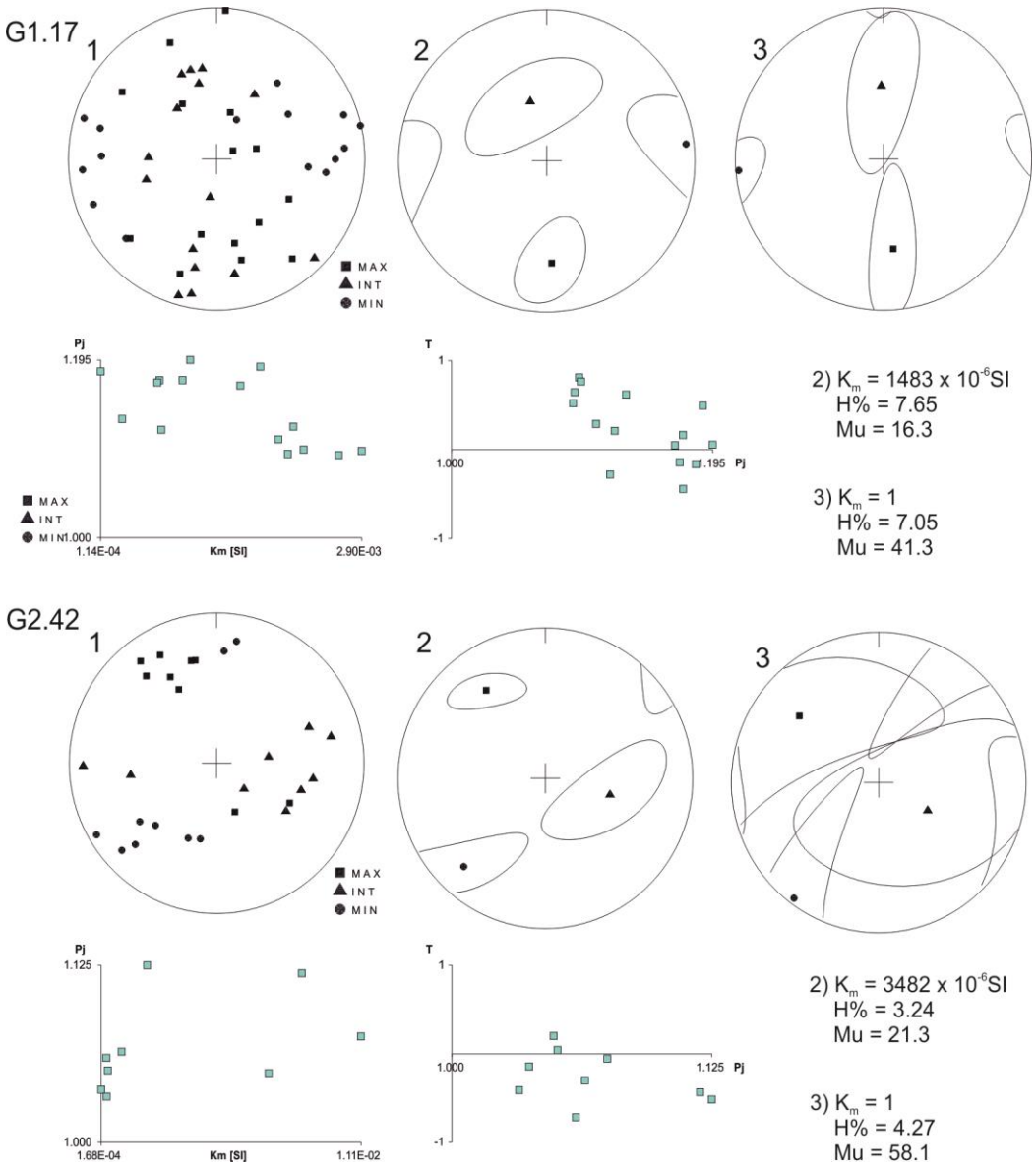


Fig. 9.19 Examples of AMS data which are interpreted to represent multiple fabrics in a single composite tensor. In both cases stereonet 1 shows sub-specimen susceptibility axes are not clustered. Stereonet 2 is the same data with three mean poles surrounded by a 95% confidence ellipse, this representation depicts reasonably well defined susceptibility axes. Stereonet 3 is the same data but normalised, in this case the confidence ellipses differ drastically, overlap and show that a simple interpretation based on Stereonet 2 would be insufficient.

The Dogs Bay area is recognised as a key locality for distinguishing this structural overprint (Fig. 9.20A). Here biotite layers and a concentric emplacement foliation dip moderately to the north and these are cross cut by a suite of NNW-SSE and NNE-SSW faults and associated NNW-SSE silicate foliations. Stereographic projections of all fabric data depict a clear relationship between AMS data and observed foliations (Figs. 9.20B, C). Figure 9.20B is a plot of all data recovered that is associated with initial emplacement of magma (inflation fabric) and tectonic deformation (NNW-SSE faults). Mean poles determined from this data (Fig. 9.20C) show an unequivocal cross cutting relationship between emplacement related fabrics (striking ESE-WNW dipping moderately north) and the tectonic overprint (NNW-SSE subvertical-east). A contoured plot of K1 axes centres almost precisely over the intersection of the two cross cutting planes and demonstrates that determined K1 vectors are tectonic in origin and formed in response to shearing.

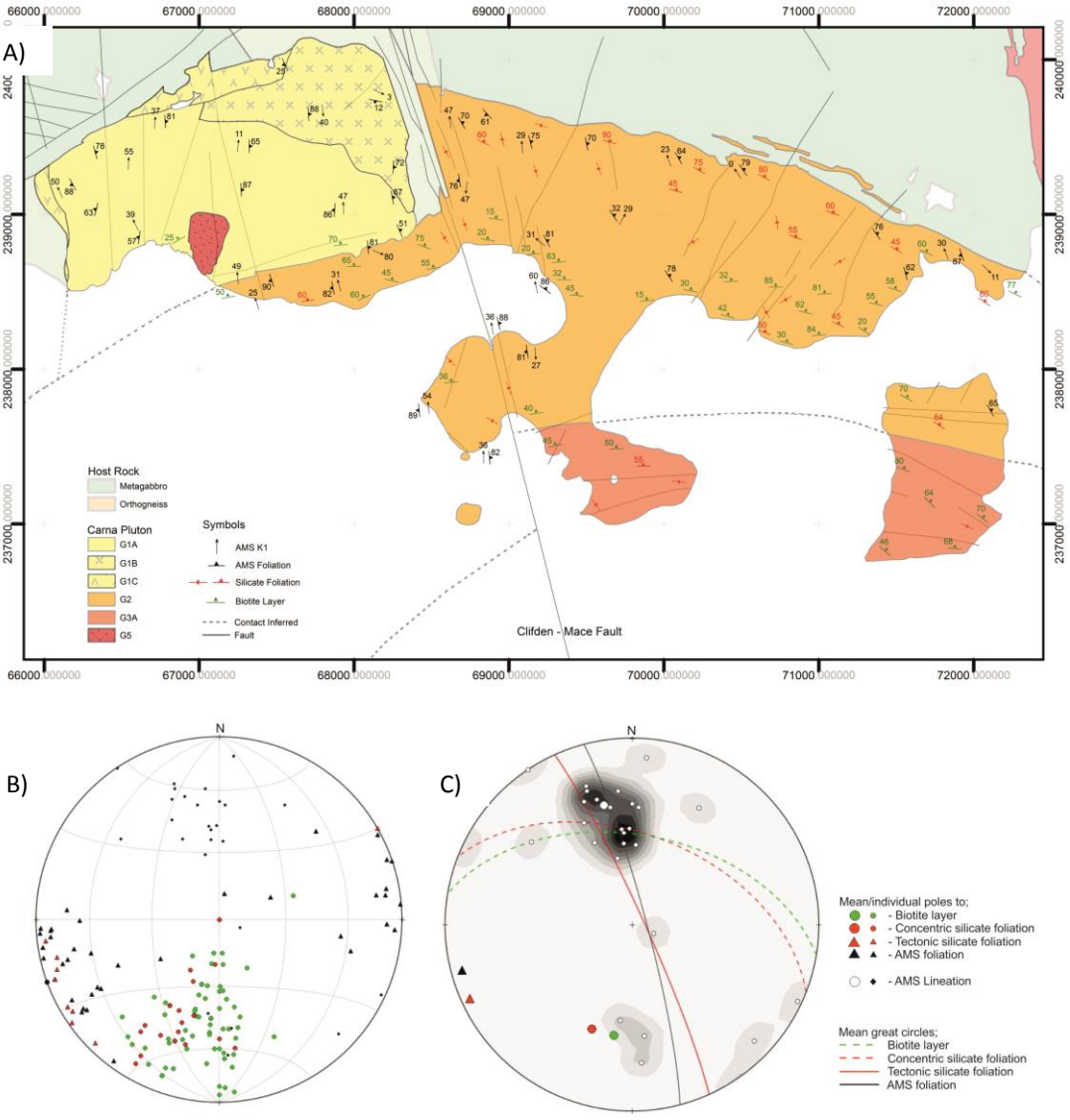


Fig. 9.20 A) Blow up map of the Dogs Bay area and summarised fabric data. B) stereonet of all data plotted in (A), (C) is the same data summarised with K1 axes of AMS contoured. Note that the mean K1 axis defined by all data lies along the intersection of the concentric ballooning fabric and the tectonic overprint.

The process of overprinting magnetic fabrics is now reasonably well understood (Graham 1954, 1966; Borradaile and Tarling 1981; Rochette and Fillion 1988; Borradaile and Sarvas 1990; Jackson and Tauxe 1991; Hrouda 1992; Borradaile and Henry 1997; Bouchez 1997; Parés *et al.* 1999; Aubourg and Robion 2002; Hrouda 2002; Parés and van der Pluijm 2002; Borradaile and Jackson 2004; Parés 2004; Borradaile and Jackson 2010). During pure shear flattening, an originally oblate fabric will stretch toward σ3 and eventually enter the prolate field, if flattening continues the strain ellipsoid will again pass back into the oblate field (Flinn 1962; Flinn 1965) (Ramsay 1967; Ramsay and Huber 1983). This process of progressive horizontal shortening has been recognised in AMS data by several authors (Bakhtari *et al.* 1998; Parés and van der Pluijm 2002; Parés 2004). In contrast to this, during simple shearing an originally oblate fabric becomes increasingly prolate parallel to σ3 on the plane of shear. As an intermediate fabric, ε1 is rotated to approximate the intersection to the two cross cutting planes (plane of shearing and original fabric) and ε2 and ε3 are rotated out of the original plane. If shearing continues ε1 rotates to become parallel to σ3 while ε2 and ε3 rotate to a mutually orthogonal position perpendicular to σ3. Again several authors have documented the development of magnetic fabrics due to overprinting of primary foliations due to simple shear. K1 (ε1) will rotate parallel to σ3 and define a magnetic stretching lineation on the shearing plane (Ferré and Améglio 2000; Hirt *et al.* 2000) or become an intermediate fabric if deformation halts prior to this (Parés and van der Pluijm 2002). Several accounts also exist where two planar features intersect to define an intersection lineation which can be detected via AMS analysis (Borradaile and Tarling 1981; Rochette and Vialon 1984), a feature best preserved in rocks with very strong primary and pervasive secondary foliations.

To determine the significance of the composite tensors detected, a biotite layer (090 45°N) in the Dogs Bay area was sampled and subjected to the full suite of magnetic analysis (G2.42). The resulting AMS tensor, the inclined biotite layer and subvertical NNW-SSE fault are modelled in Figure 9.21. K1 is orientated slightly oblique to the intersection of the tectonic and magmatic foliation planes and the K3 is close to orthogonal to the projected fault plane at a high angle to that of the biotite layer (Fig. 9.21, B). A large discrepancy between normalised and un-normalised stereographic projections indicate significant overprinting occurred (Fig. 9.19, G2.42). However, petrographic analysis of this specimen show no signs of submagmatic or solid state deformation (Fig. 9.21A). This demonstrates subtle overprinting of the original foliation (biotite layer) occurred prior to crystallisation during rotation of the magnetic tensor toward the plane of simple shear.

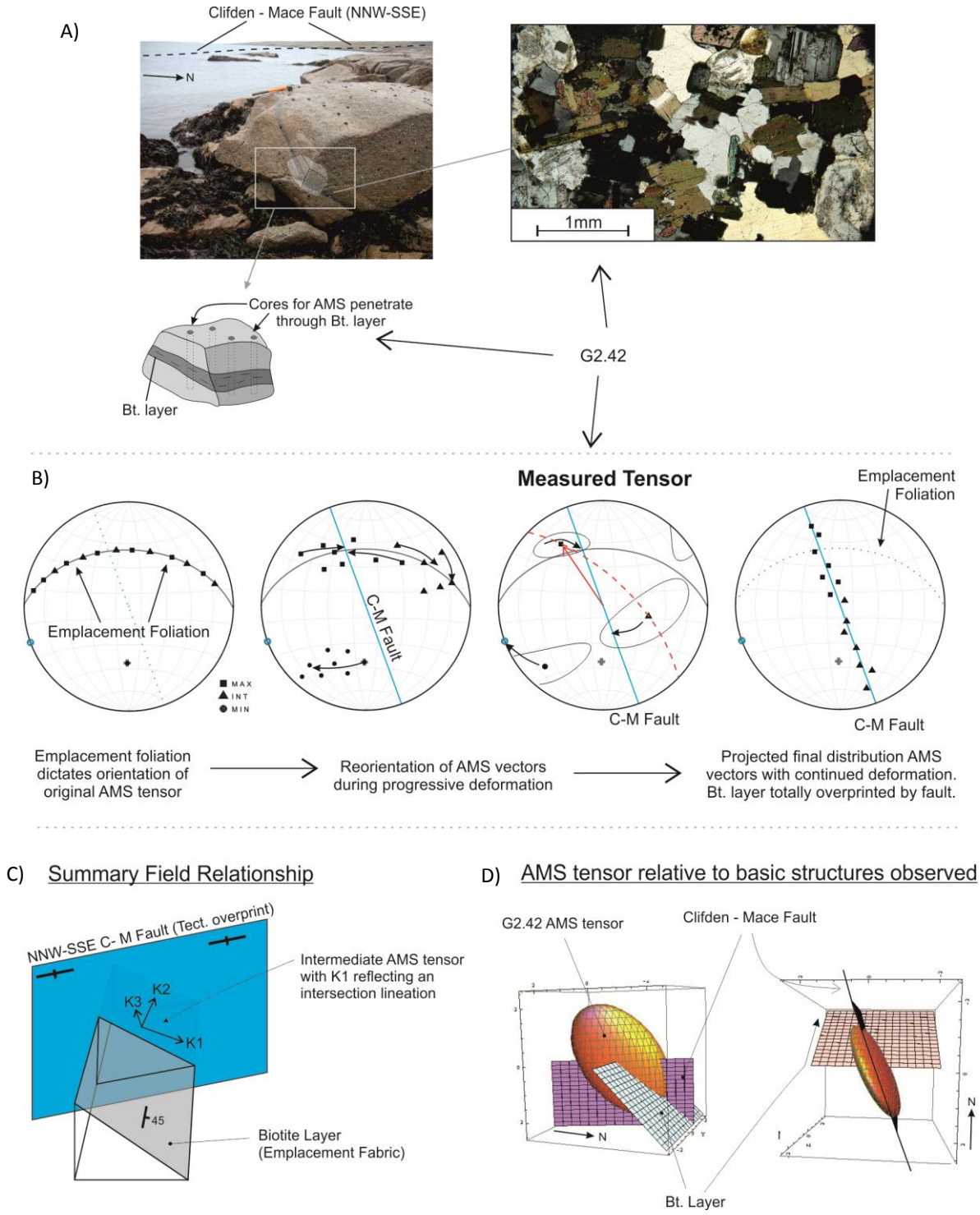


Fig. 9.21 A) Sample collected from biotite layer with no obvious tectonic deformation (Dogs Bay). B) The AMS tensor reflects a composite of an concentric emplacement and a NNW-SSE tectonic foliation. C) Simplified field relationship at sample site with fault cross cutting inclined biotite layer. D) Data shows K1 axis of AMS tensor is close to parallel to the intersection lineation defined by magmatic and tectonic foliations. Shearing must have occurred in the pre-solid state as this sample shows no evidence of brittle or low temperature deformation (A).

The CMF is a predominantly simple shear structure (Leake and Tanner 1994), it is proposed that progressive deformation caused rotation of the principal susceptibility axes (that originally

defined the primary magmatic fabric) into this plane (Fig. 9.21B). Prior to shearing the mean K3 axis were perpendicular to the foliation, K1 and K2 were randomly distributed across this plane. As deformation progressed, the K3 rotated to an orthogonal position relative to the CMF while K1 rotated into this plane from the biotite layer to produce an intermediate tensor which has K1 orientated on the intersection of the two planes and K3 defining the pole to the CMF (Fig. 9.21 B-D). Ultimately if shearing continues K1 will align with the tectonic stretching direction.

Poorly defined foliations are most sensitive to overprinting (Parés and van der Pluijm 2002). The degree of anisotropy imparted during the emplacement of magma is typically moderate to low (Bouchez 1997), in the case of the Carna Pluton ~ 7% (low-moderate). Furthermore, no competent horizon existed prior to shearing as this commenced in the sub-magmatic/magmatic state. Hence the determined AMS tensor is likely to reflect an intermediate fabric i.e. a composite of emplacement and tectonic anisotropies, rather than an intersection lineation.

The observations made above demonstrate shearing along the CMF was active during the emplacement of magma and continued after the granite had fully crystallised. Significantly the majority of shear zones show solid state top to the left displacement, but examples of submagmatic sinistral and some dextral S-C fabrics are identified. Thus shearing was concurrent with the emplacement of magma but a reverse in the sense of shear occurred prior to full crystallisation. This indicates a modification to the local stress field occurred between 412Ma and 407Ma.

9.6.2 Tectonic Controls Over Siting of the Carna Pluton

It is purported that the Carna Pluton formed by the upward movement of a "central ring complex", that this process was driven by buoyancy contrasts and stoping of the more dense country rock and that tectonic factors played a negligible role (Leake 2011). The data presented here are inconsistent with the previous hypothesis. It is proposed that the Carna Pluton is a syn-tectonic pluton. Its symmetry and siting was dictated by the net interaction of internal magma pressure, the regional stress field and local deep seated NNW-SSE and ESE-WNW structures.

New chronological data presented here show that the Roundstone and Carna Plutons had been emplaced by ~ 423Ma and ~ 409Ma respectively. As a consequence of this it is shown that

the Roundstone and Omey Plutons intruded approximately concurrently and some 10Ma before the Carna Pluton was emplaced. These data also makes it clear that the G2 facies in the Carna Pluton predates the ETG facies of the Kilkieran Pluton by ~ 10Ma, hence confirming the independence of these two intrusive bodies. Most significantly these new data substantiates the claim that both the Roundstone and Omey Plutons intruded during regional sinistral transpression (Chapters 7 & 8) and also provides an age for the Carna Pluton that allows this intrusion to be temporally related to existing regional kinematic models (i.e. (Dewey and Strachan 2003; Soper and Woodcock 2003)).

Structural data show a weak concentric inflation foliation in the Carna Pluton that is cross cut by a down temperature magmatic to solid state tectonic foliation, this is attributed to shearing along the CMF. It is significant that both sinistral and dextral shear sense indicators are associated with movement along this fault and that only sinistral shearing is recorded under low temperature solid state conditions. These data show that the Clifden-Mace Fault was active during and after the emplacement of the Carna Pluton and indicate that some modification of the ambient stress field occurred during crystallisation which caused a reversal in the direction of shearing. In light of the new chronological data discussed, this implies that the regional stress field was modified between 412-409Ma.

The CMF was active during the siting of the Carna Pluton. Following the discussion on the role of crustal structure in magma transport in Chapter 1, and in light of the geometrical relationship between this structure and the symmetry of the pluton, it is proposed that the Carna Pluton was emplaced into an active NNW-SSE shear zone which was suitably orientated to facilitate magma ascent at this time (i.e. 412Ma and earlier). A simple kinematic model (Fig. 9.22) demonstrates that a regional transpressional stress field would have facilitated magma ascent along the CMF and the onset of regional transtension would have closed this conduit.

Regional southwest-northeast directed transpression (425-410Ma, Dewey and Strachan (2003)) promoted sinistral shearing across the northwest-southeast Skird Rocks Fault (SRF) and Highland Boundary Fault (HBF). These acted as bounding structures to a regional scale fault system within which blocks bound by NNW-SSE faults underwent anticlockwise rotation (Fig. 9.22A). Regional transpressive stress resulted in a dextral transtensive regime across the CMF and N-S compression across the SRF. The intersecting SRF and CMF formed an ideal vertical conduit along which magma ascended driven by excess magma pressure. The oval NNW-SSE elongate symmetry of the pluton was controlled by the CMF as magma was preferentially transported

along this structure. Continued dextral shearing during this phase imparted magmatic to submagmatic top to the right shear sense indicators along NNW-SSE structures associated with the CMF.

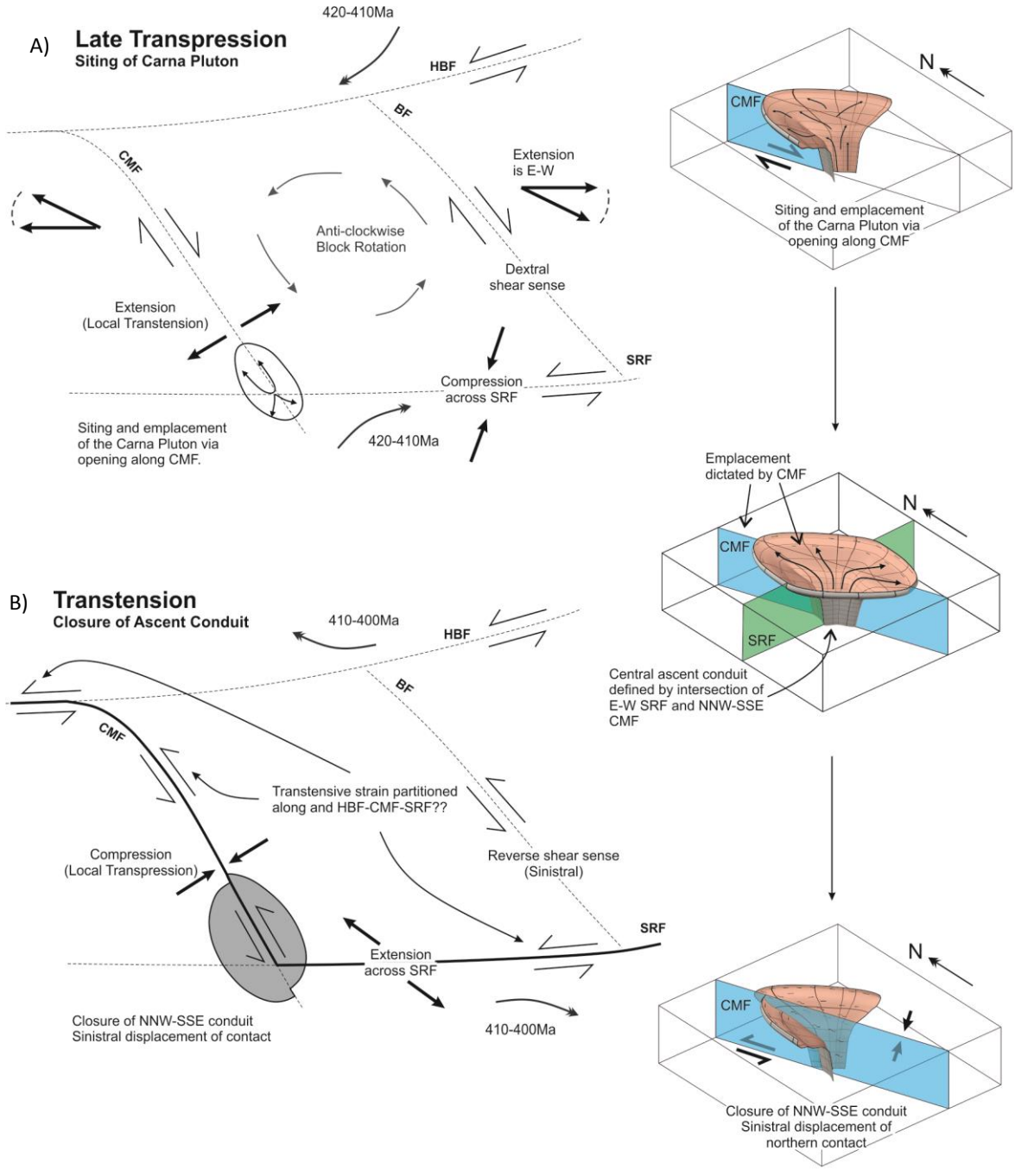


Fig. 9.22 Proposed relationship between regional stress, local structure and the construction of the Carna Pluton. A) Regional sinistral transpression promotes net E-W extension across the CMF and N-S compression across the SRF. A vertical ascent conduit forms over the intersection of these structures and magma preferentially migrates along the CMF at the site of emplacement where inflation commences. B) The transpression-transtension transition occurs between 412-409Ma as regional transtension causes net compression across the CMF and extension across the SRF. This terminates magma ascent along the CMF as the SRF provides a new path of least resistance for over-pressured magma leading to the emplacement of the Kilkieran Pluton.

The regional principal stress field rotated at ~ 410Ma and with it regional transpression evolved to northwest-southeast transtension between 410-400Ma (Dewey and Strachan 2003). Locally, this caused E-W compression and N-S extension thus reverting the CMF to a sinistral transpressive structure and the SRF to an extensional structure (Fig. 9.22B). Thus at this time magma ceased to preferentially migrate along the CMF as other, more preferable ascent conduits had opened. This initiated construction of the Kilkieran Complex immediately to the east via the SRF.

The current model hinges on the age of the Carna Pluton relative to the timing of the regional transpression to transtension transition. In essence, magma ingress was facilitated by regional transpression and terminated due to the onset of regional transtension. The current data set also requires this transition to have occurred after 412 and before 409Ma. This is remarkably consistent with the studies carried out 130km to the south in the Dingle basin which show sinistral transtension continued until about 409Ma (Richmond and Williams 2000) and also with the proposed regional model for the transpression to transtension late Caledonian transition (Dewey and Strachan 2003). Therefore, the structural and chronological data sets provided are mutually and independently consistent and demonstrate a tectonic control over the construction of the Carna Pluton.

There are several fundamental advantages to this new model. Firstly, the final model is consistent with the collected data and correlates well with those hypotheses formed for the construction of other members of the GGC (Chapters 5, 7 & 8). Secondly, the ascent and emplacement of magma is achieved via exploitation of pre-existing structural discontinuities that are shown to react in unity with the ambient stress field i.e. magma exploitation of a conduit correlates with the stress field and terminates when the system is in compression. Finally, Leake (2011) argued that magma ceased to rise due to a lack of buoyancy contrasts between facies of the Roundstone and Carna Pluton. This point of view fails to recognise that the Delaney Dome Fm. (Leake and Singh 1986; Tanner *et al.* 1989; Draut and Clift 2002) underlies much of the Connemara Bedrock. As this rock is less dense than much of the Carna and Roundstone Pluton facies, buoyancy cannot be considered a dominant driving force. Here such buoyancy and competency parameters are not favoured as sole driving forces. Instead, the dynamic interaction between deep seated structures (CMF, SRF), the ambient stress field and magma overpressure are cited as the primary factors which controlled the siting and construction of the Carna Pluton.

The predominance of sinistral shear along NNW-SSE structures after emplacement of the Carna Pluton remains enigmatic. One hypothesis is that the flip in the regional stress field at 410Ma promoted local sinistral transpression across the NNW-SSE faults. As an alternative hypothesis, progressive inflation of the Kilkieran Pluton to the east may have caused a relative northward displacement of the portion of the Connemara Metamorphic Complex bound by the Barna Fault and Clifden Mace Fault. This could have caused sinistral reactivation of the Clifden-Mace Fault. These concepts are discussed in the next chapter.

9.7 Conclusion

The Carna Pluton is an entirely a structure distinct to the adjoining Kilkieran Pluton, the former having been emplaced some 10Ma prior to the latter. The Roundstone Pluton was emplaced at 423.8 ± 3.2Ma and had fully crystallised before the Carna Pluton began to assemble at 412.8 ± 2.4Ma. Magnetic data reflects a concentric inflation foliation cross cut by a tectonic stretching lineation parallel to the CMF. Field and petrographic observations confirm this tectonic fabric developed during and after the crystallisation of the pluton and hence infer tectonic processes played a leading role in controlling the symmetry of this oval NNW-SSE orientated intrusion.

It is concluded that siting was achieved along a central ascent conduit determined by the intersection of the SRF and CMF. Emplacement progressed preferentially along the CMF which controlled the overall exposed symmetry of the intrusion. Inflation of the pluton occurred synchronously with shearing across the CMF that imparted both dextral and predominantly sinistral shear sense indicators across NNW-SSE structures. Final sinistral movement along this structure post-dated full crystallisation and was most likely caused by reactivation of the CMF as an accommodation structure during expansion of the Kilkieran Complex.

Chapter 10:

Synthesis;
The Kinematic Evolution of the Galway Granite Complex and Conclusions

10.1 Introduction

The final aim of the current work is to determine whether large orogenic-scale stress regime variations can be detected through the detailed structural evaluation of a suite of plutons emplaced intermittently during this fluctuation. Several authors have demonstrated that magma will exploit existing anisotropies in the crust as a path of least resistance, this is achievable in compressive, tensile or transcurrent regimes (Anderson 1951; Corry 1988; Hutton 1988, 1992; Hutton and Reavy 1992; Jacques and Reavy 1994; Hutton 1997; Cruden 1998; Brown and Solar 1999; Vigneresse *et al.* 1999; Stevenson 2009). The conduit orientation is determined by the net interaction between the ambient stress field at the time of intrusion, local structural features and internal magma pressure (Vigneresse *et al.* 1999; Ablay *et al.* 2008). If the ambient stress field is modified, more suitably orientated structures may be exploited as a new magma transport conduit. Thus, in a single area, plutons that were emplaced concurrently within a particular stress field should exploit similar pre-existing structures, these may contrast those used by neighbouring plutons which were emplaced at a different time within a different stress field.

The Galway Granite Complex (GGC) intruded throughout late Caledonian transpression, transtension (Dewey and Strachan 2003; Soper and Woodcock 2003) and the Acadian Orogeny (Woodcock *et al.* 2007) and between 425-380Ma (Feely *et al.* 2010). Despite the fact that the generation, ascent and emplacement of the GGC continued over such a protracted and tectonically dynamic period, no attempt has yet been made to relate the siting of these intrusions to the broader kinematic picture. This is dominantly due to the fact that until now, no detailed structural information was available from intrusions located outside of the Kilkieran Complex. The new data set presented in this thesis facilitates such an evaluation.

The kinematic regime during construction of the GGC is summarised in Section 10.2. The distribution of strain within transpressive and transtensive stress fields is discussed in Section 10.3. Section 10.4 reviews the existing structural models associated with members of the GGC. These concepts are applied to the new data presented in this thesis to synthesise the first kinematic model for the evolution of the GGC in Section 10.5. Finally the main outcomes of the current work are summarised in Section 10.6.

10.2 Late Caledonian Transtension - Transpression Transition

There is a consensus that the Caledonian Orogeny culminated in a period of dynamic sinistral transcurrent deformation during and following the final closure of the Iapetus Ocean (Soper *et al.* 1992; Torsvik *et al.* 1996). This was followed later by the Acadian Orogeny (400-390Ma in Ireland and the UK) which was an entirely separate collision event that is related to the convergence of Avalonia and Armorica and closure of the Rheic Ocean (Woodcock *et al.* 2007).

The sinistral transcurrent docking of Avalonia-Baltica and Laurentia may be divided into two episodes, i.e. transpression and transtension (Dewey and Strachan 2003; Soper and Woodcock 2003). Some ambiguity remains over the timing of the transpression-transtension transition, this is highlighted in a comparison of the literature in Dewey and Strachan (2003) and Soper and Woodcock (2003). Drawing on evidence from the Louisburgh Basin and the Corvock and Slieve Gamph Granite in Ireland (Dewey 1997), the arrival of Laurentian sediments on the Avalonian margin (Hutton and Murphy 1987; Soper and Woodcock 1990), as well as data from the Baltican - Laurentian accretionary zone and early-mid Devonian continental deposits, and associated deformation structures, in Ireland and southern Britain, Dewey and Strachan (2003) concluded the regional stress field underwent a transition from transpression to transtension at 410Ma. This is in contrast to the findings of Soper and Woodcock (2003) who argued transpression between Laurentia and Avalonia had terminated by 420Ma and was followed by a prolonged transtensive episode that lasted until the onset of Acadian deformation at 400Ma (Soper *et al.* 1987; McKerrow 1988; Meere and Mulchrone 2006). The argument for an earlier instigation of transtension is based heavily on the temporal requirement for the development of large ORS basins across southern Britain throughout the lower Devonian prior to Acadian deformation (Soper and Woodcock 2003).

Emphasising that the majority of evidence cited by Dewey and Strachan (2003) was derived from the Laurentia-Baltica convergence zone, Soper and Woodcock (2003) reconciled these contrasting models by considering a three-plate dynamic model (Soper *et al.* 1992) where Avalonia and Baltica were juxtaposed but are structurally independent. Thus transpression could have continued between Baltica and Laurentia until 410Ma while transtension between Avalonia and Laurentia ensued at 420Ma (Soper and Woodcock 2003). Other explanations are feasible. Tectonic controls on the development of Devonian sedimentary basins and associated structures have been the subject of debate. Some argue for a regional extensional regime with no significant strike slip component (McClay *et al.* 1986; Rogers *et al.* 1989) while others demonstrate basin development within a transcurrent setting is feasible (Vogt 1936; Harland 1985). Several authors

(Sanderson and Marchini 1984; McCoss 1986; Jones *et al.* 1997; Dewey *et al.* 1998; Dewey 2002) discuss the generation of shortening or extensional features in regional transtensive or transpressive regimes respectively. Hence, early Devonian transtension is not a pre-requisite for the development of sedimentary basins. In fact, the Dingle Basin is an example of one such basin which opened within a sinistrally transpressive regime between the Gorstian and early Praghian (Boyd and Sloan 2000; Richmond and Williams 2000).

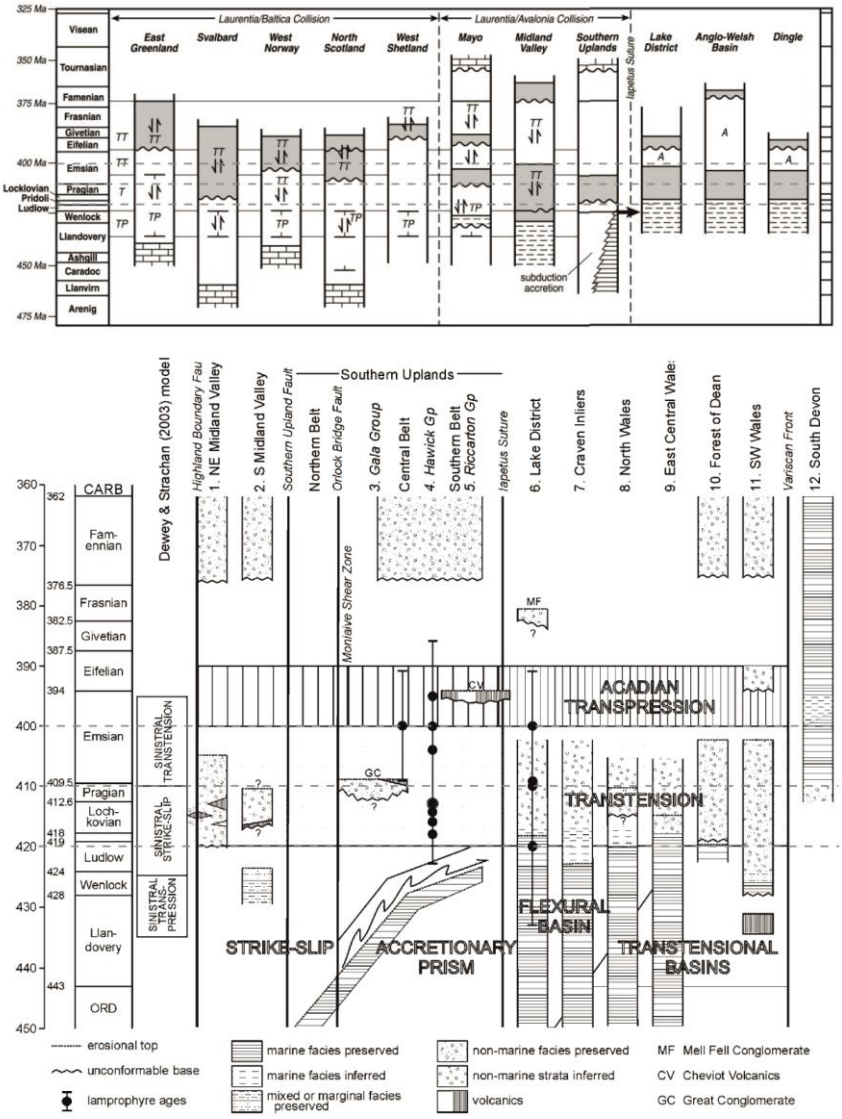


Fig. 10.1 A) Dewey and Strachan (2003) suggest transtension did not initiate until 410Ma. B) Soper and Woodcock (2003) suggest that extension between Laurentia and Avalonian stated at 420Ma.

Finally, a synthesis of data relating to late Caledonian transcurrent shearing (Dewey and Strachan 2003) shows large variations in local stress fields across the orogenic belt (Fig. 10.1). This diagram highlights that far field kinematic forces may differ along strike on an orogenic scale and

emphasises the need for the construction of local scale models based on primary field data which may be later incorporated into regional scale syntheses. The current evaluation of the GGC is one such example and provides an insight into the kinematic dynamic between 425-380Ma in this area of the Caledonian Belt.

10.3 Dynamics of Transpression and Transtension

Transpression and transtension were first considered as plate boundary kinematic processes by Harland (1971) who defined these as oblique relative movements between tectonic plates that occur intermediately between compressional-transcurrent and transcurrent-extensional kinematic regimes. More recently transpression and transtension were redefined as strike slip deformations that deviate from simple shear due to a shortening or extension component orthogonal to the zone of deformation (Dewey *et al.* 1998). Sanderson and Marchini (1984) analysed these processes and identified that any transpressive or transtensive regime may be factorised into an element of pure shear and simple shear. This work also shows that a predictable suite of structures will arise from a homogenous medium in a transpressive or transtensive regime which is dependent on the relative angle of incidence between the bounding margins of a deformation zone and the regional stress field (Fig. 10.2).

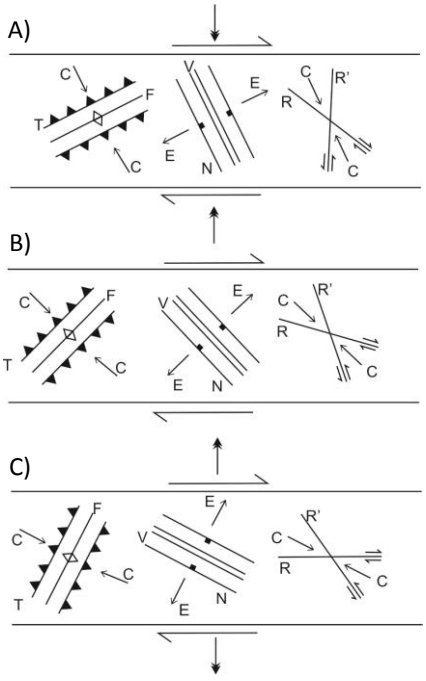


Fig. 10.2 Basic structures predicted to form in a isotropic medium within a transpressive (A), simple shear (B) and transtensive stress field (C). During transpression the net extensional vector is orientated at a low angle relative to the bounding structure. During transtension, net compression is at a low angle relative to the bounding structure. C = compression axis (σ_1); E = extension al axis (σ_3); N = normal faults; T = thrust faults; R, R' = Riedel shears/wrench faults; V = extensional fractures/dykes/veins; F = Folding.

Several graphical and numerical solutions have since been presented which allow the orientation and relative magnitudes of principal stress vectors and characteristic strain patterns to be constrained in some scenarios. McCoss (1986) provides a mathematical derivation which allows the relative magnitudes of the axes of the strain ellipsoid to be determined for infinitesimal and finite strains if volume remains constant (Fig 10.3). By modifying the bounding parameters of the deformation zone, the affect of horizontal stretching (Jones *et al.* 1997), vertical displacement of the fault blocks (Robin and Cruden 1994), or the influence of volume change (Fossen and Tikoff 1993) during deformation may be modelled. These factors are also subject to the stability and rate at which deformation progresses and whether shortening/extension is symmetric or asymmetric relative to block movements, i.e. state of transpression/transtension (Dutton 1997).

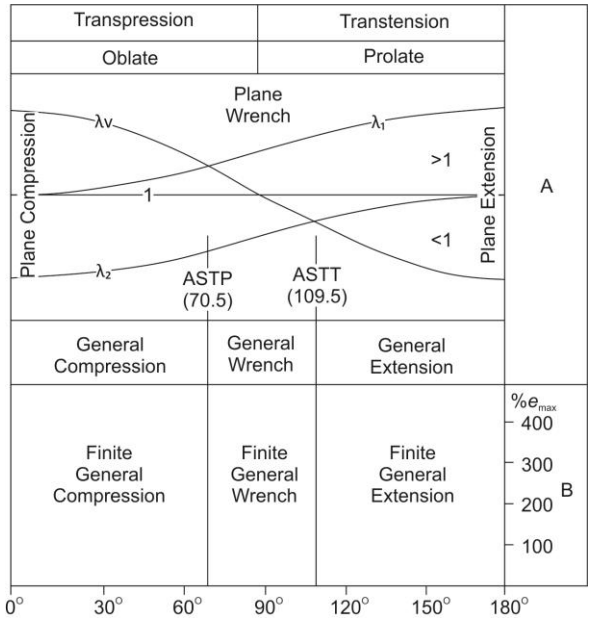


Fig. 10.3 Graphical solutions of McCoss (1986) for determining the characteristics of the infinitesimal strain ellipsoid (A) and the finite strain ellipsoid (A & B) progressively through compressive to transcurrent to extensional stress fields. In any system the transition between transtension and transpression will occur progressive through the classic "wrench tectonics" field, and in most systems some element of compression or extension is expected. Axially symmetric transpression and transtension are denoted by ASTP and ASTT respectively, λ_v is the vertical principal quadratic elongation, λ_1 and λ_2 are the horizontal principal strains. e_{max} is the maximum finite extension.

Dewey *et al.* (1998) emphasised that idealistic finite or incremental strain models are often inadequate because in reality the constants applied do not stand, and are not otherwise constrained. This is not to say that such models cannot be applied to real examples but that each scenario will have unique parameters which must be considered. With this in mind, basic transpressive/transtensive models have been applied to practical scenarios. Harland (1971) originally applied the basic transpression model to explain deformation structures in Caledonian Spitsbergen. Dias and Ribeiro (1994) revealed, through detailed strain analysis on quartzites from the Centro-Iberian Zone, western Europe, that regional transpression can generate a broad variety of fine strain ellipsoids and that this can be accounted for by taking lateral escape, volume change and axial depression into account. In a more recent synthesis of literature on Caledonian

oblique slip terranes, Dewey (2002) concluded that constrictional strains in orogenic belts, with a horizontal stretching component, are often not a product of horizontal shortening and vertical thickening but instead may be a product of a regional transtension during orogenic collapse (Dewey 1988).

The most basic model for transpression and transtension show that in a constant volume, horizontal extension or shortening is achieved by vertical thinning or thickening within the deformation zone (Sanderson and Marchini 1984). Thus, during transpression net extension is expected at a low angle to the orogenic front and during transtension any net compression is found in this same geometrical field (Fig. 10.2). Regardless of the inherent nature of the deformation zone bedrock the incident stress field will abide by these fundamental rules and this principle is applied below.

The Connemara Metamorphic Complex (CMC) represents a lithologically heterogeneous and structurally complex terrane that forms part of an accretion zone between the converging Avalonian and Laurentian margins (Leake and Tanner 1994). Idealised models which predict the deformation path and distribution of strain within an isotropic medium are not directly applicable, however the orientation of the net principal stress field vectors may be predicted. In what follows, the Highland Boundary Fault (HBF) to the north and the Skird Rocks Fault (SRF) to the south represent the large scale bounding structures to the deformation zone that is the Connemara Metamorphic Complex. The Clifden-Mace Fault (CMF) and the Barna Fault (BF) are pre-existing oblique brittle structures which act passively to accommodate simple shear along the bounding HBF and SRF.

10.4 Summary of Emplacement Models Pertaining to GGC Constituents

Prior to the intrusion of the GGC, the CMC was thrust south of the HBF over the Delaney Dome Fm. (DDF) along the Mannin Thrust. The precise timing of this thrusting remains enigmatic and may have continued up until 426 ± 10Ma, (Kennan *et al.* 1987), 447 ± 4Ma (Tanner *et al.* 1989) 457 ± 6Ma (Cliff *et al.* 1996) or as early as 462.5 ± 1Ma based on a compilation of chronological, thermal and field data (Chapter 3). Despite this ambiguity, it remains clear that the CMC was in its current position relative to the Delaney Dome Formation (DDF), and that the CMF and BF were established and active, prior to emplacement of the earliest members of the GGC (Chapter 3).

The GGC comprises six individual composite plutons that intruded the CMC throughout the mid-Silurian to Late Devonian (Fig. 10.4). These include the spatially distinct Earlier Plutons (the Omey, Inish, Letterfrack and Roundstone plutons) and the Main Batholith that comprises two structurally and temporally distinct plutons (the Carna and Kilkieran plutons). The western portion of the Kilkieran Pluton cross cuts the Carna Pluton in the east. Owing to petrographic similarities this contact is hard to identify, however the chronological and structural data presented unequivocally show these to be independent intrusive bodies (Chapter 9). At 380.1 ± 5.5Ma the Costelloe-Murvey Granite (CMG) represents the latest and a distinct constituent of the GGC which happens to cross cut the core of the Kilkieran Pluton.

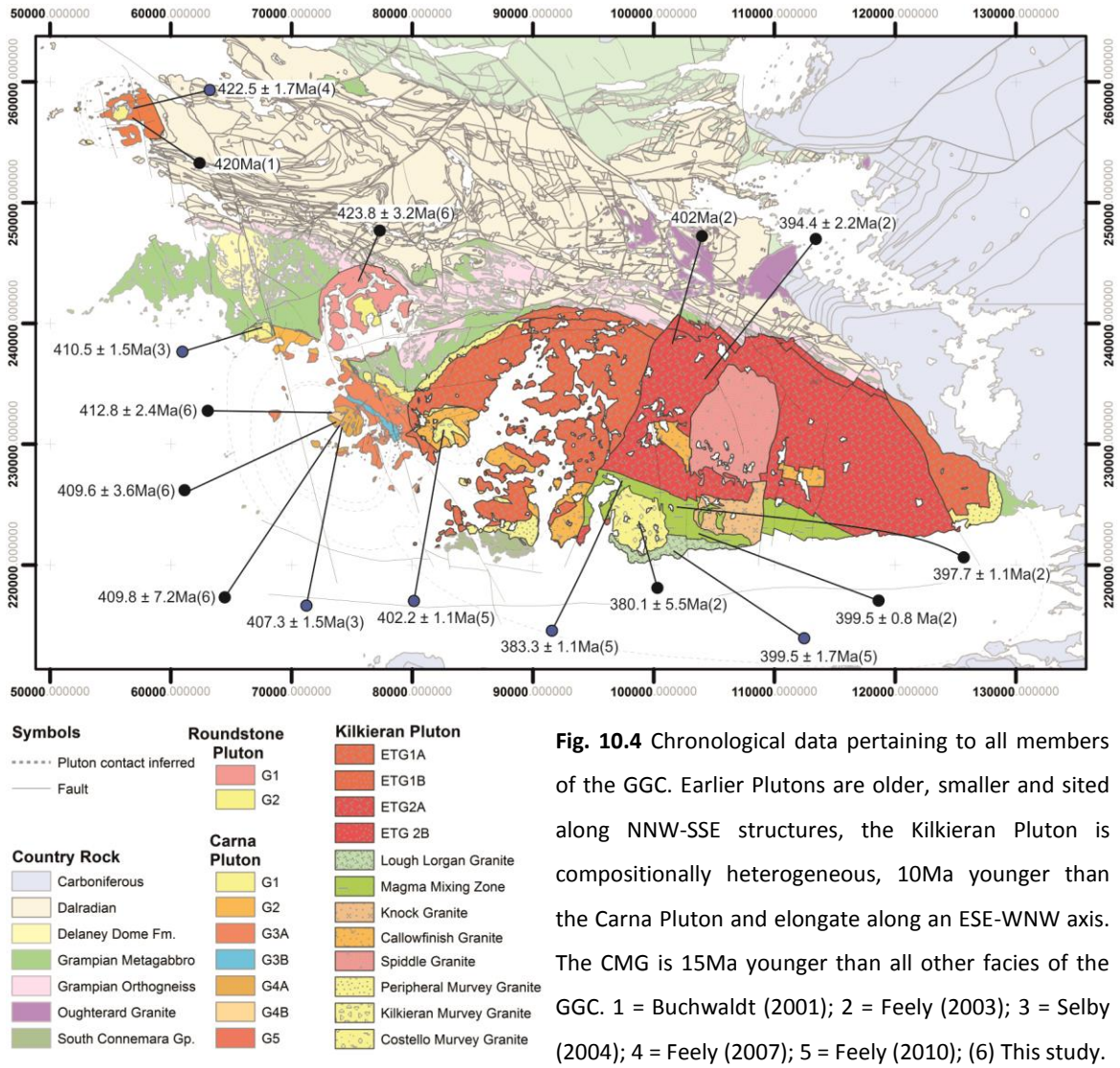


Fig. 10.4 Chronological data pertaining to all members of the GGC. Earlier Plutons are older, smaller and sited along NNW-SSE structures, the Kilkieran Pluton is compositionally heterogeneous, 10Ma younger than the Carna Pluton and elongate along an ESE-WNW axis. The CMG is 15Ma younger than all other facies of the GGC. 1 = Buchwaldt (2001); 2 = Feely (2003); 3 = Selby (2004); 4 = Feely (2007); 5 = Feely (2010); (6) This study.

The Omey Pluton (Chapter 7) has a defined floor and roof which shows emplacement was achieved laterally into the folded units of the Dalradian metasediments. This is a discordant inflated phacolith, the symmetry of which was partially controlled by the predefined structure of the host rock (D4 Connemara Anticline). Subtle cross cutting NNW-SSE shear zones were active in the submagmatic state and are cited as conduits which facilitated ascent of magma into the pluton at ~422.5Ma (Feely *et al.* 2007).

Similarly, it is proposed that the Roundstone Pluton (Chapter 8) ascended along dextrally transtensive NNW-SSE faults, in this case emplacement was controlled by the Mannin Thrust that acted as a stress barrier to ascending magma. During inflation, magma pressure exceeded the tensile strength of the bounding roof (the CMC) and brittle failure formed a faulted peripheral bounding margin to ultimately define a punched and domed laccolith fed by underlying NNW-SSE magma conduits at 420Ma.

The Carna Pluton (Chapter 9) is also controlled by a NNW-SSE shear zone. This is demonstrated by the common alignment of the CMF and the long axis of the pluton as well as petrographic, field and magmatic data that show both dextral and sinistral shearing along this structures was concurrent with magma emplacement. Construction of the pluton initiated prior to 412.8 ± 2.4Ma and a hiatus in the supply of magma occurred at 409.8 ± 7.2Ma. In contrast to those fabrics identified in the magmatic state, only sinistral NNW-SSE shearing is noted in the submagmatic to brittle state, thus this reversal of shear sense temporally coincides with the hiatus in magma supply and crystallisation of the pluton. This shear sense reversal is associated with space creation for emplacement of the Kilkieran Pluton.

In essence, the Kilkieran Pluton (Chapter 5) is a composite ESE-WNW orientated oval intrusion with a surface area of approximately 1100Km^2. It is cross cut by the Shannawona Fault in the west and Barna Fault in the east, which have juxtaposed the deeper central block against the shallower eastern and central blocks (Leake and Said 1994; Callaghan 1999; Leake 2006). A total of 7 major facies are mapped (several more minor facies are recognised) and geochronological data show a decreasing age profile from the peripheral Kilkieran Murvey Granite (402.2 ± 1.1Ma (Feely *et al.* 2010)) toward the central magma mixing zone (383.3Ma, (Feely *et al.* 2003)) which is cross cut by the Costelloe-Murvey Granite, the youngest constituent of the GGC at 380.1Ma (Feely *et al.* 2003). These data are robustly supported by field relationships (El-Desouky 1992; El-Desouky *et al.* 1996; Crowley and Feely 1997; Baxter 2000; Baxter and Feely 2002). A strong contact parallel foliation was first recognised round the intrusion by Kinahan (1869). This is a down temperature pure shear coaxial foliation which increases in intensity as the northern margin is approached and is related to continued inflation during cooling of the pluton (Baxter *et al.* 2005). The MMZ

exhibits a strong axis parallel ESE-WNW foliation and represents an east to west magma transport direction (El-Desouky *et al.* 1996). The Skird Rocks Fault strikes E-W across Galway Bay beneath the Main Batholith.

Ryan *et al.* (1995) suggest emplacement occurred in a step-over area bound by Reidel shears formed between major terrane boundaries to the north (splay off the Antrim - Galway line) and south (Skird Rocks Fault). El-Desouky *et al.* (1996) modified this interpretation and opted for a crustal pull apart model bound by the Maam Valley and Clifden-Mace Fault northwest-southeast shear couple and the SRF during regional transtension. This model was supported by Baxter *et al.* (2005) however this work highlighted the lack of evidence for non-coaxial shear along bounding margins and thus placed some ambiguity about this transtensional pull apart model. Alternatively, Leake (2006) modelled emplacement by a bifurcation along a releasing bend on the SRF and progressive northward emplacement of magma driven via stoping that was ultimately controlled by the strong WNW-ESE gneissic foliation of the host. Despite these differing opinions there is a consensus that the intrusion exploited the SRF as a conduit during ascent and emplacement.

10.5 Tectonic Controls over the GGC

The symmetry and emplacement of each pluton studied was controlled by local structural features, i.e. the Connemara Antiform, the Mannin Thrust and CMF in the respective cases of the Omey, Roundstone and Carna Plutons. However, abundant evidence for magmatic-submagmatic shearing along NNW-SSE structures is also reported in each case indicating a common underlying NNW-SSE structural control. These shear zones conjoin with larger scale prominent NNW-SSE D5 faults when traced along strike into the host rock. D5 faults are known to predate granite emplacement, are demonstrated to have been active during magma emplacement and have controlled the architecture of each pluton to some extent. As such those associated with individual plutons are cited as magma transport conduits.

In contrast to the above, all existing data which pertain to the Kilkieran Complex indicate some E-W structural control i.e. the SRF or similar. Despite multiple detailed structural studies, no significant NNW-SSE anomalies are detected and all authors to date are satisfied with the consensus that emplacement was achieved into an extensional E-W structure (El-Desouky *et al.* 1996; Crowley and Feely 1997; Baxter *et al.* 2005; Feely *et al.* 2006; Leake 2006; Feely *et al.* 2010).

New and existing chronological data presented in this thesis (summarised in Figure 10.5 and Table 10.1) support these findings and show that a temporal relationship exists between ambient regional stress fields and magma ascent conduits.

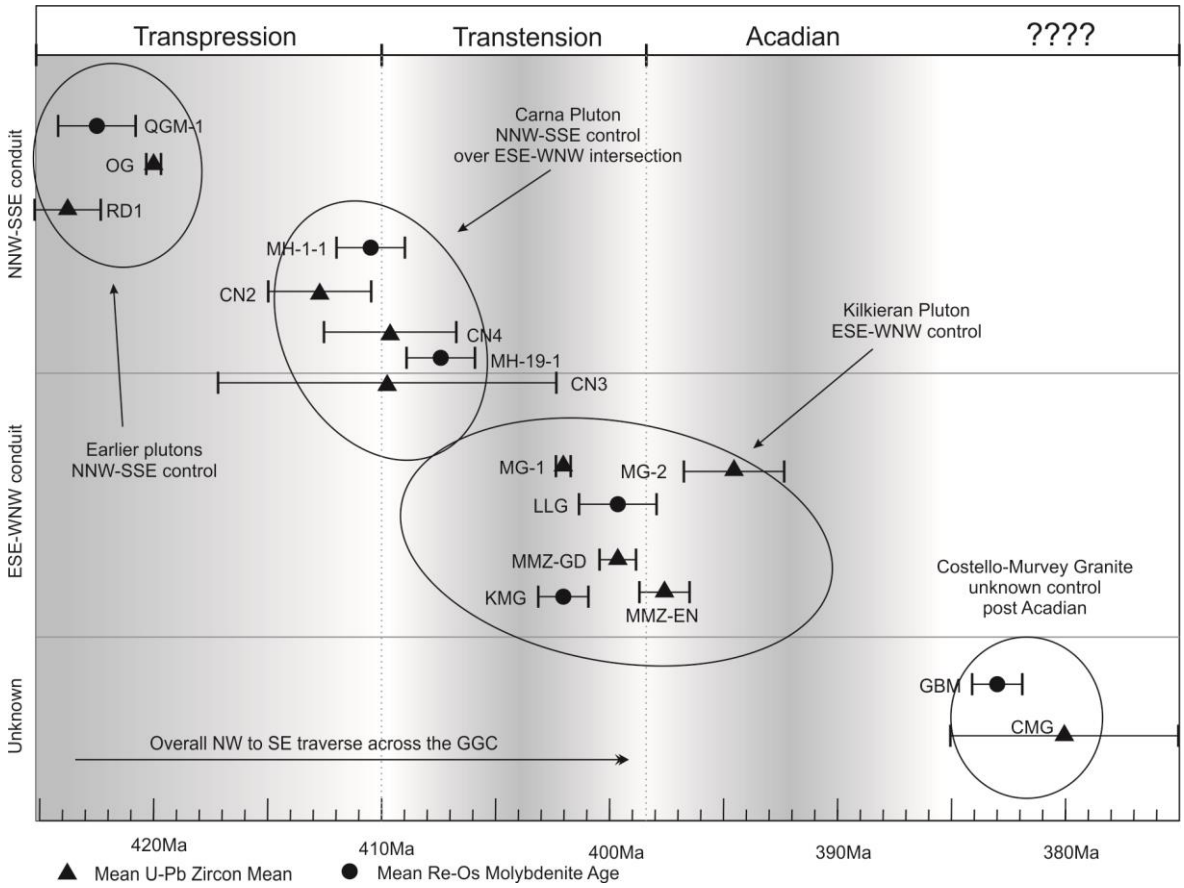


Fig. 10.5 Regional stress field evolution relative to the timing and structural controls over pluton construction. Samples projected correspond to those presented in Table 10.1 and Fig. 10.4.

Construction of the GGC occurred over four temporally distinct temporal intervals (Fig. 10.5), these intervals are associated with contrasting structural controls over granite ascent and emplacement which are, in turn, associated with differing stress regimes. The first group is that of the earliest plutons i.e. the Omey and Roundstone plutons which have similar crystallisation ages (~423Ma), sizes and NNW-SSE structural conduits. This is followed by the larger Carna Pluton (~410Ma) which is cited over the intersection of the SRF and CMF and intruded into and inflated within the NNW-SSE CMF. Significantly, exclusively ductile dextral but both ductile and brittle sinistral shear sense indicators are observed along NNW-SSE structures in this pluton, this infers a change to the local stress field during crystallisation. The Kilkieran Pluton defines the third phase of magmatism (~402-397Ma). This pluton is entirely distinct from other members of the GGC due

to its appreciable larger volume, facies heterogeneity and timing of emplacement. Most importantly, this pluton is controlled by the E-W SRF and this indicates that between 410Ma and 400Ma some modification to the stress field had occurred that promoted magma ingress along this E-W, rather than a NNW-SSE, structure. The Costelloe-Murvey Granite (380.1 ± 5.5Ma (Feely *et al.* 2003)) punctuates an independent final phase of magmatism associated with the GGC. No detailed structural data has been compiled to date, however this is notably smaller and petrographically and geochemically distinct from other facies of the Kilkieran Pluton (Buchwaldt 2001). Buchwaldt (2001) suggested that these traits reflect a magma of an entirely different petrogenic origin and indicated that it does not relate to other facies of the GGC in a simple manner.

Author	Sample ID	Pluton-Facies	Method	Age (Ma)
Buchwaldt (2001)	OG	Omey - G1	U-Pb Zircon	~ 420 (1)
Feely (2003)	CMG	Kilkieran - CMG	U-Pb zircon TIMS	380.1 ± 5.5 (2)
Feely (2003)	MMZ-GD	Kilkieran - MMZ granodiorite	U-Pb zircon TIMS	399.5 ± 0.8 (2)
Feely (2003)	MMZ-EN	Kilkieran - MMZ enclave	U-Pb zircon TIMS	397.7 ± 1.1 (2)
Feely (2003)	MG-1	Kilkieran - Megacrystic Granite	U-Pb zircon TIMS	~ 402 (2)
Feely (2003)	MG-2	Kilkieran - Megacrystic Granite	U-Pb zircon TIMS	394.4 ± 2.2 (2)
Selby (2004)	MH-1-1	Carna - G1 (at Murvey)	187Re-187Os Moly	410.5 ± 1.5 (3)
Selby (2004)	MH-19-1-1	Carna - Mace Head	187Re-187Os Moly	407.3 ± 1.5 (3)
Feely (2007)	QGM-1	Omey - G2	187Re-187Os Moly	422.5 ± 1.7 (4)
Feely (2010)	GBM	Kilkieran - MMZ (Costelloe)	187Re-187Os Moly	383.3 ± 1.1 (5)
Feely (2010)	LLG	Kilkieran - Lough Lurgan Granite	187Re-187Os Moly	399.5 ±1.7 (5)
Feely (2010)	KMG	Kilkieran - Kilkieran Murvey Granite	187Re-187Os Moly	402.2 ± 1.1 (5)
This Study	RD1	Roundstone - G1	U-Pb zircon LAICPMS	423.8 ± 3.2 (6)
This Study	CN2	Carna - G4 (Mace Head)	U-Pb zircon LAICPMS	412.8 ± 2.4 (6)
This Study	CN3	Carna - G5 (Mace Pier Granite)	U-Pb zircon LAICPMS	409.8 ± 7.2 (6)
This Study	CN4	Carna - G5 (Mace Head K-fd Breccia)	U-Pb zircon LAICPMS	409.6 ± 3.6 (6)
Not included in results presented in Figures 10.4 & 10.5				
Leggo (1966)	N.A	Omey Pluton	Rb-Sr Whole rock	388 ± 17
Leggo (1966)	N.A	Inish Pluton	Rb-Sr Whole rock	404 ± 8
Leggo (1966)	N.A	Roundstone Pluton	Rb-Sr Whole rock	395 ± 80
Pidgeon (1969)	N.A	Carna Pluton	U-Pb Zircons	420 ± 20
Buchwaldt (2001)	N.A	Kilkieran - CMG	U-Pb Zircon	380
Leggo (1966)	N.A	Oughterard Granite	Rb-Sr Whole rock	444 ± 7
Leggo (1966)	N.A	Oughterard Granite	Rb-Sr Whole rock	510 ± 35
Leggo (1966)	N.A	Galway Granite Composite	Rb-Sr Whole rock	384 ± 1
Leggo (1966)	N.A	Composite of Murvey, Carna, Screeb, Errisbeg Townland Granite	Rb-Sr Whole rock	385 ± 7

Table 10.1 Existing chronological data for the GGC. The most up-to-date and accurate of this data is projected in Figs. 10.4 & 10.5.

It is proposed that the construction of the GGC was fundamentally controlled by fluctuation of the regional stress field, the most significant of which was the termination of transpression and onset of regional transtension. The current data set shows a significant change in the local stress field occurred during crystallisation of the Carna Pluton before the Kilkieran Pluton i.e. between 412 - 407Ma. As depicted in Figure 10.5, this interpretation is tenable in the context of the temporal parameters set out in Dewey and Strachan (2003) who suggested a transition from regional transpression to transtension at 410Ma. Results of this study contrast with the findings of Soper and Woodcock (2003) (420Ma transition) despite the fact that the latter model was devised specifically for the Avalonian-Laurentian dynamic and the former for a more regional context. This conclusion is supported by the presence of a major transition between the orientation of preferred conduits between 412Ma (Carna Pluton) and 402Ma (Kilkieran Pluton) and the lack of any observable transition at 420Ma (Earlier Plutons and the Carna Pluton).

A simple wire frame diagram (Fig. 10.6) illustrates the proposed sequence of kinematic events during the construction of the GGC. Closure of the Iapetus ocean generated magma from the mid Silurian to mid Devonian due to subduction related slab dehydration, slab break-off and crustal thickening during the convergence of Avalonian, Baltica and Laurentia (Atherton and Ghani 2002; Neilson *et al.* 2009) and later decompression due to Devonian transtension (Brown *et al.* 2008). Excess magma pressure (Ablay *et al.* 2008) promoted fluid migration in the direction of least compressive stress. Thus magma ascent towards the surface along pre-existing deep seated structures was initiated, in the Connemara region these are represented by the CMF and the SRF.

Regional far field stress evolved from orogenic orthogonal shortening to sinistrally oblique compressive stress between 430-425Ma. In western Ireland, the Connemara terrane represents a deformation zone bound by the Highland Boundary Fault (HBF) and the Skird Rocks Fault (SRF). Wholesale sinistral transpressive strike slip occurred along the SRF and HBF; the deformation zone, bound by these faults, was structurally heterogeneous and decoupled along strike due to strain partitioning along NNW-SSE faults (CMF and BF). Regional transpression promoted anti-clockwise rotation of the terrane block bound by the CMF, BF, SRF and HBF (Fig. 10.6A). Thus, local dextrally transtensive stress is predicted along NNW-SSE faults while the HBF and SRF were in the compressive field. As a consequence of this local east-west extensional component, NNW-SSE shear zones presented a favourable migration conduit for ascending magma throughout regional transpression. The Omey and Roundstone Plutons were emplaced during this time (Fig. 10.6A) and are cited over NNW-SSE conduits which supplied magma to the upper crust. Emplacement was controlled by local factors (discussed above).

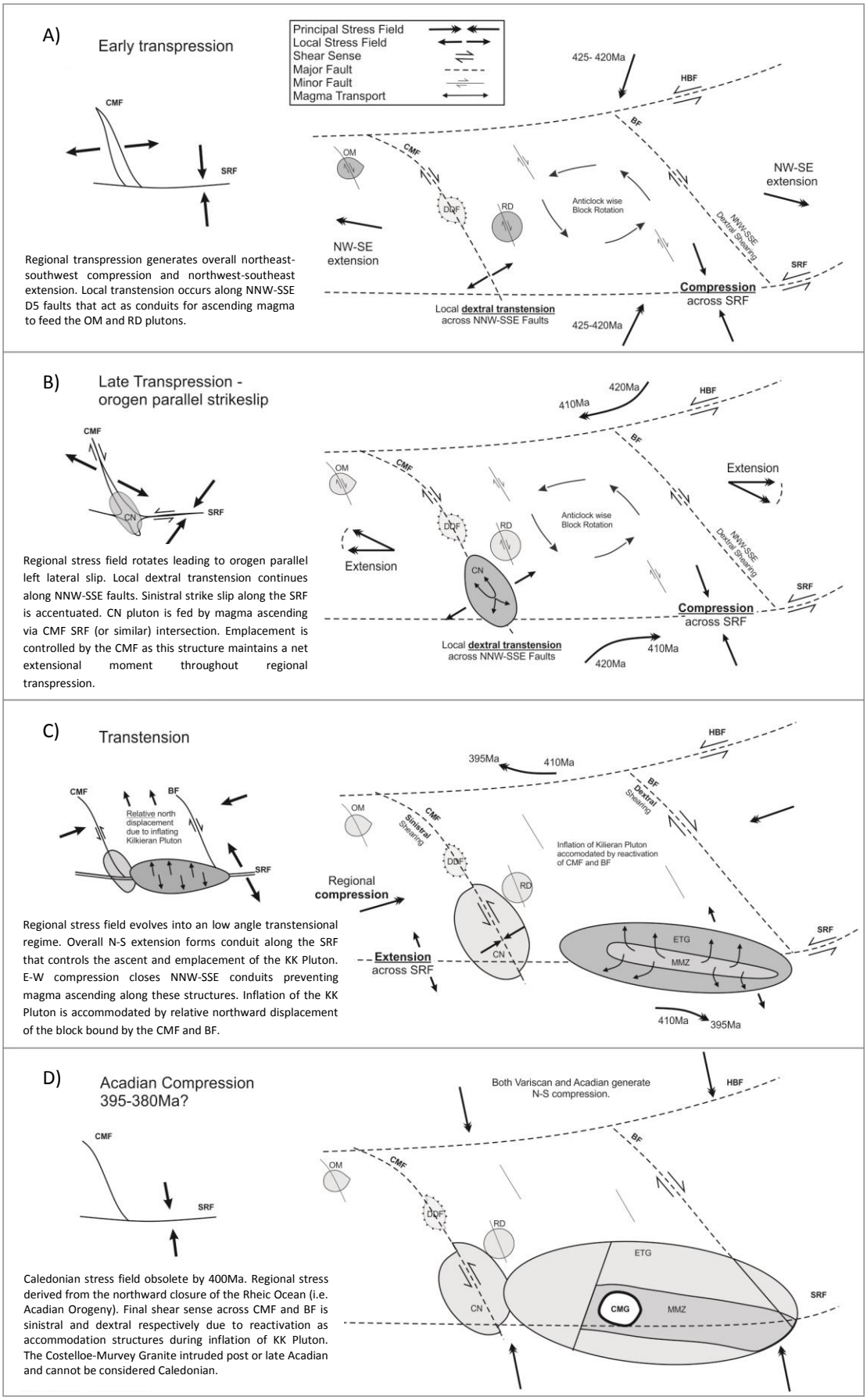


Fig. 10.6 Proposed model for the interaction of local structure, igneous intrusions and the evolution of the regional stress field from the late Silurian to mid-Devonian.

The kinematic conditions which facilitated construction of the Carna Pluton are shown in Figure 10.6B. Regional σ1 had rotated to a lower angle of incidence relative to the orogenic front and accentuated transcurrent shearing along the SRF. Reduced compression along the SRF and transtension along the intersecting CMF provided an ideal centralised ascent conduit. This intrusion preferentially exploited a NNW-SSE conduit (i.e. the CMF) during ascent and emplacement as structures of this orientation had a net extensional component at this time. The concurrency of dextral shearing (and from it the inference of local transtension) and magma emplacement is demonstrated by the presence of subtle top to the right shears and S-C fabrics at outcrop scale and the occurrence of NNW-SSE magnetic fabrics in samples with no submagmatic or solid state deformation features. As pluton construction instigated at 412Ma, it is deduced that regional sinistral transpression continued at least until this time.

Regional transpression evolved from sinistral transcurrent shear at ~410Ma to transtension before 402Ma (Fig 10.6C). Prominent submagmatic and solid state sinistral deformation along the CMF indicate that a major change in the local stress field was concurrent with a hiatus in magma supply to the Carna Pluton at ~409Ma. This is associated with a transition from transpression to transtension and construction of the Kilkieran Pluton. The Kilkieran Pluton (402-395Ma) was emplaced during regional transtension via the SRF which is suitably orientated to facilitate net extension in such a regime. In contrast to this, high angle NNW-SSE structures would experience a net E-W compressive field during northwest-southeast transtension. It is proposed that the transition from transpression to transtension imparted a net compressive stress across NNW-SSE structures, closing conduits sited along them; extensional stress across ESE-WNW structures, providing an alternative conduit for ascending magma. The larger size, prolonged activity and heterogeneity of the Kilkieran Pluton (El-Desouky 1992; Crowley and Feely 1997; Baxter and Feely 2002; Feely *et al.* 2010) may be due in part to the fact that it was cited along a deep seated structure which was subjected to wholesale opening from 410-395Ma, unlike the localised extensional fields that occurred across NNW-SSE conduits from 425-410Ma.

The predicted regional stress field during intrusion of the Costelloe-Murvey Granite (CMG, 380.1 ± 5.5 (Feely *et al.* 2003)) is illustrated in Figure 10.6D. This granite post dates all other members of the Kilkieran Pluton by ~10-20Ma, post dates the Acadian by 10Ma (Meere and Mulchrone 2006; Woodcock *et al.* 2007) and Caledonian transpression by >25Ma (Dewey and Strachan 2003). An N-S compressive stress field, due to either residual Acadian or early Variscan stress presided over this phase of magmatism (Coward 1990). Buchwaldt (2001) has presented a binary isotopic model which shows this granite could have been generated from large-scale melting of older facies of the Kilkieran Pluton. The mechanisms of emplacement and structural

controls on citing this granite remain enigmatic and are beyond the scope of the current study. However it is suggested that this is not a Caledonian Granite but is instead derived from some later event that caused re-melting of the continental crust due to ascent of hot mantle material. It is postulated that dehydration and subduction of the Rheic Ocean crust, following the Acadian Orogeny, could have generated such conditions. This hypothesis remains untested but is readily supported by U-Pb data (*pers. comm.* Helen O'Rourke, UCD) which shows a meta-igneous xenolith from the Iapetus Suture Zone to be 395Ma amongst other evidence for high grade metamorphic processes between 395-385Ma in this area.

Sinistral displacement along the CMF

A sinistrally transtensive regime between 410-400Ma would have promoted dextral shearing along the CMF. It is obvious from field observations that this is not the case. Thus, final sinistral displacement along the CMF is not comprehensively addressed in the current model.

In the model proposed above (Fig. 10.6 C), the block north of the Main Batholith, bound by the CMF and BF, was displaced northwards relative to the terrane to the east and west. This model suggests that south ward displacement of this block was prevented due to inflation of the Kilkieran Pluton in the SRF and, thus, it was displaced northwards relative to the terrain to the east and west. As a consequence of this, dextral and sinistral displacement occurred along the BF and CMF respectively, which is the relationship observed at the present day erosion level (Fig. 2.2).

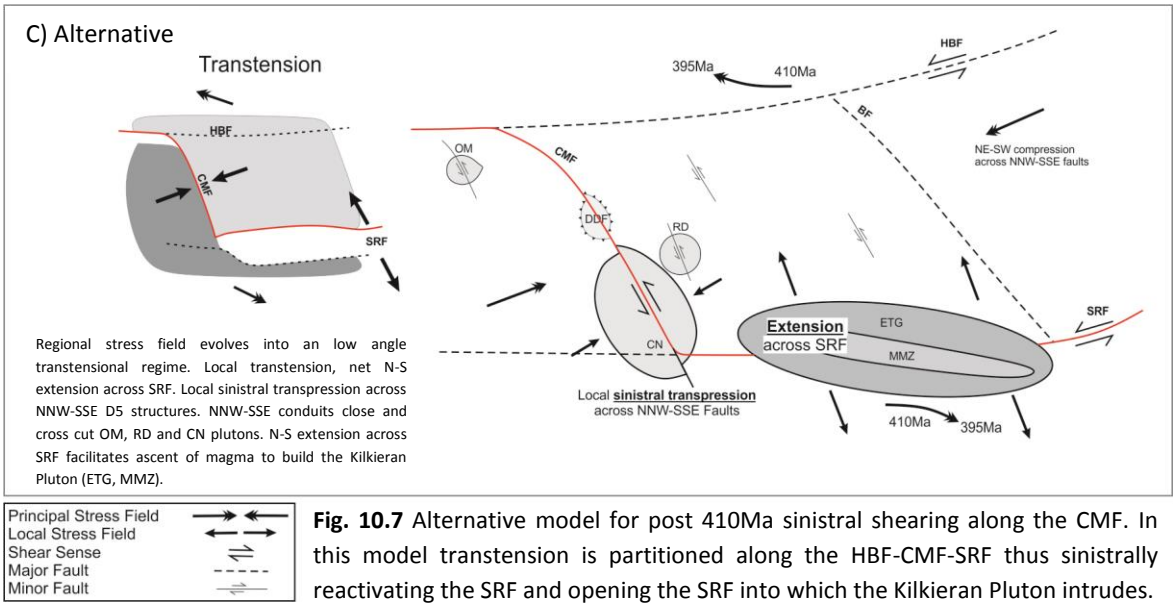


Fig. 10.7 Alternative model for post 410Ma sinistral shearing along the CMF. In this model transtension is partitioned along the HBF-CMF-SRF thus sinistrally reactivating the SRF and opening the SRF into which the Kilkieran Pluton intrudes.

An alternative model (Fig. 10.7) postulates that sinistral reactivation of the CMF was a product of regional transpression, and not directly related to inflation of the Kilkieran Pluton. This model is comparable to the inverse of a transtensional pull apart system, where the tectonic extension component is accommodated along a fault system defined by ENE-WNW and NNW-SSE structures. In this model the HBF-CMF-SRF intersect to define a fault system that preferentially partitions transtensive strain (red line in Fig. 10.7). Regional transtension shifts the defined northern block northwest as the southern block shifts southeast. This satisfies sinistral shearing along the CMF and extension along the SRF and construction of the Kilkieran Pluton but requires strain to be preferentially partitioned along the CMF rather than the more prominent and laterally continuous HBF and SRF.

10.6 Conclusions

10.6.1 Kinematic Controls on the Galway Granite Complex

A transition in the regional stress field occurred at ~410Ma, after emplacement of the earlier plutons and before the Kilkieran Pluton began to intrude. This promoted the exploitation of E-W rather than NNW-SSE faults as magma conduits. The Carna Pluton is temporally and spatially situated between these intrusions and was emplaced into a NNW-SSE structure which exhibits a reversal of shear sense shortly after this granite became emplaced. The Carna Pluton is identified as a corner stone which marks the transition in the regional stress field, after its emplacement larger volumes of magma ascended along the SRF due to NNW-SSE extension during late Caledonian regional transtension.

Two hypotheses are offered as valid explanations for late stage sinistral shearing along the CMF (Figs. 10.6C & 10.7). Neither can be substantiated based on the current data set however that of northward displacement due to inflation of the Kilkieran Pluton is preferred as it is mechanically consistent and does not require the transfer of strain from one terrane boundary to another, as is required in the first model.

The Costelloe-Murvey Granite is a distinctive pluton within the Main Batholith that happens to cross cut the Kilkieran Pluton. It post-dates the Acadian and hence cannot be considered Caledonian. Geochemical evidence suggests it may have been formed in response to melt generated during the Acadian Orogeny. It is here considered part of the Galway Granite Complex and is most likely a product of Acadian orogenesis.

10.6.2 Comment on Large Scale Petrogenic Models

Large scale petrogenetic models which attempt to account for prolonged magmatism throughout the late Caledonian Orogeny (Read 1961; Harmon and Halliday 1980; Stephens and Halliday 1984; Thirlwall *et al.* 1989; Davies and von Blanckenburg 1995; Stone *et al.* 1997; Stephens and Highton 1999; Atherton and Ghani 2002; Brown *et al.* 2008; Neilson *et al.* 2009; Baumann *et al.* 2010) are discussed in Chapter 4. Different plutons in the GGC have been related to different petrogenetic models depending on the compatibility of temporal constraints on both model and pluton (Feely *et al.* 2010). In isolation, such affiliations work, however considering the GGC is confined to a single geological terrane and intruded over such a prolonged period of time, the proposed associations are suspect. For example, south of the Orlock Bridge Fault (which is south of Connemara), the Trans-Suture Suite (Brown *et al.* 2008) should have S-type affinities and crystallised between ~400-390Ma. This is temporally compatible with the age of the Kilkieran Pluton but not tectonically, it also does not account for the occurrence of the Carna or Earlier Plutons. North of this fault, intrusions are characteristically between 420-400Ma and associated with a slab break-off, asthenospheric heat upwelling and melting of hydrous enriched lithospheric mantle (Soper 1986; Atherton and Ghani 2002; Neilson *et al.* 2009). This model is most consistent with the overall age of the GGC but fails to account for the CMG or the fact the largest phases of magmatism in Connemara occurred at the end member of its temporal parameters.

The chronological and kinematic sequence of events pertaining to the GGC is now reasonably well constrained (Inish and Letterfrack plutons remain untested, the CMG lacks a detailed structural evaluation). Definite relationships are identified which places individual intrusions in a workable context relative to the regional kinematic evolution of the Siluro-Devonian period. Therefore the validity of these data, regardless of the acceptance of larger scale interpretations, is upheld thus far. The GGC represents one of the largest late Caledonian granitoid centres in Ireland and Britain, the difficulty in resolving its petrogenic origins in the context of existing regional petrogenetic models highlights a shortfall in the current literature surrounding Caledonian events, and indeed orogenic processes, in general. Greater scrutiny of existing models based on new fieldwork and geochemical data which is used in conjunction with structural data to synthesise an improved working model is required.

Given the volume of structural, field and chronological data now available for the region, the GGC is now primed for a fresh examination of its geochemical attributes. This would aim to determine the petrogenetic evolution of this suite of granites and ultimately attempt to resolve

current larger scale ideas on the prolonged episode of magmatism that occurred at the end of the Caledonian Orogeny and throughout the Acadian Orogeny.

10.6.3 The Caveats of AMS and Implications for Other Studies

The level of sensitivity achievable when using AMS to evaluate emplacement processes and subsequent deformation makes this technique an extremely powerful tool. However, equivocal interpretations can result from poorly scrutinized data (see Appendix D for discussion). Careful analysis of AMS data and comparison of these results with basic susceptibility experiments and petrographic and field observations can resolve these issues.

Structural overprinting of the AMS tensor is a major concern when examining granitoid plutons particularly in cases where very low degrees of anisotropy are present (Bouchez 1997; Parés and van der Pluijm 2002; Just *et al.* 2004). Emplacement, inflation, crystallisation and possible later deformation events all impart potentially unique stress fields during pluton growth and tend to generate multiple fabrics which are all reflected by a single mean AMS tensor. The presence of sub-fabrics can be inferred from statistical manipulation of low field AMS data (Owens 2000) but full quantification requires much more complex and time consuming analysis on specialised equipment (e.g. Lagroix and Borradaile (2000); Aubourg and Robion (2002); Žák *et al.* (2010)). A more practical approach often applies standard AMS analysis combined with detailed traditional structural and petrographic analysis of plutonic bodies to determine the presence of sub-fabrics, the rheological state under which differing stress fields occurred and the relationship between local stress fields within a pluton and the larger scale kinematic setting. (e.g. Archanjo and Fetter (2004); Debacker *et al.* (2004); López de Luchi *et al.* (2004); Mamtani and Greiling (2005); Ono *et al.* (2010)).

In the current study, quantitative analysis of AMS data shows a progression from oblate concentric flattening fabrics in the interior of the Omey Pluton into a prolate fabric within identified NNW-SSE shear zones. The discordance of these structures and internal contacts, the presence of submagmatic microstructures and the comparable orientation of these structures to those in the host rock provides unequivocal evidence that the AMS K1 vector reflects syn-emplacement shear zones and is not a magma flow indicator (in the traditional sense). Similar results were determined from the Carna Pluton and in the case of the Roundstone plutons NNW-SSE K1 vectors were determined to be flow indicators that are ultimately tectonically controlled.

In recent years AMS has been widely applied in the analysis of plutonic bodies and in many cases resulting tensors have been interpreted as subhorizontal magma flow indicators (Stevenson *et al.* 2008; Stevenson and Bennett 2011; Magee *et al.* 2012; Petronis *et al.* 2012). Data from Magee *et al.* (2012), Petronis *et al.* (2012) and Chapter 7 of this thesis is presented below (Fig. 10.8). A comparison of these data show several similarities regarding the orientation and magnitude of AMS tensors. Significantly, in both cases K1 vectors exhibit a full spectrum of inclination angles along a single plane that is parallel to mapped faults or significant topographic lows which may be unrecognised faults.

Magee *et al.* (2012) interprets AMS data from the Ben Hiant Dolerite to reflect lateral flow fabrics, however an accompanying stereonet of the data shows that few lateral prolate tensors were detected and that the majority of K1 axes consistently trend NNW-SSE (Figs. 10.8A - C). Richey and Thomas (1930) described "north-west lines of crush, the positions of which are marked by straight-running hollows" that traverse the Ben Hiant Dolerite. It is possible that the detected AMS tensors may reflect tectonic overprinting by this faulting episode and hence don't exclusively reflect lateral magma flow as proposed by Magee *et al.* (2012). Petronis *et al.* (2012) interprets some AMS tensors from the Ross of Mull Granite as magmatic flow fabrics, that steepened during inflation, and others as tectonic overprints (Figs. 10.8F, G). Again the vast majority of K1 axes are similarly oriented (in this case NNE-SSW) and parallel local depressions and recognised faults that traverse the intrusion. AMS data from the Omey Pluton is used as an example from the current work is interpreted to reflect lateral emplacement which was overprinted by inflation and shearing along underlying ascent conduits, this is best observed in the Omey Pluton example (Figs. 10.8D, E).

The difference in interpretation is subtle but important as the authors cited differentially attribute very similar data to drastically distinct causative forces. This highlights contrasting opinions over the importance of post emplacement tectonic overprinting. In the absence of a detailed review of the work cited, it is not possible to reconcile the deductions of the three authors, however it seems probable that the AMS of samples collected in close proximity to faults is vulnerable to tectonic overprinting. Furthermore, it is clear that in all cases the K1 vectors are not dominantly subhorizontal and thus do not independently support sub-lateral emplacement models. In most cases AMS data do not show that lateral emplacement occurred as much as it infers it may have occurred but was subsequently overprinted.

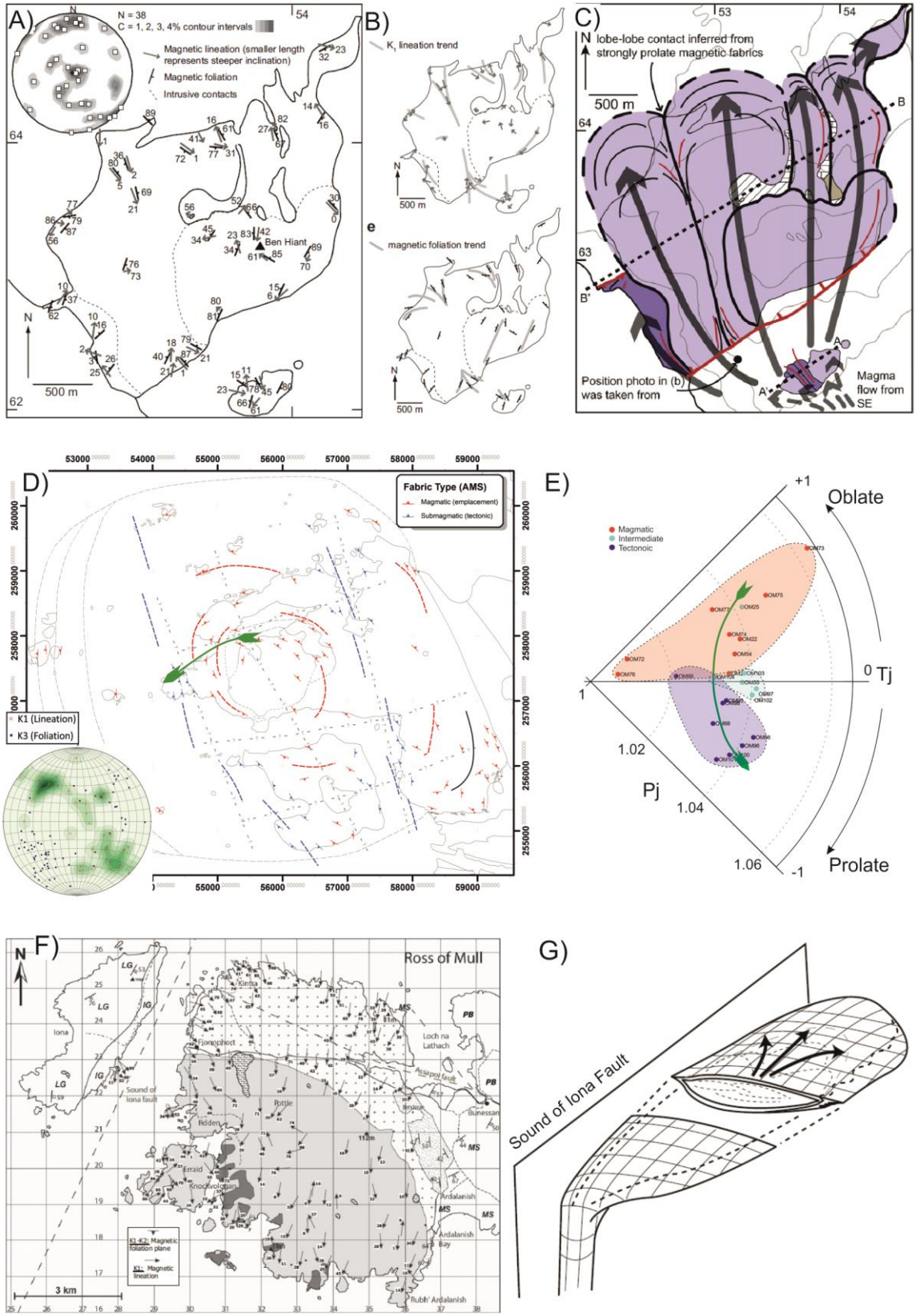


Fig. 10.8 Magee *et al.* (2012) interpreted AMS tensors from the Ben Hiant Dolerite as magmatic flow indicators (A-C) however the results of the current work show that extremely similar data (note similarities in stereographic projections) actually reflects both pluton inflation and tectonic shearing along NNW-SSE trans-plutonic faults in the Omey Pluton (D-E). Petronis *et al.* (2012) considered the AMS tensor to be a product of both tectonic and magmatic processes.

In summary, AMS needs careful analysis and comparison with traditional methods before an absolute causative force can be attributed to the net tensor. The AMS tensor is merely an ellipsoid defined by three mutually orthogonal vectors whose orientation is controlled by the net sum of all stresses applied to the host material as well as the susceptibility properties that are intrinsic to the constituent minerals. These properties cannot infer the origin of the averaged tensor. Detailed field and petrographic examination is required. Despite this, the benefits of AMS are clear as this is superior to other fabric analysis methods both in terms of accuracy and time - cost efficiency.

10.6.4 Publications arising from this Study

Contributions to Date

McCarthy, W., Reavy, R.J., Stevenson, C.T., Petronis, M.S., Feely, M. & Crowley, Q. (2012) Micro-magnets measuring macro movements - the intrusion and subsequent deformation of the Carna Granite. [Oral Presentation], Irish Geological Research Meeting, Cork, Ireland.

McCarthy, W., Reavy, R.J., Stevenson, C.T. & Petronis, M.S. (2012) A multidisciplinary approach to the interpretation of rock magnetic data; a case study from the Galway Granite Batholith. [Poster Presentation], Irish Geological Research Meeting, Cork, Ireland.

McCarthy, W., Reavy, R.J., Stevenson, C.T. & Feely, M. (2011) Emplacement of the earliest phases of the Galway Granite. [Oral Presentation], Irish Geological Research Meeting, Galway, Ireland.

McCarthy, W., Reavy, R.J., Stevenson C.T. & Feely, M. (2011) Omey - Initiation of Late Caledonian magmatism in Connemara. [Poster Presentation], Irish Geological Research Meeting, Galway, Ireland.

McCarthy, W., Reavy, R.J., Stevenson C.T.E. & Feely, M. (2011) Emplacement of the earliest phases of the Galway Granite complex. [Poster Presentation], Volcanic and Magmatic Studies Group, Cambridge, UK.

McCarthy, W., Reavy, R.J., Stevenson, C.T.E. & Feely, M. (2010) Emplacement of the Omey Granite, Co. Galway - Preliminary AMS results. [Poster Presentation], Irish Geological Research Meeting, Belfast, UK.

McCarthy, W., Reavy, R.J., Stevenson, C.T.E. & Feely, M. (2010) Construction of the Omey Granite. [Poster Presentation], Volcanic and Magmatic Studies Group AGM, Birmingham, UK.

McCarthy, W., Reavy, R.J., Stevenson, C.T.E. & Feely, M. (2010) Preliminary AMS for the Omey Granite. [Poster Presentation], Tectonic Studies Group AGM, Birmingham, UK.

Contributions in preparation

McCarthy, W.J., Reavy, R.J., Stevenson, C.T.E., Petronis, M.S., (in prep) Sub-plutonic shear zones as magma ascent conduits; Ascent and Emplacement of the Omey Pluton (intended journal; Journal of Structural Geology)

McCarthy, W.J., Stevenson, C.T.E., Petronis, M.S., Reavy, R.J., (in prep) Validity of forceful and passive emplacement concept and construction of the Roundstone Pluton (intended journal; Geology)

McCarthy, W.J., Petronis, M.S., Reavy, R.J., Stevenson, C.T.E., Crowley, Q., (in prep) A tectonic control for the Ascent and emplacement of the Carna Pluton (intended journal; Scottish Journal of Geology)

McCarthy, W.J., Reavy, R.J., Stevenson, C.T.E., Petronis, M.S., Crowley, Q., (in prep) Progressive modification to magma transport conduits due to modification to far field orogenic stress fields; A holistic structural model for the Galway Granite Complex (intended journal; Journal of the Geological Society, London)

McCarthy, W.J., Dobson, K., The feasibility of AMS as a proxy for finite strain; A principal study utilising AMS analysis and x-ray tomography (intended journal; Tectonophysics)



References;

Ablay, G. J., Clemens, J. D., and Petford, N. (2008), 'Large-scale mechanics of fracture-mediated felsic magma intrusion driven by hydraulic inflation and buoyancy pumping', *In: Thomson, K. & Petford, N. (eds) Structure and Emplacement of High-Level Magmatic Systems. Geological Society, London, Special Publications,* 302, 3-29.

Acocella, V. and Rossetti, F. (2002), 'The role of extensional tectonics at different crustal levels on granite ascent and emplacement: an example from Tuscany (Italy)', *Tectonophysics,* 354 (1–2), 71-83.

Ade-Hall, J. M., Palmer, H. C., and Hubbard, T. P. (1971), 'The Magnetic and Opaque Petrological Response of Basalts to Regional Hydrothermal Alteration', *Geophysical Journal of the Royal Astronomical Society,* 24 (2), 137-74.

Ague, J. J. and Brimhall, G. H. (1988), 'Magmatic arc asymmetry and distribution of anomalous plutonic belts in the batholiths of California: Effects of assimilation, crustal thickness, and depth of crystallization', *Geological Society of America Bulletin,* 100 (6), 912-27.

Ahmed-Said, Y. and Leake, B. E. (1996), 'The conditions of metamorphism of a grossular-wollastonite vesuvianite skarn from the Omey Granite, Connemara, western Ireland, with special inference to the chemistry of vesuvianite', *Mineralogical Magazine,* 60 (4), 541-50.

Akimoto, S. (1962), 'Magnetic properties of FeO-Fe_2O_3-TiO system as a basis of rock magnetism', *Journal of physics Society Japan,* 17 (suppl. B1), 706-10.

Aleinikoff, J. N., Zartman, R. E., Walter, M., Rankin, D. W., Lyttle, P. T., and Burton, W. C. (1995), 'U-Pb ages of metarhyolites of the Catoctin and Mount Rogers formations, Central and Southern Appalachians; evidence for two pulses of Iapetan rifting', *American Journal of Science,* 295 (4), 428-54.

Allen, P. A. and Allen, J. R. (2005), 'Basin Analysis; Principles and Applications', *Blackwell Publishing*.

Altenberger, U. and Wilhelm, S. (2000), 'Ductile deformation of K-feldspar in dry eclogite facies shear zones in the Bergen Arcs, Norway', *Tectonophysics,* 320 (2), 107-21.

Améglio, L. and Vigneresse, J. L. (1999), 'Geophysical imaging of the shape of granitic intrusions at depth: a review', *In Castro, A. Gernandez, C. Vigneresse, J.L. (eds) Understanding Granites: Integrating New and Classical Techniques, Geological Society of London, Special Publication,* 168, 39-54.

Anderson, E. M. (1936), 'The dynamics of the formation of cone-sheets, ring-dikes and cauldron-subsidence', *Proceedings of the Royal Society of Edinburgh,* 56, 128-56.

--- (1951), 'The dynamics of faulting.', *London, Oliver and Boyd*.

Anderson, T. B. and Oliver, G. J. H. (1996), 'Xenoliths of Iapetus Suture mylonites in County Down lamprophyres, Northern Ireland', *Journal of the Geological Society,* 153 (3), 403-07.

Anderton, R. (1980), 'Did Iapetus start to open during the Cambrian?', *Nature,* 286 (5774), 706-08.

--- (1980), 'Distinctive pebbles as indicators of Dalradian provenance', *Scottish Journal of Geology,* 16 (2-3), 143-52.

Anderton, R. (1982), 'Dalradian deposition and the late Precambrian–Cambrian history of the N Atlantic region: a review of the early evolution of the Iapetus Ocean', *Journal of the Geological Society,* 139 (4), 421-31.

--- (1985), 'Sedimentation and tectonics in the Scottish Dalradian', *Scottish Journal of Geology,* 21 (4), 407-36.

Angus, N. S. (1982), 'Autometasomatic gneisses of the Currywongaun-Doughruagh syntectonic intrusion, Connemara, Ireland', *Mineralogical Magazine,* 46 (411-420).

Arbaret, L., Diot, H., Bouchez, J. L., Lespinasse, P., and Saint-Blanquat, M. d. (1997), 'Analogue 3d Simple-shear experiments of magmatic biotite subfabrics.', *In: Bouchez, J.L., Hutton,*

D.H.W., Stephens, W.E., (eds.), Grantie: From Segregation of Melt to Emplacement Fabrics, Kluwer Academic Publishers, Dordrecht, 129-44.

Archanjo, C. J., Launeau, P., and Bouchez, J. L. (1995), 'Magnetic fabric vs. magnetite and biotite shape fabrics of the magnetite-bearing granite pluton of Gameleiras (Northeast Brazil)', *Physics of the Earth and Planetary Interiors,* 89 (1–2), 63-75.

Archanjo, C. J. and Fetter, A. H. (2004), 'Emplacement setting of the granite sheeted pluton of Esperança (Brasiliano orogen, Northeastern Brazil)', *Precambrian Research,* 135 (3), 193-215.

Archanjo, C. J. and Launeau, P. (2004), 'Magma flow inferred from preferred orientations of plagioclase of the Rio Ceará-Mirim dyke swarm (NE Brazil) and its AMS significance', *Geological Society, London, Special Publications,* 238 (1), 285-98.

Archanjo, C. J., Hollanda, M. H. B. M., Rodrigues, S. W. O., Neves, B. B. B., and Armstrong, R. (2008), 'Fabrics of pre- and syntectonic granite plutons and chronology of shear zones in the Eastern Borborema Province, NE Brazil', *Journal of Structural Geology,* 30, 310-26.

Archer, J. B. (1980), 'Patrick Ganly: Geology', *Irish Naturalists' Journal,* 20, 142-47.

Argyle, K. S. and Dunlop, D. J. (1990), 'Low-Temperature and High-Temperature Hysteresis of Small Multidomain Magnetites (215-540 nm)', *J. Geophys. Res.,* 95 (B5), 7069-82.

Argyle, K. S., Dunlop, D. J., and Xu, S. (1994), 'Single-domain Behavior of multidomain magnetite grains', *EOS Transactions. AGU. (abstract),* Fall meeeting (75), 196.

Arrowsmith, P. (1987), 'Laser ablation of solids for elemental analysis by inductively coupled plasma mass spectrometry', *Analytical Chemistry,* 59 (10), 1437-44.

Arrowsmith, S. J., Kendall, M., White, N., VanDecar, J. C., and Booth, D. C. (2005), 'Seismic imaging of a hot upwelling beneath the British Isles', *Geology,* 33 (5), 345-48.

Arzi, A. A. (1978), 'Critical phenomena in the rheology of partially melted rocks', *Tectonophysics,* 44 (1–4), 173-84.

Atherton, M. P. (1995), 'Granite magmatism', *Geological Society, London, Memoirs,* 16 (1), 221-35.

Atherton, M. P. and Ghani, A. A. (2002), 'Slab breakoff: a model for Caledonian, Late Granite syn-collisional magmatism in the orthotectonic (metamorphic) zone of Scotland and Donegal, Ireland', *Lithos,* 62 (3–4), 65-85.

Aubourg, C. and Robion, P. (2002), 'Composite ferromagnetic fabrics (magnetite, greigite) measured by AMS and partial AARM in weakly strained sandstones from western Makran, Iran', *Geophysical Journal International,* 151 (3), 729-37.

Aucott, J. W. (1966), 'The petrology and geochemistry of the Galway Granite in the Crook Moithan area, Connemara, Co. Galway, Eire', *PhD Thesis, University of Bristol*.

Badger, R. L. and Sinha, A. K. (1988), 'Age and Sr isotopic signature of the Catoctin volcanic province: Implications for subcrustal mantle evolution', *Geology,* 16 (8), 692-95.

Badley, M. E. (1976), 'Stratigraphy, structure and metamorphism of Dalradian rocks of the Maumturk Mountains, Connemara, Ireland', *Journal of the Geological Society,* 132 (5), 509-20.

Bagdassarov, N. and Dorfman, A. (1998), 'Granite rheology: magma flow and melt migration', *Journal of the Geological Society,* 155 (5), 863-72.

Bailey, E. B., Clough, C. T., Wright, W. B., Richey, J. E., and Wilson, G. V. (1924), 'Tertiary and Post-Tertiary Geology of Mull, Loch Aline, and Oban', *HMSO, London.*

Bailey, E. B. and McCallien, W. J. (1956), 'Composite minor intrusions and the Slieve Gullion Complex, Ireland', *Liverpool and Manchester Geological Society,* 1, 466-501.

Bailey, M. E. and Dunlop, D. J. (1983), 'Alternating field characteristics of pseudo-single-domain (2–14 μm) and multidomain magnetite', *Earth and Planetary Science Letters,* 63 (3), 335-52.

Baker, D. R. (1996), 'Granitic melt viscositites: Empierical and configurational entropy models for their calculation', *American Mineralogist,* 81, 126-34.

Bakhtari, H. R., Frizon de Lamotte, D., Aubourg, C., and Hassanzadeh, J. (1998), 'Magnetic fabrics of Tertiary sandstones from the Arc of Fars (Eastern Zagros, Iran)', *Tectonophysics,* 284 (3–4), 299-316.

Balsley, J. R. and Buddington, A. F. (1960), 'Magnetic Susceptibility Anisotropy and Fabric of some Adirondack Granite and Orthogneisses', *American Journal of Science, Bradley Volume,* 258-A, 6-20.

Barber, J. P. and Yardley, B. W. D. (1985), 'Conditions of high grade metamorphism in the Dalradian of Connemara, Ireland', *Journal of the Geological Society,* 142 (1), 87-96.

Barnichon, J. D., Havenith, H., Hoffer, B., Charlier, R., Jongmans, D., and Duchesne, J. C. (1999), 'The deformation of the Egersund–Ogna anorthosite massif, south Norway: finite-element modelling of diapirism', *Tectonophysics,* 303 (1–4), 109-30.

Barros, C. E. M., Barbey, P., and Boullier, A. M. (2001), 'Role of magma pressure, tectonic stress and crystallization progress in the emplacement of syntectonic granites. The A-type Estrela Granite Complex (Carajás Mineral Province, Brazil)', *Tectonophysics,* 343 (1–2), 93-109.

Batchelor, G. (2000), 'Introduction to fluid Mechanics', *Cambridge University Press*.

Bates, R. L. and Jackson, J. A. (1980), 'Glossary of Geology (2nd edition)', *American Geological Institute, Falls Church, Virginia*, 751.

Bathal, R. S. (1971), 'Magnetic anisotropy in rocks', *Earth Science Review,* 7, 227-53.

Baumann, C., Gerya, T. V., and Connolly, J. A. D. (2010), 'Numerical modelling of spontaneous slab breakoff dynamics during continental collision', *Geological Society, London, Special Publications,* 332 (1), 99-114.

Baxter, E. F., Ague, J. J., and Depaolo, D. J. (2002), 'Prograde temperature–time evolution in the Barrovian type–locality constrained by Sm/Nd garnet ages from Glen Clova, Scotland', *Journal of the Geological Society,* 159 (1), 71-82.

Baxter, S. (2000), 'The geology of part of the Galway Granite near Barna, Co. Galway, Ireland', *PhD Thesis, National University of Ireland Galway*.

Baxter, S. and Feely, M. (2002), 'Magma mixing and mingling textures in granitoids: examples from the Galway Granite, Connemara, Ireland', *Mineralogy and Petrology,* 76 (1), 63-74.

Baxter, S., Graham, N. T., Feely, M., Reavy, R. J., and Dewey, J. F. (2005), 'A microstructural and fabric study of the Galway Granite, Connemara, western Ireland', *Geological Magazine,* 142 (1), 81-95.

Becker, J. S. (2005), 'Recent developments in isotope analysis by advanced mass spectrometric techniques', *Journal of Analytical Atomic Spectrometry,* 20, 1173-84.

Bell, B. R. and Williamson, I. T. (2002), 'Tertiary igneous activity', *In: Trewin, N.H. (ed) The Geology of Scotland. Geological Society, London (4th edition).* 371-408.

Bell, T. H. (1998), 'Recrystallisation of biotite by subgrain rotation', *In: A. Snoke, J. Tullis, V.R. Todd (eds.), Fault related rocks - a photographic atlas. Princeton University Press, New Jersey*, 272-73.

Benn, K. (2010), 'Anisotropy of magnetic susceptibility fabrics in syntectonic plutons as tectonic strain markers: the example of the Canso pluton, Meguma Terrane, Nova Scotia', *Geological Society of America Special Papers,* 472, 147-58.

Bennett, M. C. and Gibb, F. G. F. (1983), 'Younging directions in the Dawros peridotite, Connemara', *Journal of the Geological Society,* 140 (1), 63-73.

Bergantz, G. W. (2000), 'On the dynamics of magma mixing by reintrusion: implications for pluton assembly processes', *Journal of Structural Geology,* 22 (9), 1297-309.

Berthe, D., Choukroune, P., and Jegouzo, P. (1979), 'Orthogeneiss, mylonites and non coaxial deformation of granites: the example of the South Armorican shear zone', *Journal of Structural Geology,* (1), 31-42.

BGS, B. G. S. (2007), 'Assynt. Scotland Special Sheet. Bedrock.

1:50,000 Geology Series', *British Geological Survey, Keyworth, Nottingham*.
Bina, M. and Daly, L. (1994), 'Mineralogical change and self-reversed magnetizations in pyrrhotite resulting from partial oxidation; geophysical implications', *Physics of the Earth and Planetary Interiors,* 85 (1–2), 83-99.
Blenkinsop, T. G. (2000), 'Deformation microstructures and mechanisms in minerals and rocks', *Dordrecht: Kluwer*.
Blichert-Toft, J., Chauvel, C., and Albarède, F. (1997), 'Separation of Hf and Lu for high-precision isotope analysis of rock samples by magnetic sector-multiple collector ICP-MS', *Contributions to Mineralogy and Petrology,* 127 (3), 248-60.
Bluck, B. J., Gibbons, W., and Ingham, J. K. (1992), 'Terranes', *Geological Society, London, Memoirs,* 13 (1), 1-4.
Blumenfeld, P. and Bouchez, J.-L. (1988), 'Shear criteria in granite and migmatite deformed in the magmatic and solid states', *Journal of Structural Geology,* 10 (4), 361-72.
Bolle, O., Diot, H., and Trindade, R. I. F. (2003), 'Magnetic fabrics in the Holum granite (Vest-Agder, southern most Norway): implications for the late evolution of the Sveconorwegian (Grenvillian) orogen of SW Scandinavia', *Precambrian Research,* 121, 221-49.
Borradaile, G. (1987), 'Anisotropy of magnetic susceptibility: rock composition versus strain', *Tectonophysics,* 138 (2–4), 327-29.
Borradaile, G. and Sarvas, P. (1990), 'Magnetic susceptibility fabrics in slates: Structural, mineralogical and lithological influences', *Tectonophysics,* 172 (3–4), 215-22.
Borradaile, G. and Dehls, J. F. (1993), 'Regional Kinematics inferred from magnetic subfabrics in Archean rocks in Northern Ontario, Canada', *Journal of Structural Geology,* 15 (7), 887-94.
Borradaile, G. (2001), 'Anisotropy of magnetic susceptibility, Measurement schemes', *Geophysical Research Letters,* 22, 1957-60.
Borradaile, G. and Lagroix, F. (2001), 'Magnetic fabrics reveal upper mantle flow fabrics in the Toordos ophiolite complex, Cyprus.', *Journal of Structural Geology,* 23, 1299-317.
Borradaile, G. (2003), 'Statistics of Earth Science Data', *Springer-Verlag*, 351.
Borradaile, G. J. and Tarling, D. H. (1981), 'The influence of deformation mechanisms on magnetic fabrics in weakly deformed rocks', *Tectonophysics,* 77 (1–2), 151-68.
Borradaile, G. J. and Puumala, M. A. (1989), 'Synthetic magnetic fabrics in a plasticene medium', *Tectonophysics,* 164 (1), 73-78.
Borradaile, G. J. and Werner, T. (1994), 'Magnetic anisotropy of some phyllosilicates', *Tectonophysics,* 235 (3), 223-48.
Borradaile, G. J. and Stupavsky, M. (1995), 'Anisotropy of magnetic susceptibility: Measurement schemes', *Geophys. Res. Lett.,* 22 (15), 1957-60.
Borradaile, G. J. and Henry, B. (1997), 'Tectonic applications of magnetic susceptibility and its anisotropy', *Earth-Science Reviews,* 42 (1–2), 49-93.
Borradaile, G. J. and Jackson, M. (2004), 'Anisotropy of magnetic susceptibility (AMS): magnetic petrofabrics of deformed rocks', *Geological Society, London, Special Publications,* 238 (1), 299-360.
--- (2010), 'Structural geology, petrofabrics and magnetic fabrics (AMS, AARM, AIRM)', *Journal of Structural Geology,* 32 (10), 1519-51.
Bouchez, J. L., Gleizes, G., Djouadi, T., and Rochette, P. (1990), 'Microstructure and magnetic susceptibility applied to emplacement kinematics of granites: the example of the foix pluton (French pyrenees)', *Tectonophysics,* 184 (2), 157-71.
Bouchez, J. L., Delas, C., Gleizes, G., Nédélec, A., and Cuney, M. (1992), 'Submagmatic microfractures in granites', *Geology,* 20 (1), 35-38.
Bouchez, J. L. (1997), 'Granite is never isotropic: an introduction to AMS studies of granitic rocks.', *In: Bouchez, J.L., Hutton, D.H.W., Stephens, W.E., (eds.), Grantie: From Segregation of Melt to Emplacement Fabrics, Kluwer Academic Publishers, Dordrecht*, 95-112.

Bouchez, J. L., Nguema, T. M. M., Esteban, L., Siqueira, R., and Scrivener, R. (2006), 'The tourmaline-bearing granite pluton of Bodmin (Cornwall, UK): magnetic fabric study and regional inference', *Journal of the Geological Society,* 163 (4), 607-16.

Boyd, J. D. and Sloan, R. J. (2000), 'Initiation and early development of the Dingle Basin, SW Ireland, in the context of the closure of the Iapetus Ocean', *Geological Society, London, Special Publications,* 180 (1), 123-45.

Boyle, A. P. and Dawes, I. P. (1991), 'Contrasted metamorphhic and structural evolutions across a major ductile/brittle displacement zone in NW Connemara, western Ireland', *Geologische Rundschau,* 80, 459-80.

Bradshaw, R., Plant, A. G., Burke, K. C., and Leake, B. E. (1969), 'The Oughterard Granite, Connemara, Co. Galway', *Proceedings of the Royal Irish Academy. Section B: Biological, Geological, and Chemical Science,* 68, 39-65.

Bremner, D. and Leake, B. E. (1977), 'On the western boundary of the Galway Granite', *Geological Magazine,* 114 (03), 227-28.

Bremner, D. L., Leake, B. E., and Morton, W. H. (1980), 'The Geology of the Roundstone Ultrabasic Complex, Connemara', *Proceedings of the Royal Irish Academy. Section B: Biological, Geological, and Chemical Science,* 80B, 395-433.

Bridgwater, D., Sutton, J., and Watterson, J. (1974), 'Crustal downfolding associated with igneous activity', *Tectonophysics,* 21 (1–2), 57-77.

Brown, G. C. and McClelland, W. C. (2000), 'Pluton emplacement by sheeting and vertical ballooning in part of the southeast Coast Plutonic', *Geological Society of America,* 112 (5), 708.

Brown, M. and Solar, G. S. (1998), 'Granite ascent and emplacement during contractional deformation in convergent orogens', *Journal of Structural Geology,* 20 (9–10), 1365-93.

Brown, M. and Solar, G. S. (1999), 'The mechanism of ascent and emplacement of granite magma during transpression: a syntectonic granite paradigm', *Tectonophysics,* 312 (1), 1-33.

Brown, M. (2007), 'Crustal melting and melt extraction, ascent and emplacement in orogens: mechanisms and consequences', *Journal of the Geological Society,* 164 (4), 709-30.

Brown, P. E. (1991), 'Caledonian and earlier magmatism', *Geology of Scotland., Craig, G.Y. (ed). Geological Society of London* 229-96.

Brown, P. E., Ryan, P. D., Soper, N. J., and Woodcock, N. H. (2008), 'The Newer Granite problem revisited: a transtensional origin for the Early Devonian Trans-Suture Suite', *Geological Magazine,* 145 (2), 235-56.

Brun, J. P. and Pons, J. (1981), 'Strain patterns of pluton emplacement in a crust undergoing non-coaxial deformation, Sierra Morena, Southern Spain', *Journal of Structural Geology,* 3 (3), 219-29.

Brun, J. P., Gapais, D., Cogne, J. P., Ledru, P., and Vigneresse, J. L. (1990), 'The Flamanville Granite (Northwest France): An unequivocal example of a syntectonically expanding pluton', *Geological Journal,* 25 (3-4), 271-86.

Buchwaldt, R. (2001), 'Geochronology and Nd-Sr systematics of late Caledonian Granite in western Ireland: New implications for the Caledonian Orogeny', *Geological Society of America, 36th Annual Meeting, March 12-14th.*, Session No. 20.

Buddington, A. F. (1959), 'Granite emplacement with special reference to North America.', *Bull. geol. Soc. Am.,* 70, 671-747.

Buddington, A. F. and Lindsley, D. H. (1964), 'Iron-Titanium Oxide Minerals and Synthetic Equivalents', *Journal of Petrology,* 5 (2), 310-57.

Burchardt, S., Tanner, D. C., and Krumbholz, M. (2009), 'Emplacement of the Slaufrudalur Pluton, southeast Iceland, deduced from field observations and its three-dimensional shape', *Trabajos de Geología, Universidad de Oviedo,* 29, 129-30.

Burchardt, S., Tanner, D., and Krumbholz, M. (2012), 'The Slaufrudalur pluton, southeast Iceland—An example of shallow magma emplacement by coupled cauldron subsidence and magmatic stoping', *Geological Society of America Bulletin,* 124 (1-2), 213-27.

Burgoyne, T. W. and Hieftje, G. M. (1996), 'An introduction to ion optics for the mass spectrograph', *Mass Spectrometry Reviews,* 15 (4), 241-59.

Burov, E., Jaupart, C., and Guillou-Frottier, L. (2003), 'Ascent and emplacement of buoyant magma bodies in brittle-ductile upper crust', *J. Geophys. Res.,* 108 (B4), 2177.

Bussel, M. A. (1985), 'The Centred complex of the Rio Huaura: a study of magma mixing and differentiation in high-level magma chambers', *In: Pitcher, W.S., Atherton, M.P., Cobbing, E.J., Beckinsale, R.D. (eds), Magmatism at a plate. Blackie & Sons Ltd, Glasgow*, 128-54.

Butler, R. F. (1982), 'Magnetic Mineralogy of Continental Deposits, San Juan Basin, New Mexico, and Clark's Fork Basin, Wyoming', *J. Geophys. Res.,* 87 (B9), 7843-52.

Butler, R. W. H. (1987), 'Thrust sequences', *Journal of the Geological Society,* 144 (4), 619-34.

Butler, R. W. H. (2004), 'The nature of 'roof thrusts' in the Moine Thrust Belt, NW Scotland: implications for the structural evolution of thrust belts', *Journal of the Geological Society,* 161 (5), 849-59.

Cagnoli, B. and Tarling, D. H. (1997), 'The reliability of anisotropy of magnetic susceptibility (AMS) data as flow direction indicators in friable base surge and ignimbrite deposits: Italian examples', *Journal of Volcanology and Geothermal Research,* 75 (3–4), 309-20.

Callaghan, B. (1999), 'The geology of the Shannawona Fault zone of the Galway Granite in the Casla area, Connemara, Ireland', *PhD Thesis, National University of Ireland Galway*.

--- (2005), 'Locating the Shannawona Fault: Field and Geobarometric Studies from the Galway Batholith, Western Ireland', *Irish Journal of Earth Sciences,* 23, 85-100.

Callot, J. P. and Guichet, X. (2003), 'Rock texture and magnetic lineation in dykes: a simple analytical model', *Tectonophysics,* 366 (3–4), 207-22.

Callot, J. P., Gurevitch, E., Westphal, M., and Pozzi, J. P. (2004), 'Flow patters in the Siberian traps deduced from magnetic fabric studies', *Geophysical Journal International,* 156 (3), 426-30.

Cañón-Tapia, E. (1996), 'Single-grain versus distribution anisotropy: a simple three-dimensional model', *Physics of the Earth and Planetary Interiors,* 94 (1–2), 149-58.

Castro, A. (1986), 'Structural pattern and ascent model in the Central Extremadura batholith, Hercynian belt, Spain', *Journal of Structural Geology,* 8 (6), 633-45.

Cawood, P. A., McCausland, P. J. A., and Dunning, G. R. (2001), 'Opening Iapetus: Constraints from the Laurentian margin in Newfoundland', *Geological Society of America Bulletin,* 113 (4), 443-53.

Cawood, P. A., Nemchin, A. A., Smith, M., and Loewy, S. (2003), 'Source of the Dalradian Supergroup constrained by U–Pb dating of detrital zircon and implications for the East Laurentian margin', *Journal of the Geological Society,* 160 (2), 231-46.

Cawood, P. A. and Pisarevsky, S. A. (2006), 'Was Baltica right-way-up or upside-down in the Neoproterozoic?', *Journal of the Geological Society,* 163 (5), 753-59.

Cawood, P. A., Nemchin, A. A., Strachan, R., Prave, T., and Krabbendam, M. (2007), 'Sedimentary basin and detrital zircon record along East Laurentia and Baltica during assembly and breakup of Rodinia', *Journal of the Geological Society,* 164 (2), 257-75.

Chadima, M., Cajz, V., and Týcová, P. (2009), 'On the interpretation of normal and inverse magnetic fabric in dikes: Examples from the Eger Graben, NW Bohemian Massif', *Tectonophysics,* 466 (1–2), 47-63.

Channell, J. E. T., McCabe, C., Torsvik, T. H., Trench, A., and Woodcock, N. H. (1992), 'Palaeozoic palaeomagnetic studies, in the Welsh Basin-recent advances', *Geological Magazine,* 129 (05), 533-42.

Chappell, B. W. and White, A. J. R. (1974), 'Two contrasting granite types', *Pacific Geology,* 8, 173-74.

--- (2001), 'Two contrasting granite types: 25 years later', *Australian Journal of Earth Sciences,* 48 (4), 489-99.

Charlesworth, J. K. (1963), 'Historical Geology of Ireland', *Oliver and Boyd*.

Chroston, P. N. and Max, M. D. (1988), 'Seismic anisotropy in mylonites: an example from the Mannin Thrust Zone, southwest Connemara, Ireland', *Tectonophysics,* 148 (1–2), 29-39.

Claesson, S. and Roddick, J. C. (1983), '$^{40}Ar/^{39}Ar$ data on the age and metamorphism of the Ottfjället dolerites, Särv Nappe, Swedish Caledonides', *Lithos,* 16 (1), 61-73.

Claxton, C. W. (1965), 'The petrology and geochemistry of the Galway Granite in teh Screeb-Invermore-Rosmuc area, Connemara, Eire.', *PhD Thesis, Universtiy of Hull*.

Clemens, J. D. and Mawer, C. K. (1992), 'Granitic magma transport by fracture propagation', *Tectonophysics,* 204 (3–4), 339-60.

Clemens, J. D., Petford, N., and Mawer, C. K. (1997), 'Ascent mechanisms of granitic magmas: causes and consequences', *In Holness, M.B. (ed.) Deformation-enhanced Fluid Transport in the Earths Crust and Mantle. London: Chapman & Hall*, 144-71.

Clemens, J. D. and Petford, N. (1999), 'Granitic melt viscosity and silicic magma dynamics in contrasting tectonic settings', *Journal of the Geological Society,* 156 (6), 1057-60.

Cliff, R. A., Yardley, B. W. D., and Bussy, F. (1993), 'U-Pb isotopic dating of fluid infiltration and metasomatism during Dalradian regional metamorphism in Connemara, western Ireland.', *Journal of Metamorphic Geology,* 11 (2), 185-91.

Cliff, R. A., Yardley, B. W. D., and Bussy, F. R. (1996), 'U–Pb and Rb–Sr geochronology of magmatism and metamorphism in the Dalradian of Connemara, western Ireland', *Journal of the Geological Society,* 153 (1), 109-20.

Clough, C. T., Maufe, H. B., and Bailey, E. B. (1909), 'The Cauldron-Subsidence of Glen Coe, and the Associated Igneous Phenomena', *Quarterly Journal of the Geological Society,* 65 (1-4), 611-53,NP,55-57,NP,59-69,NP,71-78.

Coats, J. S. and Wilson, J. R. (1971), 'The eastern end of the Galway Granite', *Mineralogical Magazine,* 38, 138-51.

Cobbing, E. J. (1959), 'The metamorphic petrology and structure of the district of NW of Clifden, Co. Galway', *Ph.D. Thesis University of Durham*.

--- (1968), 'The Geology of the District North-West of Clifden, Co. Galway', *Proceedings of the Royal Irish Academy. Section B: Biological, Geological, and Chemical Science,* 67, 303-25.

Cocks, L. R. M., Holland, C. H., Rickards, R. B., and Strachan, I. (1971), 'A correlation of Silurian rocks in the British Isles', *Journal of the Geological Society,* 127 (2), 103-36.

Cocks, L. R. M. and Fortey, R. A. (1982), 'Faunal evidence for oceanic separations in the Palaeozoic of Britain', *Journal of the Geological Society,* 139 (4), 465-78.

Cocks, L. R. M. and Fortey, R. A. (1990), 'Biogeography of Ordovician and Silurian Faunas.', *In: McKewrrow, W.S., Scotese, C.F. (Eds.), Palaeozoic Palaeogeography and Biogeography. Mem. Geological Society, London.,* 12, 97-104.

Cocks, L. R. M., McKerrow, W. S., and van Staal, C. R. (1997), 'The margins of Avalonia', *Geological Magazine,* 134 (5), 627-36.

Cocks, L. R. M. (2000), 'The Early Palaeozoic geography of Europe', *Journal of the Geological Society,* 157 (1), 1-10.

Compston, W., Sambridge, M. S., Reinfrank, R. F., M., M., Vidal, G., and Claesson, S. (1995), 'Numerical ages of volcanic rocks and the earliest faunal zone within the late Precambrian of east Poland', *Journal of the Geological Society, London,* 152, 599-611.

Compton, R. (1955), 'Trondhjemite batholith near Bidwell Bar, California.', *Bull. geol. Soc. Am.,* 66, 9-44.

Corry, C. E. (1988), 'Laccoliths: Mechanics of emplacement and growth', *Geological Society of America*.

Courrioux, G. (1987), 'Oblique diapirism: the criffel granodiorite/granite zoned pluton (southwest Scotland)', *Journal of Structural Geology,* 9 (3), 313-30.
Coward, M. P. (1981), 'Diapirism and gravity tectonics: report of a Tectonic Studies Group conference held at Leeds University, 25–26 March 1980', *Journal of Structural Geology,* 3 (1), 89-95.
--- (1982), 'Surge zones in the Moine thrust zone of NW Scotland', *Journal of Structural Geology,* 4 (3), 247-56.
--- (1983), 'The thrust and shear zones of the Moine thrust zone and the NW Scottish Caledonides', *Journal of the Geological Society,* 140 (5), 795-811.
--- (1985), 'The thrust structures of southern Assynt, Moine thrust zone', *Geological Magazine,* 122 (6), 595-607.
--- (1990), 'The Precambrian, Caledonian and Variscan framework to NW Europe', *Geological Society, London, Special Publications,* 55 (1), 1-34.
Crowley, Q. (1997), 'Geology and geochemistry of the Galway Granite in the Inveran sector, Western Ireland', *PhD Thesis, National University of Ireland Galway*.
Crowley, Q. and Feely, M. (1997), 'New perspectives on the order and style of granite emplacement in the Galway Batholith, western Ireland', *Geological Magazine,* 134 (4), 539-48.
Cruden, A. R. (1988), 'Deformation around a rising diapir modeled by creeping flow past a sphere', *Tectonics,* 7 (5), 1091-101.
Cruden, A. R., Koyi, H., and Schmeling, H. (1995), 'Diapiric basal entrainment of mafic into felsic magma', *Earth and Planetary Science Letters,* 131 (3–4), 321-40.
Cruden, A. R. (1998), 'On the emplacement of tabular granites', *Journal of the Geological Society,* 155 (5), 853-62.
Cruden, A. R., Tobisch, O. T., and Launeau, P. (1999), 'Magnetic fabric evidence for conduit-fed emplacement of a tabular intrusion: Dinkey Creek Pluton, central Sierra Nevada batholith, California', *J. Geophys. Res.,* 104 (B5), 10511-30.
Cruden, A. R. (2008), 'Emplacement mechanisms and structural influences of a younger granite intrusion into older wall rocks - a principal study with application to the Götemar and Uthammar granites', *Report for Svensk Kärnbränslehantering AB (Swedish Nuclear Fuel and waste Management Co.* .
Cruse, M. A. J. B. (1963), 'The geology of Renvyle, Inishbofin and Inishark, north-west Connemara, Co. Galway, Eire', *Ph.D. thesis, University of Bristol*.
Cruse, M. A. J. B. and Leake, B. E. (1968), 'The Geology of Renvyle, Inishbofin and Inishshark, NW Connemara, County Galway', *Proceedings of the Royal Irish Academy,* 67B, 1-37.
Culshaw, N. G. and Fyson, W. K. (1984), 'Quartz ribbons in high grade granite gneiss: modifications of dynamically formed quartz c-axis preferred orientation by oriented grain growth', *Journal of Structural Geology,* 6 (6), 663-68.
Cutts, K. A., Kinny, P. D., Strachan, R. A., Hand, M., Kelsey, D. E., Emery, M., Friend, C. R. L., and Leslie, A. G. (2010), 'Three metamorphic events recorded in a single garnet: Integrated phase modelling, in situ LA-ICPMS and SIMS geochronology from the Moine Supergroup, NW Scotland', *Journal of Metamorphic Geology,* 28 (3), 249-67.
Czamanske, G. K. and Mihalik, P. (1972), 'Oxidation During Magmatic Differentiation, Finnmarka Complex, Oslo Area, Norway: Part 1, The Opaque Oxides', *Journal of Petrology,* 13 (3), 493-509.
Dallmeyer, R. D. (1988), 'Polyphase tectonothermal evolution of the Scandinavian Caledonides', *Geological Society, London, Special Publications,* 38 (1), 365-79.
Dallmeyer, R. D., Strachan, R. A., Rogers, G., Watt, G. R., and Friend, C. R. L. (2001), 'Dating deformation and cooling in the Caledonian thrust nappes of north Sutherland, Scotland:

insights from $^{40}Ar/^{39}Ar$ and Rb–Sr chronology', *Journal of the Geological Society,* 158 (3), 501-12.

Daly, L. and Zinsser, H. (1973), 'Etude comparative des anisotropies de susceptibiliteet d'aimantation remanente isotherme: Consequences pour l'analyse structurale et le paleomagnetisme', *Ann. Geophys.,* 29, 189-200.

Daly, R. A. (1933), 'Igneous rocks in the depths of the earth', *McGraw Hill, New York*.

Dalziel, I. W. D. (1992), 'On the organization of American plates in the Neoproterozoic and the breakout of Laurenita', *GSA Today,* 2 (11), 240-41.

Dalziel, I. W. D. (1997), 'OVERVIEW: Neoproterozoic-Paleozoic geography and tectonics: Review, hypothesis, environmental speculation', *Geological Society of America Bulletin,* 109 (1), 16-42.

Dalziel, I. W. D. and Soper, N. J. (2001), 'Neoproterozoic Extension on the Scottish Promontory of Laurentia: Paleogeographic and Tectonic Implications', *The Journal of Geology,* 109 (3), 299-317.

Davies, H. J. and von Blanckenburg, F. (1995), 'Slab breakoff: A model of lithosphere detachment and its test in the magmatism and deformation of collisional orogens', *Earth and Planetary Science Letters,* 129 (1–4), 85-102.

Davis, B. K. and Henderson, R. A. (1999), 'Syn-orogenic extensional and contractional deformation related to granite emplacement in the northern Tasman Orogenic Zone, Australia', *Tectonophysics,* 305 (4), 453-75.

Day, R., Fuller, M., and Schmidt, V. A. (1977), 'Hysteresis properties of titanomagnetites: Grain-size and compositional dependence', *Physics of the Earth and Planetary Interiors,* 13 (4), 260-67.

de Laeter, J. R. (1998), 'Mass spectrometry and geochronology', *Mass Spectrometry Reviews,* 17 (2), 97-125.

Debacker, T. N., Robion, P., and Sintubin, M. (2004), 'The anisotropy of magnetic susceptibility (AMS) in low-grade, cleaved pelitic rocks: influence of cleavage/bedding angle and type and relative orientation of magnetic carriers', *Geological Society, London, Special Publications,* 238 (1), 77-107.

Debacker, T. N., Dewaele, S., Sintubin, M., Verniers, J., Muchez, P., Boven, A. (2005), 'Timing and duration of the progressive deformation of the Brabant Massif, Belgium', *Geologica Belgica,* 8, 20-34.

Dempster, T. J., Tanner, P. W. G., and Ainsworth, P. (1994), 'Chemical zoning of white micas; a record of fluid infiltration in the Oughterard granite, western Ireland', *American Mineralogist,* 79 (5-6), 536-44.

Dempster, T. J., Rogers, G., Tanner, P. W. G., Bluck, B. J., Muir, R. J., Redwood, S. D., Ireland, T. R., and Paterson, B. A. (2002), 'Timing of deposition, orogenesis and glaciation within the Dalradian rocks of Scotland: constraints from U–Pb zircon ages', *Journal of the Geological Society,* 159 (1), 83-94.

Derham, J. M. and Feely, M. (1988), 'A K-feldspar breccia from the Mo–Cu stock work deposit in the Galway Granite, west of Ireland', *Journal of the Geological Society,* 145 (4), 661-67.

Dewaele, S., Boven, A., Muchez, P.H. (2002), '40Ar/39Ar dating of mesothermal, orogenic mineralization in a low-angle reverse shear zone in the Lower Palaeozoic of the Anglo-Brabant fold belt, Belgium', *Transactions of the Institution of Mining and Metallurgy.,* 111, B215-B30.

Dewey, J. and Mange, M. (1999), 'Petrography of Ordovician and Silurian sediments in the western Irish Caledonides: tracers of a short-lived Ordovician continent-arc collision orogeny and the evolution of the Laurentian Appalachian-Caledonian margin', *Geological Society, London, Special Publications,* 164 (1), 55-107.

Dewey, J. F. (1971), 'A model for the Lower Palaeozoic evolution of the southern margin of the early Caledonides of Scotland and Ireland', *Scottish Journal of Geology,* 7 (3), 219-40.
--- (1988), 'Extensional collapse of orogens', *Tectonics,* 7 (6), 1123-39.
Dewey, J. F., Holdsworth, R. E., and Strachan, R. A. (1998), 'Transpression and transtension zones', *Geological Society, London, Special Publications,* 135 (1), 1-14.
Dewey, J. F. (2002), 'Transtension in Arcs and Orogens', *International Geology Review,* 44 (5), 402-39.
Dewey, J. F. and Strachan, R. A. (2003), 'Changing Silurian–Devonian relative plate motion in the Caledonides: sinistral transpression to sinistral transtension', *Journal of the Geological Society,* 160 (2), 219-29.
Dewey, J. F. (2005), 'Orogeny can be very short', *Proceedings of the National Academy of Sciences of the United States of America,* 102 (43), 15286-93.
Dewey, J. F., Dutton, B., Ryan, P.D. (1997), 'Transpression in the Irish Caledonides and the Silurian evolution of basins, plutons, fabrics and cleavage sequences', *Abstracts: Continental Transpressional and Transtensional Tectonics. Tectonic Studies Group Meeting, London*.
Dias, R. and Ribeiro, A. (1994), 'Constriction in a transpressive regime: an example in the Iberian branch of the Ibero-Armorican arc', *Journal of Structural Geology,* 16 (11), 1543-54.
Dickin, A. P. (2005), *Radiogenic Isotope Geology* (Cambridge University Press).
Dietl, C. and Koyi, H. (2011), 'Sheets within diapirs – Results of a centrifuge experiment', *Journal of Structural Geology,* 33 (1), 32-37.
Ding, X., Chen, P., Chen, W., Huang, H., and Zhou, X. (2006), 'Single zircon LA-ICPMS U-Pb dating of Weishan granite (Hunan, South China) and its petrogenetic significance', *Science in China Series D: Earth Sciences,* 49 (8), 816-27.
Dingwell, D. B. (1999), 'Granitic melt viscosities', *In: Castro, A., Fernandez, C., Vigneresse, J. L., (eds), Understanding Granites: Integrating New and Classical Techniques. Geological Society of London, Special Publications,* 168, 141-60.
Douglas, D. J. (2009), 'Linear quadrupoles in mass spectrometry.', *Mass Spectrometry Reviews,* 28 (6), 937-60.
Doukhan, J. C. (1995), 'Lattice defects and Mechanical Behaviour of Quartz SiO_2', *Journal de Physique,* 5 (11), 1809-32.
Downs-Rose, K. (1985), 'The geology of the Roundstone Intrusion, Connemara, Ireland.', *Ph.D. thesis, University of Glasgow*.
Draut, A. E. and Clift, P. D. (2002), 'The origin and significance of the Delaney Dome Formation, Connemara, Ireland', *Journal of the Geological Society,* 159 (1), 95-103.
Droop, G. T. R. and Treloar, P. J. (1981), 'Pressures of metamorphism in the thermal aureole of the Etive Granite Complex', *Scottish Journal of Geology,* 17 (2), 85-102.
Dunlop, D. J. (1972), 'Magnetic Mineralogy of Unheated and Heated Red Sediments by Coercivity Spectrum Analysis*', *Geophysical Journal of the Royal Astronomical Society,* 27 (1), 37-55.
Dunlop, D. J., Hanes, J. A., and Buchan, K. L. (1973), 'Indices of Multidomain Magnetic Behavior in Basic Igneous Rocks: Alternating-Field Demagnetization, Hysteresis, and Oxide Petrology', *Journal of geophysical Research,* 78, 1387-93.
Dunlop, D. J. (1986), 'Hysteresis Properties of Magnetite and their Dependence on Particle Size: A Test of Pseudo-Single-Domain Remanence Models', *J. Geophys. Res.,* 91 (B9), 9569-84.
Dunlop, D. J. and Ozdemir, O. (1997), 'Rock Magnetism: Fundamentals and Frontiers', *Cambridge University Press*.
Dutton, B. J. (1997), 'Finite strains in transpression zones with no boundary slip', *Journal of Structural Geology,* 19 (9), 1189-200.
Edmunds, W. M. and Thomas, P. R. (1966), 'The stratigraphy and structure of the Dalradian rocks north of Recess, Connemara, Co. Galway.', *Proceedings of the Royal Irish Academy.,* 64B, 517-29.

Edwards, J. (1984), 'Partial anhysteretic remanent magnetizations produced in rotating samples, and comparisons with corresponding rotational remanent magnetizations', *Geophysical Journal of the Royal Astronomical Society,* 77 (3), 619-37.

Eggins, S. M., Kinsley, L. P. J., and Shelley, J. M. G. (1998), 'Deposition and element fractionation processes during atmospheric pressure laser sampling for analysis by ICP-MS', *Applied Surface Science,* 127–129 (0), 278-86.

Einsele, G. (1992), 'Sedimentary Basins; Evolution, Facies, Sediment Budget', *Springer Berlin Heidelberg New York*.

El-Desouky, M. E., Feely, M., and Mohr, P. (1996), 'Diorite-granite magma mingling and mixing along the axis of the Galway Granite batholith, Ireland', *Journal of the Geological Society,* 153 (3), 361-74.

El-Desouky, M. M. (1992), 'Magma mixing in the Spiddal sector of the Galway Granite: geology, geochemistry and genetic aspects', *PhD Thesis, National University of Ireland Galway*.

Elena, G.-E., Galindo-Zaldívar, J., Simancas, F., and Expósito, I. (2003), 'Diapiric emplacement in the upper crust of a granitic body: the La Bazana Granite (SW Spain)', *Tectonophysics,* 361, 83-96.

Elias, E. M., Macintyre, R. M., and Leake, B. E. (1988), 'The cooling history of Connemara, western Ireland, from K-Ar and Rb-Sr age studies', *Journal of the Geological Society,* 145 (4), 649-60.

Elliott, D., Johnson, M.R.W. (1980), 'Structural evolution in the northern part of the Moine thrust belt, NW Scotland', *Transactions of the Royal Society of Edinburgh: Earth Sciences,* 71, 69-96.

Ellwood, B. B., Balsam, W., Burkart, B., Long, G. J., and Buhl, M. L. (1986), 'Anomalous Magnetic Properties in Rocks Containing the Mineral Siderite: Paleomagnetic Implications', *J. Geophys. Res.,* 91 (B12), 12779-90.

Ellwood, B. B., Burkart, B., Rajeshwar, K., Darwin, R. L., Neeley, R. A., McCall, A. B., Long, G. J., Buhl, M. L., and Hickcox, C. W. (1989), 'Are the Iron Carbonate Minerals, Ankerite and Ferroan Dolomite, Like Siderite, Important in Paleomagnetism?', *J. Geophys. Res.,* 94 (B6), 7321-31.

Ellwood, B. B., Terrell, G. E., and Cook, W. J. (1993), 'Frequency dependence and the electromagnetic susceptibility tensor in magnetic fabric studies', *Physics of the Earth and Planetary Interiors,* 80 (1–2), 65-74.

Emeleus, C. H., Troll, V. R., Chew, D. M., and Meade, F. C. (2012), 'Lateral versus vertical emplacement in shallow-level intrusions? The Slieve Gullion Ring-complex revisited', *Journal of the Geological Society,* 169 (2), 157-71.

Emerman, S. H. and Marrett, R. (1990), 'Why dikes?', *Geology,* 18 (3), 231-33.

Engelder, T. (1993), 'Stress Regimes in the Lithosphere', *Princeton University Press, New Jersey*.

England, R. W. (1990), 'The identification of granitic diapirs', *Journal of the Geological Society,* 147 (6), 931-33.

England, R. W. (1992), 'The genesis, ascent, and emplacement of the Northern Arran Granite, Scotland: Implications for granitic diapirism', *Geological Society of America Bulletin,* 104 (5), 606-14.

Esmaeily, D., Bouchez, J. L., and Siqueira, R. (2007), 'Magnetic fabrics and microstructures of the Jurassic Shah-Kuh granite pluton (Lut Block, Eastern Iran) and geodynamic inference', *Tectonophysics,* 439 (1–4), 149-70.

Evans, B. W. and Leake, B. E. (1970), 'The Geology of the Toombeola District, Connemara, Co. Galway.', *Proceedings of the Royal Irish Academy. Section B: Biological, Geological, and Chemical Science,* 70, 105-41.

Evans, B. W. and Leake, B. E. (1970), 'The Geology of the Toombeola District, Connemara, Co. Galway', *Proceedings of the Royal Irish Academy. Section B: Biological, Geological, and Chemical Science,* 70, 105-40.

Evans, D. J., Rowley, W. J., Chadwick, R. A., Kimbell, G. S., and Millward, D. (1994), 'Seismic reflection data and the internal structure of the Lake District batholith, Cumbria, northern England', *Proceedings of the Yorkshire Geological and Polytechnic Society,* 50 (1), 11-24.

Evans, J. A. (1996), 'Dating the transition of smectite to illite in Palaeozoic mudrocks using the Rb–Sr whole-rock technique', *Journal of the Geological Society,* 153 (1), 101-08.

Fanjat, G., Camps, P., Shcherbakov, V., Barou, F., Sougrati, M. T., and Perrin, M. (2012), 'Magnetic interactions at the origin of abnormal magnetic fabrics in lava flows: a case study from Kerguelen flood basalts', *Geophysical Journal International,* 189 (2), 815-32.

Feely, M. (1982), 'Geological, geochemical and geophysical studies on the Galway Granite in the Costelloe-Inveran sector, western Ireland.', *PhD Thesis, National University of Ireland Galway*.

Feely, M. and Högelsberger, H. (1991), 'Preliminary Fluid Inclusion Studies of the Mace Head Mo-Cu Deposit in the Galway Granite', *Irish Journal of Earth Sciences,* 11 (1), 1-10.

Feely, M., McCabe, E., and Kunzendorf, H. (1991), 'The evolution of REE profiles in the Galway Granite, western Ireland', *Irish Journal of Earth Sciences,* 11, 71-89.

Feely, M., Coleman, D. S., Baxter, S., and Miller, B. (2003), 'U-Pb zircon geochronology of the Galway Granite, Connemara, Ireland: Implications for the timing of late Caledonian tectonic and magmatic events and for correlations with Acadian plutonism in New England', *Atlantic Geology,* 39, 175-84.

Feely, M., Leake, B. E., Baxter, S., Hunt, J., and Mohr, P. (2006), 'A Geological Guid to the Granite of the Galway Batholith, Connemara, western Ireland', *Geological Survery of Ireland*.

Feely, M., Selby, D., Conliffe, J., and Judge, M. (2007), 'Re-Os geochronology and fluid inclusion microthermometry of molybdenite mineralisation in the late-Caledonian Omey Granite, western Ireland', *Applied Earth Science,* 116 (3), 143-49.

Feely, M., Selby, D., Hunt, J., and Conliffe, J. (2010), 'Long-lived granite-related molybdenite mineralization at Connemara, western Irish Caledonides', *Geological Magazine,* 147 (6), 886-94.

Femenias, O., Diot, H., Berza, T., Gauffriau, A., and Demaiffe, D. (2004), 'Asymmertical to symmetrical magnetic fabric of dikes: Paleo-flow orientations and Paleo-stresses recorded on feeder-bodies from the Motru Dyke Swarm (Romania)', *Journal of Structural Geology,* 26, 1401-218.

Feng, R., Machado, N., and Ludden, J. (1993), 'Lead geochronology of zircon by LaserProbe-inductively coupled plasma mass spectrometry (LP-ICPMS)', *Geochimica et Cosmochimica Acta,* 57 (14), 3479-86.

Ferguson, C. C. and Harvey, P. K. (1979), 'Thermally overprinted Dalradian rocks near Cleggan, Connemara Western Ireland', *Proceedings of the Geologists' Association,* 90 (1–2), 43-50.

Ferguson, C. C. and Al-Ameen, S. I. (1985), 'Muscovite breakdown and corundum growth at anomalously low $f_{H2}O$: A study of contact metamorphism and convective fluid movement around the Omey Granite, Connemara, Ireland.', *Mineral. Mag.,* 49, 505-14.

--- (1986), 'Geochemistry of Dalradian pelites from Connemara, Ireland: new constraints on kyanite genesis and conditions of metamorphism', *Journal of the Geological Society,* 143 (2), 237-52.

Ferré, E. C. and Améglio, L. (2000), 'Preserved magnetic fabrics vs. annealed microstructures in the syntectonic recrystallised George granite, South Africa', *Journal of Structural Geology,* 22 (8), 1199-219.

Ferré, E. C. (2002), 'Theoretical models of intermediate and inverse AMS fabrics', *Geophys. Res. Lett.,* 29 (7), 1127.

Fitches, W. R., Pearce, N. J. G., Evans, J. A., and Muir, R. J. (1996), 'Provenance of late Proterozoic Dalradian tillite clasts, Inner Hebrides, Scotland', *Geological Society, London, Special Publications,* 112 (1), 367-77.

Fitz Gerald, J. D. and Stünitz, H. (1993), 'Deformation of granitoids at low metamorphic grade. I: Reactions and grain size reduction', *Tectonophysics,* 221 (3–4), 269-97.

Fletcher, T. P. and Rushton, A. W. A. (2007), 'The Cambrian Fauna of the Leny Limestone, Perthshire, Scotland', *Earth and Environmental Science Transactions of the Royal Society of Edinburgh,* 98 (2), 199-218.

Flinn, D. (1962), 'On folding during three dimensional progressive deformation', *Quarterly Journal of the Geological Society London,* 118, 385-428.

Flinn, D. (1965), 'On the Symmetry Principle and the Deformation Ellipsoid', *Geological Magazine,* 102 (01), 36-45.

--- (1985), 'The Caledonides of Shetland.', *In: Gee, D.G. & Sturt, B.A. (eds) The Caledonide Orogen – Scandinavia and Related Areas. Wiley, Chichester*, 1158-71.

Floyd, J. D. (1995), 'Lithostratigraphy of the Ordovician rocks in the Southern Uplands: Crawford Group, Moffat Shale Group, Leadhills Supergroup', *Earth and Environmental Science Transactions of the Royal Society of Edinburgh,* 86 (03), 153-65.

Forien, M. and Dietl, C. (2009), 'Simultaneously ascending diapirs from different depths and different positions: a centrifuge study', *Geotectonic Research,* 96 (1), 39-52.

Fossen, H. and Tikoff, B. (1993), 'The deformation matrix for simultaneous simple shearing, pure shearing and volume change, and its application to transpression-transtension tectonics', *Journal of Structural Geology,* 15 (3–5), 413-22.

Fossen, H. and Dallmeyer, R. D. (1998), '40Ar/39Ar muscovite dates from the nappe region of southwestern Norway: dating extensional deformation in the Scandinavian Caledonides', *Tectonophysics,* 285 (1–2), 119-33.

Fossen, H. and Dunlap, W. J. (1998), 'Timing and kinematics of Caledonian thrusting and extensional collapse, southern Norway: evidence from 40Ar/39Ar thermochronology', *Journal of Structural Geology,* 20 (6), 765-81.

Fowler, M. B., Henney, P. J., Darbyshire, D. P. F., and Greenwood, P. B. (2001), 'Petrogenesis of high Ba–Sr granites: the Rogart pluton, Sutherland', *Journal of the Geological Society,* 158 (3), 521-34.

Fowler, M. B., Kocks, H., Darbyshire, D. P. F., and Greenwood, P. B. (2008), 'Petrogenesis of high Ba–Sr plutons from the Northern Highlands Terrane of the British Caledonian Province', *Lithos,* 105 (1–2), 129-48.

František, H. (1992), 'Separation of a component of tectonic deformation from a complex magnetic fabric', *Journal of Structural Geology,* 14 (1), 65-71.

Friedman, M. and Higgs, N. G. (1981), 'Calcite fabrics in experimental shear zones in mechanical behavior of crustal rocks', *American Geophysical Union Monograms,* 24, 11-27.

Friedrich, A. M., Bowring, S. A., Martin, M. W., and Hodges, K. V. (1999), 'Short-lived continental magmatic arc at Connemara, western Irish Caledonides: Implications for the age of the Grampian orogeny', *Geology,* 27 (1), 27-30.

Friedrich, A. M., Hodges, K. V., Bowing, S. A., and Martin, M. W. (1999), 'Geochronological constraints on the magmatic, metamorphic and thermal evolution of the Connemara Caledonides, western Ireland', *Journal of the Geological Society,* 156 (6), 1217-30.

Fuller, M. D. (1963), 'Magnetic Anisotropy and Paleomagnetism', *J. Geophys. Res.,* 68 (1), 293-309.

Gaillot, P., de Saint-Blanquat, M., and Bouchez, J.-L. (2006), 'Effects of magnetic interactions in anisotropy of magnetic susceptibility: Models, experiments and implications for igneous rock fabrics quantification', *Tectonophysics,* 418 (1–2), 3-19.

Gallagher, V., Feely, M., Hogelsberger, H., Jenkin, G. R. T., and Fallick, A. E. (1992), 'Geological fluid inclusion and stable isotope studies of Mo mineralisation, Galway Granite, Ireland', *Mineralium Deposita,* 27 (4), 314-25.

Gee, D. G. (1975), 'A tectonic model for the central part of the Scandinavian Caledonides.', *American Journal of Science,* 275A, 48.

Getzlaff, M. (2007), 'Fundamentals of Magentism', *Springer Berlin Heidelberg New York*.

Ghosh, S. K. (1994), 'Structural Geology: Fundamentals and Modern Developments', *Pergamon Press, London*, 598.

Gilbert, G. K. (1877), 'Report on the geology of the Henry Mountains (Utah).', *united States Geological Survey, Washington D.C.*

Giles, M. (1980), 'The petrology of the Galway Granite', *Ph.D. thesis, University of Glasgow*.

Girdler, R. W. (1961), 'The Measurement and Computation of Anisotropy of Magnetic Susceptibility of Rocks', *Geophysical Journal of the Royal Astronomical Society,* 5 (1), 34-44.

Glazner, A. F. and Bartley, J., M. (2006), 'Is stoping a volumetrically significant pluton emplacement process?', *Geological Society of America,* 118, 1185-95.

Glazner, A. F. and Bartley, J. M. (2008), 'Reply to comments on "Is stoping a volumetrically significant pluton emplacement process?"', *Geological Society of America Bulletin,* 120 (7-8), 1082-87.

Glover, B. W. and Winchester, J. A. (1989), 'The Grampian Group: a major Late Proterozoic clastic sequence in the Central Highlands of Scotland', *Journal of the Geological Society,* 146 (1), 85-96.

Gómez Barreiro, J., Wijbrans, J. R., Castiñeiras, P., Martínez Catalán, J. R., Arenas, R., Díaz García, F., and Abati, J. (2006), '40Ar/39Ar laserprobe dating of mylonitic fabrics in a polyorogenic terrane of NW Iberia', *Journal of the Geological Society,* 163 (1), 61-73.

Goodenough, K. M., Young, B. N., and Parsons, I. (2004), 'The minor intrusions of Assynt, NW Scotland: early development of magmatism along the Caledonian Front', *Mineralogical Magazine,* 68 (4), 541-59.

Goodenough, K. M., Evans, J. A., and Krabbendam, M. (2006), 'Constraining the maximum age of movements in the Moine Thrust Belt: dating the Canisp Porphyry', *Scottish Journal of Geology,* 42 (1), 77-81.

Goodenough, K. M., Millar, I., Strachan, R. A., Krabbendam, M., and Evans, J. A. (2011), 'Timing of regional deformation and development of the Moine Thrust Zone in the Scottish Caledonides: constraints from the U–Pb geochronology of alkaline intrusions', *Journal of the Geological Society,* 168 (1), 99-114.

Gorokhov, I., Semikhatov, M., Arakelyants, M., Fallick, E., Mel'nikov, N., Turchenko, T., Ivanovskaya, T., Zaitseva, T., and Kutyavin, E. (2006), 'Rb-Sr, K-Ar, H-and O-Isotope systematics of the Middle Riphean shales from the Debengda Formation, the Olenek Uplift, North Sibera', *Stratigraphy and Geological Correlation,* 14 (3), 260-74.

Graham, C. M. (1986), 'The role of the Cruachan Lineament during Dalradian evolution', *Scottish Journal of Geology,* 22 (2), 257-70.

Graham, J. W. (1954), 'Magnetic susceptibility anisotropy, an unexploited petrofabric element', *Geologcial Society of America Bulletin,* 65, 1257-58.

--- (1966), 'Significance of magnetic anisotropy in Appalachian sedimentary rocks', *In: Steinhart, J.S. and Smith, T.J. (eds.) The Earth Beneath the Continents. American Geophysical Union Geophysical Monograph* 10, 627-48.

Graham, N. T. (1997), 'Fabric studies in the Galway Granite, Ireland', *Unpublished PhD thesis, National University of Ireland, Galway*.

Grégoire, V., de Saint Blanquat, M., Nédélec, A., Bouchez, J., and Luc (1995), 'Shape anisotropy versus magnetic interactions of magnetite grains: Experiments and application to AMS in granitic rocks', *Geophys. Res. Lett.,* 22 (20), 2765-68.

Grégoire, V., Darrozes, J., Gaillot, P., Nédélec, A., and Launeau, P. (1998), 'Magnetite grain shape fabric and distribution anisotropy vs rock magnetic fabric: a three-dimensional case study', *Journal of Structural Geology,* 20 (7), 937-44.

Griffin, W. L., Austrheim, H., and Bradstad, K. (1985), 'High-pressure metamorphism in the Scandinavian Caledonides', *In: Gee, D.G. & Sturt, B.A. (eds) The Caledonide Orogen – Scandinavia and Related Areas. Wiley, Chichester*, 783-802.

Grocott, J., Arévalo, C., Welkner, D., and Cruden, A. (2009), 'Fault-assisted vertical pluton growth: Coastal Cordillera, north Chilean Andes', *Journal of the Geological Society,* 166 (2), 295-301.

Grogan, S. E. and Reavy, R. J. (2002), 'Disequilibrium textures in the Leinster Granite Complex, SE Ireland: evidence for acid-acid magma mixing', *Mineralogical Magazine,* 66 (6), 929-39.

Grount, F. F. (1918), 'The lopolith, an igneous form exempified by the Duluth gabbro', *American Journal of Science, 4th series,* 46, 516-22.

Guglielmo, G. (1994), 'Interference between pluton expansion and coaxial tectonic deformation: Three-dimensional computer model and field implications', *Journal of Structural Geology,* 16 (2), 237-52.

Guillong, M. (2004), 'Mass Sepectrometry: Laser ablation system developments and investigations on elemental fractionation', *PhD. Thesis Eidgenossischen Technischen Hochschule Zurich*.

Hacker, D. B., Petronis, M. S., Holm, D. K., and Geissman, J. W. (2007), 'Shallow Level Emplacement Mechanisms of the Miocene Iron Axis Laccolith Group, Southwestern Utah', *Geological Society of America Rocky Mountain Section,* Anuall Meeting St. George, Utah.

Haggerty, S. E. (1976), 'Opaque Mineral Oxides in Terrestrial Igneous Rocks, ' *Mineralogical Society of America, MSA, Short Course Notes,* Chapter 4.

Halliday, A. N., Stephens, W. E., Hunter, R. H., Menzies, M. A., Dickin, A. P., and Hamilton, P. J. (1986), 'Isotopic and chemical constraints on the building of the deep Scottish lithosphere', *Scottish Journal of Geology,* 21 (4), 465-91.

Halliday, A. N., Aftalion, M., Parsons, I., Dickin, A. P., and Johnson, M. R. W. (1987), 'Syn-orogenic alkaline magmatism and its relationship to the Moine Thrust Zone and the thermal state of the Lithosphere in NW Scotland', *Journal of the Geological Society,* 144 (4), 611-17.

Halliday, A. N., Graham, C. M., Aftalion, M., and Dymoke, P. (1989), 'Short Paper: The depositional age of the Dalradian Supergroup: U-Pb and Sm-Nd isotopic studies of the Tayvallich Volcanics, Scotland', *Journal of the Geological Society,* 146 (1), 3-6.

Halverson, G. P., Dudás, F. Ö., Maloof, A. C., and Bowring, S. A. (2007), 'Evolution of the 87Sr/86Sr composition of Neoproterozoic seawater', *Palaeogeography, Palaeoclimatology, Palaeoecology,* 256 (3–4), 103-29.

Hambrey, M. J. (1983), 'Correlation of Late Proterozoic tillites in the North Atlantic region and Europe', *Geological Magazine,* 120 (03), 209-32.

Hamilton, T. D., Borradaile, G. J., and Lagroix, F. (2004), 'Sub-fabric identification by standardization of AMS, an example of inferred neotectonic structures from Cyprus', *In: Martin-Hernandes, F., Lunenburg, C.M., Aubourg, C., Jackson, A. (eds.). Magnetic Fabrics. Geological Society of London Special Publications,* 238, 527-40.

Hargraves, R. B., Johnson, D., and Chan, C. Y. (1991), 'Distribution anisotropy: The cause of AMS in igneous rocks?', *Geophys. Res. Lett.,* 18 (12), 2193-96.

Harker, A. (1909), 'The Natural History of Igenous Rocks', *Cambridge University Press*.

Harland, W. B. (1971), 'Tectonic transpression in Caledonian Spitsbergen', *Geological Magazine,* 108 (01), 27-41.

--- (1985), 'Caledonide Svalbard', *In: Gee, D.G. & Sturt, B.A. (eds) The Caledonide Orogen – Scandinavia and Related Areas. Wiley, New York,* (999-1016).

Harmon, R. S. and Halliday, A. N. (1980), *Nature,* 283, 21-25.

Harris, A. L. and Pitcher, W. S. (1975), 'The Dalradian Supergroup.', *in Harris, A.L. et al. (eds) A correlation of the Precambrian rocks of the British Isles. Spec. Rep. Geological Society London., Special Report,* 6.

Harris, A. L. and Pitcher, W. S. (1976), 'The Dalradian Supergroup.', *In Harris, A.L. et al. (eds) A correlation of the Precambrian rocks of the British Isles. Spec. Rep. Geological Society London.,* 7.

Harris, A. L., Haselock, P. J., Kennedy, M. J., and Mendum, J. R. (1994), 'The Dalradian Supergroup in Scotland, Shetland and Ireland', *A revised corrolation of Precambrian rocks in the British Isles. Geological Society, London Special Reports,* 22, 21.

Harris, A. L., Baldwin, C.T., Bradbury, H.J., Johnson, H.D., Smith, R.A. (1978), 'Ensialic basin sedimentation: the Dalradian Supergroup.', *Crustal Evolution of North-western Britain and adjacent regions. Steel House Press, Liverpool.*, 115-38.

Harry, W. T. a. E., C.H. (1960), *Rept. 21st International Geological Congress, Norden, Germany,* 14, 173-81.

Hartz, E. (2000), 'Early syndepositional tectonics of East Greenland's Old Red Sandstone basin', *Geological Society, London, Special Publications,* 180 (1), 537-55.

Hartz, E. H. and Torsvik, T. H. (2002), 'Baltica upside down: A new plate tectonic model for Rodinia and the Iapetus Ocean', *Geology,* 30 (3), 255-58.

Harvery, P. K. (1967), 'The geology of the Glinsk district, Connemara, Eire', *Ph.D. Thesis University of Bristol*.

Harvey, P. K. (1967), 'The Geology of the Glinsk District, Connemara, Eire.', *Ph.D. thesis, University of Bristol*.

Haug, E. (1900), 'Les Geosynclinaus et les Aires Continentales', *Bulletin de la Societe Geologique de France,* (385), 79-105.

Hauptraan, Z. (1974), 'High Temperature Oxidation, Range of Non-Stoichiometry and Curie Point Variation of Cation Deficient Titanomagnetite Fe2.4Ti0.6O4+γ', *Geophysical Journal International,* 38 (1), 29-47.

He, B., Xu, Y.-G., and Paterson, S. (2009), 'Magmatic diapirism of the Fangshan pluton, southwest of Beijing, China', *Journal of Structural Geology,* 31 (6), 615-26.

Heider, F., Dunlop, D. J., and Soffel, H. C. (1992), 'Low-Temperature and Alternating Field Demagnetization of Saturation Remanence and Thermoremanence in Magnetite Grains (0.037 μm to 5 mm)', *J. Geophys. Res.,* 97 (B6), 9371-81.

Hellstrom, J., Paton, C., Woodhead, J., and Hergt, J. (2008), 'Iolite: software for spatially resolved LA-(quad and MC) ICPMS analysis', *Mineralogical association of Canada short course sereis 40*, 343-48.

Herbert, E., Huppert, E., Stephen, R., and Sparks, J. (1980), 'The Fluid Dynamics of a Basaltic Magma Chamber Replenished by Influx of Hot, Dense Ultrabasic Magma', *Contributions of Mineralogy & Petrology,* 75, 279-89.

Heumann, K. G., Eisenhut, S., Gallus, S., Hebeda, E. H., Nusko, R., Vengosh, A., and Walczyk, T. (1995), 'Recent developments in thermal ionization mass spectrometric techniques for isotope analysis. A review', *Analyst,* 120 (5), 1291-99.

Hext, G. R. (1963), 'The estimation of second-order tensors, with related tests and designs', *Biometrika,* 50 (3-4), 353-73.

Hibbard, J. (1988), 'Stratigraphy of the Fleur de Lys Belt, northwest Newfoundland', *In: Winchester, J.A. (ed.) Later Proterozoic stratigraphy of the northern Atlantic Regions. Blackie*, 200-11.

Higgins, A. K. and Leslie, A. G. (2000), 'Restoring thrusting in the East Greenland Caledonides', *Geology,* 28 (11), 1019-22.

Highton, A. J., Hyslop, E. K., and Noble, S. R. (1999), 'U-Pb zircon geochronology of migmatization in the northern Central Highlands: evidence for pre-Caledonian (Neoproterozoic) tectonometamorphism in the Grampian block, Scotland', *Journal of the Geological Society,* 156 (6), 1195-204.

Hippertt, J. F. M. (1993), ''V'-pull-apart microstructures: a new shear-sense indicator', *Journal of Structural Geology,* 15 (12), 1393-403.

Hirt, A. M., Julivert, M., and Soldevila, J. (2000), 'Magnetic fabric and deformation in the Navia–Alto Sil slate belt, northwestern Spain', *Tectonophysics,* 320 (1), 1-16.

Hirth, G. and Tullis, J. (1992), 'Dislocation creep regimes in quartz aggregates', *Journal of Structural Geology,* 12 (2), 145-59.

Hobbs, B. E. (1985), 'The geological significance of microfabrics', *In: H.R. Wenk (ed.), Preferred orientation in deformed metals and rocks. Academic Press, New York*.

Hodych, J. P., Cox, R.A. Kosịler, J. (2004), 'An equatorial Laurentia at 550Ma confirmed by Grenvillian inherited zircons dated by LAM ICP-MS in the Skinner Cove volcanics of Western Newfoundland: implication for inertial interchange true polar wander.', *Precambrian Research,* 129, 93-113.

Hoffman, P. F. (1991), 'Did the Breakout of Laurentia Turn Gondwanaland Inside-Out?', *Science,* 252 (5011), 1409-12.

Holder, M. T. (1979), 'An emplacement mechanism for post tectonic granites and its implications for their geochemical features', *In: Atherton, M.P., Tarney, J., (eds)., Origin of granite batholiths: geochemical evidence. Shiva Publishing*, 116-28.

Holdsworth, R. E. (1989), 'The geology and structural evolution of a Caledonian fold and ductile thrust zone, Kyle of Tongue region, Sutherland, northern Scotland', *Journal of the Geological Society,* 146 (5), 809-23.

Holdsworth, R. E., McErlean, M. A., and Strachan, R. A. (1999), 'The influence of country rock structural architecture during pluton emplacement: the Loch Loyal syenites, Scotland', *Journal of the Geological Society,* 156 (1), 163-75.

Holdsworth, R. E., Strachan, R. A., Alsop, G. I., Grant, C. J., and Wilson, R. W. (2006), 'Thrust sequences and the significance of low-angle, out-of-sequence faults in the northernmost Moine Nappe and Moine Thrust Zone, NW Scotland', *Journal of the Geological Society,* 163 (5), 801-14.

Hon, D. (1972), 'Cauldron Subsidence in Lunar Craters Ritter and Sabine', *The Lunar Science Institute, Northwestern State University Natchitoches, Louisiana, 71457*.

Horne, R. R. (1975), 'Possible Transverse Fault Control of Base Metal Mineralisation in Ireland and Britain', *The Irish Naturalists' Journal,* 18 (5), 140-44.

--- (1975), 'Transverse fault systems in fold belts and oceanic fracture zones', *Nature,* 255 (5510), 620-21.

Houk, R. S. (1986), 'Mass spectrometry of inductively coupled plasmas', *Analytical Chemistry,* 58 (1), 97A-105A.

Housen, B. A., Richter, C., and van der Pluijm, B. A. (1993), 'Composite magnetic anisotropy fabrics: experiments, numerical models and implications for the quantification of rock fabrics', *Tectonophysics,* 220 (1–4), 1-12.

Hrouda, F., Chlupáčová, M., and Rejl, L. (1971), 'The mimetic fabric of magnetite in some foliated granodiorites, as indicated by magnetic anisotropy', *Earth and Planetary Science Letters,* 11 (1–5), 381-84.

Hrouda, F. (1982), 'Magnetic anisotropy of rocks and its application in geology and geophysics', *Surveys in Geophysics,* 5 (1), 37-82.

Hrouda, F. and Jelínek, V. (1990), 'Resolution of ferrimagnetic and paramagnetic anisotropies in rocks, using combined low-field and high-field measurements', *Geophysical Journal International,* 103 (1), 75-84.

Hrouda, F. and Kahan, S. (1991), 'The magnetic fabric relationship between sedimentary and basement nappes in the High Tatra Mountains, N. Slovakia', *Phys. Earth Planet. Inter.,* 63, 71-77.

Hrouda, F. (1992), 'Separation of a component of tectonic deformation from a complex magnetic fabric', *Journal of Structural Geology,* 14 (1), 65-71.

--- (2002), 'The use of the anisotropy of magnetic remanence in the resolution of the anisotropy of magnetic susceptibility into its ferromagnetic and paramagnetic components', *Tectonophysics,* 347 (4), 269-81.

--- (2003), 'Indices for Numerical Characterization of the Alteration Processes of Magnetic Minerals Taking Place During Investigation of Temperature Variation of Magnetic Susceptibility', *Studia Geophysica et Geodaetica,* 47 (4), 847-61.

Hrouda, F., Chlupáčová, M., and Mrázová, Š. (2006), 'Low-field variation of magnetic susceptibility as a tool for magnetic mineralogy of rocks', *Physics of the Earth and Planetary Interiors,* 154 (3–4), 323-36.

Hudson, N. F. C. (1985), 'Conditions of Dalradian metamorphism in the Buchan area, NE Scotland', *Journal of the Geological Society,* 142 (1), 63-76.

Hurst, J. M., Hancock, N. J., and McKerrow, W. S. (1978), 'Wenlock stratigraphy and palaeogeography of Wales and the Welsh Borderland', *Proceedings of the Geologists' Association,* 89 (3), 197-226.

Hutton, D. H. W. (1982), 'A tectonic model for the emplacement of the Main Donegal Granite, NW Ireland', *Journal of the Geological Society,* 139 (5), 615-31.

Hutton, D. H. W. and Murphy, F. C. (1987), 'The Silurian of the Southern Uplands and Ireland as a successor basin to the end-Ordovician closure of Iapetus', *Journal of the Geological Society,* 144 (5), 765-72.

Hutton, D. H. W. (1988), 'Granite emplacement mechanisms and tectonic controls: inferences from deformation studies', *Earth and Environmental Science Transactions of the Royal Society of Edinburgh,* 79 (2-3), 245-55.

Hutton, D. H. W. (1988), 'Igneous emplacement in a shear-zone termination: The biotite granite at Strontian, Scotland', *Geological Society of America Bulletin,* 100 (9), 1392-99.

Hutton, D. H. W., Dempster, T. J., Brown, P. E., and Becker, S. D. (1990), 'A new mechanism of granite emplacement: intrusion in active extensional shear zones', *Nature,* 343 (6257), 452-55.

Hutton, D. H. W. and McErlean, M. (1991), 'Silurian and Early Devonian sinistral deformation of the Ratagain granite, Scotland: constraints on the age of Caledonian movements on the Great Glen fault system', *Journal of the Geological Society,* 148 (1), 1-4.

Hutton, D. H. W. (1992), 'Granite sheeted complexes: evidence for the dyking ascent mechanism', *Earth and Environmental Science Transactions of the Royal Society of Edinburgh,* 83 (1-2), 377-82.

Hutton, D. H. W. and Ingram, G. M. (1992), 'The Great Tonalite Sill of southeastern Alaska and British Columbia: emplacement into an active contractional high angle reverse shear zone (extended abstract)', *Transactions of the Royal Society of Edinburgh: Earth Sciences,* 83, 383-86.

Hutton, D. H. W. and Reavy, R. J. (1992), 'Strike-slip tectonics and granite petrogenesis', *Tectonics,* 11 (5), 960-67.

Hutton, D. H. W. (1996), 'The "space problem" in the emplacement of granite', *Episodes, International Union of Geological Sciences,* 19 (4), 114-19.

Hutton, D. H. W. and Alsop, G. I. (1996), 'The Caledonian strike-swing and associated lineaments in NW Ireland and adjacent areas: sedimentation, deformation and igneous intrusion patterns', *Journal of the Geological Society,* 153 (3), 345-60.

Hutton, D. H. W. and Alsop, G. I. (1996), 'The Swilly Slide: A Major Synmetamorphic, Extensional, Ductile Fault in the Dalradian of Donegal', *Irish Journal of Earth Sciences,* 15, 41-57.

Hutton, D. H. W. (1997), 'Syntectonic granites and the principle of effective stress: a general solution to the space problem', *In: Bouchez, J.L., Hutton, D.H.W., Stephens, W.E., (eds.), Grantie: From Segregation of Melt to Emplacement Fabrics, Kluwer Academic Publishers, Dordrecht*, 189-97.

Hutton, D. H. W., Brown, P. E., Grocott, J., Garde, A. A., Chadwick, B., Cruden, A. R., and Swager, C. (2000), 'Discussion on emplacement of rapakivi granite and syenite by floor depression and roof uplift in the Palaeoproterozoic Ketilidian orogen, South Greenland', *Journal of the Geological Society,* 157 (3), 701-04.

Hutton, D. H. W. and Siegesmund, S. (2001), 'The Ardara Granite: Reinflating the Balloon Hypothesis', *Zeitschrift der Deutschen Geologischen Gesellschaft,* 152 (2-4), 309-23.

Hutton, D. H. W. (2009), 'Insights into magmatism in volcanic margins: bridge structures and a new mechanism of basic sill emplacement – Theron Mountains, Antarctica', *Petroleum Geoscience,* 15 (3), 269-78.

Hyslop, E. K. and Piasecki, M. A. J. (1999), 'Mineralogy, geochemistry and the development of ductile shear zones in the Grampian Slide zone of the Scottish Central Highlands', *Journal of the Geological Society,* 156 (3), 577-89.

Ildefonse, B. and Fernandez, A. (1988), 'Influence on the concentration of rigid markers in a viscous medium on the production of preferred orientations: an experimental contribution.', *Bulletin of Geology University of Uppsala,* 14, 55-60.

Ildefonse, B., Launeau, P., Bouchez, J.-L., and Fernandez, A. (1992), 'Effect of mechanical interactions on the development of shape preferred orientations: a two-dimensional experimental approach', *Journal of Structural Geology,* 14 (1), 73-83.

Imon, R., Okudaira, T., and Fujimoto, A. (2002), 'Dissolution and precipitation processes in deformed amphibolites: an example from the ductile shear zone of the Ryoke metamorphic belt, SW Japan', *Journal of Metamorphic Geology,* 20 (3), 297-308.

Imon, R., Okudaira, T., and Kanagawa, K. (2004), 'Development of shape- and lattice-preferred orientations of amphibole grains during initial cataclastic deformation and subsequent deformation by dissolution–precipitation creep in amphibolites from the Ryoke metamorphic belt, SW Japan', *Journal of Structural Geology,* 26 (5), 793-805.

Ingold, L. M. (1936), 'The Geology of the Currywongaun-Doughruagh Area, Co. Galway', *Proceedings of the Royal Irish Academy. Section B: Biological, Geological, and Chemical Science,* 43, 135-59.

Ingram, G. M. and Hutton, D. H. W. (1994), 'The Great Tonalite Sill: Emplacement into a contractional shear zone and implications for Late Cretaceous to early Eocene tectonics in southeastern Alaska and British Columbia', *Geological Society of America Bulletin,* 106 (5), 715-28.

Ireland, T. R. (2013), 'Invited Review Article: Recent developments in isotope-ratio mass spectrometry for geochemistry and cosmochemistry', *Review of Scientific Instruments,* 84 (1), 011101.

Irving, E. (1970), 'The Mid-Atlantic Ridge at 45N. XVI. Oxidation and magnetic properties of basalts: review and discussion', *Canadian Journal of Earth Sciences,* 7, 1528-38.

Ising, G. (1942), 'On the magentic properties of varved clay', *Arkiv for Matematik, Astronomi och Fysik,* 29A, 1-37.

Jackson, M. (1991), 'Anisotropy of magnetic remanence: A brief review of mineralogical sources, physical origins, and geological applications, and comparison with susceptibility anisotropy', *Pure and Applied Geophysics,* 136 (1), 1-28.

Jackson, M., Moskowitz, B. M., and Bowles, J. (2011), 'Interpretation of Low-Temperature Data Part III: the Magnetite Verwey Transition', *The IRM Quarterly,* 20 (4), 1-11.

Jackson, M. J. and Tauxe, L. (1991), 'Anisotropy of magnetic susceptibility and remanence, developments in the characterization of tectonic, sedimentary and igneous fabric', *Revies of Geophysics, IUGG Report-Contributions in Geomagnetism, Paleomagnetism),* 29, 371-76.

Jackson, S. E., Pearson, N. J., Griffin, W. L., and Belousova, E. A. (2004), 'The application of laser ablation-inductively coupled plasma-mass spectrometry to in situ U–Pb zircon geochronology', *Chemical Geology,* 211 (1–2), 47-69.

Jacques, J. M. and Reavy, R. J. (1994), 'Caledonian plutonism and major lineaments in the SW Scottish Highlands', *Journal of the Geological Society,* 151 (6), 955-69.

Jagger, M. D. (1985), 'Teh Cashel district of Connemara, Co. Galway, Eire: an isotopic study', *Ph.D. thesis, University of Glasgow*.

Jagger, M. D., Max, M. D., Aftalion, M., and Leake, B. E. (1988), 'U-Pb zircon ages of basic rocks and gneisses intruded into the Dalradian rocks of Cashel, Connemara, western Ireland', *Journal of the Geological Society,* 145 (4), 645-48.

Jeager, J. C. and Cook, N. G. W. (1979), 'Fundamentals of Rock Mechanics', *Chapman & Hall*, 593.

Jelinek, V. (1977), 'The statistical theory of measuring anisotropy of magnetic susceptibility of rocks and its aplication', *Geophyzika, Brno*.

--- (1981), 'Characterization of the magnetic fabric of rocks', *Tectonophysics,* 79 (3–4), T63-T67.

Jelínek, V. and Pokorný, J. (1997), 'Some new concepts in technology of transformer bridges for measuring susceptibility anisotropy of rocks', *Physics and Chemistry of The Earth,* 22 (1–2), 179-81.

Jenkin, G. R. T. (1988), 'Stable isotope studies in the Caledonides of SW Connemara, Ireland', *Ph.D. thesis, University of Glasgow*.

Johnson, P. H. and Atwater, T. (1977), 'Magnetic study of basalts from the Mid-Atlantic Ridge, lat 37°N', *Geological Society of America Bulletin,* 88 (5), 637-47.

Jones, R. R., Holdsworth, R. E., and Bailey, W. (1997), 'Lateral extrusion in transpression zones: the importance of boundary conditions', *Journal of Structural Geology,* 19 (9), 1201-17.

Just, J., Kontny, A., and Dewall, H. (2003), 'Magnetic Fabric Development During Hydrothermal Alteration And Brittle Deformation In Granite From The EPS-1 Drilling, (Soultz-sous-Forets, France)', *American Geophysical Union, Fall Meeting 2003, Abstract*.

Just, J., Kontny, A., De Wall, H., Hirt, A. M., and Martín-Hernández, F. (2004), 'Development of magnetic fabrics during hydrothermal alteration in the Soultz-sous-Forêts granite from the EPS-1 borehole, Upper Rhine Graben', *Geological Society, London, Special Publications,* 238 (1), 509-26.

Just, J. and Kontny, A. (2012), 'Thermally induced alterations of minerals during measurements of the temperature dependence of magnetic susceptibility: a case study from the hydrothermally altered Soultz-sous-Forêts granite, France', *International Journal of Earth Sciences,* 101 (3), 819-39.

Kamo, S. L., Gower, C. F., and Krogh, T. E. (1989), 'Birthdate for the lapetus Ocean? A precise U-Pb zircon and baddeleyite age for the Long Range dikes, southeast Labrador', *Geology,* 17 (7), 602-05.

Kanaori, Y., Kawakami, S.-I., and Yairi, K. (1991), 'Microstructure of deformed biotite defining foliation in cataclasite zones in granite, central Japan', *Journal of Structural Geology,* 13 (7), 777-85.

Karlstrom, K. E., Miller, C. F., Kingsbury, J. A., and Wooden, J. L. (1993), 'Pluton emplacement along a ductile thrust zone, Pine Mountains, south-eastern California: Interaction between deformational and solidification processes', *Bulletin of the Geological Socitey of America,* 105, 213-30.

Keeling, B. E. (1981), 'The geochemistry of the Connemara Gneiss complex, Co. Galway, Ireland.', *Ph.D. thesis, University of Glasgow*.

Kekulawala, K. R. S. S., Paterson, M. S., and Boland, J. N. (1981), 'An Experimental Study of the Role of Water in Quartz Deformation', *In: J. Handin, N.L. Carter (eds.), Mechanical Behaviour of Crustal Rocks: The Handin Volume, American Geophysical Union*, 49-60.

Kelso, P. R., Banerjee, S. K., and Worm, H.-U. (1991), 'The effect of low-temperature hydrothermal alteration on the remanent magnetization of synthetic titanomagnetites: A case for acquisition of chemical remanent magnetization', *Journal of Geophysical Research: Solid Earth,* 96 (B12), 19545-53.

Kelso, P. R., Tikoff, B., Jackson, M., and Sun, W. (2002), 'A new method for the separation of paramagnetic and ferromagnetic susceptibility anisotropy using low field and high field methods', *Geophysical Journal International,* 151 (2), 345-59.

Kemp, A. E. S. (1987), 'Tectonic development of the Southern Belt of the Southern Uplands accretionary complex', *Journal of the Geological Society,* 144 (5), 827-38.

Kennan, P. S., Feely, M., and Mohr, P. (1987), 'The age of the Oughterard Granite, Connemara, Ireland', *Geological Journal,* 22 (4), 273-80.

Kennedy, M. J. (1975), 'Repetitive orogeny in the northeastern Appalachians-new plate models based upon Newfoundland examples', *Tectonophysics,* 28 (1–2), 39-87.

Kennedy, M. J. and Menuge, J. F. (1992), 'The Inishkea Division of northwest Mayo: Dalradian cover rather than pre-Caledonian basement. ', *Journal of the Geological Socitey, London,* 149, 167-70.

Kennedy, W. Q. (1958), 'The tectonic evolution of the Midland Valley, Scotland', *Transactions of the Geological Society of Glasgow*.

Kerr, A. D. and Pollard, D. D. (1998), 'Toward more realistic formulations for the analysis of laccoliths', *Journal of Structural Geology,* 20 (12), 1783-93.

Khain, V. E. (1985), 'Geology of the U.S.S.R.: Berlin-Stuttgard', *Gebruder Borntraeger, Berlin.*, 264.

Khan, M. A. (1962), 'The Anisotropy of Magnetic Susceptibility of Some Igneous and Metamorphic Rocks', *J. Geophys. Res.,* 67 (7), 2873-85.

Kilburn, C., Shackleton, R. M., and Pitcher, W. S. (1965), 'The stratigraphy and origin of the portaskaig boulder bed series (Dalradian)', *Geological Journal,* 4 (2), 343-60.

Kinahan, G. H. (1869), 'Explanation to accompany Sheet 105 with that portion of Sheet 114 that lies north of Galway Bay.', *Memoir of the Geological Survey of Ireland, Dubline*.

Kinahan, G. H., Nolan, J., Leonard, H., and Cruise, R. J. (1878), 'Explanatory memoir to accompany Sheets 93 and 94, with the adjoining portions of Sheets 83, 84, and 103, of the maps of the Geological Survey of Ireland.', *Memoir of the Geological Survey Ireland.*

King, R. F. (1966), 'The magnetic fabric of some Irish Granites', *Geological Journal,* 5 (1), 43-66.

Kingsley, L. (1931), 'Cauldron subsidence of the Ossipee Mountains', *American Journal of Science,* Series 5 Vol. 22 (128), 139-68.

Kinny, P. D., Friend, C. R. L., Strachan, R. A., Watt, G. R., and Burns, I. M. (1999), 'U–Pb geochronology of regional migmatites in East Sutherland, Scotland: evidence for crustal melting during the Caledonian orogeny', *Journal of the Geological Society,* 156 (6), 1143-52.

Kinny, P. D., Strachan, R. A., Friend, C. R. L., Kocks, H., Rogers, G., and Paterson, B. A. (2003), 'U–Pb geochronology of deformed metagranites in central Sutherland, Scotland: evidence for widespread late Silurian metamorphism and ductile deformation of the Moine

Supergroup during the Caledonian orogeny', *Journal of the Geological Society,* 160 (2), 259-69.

Kneller, B. C. (1991), 'A foreland basin on the southern margin of Iapetus', *Journal of the Geological Society,* 148 (2), 207-10.

Kneller, B. C., King, L. M., and Bell, A. M. (1993), 'Foreland basin development and tectonics on the northwest margin of eastern Avalonia', *Geological Magazine,* 130 (05), 691-97.

Koch, J. and Gunther, D. (2011), 'Review of the State-of-the-Art of Laser Ablation Inductively Coupled Plasma Mass Spectrometry', *Applied Spectroscopy,* 65 (5), 155A-62A.

Koukouvelas, I. and Pe-piper, G. (1991), 'The Oligocene Xanthi pluton, northern Greece: a granodiorite emplaced during regional extension', *Journal of the Geological Society,* 148 (4), 749-58.

Krabbendam, M., Strachan, R. A., Leslie, A. G., Goodenough, K. M., and Bonsor, H. C. (2011), 'The internal structure of the Moine Nappe Complex and the stratigraphy of the Morar Group in the Fannichs–Beinn Dearg area, NW Highlands', *Scottish Journal of Geology,* 47 (1), 1-20.

Krabbendam, M., Leslie, A.G. (2010), 'The Traligill Transverse Zone: Lateral variations and linkages in thrust geometry in the Assynt Culmination, Moine Thrust Belt, NW Scotland.', *In: Law, R., Butler, R.W.H., Holdsworth, R.E., Krabbendam, M, Strachan, R.A. (eds) Continental Tectonics adn Mountain Building: The legacy of Peach and Horne. Geological Society, London, Special Publications.,* 335, 335-57.

Kruhl, J. H. (1996), 'Prism- and basal-plane parallel subgrain boundaries in quartz: a microstructural geothermobarometer', *Journal of Metamorphic Geology,* 14 (5), 581-89.

Kruse, R. and Stünitz, H. (1999), 'Deformation mechanisms and phase distribution in mafic high-temperature mylonites from the Jotun Nappe, southern Norway', *Tectonophysics,* 303 (1–4), 223-49.

Kruse, R., Stunitz, H., and Kunze, K. (2001), 'Dynamic recrystallisation processes in plagioclase phenocrysts', *Journal of Structural Geology,* 23, 1781-802.

Kumpulainen, R. and Nystuen, J. P. (1985), 'Late Proteroaoic basin evolution and sedimentation in the westernmost part of Baltoscandia', *The Caledonide Orogen-Scandinavia and related area.*, 213-32.

Lagarde, J. L., Ait Omar, S., and Roddaz, B. (1990), 'Structural characteristics of granitic plutons emplaced during weak regional deformation: examples from late Carboniferous plutons, Morocco', *Journal of Structural Geology,* 12 (7), 805-21.

Lagroix, F. and Borradaile, G. J. (2000), 'Magnetic fabric interpretation complicated by inclusions in mafic silicates', *Tectonophysics,* 325 (3–4), 207-25.

--- (2000), 'Tectonics of the circum-Troodos sedimentary cover of Cyprus, from rock magnetic and structural observations', *Journal of Structural Geology,* 22 (4), 453-69.

Lambert, R. S. J. and McKerrow, W. S. (1977), 'The Grampian Orogeny', *Scottish Journal of Geology,* 12 (4), 271-92.

Lapointe, P., Morris, W. A., and Harding, K. L. (1986), 'Interpretation of magnetic susceptibility: a new approach to geophysical evaluation of the degree of rock alteration', *Canadian Journal of Earth Sciences,* 23 (3), 393-401.

Lapworth, C. (1883), 'The Secret of the Highlands', *Geological Magazine,* 10, 120-28.

Lattard, D., Engelmann, R., Kontny, A., and Sauerzapf, U. (2006), 'Curie temperatures of synthetic titanomagnetites in the Fe-Ti-O system: Effects of composition, crystal chemistry, and thermomagnetic methods', *Journal of Geophysical Research,* 111 (B12S28).

Lau, J., Herrero-Bervera, E., and Urrutia Fucugauchi, J. (2007), 'Thermally Enhanced Magnetic Fabrics of Basaltic Dikes from Kapaa Quarry, Koolau Volcano, Oahu, Hawaii, USA', *American Geophysical Union, Spring Meeting.*

Launeau, P. and Robin, P. Y. F. (1996), 'Fabric analysis using the intercept method', *Tectonophysics,* 267 (1–4), 91-119.
Launeau, P. and Cruden, A. R. (1998), 'Magmatic fabric acquisition mechanisms in a syenite: Results of a combined anisotropy of magnetic susceptibility and image analysis study', *J. Geophys. Res.,* 103 (B3), 5067-89.
Launeau, P. and Robin, P.-Y. F. (2005), 'Determination of fabric and strain ellipsoids from measured sectional ellipses—implementation and applications', *Journal of Structural Geology,* 27 (12), 2223-33.
Law, R. D. (1990), 'Crystallographic fabrics: a selective review of their applications to research in structural geology', *In: Knipe, R.J., Ruttler, R.H. (eds), Deformation mechanisms, rheology and tectonics. Geological Society Special Publication,* 54, 355-52.
Lawrence, G. (1968), 'The geochemistry of the Galway Granite Lettermullan, Co. Galway, Eire', *PhD Thesis, University of Bristol*.
Leake, B. E. (1958), 'The Cashel-Lough Wheelaun intrusion, Co. Galway', *Proceedings of the Royal Irish Academy,* 59B, 155-203.
Leake, B. E. (1963), 'A possible fossil in a graphitic marble in the Connemara Schist, Cornamona, Co. Galway, Ireland', *Geological Magazine,* 100, 44-46.
Leake, B. E. (1964), 'New Light on the Dawros Peridotite, Connemara, Ireland', *Geological Magazine,* 101 (01), 63-75.
Leake, B. E. (1969), 'The origin of the Connemara migmatites of the Cashel district, Connemara, Ireland', *Quarterly Journal of the Geological Society,* 125 (1-4), 219-76.
--- (1970), 'The fragmentation of the Connemara basic and ultrabasic intrusions', *in: Newall, G. and Rast, N. (eds) Mechanism of Igneous Intrusion. Geological Journal Special Issue,* (2), 103-22.
--- (1974), 'The crystallisation history and mechanism of emplacement of the western part of the Galway Granite, Connemara, western Ireland

', *Mineralogical Magazine*.
--- (1974), 'The crystallisation history and mechanism of emplacement of the western part of the Galway Granite, Connemara, western Ireland.', *Mineralogical Magazine,* 39, 498-513.
Leake, B. E., Tanner, P. W. G., and Senior, A. (1975), 'The Composition and Origin of the Connemara Dolomitic Marbles and Ophicalcites, Ireland', *Journal of Petrology,* 16 (1), 237-57.
Leake, B. E. (1978), 'Granite emplacement: the granites of Ireland and their origin', *In: Gowes, D.R., Leake, B.E., Crustal evolution in northwestern Britain and adjacent regions. Geolgoical Journal Special Publications,* 10 (221-248).
--- (1980), 'Some metasomatic calc-magnesian silicate rocks from Connemara, western Ireland: mineralogical control of rock composition', *American Mineralogist,* 65, 26-36.
Leake, B. E., Tanner, G. P. W., and Senior, A. (1981), 'The Geology of Connemara, 1:63,360 coloured geological map', *University of Glasgow*.
--- (1981), 'Fold traces (F3-F5) and Regional Metamorphism in the Dalradian Rocks of Connemara, 1:63,360 coloured geological map ', *University of Glasgow*.
Leake, B. E., Geoff Tanner, P. W., Singh, D., and Halliday, A. N. (1983), 'Major southward thrusting of the Dalradian rocks of Connemara, western Ireland', *Nature,* 305 (5931), 210-13.
Leake, B. E., Tanner, P. W. G., Macintyre, R. M., and Elias, E. (1984), 'Tectonic position of the Dalradian rocks of Connemara and its bearing on the evolution of the Midland Valley of Scotland', *Earth and Environmental Science Transactions of the Royal Society of Edinburgh,* 75 (02), 165-71.
Leake, B. E. (1986), 'The geology of SW Connemara, Ireland: a fold and thrust Dalradian and metagabbroic-gneiss complex', *Journal of the Geological Society, London,* 143, 221-36.

Leake, B. E. and Singh, D. (1986), 'The Delaney Dome Formation, Connemara, W. Ireland, and the Geochemical Distinction of Ortho- and Para-Quartzofeldspathic Rocks', *Mineralogical Magazine,* 50, 205-15.

Leake, B. E. (1988), 'Comments on the age of the oughterard granite, Connemara, Ireland', *Geological Journal,* 23 (3), 271-72.

Leake, B. E. (1989), 'The metagabbros, orthogneisses and paragneisses of the Connemara complex, western Ireland', *Journal of the Geological Society,* 146 (4), 575-96.

Leake, B. E. and Said, Y. A. (1994), 'Hornblende barometry of the Galway batholith, Ireland: an empirical test', *Mineralogy and Petrology,* 51 (2), 243-50.

Leake, B. E. and Tanner, G. P. W. (1994), 'The Geology of the Dalradian and Associated Rocks of Connemara, Western Ireland.', *Royal Irish Academy*.

Leake, B. E. (2006), 'Mechanism of emplacement and crystallisation history of the northern margin and centre of the Galway Granite, western Ireland', *Earth and Environmental Science Transactions of the Royal Society of Edinburgh,* 97 (01), 1-23.

Leake, B. E. (2011), 'Stoping and the mechanisms of emplacement of the granites in the Western Ring Complex of the Galway granite batholith, western Ireland', *Earth and Environmental Science Transactions of the Royal Society of Edinburgh,* 102 (01), 1-16.

Lee, D. and Halliday, A. N. (1995), 'Hafnium-tungsten chronometry and the timing of terrestrial core formation', *Nature,* 378, 771-74.

Leggett, J. K., McKerrow, W. S., and Eales, M. H. (1979), 'The Southern Uplands of Scotland: A Lower Palaeozoic accretionary prism', *Journal of the Geological Society,* 136 (6), 755-70.

Leggett, J. K., McKerrow, W. S., and Soper, N. J. (1983), 'A model for the crustal evolution of southern Scotland', *Tectonics,* 2 (2), 187-210.

Leggo, P. J. (1963), 'The geology and mineralogy of the Maam Cross-Screeb district, Connemara, Eire', *PhD Thesis, University of Bristol*.

Leggo, P. J., Compston, W., and Leake, B. E. (1966), 'The geochronology of the Connemara granites and its bearing on the antiquity of the Dalradian Series', *Quarterly Journal of the Geological Society,* 122 (1-4), 91-116.

Lejeune, A.-M. and Richet, P. (1995), 'Rheology of crystal-bearing silicate melts: An experimental study at high viscosities', *J. Geophys. Res.,* 100 (B3), 4215-29.

Lindsley, D. H. (1976), 'The crystal chemistry and structure of oxide minerals as exemplified by the Fe-Ti oxides, and experimental studies of oxide minerals', *Oxide Minerals, 1st edition, Mineralogical Society of America, Washington DC.*, 69-106.

--- (1991), 'Oxide Minerals: Petrologic and Magnetic Significance', *Reviews in Mineralogy; Mineralogical Society of America,* 25.

Lloyd, G. E. and Knipe, R. J. (1992), 'Deformation mechanisms accommodating faulting of quartzite under upper crustal conditions', *Journal of Structural Geology,* 14 (2), 127-43.

Lloyd, G. E. (2004), 'Microstructural evolution in a mylonitic quartz simple shear zone: the significant roles of dauphine twinning and misorientation', *In: G.I. Alsop, R.E. Holdsworth, K. McCaffrey, M. Hand (eds.), Transports and flow processes in shear zones. Geological Society of London Special Publications,* 224, 39-61.

Long, C. B. and McConnell, B. (1995), 'Bedrock Geology, 1:100,000 Series', *Geological Survery of Ireland,* Sheet 10 (Bedrock of Connemara).

López de Luchi, M. G., Rapalini, A. E., Siegesmund, S., and Steenken, A. (2004), 'Application of magnetic fabrics to the emplacement and tectonic history of Devonian granitoids in central Argentina', *Geological Society, London, Special Publications,* 238 (1), 447-74.

Lowrie, W. and Fuller, M. (1971), 'On the Alternating Field Demagnetization Characteristics of Multidomain Thermoremanent Magnetization in Magnetite', *J. Geophys. Res.,* 76 (26), 6339-49.

Lowrie, W. and Heller, F. (1982), 'Magnetic properties of marine limestones', *Rev. Geophys.,* 20 (2), 171-92.
Lowrie, W. (1990), 'Identification of ferromagnetic minerals in a rock by coercivity and unblocking temperature properties', *Geophysical Research Letters,* 17 (2), 159-62.
Ludwig, K. R. and Mundil, R. (2002), 'Extracting reliable U-Pb ages and errors from complex populations of zircons from Phanerozoic tuffs', *12th Goldschmidt Conference, Abstract*.
Lüneburg, C. M., Lampert, S. A., Lebit, H. D., Hirt, A. M., Casey, M., and Lowrie, W. (1999), 'Magnetic anisotropy, rock fabrics and finite strain in deformed sediments of SW Sardinia (Italy)', *Tectonophysics,* 307 (1–2), 51-74.
MacDonald, R. and Fettes, D. J. (2007), 'The tectonomagmatic evolution of scotland', *Transactions of the Royal Society of Edinburgh: Earth Sciences,* 97, 213-95.
Madden, J. S. (1987), 'Gamma-ray spectrometric studies of the main Galway Granite, Connemara, western Ireland', *Unpublished PhD Thesis, National University of Ireland*.
Magee, C. (2011), 'Emplacement of sub-volcanic cone sheet intrusions', *Ph.D. thesis, University of Birmingham*.
Magee, C., Stevenson, C. T. E., O'Driscoll, B., and Petronis, M. S. (2012), 'Local and regional controls on the lateral emplacement of the Ben Hiant Dolerite intrusion, Ardnamurchan (NW Scotland)', *Journal of Structural Geology,* 39 (0), 66-82.
Mahon, K. I., Harrison, T. M., and Drew, D. A. (1988), 'Ascent of a Granitoid Diapir in a Temperature Varying Medium', *J. Geophys. Res.,* 93 (B2), 1174-88.
Mamtani, M. A. and Greiling, R. O. (2005), 'Granite emplacement and its relation with regional deformation in the Aravalli Mountain Belt (India)—inferences from magnetic fabric', *Journal of Structural Geology,* 27 (11), 2008-29.
Manual, N., Fujino, K., and Samanta, S. (1997), 'Development of quartz ribbons in quartzofeldspathic granulites', *Journal of Earth System Science,* 106 (4), 225-36.
Marsh, B. D. (1982), 'On the mechanics of igneous diapirism, stoping, and zone melting', *American Journal of Science,* 282 (6), 808-55.
Marshall, M. and Cox, A. (1972), 'Magnetic changes in pillow basalts due to sea floor weathering', *J. Geophys Res.,* 77, 6459-69.
Martin-Hernandez, F. and Ferre, E. C. (2006), 'Separation of paramagnetic and ferrimagnetic anisotropies: A review', *Journal of Geophysical Research,* 112 (B03105), 1-16.
Marzec, L. (1927), 'Les plis diapirs et le diapirisme en general.', *C.R. Seances Inst. Geol. Roumanie,* 6, (1914-15), 226-270.
Maslov, A. V., Erdtmann, B. D., Ivanov, K. S., Ivanov, S. N., and Krupenin, M. T. (1997), 'The main tectonic events, depositional history, and the palaeogeography of the southern Urals during the Riphean-early Palaeozoic', *Tectonophysics,* 276 (1–4), 313-35.
Mattinson, J. M. (2005), 'Zircon U–Pb chemical abrasion (bCA-TIMSQ) method: Combined annealing and multi-step partial dissolution analysis for improved precision and accuracy of zircon ages', *Chemical Geology,* 220, 47-66.
Max, M. D. (1978), 'The Galway Granite', *Bulletin of the Geological Survey of Ireland,* 2, 431-51.
Max, M. D., Long, C. B., and Geoghegan, M. A. (1978), 'The Galway Granite', *Geolgoical Survey of Ireland Bulletin,* 2, 223-33.
Max, M. D., Ryan, P. D., and Inamdar, D. D. (1983), 'A magnetic deep structural geology interpretation of Ireland', *Tectonics,* 2 (5), 431-51.
McCaffrey, K. J. W. (1992), 'Igneous emplacement in a transpressive shear zone: Ox Mountains igneous complex', *Journal of the Geological Society,* 149 (2), 221-35.
McCaffrey, K. J. W. and Petford, N. (1997), 'Are granitic intrusions scale invariant?', *Journal of the Geological Society,* 154 (1), 1-4.
McCann, T. and Krawczyk, C. M. (2001), 'The Trans-European Fault: a critical reassessment', *Geological Magazine,* 138 (1), 19-29.

McCay, G. A., Prave, A. R., Alsop, G. I., and Fallick, A. E. (2006), 'Glacial trinity: Neoproterozoic Earth history within the British-Irish Caledonides', *Geology,* 34 (11), 909-12.

McClay, K. R., Norton, M. G., Coney, P., and Davis, G. (1986), 'Collapse of the Caledonide orogen and the Old Red Sandstone', *Nature,* 343, 147-49.

McCoss, A. M. (1986), 'Simple constructions for deformation in transpression/transtension zones', *Journal of Structural Geology,* 8 (6), 715-18.

McGloin, J. (1988), 'The geology of the Carraroe Peninsula, Connemara, Co. Galway', *B.Sc Thesis, National University of Ireland, Galway*.

McKerrow, W. S. (1962), 'THE CHRONOLOGY OF CALEDONIAN FOLDING IN THE BRITISH ISLES', *Proceedings of the National Academy of Sciences,* 48 (11), 1905-13.

McKerrow, W. S., Leggett, J. K., and Eales, M. H. (1977), 'Imbricate thrust model of the Southern Uplands of Scotland', *Nature,* 267 (5608), 237-39.

McKerrow, W. S. (1988), 'The development of the Iapetus Ocean from the Arenig to the Wenlock', *Geological Society, London, Special Publications,* 38 (1), 405-12.

McKerrow, W. S. (1988), 'Wenlock to Givetian deformation in the British Isles and the Canadian Appalachians', *Geological Society, London, Special Publications,* 38 (1), 437-48.

McKerrow, W. S., MaC Niocaill, C., and Dewey, J. F. (2000), 'The Caledonian Orogeny redefined', *Journal of the Geological Society,* 157 (6), 1149-54.

McKerrow, W. S., Campbell, C.J. (1960), 'The stratigraphy and structure of the Lower Palaeozoic rocks of north-west Galway', *Proceedings of the Royal Society of Dublin,* 1, 27-52.

McKerrow, W. S., Dewey, J.F. Scotese, C.R., (1991), 'The Ordovician and Silurian development of the Iapetus Ocean, in Bassett.', *M.G. (ed), The Murchison Symposium, Special Paper in Palaeontology.,* 44, 165-78.

McLeod, G. W., Dempster, T. J., and Faithfull, J. W. (2011), 'Deciphering Magma-Mixing Processes Using Zoned Titanite from the Ross of Mull Granite, Scotland', *Journal of Petrology,* 52 (1), 55-82.

Meere, P. A. and Mulchrone, K. F. (2006), 'Timing of deformation within Old Red Sandstone lithologies from the Dingle Peninsula, SW Ireland', *Journal of the Geological Society,* 163 (3), 461-69.

Meert, J. G. (2003), 'A synopsis of events related to the assembly of eastern Gondwana', *Tectonophysics,* 362 (1–4), 1-40.

Meighan, D. (2003), 'The Caledonian Newry Complex, NE Ireland: new U-Pb ages, a subsurface extension and magmatic epidote', *Joint meeting: Geological Society of America - Northeastern Section - Atlantic Geoscience Society*, 79.

Meighan, I. G. (1976), 'A revision of the Tertiary granites in the E. Mournes Centre', *Journal of the Geological Society, London,* 132, 700.

Meighan, I. G., Gibson, D., and Hood, D. N. (1984), 'Some aspects of Tertiary acid magmatism in NE Ireland', *Mineralogical Magazine,* 48, 351-63.

Merriman, R. J., Rex, D. C., Soper, N. J., and Peacor, D. R. (1995), 'The age of Acadian cleavage in northern England, UK: K–Ar and TEM analysis of a Silurian metabentonite', *Proceedings of the Yorkshire Geological and Polytechnic Society,* 50 (3), 255-65.

Miller, C. A. and Barton, M. (1992), 'The Egersund Dike System, SW Norway: An example of high pressure evolution of tholeiites.', *EOS Transactions. AGU. (abstract)*, 338.

Miller, C. F., Watson, E. B., and Harrison, T. M. (1988), 'Perspectives on the source, segregation and transport of granitoid magmas', *Earth and Environmental Science Transactions of the Royal Society of Edinburgh,* 79 (2-3), 135-56.

Miller, R. B. and Paterson, S. R. (1999), 'In defense of magmatic diapirs', *Journal of Structural Geology,* 21 (8–9), 1161-73.

Min, K., Renne, P. R., and Huff, W. D. (2001), '40Ar/39Ar dating of Ordovician K-bentonites in Laurentia and Baltoscandia', *Earth and Planetary Science Letters,* 185 (1–2), 121-34.

Molyneux, S. J. and Hutton, D. H. W. (2000), 'Evidence for significant granite space creation by the ballooning mechanism: The example of the Ardara pluton, Ireland', *Geological Society of America Bulletin,* 112 (10), 1543-58.

Morin, J. (1950), 'Magnetic susceptibility of αFe_2O_3 and ΥFe_2O_3 ', *Physical Review,* 78, 819-20.

Morris, W. A., Briden, J. C., Piper, J. D. A., and Sallomy, J. T. (1973), 'Palaeomagnetic studies in the British Caledonides, V-Miscellaneous new data', *Royal Astronomical Society Geophysical Journal,* 34, 69-106.

Morris, W. A. (1976), 'Transcurrent motion determined paleomagnetically in the Northern Appalachians and Caledonides and the Acadian Orogeny', *Canadian Journal of Earth Sciences,* 13 (9), 1236-43.

Morris, W. A. and Tanner, P. W. G. (1977), 'The use of paleomagnetic data to delineate the history of the development of the Connemara Antiform', *Canadian Journal of Earth Sciences,* 14 (11), 2601-13.

Morton, W. H. (1964), 'The petrology and structure of the basic igneous complex at Roundstone, Co. Galway, Eire.', *Ph.D. thesis, University of Manchester*.

Moskowitz, B. M. (1981), 'Methods for estimating Curie temperatures of titanomagnetites from experimental Js-T data', *Earth planet Sci. Lett.,* 53 (84-88).

Moskowitz, B. M. (1987), 'Towards resolving the inconsistencies in characteristic physical properties of synthetic titanomaghemites', *Physics of the Earth and Planetary Interiors,* 46 (1–3), 173-83.

Mulchrone, K. F., Grogan, S., and De, P. (2005), 'The relationship between magmatic tiling, fluid flow and crystal fraction', *Journal of Structural Geology,* 27 (2), 179-97.

Müller, A., Leiss, B., Ullemeyer, K., and Breiter, K. (2011), 'Lattice-preferred orientations of late-Variscan granitoids derived from neutron diffraction data: implications for magma emplacement mechanisms', *International Journal of Earth Sciences,* 100 (7), 1515-32.

Murphy, T. (1952), 'Measurements of gravity in Ireland: Gravity survey of central Ireland', *Dublin Institute of Advanced Studies, Geophysics Memoirs 2*.

Mykura, W. (1976), 'British Gregional Geology. Orkney and Shetland.', *HMSO, Edinburgh.*

Nagata, T. (1961), 'Rock Magnetism', *Maruzen, Tokyo*.

Neilson, J. C., Kokelaar, B. P., and Crowley, Q. G. (2009), 'Timing, relations and cause of plutonic and volcanic activity of the Siluro-Devonian post-collision magmatic episode in the Grampian Terrane, Scotland', *Journal of the Geological Society,* 166 (3), 545-61.

Neuman, R. B. (1967), 'Bedrock geology of the Shin Pond and Stacyville Quadrangles, Penobscot County, Maine', *United States Geological Survey, Progessional Paper,* 524 (1), 37.

Neves, S. P., Araujo, A. M. B., Correia, P. B., and Mariano, G. (2003), 'Magnetic fabrics in the Cabanas Granite (NE Brazil): interplay between emplacement and regional fabrics in a dextral transpressive regime', *Journal of Structural Geology,* 25, 441-53.

Nicholson, P. G. (1993), 'A basin reappraisal of the Proterozoic Torridon Group, northwest Scotland.', *In. Frostick, L.E., Steel, R.J. (eds) Tectonic Controls and Signatures in Sedimentary Successions. Blackwell Scientific Publications*, 183-202.

Nikishin, A. M., Ziegler, P. A., Stephenson, R. A., Cloetingh, S. A. P. L., Furne, A. V., Fokin, P. A., Ershov, A. V., Bolotov, S. N., Korotaev, M. V., Alekseev, A. S., Gorbachev, V. I., Shipilov, E. V., Lankreijer, A., Bembinova, E. Y., and Shalimov, I. V. (1996), 'Late Precambrian to Triassic history of the East European Craton: dynamics of sedimentary basin evolution', *Tectonophysics,* 268 (1–4), 23-63.

Nilsen, T. H. and Sylvester, A. G. (1999), 'Strike-slip basins; Part 1', *The Leading Edge,* 18 (10), 1146-52.

--- (1999), 'Strike-slip basins; Part 2', *The Leading Edge,* 18 (11), 1258-67.

Nishitani, T. and Kono, M. (1983), 'Curie temperature and lattice constant of oxidized titanomagnetite', *Geophysical Journal of the Royal Astronomical Society,* 74 (2), 585-600.

Noble, S. R., Hyslop, E. K., and Highton, A. J. (1996), 'High-precision U–Pb monazite geochronology of the c. 806 Ma Grampian Shear Zone and the implications for the evolution of the Central Highlands of Scotland', *Journal of the Geological Society,* 153 (4), 511-14.

Noble, S. R., Tucker, R.D., Pharaoh, T.C. (1993), 'Lower Palaeozoic adn Precambrian igneous rocks from eastern England, and their bearing on late Ordovician closure of the Tornquist Sea: constraints from U-Pb and Nd isotopes.', *Geological Magazine,* 130, 835-46.

Nosova, A. A., Veretennikov, N.V. & Levsky, L.K. (2005), 'Nature of the mantle source and specific features of crustal contamination of Neoproterozoic flood basalts of the Volhynia Province (Nd–Sr isotopic and ICP-MS geochemical data).', *Transactions (Doklady) of the Russian Academy of Sciences,* 401A, 433-92.

Nye, J. F. (1957), 'Physical properties of crystals', *Oxford University Press*, 322.

O'Driscoll, B., Troll, V. R., Reavy, R. J., and Turner, P. (2006), 'The Great Eucrite intrusion of Ardnamurchan, Scotland: Reevaluating the ring-dike concept', *Geology,* 34 (3), 189-92.

O'Reilly, W. (1976), 'Magnetic minerals in the crust of the Earth', *Reports on Progress in Physics,* 39 (9), 857.

O'Reilly, W. (1984), 'Rock and mineral magnetism', *Blackie*.

O'Driscoll, B., Stevenson, C. T. E., and Troll, V. R. (2008), 'Mineral Lamination Development in Layered Gabbros of the British Palaeogene Igneous Province: A Combined Anisotropy of Magnetic Susceptibility, Quantitative Textural and Mineral Chemistry Study', *Journal of Petrology,* 49 (6), 1187-221.

Oliver, G. J. H., Wilde, S. A., and Wan, Y. (2008), 'Geochronology and geodynamics of Scottish granitoids from the late Neoproterozoic break-up of Rodinia to Palaeozoic collision', *Journal of the Geological Society,* 165 (3), 661-74.

Ono, T., Hosomi, Y., Arai, H., and Takagi, H. (2010), 'Comparison of petrofabrics with composite magnetic fabrics of S–C mylonite in paramagnetic granite', *Journal of Structural Geology,* 32 (1), 2-14.

Ordóñez Casado, B., Gebauer, D., Schäfer, H. J., Ibarguchi, J. I. G., and Peucat, J. J. (2001), 'A single Devonian subduction event for the HP/HT metamorphism of the Cabo Ortegal complex within the Iberian Massif', *Tectonophysics,* 332 (3), 359-85.

Orlický, O. (1990), 'Detection of magnetic carriers in rocks: results of susceptibility changes in powdered rock samples induced by temperature.', *Physics of the Earth and Planetary Interiors,* 63, 66-70.

Owens, W. H. (1973), 'Strain modification of angular density distributions', *Tectonophysics,* 16 (3–4), 249-61.

--- (1974), 'Mathematical model studies on factors affecting the magnetic anisotropy of deformed rocks', *Tectonophysics,* 24 (1–2), 115-31.

Owens, W. H. and Bamford, D. (1976), 'Magnetic, Seismic, and other Anisotropic Properties of Rock Fabrics', *Philosophical Transactions of the Royal Society of London. Series A, Mathematical and Physical Sciences,* 283 (1312), 55-68.

Owens, W. H. and Rutter, E. H. (1978), 'The development of magnetic susceptibility anisotropy through crystallographic preferred orientation in a calcite rock', *Physics of the Earth and Planetary Interiors,* 16 (3), 215-22.

Owens, W. H. (1994), 'Laboratory drilling of field-orientated block samples', *Journal of Structural Geology,* 16 (12), 1719-21.

--- (2000), 'Statistical analysis of normalized and unnormalized second‐rank tensor data, with application to measurements of anisotropy of magnetic susceptibility', *Geophys. Res. Lett.,* 27 (18), 2985-88.

--- (2000), 'Error estimates in the measurement of anisotropic magnetic susceptibility', *Geophysical Journal International,* 142 (2), 516-26.

Özdemir, Ö., Dunlop, D. J., and Moskowitz, B. M. (1993), 'The effect of oxidation on the Verwey transition in magnetite', *Geophys. Res. Lett.,* 20 (16), 1671-74.

Panahi, A. and Young, G. M. (1997), 'A geochemical investigation into the provenance of the Neoproterozoic Port Askaig Tillite, Dalradian Supergroup, western Scotland', *Precambrian Research,* 85 (1–2), 81-96.

Pankhurst, R. J. (1970), 'The geochronology of the 'younger' basic complexex of northeast Scotland.', *Scottish Journal of Geology,* 6 (83), 25.

Parés, J. M., van der Pluijm, B. A., and Dinarès-Turell, J. (1999), 'Evolution of magnetic fabrics during incipient deformation of mudrocks (Pyrenees, northern Spain)', *Tectonophysics,* 307 (1–2), 1-14.

Parés, J. M. and van der Pluijm, B. A. (2002), 'Evaluating magnetic lineations (AMS) in deformed rocks', *Tectonophysics,* 350 (4), 283-98.

--- (2002), 'Phyllosilicate fabric characterization by Low-Temperature Anisotropy of Magnetic Susceptibility (LT-AMS)', *Geophys. Res. Lett.,* 29 (24), 2215.

Parés, J. M. (2004), 'How deformed are weakly deformed mudrocks? Insights from magnetic anisotropy', *Geological Society, London, Special Publications,* 238 (1), 191-203.

Park, R. G. and Tarney, J. (1987), 'The Lewisian complex: a typical Precambrian high-grade terrain?', *Geological Society, London, Special Publications,* 27 (1), 13-25.

Park, R. G., Stewart, A. D., and Wright, D. T. (2002), 'The Hebridean Terrane.', *In: Trewin, N.H. (ed) The Geology of Scotland. Geological Society, London.*, 45-80.

Parslow, G. R. and Randall, B. A. O. (1973), 'A gravity survey of the Cairnsmore of Fleet granite and its environs', *Scottish Journal of Geology,* 9 (3), 219-31.

Parsons, T. and Thompson, G. A. (1991), 'The Role of Magma Overpressure in Suppressing Earthquakes and Topography: Worldwide Examples', *Science,* 253 (5026), 1399-402.

Passchier, C. W. (1982), 'Mylonitic deformation in the Saint-Barthelemy Massif, French Pyrenees, with emphasis on the genetic relationship between ultra mylonite and pseudotachylyte.', *GUA Papers of Geology,* 1 (16), 1-173.

Passchier, C. W. and Trouw, R. A. J. (2005), 'Microtectonics', *Springer Berlin Heidelberg New York,* 2.

Paterson, S. R., Vernon, R. H., and Othmar, T. T. (1988), 'A review of criteria for the identification of magmatic and tectonic foliations in granitoids', *Journal of structural Geology,* 11 (3), 349-63.

Paterson, S. R., Vernon, R. H., and Tobisch, O. T. (1989), 'A review of criteria for the identification of magmatic and tectonic foliations in granitoids', *Journal of Structural Geology,* 11 (3), 349-63.

Paterson, S. R. and Tobisch, O. T. (1992), 'Rates of processes in magmatic arcs: implications for the timing and nature of pluton emplacement and wall rock deformation', *Journal of Structural Geology,* 14 (3), 291-300.

Paterson, S. R. and Fowler, K. T. (1993), 'Re-examining pluton emplacement processes', *Journal of Structural Geology,* 15 (2), 191-206.

Paterson, S. R. and Vernon, R. H. (1995), 'Bursting the bubble of ballooning plutons: A return to nested diapirs emplaced by multiple processes', *Geological Society of America Bulletin,* 107 (11), 1356-80.

Paterson, S. R., Fowler Jr, T. K., Schmidt, K. L., Yoshinobu, A. S., Yuan, E. S., and Miller, R. B. (1998), 'Interpreting magmatic fabric patterns in plutons', *Lithos,* 44 (1–2), 53-82.

Paterson, S. R., Pignotta, G. S., and Vernon, R. H. (2004), 'The significance of microgranitoid enclave shapes and orientations', *Journal of Structural Geology,* 26 (8), 1465-81.

Paterson, S. R., Pignotta, G. S., Farris, D., Memeti, V., Miller, R. B., Vernon, R. H., and Žák, J. (2008), 'Is stoping a volumetrically significant pluton emplacement process?: Discussion', *Geological Society of America Bulletin,* 120 (7-8), 1075-79.

Paton, C., Hellstrom, J., Paul, B., Woodhead, J., and Hergt, J. (2011), 'Iolite: Freeware for the visualisation and processing of mass spectrometric data', *Journal of Analytical Atomic Spectrometry,* 26 (12), 2508-18.

Paul, W. and Steinwedel, H. (1953), 'Ein neues Massenspektrometer ohne Magnetfeld', *Zeitschrift fur Naturforschung A,* 8 (7), 488-50.

Petford, N. (1996), 'Dykes or diapirs?', *Geological Society of America Special Papers,* 315, 105-14.

Petford, N., Clemens, J. D., and Vigneresse, J. L. (1997), 'Application of information theory to the formation of granitic rocks', *In Bouchez, J.L., Hutton, D. & Stephens, W.E. (eds) Granite From Melt Segregation to Emplacement Fabrics. Dordrecht: Kluwer Academic Publishers.*, 3-10.

Petford, N. and Clemens, J. D. (2000), 'Granites are not diapiric!', *Geology Today,* 16 (5), 180-84.

Petford, N., Cruden, A. R., McCaffrey, K. J. W., and Vigneresse, J. L. (2000), 'Granite magma formation, transport and emplacement in the Earth's crust', *Nature,* 408 (6813), 669-73.

Petford, N. (2003), 'Rheology of Granitic Magmas During Ascent and Emplacement', *Annual Review of Earth and Planetary Sciences,* 31, 399-427.

Petronis, M. S., O'Driscoll, B., and Lindline, J. (2011), 'Late stage oxide growth associated with hydrothermal alteration of the Western Granite, Isle of Rum, NW Scotland', *Geochem. Geophys. Geosyst.,* 12 (1), Q01001.

Petronis, M. S., O'Driscoll, B., Stevenson, C. T. E., and Reavy, R. J. (2012), 'Controls on emplacement of the Caledonian Ross of Mull Granite, NW Scotland: Anisotropy of magnetic susceptibility and magmatic and regional structures', *Geological Society of America Bulletin,* 124, 906-27.

Petrovský, E., Kapi, and ka, A. (2006), 'On determination of the Curie point from thermomagnetic curves', *J. Geophys. Res.,* 111 (B12), B12S27.

Petrus, J. A. and Kamber, B. S. (2012), 'VizualAge: A Novel Approach to Laser Ablation ICP-MS U-Pb Geochronology Data Reduction', *Geostandards and Geoanalytical Research,* 36 (3), 247-70.

Pharaoh, T. C., Merriman, R. J., Webb, P. C., and Beckinsale, R. D. (1987), 'The concealed Caledonides of eastern England: preliminary results of a multidisciplinary study', *Proceedings of the Yorkshire Geological Society,* 46 (4), 355-69.

Pharaoh, T. C., Brewer, T. S., and Webb, P. C. (1993), 'Subduction-related magmatism of Late Ordovician age in eastern England', *Geological Magazine,* 130 (5), 647-56.

Pharaoh, T. C. (1999), 'Palaeozoic terranes and their lithospheric boundaries within the Trans-European Suture Zone (TESZ): a review', *Tectonophysics,* 314 (1–3), 17-41.

Piazolo, S., Bons, P. D., and Passchier, C. W. (2002), 'The influence of matrix rheology and vorticity on fabric development of populations of rigid objects during plane strain deformation', *Tectonophysics,* 351, 315-29.

Pickering, K. T., Bassett, M. G., and Siveter, D. J. (1988), 'Late Ordovician–early Silurian destruction of the Iapetus Ocean: Newfoundland, British Isles and Scandinavia—a discussion', *Earth and Environmental Science Transactions of the Royal Society of Edinburgh,* 79 (04), 361-82.

Pidgeon, R. T. (1969), 'Zircon U-Pb ages from the Galway granite and the Dalradian, Connemara, Ireland', *Scottish Journal of Geology,* 5 (4), 375-92.

Pisarevsky, S. A., Wingate, M. T. D., Powell, C. M., Johnson, S., and Evans, D. A. D. (2003), 'Models of Rodinia assembly and fragmentation', *Geological Society, London, Special Publications,* 206 (1), 35-55.

Pitcher, W. S. (1953), 'The Rosses granitic ring-complex, County Donegal, Eire', *Proceedings of the Geologists' Association,* 64 (3), 153-IN2.

Pitcher, W. S. and Bussell, M. A. (1977), 'Structural control of batholithic emplacement in Peru: a review', *Journal of the Geological Society,* 133 (3), 249-55.

Pitcher, W. S. (1979), 'The nature, ascent and emplacement of granitic magmas', *Journal of the Geological Society,* 136 (6), 627-62.
Pitcher, W. S. (1982), 'Granite type and tectonic environment', *In: Hsu, K.J. (ed.) Mountain Building Processes. Academmic Press, London*, 19-40.
Pitcher, W. S., Atherton, M. P., Cobbing, E. J., and Beckinsale, R. D. (1985), 'Magmatism at a plate', *Blackie & Sons Ltd. Glasgow*.
Pitcher, W. S. (1987), 'Granites and yet more granites forty years on.', *Geol. Rdsch,* 76, 51-79.
--- (1993), 'The Nature and Origin of Granite', *Chapman & Hall*.
--- (1997), 'The nature and origin of Granite (2nd edition)', *Chapman & Hall*.
Plant, A. G. (1968), 'The geology of the Leam-Shannawona district, Connemara, Ireland.', *PhD Thesis, University of Bristol*.
Platt, J. P. and Vissers, R. L. M. (1980), 'Extensional structures in anisotropic rocks', *Journal of Structural Geology,* 2 (4), 397-410.
Pollard, D. D. and Johnson, A. M. (1973), 'Mechanics of growth of some laccolithic intrusions in the Henry mountains, Utah, II: Bending and failure of overburden layers and sill formation', *Tectonophysics,* 18 (3–4), 311-54.
Pollard, D. D. and Muller, O. H. (1976), 'The Effect of Gradients in Regional Stress and Magma Pressure on the Form of Sheet Intrusions in Cross Section', *J. Geophys. Res.,* 81 (5), 975-84.
Poprawa, P., Šliaupa, S., Stephenson, R., and Lazauskien�โ, J. (1999), 'Late Vendian–Early Palæozoic tectonic evolution of the Baltic Basin: regional tectonic implications from subsidence analysis', *Tectonophysics,* 314 (1–3), 219-39.
Potter, D. K. and Stephenson, A. (1988), 'Single domain particles in rocks and magnetic fabric analysis', *Geophys. Res. Lett.,* 15 (10), 1097-100.
Prave, A. R. (1999), 'The Neoproterozoic Dalradian Supergroup of Scotland: an alternative hypothesis', *Geological Magazine,* 136 (06), 609-17.
Prave, A. R., Strachan, R. A., and Fallick, A. E. (2009), 'Global C cycle perturbations recorded in marbles: a record of Neoproterozoic Earth history within the Dalradian succession of the Shetland Islands, Scotland', *Journal of the Geological Society,* 166 (1), 129-35.
Pressler, R. E., Schneider, D. A., Petronis, M. S., Holm, D. K., and Geissman, J. W. (2007), 'Pervasive horizontal fabric and rapid vertical extrusion: Lateral overturning and margin sub-parallel flow of deep crustal migmatites, northeastern Bohemian Massif', *Tectonophysics,* 443 (1–2), 19-36.
Pringle, J. (1939), 'The Discovery of Cambrian Trilobites in the Highland Border Rocks Near Callander Perthshire.', *Report to the British Association for the Advancement of Science*, 252.
Pryer, L. L. (1993), 'Microstructures in feldspars from a major crustal thrust zone: The Grenville Front, Ontario, Canada', *Journal of Structural Geology,* 15 (1), 21-36.
Pryer, L. L. and Robin, P. Y. F. (1995), 'Retrograde metamorphic reactions in deforming granites and the origin of flame perthite', *Journal of Metamorphic Geology,* 13 (6), 645-58.
Ramberg, H. (1970), 'Model studies in relation to intrusion of plutonic bodies', *In: Newall, G. and Rast, N. (eds) Mechanism of Igneous Intrusion. Geological Journal Special Issue*, 261-86.
--- (1981), 'Gravity, Deformation on the Earths's Crust in Theory, Experiments and Geological Applications', *Academic Press, New York*, 214.
Ramsay, D. M. and Huber, M. I. (1983), 'London Academic Press', *The techniques of modern structural geology,* 1.
Ramsay, J. G. (1967), 'Folding and Fracturing of Rocks ', *McGraw Hill, New York*.
Ramsay, J. G. (1989), 'Emplacement kinematics of a granite diapir: the Chindamora batholith, Zimbabwe', *Journal of Structural Geology,* 11 (1–2), 191-209.

Read, H. H. (1961), 'Aspects of Caledonian magmatism in Britain', *Liverpool and Manchester Geological Society,* 2, 653-83.
Readman, P. W. and O'Reilly, W. (1970), 'The synthesis and inversion of non-stoichiometric titanomagnetites', *Phys. Earth Planet. Inter.,* 4, 121-28.
--- (1972), 'Magnetic properties of oxidized (cation deficient) titanomagnetite (Fe, Ti, *A*)3 O4', *J. Geomagn. Geoelectr.,* 24, 69-90.
Reavy, R. J. (1989), 'Structural controls on metamorphism and syn-tectonic magmatism: the Portuguese Hercynian collision belt', *Journal of the Geological Society,* 146 (4), 649-57.
Reynolds, D. L. (1951), 'The Geology of Slieve Gullion, Foughill and Carrickarnan: an actualistic interpretation of a Tertiary Gabbro-Granophyre Complex', *Transactions of the Royal Society of Edinburgh: Earth Sciences,* 52, 86-143.
--- (1956), 'Calderas and ring complexes', *Verhandeling van het koninklijk Nederlands Geologisch Mijnbouwkundig Genootschap,* 16, 355-79.
Richey, J. E. (1928), 'The Structural Relations of the Mourne Granites, Northern Ireland', *Quarterly Journal of the Geological Society,* 83 (1-5), 653-88,NP-NP.
Richey, J. E. and Thomas, H. H. (1930), 'The geology of Ardnamurchan, northwest Mull and Coll', *Memoir of the Geological Survey Scotland, HMSO*, 393.
Richey, J. E. (1932), 'Tertiary ring structures in Britain', *Transactions of the Geological Society of Glasgow,* 19, 42-140.
Richmond, L. K. and Williams, B. P. J. (1998), 'Fluvial-aeolian interactions and Old Red Sandstone basin evolution, Northwest Dingle Peninsula, Co. Kerry, Southwest Ireland', *Unpublished PhD thesis, University of Aberdeen*.
Richmond, L. K. and Williams, B. P. J. (2000), 'A new terrane in the Old Red Sandstone of the Dingle Peninsula, SW Ireland', *Geological Society, London, Special Publications,* 180 (1), 147-83.
Roberts, A. M., Smith, D. I., and Harris, A. L. (1984), 'The structural setting and tectonic significance of the Glen Dessary Syenite, Inverness-shire', *Journal of the Geological Society,* 141 (6), 1033-42.
Robertson, D. J. (1988), 'Paleomagnetism of the Connemara gabbros, western Ireland', *Geophysical journal of the Royal Astronomical Society, London,* 94, 51-64.
Robin, P.-Y. F. and Cruden, A. R. (1994), 'Strain and vorticity patterns in ideally ductile transpression zones', *Journal of Structural Geology,* 16 (4), 447-66.
Robin, P.-Y. F. (2002), 'Determination of fabric and strain ellipsoids from measured sectional ellipses — theory', *Journal of Structural Geology,* 24 (3), 531-44.
Robion, P., Averbuch, O., and Sintubin, M. (1999), 'Fabric development and metamorphic evolution of lower Palaeozoic slaty rocks from the Rocroi massif (French–Belgian Ardennes): new constraints from magnetic fabrics, phyllosilicate preferred orientation and illite crystallinity data', *Tectonophysics,* 309 (1–4), 257-73.
Roche, O., Druitt, T. H., and Merle, O. (2000), 'Experimental study of caldera formation', *J. Geophys. Res.,* 105 (B1), 395-416.
Rochette, P. and Vialon, P. (1984), 'Development of planar and linear fabrics in Dauphinois shales and slates (French Alps) studied by magnetic anisotropy and its mineralogical control', *Journal of Structural Geology,* 6 (1–2), 33-38.
Rochette, P. (1987), 'Magnetic susceptibility of the rock matrix related to magnetic fabric studies', *Journal of Structural Geology,* 9 (8), 1015-20.
--- (1988), 'Inverse magnetic fabric in carbonate-bearing rocks', *Earth and Planetary Science Letters,* 90 (2), 229-37.
Rochette, P. and Fillion, G. (1988), 'Identification of multicomponent anisotropies in rocks using various field and temperature values in a cryogenic magnetometer', *Physics of the Earth and Planetary Interiors,* 51 (4), 379-86.

Rochette, P., Jackson, M. J., and Aubourg, C. (1992), 'Rock magnetism and the interpretation of anisotropy of magnetic susceptibility', *Reviews of Geophysics,* 30, 209-26.

Rochette, P., Aubourg, C., and Perrin, M. (1999), 'Is this magnetic fabric normal? A review and case studies in volcanic formations', *Tectonophysics,* 307 (1–2), 219-34.

Rock, N. M. S., Cooper, C., and Gaskarth, J. W. (1986), 'Late Caledonian subvolcanic vents and associated dykes in the Kirkcudbright area, Galloway, south-west Scotland', *Proceedings of the Yorkshire Geological Society,* 46 (1), 29-37.

Rock, N. M. S., Gaskarth, J. W., and Rundle, C. C. (1986), 'Late Caledonian Dyke-Swarms in Southern Scotland: A Regional Zone of Primitive K-Rich Lamprophyres and Associated Vents', *The Journal of Geology,* 94 (4), 505-22.

Roddick, J. C., Loveridge, W. D., and Parrish, R. R. (1987), 'Precise UPb dating of zircon at the sub-nanogram Pb level', *Chemical Geology: Isotope Geoscience section,* 66 (1–2), 111-21.

Rogers, D. A., Marshall, J. E. A., and Astin, T. R. (1989), 'Short Paper: Devonian and later movements on the Great Glen fault system, Scotland', *Journal of the Geological Society,* 146 (3), 369-72.

Rogers, G. and Dunning, G. R. (1991), 'Geochronology of appinitic and related granitic magmatism in the W Highlands of Scotland: constraints on the timing of transcurrent fault movement', *Journal of the Geological Society,* 148 (1), 17-27.

Rogers, G., Paterson, B. A., Dempster, T. J., and Redwood, S. D. (1994), 'U-Pb geochronology of the 'Newer' Gabbros, NE Grampians (abstract).', *Caledonian Terrane Relationships in Britain, Keyworth.*

Rogers, G., Kinny, P. D., Strachan, R. A., Friend, C. R. L., and Paterson, B. A. (2001), 'U–Pb geochronology of the Fort Augustus granite gneiss: constraints on the timing of Neoproterozoic and Palaeozoic tectonothermal events in the NW Highlands of Scotland', *Journal of the Geological Society,* 158 (1), 7-14.

Roman-Berdiel, T., Gapais, D., and Brun, J. P. (1995), 'Analogue models of laccolith formation', *Journal of Structural Geology,* 17 (9), 1337-46.

Román-Berdiel, T., Aranguren, A., Cuevas, J., Tubía, J. M., Gapais, D., and Brun, J.-P. (2000), 'Experiments on granite intrusion in transtension', *Geological Society, London, Special Publications,* 174 (1), 21-42.

Roman Berdiel, T., Gapais, D., and Brun, J.-P. (1997), 'Granite intrusion along strike-slip zones in experiment and nature', *American Journal of Science,* 297 (6), 651-78.

Rooney, A. D., Chew, D. M., and Selby, D. (2011), 'Re-Os geochronology of the Neoproterozoic-Cambrian Dalradian Supergroup of Scotland and Ireland: Implications for Neoproterozoic stratigraphy, glaciations and Re-Os systematics.', *Precambrian Research,* 185, 202-14.

Roscoe, R. (1952), 'The viscosity of suspensions of rigid spheres', *British Journal of Applied Physics,* 3, 267.

Rosenberg, C. L. and Stünitz, H. (2003), 'Deformation and recrystallization of plagioclase along a temperature gradient: an example from the Bergell tonalite', *Journal of Structural Geology,* 25 (3), 389-408.

Rosenberg, C. L. and Handy, M. R. (2005), 'Experimental deformation of partially melted granite revisted: implications for the continental crust', *Journal of Metamorphic Geology,* 23, 19-28.

Rubin, A. M. (1998), 'Dike ascent in partially molten rock', *J. Geophys. Res.,* 103 (B9), 20901-19.

Rushmer, T. (1995), 'An experimental deformation study of partially molten amphibolite: Application to low-melt fraction segregation', *J. Geophys. Res.,* 100 (B8), 15681-95.

Ryall, P. J. C. and Ade-Hall, J. M. (1975), 'Radial Variation of Magnetic Properties in Submarine Pillow Basalt', *Canadian Journal of Earth Sciences,* 12 (12), 1959-69.

Ryan, M. P. (1993), 'Neutral Buoyancy and the Structure of Mid-Ocean Ridge Magma Reservoirs', *J. Geophys. Res.,* 98 (B12), 22321-38.

Ryan, P. D. and Dewey, J. F. (1991), 'A geological and tectonic cross-section of the Caledonides of western Ireland', *Journal of the Geological Society,* 148 (1), 173-80.

Ryan, P. D., Soper, N. J., Snyder, D. B., England, R. W., and Hutton, D. H. W. (1995), 'The Antrim–Galway Line: a resolution of the Highland Border Fault enigma of the Caledonides of Britain and Ireland', *Geological Magazine,* 132 (02), 171-84.

Ryan, P. D. and Dewey, J. F. (2004), 'The South Connemara Group reinterpreted: a subduction-accretion complex in the Caledonides of Galway Bay, western Ireland', *Journal of Geodynamics,* 37 (3–5), 513-29.

Sanderson, D. J. and Marchini, W. R. D. (1984), 'Transpression', *Journal of Structural Geology,* 6 (5), 449-58.

Sawaki, Y., Kawai, T., Shibuya, T., Tahata, M., Omori, S., Komiya, T., Yoshida, N., Hirata, T., Ohno, T., Windley, B. F., and Maruyama, S. (2010), '87Sr/86Sr chemostratigraphy of Neoproterozoic Dalradian carbonates below the Port Askaig Glaciogenic Formation, Scotland', *Precambrian Research,* 179 (1–4), 150-64.

Saylor, B. Z., Kaufman, A. J., Grotzinger, J. P., and Urban, F. (1998), 'A composite reference section for terminal proterozoic strata of southern Namibia', *Journal of Sedimentary Research,* 68 (6), 1223-35.

Scaillet, B., Holtz, F., Pichavant, M., and Schmidt, M. (1996), 'Viscosity of Himalayan leucogranites: Implications for mechanisms of granitic magma ascent', *J. Geophys. Res.,* 101 (B12), 27691-99.

Scaillet, B., Whittington, A., Martel, C., Pichavant, M., and Holtz, F. (2000), 'Phase equilibrium constraints on the viscosity of silicic magmas, 2. Implications for mafic–silicic mixing processes.', *In: Barbarin, B., Stephens, W.E., Bouchez J.L., Clarke, D.B., Cuney, M., Martin, H. (eds.), The Origin of Granites and Related Rocks. Transactions of the Royal Society of Edinburgh: Earth Sciences 91, Bristol*, 61-72.

Schofield, N., Heaton, L., Holford, S. P., Archer, S. G., Jackson, C. A.-L., and Jolley, D. W. (2012), 'Seismic imaging of 'broken bridges': linking seismic to outcrop-scale investigations of intrusive magma lobes', *Journal of the Geological Society,* 169 (4), 421-26.

Schümmer, P. (1979), 'Mechanics of Non-Newtonian Fluids. Von W. R. Schowalter. Pergamon Press, Oxford–Frankfurt 1978. 1. Aufl., IX, 300 S., zahlr. Abb. u. Tab., geb., $ 35.00', *Chemie Ingenieur Technik,* 51 (7), 766-66.

Scotese, C. R. and McKerrow, W. S. (1990), 'Revised World maps and introduction', *Geological Society, London, Memoirs,* 12 (1), 1-21.

Selby, D., Creaser, R. A., and Feely, M. (2004), 'Accurate and precise Re-Os molybdenite dates from the Galway Granite, Ireland. Critical comment on "Disturbance of the Re-Os chronometer of molybdenites from the late-Caledonian Galway Granite, Ireland, by hydrothermal fluid circulation" by Suzuki *et al., Geochemical Journal*, 35, 29-35, 2001', *Geochemical Journal,* 38, 291-94.

Senior, A. and Leake, B. E. (1978), 'Regional Metasomatism and the Geochemistry of the Dalradian Metasediments of Connemara, Western Ireland', *Journal of Petrology,* 19 (3), 585-625.

Sherlock, S. C., Kelley, S. P., Zalasiewicz, J. A., Schofield, D. I., Evans, J. A., Merriman, R. J., and Kemp, S. J. (2003), 'Precise dating of low-temperature deformation: Strain-fringe analysis by 40Ar-39Ar laser microprobe', *Geology,* 31 (3), 219-22.

Shigematsu, N. (1999), 'Dynamic recrystallization in deformed plagioclase during progressive shear deformation', *Tectonophysics,* 305 (4), 437-52.

Siebel, W., Trzebski, R., Stettner, G., Hecht, L., Casten, U., Hohndorf, A., and Muller, P. (1997), 'Granitoid magmatism of the NW Bohemian massif revealed: gravity data, composition, age relations and phase concept', *Geol. Rundsch.,* 86, S45-S63.

Simpson, C. (1985), 'Deformation of granitic rocks across the brittle-ductile transition', *Journal of Structural Geology,* 7 (5), 503-11.

Smith, D. C. and Lappin, M. A. (1989), 'Coesite in the Straumen kyanite-eclogite pod, Norway', *Terra Nova,* 1 (1), 47-56.

Smith, D. I. and Watson, J. (1983), 'Scale and movement on the Great Glen Fault, Scotland.', *Geology,* 11, 523-26.

Snowden, P. A. and Snowden, D. V. (1981), 'Petrochemistry of the late Archean granites of thc Chindamora batholith, Zimbabwe', *Precambrian Research,* 16, 103-29.

Soper, N. J. and Hutton, D. H. W. (1984), 'Late Caledonian sinistral displacements in Britain: Implications for a three-plate collision model', *Tectonics,* 3 (7), 781-94.

Soper, N. J. (1986), 'The Newer Granite problem: a geotectonic view', *Geological Magazine,* 123 (03), 227-36.

Soper, N. J., Webb, B. C., and Woodcock, N. H. (1987), 'Late Caledonian (Acadian) transpression in north-west England: timing, geometry and geotectonic significance', *Proceedings of the Yorkshire Geological Society,* 46 (3), 175-92.

Soper, N. J. (1988), 'Timing and geometry of collision, terrane accretion and sinistral strike-slip events in the British Caledonides', *Geological Society, London, Special Publications,* 38 (1), 481-92.

Soper, N. J. and Woodcock, N. H. (1990), 'Silurian collision and sediment dispersal patterns in southern Britain', *Geological Magazine,* 127 (6), 527-42.

Soper, N. J., Strachan, R. A., Holdsworth, R. E., Gayer, R. A., and Greiling, R. O. (1992), 'Sinistral transpression and the Silurian closure of Iapetus', *Journal of the Geological Society,* 149 (6), 871-80.

Soper, N. J. (1994), 'Was Scotland a Vendian RRR junction?', *Journal of the Geological Society,* 151 (4), 579-82.

--- (1994), 'Neoproterozoic sedimentation on the northeast margin of Laurentia and the opening of Iapetus', *Geological Magazine,* 131 (03), 291-99.

Soper, N. J. and England, R. W. (1995), 'Vendian and Riphean rifting in NW Scotland', *Journal of the Geological Society,* 152 (1), 11-14.

Soper, N. J., Harris, A. L., and Strachan, R. A. (1998), 'Tectonostratigraphy of the Moine Supergroup: a synthesis', *Journal of the Geological Society,* 155 (1), 13-24.

Soper, N. J., Ryan, P. D., and Dewey, J. F. (1999), 'Age of the Grampian orogeny in Scotland and Ireland', *Journal of the Geological Society,* 156 (6), 1231-36.

Soper, N. J. and Woodcock, N. H. (2003), 'The lost Lower Old Red Sandstone of England and Wales: a record of post-Iapetan flexure or Early Devonian transtension?', *Geological Magazine,* 140 (6), 627-47.

Spencer, A. M. (1971), 'Late Pre-cambrian Glaciation In Scotland', *Geological Society, London, Memoirs,* 6 (1), 5-102.

Stacey, F. D. (1960), 'Magnetic Anisotropy of Rocks', *Journal of Geophysical Research,* 54, 2429-42.

Steenken, A., Siegesmund, S., and Heinrichs, T. (2000), 'The emplacement of the Rieserferner Pluton (Eastern Alps, Tyrol): constraints from field observations, magnetic fabrics and microstructures', *Journal of Structural Geology,* 22 (11–12), 1855-73.

Stephens, W. E. and Halliday, A. N. (1984), 'Geochemical contrasts between late Caledonian granitoid plutons of northern, central and southern Scotland', *Earth and Environmental Science Transactions of the Royal Society of Edinburgh,* 75 (02), 259-73.

Stephens, W. E. (1992), 'Spatial, compositional and rheological constraints on the origin of zoning in the Criffell pluton, Scotland', *Earth and Environmental Science Transactions of the Royal Society of Edinburgh,* 83 (1-2), 191-99.

Stephens, W. E. and Highton, I. (1999), 'The Caledonian Igneous Rocks of Great Britain: an introduction. ', *Caledonian Igneous Rocks of Britain by Stephenson, D., Bevins, R.E., Millward, D.,Highton, A.J., Parsons, I., Stone, P., Wadsworth, W.J. (eds). Geological Conservation Review Series: Joint Nature Conservation Committee*, 17-19.

Stephenson, A. (1994), 'Distribution anisotropy: two simple models for magnetic lineation and foliation', *Physics of the Earth and Planetary Interiors,* 82 (1), 49-53.

Stevens, N. C. (1958), 'Ring-structures of the Mt. Alford district south-east Queensland', *Journal of the Geological Society of Australia,* 6, 37-49.

Stevenson, C. T. E. (2004), 'Granite Emplacement and Magam Flow in Contrasting Tectonic Environments using Anisotropy of Magnetic Susceptibility', *Ph.D. thesis, University of Birmingham*.

Stevenson, C. T. E., Owens, W. H., and Hutton, D. H. W. (2007), 'Flow lobes in granite: The determination of magma flow direction in the Trawenagh Bay Granite, northwestern Ireland, using anisotropy of magnetic susceptibility', *Geological Society of America Bulletin,* 119 (11-12), 1368-86.

Stevenson, C. T. E., Owens, W. H., Hutton, D. H. W., Hood, D. N., and Meighan, I. G. (2007), 'Laccolithic, as opposed to cauldron subsidence, emplacement of the Eastern Mourne pluton, N. Ireland: evidence from anisotropy of magnetic susceptibility', *Journal of the Geological Society,* 164 (1), 99-110.

Stevenson, C. T. E. (2008), 'A Revised intrusion sequence for the Donegal Batholith: evidence from its aureole in Lettermacaward', *Irish Journal of Earth Sciences,* 26, 33-43.

Stevenson, C. T. E., Hutton, D. H. W., and Price, A. R. (2008), 'The Trawenagh Bay Granite and a new model for the emplacement of the Donegal Batholith', *Earth and Environmental Science Transactions of the Royal Society of Edinburgh,* 97 (4), 455-77.

Stevenson, C. T. E., O'Driscoll, B., Holohan, E. P., Couchman, R., Reavy, R. J., and Andrews, G. D. M. (2008), 'The structure, fabrics and AMS of the Slieve Gullion ring-complex, Northern Ireland: testing the ring-dyke emplacement model', *Geological Society, London, Special Publications,* 302 (1), 159-84.

Stevenson, C. T. E. (2009), 'The relationship between forceful and passive emplacement: The interplay between tectonic strain and magma supply in the Rosses Granitic Complex, NW Ireland', *Journal of Structural Geology,* 31 (3), 270-87.

Stevenson, C. T. E. and Bennett, N. (2011), 'The emplacement of the Palaeogene Mourne Granite Centres, Northern Ireland: new results from the Western Mourne Centre', *Journal of the Geological Society,* 168 (4), 831-36.

Stewart, A. D. (1982), 'Late Proterozoic rifting in NW Scotland: the genesis of the 'Torridonian'', *Journal of the Geological Society,* 139 (4), 413-20.

--- (2002), 'The Later Proterozoic Torridonian Rocks of Scotland: their Sedimentology, Geochemistry and Origin.', *Geological Society, London, Memoirs.,* 24.

Stewart, M., Strachan, R. A., Martin, M. W., and Holdsworth, R. E. (2001), 'Constraints on early sinistral displacements along the Great Glen Fault Zone, Scotland: structural setting, U–Pb geochronology and emplacement of the syn-tectonic Clunes tonalite', *Journal of the Geological Society,* 158 (5), 821-30.

Stille, H. (1924), 'Grundfragen der vergleichenden Tektonik.', *Gebruder Borntraeger, Berlin.*

Stipp, M., Stünitz, H., Heilbronner, R., and Schmid, S. M. (2002), 'The eastern Tonale fault zone: a 'natural laboratory' for crystal plastic deformation of quartz over a temperature range from 250 to 700 °C', *Journal of Structural Geology,* 24 (12), 1861-84.

Stone, P., Floyd, J. D., Barnes, R. P., and Lintern, B. C. (1987), 'A sequential back-arc and foreland basin thrust duplex model for the Southern Uplands of Scotland', *Journal of the Geological Society,* 144 (5), 753-64.

Stone, P. (1995), 'Geology of the Rhinns of Galloway.', *Memoir of the British Geological Survery. HMSO, London.*

Stone, P., Kimbell, G. S., and Henney, P. J. (1997), 'Basement control on the location of strike-slip shear in the Southern Uplands of Scotland', *Journal of the Geological Society,* 154 (1), 141-44.

Storetvedt, K. M. (1966), 'Remanent magnetization of some dolerite intrusions in the Egersund area, southern Norway.', *Geophysica Norvegica,* 26, 1-17.

Strachan, R. A. and Holdsworth, R. E. (1988), 'Basement–cover relationships and structure within the Moine rocks of central and southeast Sutherland', *Journal of the Geological Society,* 145 (1), 23-36.

Strachan, R. A., Holdsworth, R. E., Friderichsen, J. D., and Jepsen, H. F. (1992), 'Regional Caledonian structure within an oblique convergence zone, Dronning Louise Land, NE Greenland', *Journal of the Geological Society,* 149 (3), 359-71.

Strachan, R. A., Smith, M., Harris, A. L., and Fettes, D. J. (2002), 'The Geology of Scotland; The Northern Highland and Grampian Terranes', *The Geological Society, London*.

Strachan, R. A. and Evans, J. A. (2008), 'Structural setting and U–Pb zircon geochronology of the Glen Scaddle Metagabbro: evidence for polyphase Scandian ductile deformation in the Caledonides of northern Scotland', *Geological Magazine,* 145 (3), 361-71.

Stunitz, H. (1998), 'Syndeformational recrystallization - dynamic or compositionally induced?', *Contributions of Mineralogy & Petrology,* 131 (219-236).

Stünitz, H. and Gerald, J. D. F. (1993), 'Deformation of granitoids at low metamorphic grade. II: Granular flow in albite-rich mylonites', *Tectonophysics,* 221 (3–4), 299-324.

Suess, E. (1906), 'The face of the earth (English Translation)', *Translated by the H.B.C. Sollas, Oxford*.

Sundvoll, B. (1987), 'The age of the Egersund dyke swarm, SW Norway. Some tectonic implications.', *Terra Cognita (abstract),* 7 (108).

Suzuki, K., Feely, M., and O'Reilly, C. (2001), 'Disturbance of the Re-Os chronometer of molybdenites from the late-Caledonian Galway Granite, Ireland, by hydrothermal fluid circulation', *Geochemical Journal,* 35, 29-35.

Takada, A. (1989), 'Magma transport and reservoir formation by a system of propagating cracks', *Bulletin of Volcanology,* 52 (2), 118-26.

Takeda, Y.-T. and Obata, M. (2003), 'Some comments on the rheologically critical melt percentage', *Journal of Structural Geology,* 25 (5), 813-18.

Tanner, G. (2008), 'Tectonic significance of the Highland Boundary Fault, Scotland', *Journal of the Geological Society,* 165 (5), 915-21.

Tanner, G. P. W., Shackleton, R. M., and Rogers, G. (1997), 'New constraints upon the structural and isotopic age of the Oughterard Granite and on the timing of events in the Dalradian rocks of Connemara, western Ireland.', *Geological Journal,* 32, 247-63.

Tanner, P. W. G. (1967), 'The Dalradian of Connemara, Eire.', *11th Annual Report Research Institute of Arfican Studies, Leeds.*, 26-28.

Tanner, P. W. G. and Shackleton, R. M. (1979), 'Structure and stratigraphy of the Dalradian rocks of the Bennabeola area, Connemara, Eire', *Geological Society, London, Special Publications,* 8 (1), 243-56.

Tanner, P. W. G. (1981), 'Serial cross-sections through the Bennabeola area, Connemara. 1:50,000 in colour.', *University of Glasgow.*

Tanner, P. W. G. (1981), 'Dalradian Geology of the Bennabeola area, Co. Galway. 1:50,000 in coloured geological map.', *University of Glasgow*.

Tanner, P. W. G., Dempter, T. J., and Dickin, A. P. (1989), 'Short Paper: Time of docking of the Connemara terrane with the Delaney Dome Formation, western Ireland', *Journal of the Geological Society,* 146 (3), 389-92.

Tanner, P. W. G. (1990), 'Structural age of the Connemara gabbros, western Ireland', *Journal of the Geological Society,* 147 (4), 599-602.

Tanner, P. W. G. and Sutherland, S. (2007), 'The Highland Border Complex, Scotland: a paradox resolved', *Journal of the Geological Society,* 164 (1), 111-16.

Tanner, P. W. G. and Thomas, P. R. (2009), 'Major nappe-like D2 folds in the Dalradian rocks of the Beinn Udlaidh area, Central Highlands, Scotland', *Earth and Environmental Science Transactions of the Royal Society of Edinburgh,* 100 (04), 371-89.

Tarling, D. H. and Hrouda, F. (1993), 'The Magnetic Anisotropy of Rocks', *Chapman & Hall*.

Tarney, J. and Jones, C. E. (1994), 'Trace element geochemistry of orogenic igneous rocks and crustal growth models', *Journal of the Geological Society,* 151 (5), 855-68.

Tauxe, L. (1998), 'Paleomagnetic principles and practice', *Kluwer Academic Publishers, Dordrecht*, 299.

Taylor, H. (1980), *Earth planet. Sci. Lett.,* 47, 243-54.

Thirlwall, M. F. (1982), 'Systematic variation in chemistry and Nd-Sr isotopes across a Caledonian calc-alkaline volcanic arc: implications for source materials', *Earth and Planetary Science Letters,* 58 (1), 27-50.

--- (1986), 'Lead isotope evidence for the nature of the mantle beneath Caledonian Scotland', *Earth and Planetary Science Letters,* 80 (1–2), 55-70.

--- (1988), 'Geochronology of Late Caledonian magmatism in northern Britain', *Journal of the Geological Society,* 145 (6), 951-67.

Thirlwall, M. F., Stephens, W. E., and Shand, P. (1989), 'Calc-alkaline magmagenesis in the Scottish Southern Uplands forearc: a Pb-Sr-Nd isotope study', *Terra abstracts,* 1, 178.

Thomas, C., W., Graham, C., M., Ellam, R., M., and Fallick, A., E. (2004), '$^{87}Sr/^{86}Sr$ chemostratigraphy of Neoproterozoic Dalradian limestones of Scotland and Ireland: constraints on depositional ages and time scales', *Journal of the Geological Society,* 161 (2), 229-42.

Thompson, R. and Oldfield, P. (1986), 'Environmental Magnetism', *Allen & Unvin, London*.

Thomson, K. and Petford, N. (2008), 'Structure and Emplacement of High-level Magmatic Systems', *Geological Society Special Publication* 302.

Todd, S. P., Boyd, J. D., Sloan, R. J., and Williams, B. P. J. (1990), 'Sedimentology an tectonic setting of the Siluro-Devonian rocks of the Dingle Peninsula, SW Ireland.', *Field Excursion Guide, 13th International Sedimentological Congress, Nottingham, U.K.*

Todd, S. P. (2000), 'Taking the roof off a suture zone: basin setting and provenance of conglomerates in the ORS Dingle Basin of SW Ireland', *Geological Society, London, Special Publications,* 180 (1), 185-222.

Toghill, P. (1992), 'The Shelveian event, a late Ordovician tectonic episode in Southern Britain (Eastern Avalonia)', *Proceedings of the Geologists' Association,* 103 (1), 31-35.

Torsvik, T. H., Løvlie, R., and Storetvedt, K. M. (1983), 'Multicomponent magnetization in the helmsdale granite, north Scotland; geotectonic implication', *Tectonophysics,* 98 (1–2), 111-29.

Torsvik, T. H., Smethurst, M. A., Briden, J. C., and Sturt, B. A. (1990), 'A review of Palaeozoic palaeomagnetic data from Europe and their palaeogeographic implications', *In: McKerrow, W.S. & Scotese, C.R. (eds) Palaeozoic Palaeogeography and Biogeography. Geological Society, London, Memoirs,* 12, 25-41.

Torsvik, T. H., Ryan, P. D., Trench, A., and Harper, D. A. T. (1991), 'Cambrian-Ordovician paleogeography of Baltica', *Geology,* 19 (1), 7-10.

Torsvik, T. H. and Trench, A. (1991), 'Ordovician magnetostratigraphy: Llanvirn-Caradoc limestones of the Baltic platform', *Geophysical Journal International,* 107 (1), 171-84.

Torsvik, T. H. and Trench, A. (1991), 'The Ordovician history of the Iapetus Ocean in Britain: new palaeomagnetic constraints', *Journal of the Geological Society,* 148 (3), 423-25.

Torsvik, T. H., Trench, A., Svensson, I., and Walderhaug, H. J. (1993), 'Palaeogeographic significance of mid-Silurian palaeomagnetic results from southern Britain—major revision of the apparent polar wander path for eastern Avalonia', *Geophysical Journal International,* 113 (3), 651-68.

Torsvik, T. H., Smethurst, M. A., Meert, J. G., Van der Voo, R., McKerrow, W. S., Brasier, M. D., Sturt, B. A., and Walderhaug, H. J. (1996), 'Continental break-up and collision in the Neoproterozoic and Palaeozoic — A tale of Baltica and Laurentia', *Earth-Science Reviews,* 40 (3–4), 229-58.

Torsvik, T. H. (1998), 'Palaeozoic Palaeogeography: A North Atlantic viewpoint.', *Geol. For. Forh.,* 120, 10.

Torsvik, T. H. and Rehnström, E. F. (2003), 'The Tornquist Sea and Baltica–Avalonia docking', *Tectonophysics,* 362 (1–4), 67-82.

Townend, R. (1966), 'The Geology of some Granite Plutons from Western Connemara, Co. Galway.', *Proceedings of the Royal Irish Academy. Section B: Biological, Geological, and Chemical Science,* 65, 157-202.

Treloar, P. J. (1977), 'The stratigraphy, geochemistry and metamorphism of the rocks of the Recess area, Connemara, Eire.', *Ph.D. thesis, University of Glasgow*.

--- (1982), 'The stratigraphy and structure of the rocks of the Lissoughter area, Connemara,' *Proceedings of the Royal Irish Academy.,* 82B, 83-107.

Trench, A. and Torsvik, T. H. (1992), 'The closure of the Iapetus Ocean and Tornquist Sea: new palaeomagnetic constraints', *Journal of the Geological Society,* 149 (6), 867-70.

Tribe, I. R. and D'Lemos, R. S. (1996), 'Significance of a hiatus in down-temperature fabric development within syn-tectonic quartz diorite complexes, Channel Islands, UK', *Journal of the Geological Society,* 153 (1), 127-38.

Trindade, R. I. F., Raposo, M. I. B., Ernesto, M., and Siqueira, R. (1999), 'Magnetic susceptibility and partial anhysteretic remanence anisotropies in the magnetite-bearing granite pluton of Tourão, NE Brazil', *Tectonophysics,* 314 (4), 443-68.

Trindade, R. I. F., Bouchez, J.-L., Bolle, O., Nédélec, A., Peschler, A., and Poitrasson, F. (2001), 'Secondary fabrics revealed by remanence anisotropy: methodological study and examples from plutonic rocks', *Geophysical Journal International,* 147 (2), 310-18.

Trzebski, R., Behr, H. J., and Conrad, W. (1997), 'Subsurface distribution and tectonic setting of the late-Variscan granites in the northwestern Bohemian Massif', *Geologische Rundschau,* 86 (0), S64-S78.

Tullis, J. and Yund, R. A. (1987), 'Transition from cataclastic flow to dislocation creep of feldspar: Mechanisms and microstructures', *Geology,* 15 (7), 606-09.

--- (1991), 'Diffusion creep in feldspar aggregates: experimental evidence', *Journal of Structural Geology,* 13 (9), 987-1000.

Usui, Y., Nakamura, N., and Yoshida, T. (2006), 'Magnetite microexsolutions in silicate and magmatic flow fabric of the Goyozan granitoid (NE Japan): Significance of partial remanence anisotropy', *J. Geophys. Res.,* 111 (B11), B11101.

Vahid, A., Mohammad-Vali, V., Reza, D., and Jamal, R. (2011), 'The field and microstructural study of Malayer plutonic rocks, west of Iranb', *JGeope,* 1, 59-69.

Valley, P. M., Hanchar, J. M., and Whitehouse, M. J. (2011), 'New insights on the evolution of the Lyon Mountain Granite and associated Kiruna-type magnetite-apatite deposits, Adirondack Mountains, New York State', *Geosphere,* 7 (2), 357-89.

van Breemen, O., Aftalion, M., Pankhurst, R. J., and Richardson, S. W. (1979), 'Age of the Glen Dessary Syenite, Inverness-shire: diachronous Palaeozoic metamorphism Across the Great Glen', *Scottish Journal of Geology,* 15 (1), 49-62.

van Breemen, O. and Bluck, B. J. (1981), 'Episodic granite plutonism in the Scottish Caledonides', *Nature,* 291 (5811), 113-17.

Van den Eckhout, B., Grocott, J., and Vissers, R. (1986), 'On the role of diapirism in the segregation, ascent and final emplacement of granitoid magmas-Discussion.', *Tectonophysics,* 127, 161-69.

Van der Molen, I. and Paterson, M. S. (1979), 'Experimental deformation of partially-melted granite', *Contributions to Mineralogy and Petrology,* 70 (3), 299-318.

van der Voo, R. and Scotese, C. (1981), 'Paleomagnetic evidence for a large (2,000 km) sinistral offset along the Great Glen fault during Carboniferous time', *Geology,* 9 (12), 583-89.

van Staal, C. R., Dewey, J. F., Niocaill, C. M., and McKerrow, W. S. (1998), 'The Cambrian-Silurian tectonic evolution of the northern Appalachians and British Caledonides: history of a complex, west and southwest Pacific-type segment of Iapetus', *Geological Society, London, Special Publications,* 143 (1), 197-242.

Vassallo, J. J. and Wilson, C. J. L. (2002), 'Palaeoproterozoic regional-scale non-coaxial deformation: an example from eastern Eyre Peninsula, South Australia', *Journal of Structural Geology,* 24 (1), 1-24.

Vauchez, A., Pacheco Neves, S., and Tommasi, A. (1997), 'Transcurrent shear zones and magma emplacement in Neoproterozoic belts of Brazil.', *In: Bouchez, J.L., Hutton, D.H.W., Stephens, W.E., (eds.), Grantie: From Segregation of Melt to Emplacement Fabrics, Kluwer Academic Publishers, Dordrecht*, 275-94.

Vaughan, A. P. M. (1996), 'A tectonomagmatic model for the genesis and emplacement of Caledonian calc-alkaline lamprophyres', *Journal of the Geological Society,* 153 (4), 613-23.

Vegas, N., Naba, S., Bouchez, J., and Jessell, M. (2008), 'Structure and emplacement of granite plutons in the Paleoproterozoic crust of Eastern Burkina Faso: rheological implications', *International Journal of Earth Sciences,* 97 (6), 1165-80.

Verniers, J., Pharaoh, T., André, L., Debacker, T. N., De Vos, W., Everaerts, M., Herbosch, A., Samuellson, J., Sintubin, M., and Vecoli, M. (2002), 'The Cambrian to mid Devonian basin development and deformation history of Eastern Avalonia, east of the Midlands Microcraton: new data and a review', *Geological Society, London, Special Publications,* 201 (1), 47-93.

Vernon, R. H. (1987), 'A Microstructural indicator of shear sense in volcanic rocks and its relationship to porphyroblast rotation in metamorphic rocks', *Journal of Geology,* 95, 127-33.

Vernon, R. H. and Paterson, S. R. (1993), 'The Ardara pluton, Ireland: deflating an expanded intrusion', *Lithos,* 31 (1–2), 17-32.

Vernon, R. H. (2000), 'Review of Microstructural Evidence of Magmatic and Solid-State Flow', *Visual Geosciences,* 5 (2), 1-23.

--- (2004), 'A practical guide to Rock Microstructure', *Cambridge University Press*, 43-165.

Verwey, E. J. W. (1939), 'Electronic Conduction of Magnetite (Fe3O4) and its Transition Point at Low Temperatures', *Nature,* 144, 327-28.

Verwey, E. J. W. and Haayman, P. W. (1941), 'Electronic conductivity and transition point of magnetite ("Fe3O4")', *Physica,* 8 (9), 979-87.

Vigneresse, J.-L., Tikoff, B., and Améglio, L. (1999), 'Modification of the regional stress field by magma intrusion and formation of tabular granitic plutons', *Tectonophysics,* 302 (3–4), 203-24.

Vigneresse, J. L. (1990), 'Use and misuse of geophysical data to determine the shape at depth of granitic intrusions', *Geological Journal,* 25 (3-4), 249-60.

Vigneresse, J. L., Barbey, P., and Cuney, M. (1996), 'Rheological Transitions During Partial Melting and Crystallization with Application to Felsic Magma Segregation and Transfer', *Journal of Petrology,* 37 (6), 1579-600.

Vigneresse, J. L. and Tikoff, B. (1999), 'Strain partitioning during partial melting and crystallizing felsic magmas', *Tectonophysics,* 312 (2–4), 117-32.

Vigneresse, J. L. and Clemens, J. D. (2000), 'Granitic magma ascent and emplacement: neither diapirism nor neutral buoyancy', *In: Vendeville, B., Mart, Y., Vigneresse, J.L. (eds) Salt,*

Shale and Igneous Diapirs in and Around Europe. Geological Society London, Special Publications, (174), 1-19.

Vigneresse, J. L. (2005), 'A new paradigm for granite generation', *Transactions: Earth Sciences,* 95 (1-2), 11-22.

Vincenz, S. A. (1965), 'Frequency Dependence of Magnetic Susceptibility of Rocks in Weak Alternating Fields', *J. Geophys. Res.,* 70 (6), 1371-77.

Vogt, T. (1936), 'Orogenesis in the Region of Palaeozoic Folding of Scandinavia and Spitsbergen', *In: Report of the 16th International Geologic Congress, Washington,* 1933, 953-55.

Wager, L. R. and Andrew, G. (1930), 'The Age of the Connemara Schists and of their Metamorphism', *Geological Magazine,* 67 (06), 271-75.

Wager, L. R. (1932), 'The Geology of the Roundstone District, County Galway.', *Proceedings of the Royal Irish Academy. Section B: Biological, Geological, and Chemical Science,* 41, 46-71.

--- (1939), 'Outline of the geology of Connemara', *Proceedings of the Geologists' Association, London,* 50, 346-51.

Wager, L. R. (1967), 'Layered igneous rocks: San Francisco', *W.H. Freeman and Company*, 588.

Wager, L. R. and Brown, G. M. (1968), 'Layered igneous rocks', *Oliver and Boyd, Edinburgh*, 588.

Walker, G. P. L. and Leedal, G. P. (1954), 'The Barnesmore granite complex, County Donegal', *Scientific Proceedings of the Royal Dublin Society,* 26, 207-43.

Watt, G. R. and Thrane, K. (2001), 'Early Neoproterozoic events in East Greenland', *Precambrian Research,* 110 (1–4), 165-84.

Weertman, J. (1971), 'Theory of Water-Filled Crevasses in Glaciers Applied to Vertical Magma Transport beneath Oceanic Ridges', *J. Geophys. Res.,* 76 (5), 1171-83.

Weinberg, R. F. and Podladchikov, Y. (1994), 'Diapiric ascent of magmas through power law crust and mantle', *J. Geophys. Res.,* 99 (B5), 9543-59.

Weinberg, R. F. (1996), 'Ascent mechanism of felsic magmas: news and views', *Geological Society of America Special Papers,* 315, 95-103.

Whalen, J. B. and Chappell, B. W. (1988), 'Opaque mineralogy and mafic mineral chemistry of I- and S-type granites of the Lachan fold belt, southeast Australia', *American Mineralogist,* 73, 281-96.

Whitcombe, D. N. and Maguire, P. K. H. (1981), 'A seismic refraction investigation of the Charnian basement and granitic intrusions flanking Charnwood Forest', *Journal of the Geological Society,* 138 (6), 643-51.

Wiedenbeck, M., Hanchar, J. M., Peck, W. H., Sylvester, P., Valley, J., Whitehouse, M. J., Kronz, A., Morishita, Y., Nasdala, L., Fiebig, J., Franchi, I., Girard, J. P., Greenwood, R. C., Hinton, R., Kita, N., Mason, P. R. D., Norman, M., Ogasawara, M., Piccoli, P. M., Rhede, D., Satoh, H., Schulz-Dorbick, B., Skar, O., Spicuzza, M. J., Terada, K., Tindle, A., Togashi, S., Vennemann, T., Xie, Q., and Zheng, Y. F. (2004), 'Further Characterisation of the 91500 Zircon Crystal', *Geostandards and Geoanalytical Research,* 28 (1), 9-39.

Wilcox, R. E., Harding, T. P., and Seely, D. R. (1973), 'Basin wrench tectonics', *Bulletin American Association of Petroleum Geologists,* 57, 74-96.

Williams, D. M., Armstrong, H. A., and Harper, D. A. T. (1989), 'The age of the South Connemara Group, Ireland, and its relationship to the Southern Uplands Zone of Scotland and Ireland', *Scottish Journal of Geology,* 24 (3), 279-87.

Williams, Q. and Tobisch, O. T. (1994), 'Microgranitic enclave shapes and magmatic strain histories: Constraints from drop deformation theory', *J. Geophys. Res.,* 99 (B12), 24359-68.

Wilson, J. R. (1969), 'The Geology of the Galway Granite, northwest of Galway City', *Ph.D. thesis, University of Bristol*.

Wolff, J. A., Ellwood, B. B., and Sachs, S. D. (1989), 'Anisotropy of magnetic susceptibility in welded tuffs: application to a welded-tuff dyke in the tertiary Trans-Pecos Texas volcanic province, USA', *Bulletin of Volcanology,* 51 (4), 299-310.

Wones, D. R. and Eugster, H. P. (1965), 'Stability of Biotite: Experiment, Theory and Application', *The American Mineralogist,* 50, 1228-72.

Woodcock, N. H. (1990), 'Sequence stratigraphy of the Palaeozoic Welsh Basin', *Journal of the Geological Society,* 147 (3), 537-47.

--- (1991), 'The Welsh, Anglian and Belgian Caledonides compared.', *Annales de la Societe Geologique de Belgique.,* 114, 5-17.

Woodcock, N. H. and Pharaoh, T. C. (1993), 'Silurian fades beneath East Anglia', *Geological Magazine,* 130 (05), 681-90.

Woodcock, N. H. and Strachan, R. (2000), 'Geological history of Britain and Ireland', *Cambridge, Blackwell Science*, 423.

Woodcock, N. H., Soper, N. J., and Strachan, R. A. (2007), 'A Rheic cause for the Acadian deformation in Europe', *Journal of the Geological Society,* 164 (5), 1023-36.

Woodcock, N. H. and Strachan, R. A. (2012), 'Geological History of Britain and Ireland', *Blackwell Publishing*.

Woodcock, N. H., Soper, N.J. (2006), 'The Acadian Orogeny: the mid-Devonian Phase that formed slate belts in England and Wales', *Brenchley, P.J. & Rawson, P.F (eds) The Geology of England and Wales. Geological Society. London*, 131-46.

Woodhead, J. (2008), 'A GUIDE TO DEPTH PROFILING AND IMAGING APPLICATIONS OF LA–ICP–MS', *Mineralogical association of Canada short course sereis 40*, 135-45.

Worm, H.-U. and Banerjee, S. K. (1984), 'Aqueous low-temperature oxidation of titanomagnetite', *Geophysical Research Letters,* 11 (3), 169-72.

Wright, H. M. N. and Weinberg, R. F. (2009), 'Strain localization in vesicular magma: Implications for rheology and fragmentation', *Geology,* 37 (11), 1023-26.

Wright, P. C. (1961), 'The petrology and geochemistry of the Galway Granite, of the Carna district, Connemara, Eire', *Ph.D. Thesis University of Bristol*.

--- (1963), 'The Petrology, Chemistry and Structure of the Galway Granite of the Carna Area, Co. Galway', *Proceedings of the Royal Irish Academy. Section B: Biological, Geological, and Chemical Science,* 63, 239-64.

Xu, S. and Dunlop, D. J. (1995), 'Toward a better understanding of the Lowrie-Fuller test', *J. Geophys. Res.,* 100 (B11), 22533-42.

Yardley, B. W. D. (1976), 'Deformation and metamorphism of Dalradian rocks and the evolution of the Connemara Cordillera', *Journal of the Geological Society,* 132 (5), 521-42.

Yardley, B. W. D. (1980), 'Metamorphism and orogeny in the Irish Dalradian', *Journal of the Geological Society,* 137 (3), 303-09.

Yardley, B. W. D., Barber, J. P., Gray, J. R., and Taylor, W. E. G. (1987), 'The Metamorphism of the Dalradian Rocks of Western Ireland and its Relation to Tectonic Setting [and Discussion]', *Philosophical Transactions of the Royal Society of London. Series A, Mathematical and Physical Sciences,* 321 (1557), 243-70.

Yoshinobu, A. S. and Barnes, C. G. (2008), 'Is stoping a volumetrically significant pluton emplacement process?: Discussion', *Geological Society of America Bulletin,* 120 (7-8), 1080-81.

Young, D. G. G. (1974), 'Donegal Granite - gravity analysis', *Proceedings of the Royal Irish Academy. Section B-Biological, Geological and Chemical Science,* 74, 63-73.

Zagorevski, A., Van Staal, C. R., McNicoll, V., and Rogers, N. (2007), 'Upper Cambrian to Upper Ordovician peri-Gondwanan Island arc activity in the Victoria Lake Supergroup, Central Newfoundland: Tectonic development of the northern Ganderian margin', *American Journal of Science,* 307 (2), 339-70.

Žák, J., Hrouda, F., and Holub, F. V. (2010), 'Plane-confined magnetic lineations in mingled mafic and felsic magmas, the Sázava pluton, Bohemian Massif', *Journal of Volcanology and Geothermal Research,* 190 (3–4), 312-24.

Zaniewski, A., Reavy, R. J., and Harris, A. L. (2006), 'Field relationships and emplacement of the Caledonian Ross of Mull Granite, Argyllshire', *Scottish Journal of Geology,* 42 (2), 179-89.

Ziegler, P. A. and Kent, P. (1982), 'Faulting and Graben Formation in Western and Central Europe [and Discussion]', *Philosophical Transactions of the Royal Society of London. Series A, Mathematical and Physical Sciences,* 305 (1489), 113-43.

Zwaan, B. K., Van Roemund, H.L.M. (1990), 'A rift-related mafic dyke swarm in the Corrovarre Nappe of the Caledonian Middle Allochthon, Troms, North Norway, and its tectonometamorphic evolution.', *Nor. Geol. Unders. Bull.,* 419, 20.